

**Complex transcription of the utrophin gene: A study
of short utrophin isoforms**

Cecilia Jiménez-Mallebrera

June 2001

Thesis submitted for the degree of Doctor of Philosophy
in the University of London

MRC Human Biochemical Genetics Unit
The Galton Laboratory
Department of Biology
University College London
University of London

ProQuest Number: U643808

All rights reserved

INFORMATION TO ALL USERS

The quality of this reproduction is dependent upon the quality of the copy submitted.

In the unlikely event that the author did not send a complete manuscript and there are missing pages, these will be noted. Also, if material had to be removed, a note will indicate the deletion.



ProQuest U643808

Published by ProQuest LLC(2016). Copyright of the Dissertation is held by the Author.

All rights reserved.

This work is protected against unauthorized copying under Title 17, United States Code.
Microform Edition © ProQuest LLC.

ProQuest LLC
789 East Eisenhower Parkway
P.O. Box 1346
Ann Arbor, MI 48106-1346

Summary

Utrophin is the autosomal homologue of dystrophin. Transcription from the utrophin gene involves at least five promoters that regulate the expression of two full-length and three short transcripts (G-utrophin, Up71 and Up 140). The skeletal muscle full-length form has been well studied because it has a potential role in the treatment of Duchenne Muscular Dystrophy. However, there is little information on the short forms, particularly their patterns of expression and function. The aim of this project was to characterise the short utrophin forms at the mRNA and protein levels and to look for other utrophin transcripts. Mice knocked-out for full-length utrophin (UKO^{ex6}) were used as an experimental system. These mice lack full-length utrophin but it was expected that they would express all the short forms.

In order to examine the distribution of utrophin protein in UKO^{ex6} mice, polyclonal antibodies were raised against different regions of the protein. Western blotting and immunofluorescence studies, using these antibodies, confirmed that full-length utrophin is absent in UKO^{ex6} tissues and identified two novel short forms Up120 and Up109. These studies also showed that while Up140 and Up71 appear not to be translated, the other short forms are translated in a tissue specific fashion. G-utrophin is neuronal specific; Up120 is expressed specifically in kidney glomeruli; Up109 was identified in foetal hands/feet and appears to localise to the epidermis. A cDNA for Up109 was isolated by 5' RACE; this contains 460bp of unique sequence encoding 5'UTR and 17 amino acids.

Immunological studies confirmed that the full-length form is the major utrophin in skeletal muscle, and demonstrated that this form is also the most abundant in kidney and testis. In the testis, full-length utrophin localises to intertubular tissue and to Leydig cells. Western blot analysis suggested that a novel isoform(s) is expressed in the testis, however, this could not be confirmed by immuno-histochemistry. Weak signal detected at the neuromuscular junction in UKO^{ex6} adult muscle was interpreted as being due to a short isoform, perhaps Up140.

In contrast to the apparently limited distribution of short forms as proteins, mRNA *in situ* hybridisation experiments to control and UKO^{ex6} embryo sections showed that they are transcribed abundantly throughout development. Short transcripts are first detected by 8.5 dpc in the neural tube and appear to comprise the majority of utrophin expression during development. Sites of high expression of full-length utrophin mRNA during development are tongue, choroid plexus and the outflow of the heart. A comparison of the mRNA and protein distributions suggests that the transcription of short utrophin mRNAs is not matched by their translation (this is particularly true for Up140 and Up71). The significance of this important observation and possible roles for the short transcripts are discussed. The developmental studies also revealed three novel sites of utrophin expression - pyloric sphincter, the urethra and the semicircular canals.

Summary

Utrophin is the autosomal homologue of dystrophin. Transcription from the utrophin gene involves five promoters that regulate the expression of two full-length and three short transcripts. The skeletal muscle isoform has been well studied because it has a potential role in the treatment of Duchenne Muscular Dystrophy. However, there is little information on the short isoforms, particularly their patterns of expression and function. The aim of this project was to characterise the short utrophin isoforms at the mRNA and protein levels and to look for other utrophin transcripts. Mice knocked-out for full-length utrophin (UKO^{ex6}) were used as the experimental model. These mice lack full-length utrophin but it was believed that they would express all the short isoforms.

In order to examine the distribution of utrophin protein in UKO^{ex6} mice, polyclonal antibodies were raised against different regions of the protein. Western blotting and immunofluorescence to tissue sections confirmed that full-length utrophin is absent in UKO^{ex6} tissues and showed that while Up140 and Up71 appear not to be translated, some short isoforms are translated in a limited fashion. Two of these isoforms, Up120 and Up109, had not been reported previously. Up120 is a kidney specific isoform and Up109 might be a foetal isoform. Up109 cDNA, which contains novel sequence in intron 55, was isolated by 5' RACE.

Immunological analysis of a selection of tissues showed that the full-length form is the major utrophin in skeletal muscle, kidney and testis and revealed that in the latter full-length utrophin localises to the intertubular tissue and to the Leydig cells. Surprisingly, weak utrophin signal could be detected at the neuromuscular junction in UKO^{ex6} adult muscle.

In contrast to the restricted expression of short isoforms as proteins, mRNA *in situ* hybridisation experiments using probes to different regions of utrophin mRNA showed that short utrophin isoforms are transcribed abundantly throughout development. Thus, for these isoforms the abundance of mRNA is not matched by that of the protein. The significance of this observation and possible roles for the short transcripts are discussed.

Acknowledgements

I would like to thank my supervisor Prof. Yvonne Edwards for her dedication and encouragement throughout this period and more important, for teaching me how to be a good scientist.

I would like to take this opportunity to thank the members of my group at the MRC Human Biochemical Genetics Unit with whom I shared very nice and busy times, Katie, Ira, Sinthuja, Kim, Eleni, Michelle, Harry, Felicity, and Constanze, and give a special thanks to Wendy Putt and James Wilson for their enormous help with this work.

I am very grateful to Prof. Kay Davies and her group in Oxford for the gift of a colony of UKO^{ex6} mice and antibodies, technical advice, useful interactions and interest in the progress of this project. I would like to express my gratitude to Dr. Susan Brown for her generous help with the immuno-histochemistry and kind advice.

I would like to give my most heartfelt thanks to my parents and my brother who with their love and sacrifice have made it possible for me to pursue these studies.

Finally, a big thank you to David for his love, patience and support.

This work has been funded by the “Association Française contre les Myopathies” and the European Commission.

Contents

	Page
Summary	2
Acknowledgements	3
Contents	4
List of Figures	9
List of Tables	13
Abbreviations	14
Chapter One : Introduction	18
1.1 Cloning of full-length utrophin cDNA	19
1.2 The utrophin gene	20
1.3 The utrophin protein structure	22
1.4 Utrophin related proteins	29
spectrin	29
α -actinin	30
dystrobrevin	32
Dystrophin related protein 2 (DRP2)	33
1.5 The dystrophin isoforms	35
Muscle isoform	35
Brain isoform	35
Cerebellar isoform	37
Lymphoid isoform	37
Dp71 isoform	38
Dp116 isoform	40
Dp140 isoform	41
Dp260 isoform	41
1.6 Alternative splicing of the dystrophin transcripts	43
1.7 Function of dystrophin isoforms and animal models	46
<i>mdx</i> mice	46
<i>mdx</i> ^{3CV} mice	48
DMD ^{ex52} mice	48
Function of full-length dystrophin	49
Function of short dystrophin isoforms	50
1.8. The utrophin isoforms	54
Full-length utrophin A	54

	Page
<i>-Full-length utrophin A promoter</i>	60
<i>-Regulation of expression of full-length utrophin A in skeletal muscle</i>	61
<i>-Structure and function of 395kDa utrophin -DAP complex at the NMJ</i>	64
<i>-Structure and function of 395kDa utrophin -DAP complex in non-muscle tissues</i>	67
Full-length utrophin B	70
N-utrophin	70
G-utrophin	71
Up140 isoform	72
Up71 isoform	74
1.9 Expression of utrophin mRNAs during embryonic development	77
1.10 Function of utrophin isoforms and animal models	78
UKO ^{ex6} mice	78
UKO ^{ex64} mice	81
dko ^{ex6} and dko ^{ex64} mice	82
1.11 DMD	85
DMD: mutations	85
DMD: therapies	87
Aims and objectives	96
Chapter two: Materials and Methods	98
2.1 Materials	98
Standard reagents	98
Enzymes	98
Electrophoresis reagents	98
Miscellaneous	98
Common buffers	99
Microbiology media	99
Bacterial strains	100
2.2 Methods	100
DNA precipitation and assay of concentration	100
RNA precipitation and assay of concentration	100
Restriction enzyme digests	101
DNA ligations	101
Transformation of competent cells	101
Plasmid DNA preparation	102

	Page
Agarose gel electrophoresis and recovery of DNA fragments	102
Isolation of RNA	103
Preparation of cDNA by reverse transcription and RT-PCR	103
RNA formaldehyde-agarose electrophoresis	106
DNA sequencing	106
Preparation and analysis of protein	108
Production of Mupa antibodies	109
Western blotting	117
5' RACE	119
Genomic library screening	123
Southern blotting	125
Fluorescent immuno-histochemistry	125
mRNA <i>in situ</i> hybridisation to embryo sections	127
Chapter Three: Production of the Mupa antibodies	134
Results	134
3.1 General comments	134
3.2 Preparation of utrophin constructs	138
3.3 Small scale production of GST-fusion proteins	142
3.4 Large scale production of GST-fusion proteins	152
3.5 Rabbit Immunisations	159
3.6 Isolation of immunoglobulins from serum	160
3.7 Affinity purification	162
Discussion	166
3.8 General comments	166
3.9 Thoughts on antibody affinity purification methods	168
Chapter Four: Western blots and 5' RACE	170
Results: Western blots	170
4.1 General comments	170
4.2 Western blot analysis of a selection of tissues	179
kidney	179
Brain	184
Skeletal muscle	190
Testis	193
Foetal hands	196
4.3 Summary of results	200

	Page
Results:5' RACE	202
4.4 5' RACE in the region of exons 54 and 55	202
4.5 5' RACE in the region of exons 56 and 57	211
4.6 Characterisation of the novel 109kDa isoform (Up109)	219
5' novel sequence of Up109	219
Expression of Up109 mRNA	221
Position of Up109 first exon in the utrophin gene	224
5' flanking sequence of Up109	230
Discussion	234
4.7 General comments	234
4.8 The origin of multiple bands seen on Western blots	235
Degradation of full-length utrophin	235
Cross-reactivity with related proteins	236
Other cross-reactivities	240
4.9 Short utrophin isoforms	242
Are Up140 and Up71 translated?	242
Confirmation that G-utrophin is a neuronal specific utrophin isoform	248
Where is the promoter of Up120?	250
Does Up120 have a role in kidney?	251
A novel short isoform(s) expressed in testis	252
Up109: A novel foetal utrophin isoform	252
Thoughts on the function of Up109	255
Up109 proximal promoter	255
Chapter 5: Immuno-histochemistry	258
Results	258
5.1 General comments	258
5.2 Immuno-histochemical analysis of a selection of tissues	258
Adult skeletal muscle	258
Foetal skeletal muscle	278
Adult kidney	281
Adult testis	286
Foetal hands	291
Discussion	296
5.3 Utrophin isoforms in skeletal muscle	296
5.4 Full-length utrophin and Up120 are expressed in kidney	304

	Page
5.5 Full-length utrophin is expressed in testis intertubular tissue and in Leydig cells	309
5.6 Expression of utrophin isoforms in the skin	315
Chapter 6: Expression of utrophin mRNAs during embryogenesis	318
Results	318
6.1 General comments	318
6.2 mRNA <i>in situ</i> hybridisation	321
6.3 Summary of results	347
Discussion	351
6.4 General comments	351
6.5 Utrophin mRNAs detected in selected tissues	352
Neural tube	352
Dorsal-root and cranial ganglia	354
Choroid plexii	355
Tongue	356
Limb bud/digits	357
Semicircular canals	358
Pyloric sphincter	361
Urogenital system	362
6.6 Final remarks	365
Chapter 7: Final Results and conclusions	371
7.1 General conclusions	371
7.2 Other genes containing alternative promoters	374
7.3 If short utrophins are not translated do they have another function?	378
7.4 Implications for manipulation of utrophin transcription in DMD patients	381
7.5 Utrophin and disease	383
References	386

List of Figures

	Page
Fig 1.1 Comparison between utrophin and dystrophin proteins	23
Fig 1.2 Structure of the utrophin protein	24
Fig 1.3 Structure of the known isoforms of dystrophin	36
Fig 1.4 Structure of the known isoforms of utrophin	55
Fig 1.5 395kDa Utrophin-DAP complex at the neuromuscular junction	65
Fig 1.6 395kDa Utrophin-DAP complex at the membrane of a epithelial cell	69
Fig 3.1 Positions of the aa sequences corresponding to the utrophin proteins utr-1, -2,-3 and -4	137
Fig 3.2 RT-PCR amplification of the utrophin sequences corresponding to utr proteins and structure of the pGEX vector	139
Fig 3.3 Restriction digests of plasmid DNAs of GSTutr recombinants	141
Fig 3.4 Diagram of the small scale preparation of GST-fusion proteins procedure	143
Fig 3.5 SDS PAGE of small scale preparation of GSTutr-1 and GSTutr-2 stained with Coomassie blue	144
Fig 3.6 SDS PAGE of small scale preparation of GSTutr-3 and GSTutr-4 stained with Coomassie blue	145
Fig 3.7 Preparation of GSTutr-2 using different IPTG concentrations and induction times	147
Fig 3.8 Preparation of GSTutr-2 using different Triton X-100 concentrations	149
Fig 3.9 Preparation of GSTutr-2 using optimal conditions	151
Fig 3.10 Diagram of the large scale preparation of GST fusion proteins procedure	153
Fig 3.11 SDS PAGE of large scale preparation of GSTutr-3 stained with Coomassie blue	154
Fig 3.12 SDS PAGE of purified proteins utr-1,utr-3 and utr-4 stained with Coomassie blue	156
Fig 3.13 Western blot analysis of purified proteins utr-1, utr-3 and utr- 4 using utrophin specific antibodies	158
Fig 3.14 Graphical representation of the immune response of rabbit Wendy immunised with utr-3	161
Fig 3.15 SDS PAGE of isolated IgGs from Wendy serum stained with Coomassie blue	163
Fig 3.16 SDS PAGE of fractions after affinity purification of Mupa-2 stained with Coomassie blue and OD of these fractions	164

	Page
Fig.4.1 SDS PAGE of mouse tissue extracts stained with Coomassie blue	172
Fig 4.2 A Positions of aa sequences used to raise the Mupa antibodies, Mancho-3, Urd40, Ut43,"COOH-ter" and K5B1	173
Fig 4.2 B Minimum sizes of polypeptides that could be detected with the COOH-ter antibodies	177
Fig 4.3 Western blot of tissue extracts using Mupa-2 and without the primary antibody	174
Fig 4.4 Western blot of adult and foetal kidney and adult lung extracts	180
Fig 4.5 aa alignment of the utrophin sequence used to raise Mupa-1 and β -spectrin	181
Fig 4.6 Western blot of adult brain extracts	186
Fig 4.7 aa alignment of the utrophin sequence used to raise Mupa-1 and T-plastin	188
Fig 4.8 Western blot of adult skeletal muscle extracts	191
Fig 4.9 aa alignment of the utrophin sequence used to raise Mupa-1 and α -actinin	192
Fig 4.10 Western blot of adult testis extracts	195
Fig 4.11 Western blot of 16.5 dpc hands extracts	197
Fig 4.12 SDS PAGE of UKO ^{ex6} foetal hands extracts stained with Coomassie blue and immunoblotted with Mupa-2 and Urd40	199
Fig 4.13 RNA preparations from adult kidney and foetal hands	203
Fig 4.14 Outline of the 5' RACE procedure	204
Fig 4.15 Position of primers used in 5' RACE in the region of exons 54-55	205
Fig 4.16 First and second round PCR products using UT56R1, UT55R2 and UT55R3	207
Fig 4.17 <i>EcoRI/HindIII</i> and <i>PstI</i> digests of DNAs from foetal hands 5' RACE recombinants	209
Fig 4.18 Position of primers used in 5' RACE in the region of exons 56-57	212
Fig 4.19 First and second round PCR products using UT59R1, UT58R2 and UT57R3	214
Fig 4.20 Second round PCR at 58 °C using either UT58R2 or UT57R3 and electrophoresis of the gel extracted major bands	215

	Page
Fig 4.21 Extent of the mRNA sequences isolated by 5' RACE in the regions of exons 56-57	217
Fig 4.22 Sequencing of the 900bp and 600bp foetal hands and kidney 5' RACE products	218
Fig 4.23 The 5' novel sequence of Up109	220
Fig 4.24 RT-PCR of mouse cDNAs using Up109 specific primers	223
Fig 4.25 Alternative splicing in the first exon of Up109	225
Fig 4.26 <i>EcoRI</i> digestion of the genomic recombinant U109G-2; sequencing and PCR amplification of a major 6.8kb fragment	227
Fig 4.27 Relative positions of exons 55, 56 and Up109 and G-utrophin 1 st exons on the genomic sequence AC073979	229
Fig 4.28 5' flanking sequence of Up109	232
Fig 5.1 Control skeletal muscle sections labelled with Mupa-1	260
Fig 5.2 <i>mdx</i> skeletal muscle sections labelled with Mupa-1	261
Fig 5.3 <i>mdx</i> skeletal muscle sections labelled with Mupa-2 and control sections labelled with Mupa-3	262
Fig 5.4 C57Bl skeletal muscle sections labelled with second antibody only and with pre-immune serum	264
Fig 5.5 Double labelling of C57Bl skeletal muscle sections for dystrophin and utrophin	265
Fig 5.6 Labelling of blood-vessels and nerves with Mupa-1 and -2	267
Fig 5.7 C57Bl and UKO ^{ex6} skeletal muscle sections labelled with Mupa-1 using 2 or 5 sec exposure time	269
Fig 5.8 C57Bl and UKO ^{ex6} skeletal muscle sections labelled with Urd40 using 2 or 5 sec exposure time	270
Fig 5.9 C57Bl and UKO ^{ex6} skeletal muscle sections labelled with Mupa-2 using 2 sec exposure time	271
Fig 5.10 RT-PCRs of C57Bl and UKO ^{ex6} cDNAs between exons 4 and 8	273
Fig 5.11 RT-PCRs of C57Bl and UKO ^{ex6} cDNAs in the 5' region of utrophin	275
Fig 5.12 Labelling of C57Bl and UKO ^{ex6} skeletal muscle sections with α - and β -dystroglycan, α -sarcoglycan and dystrophin antibodies	277
Fig 5.13 C57Bl and UKO ^{ex6} foetal muscle sections labelled with Mupa-1, Mupa-3 and Urd40	279
Fig 5.14 C57Bl and UKO ^{ex6} foetal muscle sections labelled for dystrophin	280

	Page
Fig 5.15 C57Bl and UKO ^{ex6} kidney sections labelled with Mupa-1	283
Fig 5.16 C57Bl and UKO ^{ex6} kidney sections labelled with Mupa-3	284
Fig 5.17 C57Bl and UKO ^{ex6} kidney sections labelled with Mupa-3 using a biotin-streptavidin amplification system	285
Fig 5.18 C57Bl and UKO ^{ex6} kidney sections labelled for dystrophin	287
Fig 5.19 C57Bl and UKO ^{ex6} testis sections labelled with Mupa-1	288
Fig 5.20 C57Bl and UKO ^{ex6} testis sections labelled with Mupa-2	289
Fig 5.21 C57Bl and UKO ^{ex6} testis sections labelled with Mupa-3	290
Fig 5.22 C57Bl and UKO ^{ex6} 15.5 dpc hands sections labelled with Mupa-2 and -3 and anti-collagen I antibody	292
Fig 5.23 C57Bl and UKO ^{ex6} 16.5 dpc hands sections labelled with Mupa-1 and -3 and anti-collagen I antibody	294
Fig 6.1 Position of riboprobes used for mRNA <i>in situ</i> hybridisation	323
Fig 6.2 RT-PCRs of the utrophin sequences corresponding to the riboprobes and structure of pAMP vector	324
Fig 6.3 Orientation of typical sections	326
Fig 6.4 Hybridisation to 8.5 dpc embryos	328
Fig 6.5 Hybridisation to 9.5-10.5dpc embryos	329
Fig 6.6 Hybridisation to 10.5dpc and 12.5 dpc embryos in the region of the neural tube.	331
Fig 6.7 Utrophin mRNA expression in the developing limb	333
Fig 6.8 Utrophin mRNA expression in trigeminal ganglia	335
Fig 6.9 Utrophin mRNA expression in dorsal-root ganglia	336
Fig 6.10 Hybridisation to 12.5dpc embryos in the head and heart regions	337
Fig 6.11 Hybridisation to 14.5 and 15.5 dpc embryos	340
Fig 6.12 Utrophin mRNA expression in the developing digits	341
Fig 6.13 Utrophin mRNA expression in the semicircular canals	343
Fig 6.14 Utrophin mRNA expression in the kidney, pyloric sphincter, testis and urethra	344
Fig 6.15 Utrophin mRNA expression in the choroid plexii	346
Fig 6.16 Hybridisation to 14.5dpc embryos in the facial region	348

List of Tables

		Page
Table 1.1	Summary of expression of dystrophin isoforms	44
Table 1.2	Summary of expression of utrophin isoforms	56
Table 2.1	Sequence of primers used in RT-PCR experiments	105
Table 2.2	Sequence of primers used for the production of the Mupa antibodies	110
Table 2.3	Primary antibodies used in Western blots and immuno-histochemistry	118
Table 2.4	Sequence of primers used in 5' RACE experiments	121
Table 2.5	Sequence of primers used to produce the riboprobes for mRNA <i>in situ</i> hybridisation	130
Table 4.1	Classification of polypeptides seen on Western blots	176
Table 4.2	Summary of Western blots results	201
Table 6.1	Summary of mRNA <i>in situ</i> hybridisation results	349
Table 6.2	Major foetal tissues expressing utrophin mRNAs	369

Abbreviations

aa	amino acids
Amp	ampicillin
ABS	actin binding sites
AChE	acetylcholine esterase
AChR	acetylcholine receptors
ATP	adenosine triphosphate
UAP	Universal anchor primer
BMD	Beckers muscular dystrophy
BLAST	basic local alignment tool
bp	base pair
BSA	bovine serum albumin
c.	circa
CaM	calmodulin
CD	circular dichroism
cDNA	complementary deoxyribonucleic acid
CH	calponin homology
Ci	curie
CNS	central nervous system
COOH	carboxyl terminus
cpm	counts per minute
DAP	dystrophin associated protein
DAPI	4', 6-diamidino-2-phenylindole
dCTP	deoxycytidine-5' triphosphate
DEPC	diethylpyrocarbonate
dGTP	deoxyguanosine-5' triphosphate
dH ₂ O	distilled water (milli-RO plus)
ddH ₂ O	deionised and distilled water (milli-Q plus)
dko	double dystrophin-utrophin deficient mouse
DMD	Duchenne muscular dystrophy
DNA	deoxyribonucleic acid
dNTP	deoxynucleoside triphosphate
dpc	days post-coitum
DRP	dystrophin related protein
DTT	dithiothreitol

Dko mice = *mdx*; *utrn*^{-/-} mice

DMD gene dystrophin gene 14

dTTP	deoxythymidine-5' triphosphate
ECL	enhanced chemiluminescence
EDTA	ethylenediaminetetraacetic acid
EKLF	erythroid kruppel-like factor
ERG	electroretinogram
EST	expressed sequence tags
EtBr	Ethidium Bromide
F	filamentous
Fig	figure
F-L	full length
g	grams
GCR	glucocorticoid response
GFP	green fluorescent protein
GSP	gene specific primer
hr	hour
HRP	horse radish peroxidase
IgG	Immunoglobulin
ILM	inner limiting membrane
IPTG	isopropyl- β -D-thiogalactoside
Kb	kilobases
kDa	kilo Daltons
K	1000x rpm
LB	laurita bautaria
M	molar
Mb	megabases
MCS	multiple cloning site
MDCK	Madin-Darby canine kidney
mdx	dystrophin deficient mice
mGluR	metabotropic glutamate receptor
min	minute
mM	millimolar
M-MLV RT	Moloney murine leukemia virus reverse transcriptase
MOPS	3-(N-morpholino) propane sulphonic acid.
MRC	Medical Research Council
MRF	myogenic regulatory factors
mRNA	messenger ribonucleic acid
mt	mitochondrial

MTJ	myotendinous junction
Mupa	mouse utrophin polyclonal antibody
MuSK	muscle specific receptor tyrosine kinase
mw	molecular weight
NaAC	sodium acetate
NaCl	sodium chloride
ng	nanograms
NH ₂	amino terminal
nm	nanometer
NMJ	neuro-muscular junction
nNOS	neuronal nitric oxide synthase
nt	nucleotides
°C	degrees centigrade
OD	optical density
o/n	overnight
OPL	outer plexiform layer
ORF	open reading frame
PAGE	polyacrylamide gel electrophoresis
PCR	polymerase chain reaction
pfu	plaque forming unit
PGM	phosphoglucomutase
PH	pleckstrin homology
PSM	phage storage medium
RACE	rapid amplification of cDNA ends
RNA	ribonucleic acid
RNAse	ribonuclease
rpm	revolutions per minute
RT	reverse transcriptase
rt	room temperature (23 °C)
RT-PCR	reverse transcription polymerase chain reaction
SDS	sodium dodecyl sulphate
sec	second
SSC	sodium chloride/sodium citrate buffer
SN	supernatant
TBE	tris/borate/EDTA buffer
TdT	terminal deoxynucleotidyl transferase
TEMED	N,N,N ¹ ,N ¹ -tetramethylethylenediamine

T _m	melting temperature
Tris	2-amino-2(hydromethyl)-propane-1,3-diol
U	units
UKO ^{ex6}	utrophin knockout (exon 6)
UTR	untranslated sequence
UTRN	utrophin gene
UV	ultra violet
v/v	volume to volume
W	watts
w/v	weight per volume
YAC	yeast artificial chromosome
Yap	yes kinase associated proteins
μg	microgram
μm	micromolar
μl	microlitre

UKO mice = *utrn*^{-/-} mice

Chapter 1

Introduction

In 1986 it was established that deletions and mutations of the X-linked DMD gene which resulted in deficiency of its product - dystrophin, were the cause of Duchenne muscular dystrophy (DMD) (Monaco et al., 1986). Since then the research community has worked towards possible therapies for this fatal disease (e.g. Cox et al., 1993a; Tinsley et al., 1996). A promising strategy which is under investigation is the upregulation of the dystrophin homologue, utrophin. The structural and functional similarities between utrophin and dystrophin have led to the proposal that utrophin can replace dystrophin in the dystrophin deficient muscle (Tinsley et al., 1996; Rafael et al., 1998). The strength of the relationship between the two genes has been further highlighted in recent years by the isolation of short products of the utrophin gene which are homologues of the short isoforms encoded by the dystrophin gene.

The short utrophin isoforms are the topic of this thesis. In this introductory chapter I will consider the cloning of the utrophin gene and the structure and expression of full-length utrophin mRNA and protein, making comparisons with dystrophin when appropriate. Other members of the spectrin/dystrophin superfamily which are relevant to the findings reported in this thesis will also be described briefly. I will then discuss the short dystrophin isoforms whose existence prompted the search for the short utrophin isoforms. The identification of the short utrophins and the state of knowledge about their patterns of expression before the present study was undertaken, is also described in this chapter. The functional significance of these isoforms will be

discussed in the context of the utrophin and utrophin-dystrophin deficient mice. Particular attention will be paid to the mice “knocked-out” in exon 6 of utrophin (UKO^{ex6}), (Deconinck et al., 1997a). These mice are deficient for full-length utrophin but are expected to express the short utrophins and represent a key resource used in this thesis.

Finally, progress in current research towards developing a therapy for DMD will be discussed.

1.1 Cloning of full-length utrophin cDNA

In this section I will briefly set the work in its historic context by summarising the cloning and chromosome mapping of the utrophin gene. In the following sections (1.2 and 1.3), the structure of full-length utrophin mRNA and protein are reviewed in some detail since this information is essential i) to understand the strategies used in this study for designing antibodies and riboprobes, ii) so that the relationship between exons and protein domains is clear and iii) so that the functional protein domain structure of the short isoforms is clear.

The cloning and sequencing of the human utrophin cDNA was completed in 1992 using cDNA libraries prepared from a glioma cell line (Tinsley et al., 1992) and from placenta mRNAs (Fairbrother thesis, 1993). A mouse utrophin cDNA was isolated from a smooth muscle cell line (BC3H1) and from adult mouse lung cDNA libraries using a sequence from the 3' end of the human cDNA (Guo et al., 1996). The mouse and the human

sequences share 84% identity at the nucleotide level and 87% identity at the amino acid level

The size of the utrophin mRNA is 13 Kb, it contains an open reading frame of 10,299 bp and a 550 bp 5' untranslated sequence (UTR). A consensus polyadenylation sequence is found 2Kb downstream of the stop codon (Tinsley et al., 1992). The utrophin mRNA is slightly smaller than the DMA cDNA, 13Kb versus 14Kb. This difference can be explained by the slightly longer coding region (11Kb) and 3' UTR (2.7Kb) of the DMD mRNA compared to the utrophin mRNA (Koenig et al., 1987).

The gene encoding human utrophin was initially located to chromosome 6q21-ter by Southern blotting analysis of a panel of human-rodent somatic cell hybrid DNAs (Love et al., 1989). This position was subsequently refined by Buckle et al. (1990) to 6q24 by radioactive *in situ* hybridisation to human metaphase chromosomes. The mouse utrophin gene was located to chromosome 10 by linkage analysis of DNAs from an interspecific backcross (C57Bl/6 x SPE) F1 x C57Bl or (BALB/c x SPE) F1 x BALB/c (Buckle et al., 1990). This finding caused some excitement at the time because this position is close to the dystrophin muscularis (*dy*) locus, which confers a severe neuromuscular recessive disorder. However, analysis of *dy* muscle showed normal levels of utrophin protein and indeed subsequently, merosin (laminin alpha 2) deficiency was shown to be the primary defect in *dy* mice (Sunada et al., 1994).

1.2 The utrophin gene (*UTRN/Utrn*)

The structure of the utrophin gene has been determined in part. It spans 900Kb of genomic DNA, is multiexonic and is likely to be very similar in

complexity and structure to the DMD gene (Pearce et al., 1993) whose intron/exon structure is fully known (Roberts et al., 1992, 1993; Fairbrother thesis, 1993). The DMD gene spans 2.4 Mb, it is the largest known gene, and comprises 79 exons. The size of the introns varies from a few base pairs to 400Kb (Koenig et al., 1989; Bar et al., 1990; Roberts et al., 1992). It is possible to determine the positions of the same exon/exon boundaries in the utrophin gene by direct alignment of the utrophin and dystrophin coding sequences. The exon numbering system used for utrophin in this thesis is based on the corresponding dystrophin exon numbers. However, it should be remembered that there is some lack of alignment in several regions where exons present in dystrophin are absent in utrophin - these are - exons 9 and 10, corresponding to the hinge region 1; exons 40 to 43, spectrin repeat 15, and exons 48 to 52, spectrin repeat 19 and hinge region 3 (Fig 1.1).

In addition, Pearce et al. (1993) showed that the 5' UTR of utrophin consists of two closely spaced exons and that the translation initiation codon is in the second exon. These two most 5' exons are separated from the cluster of the next three downstream exons by 120-140Kb of genomic sequence (Pearce et al., 1993). This is a different architecture to that found in the dystrophin gene. The 5' UTR of the dystrophin cDNA is shorter (209bp vs 550bp) and comprises a single exon (Koenig et al., 1987).

The 5' flanking sequence containing proximal promoter regions of utrophin gene has been cloned and sequenced (Dennis et al., 1996) and I will describe it later in this chapter.

1.3 Utrophin protein structure

Full-length human utrophin protein comprises 3433 amino acids (aa), (3429 aa in mouse) with a molecular weight of 395kDa (Tinsley et al., 1992). There are four major structural domains; an actin-binding domain at the NH₂-terminus, a central rod domain made up of coiled-coil repeats, a cysteine-rich domain and a COOH-terminal domain (Fig 1.1).

The actin-binding domain of utrophin is related to the actin-binding domains of other members of the spectrin superfamily, spectrin and α -actinin and of other actin-binding proteins such as fimbrin, filamin and plectin. It consists of two calponin homology (CH) domains each of circa (c.) 100 aa (Fig 1.2). CH domains were first identified in the muscle regulatory protein calponin by X-ray crystallography and consist of 4 α -helices (Carugo et al., 1997). The first CH domain (CH1) in utrophin extends from aa 34 to aa 131 and the second (CH2) from aa 147 to aa 260. The CH1 domain is more closely similar to the CH domain of other actin-binding proteins than it is to the adjacent CH2 domain. This suggests that CH1 and CH2 arose from intragenic duplication early in the evolution of the spectrin superfamily and have subsequently diverged in sequence (Stradal et al., 1998).

Sequence comparisons between utrophin and α -actinin (Tinsley et al., 1993b) identified three actin-binding sites; the first two sites (ABS1 and ABS2) are located in CH1 and the third site, ABS3, is located in CH2, (Fig 1.2), (Stradal et al., 1998). Actin sedimentation assays and antibody-blocking studies showed that the major actin-binding activity lies in the CH1 region and that the ABS2 domain is critical for the binding of actin whereas ABS1 and ABS3 have

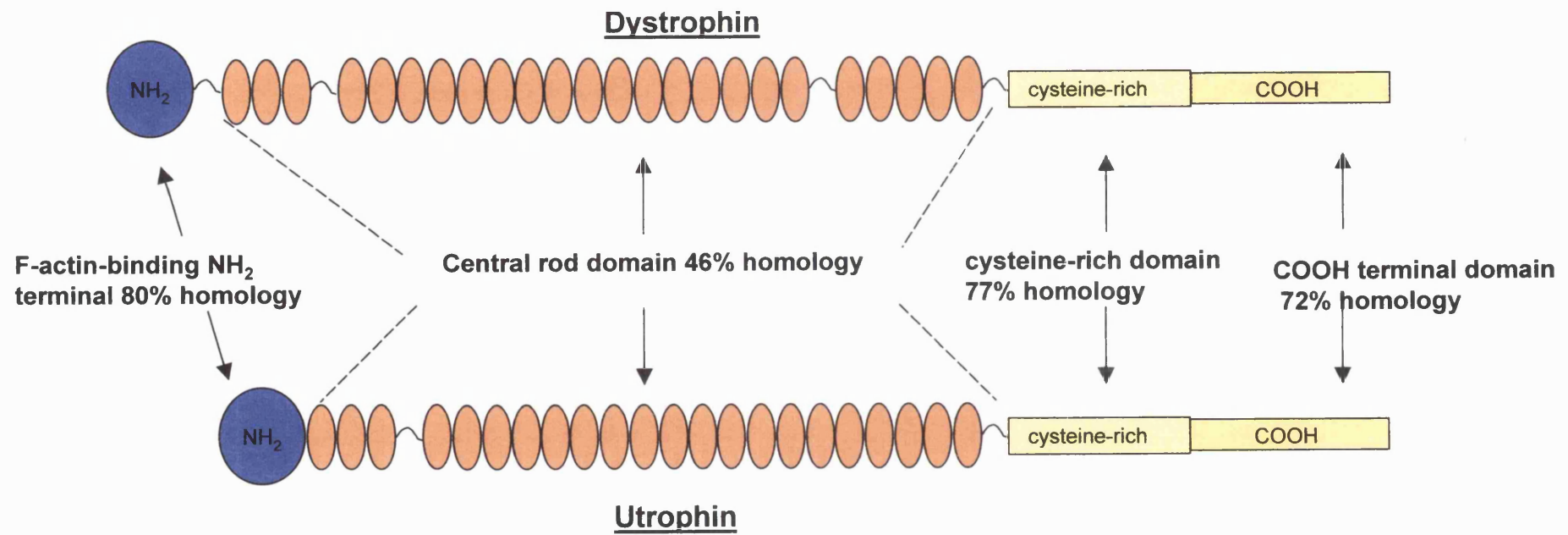



Fig 1.1. A diagram comparing the utrophin and dystrophin proteins.

 =coiled-coil repeats (110 aa)
  = hinge region

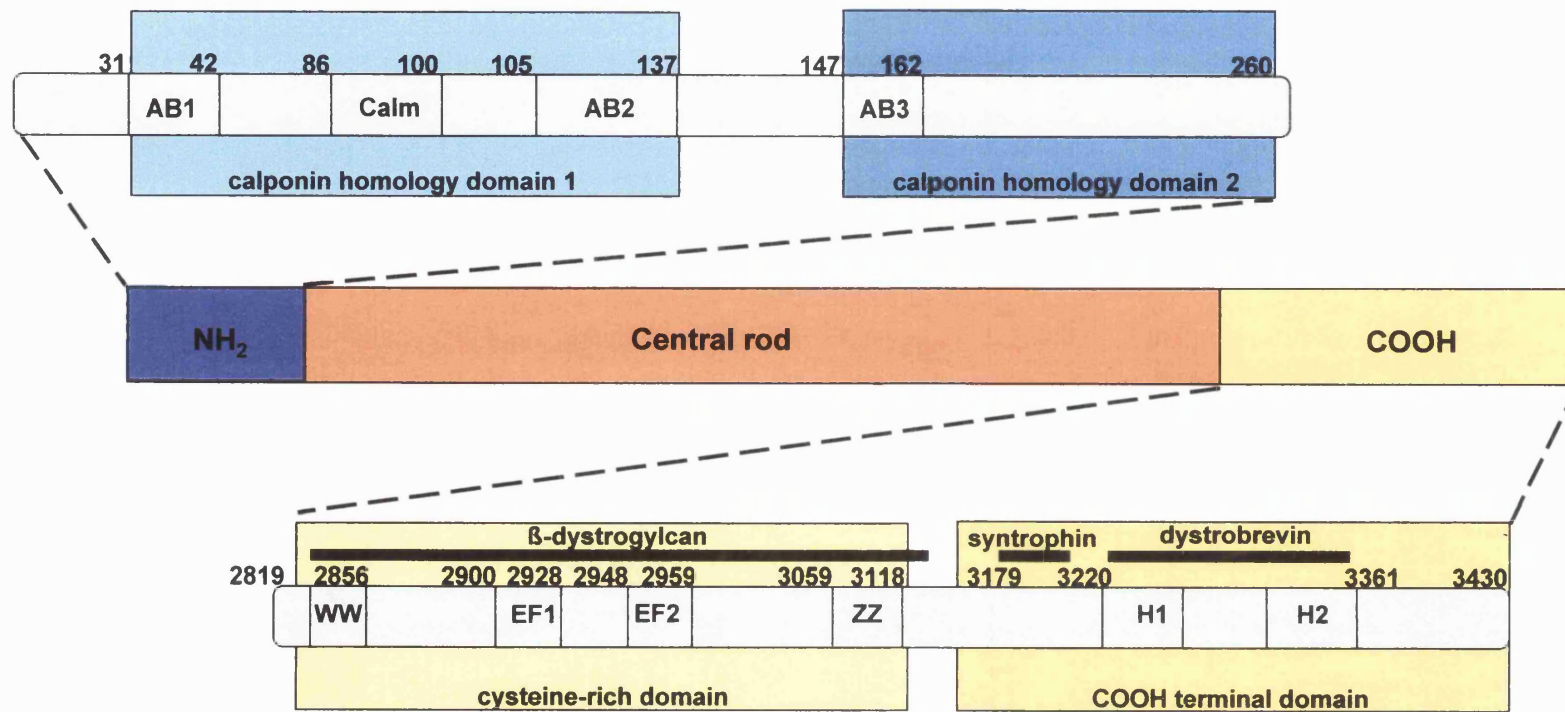


Fig 1.2 A diagram showing the detailed structure of the utrophin protein (adapted from Winder et al., 1995)

rather supporting and stabilising roles (Keep et al., 1999; Morris et al., 1999; Moores et al., 2000).

The NH₂-terminal CH1 domain also contains a calmodulin binding site which is thought to regulate the binding to actin in a calcium dependant fashion (Fig 1.2, Winder et al., 1995).

The NH₂-terminal domain of dystrophin shares the 3 conserved actin-binding domains and shows 80% homology with utrophin (Tinsley et al., 1993b). Both utrophin and dystrophin have higher affinity for the β isoform of F-actin (cytoskeletal) than for the α isoform (skeletal muscle). However, some functional differences exist between the actin binding domains, for example utrophin shows a higher binding affinity for F-actin than the corresponding region of dystrophin (Winder et al., 1995). This probably reflects differences in the regulation of the binding to F-actin and in the actual biochemical mechanism. For example, in utrophin, the binding to F-actin is calcium dependant whereas in dystrophin, binding is calcium independent (Winder et al., 1995).

In addition, dystrophin displays actin-binding activity associated with the rod region, repeats 11 to 17 (Amann et al., 1998), which increases the affinity between dystrophin and F-actin. The corresponding region of utrophin lacks this additional actin binding activity because of the relatively acidic nature of the repeats in utrophin (Amann et al., 1999).

However, the most NH₂-terminal 28 aa of utrophin, which show no homology to dystrophin, appear to be important for maximising binding to actin (Moores et al., 2000) and it has been proposed that this sequence plays a

similar stabilising role to the actin-binding domain in the rod region of dystrophin (Moore et al., 2000).

The central rod domain of utrophin consists of 22 coiled-coil repeats which are characteristic of all members of the spectrin superfamily. Each repeat consists of 99 to 110 aa arranged in 3 α -helices separated by two long loops which fold into a coil-coiled structure. It is believed that this rod domain confers flexibility and elasticity to the protein (Koenig et al., 1990). It is in this region that the homology between utrophin and dystrophin is lowest (46%). Utrophin has 22 repeats interrupted by two proline-rich hinge regions whereas dystrophin has 24 repeats and four hinge regions (Fig 1.1). Direct comparison of the coding sequences of utrophin and dystrophin reveals that repeats 15 and 19 and hinge region 1 and 3 are present in dystrophin but are absent in utrophin (Tinsley et al., 1992).

The COOH-terminal cysteine rich domain contains three motif sequences, a WW domain, two EF-Hand domains, and a ZZ domain. The level of homology in this region between utrophin and dystrophin is 77% (Fig 1.1). The WW domain consists of the consensus sequence XPPXY (Chen and Sudol 1995). This domain is known to be involved in protein/protein interactions and is the site where utrophin and dystrophin interact with the membrane-associated glycoprotein β -dystroglycan (Fig 1.2). This interaction involves the COOH-terminus of β -dystroglycan (Jung et al., 1995; Rosa et al., 1996; de Vignano et al., 2000) which also contains a WW domain sequence of PPPYVPP. β -dystroglycan is a member of the dystrophin associated proteins (DAPs). These proteins form a complex with utrophin at the neuromuscular junction (NMJ) (Matsumura et al., 1992) and with dystrophin at the sarcolemma (Campbell et

al., 1989) in skeletal muscle. Amongst the DAPs there is an extracellular protein- α -dystroglycan (156kDa), various transmembrane proteins - β -dystroglycan, sarcoglycans (SG), (50kDa, 43kDa, 35kDa, 32kDa), sarcospan (25kDa) and cytoplasmic proteins: dystrobrevin (94kDa) and syntrophin (59kDa), (Blake et al., 1996b; Sadoulet-Puccio et al., 1996; Nigro et al., 1997; Crosbie et al., 1997).

The WW domain of utrophin is very similar to that described for the Yes kinase-associated protein YAP65. YAP65 complexes with a proline rich peptide via the WW domain in a similar manner to utrophin's interaction with β -dystroglycan (Macias et al., 1996).

EF-Hand motifs bind calcium and are implicated in the calcium dependant regulation of a variety of intracellular activities such as protein phosphorylation. Winder et al. (1997) using $^{45}\text{Ca}^{2+}$ gel overlay assays showed that the COOH-terminal EF-Hand of dystrophin binds weakly to calcium, this has not been demonstrated yet for utrophin. The EF-Hand motifs in utrophin and dystrophin are also involved in the interaction with β -dystroglycan (Huang et al., 2000; di Vignano et al., 2000).

The ZZ domain is so named in reference to the WW domain and because of its similarity to zinc finger domains found in other proteins. (Ponting et al., 1996; Winder et al., 1997). In utrophin and dystrophin the ZZ domain contains two pairs of conserved cysteine residues with a sequence motif of C-X₂-C. These are sequences that fold to form domain structures in the presence of zinc ions, each of which are positioned in a tetrahedral arrangement with four Cys or His ligands. The zinc fingers in utrophin and dystrophin contain only 4 of the 6 conserved Cys residues found in classical ZZ fingers, the others being

replaced by Ser and His. From ^{65}Zn overlay assays there is some evidence that utrophin binds zinc (Winder, et al., 1997) and that binding involves the His residue (Ponting et al., 1996). In addition to binding Zn ions, these motifs have been shown to mediate protein-protein interactions such as transcription factors binding (e.g. adapter protein p300 and TFIIB, Ponting et al., 1996). It has also been demonstrated recently that the ZZ domain of utrophin binds calmodulin (de Vignano et al., 2000) as does the dystrophin ZZ domain (Anderson et al., 1996). The precise role of the ZZ domain is unclear although there is now good evidence that it participates indirectly in the interaction between utrophin or dystrophin and β -dystroglycan (Winder et al., 1997; James et al., 2000; de Vignano et al., 2000). It has been proposed that the binding of utrophin to β -dystroglycan could be regulated by variations in calcium concentration via calmodulin and the ZZ domain (de Vignano et al., 2000).

Finally, the COOH-terminal domain (72% homology with dystrophin) consists of a pair of highly conserved coiled-coil helices, which are predicted to form parallel dimers (Fig 1.1). Protein-protein interactions in this region are facilitated by the presence of proline residues which confer flexibility (Morris et al., 1998). Utrophin interacts with the intracellular DAPs; dystrobrevins and syntrophins via the COOH-terminal domain (Fig 1.2), (Kramarcy et al., 1994; Peters et al., 1997; Sadoulet-Puccio et al., 1996; Adams et al., 1993), the two helices in utrophin forming a heterodimer with the corresponding helices in dystrobrevin (de Vignano et al., 2000).

1.4 Utrophin related proteins

Utrophin and dystrophin are members of the spectrin super-family that includes spectrin, α -actinin, dystrobrevin and dystrophin-related protein 2 (DRP2). In this section, the structure and expression of spectrin and α -actinin are described in order to emphasise their strong domain homology to utrophin. This is important since this structural homology results in antibody crossreactivity as described in Chapter 4. In addition, dystrobrevin and DRP2 are briefly described because they are, potentially, functional substitutes for short utrophins (see discussions to Chapters 5 and 7).

Spectrin Spectrin is the major component of the membrane skeleton of the eukaryotic cell and is highly conserved throughout evolution. The spectrin molecule consists of two non-identical subunits, α and β , which are encoded by different genes *SPTA1* and *SPTB*. α and β chains are assembled into head-to-tail heterodimers and two dimers further assembled into a tetramer which constitutes the functional unit. There are two major isoforms of spectrin, the erythrocytic form, expressed only in erythrocytes, and the general non-erythrocytic form, which is found in several tissues and is abundant in the brain. In addition there is a minor neuromuscular junction specific isoform which co-localises with AChR (Bloch et al., 1989).

The function of spectrin in erythrocytes is to stabilise the membrane; defects or deficiency in spectrin result in haemolytic anaemias (Hu R et al., 1992). Non-erythroid spectrin has been implicated in several biological processes such as formation and maintenance of cell-cell junctions and other specialised cell domains and exocytosis; it is particularly abundant

in brain tissue perhaps because neurones have extensive plasma membrane surfaces (Hu R. et al., 1992).

The β chain (250-270kDa) of both isoforms contains two CH domains at their NH₂-terminus followed by 16 complete repeats, a partial repeat and a serine-domain at the COOH-terminus (Pascual et al., 1997). The α chain (c. 280Kda) has a partial spectrin repeat at the NH₂-terminus, 20 complete spectrin repeats, a Src-homology 3 (SH3) domain within the 9th repeat and a calmodulin-like domain at the COOH-terminus. The erythrocytic and non-erythrocytic isoforms are slightly different in that the β chain of the non-erythrocytic isoform contains an additional proline/serine-rich region and a pleckstrin-homology (PH) domain prior to the common C-terminal serine-rich domain and the α chain of the non-erythrocytic isoform contains a calmodulin-binding site inside the 10th repeat which is absent in the erythrocytic isoform (Pascual et al., 1997).

The α and β subunits are encoded by different genes: the α erythrocytic and non erythrocytic chains are encoded by the *SPTA1* gene (human chromosome 1q21, mouse chromosome 1) and by the *SPTAN1* gene (human chromosome 9q33, mouse chromosome 2) respectively. The β -erythrocytic chain gene, *SPTB*, is located on chromosome 14q23, mouse chromosome 12, and the β non-erythrocytic chain gene, *SPTBN1* is on chromosome 2p21, mouse chromosome 11 (GeneCards, <http://bioinfo.weizmann.ac.il>).

α -actinin α -actinin (104kDa) consists of two CH domains at its N-terminus, 4 repeats and a calmodulin like, calcium binding, motif at the COOH-terminus (Pascual et al., 1997). The functional unit consists of a homodimer arranged in an antiparallel fashion (Suzuki et al., 1976). Several muscle and

non-muscle isoforms have been identified - two muscle isoforms α -actinin 2 and 3 (encoded by two separate genes on chromosomes 1q42 and 11q13 respectively) and two non-muscle isoforms - α -actinin 1 and 4 (encoded by genes on chromosomes 14q24 and 19q13). The mouse orthologues of α -actinin -2, -3 and -4 have been cloned and sequenced (*Actn4* gene is on chromosome 7, *Actn 2* gene on chromosome 13, and the position of the *Actn 3* is unknown; GeneCards, <http://bioinfo.weizmann.ac.il>).

The muscle isoforms are the major components of the Z-disks in striated muscle and of the dense bodies and plaques of smooth muscles whereas the non-muscle isoforms are distributed along microfilaments bundles and mediate their attachment to the membrane adherens-type junctions (McKay et al., 1997). Muscle and non-muscle α -actinin isoforms differ in their sensitivity to calcium, such that the binding of non-muscle isoform to actin is calcium dependent whereas the binding of the muscle isoform seems to be calcium independent (Burridge et al., 1981; Duhaiman et al., 1984). This is analogous to the actin binding of utrophin and dystrophin, where utrophin binding to actin appears to be calcium dependent whereas dystrophin binding is calcium insensitive.

The gene encoding α -actinin localises to chromosome 14q24 in close proximity to the gene encoding erythroid β -spectrin; physical linkage between the genes for α -actinin and β -spectrin suggests that a single ancestral gene may have generated the two genes by partial gene duplication (Yousoufian et al., 1990). More recent phylogenetic studies (Pascual et al., 1997) have shown that α -actinin was the ancestral source of the repeats in the spectrin/dystrophin superfamily.

Dystrobrevin

Dystrobrevin is both a dystrophin-related protein and a dystrophin-associated protein first identified as an 87 kDa postsynaptic protein that co-purifies with AChR from the electric organ of *Torpedo californica* (Carr et al., 1989). Dystrobrevin has weak homology to the cysteine rich and COOH-terminal domains of dystrophin and utrophin. It contains a cysteine-rich domain without a WW domain but has the carboxy-terminal coiled-coils and a unique region that is phosphorylated on tyrosine (Wagner et al., 1993).

The human α -dystrobrevin gene, *DTN*, is on chromosome 18q12, mouse chromosome 18, (Sadoulet-Puccio et al., 1996; Blake et al., 1996a) and appears to be transcriptionally regulated by more than one promoter (Ambrose et al., 1997; Holtzfeind et al., 1999) giving rise to three isoforms, α -dystrobrevin-1,-2 and -3 (Blake et al., 1996a; Sadoulet-Puccio et al., 1996).

α -Dystrobrevin-1 is the largest isoform (mRNA 7.5Kb) and is most similar to the torpedo 87kDa protein. α -Dystrobrevin-2 (mRNA 5Kb) and dystrobrevin-3 (mRNA 1.8Kb) are successive COOH-terminal truncations of α -dystrobrevin-1 which lack the tyrosine kinase substrate domain and both the tyrosine kinase substrate domain and coiled-coil domains respectively (Blake et al., 1996a; Nawrotzki et al., 1998).

The three isoforms have a different tissue distribution; α -dystrobrevin-3 is confined to skeletal and cardiac muscle, α -dystrobrevin-1 is expressed in several tissues including kidney and brain and at low levels in skeletal muscle; α -dystrobrevin-2 is also expressed in all these tissues and is more abundant in skeletal muscle than α -dystrobrevin-1. The two larger dystrobrevins bind directly to syntrophin at a site homologous to the syntrophin-binding sites in utrophin/dystrophin; they also bind to dystrophin and utrophin via their coiled-

coil domains (Blake et al., 1996a; Peters et al., 1997; Sadoulet-Puccio et al., 1997). α -dystrobrevin-3 which lacks both the syntrophin and dystrophin binding sites, is not thought to play a role in the formation of the DAP complex (Nawrotzki et al., 1998, Ambrose et al., 1997).

α -dystrobrevin-1 interacts with dystrophin at the sarcolemma and with utrophin at the NMJ, while α -dystrobrevin-2 is thought to bind to dystrophin only at both locations (Peters et al., 1997) α -dystrobrevin-1 is likely to be involved in the maturation and stabilisation of the NMJ since in α -dystrobrevin knock-out mice the AChRs clusters are disordered and these animals develop muscular dystrophy (Grady et al., 1999, 2000).

A second dystrobrevin gene (*DNTB*) on human chromosome 2p22 (mouse chromosome 12) has been identified. The *DNTB* gene encodes a protein, β -dystrobrevin, which is expressed in a broader range of tissues than the α -dystrobrevins (Peters et al., 1997, Blake et al., 1998, Puca et al., 1998).

Both α -dystrobrevin isoforms and β -dystrobrevin have been found in association with utrophin in several non-muscle tissues such as kidney and brain (Blake et al., 1999; Loh et al., 2000).

Dystrophin related protein 2 (DRP2) During the course of a phylogenetic study, in which the COOH-terminal domains of dystrophin and utrophin from a wide spectrum of animal species were being compared, a novel class of dystrophin/utrophin related protein, designated dystrophin related protein 2 (DRP2), was identified in fish (Roberts et al., 1996).

A search for DRP2 in mammals led to the identification of orthologous sequences in man and mouse (Roberts et al., 1996). The *DRP2* gene localises

to Xq22 (Roberts et al., 1996), encodes an mRNA of 7 Kb which contains a 5' UTR of 340 bp, an open reading frame of 2862 bp and a 3' UTR of 3.9 Kb. The DRP2 protein has a molecular weight of 110 kDa and contains a short proline rich NH₂-terminal domain, followed by sequences homologous with the last 2 repeats of the rod region and the cysteine-rich and COOH terminal domains of utrophin and dystrophin (Roberts et al., 1996). The homology to utrophin in this region is 63% which is lower than the homology between utrophin and dystrophin in the same region (75%). In addition, phylogenetic analysis shows that utrophin and dystrophin are more closely associated with each other than either are to DRP2 suggesting that DRP2 diverged from the spectrin lineage at an earlier stage (Roberts et al., 1996).

DRP2 is almost exclusively expressed in the CNS, in particular in the brain regions including olfactory bulb, cortex striatum, cerebellum and hippocampus and the spinal cord. It is also expressed in some peripheral tissues including the eye, ovaries, epididymus, testis colon and weakly in kidney (Roberts et al., 1996, Dixon et al., 1997). In the brain, immuno-histochemical studies have shown that DRP2 protein is associated with membrane fractions and is enriched in postsynaptic densities (PSD), particularly in regions involved in cholinergic synaptic transmission. This pattern of expression in the CNS resembles that of dystrophin. DRP2 contains the domains necessary for interactions with dystroglycan, dystrobrevins and syntrophins and there is some evidence for an association between DRP2 and β 1-syntrophin.

1.5 The dystrophin isoforms

A striking feature of dystrophin transcription is the encodement of multiple isoforms transcribed from different promoters (Fig 1.3). Three and maybe four promoters regulate the expression of three 427kDa “full-length” isoforms and four internal promoters drive the expression of four COOH-terminal short isoforms. The structural homology with utrophin was emphasised by finding that the position of at least one, and perhaps three, of these promoters was conserved between the two genes. The structure, expression and function of the dystrophin isoforms is considered in sections 1.5, 1.6 and 1.7 in order to allow comparison with the utrophin forms bearing in mind the evolutionary relationship between these two proteins.

Muscle isoform The muscle full-length dystrophin is transcribed from a promoter situated c. 310Kb from dystrophin exon 2 and is active in skeletal, cardiac and smooth muscle and in brain (Chelly et al., 1990).

Brain isoform The brain specific isoform, also known as cortical or cerebral dystrophin or C-dystrophin (Nudel et al., 1989), is transcribed from a promoter 90Kb upstream from the muscle promoter and 400Kb from exon 2 (Boyce et al., 1991). This transcript is tightly restricted to cortical and hippocampal neuronal cells and contains a unique first exon encoding 344 bp of

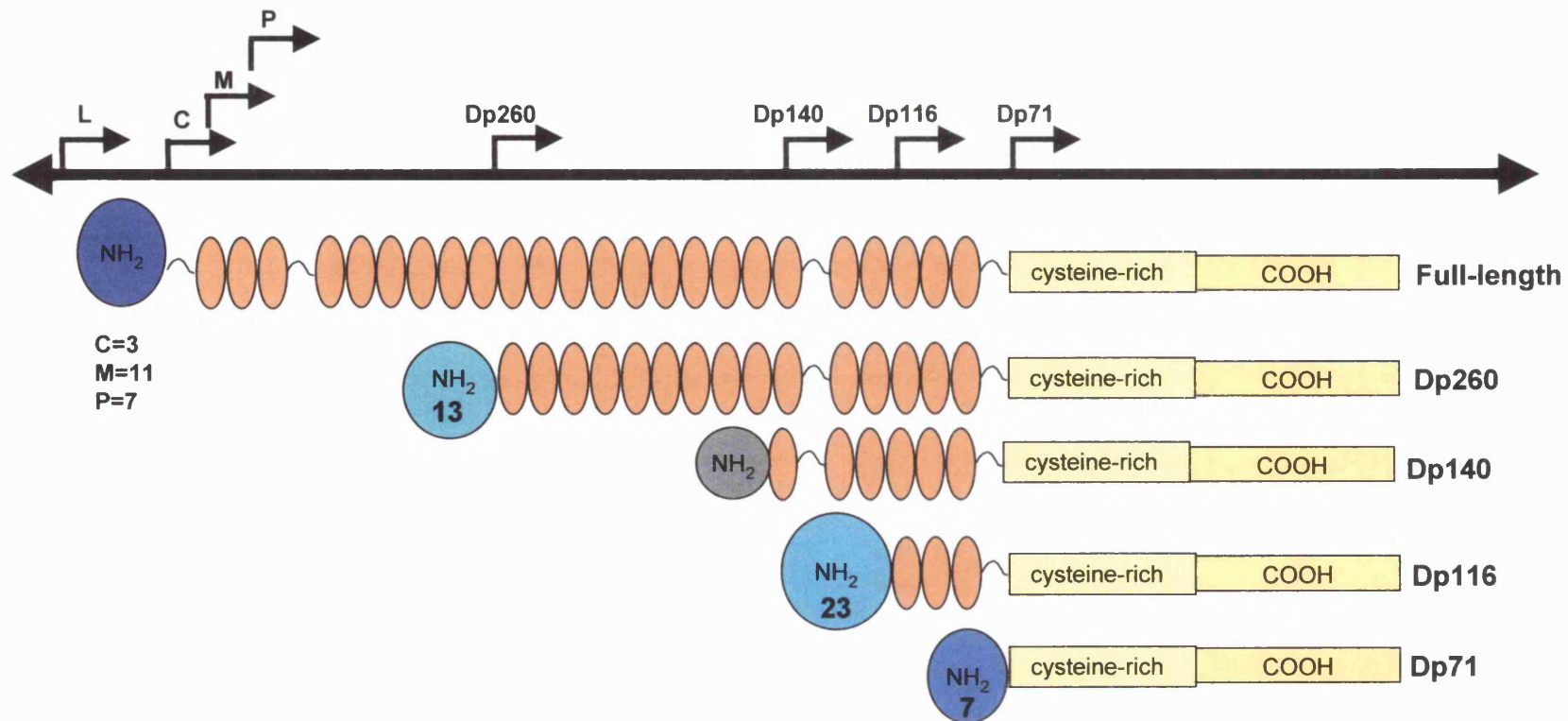


Fig 1.3 Upper. The positions of the transcription start sites of the 8 known dystrophin mRNAs are shown relative to their protein structure. Lower. The structure of each isoform. The NH₂-terminal domains are coloured blue if they contain novel aa encoded by the first exon; the number of aa is indicated. In the case of Dp140, coloured grey, the first exon encodes only 5' UTR. The four NH₂- isoforms shown are L= Lymphoid, C= Cerebral, M= Muscle and P= Purkinje.

5' UTR and 3 aa which are different from those encoded by the muscle transcript exon 1 (Chelly et al., 1990; Lidov et al., 1990; Bies et al., 1992).

Cerebellar isoform A full-length form with a novel first exon encoding 270bp of 5' UTR and a novel NH₂ terminus comprising 7 aa is expressed only in Purkinje cells of the cerebellum. The position of the first exon of the Purkinje specific transcript lies in the middle of the intron between muscle-type exon 1 and exon 2 (Gorecki et al., 1992; Abdulrazzak et al., 2001).

Lymphoid isoform A further full-length isoform of dystrophin (L-dystrophin) was identified in cultured lymphoblastoid cells from a DMD patient with a deletion extending from the 5' end of the gene to exon 2 (Nishio et al., 1994). The position of the promoter for L-dystrophin was mapped more than 500Kb upstream of the brain promoter, thereby adding 500Kb to the size of the dystrophin gene (Nishio et al., 1994). This novel first exon encodes 46 bp of 5' UTR which are spliced directly to exon 3 with the creation of a possible ATG initiation codon within exon 3 (Nishio et al., 1994). There have been no further studies of this isoform.

There is now good evidence for selective mechanisms that regulate the expression of full-length dystrophin from these alternative 5' promoters. For example, in cardiac muscle, in contrast to skeletal muscle, only the muscle specific promoter is active. As a consequence, mutations (and deletions) at the 5' end of the DMD gene in the region of the muscle promoter result in a progressive heart disease without skeletal muscle myopathy (Muntoni et al., 1993, 1995; Milasin et al., 1996; Ferlini et al., 1999). This disorder, X-linked

dilated cardiomyopathy (XLDC), is allelic to DMD. In the skeletal muscle of affected males full-length dystrophin is transcribed, by a compensatory mechanism, from the brain and purkinje specific promoters allowing the muscle to escape the dystrophic changes (Milasin et al., 1996, Muntoni et al., 1995).

In addition to the three full-length transcripts described above the dystrophin gene locus also contains internal promoters that regulate expression of at least four short transcripts, Dp71, Dp116, Dp140 and Dp260. The protein products of these transcripts do not have the NH₂-terminal region but share the same COOH-terminal and cysteine-rich domains and in some cases part of the long central rod like domain (Fig 1. 3). These isoforms were identified as unusual bands on Western or Northern blots and their cDNAs were recovered either by deliberate screening of tissue specific cDNA libraries or by 5' RACE.

Dp71 isoform A short isoform of dystrophin, Dp71, was initially identified as a 6.5 Kb dystrophin transcript on Northern blots. Transcription of Dp71 is initiated approximately 8Kb upstream from the intron62/exon 63 boundary (Hugnot et al., 1992; Lederfein et al., 1992) and the transcript encodes a 5' UTR of 80 nt and 7 novel aa spliced to exon 63 (Fig 1.3). The size of the transcript is 4.8 Kb (not 6.5Kb as initially estimated by Northern blotting) and the protein, with a molecular weight of 70.8kDa, contains the cysteine rich and carboxy-terminal domains. The isoform was designated Dp71 to reflect its molecular weight.

Dp71 mRNA has been detected by Northern blotting in several tissues including brain, liver, testis, lung and kidney and cell lines such as Schwannoma

and glioma C6 cells (Bar et al., 1990; Blake et al., 1992). Dp71 polypeptide has been detected by Western blotting in a similar range of tissues and cell lines and shows some developmental regulation; for example, Dp71 is expressed in foetal skeletal muscle but not in adult muscle (Blake et al., 1992; Hugnot et al., 1992; Schofield et al., 1994; Loh et al., 2000). The expression of Dp71 mRNA during mouse embryonic development was analysed more fully by mRNA *in situ* hybridisation using a riboprobe specific for the unique first exon (Schofield et al., 1994). Dp71 mRNA was detected at 11.5 dpc in the floor-plate and in the whole length of the neural tube by 12.5 dpc. It is also expressed in condensing mesenchyme in regions of the maxilla and mandible, in developing teeth and in liver. In the neonate brain, Dp71 mRNA is found in the ventral midbrain and caudate putamen. In an independent study, Dp71 mRNA was detected in glomeruli, tubules and collecting ducts of the developing kidney as well as in the developing eye (Durbeej et al., 1997).

Antibodies raised against different regions of the dystrophin protein have been used to determine the subcellular localisation of Dp71. In these studies the use of dystrophin deficient mice, *mdx*, has been particularly useful. The findings can be summarised in brief as follows; in foetal skeletal muscle Dp71 is expressed at the sarcolemma of myotubes before the “switching-on” of full-length dystrophin but its expression declines towards birth (Tennyson et al., 1996; Lin S. et al., 2000); Dp71 is the most abundant dystrophin isoform in retina (Rodius et al., 1997; Arsanto et al., 1999) where it localises to the outer and inner plexiform and nuclear layers and to the cytoplasm of Müller cells (Rodius et al., 1997; Claudepierre et al., 2000). In the brain, Dp71 is located in the choroid plexii, ependymal lining of the ventricles, olfactory bulb,

hippocampal regions and cerebral cortex. In the cerebellum, Dp71 is found in the molecular, granular and Purkinje layers in glial cells (Lambert et al., 1993; Jung et al., 1993; Gorecki et al., 1995). This isoform is also found in glial cells of the cerebral cortex in contrast to full-length dystrophin which is expressed only in neurones (Blake et al., 1999).

Dp116 isoform A second dystrophin short isoform, Dp116, is transcribed from a promoter within intron 55 (Byers et al., 1993). The Dp116 novel first exon contains more than 200 nucleotides of 5' UTR and coding sequence for 23 unique aa (Fig 1.3) (Schofield et al., 1994). Dp116 protein (116kDa) consists of three spectrin repeats, the cysteine rich domain and the carboxy-terminal domain.

Northern blot analysis showed that expression is confined to glioma, Schwannoma and oligodendroglioma cells (Byers et al., 1993; Schofield et al., 1994). Dp116 is a rare transcript during embryogenesis as judged by mRNA *in situ* hybridisation experiments using a Dp116 specific probe; mRNA was only weakly detected in the liver by 12.5 dpc and in brain after birth (Schofield et al., 1994).

In adults, Dp116 protein is expressed in peripheral nerves and immuno-histochemical analysis showed that Dp116 localises to a thin rim around the outside of the myelinated fibre (Byers et al., 1993). It also appears to be expressed in the inner ear. Western blots of control and *mdx* mice cochlea and immuno-histochemistry have shown that Dp116 is expressed in both types of hair cells in the cochlea alongside full-length dystrophin; in these cells Dp116 predominates at synaptic regions (Dodson et al., 1995).

Dp140 isoform The 140kDa polypeptide, Dp140, is encoded by a 7.5Kb mRNA transcribed from a promoter within intron 44. A unique non-coding first exon (110bp) is spliced to exon 45 (Lidov et al., 1995). Dp140 contains the last 6 repeats of the rod domain, the cysteine-rich and the COOH-terminal domains of the dystrophin protein (Fig 1.3) (Lidov et al., 1995).

Expression of Dp140 protein is restricted to foetal kidney, retina and brain (Lidov et al., 1998; Rodius et al., 1997); in the latter, Dp140 protein accumulates in the olfactory bulb and leptomeningeal surfaces (Lidov et al., 1995). The expression of Dp140 mRNA and protein in the developing kidney has been analysed in some detail by mRNA *in situ* hybridisation, using a Dp140 specific probe, and by immuno-histochemistry, using several anti-dystrophin COOH-terminal antibodies, (Durbeej et al., 1997). By 15 dpc, Dp140 mRNA and protein accumulate in the comma-shaped tubules at the basal side of the epithelial cells next to the basal membrane, no expression is detected in collecting ducts or glomeruli. Dp140 is absent from the adult kidney which indicates that in this tissue this isoform is most important during morphogenesis (Durbeej et al., 1997).

Dp260 isoform The identification of the Dp260 isoform was prompted by clinical observations concerning DMD patients. Some patients have an ocular phenotype characterised by an abnormal electroretinogram (ERG) with a reduced b-wave amplitude (Pillers et al., 1993; Fitzgerald et al., 1994). This is suggestive of abnormal signal transmission across the outer plexiform layer (OPL) of the retina and it was of interest to find an associated loss of dystrophin immunoreactivity at the post-synaptic region of the OPL in

eye sections from these patients (Pillers et al., 1993, Miike et al., 1989; Tamura et al., 1993). The observation that *mdx* mice have a normal ERG b-wave while the *mdx*^{3cv} mouse has a dramatically reduced b-wave, implicated an isoform transcribed from a promoter situated between exon 23 (position of the mutation in *mdx* mice) and 65 (position of the mutation in *mdx*^{3cv}).

This prediction was confirmed by the detection of a novel 260kDa band on Western blots of mouse retina extract which could be detected using an antibody raised against an exon 32 fusion protein whereas an antibody against an exon 28 protein did not detect this isoform (D'Souza et al., 1995). The corresponding mRNA was recovered by 5' RACE and sequence analysis revealed that the transcriptional start site was likely to lie within intron 29. The unique first exon contains 211bp of 5' UTR and 13 aa and is spliced to exon 30 (D'Souza et al., 1995). The Dp260 isoform is the longest of the short dystrophins and consists of 15 spectrin repeats, 2 hinge regions and the cysteine and COOH-terminal domains (Fig 1.3). Western blot analysis of retinal extracts prepared at different stages of mouse development showed that Dp260 protein levels increase perinatally (Rodius et al., 1997). Reverse transcription PCR (RT-PCR) indicates that the Dp260 transcript is expressed strongly in retina and weakly in brain and heart, with no expression in a variety of other somatic tissues (D'Souza et al., 1995).

The expression profile of the different dystrophin isoforms was reviewed by Tokarz et al. (1998) using RT-PCR; full-length dystrophin mRNA and the short transcripts were amplified from a wide selection of mouse adult tissues suggesting that their expression might be wider than previously estimated by Northern and/or Western blotting. This finding was perhaps not surprising since

RT-PCR is a very sensitive technique and trace amounts of mRNA may be amplified.

In summary, there is firm evidence that the short dystrophin isoforms are transcribed and translated in numerous tissues; while Dp71 is widely distributed, expression of Dp116, Dp140 and Dp260 seems more restricted. In all four cases, the patterns of mRNA and protein expression show some correlation.

The expression pattern of the dystrophin isoforms is summarised in Table 1.1.

1.6 Alternative splicing of the dystrophin transcripts

Multiple splice forms have been identified for all the dystrophin transcripts; alternative splicing occurs in a tissue and developmental stage specific manner.

The isoform designated Apo-dystrophin 3 (Apo-dys 3) is a splice variant of Dp71. Regular mis-splicing of intron 70 results in sequence from the 3' end of intron 70 being retained. The subsequent downstream sequence is no longer in frame resulting in premature termination of translation at a stop codon positioned in exon 71 and a unique 3' UTR sequence (Tinsley et al., 1993a; Blake et al., 1992). The overall length of Apo-dys3 mRNA is 2.2 Kb (Tinsley et al., 1993a). Apo-dys 3 mRNA has been RT-PCR amplified from a variety of foetal tissues and embryonic stem cells (Tinsley et al., 1993a).

In addition, Dp71 transcripts can be spliced for exon 71 and/or exon 78 so that four Dp71 isoforms can be produced (normal, -71,-78,-71 and -78), (Prigojin et al., 1993). This splicing is tissue specific; heart contains only

TISSUE	Dp427				Dp260*			Dp140				Dp116				Dp71			
	RT	N	IS	W	RT	N	W	RT	N	IS	W	RT	N	IS	W	RT	N	IS	W
a. brain	+	+	+	+	+	-	-	+	+	-	+	+	-	-	-	+	+	+	+
f. brain	+	+	+	+	nt	-	-	nt	-	-	-	nt	-	+	+	+	-	+	-
a. heart	+	+	+	+	+	-	-	+	-	-	-	+	-	-	-	+	+	-	+
a. eye	+	nt	-	+	+	nt	+	+	nt	-	+	+	nt	-	+	+	nt	+	+
a. smooth muscle	+	+	+	+	+	-	-	+	-	-	-	+	-	-	-	+	-	+	+
a. liver	+	-	-	-	+	-	-	+	-	-	-	-	-	+	+	+	+	+	+
a. kidney	+	-	nt	-	+	-	-	+	-	-	-	+	-	nt	-	+	+	+	+
f. kidney	nt	-	-	-	nt	-	-	+	+	+	+	nt	-	-	-	+	+	+	+
a. lung	+	-	-	-	+	-	-	+	-	-	-	+	-	-	+	+	+	-	-
a. skeletal muscle	+	+	+	+	+	+	-	+	-	nt	-	+	-	nt	-	+	-	nt	-
f. skeletal muscle	+	+	+	+	nt	-	-	nt	-	-	-	nt	-	-	-	+	+	-	+
a. spleen	+	-	-	-	+	-	-	+	-	-	-	+	-	-	-	+	-	-	+
a. testis	+	-	-	-	+	-	-	+	-	-	-	+	-	-	-	+	+	-	+
a. cochlea	nt	nt	-	+	nt	nt	-	nt	nt	-	-	nt	nt	-	+	nt	nt	-	-
glioma cells	nt	-	nt	-	nt	-	-	nt	-	nt	-	nt	+	nt	+	nt	+	nt	+
schwann cells	nt	-	nt	-	nt	-	-	nt	-	nt	-	nt	+	nt	+	nt	+	nt	+

Table 1.1 Summary of expression of the dystrophin isoforms. RT=RT-PCR; N=Northern blotting; IS= mRNA *in situ* hybridisation; W= Western blotting. a= adult; f=foetal; Data taken from Chelly et al. (1990), Nudel et al. (1989), Lederfein et al. (1992); Bar et al. (1990), Blake et al. (1992), Schofield et al. (1994), Durbeej et al. (1997), Rodius et al. (1997), Byers et al. (1993), Lidov et al. (1995), D'Souza et al. (1995), Tokarz et al. (1998).

* where *in situ* hybridisation results are given, these have been acquired using transcript specific riboprobes. In the case of Dp260, these experiments have not been carried out.

transcripts with exon 71 spliced out and liver with exon 78 spliced out; brain, muscle, kidney, retina and testis contain a mixture of all four isoforms (Geng et al., 1991; Roberts et al., 1992; Austin et al., 2000). Dp140 is subject to a similar pattern of tissue specific alternative splicing (Lidov et al., 1997). The highly regulated tissue and temporal specific pattern of splicing implies that the different spliced forms must have varied properties and functions.

The splicing out of exon 78 alters the reading frame so that the last 13 aa of the protein sequence are replaced by 31 aa followed by a stop codon (Geng et al., 1991; Lederfein et al., 1992). This unique alternative COOH-terminus aa sequence, which is conserved in the mouse, is more hydrophilic than the “plus exon 78” terminus and this might have implications for the association of Dp71 with membranes. However, another role has been proposed for the alternative splicing of exons 71/78 which involves the subcellular distribution of Dp71 isoforms. Gonzalez et al. (2000) fused the four alternative Dp71 cDNAs to the 3' end of the green fluorescent protein (GFP) gene and transfected HeLa, C2C12 and neuroblastoma cells with the various constructs. The Dp71 isoform lacking both exons 71 and 78 localised exclusively to the cytoplasm whereas the variants containing the exons showed a predominant nuclear localisation. These authors proposed that the protein domains within exon 71 and 78 might contain a nuclear localising signal (NLS) although, a consensus NLS could not be identified. However, a phosphorylation site for p34^{cdc2} protein kinase is present in exon 78 and this might regulate nuclear import (Milner et al., 1993) and thus those isoforms with exon 78 might be phosphorylated and transported whereas those without, would remain in the cytoplasm. It is relevant to note that

another dystrophin-related protein is also expressed in the nuclear compartment; β -dystrobrevin (Blake et al., 1999).

Phosphorylation could also modulate protein-protein interactions of the isoforms with DAPs. This mechanism operates in other proteins such as ankyrin (Bennett et al., 1990).

1.7 Function of dystrophin isoforms and animal models

Valuable information regarding the function of full-length and short dystrophin isoforms has emerged from the study of mouse models deficient for dystrophin. The key features of these mice are summarised below, prior to describing what is known about the functions of the dystrophin isoforms.

***mdx* mice** The *mdx* mouse is a naturally occurring mouse model for DMD which carries a nonsense mutation in exon 23 of the dystrophin gene (Sicinski et al., 1989; Bulfield et al., 1984). This mutation results in markedly reduced mRNA levels, probably due to degradation of the truncated mRNA by nonsense mediated mRNA decay (NMD) (Frischmeyer et al., 1999 and see section 6.1), and total absence of full-length dystrophin.

mdx mice show few of the clinical features observed in DMD patients however, their muscles show dystrophic changes which appear by the third week of age and include fibre necrosis, accumulation of macrophages and elevated serum creatine kinase levels. While the mice are mobile and agile several tests have shown that *mdx* muscles are weaker than those from control mice (Stedman et al., 1991). In contrast to DMD patient muscle, *mdx* muscle can undergo a very successful muscle regeneration with the appearance of new

small calibre centrally nucleated fibres. Upregulation of muscle transcription factors appears to be an integral part of this process evidenced by the finding that *mdx* mice that also lack the MyoD transcription factor, show a more severe phenotype and reduced levels of muscle regeneration (Megenny et al., 1996). Despite active regeneration, by 18 months the regenerative capacity of the *mdx* diaphragm runs out and muscle starts to be replaced by fat and connective tissue. By 24 months the regenerative capacity of the soleus muscles is also compromised (Bulfield et al., 1984), however, it is at this stage that *mdx* mice start to die of natural death (Bulfield et al., 1984).

One explanation for the mild phenotype of the *mdx* mouse is that the total force placed on the muscle of a mouse is much smaller (because of their smaller size) than the force that human muscles must support. For this reason, a dog model, the dystrophic golden retriever (GRMD), represents an attractive alternative, because of its larger size. These spontaneous dystrophic dogs have a single base pair change in the 3' consensus splice site of intron 6 which results in the skipping of exon 7 and the premature termination of translation at a stop codon in exon 8 (Sharp et al., 1992). However, it appears that there is considerable phenotypic variability between GRMD litters and this combined with the financial burden of maintaining kennels has led to the preference of mouse models.

The relatively mild phenotype displayed by *mdx* mice has also been explained in a variety of other ways including a more efficient use of short dystrophin isoforms and a more efficient recruitment of other members of the gene family such as utrophin. Utrophin is thought to be important in the sparing

of the extraocular muscles (EOM) in *mdx* mice and DMD patients (Khurana et al., 1995a; Porter et al., 1998b).

***mdx*^{3CV}** The *mdx*^{3CV} mutant has also been investigated in detail (Chapman et al., 1989). The mutation (which was induced by chemical mutagenesis) was located to intron 65 and shown to result in the creation of a novel splice acceptor site. The aberrant splicing leads to the introduction of 14bp of intronic sequence to the 5' end of exon 65 and a frameshifted mRNA which terminates prematurely at a stop codon 145 aa downstream. Both full-length and short dystrophin transcripts were undetectable and mRNA levels were estimated to be <20% of normal levels. Similarly, polypeptides corresponding to full-length dystrophins and Dp71 were not detected by Western blotting (Cox et al., 1993b; Lidov et al., 1995). Thus *mdx*^{3CV} mice are deficient for all dystrophin isoforms.

mdx^{3CV} mice are difficult to breed and show a reduced neonatal survival (Chapman et al., 1989). Those that survive show muscle pathology by four weeks of age which is similar to that of the *mdx* mouse. This includes cellular infiltration, necrosis and regenerating fibres. Greater variation in fibre size is seen in *mdx*^{3CV} compared to *mdx* (Cox et al., 1993b).

DMD^{ex52} An additional dystrophin mutant was generated by targeting exon 52 by homologous recombination, DMD^{ex52} (Araki et al., 1997). These mice are deficient for full-length dystrophin, Dp260 and Dp140 but express Dp116 and Dp71. The overall phenotype of these mice more closely resembles that of *mdx* than of *mdx*^{3CV}. This suggests that deficiency of Dp71 and/or Dp116

is responsible for the decreased neonatal survival and variability in fibre size seen in *mdx*^{3CV} mice.

Function of full-length dystrophin Physiological and histological studies of the muscles of the dystrophin-deficient mice described above and of DMD patients have led to the suggestion that in skeletal muscle full-length dystrophin maintains the integrity of the sarcolemma despite repeated cycles of muscle contraction and relaxation (Suzuki et al., 1992). This is achieved by the dystrophin molecule by forming a link between the internal actin cytoskeleton of the muscle fibre and the extracellular matrix (ECM) via a complex of dystrophin associated proteins (DAPs) (Campbell et al., 1989; Ohlendieck et al., 1991b). However, the progressive nature of DMD indicates that dystrophin exerts its protective function over an extended time period and that it might also be involved in postnatal muscle length growth (Brown and Lucy 1993).

Dystrophin also appears to be important for targeting the muscle specific isoform of nNOS (nNOS_μ, Kobzik et al., 1994) to the sarcolemma via the PDZ domain of syntrophin (Brenman et al., 1996; Kameya et al., 1999). At the sarcolemma, nNOS is important in the regulation of muscle blood-flow during exercise by controlling the vasoconstrictor response to activation of α -adrenergic receptors (Thomas et al., 1998). In the absence of dystrophin, nNOS is mislocalized to the interior of the muscle fibre where it cannot modulate contraction induced vasoconstriction (Brenman et al., 1995). This is believed to result in muscle ischemia during exercise and therefore to contribute to the muscle pathology of *mdx* mice and DMD patients (Thomas et al., 1997; Sander et al., 2000, Rafael and Brown 2000).

In brain, full-length dystrophin is thought to have a role in the stabilisation or clustering of neurotransmitter receptors. Evidence for this comes from comparing the clustering of GABA receptors in the brains of control and *mdx* mice (Knuesel et al., 1999). More recently, Knuesel et al. (2001) have shown that in the brain of an induced experimental model of temporal lobe epilepsy, dystrophin expression changes in a way that implies it has a role in synaptic and morphogenetic rearrangements in adult CNS neurones.

Function of short dystrophin isoforms

As mentioned earlier, the function of the short dystrophin isoforms is not yet understood. They all lack the actin-binding domain and some or the entire rod domain, therefore, they are not likely to interact with the actin cytoskeleton. However, they all contain the cysteine-rich and carboxy-terminal domains which contain the binding sites for the DAPs which in turn anchor dystrophin to the cell membrane. The most 3' terminal sequences also contain calmodulin binding and phosphorylation sites (Yoshida et al., 1996). Thus, the short isoforms are more likely to be part of membrane complexes involved in signalling processes rather than playing a structural role.

There is a growing body of evidence that the short dystrophins are important to normal cell function. This is well illustrated by the observation that the mental retardation (MR) seen in one third of DMD and BMD patients is more frequently associated with deletions (and point mutations) towards the 3' end of the gene that affect expression of the COOH-terminal isoforms (Lenk et al., 1993; Bushby et al., 1995; Moizard et al., 1998; Bardoni et al., 2000). Verbal intelligence and cognitive facilities are particularly affected and seem to be a

primary consequence of deficiency since they are not associated with the stage or severity of the disease. Although the molecular mechanisms leading to MR are not known there is good evidence that it is associated with the short transcripts Dp140 and Dp71 which are expressed in brain. Bushby et al. (1995) found a significant difference in the full-scale intellectual quotient (IQ) between patients with deletions at the 5' and 3' ends of the dystrophin gene. None of the patients with 5' deletions showed mental retardation whereas all showed deletions at the 3' end, but of different size and extent. These results were confirmed by Moizard et al. (1998) who carried out a thorough psychological analysis of 49 DMD patients and correlated the results with the position of the deletions in the dystrophin gene relative to Dp140 and Dp71 regions. Although a statistically significant association could not be established, Moizard and colleagues (1998) proposed three patterns of MR based on their study and previous data; absence of full-length dystrophin only, caused by mutations at the 5' end of the gene, results in moderate MR; more distal mutations, affecting full-length dystrophin and Dp140, are associated with a reduced verbal intelligence and cognitive impairment; mutations in the Dp71 region, affecting all isoforms, result in a severe cerebral dysfunction. Thus it appears that the absence of more than one brain dystrophin isoform resulting from distal mutations has a cumulative effect which explains the gradation of mental/cognitive dysfunction seen in DMD patients.

In contrast to the muscle weakness, the MR is not progressive but is present at birth which suggests that it might be the consequence of a developmental event. The expression profiles of Dp140 and Dp71 in brain differ. Dp140 is found in olfactory bulb and leptomeningeal surfaces (Lidov et al.,

1995) whereas Dp71 is expressed in the ependymal lining of the ventricles, cerebral cortex and the hippocampal dentate gyrus which is involved in some memory and cognitive processes (Gorecki et al., 1995). Dp71 appears to be part of a glial cell complex with α -dystrobrevin-1; this differs from full-length dystrophin which is confined to neurones in hippocampus and cerebral cortex and appears to be associated with β -dystrobrevin (Blake et al., 1999). Thus, the roles of the short dystrophin isoforms in the brain are likely to differ from that of full-length dystrophin.

In skeletal muscle, overexpression of Dp71 is able to restore the DAP complex to the sarcolemma of *mdx* and dystrophin-utrophin double deficient mice (dko^{ex6} , see section 1.10) (Cox et al., 1994; Rafael et al., 2000). However, this does not alleviate the muscle degeneration seen in these mutant mice which suggests that the role of full-length dystrophin cannot be fulfilled by the cysteine-rich and COOH-terminal domains solely.

In the retina, at least three short dystrophin isoforms are expressed (Rodius et al., 1997). Dp260 is expressed in photoreceptor cells in the outer plexiform layer (OPL) where it interacts with β -dystroglycan (D'Souza et al., 1995). Dp260 appears to be important for the localisation of the DAP complex within the photoreceptor terminals since in DMD^{ex52} mouse retina, β -dystroglycan disappears from the OPL (Kameya et al., 1997). The similarity in the expression profiles of Dp260 and metabotropic glutamate receptor (mGluR6) during retina formation has suggested that Dp260 could be involved in the development of this neural tissue (Nomura et al., 1994). This view is based on the observation that mGluR6 expression has been correlated with

establishment of synaptic connections between photoreceptors and bipolar cells (Nomura et al., 1994).

In contrast to Dp260, Dp71 is preferentially found in the inner limiting membrane, probably in the end feet of Müller glial cells (Claudepierre et al., 2000). Müller cells contribute to the generation of a b-wave by their ability to carry large currents of K^+ ion through specific K^+ channels. Claudepierre et al. (2000) showed that β -dystroglycan, δ - and γ -sarcoglycans and α -syntrophin are co-expressed with Dp71 in Müller cells. Thus, Dp71 could be part of a Müller cell specific DAP complex and this complex may have a role in maintaining the shape of the Müller cells via interactions with laminin in the extracellular matrix or perhaps be involved in clustering of ion channels in the cell membrane. It is possible that the abnormal ERG seen in DMD patients is not due simply to the altered expression of Dp260. Indeed, DMD^{ex52} mice have impaired expression of both Dp260 and Dp140 but have a relatively normal b-wave compared to *mdx*^{3CV} (which lack all dystrophin isoforms); so it seems that Dp260 and Dp140 are not directly responsible for the reduced b-wave and that Dp71 may also be important for normal retinal function.

Dp116 has been shown to form specific complexes in glioma, Schwannoma and oligodendroma cells. For example, in peripheral nerve Dp116, β -, δ - ϵ -sarcoglycans and dystroglycan are expressed in the membrane of the outermost layer of Schwann cells (Imamura et al., 2000). However, the functional significance of this complex is not clear since neither *mdx*^{3CV} mice nor β -sarcoglycan and/or δ -sarcoglycan deficient animals show peripheral nerve abnormalities. There is one report of a deletion affecting the region of Dp116 first exon and dystrophin exon 56 that cosegregates with mental retardation in a

Japanese dystrophinopathy family (Chen D. et al., 1999). Because of its preferential expression in Schwann cells it has been proposed that Dp116 is involved in nerve conduction velocity (Byers et al., 1993). However, patients with a deletion in the region of exon 56 do not have sensory or motor nerve conduction abnormalities (Chen D. et al., 1999).

1.8 The utrophin isoforms

In comparison with dystrophin, five promoters of utrophin transcription have been identified, by work carried out at the MRC Human Biochemical Genetics Unit and in several other laboratories (Fig 1.4; Table 1.2); two of these regulate the expression of 395kDa forms, while three internal promoters drive the expression of short mRNAs, G-utrophin, Up140 and Up71. It is of considerable interest that the positions of the internal promoters within the genes are conserved between dystrophin and utrophin.

In the following sections (1.8, 1.9 and 1.10) a comprehensive account of what was known about the various utrophin mRNAs before this study was undertaken is given. Comparisons with dystrophin are made when relevant. Most of the published information concentrates on the full-length form and much less is known/published about the short utrophins.

Full-length utrophin A Full-length utrophin A (395kDa) is encoded by a 13Kb mRNA transcribed from a CpG island at the 5' end of the gene. In a few published papers the identification of the 395kDa form is unequivocal and can be recognised by size (Northern and Western blotting) or by using probes/primers/antibodies specific for the 5' end of the cDNA or the NH₂-terminus of the protein (mRNA *in situ* hybridisation, RT-PCR, immunohistochemistry). However, in some reports the identity of the transcript/isoform(s) is uncertain. This is particularly true for many of the descriptions of utrophin in foetal tissues (see section 1.9).

There is evidence from Northern blotting for the expression of full-length utrophin mRNA in adult and foetal skeletal muscle (Love et al., 1991), placenta and several adult non-muscle tissues including brain,

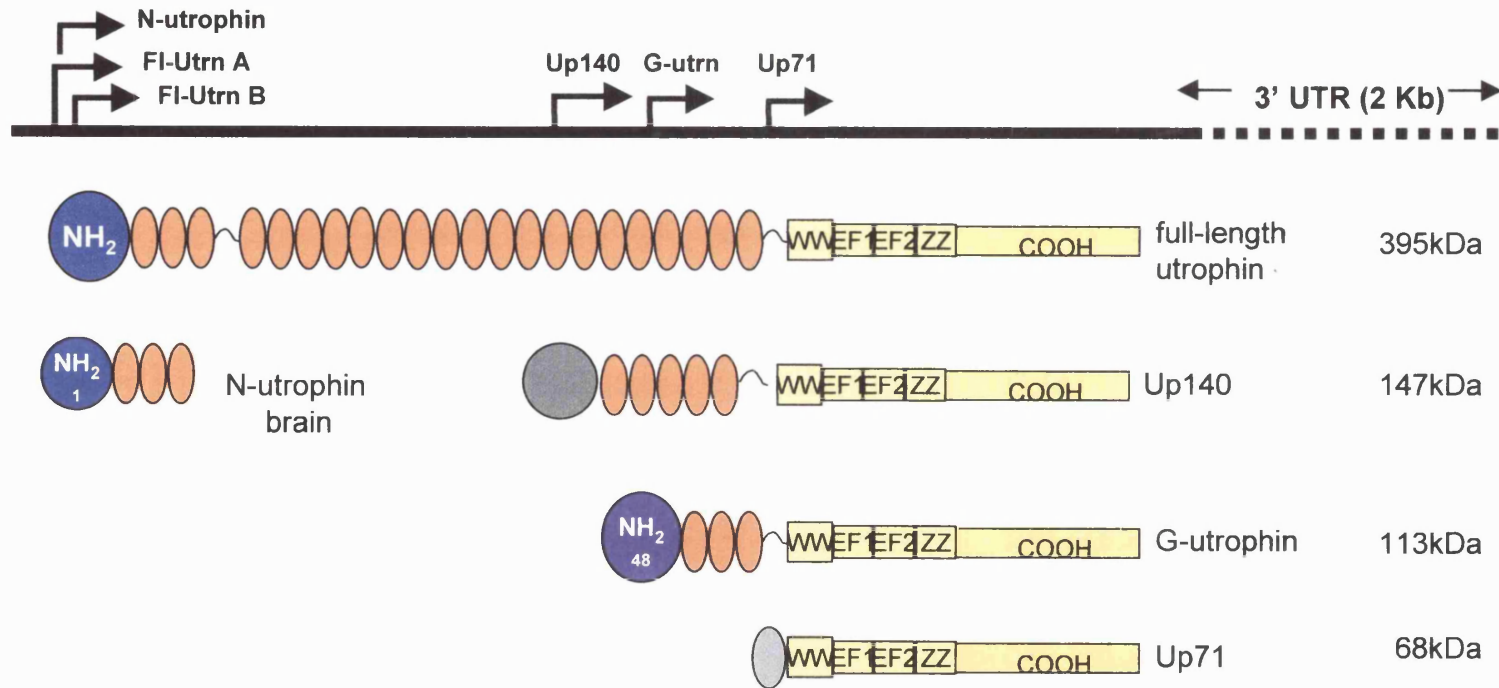


Fig 1.4 Upper. The positions of the transcription start sites of the 5 known utrophin isoforms are shown relative to the protein structure. Lower. Shows the structure of each isoform. The NH₂-terminal domains are coloured blue if these contain novel aa encoded by the first exon; the number of aa is indicated. In the case of Up140 and Up71, coloured grey, the first exon encodes only 5' UTR. Taken from Wilson (thesis 2000).

Name	mRNA (Kb)	protein (kDa)	mRNA expression pattern	protein expression pattern*
Fl-utrn A	13	395	skeletal muscle (N,RT, IS) smooth muscle (N) heart (N, RT) brain (IS, N, RT) lung (N, RT), liver (N,RT) testis (N, RT), kidney (N, RT) placenta (N), retina (RT)	skeletal muscle (W) smooth muscle (W) heart (W) brain (W) lung (W), liver (W) kidney (W) placenta (W), retina (W)
Fl-utrn B	13	395	heart, skeletal muscle, pancreas lung, kidney (N)	nt
N-utrn	3.7 (3.4)	62	glioma cell line (N)	glioma cell line (W)
G-utrophin	5.5	113	cortex, olfactory bulb, caudate putamen, ganglia (IS)	nt
Up140	6.75	147	skeletal muscle, lung, kidney liver, thymus, testis (RT)	skeletal muscle (W)
Up71	4	68	skeletal muscle, lung, kidney liver, thymus, testis (RT)	brain, nerve blood-vessels (W)

Table 1.2 Summary of the utrophin isoforms; the major sites of expression of the corresponding mRNAs and proteins are shown. Fl-utrn= full-length utrophin; nt = not tested. RT=RT-PCR; N=Northern blotting; IS= mRNA *in situ* hybridisation
W= Western blotting.

* Other tissues as in the mRNA expression column have been tested but no band was reported.

heart, liver, testis, kidney and lung (Durbeej et al., 1999; Lumeng et al., 1999). The full-length transcript has also been detected in several cell lines including smooth muscle (BC3H-1), kidney (COS-7) and adult and embryonic brain cells (EMB, AMB), (Nguyen et al., 1992). Full-length utrophin mRNA was amplified in numerous human and mouse adult and foetal tissues including testis, lung, brain, muscle, kidney and liver using primers at the 5' end of the utrophin cDNA (Wilson et al., 1999).

At the protein level, Western blotting has shown that the 395kDa utrophin is translated in a large number of adult tissues with highest levels of protein in lung, kidney and liver and the weakest in brain and skeletal muscle (Love et al.; 1989; Matsumura et al., 1993b; Lumeng et al., 1999). The 395kDa isoform is also present in a variety of cell lines including, C6 glioma cells, HeLa cells, Schwannoma cells, COS-1 kidney cells, fibroblasts and a hybridoma cell line (Nguyen et al., 1992).

Immuno-histochemical analysis of skeletal muscle sections using antibodies raised against the NH₂-terminus of utrophin has shown that in adult skeletal muscle, 395kDa utrophin is expressed at the neuromuscular junction (NMJ), myotendinous junction (MTJ), blood-vessels, intramuscular nerves and capillaries (Nguyen et al., 1995). Dystrophin in adult muscle is mainly expressed at the sarcolemma (Ervasti et al., 1991, Ervasti and Campbell 1991) but is also found at both the MTJ and the NMJ (Law et al., 1994). At the NMJ utrophin and dystrophin occupy different sites; utrophin localises to the peaks of the synaptic folds in close proximity to acetylcholine receptors (AChR) whereas dystrophin is located at the troughs of these folds where there is a high concentration of sodium channels (Bewick et al., 1992). Full-length utrophin is also expressed at

the sarcolemma of regenerating fibres and of dystrophin deficient fibres and in other inflammatory myopathies (e.g Helliwell et al., 1992).

In skeletal muscle, utrophin is developmentally regulated. Immunohistochemical analysis of human foetal muscle has shown utrophin at the sarcolemma of myotubes from 9 weeks gestation with maximum levels achieved by 18 weeks gestation. After this time, there is a decrease in expression such that by 26 weeks gestation utrophin is almost undetectable (Clerk et al., 1993; Mora et al., 1996). A similar developmental pattern is seen in mouse and rat foetal muscle (Khurana et al., 1991; Koga et al., 1993; Lin S. et al., 2000). This developmental pattern contrasts with that of dystrophin which is expressed from 8 weeks gestation and increases steadily towards birth (Khurana et al., 1991; Clerk et al., 1992; Mora et al., 1996). In foetal muscle utrophin is also detected in blood-vessels and peripheral nerves. Expression at these sites, in contrast to the sarcolemma, is not developmentally regulated and persists in the adult.

In cardiac muscle, 395kDa utrophin has been detected in the intercalated discs, transverse T-tubules and Purkinje fibres (Pons et al., 1994), however, in a recent report Sewry et al. (2001) reported that the major site of expression in the heart is the vascular system. In contrast to utrophin, dystrophin is found at the plasma membrane of the cardiomyocytes (Tanaka et al., 1990; Byers et al., 1991). The 395kDa form is apparently upregulated in dystrophin-deficient cardiomyocytes and appears at the sarcolemma (Fanin et al., 1999); this upregulation is unable to prevent myocardial dysfunction.

The occurrence of cognitive/mental impairment in some DMD patients prompted interest in not only brain dystrophin but also brain utrophin. A

systematic study of brain utrophin by mRNA *in situ* hybridisation using a panel of riboprobes and immuno-histochemistry using a panel of antibodies confirmed that the 395kDa mRNA and protein are expressed in choroid plexus and cerebral vasculature (Knuesel et al., 2000; Khurana et al., 1992; Kamakura et al., 1994). The 395kDa utrophin is abundant in the neurones of the ventral cochlear nucleus and the mesencephalic trigeminal nucleus of the brainstem and is also found in the cerebral cortex. Immuno-histochemistry and confocal microscopy revealed that in the epithelial cells of the choroid plexus utrophin localises to the basolateral membrane; in neurones utrophin localises to the cell membrane and proximal dendrites (Knuesel et al., 2000).

This distribution is different to that of dystrophin which accumulates in the Purkinje cells of the cerebellum and in cortical and hippocampal pyramidal cells (Knuesel et al., 2000; Chelly et al., 1990; Gorecki et al., 1991, 1992). In the cerebral cortex utrophin and dystrophin are expressed in different populations of neurones. The *mdx* brain shows no signs of upregulation of utrophin, or of expression of utrophin at sites normally occupied by dystrophin as has been reported for skeletal muscle (e.g. Helliwell et al., 1992).

Lung shows one of the highest levels of utrophin expression. The 395kDa form is abundant in endothelial cells (Matsumura et al., 1993b) and in epithelial and smooth muscle cells (Durbeej et al., 1999). It is difficult to ascertain from the data presented in these reports whether the expression of other utrophin isoforms could be excluded.

In kidney, Raats et al. (2000) clearly demonstrated, using an NH₂-terminal antibody, that 395kDa utrophin is the major isoform in this tissue and

that it localises to the processes of podocytes, specialised epithelial cells in kidney glomerular wall, and in the basal side of tubular epithelial cells.

In summary, full-length utrophin is ubiquitously expressed in adult tissues and is found most commonly at specialised cell-cell or cell-extracellular matrix contact regions such as the basolateral membrane of epithelial cells, the foot-processes of kidney podocytes, the somato-dendritic compartment of neurones and the intercalated discs of the heart

Full-length utrophin A promoter The proximal promoter of full-length utrophin A lies in an unmethylated CpG island (224bp) which extends across the first exon (Dennis et al., 1996). Within the human promoter there are several non conserved binding sites for the ubiquitous transcription factor Sp1 but no TATA box or CAAT motif (Dennis et al., 1996). Both the human and the mouse promoters contain an E-box, a recognition sequence for the muscle specific transcription factors of the MyoD family (Davis et al., 1989; Wright et al., 1989), and an N-box, a motif that occurs in promoter regions of genes expressed at muscle-nerve synapses (NMJ), for example the acetylcholine receptor δ subunit (Koike et al., 1995) and β 2-syntrophin (Peters et al., 1994). 0.9 Kb of 5' flanking sequence, which includes both the E box and N box, is sufficient to drive transcription of a reporter gene in transfected cell lines. The transcriptional activator GABP has been shown to bind to the N-box of utrophin and increase its expression in cultured myotubes (Gramolini et al., 1999a).

The muscle specific promoter of dystrophin lacks an N-box even though it is expressed at the NMJ (there are four E-boxes, MEF-1 and MEF-2 binding sites, a CarG box and a MCAT motif, Klamut et al., 1990, 1997; Boxer et al.,

1989; Navankasattusas et al., 1992; Mar et al., 1990; Lassar et al., 1991).

However, as described previously, utrophin localises to the crest of the synaptic folds in association with clusters of AChR, whereas dystrophin is found at the depths of the folds. Thus, the presence of an N-box is associated with expression at the synaptic contact point.

Very recent studies of the full-length utrophin A promoter have shown that the Sp binding sites bind to Sp1 and Sp3 transcription factors and that the most 3' GC site behaves as a basal promoter element while the two upstream sites are required for full promoter activity (Galvagni et al., 2001). The binding of Sp1 and Sp3 to the GC boxes activates transcription. Interestingly, mutations in the N-box prevented Sp1 and Sp3 from activating transcription and led to the proposal that Sp1 and Sp3 might interact with a factor that binds to the N-box. Indeed, Galvagni et al. (2001) demonstrated that GABP and Sp1 and Sp3 physically interact and act synergistically to induce expression of the utrophin A transcript.

Regulation of expression of full-length utrophin A in skeletal muscle The postsynaptic membrane at the NMJ is a highly differentiated region associated with the accumulation of various organelles, including distinctive myonuclei which seem to transcribe mRNAs specific to their location (Gramolini et al., 1997). At the NMJ utrophin mRNA is transcribed at comparable levels to other synaptic transcripts including AChR (Duclert et al., 1996), rapsyn and agrin (Moscoso et al., 1995, Gramolini et al., 1997).

Transfection studies using a utrophin A promoter-reporter gene construct have helped to identify the regulatory elements that are important for expression

of utrophin by synaptic nuclei (Gramolini et al., 1997; Galvagni et al., 2000, 2001). These experiments showed that proteins which bind to E-box and N-box motifs are essential for correct expression. One such protein is agrin - it is released by neurones and induces a two-fold increase in the level of utrophin in C2 myotubes (Gramolini et al., 1998). In co-transfection experiments, agrin appeared to act directly on the utrophin promoter and the sensitivity to agrin was abolished if the N-box and E-box containing regions were deleted (Gramolini et al., 1997).

Heregulin is another nerve derived factor which might regulate the 395kDa utrophin A promoter. Heregulin is known to influence the localisation and regulation of AChRs. AChR subunit genes are selectively expressed at the NMJ through the interaction of heregulin with ErbB2 and ErbB3 receptors (Moscoso et al., 1995), which in turn results in the transcriptional activation of the AChR promoters through GABP binding to the N-box. A series of experiments by Gramolini et al. (1999a) have shown that the ectopic expression of heregulin and GABP α and β also increases the expression of utrophin at the NMJ in cultured myotubes. This view finds support in the work of Galvagni et al. (2000) who showed, as mentioned earlier, that GABP interacts with Sp1/3 transcription factors to increase transcription from the full-length utrophin A promoter.

Expression of utrophin at the sarcolemma is developmentally regulated. There is a considerable body of evidence to show that transcription factors belonging to the MyoD family acting via E-box elements regulate the large increase in the expression of genes encoding cytoskeletal and membrane proteins including dystrophin and the AChR genes (Tennyson et al., 1996).

However, these transcription factors are not the major regulators of utrophin expression in the developing muscle. Major increases in the MyoD factors during muscle differentiation or following experimental denervation are not associated with major increases in utrophin expression (Gramolini et al., 1999c). The idea that the E-box and N-box elements of the utrophin promoter act in a synergistic manner to regulate the expression of the utrophin gene (Gramolini et al., 1999c) is a more attractive possibility. The E-box and N-box elements are found in close proximity in the 395kDa utrophin A promoter in a configuration similar to that in the AChR δ - and ϵ - subunit promoters (Chan et al., 1999).

The mechanisms leading to the accumulation of utrophin at the sarcolemma during the early stages of development are not well understood but are likely to operate at the post-transcriptional level. Gramolini et al. (1999c) proposed a model based on competition for binding sites in the DAP complex. In brief, levels of expression of the DAPs are relatively constant during myogenesis. During the early stages of muscle development, when dystrophin levels are low, utrophin protein is stable because is bound to the DAP complex; when levels of dystrophin increase, dystrophin binds preferentially to the DAP complex and utrophin protein levels at this location decline. This is supported by the observation that in DMD patients levels of utrophin protein increase without an increase in the levels of its mRNA (Gramolini et al., 1999b).

A similar competitive model is seen for spectrin in developing erythrocytes and explains the presence of distinct spectrin isoforms within the membrane cytoskeleton at different stages of development (Coleman et al., 1989).

Structure and function of the 395kDa utrophin-DAP complex at the NMJ In adult skeletal muscle the 395kDa utrophin at the NMJ forms a complex with synapse specific DAPs including agrin - a nerve-derived signalling molecule that triggers post-synaptic differentiation and binds to α -dystroglycan, and rapsyn - an intracellular molecule that binds to the complex via β -dystroglycan and is required for AChR clustering (Matsumura et al., 1992).

The current model of 395kDa utrophin-DAP complex at the NMJ is shown diagrammatically in Fig. 1.5 which shows the stoichiometry of the complex with one utrophin, one dystrobrevin molecule and two syntrophin molecules, one of the latter bound directly to utrophin and the other to a member of the dystrobrevin family.

Several pieces of evidence suggest that this complex is important for the structure and maturation of the NMJ. For example, the postsynaptic apparatus fails to form in mutant mice lacking either agrin (Gautman et al., 1996), rapsyn (Gautman et al., 1999) or muscle specific receptor tyrosine kinase (MusK), (DeChiara et al., 1996). Dystroglycan is also important for assembly of the AChR cluster-associated basal membrane. Although dystroglycan null mice, $DG^{-/-}$, die before muscles form (Williamson et al., 1997) myotubes can be generated from $DG^{-/-}$ embryonic stem cells; using such cells two independent studies have shown (Grady et al., 2000; Jacobson et al., 2001) that in the absence of dystroglycan, the structure of AChR clusters is abnormal and expression of laminin-5 and perlecan (heparan sulphate proteoglycan 2) at the extracellular matrix (ECM) are reduced.

A detailed analysis of the NMJ of dystrobrevin mutant mice (Grady et al., 2000) has revealed that while dystrobrevin is apparently dispensable for AChR

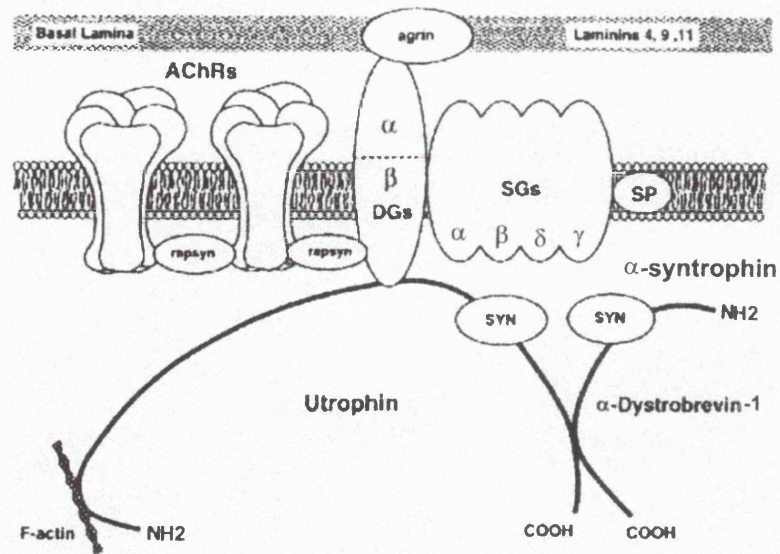


Fig 1.5 Schematic representation of the 395kDa utrophin-DAP complex at the muscle NMJ in association with acetyl-choline receptors (AChR). This complex includes utrophin, rapsyn, sarcoglycans (SG), dystroglycans (DG), sarcospan (SP), α -syntrophin (SYN) and α -dystrobrevin-1. Modified from Grady et al. (2000)

clustering, it is necessary for the maintenance of those clusters. This explains why NMJs initially form normally but the post-synaptic apparatus matures abnormally. These mice also have an abnormal “patchy” distribution of 395kDa utrophin and agrin which indicates that α -dystrobrevin might also have a role in the arrangement of these proteins at the NMJ.

Mice lacking α -syntrophin also shown an abnormal post-synaptic membrane structure with reduced density of AChR, acetyl-cholinesterase and utrophin (Adams et al., 2000) which suggest that at the NMJ utrophin is preferentially associated with the α - isoform of syntrophin.

All the data in the literature indicate that 395kDa utrophin at the NMJ is important for the maintenance of AChR clusters (Froehner et al., 1991; Phillips et al., 1993; Peters et al., 1994). Utrophin levels are reduced in inherited and acquired AChR deficiencies (Slater et al., 1997). Furthermore, the only detectable abnormality in utrophin null mice (UKO^{ex6} and UKO^{ex64}, section 1.10) is a drastic reduction in the density of AChR (<40% normal levels) probably due to a decrease in the available area of the post-synaptic folds. In these mice, the full-scale effect of the loss of utrophin seems to be masked by the compensatory effect of dystrophin, since in utrophin-dystrophin double mutants (dko, section 1.10) postsynaptic folding is virtually non existing and in one of the strains of dko mice, dko^{ex64}, the expression of some of the members of the NMJ DAP complex including dystrobrevin, β 2-syntrophin and sarcospan (Grady et al., 1997b; Crosbie et al., 1999), is reduced. The levels of these proteins were not examined in dko^{ex6} mice. Thus, it appears that 395kDa utrophin might be dispensable for the formation of the NMJ but is necessary for the correct folding

of the muscle membrane at the motor end plate and for the distribution of AChR clusters and other proteins at the NMJ.

Structure and function of the 395kDa utrophin-DAP complex in non-muscle tissues

There is less information regarding the function of full-length utrophin in non-muscle cells. Several members of the DAP complex are expressed in non-muscle tissues. For example, dystroglycan is found in lung, kidney, brain and testis (Durbeej et al., 1998, 1999), α - and β -dystrobrevin in brain and kidney (Blake et al., 1999), β -, δ -, γ -sarcoglycans and sarcospan in lung (Durbeej et al., 1999), ϵ -sarcoglycan in kidney, and α -, β 1- and β 2-syntrophins in brain and kidney (Blake et al., 1999; Loh et al., 2000; Kachinsky et al., 1999). Thus, it is likely that in these tissues 395kDa utrophin will be part of a DAP complex which may link the cytoskeleton to the ECM as in the NMJ.

The composition of such complexes has been analysed in detail in lung (Durbeej et al., 1999), brain (Blake et al., 1999) and kidney (Durbeej et al., 1999; Loh et al., 2000; Kachinsky et al., 1999). These studies provide clues on the potential function of full-length utrophin at sites other than the NMJ.

While the 395kDa utrophin has been demonstrated in all of these tissues by Western blotting (Love et al., 1991; Lumeng et al., 1999; Raats et al., 2000), all the above mentioned studies were carried out using antibodies against the COOH-terminus of utrophin and thus the presence and participation of short isoforms in similar complexes cannot be excluded.

It appears that in various tissues the 395kDa utrophin is preferentially found in specialised regions of the cell membrane in areas of cell-cell or cell-ECM contact (e.g. Kachinsky et al., 1999; Raats et al., 2000). As an example, I

will describe the 395kDa utrophin-DAP complex in kidney epithelial cells pooling together the data from the work of Durbeej et al. (1999), Loh et al. (2000) and Kachinsky et al. (1999). This tissue is of particular interest since it has been a focus of investigation in the present study on the short utrophin isoforms. In adult kidney, full-length utrophin is expressed at the basolateral membrane of polarised epithelial cells where it forms a complex with ϵ -sarcoglycan, β -dystrobrevin and β 2-syntrophin. This complex, which is diagrammatically represented in Fig 1.6, may link the cytoskeleton of the epithelial cell to laminin-1 or agrin which are both found in the glomerular extracellular matrix (Raats et al., 2000; Durbeej et al., 1998). In foetal kidney, dystroglycan is also part of this complex but dystroglycan is absent from the adult tissue. The α -, β -, γ , δ sarcoglycans and sarcospan, which take part in the NMJ complex, are not expressed in kidney epithelial cells; thus, the epithelial cell 395kDa utrophin - DAP complex may be seen as a simplified version of the NMJ complex or it is still possible that novel proteins similar to dystroglycan and sarcoglycans which take part in the complex have yet to be identified.

The polarised distribution of full-length utrophin suggests that the 395kDa utrophin A-DAP complex might have a role in the maintenance of the cell polarity by recruiting specific proteins exclusively to the basolateral membrane; this complex might also have a role in the formation of signalling complexes via interactions of molecules such as nNOS with syntrophin (Kramarcy et al., 2000).

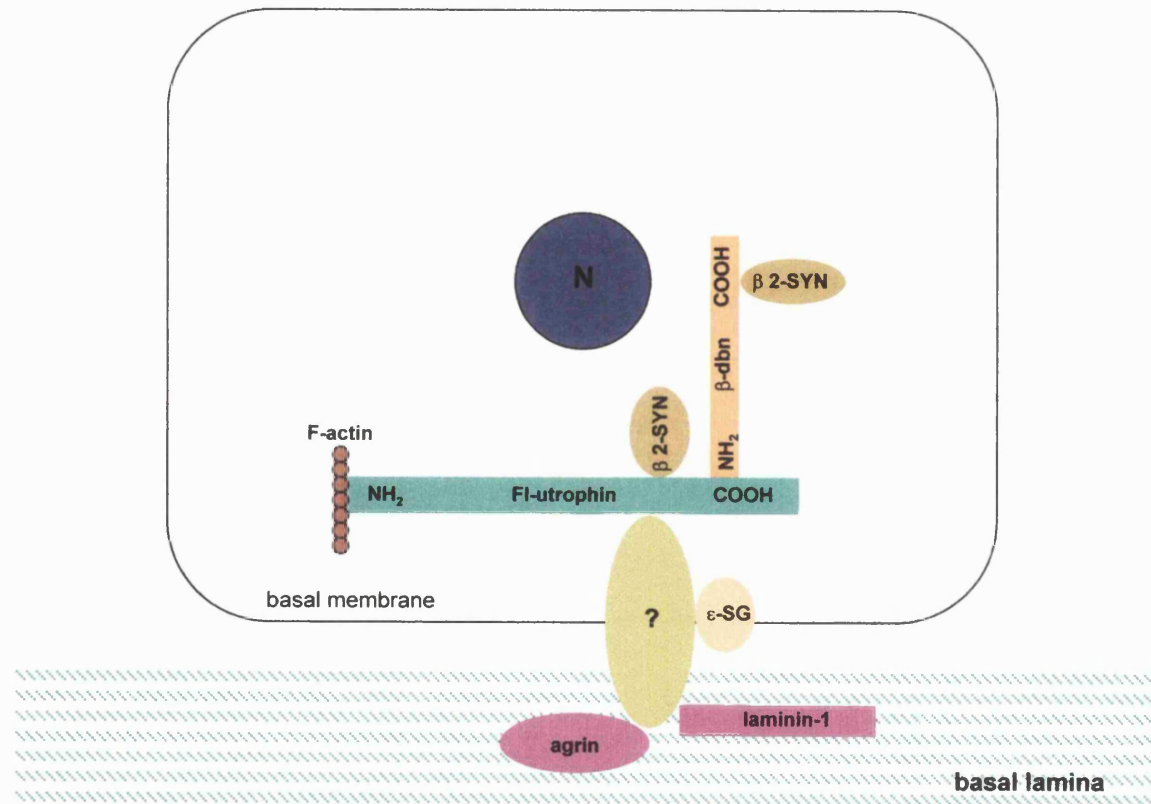


Fig 1.6 Diagrammatic representation of the 395kDa utrophin-DAP complex at the basal membrane of a kidney epithelial cell. N=nucleus; SYN=syntrophin; SG=sarcoglycan; dbn=dystrobrevin

Full-length utrophin B A second 5' full-length utrophin promoter has been identified which transcribes an alternative full-length utrophin isoform from a position 50Kb upstream of exon 3 within the 120Kb intron 2 (Burton et al., 1999). This transcript has a conserved novel first exon (1B) (Fig 1.4), which has a translation initiation codon in the same reading frame as utrophin exon 3, to which it is spliced, and which encodes 31 unique aa. Full-length utrophin B is 13Kb long and is also ubiquitously expressed; however, the pattern of expression is not identical to the 395kDa utrophin A, since it is more abundant in heart and less abundant in kidney. Both mRNAs are equally abundant in skeletal muscle (Table 1.2).

The proximal promoter region of utrophin B is devoid of a TATA or CAAT boxes, is not GC rich and does not contain Sp binding sites, E- or N-boxes.

In addition to the two full-length isoforms of utrophin, several short utrophin transcripts have been identified (Fig 1.4). Here work is at a relatively early stage and it is not always clear that these forms of utrophin are transcribed and translated.

N-utrophin N-utrophin is a 65kDa polypeptide expressed in glioma cells. It was first recognised on Western blots using an NH₂-terminal anti-utrophin antibody (Nguyen et al., 1995) and then isolated from a C6 glioma cell cDNA library (Zuellig et al., 2000). N-utrophin comprises the NH₂-terminal region of the full-length protein up to the exon14/intron 14 boundary. However, this sequence is followed by 3 bp of intron 14 which on translation give rise to a novel COOH-terminus and a unique 3' UTR which contains alternative

polyadenylation signals (Zuellig et al., 2000) (Table 1.2). Use of these alternative poly-A addition sites gives rise to two mRNA species of 3.7Kb and 3.4Kb. Zuellig et al. (2000) showed that a recombinant fragment corresponding to N-utrophin aa sequence binds F-actin *in vitro*. There have been no other reports of expression of N-utrophin in any other cell type or tissues.

G-utrophin G-utrophin mRNAs is 5.5Kb long and encodes a novel first exon of 341 bp preceding sequence corresponding to exon 56 of full-length utrophin. The novel first exon comprises 197bp of 5' UTR and a stretch of 48 unique aa (Fig 1.4). The predicted size of the polypeptide encoded by this transcript is 113kDa (Blake et al., 1995). Since the point of divergence between the novel transcript and full-length utrophin lies exactly in the same position that the Dp116 transcript diverges from the dystrophin full-length sequence, (i.e. the junction between intron 55 and exon 56), G-utrophin can be regarded as the homologue of Dp116. The unique 5' sequences of Dp116 and G-utrophin do not have significant similarity except for a conserved potential phosphorylation site which may modulate the assembly of cytoskeletal complexes.

RNase protection assays showed that G-utrophin is confined to brain where it is five times more abundant than full-length utrophin (Blake et al., 1995). The localisation of G-utrophin mRNA to specific brain regions; cerebral cortex, caudate putamen, amygdala, hypothalamus, olfactory bulb and in pontine, facial and vestibular nuclei, has been determined by mRNA *in situ* hybridisation using a G-utrophin specific probe (Blake et al., 1995). The name G-utrophin was chosen because of its abundant expression in ganglia (Blake et al., 1995) (Table 1.2).

The 5' UTR of G-utrophin contains four in frame ATG codons associated with weak Kozak consensus sequences. This observation led to the suggestion that G-utrophin was poorly translated although this was not investigated thoroughly. When the present study was started there were no reports of G-utrophin protein and the position of its transcription initiation start site and promoter within intron 55 was unknown.

Up140 isoform The clear structural homologies between utrophin and dystrophin and the identification of G-utrophin as homologue of the short dystrophin isoform Dp116 led to the search for other short utrophin isoforms corresponding to known dystrophin isoforms.

These investigations led to the identification of Up140 and Up71, potential homologues of Dp140 and Dp71, by Wilson et al. (1999) in the MRC Human Biochemical Genetics Unit labs. Both human and mouse sequences were recovered by 5' RACE.

Up140 mRNA is 6.75Kb long and has a unique first exon of 507 nt which is contiguous with exon 45 of full-length utrophin. Thus, the transcription initiation start site lies within intron 44. The Up140 unique sequence does not contain a translation initiation codon and the first conserved ATG lies in exon 47. This means that the 5' UTR of Up140 is long (886bp), a feature shared by Dp140. However, Dp140 and Up140 differ in that while the unique 5' sequence of Up140 lies immediately adjacent to the intron44/exon45 boundary, the unique 5' sequence of Dp140 lies at some distance upstream (not determined) within intron 44 (Lidov et al., 1995). The conceptual translation of Up140 from the conserved ATG predicts a protein of 147kDa comprising the last five spectrin

repeats and the cysteine-rich and COOH-terminal domains of utrophin (Fig 1.4). Thus, Up140 protein would have the potential to interact with β -dystroglycan, dystrobrevins and syntrophins.

RT-PCR using Up140 specific primers showed that this short mRNA is expressed in a range of tissues. mRNA levels are relatively high in foetal lung, brain and muscle and in adult lung, kidney and liver with some differences in intensities of amplified products between mouse and men (Table 1.2). Up140 was not abundant in adult skeletal muscle. Since this was only a semiquantitative PCR method it is difficult to judge the concentration of RNA in each preparation. However, the Up140 transcript was not detected on Northern blots from a variety of adult tissues (Blake et al., 1995; Lumeng et al., 1999), although G-utrophin 5.5Kb mRNA was seen.

Exon 71 of Up140 is alternatively spliced in a tissue specific manner (Wilson et al., 1999). The unspliced Up140 form is the major isoform in most tissues except for adult skeletal muscle where the spliced form predominates. This is an interesting observation because differential splicing of exon 71 in the dystrophin homologue Dp140 has also been described. The pattern of Dp140 is also tissue specific, for example, the spliced form is the most abundant form in cerebellum but the unspliced form is the predominant form in kidney. Dp140 is also differentially spliced for exon 78 but there is no evidence of splicing of Up140 exon 78.

The proximal promoter region of human Up140 is devoid of appropriately positioned TATA and CCAAT boxes. There are binding sites for the ubiquitous transcription factors Sp1 and AP1, four GATA motifs and binding sites for MEF-2, PIT1, an anterior pituitary enhancer, and two glucocorticoid response

elements (found in genes expressed in testis, ovaries and kidney). An E-box (MyoD/Myf binding site) such as the one found in the proximal promoter of full-length utrophin A, occurs near the transcriptional start site. Thus, the proximal promoter of Up140 appears to contain a mixture of binding sites for ubiquitous and tissue specific transcription factors, although thus far, this promoter has not been tested for biological activity.

A search of the literature reveals little evidence for translation of Up140. Peters et al. (1997) describe a polypeptide of the correct size, seen after affinity purification of skeletal muscle extracts and Lumeng et al. (1999) detected a similar 140kDa polypeptide in mouse adult testis and muscle (Table 1.2). A more thorough exploration of whether Up140 is translated or not was an objective of this thesis.

Up71 isoform A search for a utrophin homologue of dystrophin Dp71 led to the identification of a short transcript, designated Up71, in foetal brain (Wilson et al., 1999). Up71 mRNA has a unique first exon of 169 nt which is spliced to exon 63. This is the same structure as dystrophin. However, the novel 5' exon and presumably the proximal promoter of Up71 lies immediately adjacent to the intron/exon boundary whereas the first exon and promoter of Dp71 lie somewhere within intron 62 (Hugnot et al., 1992; Lederfein et al., 1992). The Up71 first exon encodes 5' UTR sequence and translation begins at a conserved ATG codon in the adjacent exon 63. Translation of the coding sequence predicts that Up71 contains the cysteine rich and carboxy terminal domains (Fig 1.4).

RT-PCRs using specific primers shows that Up71 mRNA is present in several adult and foetal tissues. There is little evidence of a tissue specificity in its distribution (Table 1.2) although amplification from adult skeletal muscle mRNA is relatively poor.

As in the case of Up140, exon 71 is alternatively spliced in a tissue specific manner – however in the case of Up71 the spliced form predominates in foetal brain and lung and the unspliced form in foetal muscle (Wilson et al., 1999). Thus, differential splicing of the short utrophin isoforms appears to be both tissue and isoform specific. The significance of the splicing of exon 71 in Up140 and Up71 is unknown; Wilson et al. (1999) noted that this exon lies in close proximity to the binding sites for dystrobrevin and syntrophin and thus splicing might have some implications for the interactions with those two proteins.

Wilson (thesis, 2000) made a limited investigation of the Up71 promoter. There are no TATA and CCAAT boxes although there is a CACCC box at -503. This latter element is known to be functionally important in the transcription of the β -globin gene for example (Mantovani et al., 1988). Two potential Sp1 binding sites, four GATA sites, four GCR elements, two c-Myb, two PIT1 sites, a CREB site and an E-box were also identified on the basis of sequence comparison with a transcription factors database (Wilson, thesis 2000). Thus, the promoter of Up71 contains a mixture of ubiquitous and tissue specific factors pointing to a widespread pattern of expression with some tissue specific variations. However, this promoter has not been investigated for biological activity.

Polypeptides of a size appropriate for Up71 have been described in peripheral nerve (Fabbrizio et al., 1995), blood-vessels (Rivier et al., 1997) and brain (Lumeng et al., 1999), (Table 1.2) – however, a comprehensive examination of the pattern of Up71 translation has not been undertaken thus far.

In summary, one short NH₂-terminal and three short COOH-terminal utrophin isoforms exist, N-utrophin, G-utrophin, Up140 and Up71. Studies at the mRNA level indicate that N-utrophin is confined to glial cells, G-utrophin to neuronal cells while Up140 and Up71 are more ubiquitously expressed. Investigation of the utrophins at the protein level has not been undertaken in a deliberate manner and therefore very little is known about their translation or about their possible functions.

The function of N-utrophin remains enigmatic, although, as mentioned earlier, it can bind F-actin *in vitro* (Zuellig et al., 2000). In addition, recombinant dystrophin sequences (encoding a protein fragment equivalent to N-utrophin) transfected into *mdx* muscle fibres have been shown to localise to the sarcolemma (Dunckley et al., 1994) and are able to interact *in vitro* with membrane phosphatidylserine via the rod domain repeat 2 (Dewolf et al., 1997). Thus, Zuellig et al. (2000) speculated that N-utrophin may be able to interact simultaneously with the actin cytoskeleton and with the cell membrane.

The three COOH-terminal forms encode the domains necessary for taking part in complex interactions with DAPs and potentially have a role in establishing specialised DAP complexes. For example G-utrophin in neurones could be complexed with syntrophin and take part in a signalling process via nNOS bound to syntrophin (Hashida-Okomura et al., 1999).

1. 9 Expression of utrophin mRNAs during embryonic development

The distribution of utrophin transcripts in foetal and adult tissues was investigated by Love et al. (1991) using slot blot and a probe corresponding to the 3' end of the utrophin cDNA. In general, utrophin mRNA was detected at higher levels in foetal (placenta, skeletal muscle, intestine, heart and liver) than in adult tissues (skeletal muscle, liver, heart and testis). However, the probe used would detect all utrophin transcripts and thus it is not clear whether full-length utrophin or short transcripts are detected in each tissue.

mRNA *in situ* hybridisation has been used to determine the distribution of utrophin transcripts in mouse embryos at different stages of development (Schofield et al., 1993). A probe designed from the 3' UTR was used and thus the utrophin detected could correspond to full-length utrophin mRNA, short transcripts or both. Utrophin transcripts are first detected at 8.5dpc in the most medial part of the neural groove. In the neural tube, utrophin mRNAs are abundant along its whole length at 9.5dpc but become restricted to the most caudal end by 12.5 dpc. Utrophin mRNAs distribution becomes broader as development proceeds. At 12.5 dpc utrophin mRNAs are abundant in cranial and spinal ganglia. By 14.5 dpc the highest levels of utrophin mRNA expression are found in the tendon primordia of the digits and utrophin mRNAs are also found in ossifying facial cartilages, choroid and stomach plexii, vibrissae, kidney and testis (Schofield et al., 1993), (developmental expression will be discussed in more detail in chapter 6).

Full-length dystrophin mRNA is less abundant than utrophin mRNAs in the mouse embryo (Houzelstein et al., 1992 and Schofield et al., 1993). Expression of DMD mRNA overlaps with that of utrophin mRNA in Rathke's

pocket and in the aortic region of the heart outflow. DMD mRNA is abundant in mesodermal derivatives such as developing cardiac and skeletal muscles. DMD mRNA is also found in smooth muscle, in the wall of the stomach and intestine, and in the CNS where it localises to the forebrain, cerebellum, hypothalamus.

1.10 Function of utrophin isoforms and animal models

As mentioned earlier, very little is known about the cellular roles of full-length utrophin and short isoforms. A promising source of information regarding these roles are the animal models of utrophin deficiency which are described below.

Utrophin knock-out mice (UKO^{ex6}) No naturally occurring diseases of man or mouse have been identified that result from mutations in the utrophin gene. This may not be surprising since such mutations would be inherited in an autosomal recessive way and would be very rare and may be expected to involve compound heterogeneity (with each of the affected alleles carrying a different mutation). In addition, it is not clear whether the utrophin gene shows the same propensity to deletions as dystrophin. This high frequency of deletions in the dystrophin gene is ascribed to the very large size of certain introns but clearly overall intron size is smaller in utrophin.

In order to investigate the functional significance of utrophin two mice were created carrying null mutations in exon 6 and in exon 64 (referred to throughout as UKO^{ex6} and UKO^{ex64} respectively, Deconinck et al., 1997a; Grady et al., 1997a). In both cases, the mice were created by insertional mutation and homologous recombination in embryonic stem cell lines.

As mentioned earlier, exon numbering in this thesis is based on the comparison with the dystrophin sequence. Deconinck et al. (1997a) describe the targeted exon of the UKO^{ex6} mouse as exon 7. In the present study, RT-PCR analysis of UKO^{ex6} tissues and sequencing of the amplified products show that the exon described as exon 6 in the dystrophin gene is the targeted exon. This discrepancy arises because the 5' UTR of utrophin A comprises sequence from two exons (Pearce et al., 1993) compared to the single exon in the DMD gene. Thus, the Oxford team have counted from the most 5' exon of utrophin A rather than using the standard dystrophin numbering. In this thesis I will retain the dystrophin exon numbering since this scheme is important for the comparative interpretation of the short utrophin isoforms.

The UKO^{ex6} mice were not expected to have altered expression of the short utrophin isoforms (although there was not direct evidence for this). For this reason, they were potentially an invaluable and crucial resource for the study of such isoforms.

Perhaps unexpectedly, UKO^{ex6} mice were reported to be within the normal range in size and appearance, which suggests that embryonic development proceeds normally. They feed well and gain weight after birth. The earliest reports (Deconinck et al., 1997a) indicated that the UKO^{ex6} mice were indistinguishable from wild-type mice and heterozygote littermates. There are no signs of abnormal breathing, locomotor behaviour and no indication of muscle weakness. UKO^{ex6} mice breed and reproduce as well as the control wild-type C57BL6/J strain which suggests that utrophin does not affect the smooth muscle function of the uterus (Deconinck et al., 1997a).

The inserted mutation leads to the skipping of the targeted exon in UKO^{ex6} tissues and the introduction of a premature stop codon in the adjacent exon. This in turn results in substantially reduced utrophin mRNA levels in UKO^{ex6} tissues compared to control mice.

Western blotting analysis of UKO^{ex6} tissues showed that in contrast to wild type mice and heterozygotes, full-length utrophin was completely absent in tissues where utrophin expression is normally high and histological examination of those tissues showed no obvious abnormalities. Levels of protein in urine were normal, indicative of proper glomerular filtration, and levels of muscle creatine kinase in the serum were also normal, indicating that there is no degeneration of cardiac or skeletal muscle (Deconinck et al., 1997a). The levels of full-length dystrophin, Dp71, α -sarcoglycan and β -dystroglycan protein were assessed in several tissues such as skeletal and cardiac muscle, brain, lung and kidney by immuno-histochemistry and Western blotting and were comparable to those found in wild type and heterozygotes littermates.

The absence of full-length utrophin at the NMJ was also demonstrated immuno-histochemically. In contrast to mice deficient for dystrophin (*mdx*), the synaptic levels of α -sarcoglycan and β -dystroglycan were not reduced nor was the AChR-associated protein rapsyn.

Nonetheless, two abnormalities are apparent at the NMJ in these knock-out mice; a reduction in the number of AChRs and in the number of folds at the post-synaptic membrane. These features are probably related; the AChRs are concentrated in the region of the folds of the post-synaptic membrane closest to the extracellular space and a reduction in the number of folds will reduce the amount of space available to accommodate AChRs (Deconinck et al., 1997a).

Synaptic function in UKO^{ex6} mice is normal except for a reduction of the post-synaptic current in some muscles (Deconinck et al., 1997a). This is in striking contrast to the ablation of several other post-synaptic molecules including rapsyn (Gautam et al., 1995) agrin (Gautam et al., 1995) and MuSK (DeChiara et al., 1996) where there is a failure in both synaptogenesis and specialisation of the postsynaptic membrane.

The expression of short utrophin isoforms was not deliberately examined in these first studies of UKO^{ex6} mice, thus, left open the possibility that short utrophin isoforms may be influencing the UKO^{ex6} mice phenotype.

Utrophin knock-out mice (UKO^{ex64}) Simultaneous to the publication of the UKO^{ex6} mice, a group in St.Louis (Grady et al., 1997a) reported the generation of a second utrophin null mice. In this case, the insertional mutation was in exon 64 in a position corresponding to the beginning of the cysteine-rich domain.

RT-PCR of mRNA from UKO^{ex64} tissue showed that the mutated RNA was deleted for the targeted exon 64 and for the preceding exon 63. This deletion leads to a frameshift and introduces a stop codon 1.7Kb upstream of the wild type stop codon. In theory, such mutated transcript could encode a truncated utrophin protein lacking the cysteine-rich and COOH domains. However, Western blotting of UKO^{ex64} tissue extracts failed to detect such a protein. No reference was made to the presence/absence of short utrophin isoforms in these mice (Grady et al., 1997a). The expectation is that the synthesis of all isoforms would be disrupted.

Despite the likely absence of all utrophin forms, the UKO^{ex64} mice develop normally and are fertile, show no behavioural, motor or cardiorespiratory abnormalities, urinary function is normal and their blood-brain barrier seems intact. It is reported that UKO^{ex64} females bear normal size litters and raise them appropriately (Grady et al., 1997a). Sections of various tissues from heterozygotes and homozygotes UKO^{ex64} mice were analysed by immunohistochemistry using a combination of NH₂- and COOH-terminal utrophin specific antibodies. No utrophin immunoreactivity was seen in any of the homozygous UKO^{ex64} tissues tested although heterozygotes expressed utrophin indistinguishably from controls.

UKO^{ex64} mice show the same general phenotype as the UKO^{ex6} mice with a reduction in the folding of the postsynaptic membrane and in the density of AChR at the NMJ. The members of the synaptic DAP complex appear to be normally distributed in UKO^{ex64} NMJ as well as in the lung.

The lack of apparent phenotype in both strains of utrophin null mice led to the proposal that dystrophin and utrophin have complementary roles and that dystrophin can compensate for the lack of utrophin. Grady et al. (1997a) looked for dystrophin in tissues that normally express abundant utrophin such as lung and kidney and did not find evidence for increased expression.

Nevertheless, this hypothesis was tested more rigorously by both the Oxford and the St.Louis teams with the generation of mice deficient for both utrophin and dystrophin.

Utrophin-dystrophin doubly deficient mice (dko^{ex6}, dko^{ex64}) Doubly (utrophin and dystrophin) deficient mouse were generated by crossing female

mdx mice with male utrophin deficient mice (either UKO^{ex6} or UKO^{ex64}) (Deconinck et al., 1997b; Grady et al., 1997b). The resulting F1 offspring were further interbred to produce homozygous dko. Both types of dko mice have a remarkably more severe phenotype than either of the single knock-outs and show many of the clinical features of DMD patients; short stature, weight loss, joint contractures, kyphosis, muscle weakness, lack of motility, abnormal breathing pattern and abnormal field behaviour. All mice succumb to a premature death by 20 weeks and respiratory failure is the most likely cause (Deconinck et al., 1997b; Grady et al., 1997b). Histological comparison of muscle sections (diaphragm, tibialis anterioris, gastrocnemius, quadriceps, soleus, extensor digitorum longus and paraspinal muscles) from *mdx* and dko littermates reveals that the onset of the dystrophic phenotype is earlier in dko mice, 6 days after birth, than in *mdx* mice, around 3-4 weeks of age, corresponding to the time when utrophin expression disappears from the sarcolemma (Deconinck et al., 1997b). By 6 days, there are large areas of necrosis with accumulation of connective tissue and little or no signs of regeneration. Muscle regeneration was first evident at two weeks of age but the pathology progresses such that by ten weeks there is severe muscle degeneration and fibrosis (Deconinck et al., 1997b; Grady et al., 1997b). There is virtually no folding of the postsynaptic membrane at the NMJ in these mice.

The dko muscle fibres show a pattern of protein expression typical of developing muscle (Deconinck N. et al., 1998), with the loss of fast fibre type differentiation. There was a shift towards slower MHC isoforms in extensor digitorum longus and diaphragm muscles (Deconinck N. et al., 1998) compared with these muscles from *mdx* littermates, and all fibres stained evenly for the

mitochondrial enzyme NADH-tetrazolium reductase in contrast to C57Bl and *mdx* muscle sections which showed the characteristic “patchwork” pattern of normal muscles, oxidative (slow type I) and glycolytic (fast, type II), (Rafael et al., 2000).

There are few differences, if any, between the *dko*^{ex6} and *dko*^{ex64} mice. However, a cardiomyopathy was detected in *dko*^{ex64} that is not seen in *dko*^{ex6}. This takes the form of an abnormal electrocardiogram associated with a decrease in neuronal nitric oxide synthase and an increase in induced nitric oxide synthase (iNOS) in the cardiac muscle of these mice (Bia et al., 1999).

dko mice also confirmed that the sparing of the extraocular muscles in *mdx* mice is due to the protective effect of utrophin. It had been recognised that in the absence of dystrophin, utrophin is present at threefold normal levels in extraocular muscles and that these are the only *mdx* skeletal muscles unaffected by dystrophic changes; in contrast, when both dystrophin and utrophin are absent, as in *dko* mice, severe pathological changes are seen in these muscles (Porter et al., 1998). Using this observation, it could be argued that perhaps utrophin attenuates the severity of the dystrophy more generally in *mdx* mice and by analogy in DMD muscle.

The strain of *mdx* mice used to produce the *dko* mice has normal expression of the COOH-terminal isoforms of dystrophin. To test whether such isoforms were upregulated in *dko* non-muscle tissues, Deconinck et al. (1997b) analysed lung and brain extracts with antibodies against the COOH-terminus of dystrophin and found some indication that Dp71 was upregulated in *dko*^{ex6} compared to wild type or *mdx* or UKO^{ex6}. Thus, this suggests that short dystrophins might be compensating for the absence of the full-length isoforms

of utrophin and dystrophin. To investigate this further, UKO^{ex6} were mated into a *mdx*^{3CV} background to produce UKO^{ex6}; *mdx*^{3CV} mice (deficient for full-length utrophin and all dystrophins) (Rafael et al., 1999). These mice developed the same clinical features as dko mice and these were not increased in severity. The histological picture was identical to the dko^{ex6} mice. This could be taken to indicate that short dystrophins do not play crucial roles in those tissues. However, these mice do express short utrophin isoforms and it remains to be seen what the effects of the complete absence of all utrophin and dystrophin isoforms (by crossing UKO^{ex64} with *mdx*^{3CV} mice) would be.

1.11 DMD

Utrophin became the focus of research in the context of Duchenne Muscular Dystrophy because of its therapeutical potential in the treatment of this condition. In this section, an overview of the evidence which suggests that upregulation of the utrophin gene could compensate for the absence of dystrophin is given. However, before this evidence is reviewed, it seems appropriate to describe briefly the structural abnormalities/mutations of the dystrophin gene which lead to DMD/BMD and the alternative therapies which are being investigated.

DMD mutations Dystrophin associated muscular dystrophies range from the severe Duchenne, DMD, to the milder Becker dystrophy, BMD, with an incidence of 1 in 3500 and 1 in 18500 live male births respectively (Emery 1991). One third of the cases of DMD are caused by *de novo* mutations which are not detectable in the mother and there is no family history (Danieli et al., 1984). The large size of the DMD gene renders it particularly susceptible to recombination, inaccuracies in replication and mutation and explains the high mutation rate. Deletions of one or more exons occur in 60-65% of DMD/BMD patients (Read et al., 1988; Bushby et al., 1999). 6% of patients show duplications of exons and the remainder show small mutations (Hu X. et al., 1990). There is no correlation between the extent of the deletion and the severity of disease (Davies et al., 1988; England et al., 1990). For example, a family was reported

to carry a deletion that spanned 700Kb of the DMD locus including 46% of the coding sequence (England et al., 1990). Members of this family were however only mildly affected and included a man of 61 still ambulant. The reason for this mild phenotype appeared to be due to the retention of both the NH₂- and COOH-terminal domains of the protein which retain their function even though the majority of the rod domain was lost (England et al., 1990).

There is a correlation between the effect of the deletion on the reading frame of the mutated DMD transcript and the severity of the muscular dystrophy; DMD results when deletions lead to a frameshift and a premature termination of translation. In those cases where exons at either side of the deletion are spliced and retain the reading frame the milder phenotype of BMD results. In DMD no protein is produced; in BMD a shortened protein product may be seen (Liechti-Gallati et al., 1989; Koenig et al., 1989; Nicholson et al., 1993). There are additional differences in clinical presentation depending on whether in-frame deletions remove the NH₂-terminus, the rod domain or the COOH-terminus and depending on the amount and quality of the truncated protein produced (Beggs et al., 1991; Nicholson et al., 1993; Muntoni et al., 1994). Deletions which remove part or all of the NH₂-and COOH-terminal domains result in a more severe phenotype. Deletions around exons 45 to 59 are frequent amongst typical BMD cases (Beggs et al., 1991; Bushby et al., 1993).

The most distinctive feature of DMD is a progressive proximal muscular dystrophy with characteristic pseudohypertrophy of the calves. In muscle biopsies of DMD individuals there is myofibre degeneration with fibrosis and fat infiltration and their blood shows a marked elevation of creatine kinase levels.

To give an idea of the typical progression of DMD I will cite the study of Boland et al. (1996) who analysed a cohort of 33 male patients. The mean age at DMD diagnosis was 4 years; wheelchair dependency emerged at a median age of 10 years; cardiac muscle failure developed in 15% of patients at c. 21 years and was seen in almost 95% of cases by the last years of life; smooth muscle dysfunction in the digestive or urinary tract occurred in 21% and 6% of patients respectively at a median age of 15 years and death occurred at a median age of 17 years.

DMD: therapies Although at present there is no cure for DMD/BMD several avenues are being explored which might provide possible treatments, some of these remain at the stage of animal and experiments but in some cases clinical trials have been proposed.

Potential therapies were recently reviewed by Allamand and Campbell, (2000). One of these involves myoblast transfer from healthy donors to patients by injection into muscle. Initially, this was considered as a very promising approach, however, clinical trials showed limited success only, due to poor survival of the injected myoblasts as a result of inflammation (Partridge et al., 1998). This has not been abandoned entirely and some functional benefit has been achieved in immunosuppressed *mdx* mice (Brussee et al., 1999). Indeed, a Phase I clinical trial is underway, involving immunosuppressed patients, led by Dr. J.P. Tremblay group in Canada (Tremblay, 2000). Systemic introduction of bone marrow stem cells may offer a promising alternative to myoblasts; Gussoni et al. (1999) injected irradiated female *mdx* mice with bone marrow cells from normal mice; over a twelve-weeks period some of the

transplanted stem cells had been recruited to form muscle and expression of dystrophin was demonstrated. Multipotent muscle-derived stem cells and blood-born macrophages might constitute another source of muscle cell precursors (Torrente et al., 2001; Lescaudron et al., 1999).

The feasibility of gene replacement has been explored during the last ten years using the *mdx* mouse and more recently the dko mice as model systems (these experiments are reviewed in Rafael and Brown 2000). Studies have shown that overexpression of a full-length dystrophin in *mdx* mice prevents the development of the dystrophic changes (Cox et al., 1993a). The vector that is favoured for gene delivery is the adeno-associated virus (AAV), however AAV is limited by the size of insert DNA it can carry (c.5 Kb maximum). This difficulty has been largely overcome by designing mini-genes modelled on the structure of a dystrophin mRNA in mildly affected BMD patients. Some of these patients have very large deletions in which coding sequence for the majority of the central rod domain is removed (England et al., 1990). Expression of such truncated minigenes, controlled by a strong muscle promoter, prevents the development of dystrophic pathology in transgenic *mdx* and dko mice (Rafael et al., 1994, 1996, 2000 ; Wells et al., 1995).

Scientists at the University of Pittsburgh have recently injected AAV carrying a dystrophin minigene, directly into the calf muscles of *mdx* mice. This resulted in the expression of functional protein in almost 90% of the treated muscle tissue and expression has lasted at least one year (Wang B. et al., 2000). The use of AAV gene transfer is more advanced in the context of other muscular dystrophies such as limb-girdle muscular dystrophy, LGMD, because of the smaller size of their cDNAs; a phase I clinical trial using sarcoglycan

constructs is underway (encoding for the α -, β -, γ - and δ - isoforms) (Stedman et al., 2000).

Other therapeutic approaches are directed towards modifying the processing of the dystrophin pre-mRNA in order to obtain a dystrophin transcript that will be translated into a Becker-type protein and result in a mild clinical presentation. This alternative has been investigated using antisense oligoribonucleotides (Mann et al., 2001) and chimeric RNA-DNA oligonucleotides to induce skipping of the mutated exon. Using the latter technology, two recent reports demonstrated the rescue of dystrophin expression in *mdx* mice and in the dog model GRMD skeletal muscle (Bartlett et al., 2000; Rando et al., 2000).

For patients with nonsense mutations rather than deletions another approach holds some promise; aminoglycoside antibiotics such as gentamicin can be used to overcome a nonsense mutation allowing the translation machinery to read through the stop codon. Restoration of dystrophin levels to 10-20% of normal was achieved in *mdx* mice after subcutaneous injection of gentamicin (300ug/ml) (Barton-Davies 1999). This treatment could prove efficient in the 3-10% of DMD patients with nonsense mutations.

Upregulation of utrophin An alternative molecular genetic approach, which departs from strategies involving gene constructs in viral vectors, has been to consider the upregulation of utrophin as therapy. Therapies based on the introduction of a functional dystrophin gene have two major disadvantages. Firstly, exogenous dystrophin may elicit an immune response that could undermine the beneficial effects of the dystrophin transgene. In fact, antibodies

against dystrophin were detected as early as 10 days after inoculation of *mdx* mice muscle with a dystrophin transgene (Lochmüller et al., 1996). The second disadvantage refers to the inherent problems in gene therapy - that is efficiency of delivery and transduction and safety. In theory, these two problems could be circumvented if a protein that could functionally replace dystrophin and which is normally expressed in dystrophin deficient muscle was used instead. Could utrophin be this protein? Utrophin meets these criteria and several experimental findings support this idea.

Firstly, utrophin is not foreign to DMD patients and thus expression of exogenous utrophin will not result in inflammation. This has been demonstrated in a comparative study where injection of a utrophin minigene in AAV into immunocompetent *mdx* mice muscle resulted in a significantly greater transgene persistence (due to reduced inflammation) compared to a similar dystrophin minigene (Ebihara et al., 2000).

Secondly, utrophin and dystrophin have significant structural and functional similarities. Utrophin can bind F-actin and associates with DAPs in a similar way to dystrophin at the sarcolemma and therefore is able to provide the link between the muscle fibre cytoskeleton and the ECM which gives the cell mechanical protection (Campbell et al., 1989; Winder et al., 1995; Matsumura et al., 1992).

Thirdly, in foetal skeletal muscle and in regenerating and mature fibres of disease muscle (DMD, BMD, polymyositis, dermatomyositis and severe childhood autosomal recessive, Duchenne like muscular dystrophy, SCARM) utrophin is upregulated and redistributed to the sarcolemma (Helliwell et al., 1992; Khurana et al., 1991; Tanaka et al., 1991; Karpati et al., 1993; Matsumura

et al., 1992; Sewry et al., 1994b; Taylor et al., 1997). It has been proposed that utrophin expression in dystrophin deficient muscle is due to failure to down-regulate utrophin after birth or to the activation of a foetal pattern of gene expression associated with fibre regeneration. However, there is evidence that utrophin is expressed in DMD/BMD mature fibres that do not express foetal myosin and that expression of utrophin increases with the age of the patient; these observations indicate that upregulation of utrophin is a specific response to the loss of dystrophin although the mechanism is not yet known (Taylor et al., 1997). Clearly, in DMD patients the endogenous upregulation of utrophin is not sufficient to prevent necrosis but it may lessen the extent of the damage at least in small calibre fibres and extraocular muscle since these show minimal pathological changes in DMD and *mdx* muscles (Matsumura et al., 1992; Khurana et al., 1995a).

Finally, amongst gene families there are many examples where different members can successfully compensate for the absence of each other. This is the case amongst the mouse engrailed genes (*En*) which are key regulators of neural development. In *En-1* mutant mice, expression of a transgene containing *En-2* sequences, under the control of the *En-1* promoter, rescues the phenotype (Hanks et al., 1995). There is evidence that *Myf-5* substitutes for the absence of *MyoD* during myogenesis in the *MyoD* null mice; in these mice, *Myf-5* levels were four fold higher than in normal circumstances (Rudnicki et al., 1992, 1995).

There is a growing body of evidence that utrophin protects the dystrophin deficient fibre. Transgenic expression of full-length utrophin and mini-gene constructs in *mdx* mice (Tinsley et al., 1996, 1998).

leads to a significant decrease in the dystrophic muscle phenotype. In both cases expression of the transgene decreased the level of muscle creatine kinase in serum, led to a decrease in the observed number of centralised nuclei fibres and restored all the components of the DAP complex at the sarcolemma. This was true even for the diaphragm which is the most severely affected muscle group in *mdx* mice. Physiological parameters such as force generation were also improved (Deconinck N. et al., 1997; Tinsley et al., 1998). These studies clearly showed that at least in mice, utrophin is able to functionally replace dystrophin. The extent of the recovery as judged by a series of mechanical and histological parameters was larger when the full-length utrophin transgene was used compared to the truncated transgene (Tinsley et al., 1996, 1998).

In addition, all of the DMD-like signs in *dko^{ex6}* mice (section 1.10) are prevented by the expression of the truncated utrophin in skeletal muscle (Rafael et al., 1998; Wakefield et al., 1998). There was no evidence of muscle weakness or kyphosis and the mice lived a normal life span. Utrophin was seen throughout the sarcolemma alongside a completely restored DAP complex. Expression of the utrophin transgene also prevented the abnormal expression of foetal muscle proteins seen in untreated *dko^{ex6}* mice.

Some progress has already been made using adeno-associated viral vectors (AAVs) to deliver high levels of utrophin to muscle. Gilbert et al. (1998) designed a AAV/utrophin vector containing the truncated utrophin transgene under the transcriptional control of the cytomegalovirus promoter (CMV). When this construct was used to inoculate *mdx* muscles, recombinant utrophin was expressed in the fibres near the site of injection, at levels markedly higher than

endogenous utrophin and localised to the sarcolemma restoring normal levels of DAPs. Because of the discrete localisation of exogenous utrophin at the immediate area of injection it is questionable whether this procedure will be useful in practice.

Ideally, it would be more attractive to achieve high levels of utrophin across the whole body musculature. One possibility is to use small molecules to regulate promoter activity. This approach has found some success in the upregulation of foetal haemoglobin in β -thalassaemia patients (Perrine et al., 1993; Rodgers et al., 1993) where compounds such as butyrate, 4-phenylbutyrate and hydroxyurea have been used. The molecular basis of their mode of action is not clear yet. It has been proposed that the butyrate compounds act by maintaining open chromatin formations by inhibiting histone deacetylases and thus facilitating transcription (Kruh et al., 1982). However, more recent work suggests that butyrate compounds exert their effect on the γ -globin gene expression via an intracellular signalling pathway involving soluble guanylate cyclase (sGC) and cGMP-dependent protein kinase (PKG), (Ikuta et al., 2001). The same compounds have been used to reactivate transcription of the FMR1 gene in lymphoblastoid cell lines from patients with Fragile X syndrome where expression of the FMR1 gene has been silenced by methylation (Chiurazzi et al., 1999). Furthermore, 4-phenylbutyrate has been approved for use in patients with cystic fibrosis to increase expression of the Δ F508 variant CFTR protein (Rubenstein et al., 1998).

There is some evidence to suggest that L-arginine and NO may induce high levels of utrophin in muscle. This appears to be due to NO acting as a signalling molecule to activate expression of foetal genes. During foetal life, the

foetal Krebs and urea cycles are attenuated (Harris, Crabb, 1997) and in this situation, L-arginine, which would normally be metabolised through these cycles, is diverted through the NOS pathway to yield NO, NADP⁺ and L-citrulline (L-arginine + NADPH = L-citrulline + NO + NADP⁺) leading to a higher level of NO in foetal tissues compared to adult tissues (Chaubourt et al., 1999, 2000).

A recent study pointed out a potential mechanism for endogenous upregulation of utrophin involving cytokines released during the immune response against an adenovirus vector carrying only reporter genes (Yamamoto et al., 2000). During a series of experiments carried out to assess the transduction efficiency of different AAV vectors in muscle, Yamamoto and colleagues (2000) found that *mdx* mice injected with the AAV vectors showed, unexpectedly, signs of muscle recovery associated with an increase in utrophin expression at the sarcolemma. This effect was abolished if the activity of CD4 T-lymphocytes was attenuated.

A large-scale search for small molecules that may upregulate utrophin is currently underway in collaboration with the Association Française contre les Myopathies (AFM).

In order to design an efficient strategy for the replacement of dystrophin it is important to know how much utrophin is needed to fully protect muscles from disease. It is difficult to estimate this value since the physiological differences between man and mouse mean that what is good for mice might be insufficient for humans. For example, the heart is not affected in *mdx* mice, in contrast to humans, and this is due to the 4 fold increase in utrophin expression in cardiac muscle (Matsumura et al., 1992). However, a similar 4 fold increase in hearts of

DMD patients is not sufficient to rescue the cardiac phenotype in those patients (Fanin et al., 1999). Quantitative analysis by immunoblot of the upregulation of utrophin which occurs naturally in DMD muscle showed a >10 fold increase in protein above normal levels (Karpati et al., 1993). However, such large increases may not be necessary. The recovery of the dystrophic *mdx* phenotype after introduction of the full-length utrophin transgene (Tinsley et al., 1998) largely depended on the amount of full-length utrophin expressed. In the utrophin transgenic experiments, one of the lines showed a two fold increase in utrophin and this was sufficient to give a normal muscle phenotype. Tinsley et al. (1998) estimated that in muscle, utrophin expression need only be induced to the normal levels found naturally in some non-muscle tissues such as kidney, to prevent muscular dystrophy.

Aims and Objectives

Several groups are currently assessing utrophin as a functional replacement for dystrophin in dystrophin deficient muscle (section 1.11), however, the description of this autosomal homologue of dystrophin is incomplete. In a collaborative work between my lab and Professor Kay Davies's group in Oxford a short isoform designated G-utrophin was identified and at the start of this project two other short isoforms Up71 and Up140 were isolated also in our lab. However, none of these short utrophin forms has been investigated in detail.

It is clear from the literature (reviewed in sections 1.8 and 1.9) that the data regarding the expression profiles of the known short utrophins, G-utrophin, Up140 and Up71, are unfinished and that there is considerable uncertainty about whether these mRNAs are translated. Consideration of the published information indicated that this omission could be partly ascribed to the focus on skeletal muscle and the comparison with dystrophin, but could also be attributable to lack of reliable/convenient antibodies and problems associated with protein degradation.

It is also of some interest to ask whether other short forms, additional to those already known, are transcribed from the utrophin gene. For example, an isoform, Dp260, is transcribed for the dystrophin gene (see section 1.5) which is apparently unique to dystrophin and has not been encountered for utrophin.

Thus, the overall aim of this thesis was to provide data on the mRNA expression profiles and protein distributions for each short isoform in differentiated and developing tissues and to search for as yet unidentified short isoforms. These objectives were greatly facilitated and prompted by the

generation of utrophin deficient mice and the establishment of a colony of these mice at UCL (gift from Prof. Kay Davies).

Aims:

1 Analysis of UKO^{ex6} mice; these mice are deficient for full-length utrophin but in theory might be expected to express the short isoforms. If this proved to be the case, the UKO^{ex6} mice would be a valuable resource to aid in the firm identification and characterisation of short isoforms.

2 To search for polypeptides corresponding to the known short transcripts, Up140, G-utrophin and Up71 by Western blotting. In order to achieve this aim it was crucial to raise a panel of utrophin-specific polyclonal antibodies.

3 To look for as yet unidentified novel forms. It was hoped that analysis of UKO^{ex6} tissues by Western blotting would unequivocally identify novel isoforms and that information on size would allow the isolation of the corresponding cDNAs using the strategy of 5' RACE.

4 To investigate the cellular and subcellular distribution of the short isoforms, in a few selected tissues by means of fluorescent immunohistochemistry using the new antibodies.

5 To examine the expression of the short utrophin transcripts during mouse development using UKO^{ex6} embryos and mRNA *in situ* hybridisation. For this purpose it was planned to generate a panel of riboprobes that would discriminate the short transcripts and tell us something about their distribution.

Chapter 2

Materials and Methods

2.1 Materials

Standard reagents Analar grade reagents were supplied by BDH/Merck, Fisons and Sigma.

Enzymes Restriction enzymes were supplied by Life Technologies (Gibco, BRL), Roche-Boehringer Mannheim and New England Biolabs. All other enzymes were obtained from Roche-Boehringer Mannheim and Life Technologies (Gibco-BRL) with the exception of Taq polymerase from Advanced Biotechnologies, Sequenase and Thermo Sequenase from Amersham Pharmacia Biotech.

Electrophoresis reagents Agarose was supplied by Life Technologies. Acrylamide from BIO-RAD was used and TEMED and ammonium Persulphate from Merck-BDH.

Miscellaneous All dNTPs and random hexamers were supplied by Amersham Pharmacia Biotech. DNA preparation, gel extraction and PCR clean up kits came from Qiagen. Tween 20, Ponceau S and antibiotics were from Sigma. RNase inhibitor was from Boehringer Mannheim and RNAzol B from Biogenesis. Hybond-N, Hybond-ECL, [α ³²PdCTP], ³³P and ³⁵S were supplied by ICN.

The 1Kb DNA marker used to size DNA fragments in agarose gels was from Life Technologies. Protein markers used to size polypeptides in Western blots were obtained from Life Technologies, New England Biolabs, BIO-RAD and Boehringer Mannheim. ECL Western blotting detection reagents were

obtained from Amersham Pharmacia Biotech. Second antibody anti-mouse and anti-rabbit immunoglobulins were obtained from DAKO.

Common Buffers

100xDenhardt's: 2% ficoll, 2% polyvinylpyrrolidone, 2% BSA

10 X PBS (pH 7.4): 1.37M NaCl, 17mM KH₂PO₄, 100mM Na₂HPO₄, 27mM KCl.

10 X TBS (pH 7.5): 150mM NaCl, 50mM Tris-HCl

'Phenol': refers to phenol equilibrated with TE, pH7.5

'Polyacrylamide': refers to a 37.5:1 mixture of acrylamide and bis-acrylamide (BIO-RAD) for SDS electrophoresis. A 19:1 mixture of acrylamide and bis-acrylamide (BIO-RAD)

PSM: 100mM NaCl, 8mM MgSO₄, 50mM Tris-HCl, pH7.5 with citric acid, 2% gelatin.

10xTBE: 890mM Tris-HCl, 890mM boric acid, 20mM EDTA.

1xTE: 10mM Tris-HCl and 1mM EDTA, pH7.5

10 x NTE: 1M Tris-HCl, 0.5M EDTA, pH7.5

20 x SSC: 3M NaCl, 0.3M sodium citrate, pH7

Microbiology media Tryptone, Yeast Extract and Bacto agar were all from Difco

L-broth (per litre): 10g Tryptone, 5g Yeast Extract, 5g NaCl, 2g glucose

L-agar (per litre): as L-broth plus 14g Bacto agar and without glucose

L-agarose (per litre): as L-broth plus 7g agarose and without glucose

LM-broth (per litre): 10g tryptone, 5g yeast extract, 5g NaCl, 2g MgSO₄.7H₂O

LM-agarose (per litre): as LM-broth with 7g agarose added.

LM-agar (per litre): as LM-broth with 14g Bacto agar

2YT-broth (per litre): 16g tryptone, 10 g yeast extract, 5g NaCl

Ampicillin: working concentration is 10ug/ml

Bacterial strains

LE392 (host for λ -DASH) grown in LM-broth with 0.2% maltose

DH5- α (host for puc19 and pAMP)

BL21 (host for pGEX)

2.2 Methods

All solutions for nucleic work were sterilised by autoclaving (15psi, 121°C for 20-25 minutes) or by filter sterilisation (through 0.22 μ m pore size 'Acrodisc' filters, Gelman Sciences). Glassware was also sterilised by autoclaving. For RNA work, water, glassware and where possible, reagents were treated overnight with 0.1% diethylpyrocarbonate (DEPC) at 37°C before autoclaving. All autoradiography was carried out by exposure of MR-1 X-ray film (Kodak), at room temperature for ^{33}P and with an intensifying screen at -70°C for ^{32}P . Disposable gloves were worn for all experiments.

DNA precipitation and assay of concentration DNA precipitations were routinely performed by the addition of 3M sodium acetate, pH5.5 to a final concentration of 0.3M and 2 volumes of 100% ethanol before chilling overnight at -20°C. Precipitated DNA was recovered by centrifugation at 16,000g (14,000 rpm in an eppendorf 5402 centrifuge) at 4°C and washed in 70% (v/v) ethanol before air drying and resuspending in double distilled water or TE. DNA was quantified by measurement of absorbance at 260nm; 1OD unit is 50 μgml^{-1} (the ratio of OD₂₆₀/OD₂₈₀ should be 1.8 for pure DNA).

RNA precipitation and assay of concentration RNA precipitations were performed as for DNA but using solutions prepared for RNA use only, 2.5

volumes of 100% ethanol and the RNA was resuspended in 5mM Tris-HCl pH=8, 1mM EDTA. RNA was quantified by measurement of absorbance at 260nm; 1OD unit is 40 μ gml⁻¹ (the ratio of OD₂₆₀/OD₂₈₀ should be > 1.7 for pure RNA).

Restriction enzyme digests: Digests were performed using the incubation buffers provided and according to the conditions recommended by the manufacturers. In most cases incubation took place in a water bath at 37°C.

DNA Ligations

Ligation of insert to pGEX DNA RT-PCR products and pGEX DNA were digested with the appropriate pair of restriction enzymes (section 3.2) and ethanol precipitated. An aliquot of the digested and purified DNAs was visualized with ethidium bromide and an appropriate ratio of vector DNA to RT-PCR products were ligated o/n at 16° C using T4 DNA ligase in a 20ul volume.

Ligation of insert to pAMP DNA The pAMP vector was used together with the CLONEAMP® (Life Technologies) system for rapid directional cloning of PCR products using uracil DNA glycosylase (UDG) according to manufacturer's instructions. In this system, primers for RT-PCR are designed to include deoxy-UMP residues at their 5' end. After amplification, the PCR products (10 to 50 ng) are treated with 1 U of UDG at 37 °C in a water bath for 30 min; this disrupts base pairing and exposes 3' overhangs which anneal to complementary ends in the pAMP vector.

Transformation of competent cells

Transformation of BL21 cells An individual colony was picked from an L-agar plate and grown o/n at 37 °C in 10ml of 2YT medium with shaking. Next day, 40 ml of 2YT medium were inoculated with 1ml of the o/n culture and

grown at 37 °C for 2 hr or until the OD₆₀₀ of the culture reached 0.6. The cells were harvested by centrifugation at 500g for 5 min at rt (room temperature) and gently resuspended in 20 ml of ice-cold, freshly prepared and sterilised by filtering 100mM CaCl₂ in 10mM Tris/HCl pH 7.5. The cell suspension was left to stand on ice for 20 min, spun down as before and finally resuspended in 4ml of the CaCl₂ solution and kept at 4 °C until use and discarded after 48 hrs.

Transformation of competent DH5α cells. 2ul of ligation reaction (see above "ligation of insert into pAMP DNA") were mixed with 100ul of competent DH5α cells (LifeTechnologies) and incubated on ice for 30 min. Cells were then heat shocked for 30 sec at 37 °C, placed back on ice for 2 min, resuspended in 300ul of LB and incubated with shaking at 37°C for 1 hr. After this time, transformed cells were spread on an L-agar plate with ampicillin and grown o/n at 37°C.

Plasmid DNA preparation Plasmid DNA was prepared using the Maxiprep (200 ml cultures and a yield of 200-500ug) or Miniprep (3ml cultures and yield of 15-30ug) kits from Qiagen following manufacturer's instructions.

Agarose gel electrophoresis and recovery of DNA fragments DNA fragments were resolved in 0.5-2% agarose gels, which were poured and run in a 1x TBE buffer solution and cast in an 18x10cm or 4x11cm flatbed moulds. Gels were routinely run at 10Vcm⁻¹. DNA fragments were visualised by ethidium bromide staining (at a concentration of 100ngml⁻¹ in both the gel and buffer) and ultra-violet transillumination. DNA fragments required for cloning or sequencing were excised from the agarose gel and purified using the QIAquick gel extraction kit or for the purification of PCR products, the QIAquick PCR purification kit was also used.

Isolation of RNA

All equipment used in this procedure was rinsed in 0.1% DEPC water and all reagents DEPC-treated and sterilised by autoclaving where possible. Typical concentrations of extracted RNA from tissues were 5-8mgml⁻¹. RNA was extracted from human and mouse adult and foetal tissues using RNazol B (Biogenesis), a solution containing guanidium thiocyanate and Phenol, using the procedure described by the manufacturer. The method involves the grinding of the tissue under liquid nitrogen and homogenisation in either hand operated glass homogeniser or an electric Silverson homogeniser using a sterile 1cm diameter grinder (Silverson, Ltd UK). 2mls of RNazol B was used for each 100mg tissue, extraction with 0.1% volume chloroform to each volume of homogenate, precipitation of the aqueous phase with one volume of isopropanol, centrifugation to collect the precipitate and washing with 75% ethanol. The RNA was re-suspended in 5mM Tris-HCl, 1mM EDTA pH8.

Preparation of cDNA by reverse transcription and RT-PCR

All procedures were carried out on ice. First strand cDNA was prepared from RNA using Life Technologies M-MLV reverse transcriptase enzyme. 5µg of total RNA was mixed with 7µl of 5x reverse transcriptase buffer (0.25M Tris-HCl pH8.3, 0.375M KCl, 15mM MgCl₂), 3.5µl 0.1 M DTT (both supplied by Life Technologies), 2µl 20mM dNTPs, 50pmoles random hexamer primers, 1µl (10 units ml⁻¹) RNase inhibitor and the volume made up to 33µl with DEPC-treated water. The mix was heated at 65°C for 10 minutes, placed on ice and 2µl of reverse transcriptase added. The reaction was incubated at 42°C for 90 minutes. Samples were stored at -20°C.

RT-PCR was performed using 3-5µl of the first strand cDNA.

Amplification reactions utilised *Taq* enzyme with 10x Buffer V (100mM Tris-HCl

pH 8.8, 500mM KCl, 15mM MgCl₂ and 1% Triton-X 100; supplied by Advanced Technologies). cDNA was amplified by PCR in a 50 µl reaction volume containing 1x Buffer V, 0.5µl 5mM dNTPs, 25pmoles of both forward and reverse primers and 2.5 units (U) of *Taq* enzyme. The reaction was heated to 94°C for 5 minutes and amplified under conditions calculated for each primer. The annealing temperature for each PCR amplification was worked out using the formula.

$$T_m = 69.3 + 0.41(\% \text{ G+C}) - 650/\text{length of the primer.}$$

The T_m used for each amplification is the average of the T_m for the forward and reverse primers minus 5°C. All RT-PCRs were amplified using a Phoenix thermal cycler with heated lid (HelenaBioSciences) using the following program: Denaturing step (94°C, 30sec), annealing step (T_m -5°C, 30sec), extension step (72°C, 45secs), final extension step (72°C, 4 min).

RT-PCR primers used to amplify exons in the 5' region of utrophin cDNA are listed in Table 2.1; those used for the production of the Mupa antibodies in Table 2.2; primers used in Up109 specific RT-PCRs in Table 2.4 and finally, primers used to generate riboprobes in Table 2.5.

Primer	Sequence	T_m
UT2-F	5'-CTGATGAACACAATGATGTACAG-3'	52°C
UT4-F	5'-AAACAATGTCAACCGAGTGC-3'	55°C
UT8-F	5'-TCAGCAAGTCACGATAGATGCC-3'	55°C
UT5-R	5'-CCTCCAATATTCACCAAGTCC -3'	53°C
UT8-R	5'-AAGCACCTCAAACAGAGACG-3'	55°C
UT12-R	5'-TTCTGCAGCTCCATCAGAGCG-3'	56°C
UT15-R	5'-TCCAAAGCCTCTTCCTTTTCGG-3'	55°C

Table 2.1 Primer pairs used to carry out RT-PCRs at the 5' of the utrophin cDNA and referred to in chapter 5, Figs 5.10 and 5.11.

RNA formaldehyde-agarose gels

All the equipment was kept for RNA use only and treated with 0.1% DEPC and the reagents were prepared using DEPC treated H₂O. Gels for RNA were prepared and run using MOPS buffer (20mM MOPS, 5mM NaAc3H₂O, 1mM EDTA). 1% agarose gels with 17% formaldehyde were run. RNA preparations were mixed with 5 volumes of RNA loading buffer (53% formamide (v/v), 17% formaldehyde (v/v), 7% glycerol, 20mM MOPS, 5mM NaAc3H₂O, 1mM EDTA and bromophenol blue) and heated in a 65 °C water bath for 10 min before being loaded in the gel. RNA was visualised with ethidium bromide (1mg/ml).

DNA sequencing

PCR products and pUC19, pAMP and pGEX cloned fragments were sequenced using dideoxynucleotide chain-termination (Sanger *et al.*, 1977) using either the Advanced Biosystems dye terminator cycle sequencing kit, or the Amersham Pharmacia Biotech Thermo Sequenase radiolabelled terminator cycle sequencing kit, both according to the manufacturers instructions. Details of primers used for sequencing are given in Tables 2.2, 2.4 and 2.5. In brief, DNA fragments were synthesised using Amplitaq (for fluorescent sequencing) or Thermosequenase DNA polymerase (for radioactive sequencing), a denatured double stranded template (50-500ng of the DNA to be sequenced) and a primer to initiate the reaction. The reaction terminates with the incorporation of a chain-terminating dideoxynucleoside triphosphate, which is either ³³P- labelled or fluorescently- labelled.

Radioactive sequencing

Radioactive sequencing was carried out using the Thermo Sequenase radio-labelled terminator cycle sequencing kit (Amersham Pharmacia Biotech) following manufacturer's instructions. The reactions were carried out in a Phoenix thermocycler using the following

conditions and 40 sequencing cycles: Denaturing step (95°C, 30 seconds), annealing step (T_m of primer, 30 seconds), extension step (72°C, 60 seconds)

At the end of the sequencing reaction, 4µl of stop solution (95% formamide, 20mM EDTA, 0.05% bromophenol blue, 0.05% xylene cyanol FF) was added to the reactions.

Electrophoresis was carried out using BIO-RAD sequencing apparatus. Radiolabelled fragments were run on a denaturing polyacrylamide gel (8% 19:1 acrylamide/bisacrylamide) containing 6M urea and polymerised with 1.7% (v/v) TEMED and 25% (w/v) ammonium persulphate. After polymerisation, the gel was warmed to 40-50°C. Samples were denatured at 80°C for five minutes prior to loading and routinely 2µl of the sample was loaded using a 48- well shark's tooth comb. The sequencing gel was electrophoresed at a constant 50°C (40-50W) in 1x TBE buffer. The gel was transferred to 3mm Whatmann paper and dried in an 80°C oven for 45-60 minutes. The gel was exposed to X-ray film for between 12-48 hours, at rt.

Fluorescent sequencing DNA was sequenced using BigDye™ and D-Rhodamine™ fluorescently labelled terminators, provided with the Advanced Biosystems dye terminator cycle sequencing ready reaction mix kit. Cycling was performed on a Phoenix Thermocycler machine using the following conditions and 25 cycles of sequencing: Denaturing step (96°C, 30 seconds), annealing step (T_m of primer, 15 seconds), extension step (60°C, four minutes).

Fluorescently labelled fragments were electrophoresed on the ABI377 automatic DNA sequencer (Advanced Biosystems) at 30W and 45°C for 12 hours. Data was collected using 377collection software and analysed using

Sequencing Analysis version 3.0 and sequence navigator version 1.0.1 software.

Preparation and analysis of proteins

Protein extraction All equipment used in this procedure was sterilised by autoclaving where possible. All human and mouse adult and foetal tissues were ground using a pestle and mortar under liquid nitrogen. Protein was extracted using protein extraction buffer (SDS 10% (w/v), EDTA 10% (w/v), glycerol 5% (v/v), 5% β -mercaptoethanol (v/v) and 50mM Tris-HCl pH 6.8) by homogenisation of the tissue in either hand operated glass homogeniser or an electric Silverson homogeniser using a sterile 1cm diameter grinder (Silverson, Ltd UK). 1ml of protein extraction buffer was used for each 100mg tissue. After homogenisation each sample was boiled (100°C) for two minutes, snapped cooled on ice before centrifugation at 13000g for 30 minutes. The supernatants were stored at -70°C until use (not longer than two weeks).

SDS-PAGE was carried out in a vertical slab electrophoresis unit (16 cm long, 18 cm wide, Hoefer, Amersham Pharmacia Biotech) using the discontinuous Tris-Cl/ Tris-glycine buffer system of Laemmli (1970). Protein extracts (50 μ g of protein were routinely analysed on Western blots, chapter 4) were mixed with four volumes of SDS loading buffer (20% glycerol, 2% SDS, 5% β -mercaptoethanol, 0.05% bromophenol blue in the stacking gel buffer), heated at 100°C for 4 minutes and electrophoresed in 5-15% gradient Tris-glycine/SDS gel, for 16 hours at 60V in running buffer (25mM Tris, 195mM glycine and 0.5% SDS). The gels were then stained for protein with Coomassie Brilliant Blue (0.2% in 10% acetic acid) and destained in 10% (v/v) acetic acid and 10% (v/v) methanol.

Production of Mupa antibodies The production of the Mupa utrophin-specific antibodies is described in detail in chapter 3. The utrophin fusion proteins were synthesised (primers used are listed in Table 2.2) using the pGEX-4T-1 vector and the GST Gene Fusion System (Amersham Pharmacia Biotech).

Small scale preparation of GSTutrn fusion proteins Positive recombinants were maintained and propagated in BL21 cells on streaking L-agar plates with ampicillin. Individual colonies were grown in 2 ml of 2YT medium with ampicillin for approximately two hours at 32-35 °C, until they reached an optical density (OD) of 0.6 at 600nm, with shaking (200rpm). At this stage, isopropyl- β -D-galactoside (IPTG, Amersham Pharmacia Biotech) was added to a final concentration of 0.1mM, to induce protein synthesis, and cultures were grown for 1.5 further hrs. After this time, the cultures were collected in a 1.5ml eppendorf tube, centrifuged at 14000 rpm (14K) in a microcentrifuge for 5 sec and the cells were resuspended in 300ul of 1x PBS. An aliquot was removed for analysis, fraction A (see Fig 3.5 and Fig 3.10).

The cells were then disrupted by sonication (Soniprep, SANYO) on ice using repetitive bursts of 5 sec (5 μ m amplitude) and the pellet which consists of cell debris and insoluble proteins was discarded after keeping a small aliquot for analysis (fraction B) (see Fig 3.5 and 3.10). Glutathione-Sepharose 4B (Amersham Pharmacia Biotech) was then added to the supernatant and allowed to bind to the fusion proteins for 5min at rt. The unbound proteins were discarded after two short centrifugation steps. Reduced glutathione (Amersham Pharmacia Biotech) was then added and the samples were incubated for 5 min at rt, spun down at 14K for 3 min. The eluted fusion proteins were recovered in

Primer	Sequence	Tm	PCR Size
utr-1F utr-1R	5'-GGATCCAGATCTGATGAACACAATGATG-3' 5'-CTCGAGTTCCTCTAGCGCTATCTGGTAG-3'	60°C	890bp
utr-2F utr-2R	5'-GGATCCAAGGAACTAAGTGTCAGTGTCCG-3' 5'-CTCGAGGGTTTGTCCGTTTGATTGATTGAG-3'	60°C	575bp
utr-3F utr-3R	5'-GAATTCAAATCTGCTAGCATCAGGGCC-3' 5'-GCTGCTGAGATATCATCTTCC-3'	60°C	587bp
utr-4F utr-4R	5'-GAATTCCTTTTCTGGAAGAACAGCAAAG-3' 5'-CTCGAGAGATGCTGCCTGGTGGAACTG-3'	58°C	880bp
PGEX-F (s) PGEX-R (s)	5'-GGGCTGGCAAGCCACGTTTGGTG-3' 5'-CCGGGAGCTGCATGTGTCAGAGG-3'	60°C	

Table 2.2 Primer pairs used to RT-PCR amplify the utrophin sequences encoding the regions utr-1, 2, 3 and 4 used to raise the Mupa antibodies and referred to in chapter 3. (s)=PGEX-4T-1 vector specific sequencing primers.

the supernatant. The GSTutrn fusion proteins were analysed by SDS PAGE and Coomassie blue staining (see Figs 3.5 to 3.9).

Large scale preparation of GSTutrn fusion proteins and purification

Positive recombinants were grown in 2 ml of 2YT with ampicillin o/n at 37° C with shaking (200 rpm). Each of these cultures was diluted 1:100 in 200ml of 2YT medium with ampicillin and grown at 32° C, 200 rpm, for 3 hrs or until they reached an OD at 600nm of 0.6. After this time, IPTG was added to a final concentration of 0.1mM and protein synthesis was induced for 4 hrs at 32° C, 200 rpm. The cultures were then transferred to 200ml containers and the cells were harvested by centrifugation at 8K rpm for 10 min at 4 ° C. The supernatant was discarded and the cells were gently resuspended in 1x PBS (1 ml per 20 ml of initial culture).

Cells were thoroughly sonicated on ice in short repetitive bursts (10 sec each, 5µm amplitude,) to disrupt cells. After sonication, Triton X-100 (Sigma) was added to a final concentration of 1%, to aid to the solubilization of the fusion proteins and the bacterial sonicates were incubated with inversion for 30 min at rt. After this time, the cell debris and insoluble proteins were pelleted by centrifugation at 10K rpm for 10 min at 4 ° C. The supernatant was clarified by filtering through a 0.45µm sterile filter unit (Nunc). The filtrate was then ready to be applied to the column. A 500ul bed volume (to purify of 2.5ug of protein from 1l of starting culture) column was prepared from a 75% slurry of Glutathione-Sepharose 4B. The column (5 ml polystyrene disposable columns BIO-RAD) was carefully packed with the Sepharose to avoid trapping air bubbles, equilibrated with 1x PBS and kept at 4 °C upright until use.

The filtered supernatant was added to the column, run through and recycled twice. Unbound proteins were removed by washing three times with 5 ml of 1x PBS. After the washes 25 units (U) of thrombin protease (Amersham Pharmacia Biotech) were added to the column and allowed to enter the Sepharose bed. The bottom and top caps of the column were replaced and the column was incubated with thrombin o/n, approximately 16 hrs, at rt. The utrophin proteins (utrⁿ-1,-3 and -4), were eluted in 500ul of 1 x PBS, analysed by SDS PAGE and Coomassie blue staining and their concentrations determined spectrophotometrically.

Immunisations Immunisations and bleedings were carried out by UCL Biological Services staff following an approved protocol after consultation with UCL Biological Services Chief Veterinary. Briefly, 0.5ug of utrophin proteins were diluted in 1x PBS (to a final volume of 500 µl) and mixed with an equal volume of Freund's complete adjuvant (FCA, Sigma) for the first immunisation and Freund's incomplete adjuvant (FIA, Sigma) for the boosts. Rabbits were injected subcutaneously in four sites (250ul each) and 2ml samples, test bleeds, were collected for analysis from the marginal ear vein prior to each immunisation.

The immunisation protocol adopted was as follows: the first immunisation was followed by two boosts at 3 weeks and 6 weeks after the first injection. 14 days later a test bleed was collected for analysis and a third boost was injected two weeks later. The rabbits were rested for 10 days and anaesthetised and exsanguinated after that time (less than 12 w after first injection).

The sera from the test bleeds and the final bleed (c. 150ml) was separated as follows: the blood was initially clotted at 37°C for 30min-1hr and

then the clot was separated from the sides of the container and the blood was allowed to continue clotting o/n at 4 °C. The serum was then separated from the clot and any insoluble material was removed by centrifugation at 1000g for 10 min. The serum was recovered and stored at -20°C.

ELISA The immune responses to the utrn antigens were monitored using a standard enzyme-linked immunoabsorbent assay (ELISA) method. Briefly, the antigens, diluted to 10ug/ml in 0.1M sodium bicarbonate at pH 9.6, were bound to a 96 flat-bottom wells plate o/n at 4°C with end-to-end rocking (throughout the procedure). The plate was washed three times with PBST before adding 100ul of 1% BSA solution to each well to block non-specific interactions. Undiluted serum and a series of dilutions were tested; ½, ¼ to 1/32 and 1/64. The plate was incubated with 100ul of the serum dilutions per well for 2hr at rt, then washed vigorously (6 times) with PBST. Goat anti-rabbit IgGs (horseradish peroxidase (HRP) conjugated, DAKO) were added to the samples (100ul/well) and incubated for 1hr at rt. After washing with PBST (3 x), 100ul of the peroxidase substrate, o-phenylenediamine dihydrochloride (OPD, Sigma), were added to each well and incubated for 5-10 min until a yellow colour appeared. The colorimetric reaction was stopped with 10% sulphuric acid. The OD was read at 492nm on a Anthos plate reader 2001 (Anthos Labtec Instruments) and the data were corrected by subtracting from the samples readings the reading of control samples incubated with the second antibody only.

Isolation of immunoglobulins from serum 10 ml of serum were mixed with 1.4g of anhydrous sodium sulphate (Sigma), mixed vigorously and incubated at 37°C for 40 min, inverting occasionally to ensure that the sodium sulphate

remained in solution. The mixture was centrifuged at 5000rpm for 15 min at rt and the supernatant was discarded (keeping an aliquot for analysis). The pellet was resuspended in 5 ml of dH₂O and 0.7 g of sodium sulphate were added. The solution was mixed vigorously and incubated at 37°C for 40 min. The pellet was collected by centrifugation at 5K for 15 min at rt and dissolved in 2.5 ml of dH₂O. 0.35g of sodium sulphate were added and the sample processed as before. The final pellet which should contain c. 90% of IgG was dissolved in 10 ml of 1 X PBS. The yield of IgG was calculated spectrophotometrically.

Preparation of affinity columns Affinity columns were prepared by immobilising utrn- 1,-3 and -4 proteins to AminoLink® or SulfoLink® coupling gels (Pierce). Both gels consist of a cross-linked agarose matrix (4% for AminoLink® and 6% for SulfoLink®) but use a different coupling chemistry. The agarose support in AminoLink® gel has been activated to form aldehyde groups that will react with primary amines in proteins. Reductive amination of the resulting Schiff bases (using cyanoborohydride) results in a stable covalent bond between the agarose and the ligand protein. On the other hand, SulfoLink® coupling gel consists of an agarose matrix with an iodoacetyl group at its end which reacts with reduced sulphydryls in the protein ligand to form a covalent thioether bond.

Preparation of AminoLink® affinity columns 4 ml of degassed 50% slurry of AminoLink® gel were packed into a 5ml polystyrene column (Pierce), being careful not to trap air bubbles, and allowed to set. Porous discs (Pierce) were placed underneath and above the gel to prevent the gel from drying. The column was then equilibrated with 2.5 bed volumes (5 ml) of AminoLink® coupling buffer (0.1M sodium phosphate, 0.15M NaCl, pH 7.2) and the bottom

cap was placed. 10 mg of utrn-1 and -3, that had been previously dialysed against AminoLink® coupling buffer, were added to the column together with 40ul of 5M solution of sodium cyanoborohydride (Sigma). The top and bottom caps were placed and the column was incubated in a rotating shaker for 6 hrs at rt to allow the ligand to bind to the gel. After this time, the column was placed upright and washed with 5 ml of AminoLink® coupling buffer. Unoccupied binding sites were blocked with 1M Tris-HCl pH7.4 for 30 min at rt with rotation. The column was washed finally with 20 ml of 1M NaCl, filled with 0.05% sodium azide solution in dH₂O, the bottom and top caps replaced and stored upright at 4 °C until use.

Preparation of SulphoLink® affinity columns The sulphhydryl groups of GSTutrn-4 were reduced prior to immobilisation as follows: 10mg of GSTutrn-4 were applied to a polyacrylamide desalting column (Pierce) previously equilibrated with 0.1 M sodium phosphate and 5mM EDTA pH 6.0. The displaced buffer was discarded and GSTutrn-4 was eluted in 1ml fractions in 0.1 M sodium phosphate and 5mM EDTA pH 6.0. The protein content of the fractions was determined spectrophotometrically and the fractions containing GSTutrn-4 were selected and pooled. Dry 1,4-dithio-threitol (DTT) was added to the protein solution to a final concentration of 25mM. The tube was wrapped in aluminium foil and the mixture was incubated at 37°C for 1.5hrs. After that time, the mixture was applied again to a desalting column equilibrated with SulphoLink® coupling buffer (50mM Tris-HCl, 5mM EDTA pH 8.5) and eluted in 1 ml SulphoLink® coupling buffer fractions. The three first fractions (free from DTT) were pooled and used to prepare the SulphoLink® affinity column. A 5 ml bed volume SulphoLink® affinity column was packed and equilibrated with 25

ml of SulphoLink® coupling buffer. The bottom cap was replaced and the reduced GSTutrn-4 protein in coupling buffer was added to the column. The top cap was replaced and the mixture was incubated for 15 min at rt on a rotating shaker and a further 30 min standing upright. The caps were removed and the column allowed to drain. The column was washed with 15 ml of SulphoLink® coupling buffer. Non-specific binding sites were blocked with 5 ml of 50mM cysteine solution in SulphoLink® coupling buffer for 15 min at rt on a rotating shaker. The blocking solution was drained and the column finally washed in 80 ml of 1 M NaCl and 80 ml of storage buffer (see in AminoLink® method above). The column was stored in storage buffer upright until use.

Affinity purification

Purification of Mupa-1 and Mupa-2 using AminoLink® affinity column.

Before use, the affinity column was equilibrated to rt, the storage solution was drained and the column was washed with 10 ml of 1 x PBS. 1ml of purified IgG solution, diluted in 1x PBS to 6 mg/ml (utrn-1) and 4mg/ml (utrn-3), were applied to the column. This was followed with the application of 200ul of 1 x PBS to ensure that sample had entered the gel. The closed column was incubated upright for 1hr at rt. Unbound IgGs were washed off with 1 column volume of 1x PBS and collected each time for analysis. This was repeated 8 times for Mupa-1 (48 mg of IgGs) and 7 times for Mupa-2 (28mg of IgGs). The column was finally washed with 7 column volumes of 1x PBS. Elution of the specific IgGs was carried out using Immunopure® IgG elution buffer (Pierce) which is a glycine-based buffer with a pH 2.8. 900ul fractions were collected into 100ul of 1M Tris pH 9.0 to neutralise the pH of the fractions. The IgG content of each fraction was determined spectrophotometrically and the fractions that

contained the antibody were pooled and dialysed against 1x PBS. 2.2mg of purified Mupa-2 and 4.4 mg of Mupa-1 were purified in this way.

Purification of Mupa-3 using SulphoLink® affinity column

This method only differs from the one described above in that the total volume of IgG solution to be purified was added together to the column instead of 1 ml at a time. Briefly, 4 ml of a 5.5 mg/ml solution of Mupa-3 IgGs (22 mg) were added to the SulphoLink® affinity column. An additional 200ul of 1 X PBS were added to the column as before. The top cap was replaced and the column was incubated at rt for 1 hr. The unbound protein was washed with 25 ml of 1 x PBS and the wash collected. The antibody was eluted as above. A total of 2.6mgs of purified antibody were recovered.

Western blotting After SDS PAGE the gels were immunoblotted and stained with Ponceau S (0.5% in 1% acetic acid). Prior to blotting, gels were equilibrated in 20% methanol, 20mM Tris, 150mM glycine. Proteins were then transferred onto Hybond ECL nitrocellulose membranes (Amersham, Pharmacia Biotech) using a BIO-RAD electro-blotting apparatus, and 40-50 mA for 7 hours. Non-specific binding of the antibodies to protein was prevented by blocking the membranes in 5% dry-skimmed milk dissolved in 0.1% Tween 20 – TBS (TBST) o/n at 4°C. The blocking solution was discarded and the membranes were incubated with the working dilution of the primary antibodies (diluted in 5% dry-skimmed milk TBST) (see Table 2. 3) for 1-2hrs at rt with shaking. The membranes were washed twice for 5 minutes each with TBST and twice with 5% milk TBST (5 minutes each). A 1/2000 dilution in 5% dry-skimmed milk TBST of horseradish peroxidase conjugated goat anti-rabbit IgG

Antibody	Specificity	Supplier	Wb dil.	IHC dil.	Reference
Mupa-1 (p)	mo utrophin (aa 24-320)		1/1000	1/800	
Mupa-2 (p)	mo utrophin (aa 2543-2738)		1/750	1/200	
Mupa-3 (p)	mo utrophin (aa 3095-3390)		1/1000	1/800	
Urd40 (p)	mo utrophin (aa 2519-2867)	Dr. Derek Blake (Dept. of Human Anatomy and Genetics, Oxford)	1/250	1/100	Blake et al. (1999)
Mancho-3 (m)	hu utrophin (aa 3101-3430)	Prof. G.Morris (NEWI, Wrexham)	1/100		Nguyen et al. (1991)
P6 (p)	modystrophinaa 2884-3097)	Dr. S.Brown (Hammersmith Hospital, London)		1/300	Sherratt et al. (1992)
Collagen- I (p)	mo collagen type I	Biodesign (Maine, USA)		1/20	Demarchez et al. (1987)
NCL-DYS2 (m)	hu dystrophin (aa 3668-3685)	Novocastra Laboratories (Newcastle Upon Tyne)		1/10	Nicholson et al. (1992)
NCL-b-SARC (m)	hu β -sarcoglycan (aa 89-152)	Novocastra Laboratories (Newcastle Upon Tyne)		1/100	Bönnemann et al. (1995) Lim et al. (1995)
NCL-b-DG (m)	hu β -dystroglycan (aa 879-894)	Novocastra Laboratories (Newcastle Upon Tyne)		1/100	Cullen et al. (1994) Bewick et al. (1993)
VIA4-1(m)	rabbit WGA purified skeletal muscle membranes	Upstate biotechnology (New York, USA)		1/50	Ervasti et al. (1990,1991) Ohlendieck et al (1991)

Table 2.3 List of primary antibodies used in Western blotting (Wb) and Immuno-histochemistry (IHC).p= polyclonal; m= monoclonal; mo=mouse; hu=human; rab=rabbit; dil.=dilution; fp=fusion protein.

(DAKO) was applied to the blots and incubated with shaking for 1hr at rt. The membranes were finally washed 4 times for 5 minutes each with TBST.

Western blotting using the monoclonal Mancho-3 was performed using a slightly modified procedure. The membranes were blocked in 5% dried skimmed milk in 1 X PBS with 0.1% Tween20 (PBST) o/n at 4°C. Excess block was removed by washing the membranes four times each for five minutes in PBST followed by two further five minute washes in 1x PBS. The membranes were incubated with Mancho-3 at rt with shaking for two hours. After washing the membranes were incubated with the second antibody, horse- radish peroxidase (HRP)-conjugated anti-mouse IgGs (1:1000 dilution in 5% dried skimmed milk in PBST) for 1 hr at rt with shaking. The final washes incorporated one extra 0.5M NaCl₂ wash after the PBST washes.

In all cases, detection of specific polypeptides was carried out using an enhanced chemical luminescence Western blotting detection system (Amersham Pharmacia Biotech) following the manufacturers instructions. The immunoblotted membranes were transferred into plastic bags and an equal volume of the enhancer and the luminol were added to the membrane and mixed well for exactly one minute. Excess liquid was drained and the membranes were placed protein side up in a light-tight cassette. Three layers of the blue X-ray film were placed on top of the membranes, the cassette securely closed and the film exposed for varying times ranging from 15 min to two hours prior to development.

5' RACE Rapid amplification of cDNA ends (5' RACE) was carried out using the GIBCO BRL 5' RACE system (version 2.0) following the manufactures instructions. These experiments are described in chapter 4

section 4.4 and 4.5, an outline of the procedure is shown in Fig 4.14 and details of primers and annealing temperatures used in each 5' RACE reaction are listed in Table 2.4. In brief, first strand cDNA is synthesised from total RNA using a gene-specific primer and SUPERSCRIPT™ II reverse transcriptase. The primer, 1.5 µg of total RNA and DEPC-H₂O were heated at 70°C for ten minutes and chilled on ice. Other components were added to produce a reaction mix containing 20mM Tris-HCl (pH 8.4), 50mM KCl, 2.5mM MgCl₂, 10mM DTT, 100mM cDNA primer, and 400µM each of dATP, dCTP, dGTP, dTTP. The reaction mix was incubated at 42°C for one minute. 1µl (200 units) of the SUPERSCRIPT™ II RT was added, mixed and incubated at 42°C for 60 minutes.

The reverse transcription reaction was stopped by incubating at 70°C for 15 minutes, the RNA template was digested by treatment with RNase H and RNase at 37°C for 30 minutes. Following brief centrifugation, the reaction mix, was passed through a Glassmax column. Prior to application to the column 120µl of binding solution (6M NaI) was added to the newly synthesised cDNA. The column was centrifuged at 13000g for 20 seconds, the flow-through collected and kept at -20°C. The column was washed four times with the wash buffer (supplied by manufacturers), and twice with 70% ethanol to remove any unincorporated dNTPs, gene-specific primer and proteins. The cDNA was eluted from the column with 50µl of sterilised, distilled H₂O at 65°C by centrifugation at 13000g for 20 seconds.

A homopolymeric poly-C tail was added to the 3' end of the cDNA using terminal deoxynucleotidyl transferase (TdT). TdT tailing creates the binding site for the abridged anchor primer on the 3' end of the cDNA. A reaction mix

5' RACE			
Primer	Sequence	Annealing Temperature	
UT56R1	5'- GCTTCCTCAGAATTCC -3'	45°C	Exons 54-55 RACE
UT55R2	5'-CAUCAUCAUCAUGCATCGGCCAGCACATTTGC -3'	55°C	
UT55R3	5'-CAUCAUCAUCAUCCTCCAAGGCACTCTGTG -3'	55°C	
UT59R1	5'- CGATCTTCTGGGCTCTCTCC-3'	56°C	Exons 56-57 RACE
UT58R2	5'- CAUCAUCAUCAUCCTTTAGCTCACGTCTCAGCAC-3'	56°C	
UT57R3	5'- CAUCAUCAUCAUGGTTCCATTTCTCAGCACTGG-3'	56°C	
Anchor primer	5'-GGCCACGCGTCTGACTAGTACGG ₁₈ -3'	60°C	Universal Primers
Universal primer	5'-CUACUACUACUAGGCCACGCGTCTGACTAGTAC -3'	57°C	

Sequencing and RT-PCR			
Up109F1	5'-TGAGACCAAACCTCTAAGCCTGG -3'	56°C	Sequencing + RT- PCR
Up109R1	5'-TTGTTGCTTCCTCAGAATTCCC -3'	56°C	Sequencing
Up109Rs1	5'- CTGTTCTCTTCAGAGCC -3'	55°C	
M13F	5'- CCCAGTCACGACGTTGTAAAACG-3'	55°C	Sequencing
M13R	5'- AGCGGATAACAATTTACACAGG-3'	55°C	
pgmF	5'-AAGATCCGCATAGACGCCAT-3'	52°C	RT-PCR
pgmR	5'-GTGCTTGCCCAGAATCATGT-3'	52°C	RT-PCR

Table 2.4 Primers used in 5' RACE experiments and for sequencing and RT-PCR amplification of the novel Up109 sequence. All are referred to in chapter 4.

containing the cDNA in 10mM Tris-HCl (pH 8.4). 25mM KCl, 1.5mM MgCl₂, 200μM dCTP was prepared and incubated at 94°C for three minutes. The mix was placed on ice and 1μl of TDT added. After incubation at 37°C for ten minutes, the reaction was stopped by heat inactivation at 65°C for ten minutes.

PCR amplification was carried out using Taq polymerase, a nested gene-specific primer corresponding to a site located within the cDNA molecule, and a novel deoxyinosine- containing anchor primer provided with the kit. The thermal cycler was preheated to 94°C prior to use and reaction mixes were prepared on ice. The first round of amplification used the abridged anchor primer in a reaction mix of final composition, 20mM Tris-HCl, 50mM KCl, 1.5mM MgCl₂, 400mM gene-specific primer (termed either GSP 1 or GSP2), 400mM abridged anchor primer, 200μM each of dATP, dCTP, dGTP and dTTP, tailed cDNA and 2.5 units of Taq polymerase. The reaction was heated at 94°C for 5 minutes and then cycled for 30 cycles using conditions established for each primer pair on a Phoenix thermocycler as follows: Denaturation step (94°C, 45 seconds), annealing of primer (55°C to 57°C, 45 seconds), primer extension (72°C, 90 seconds), final extension (72°C, 5 minutes).

10μl of the first 5' RACE product was analysed on a 2% agarose gel. In general, no product was visible at this stage.

The second round of amplification was carried out using second nested gene-specific primer (GSP2) and 1/50, 1/100 and 1/200 dilutions (in double distilled water, ddH₂O) of the first amplification product as template. The PCR mix for each sample contained the following, 20mM Tris-HCl (pH8.4), 50mM KCl, 1.5mM MgCl₂. 200nM GSP2. 200nM UAP (universal anchor primer) 200μM each of dATP, dTTP, dGTP and dCTP, diluted first round PCR product

and 2.5 units of Taq DNA polymerase. UAP primer includes a deoxy-uracil containing sequence at its 5' end for uracil DNA glycosylase mediated cloning. The reactions were heated at 94°C for 5 minutes and then cycled as in the first round PCR.

Genomic library screening

Preparation of ³²P-labelled probes DNA fragments were labelled using the Rediprime II kit (Amersham Life Sciences) which contains a dried stable labelling mix of dATP, dTTP, dGTP, Klenow enzyme and random primers. Denatured DNA (2.5-25ng) was added to the labelling mix, together with 5µl of [α -³²P]dCTP. After incubation at 37°C for 30 minutes, unincorporated [α -³²P]dCTP and primers were removed by passing through a sepharose G50 column. The labelled probe was eluted with 450µl of TE. Incorporation was generally 60-80%. The probe was denatured by boiling for 5 minutes before addition to the hybridising solution and filters.

Genomic library screening A λ -DASH mouse genomic library was screened using a ³²P- labelled *EcoRI/HindIII* 540 bp fragment of Up109 that contained 460 bp of unique sequence and the first 80 bp of exon 56. The phage were transfected into E-coli LE392 grown in LM-broth with 0.2% maltose. The library was titrated to determine the number of plaque forming units (pfu) per ml of stock and 3ml of an overnight E-coli culture were mixed with 10⁵ pfu of phage. Cells were incubated at 37°C for 20 minutes. 7mls of LM-agarose was added to the cells and the phage gently mixed before pouring onto a 142mm plate of LM-agar. Plates were incubated at 37°C overnight. Further screens were performed using 90mm plates, 200µl of cells from an overnight culture and the appropriate number of phage particles.

The lifts of the filters were carried out in duplicate using a standard method. Non-symmetrical registration marks were made to allow orientation of the filters. Briefly, filters were successively treated with the following solutions: 2x SSC, denaturing solution (1.5M NaCl, 0.5M NaOH), neutralising solution (1.5M NaCl, 0.5M Tris-HCl; pH7.5) and finally rinsed in 2x SSC before being air-dried and baked at 80°C for 2 hours in order to fix the DNA to the membranes. Filters were prehybridised and then hybridised with a labelled probe at 65°C. Prehybridisation took place for 4 hours in a hybridisation solution containing 10x Denhardt's, 4x SSC, 0.1% SDS, 10mM saturated Ppi and 0.1mg/ml denatured herring sperm). The denatured probe was added to the solution, mixed thoroughly and hybridised overnight at 65°C. After hybridisation, filters were washed in a solution of 2xSSC/0.1% SDS at rt for 30 minutes. Further washes (2x15 minutes) at higher stringency were then performed: generally 0.2xSSC/0.1%SDS and then 0.1xSSC/0.1%SDS at 65°C as for the hybridisation. Filters were blotted on 3MM Whatmann paper to remove excess fluid, wrapped in cling film and autoradiographed with X-ray film and an intensifying screen at -70°C.

Positive recombinants were identified by duplicate signals from both filters. These were picked as agar plugs after aligning the autoradiographs with the plates. Plugs were placed into 500µl of PSM and 10µl of chloroform. This phage stock was kept at 4°C overnight to allow the phage to diffuse from the agar before plating out at 200- and 500 fold dilutions for re-screening. Successive rounds were performed until the phage was picked plaque pure.

For maxi-preparations of homogenous λDASH bacteriophage DNA, 10⁵ pfu were plated on 90mm LM-agar plates. 5x10⁸ pfu were adsorbed to 3mls of

an overnight culture of LE 392 cells, in the same way as described earlier. The phage and cell mix was added to 200ml of LM-broth and incubated at 37°C for up to 5 hours, until cell lysis was obvious. 2ml of chloroform was added and the culture incubated at 37°C for 20 minutes. λ -DASH bacteriophage DNA was extracted using the QIAGEN lambda maxi purification kit according to the manufacturers instructions. Yields of 500 μ g per 200 ml culture were routinely obtained.

Southern blotting After electrophoresis in agarose gels, DNA was denatured by submerging the gel in 1.5M NaCl, 0.5M NaOH for 30 minutes and neutralised by submerging in 1.5M NaCl, 0.5M Tris-HCl pH7.5 for 60 minutes. The DNA was blotted (Southern, 1975) onto a nylon filter (Hybond-N, Amersham) by capillary action of 20xSSC for 16-24 hours. Filters were then baked at 80°C for 2 hours to bind the DNA to the filter.

Hybridisations of Southern blots were carried out in sealed bags in a 65°C water bath in the pre-hybridisation solution described in section genomic library screening. The denatured probe was then added and the filter hybridised overnight at either 65°C or 55°C depending on the expected level of homology between the probe and the blotted DNA.

After hybridisation the filters were washed to a final stringency of 0.1 x SSC, 0.1% SDS at 65°C.

Fluorescent immuno-histochemistry

Tissue and section preparation Freshly dissected adult and foetal tissues were embedded in embedding compound (OCT, Raymond A Lamb) and frozen in liquid nitrogen-cooled isopentane. 7 μ m serial sections were cut on a cryostat

(OTF cryostat, Bright) and collected onto SuperFrost Plus slides (BDH-Merck), air-dried and stored at -70°C .

All reagents were diluted in 1x PBS unless otherwise stated. All incubations were carried out at rt in a humid chamber (Raymond A Lamb). Sections were washed between steps in 1x PBS.

Procedure used with polyclonal antibodies Sections were blocked in 10% (v/v) normal donkey serum (Jackson Immunoresearch) for 20 min before incubating in primary antibody (see Table 2.3) for 1hr. The slides were then briefly washed three times in 1 x PBS and incubated in 1/200 dilution of biotinylated anti-rabbit Ig (Amersham-Pharmacia Biotech) for 45 min. After that time, slides were washed as before and incubated in 1/200 dilution of Texas-Red- or fluorescein-conjugated streptavidin (Amersham-Pharmacia Biotech) for 20 min. Slides were finally washed three times in 1 x PBS and mounted with one drop of Vectashield-DAPI (Vector Laboratories) and viewed under a fluorescence microscope (Leica or Zeiss).

A modified procedure was employed when, using a biotin-streptavidin amplification step, high non-specific background became a problem. In this case, sections were blocked in 10% (v/v) foetal calf serum for 20 min, incubated in the diluted primary antibodies for 1 hr and after three washes in 1x PBS, incubated in 1/75 dilution of fluorescein-conjugated anti-rabbit IgG (Vector Laboratories) for 45 min. Following manufacturer's indications, this second antibody was diluted in 1 x PBS containing 2% normal mouse serum to prevent cross-reactivities with IgG's present in the tissue. Excess second antibody was removed by washing the slides three times in 1 x PBS and the sections were finally mounted with Vectashield-DAPI (Vector Laboratories). Testis sections

were fixed prior to staining in 100% acetone at -20°C for 7 min and rinsed in 1 x PBS before applying the blocking solution.

Procedure used with monoclonal antibodies The M.O.M. immunodetection kit (Vector Laboratories) was used with the mouse monoclonal antibodies listed in [†]Table 2.3 to prevent non-specific background due to the presence of mouse immunoglobulins in the tissues. The working dilutions of reagents were prepared and the kit was used according to manufacturer's instructions. Briefly, sections were incubated in M.O.M.[™] mouse IgG blocking reagent for 1 hr followed by two washes for 2 min in 1 x PBS. Sections were then incubated for 5 min in working solution of M.O.M.[™] diluent followed by incubation for 30 min with the corresponding primary antibodies which had been diluted in M.O.M.[™] diluent. Sections were washed as before and incubated with M.O.M.[™] biotinylated anti-mouse IgG reagent for 10 min and washed again twice in 1x PBS for 2 min. Fluorescein-conjugated avidin was applied to the sections which were incubated for 5 min; sections were mounted in Vectashield-DAPI (Vector Laboratories).

mRNA in situ hybridisation to embryo sections using radiolabelled

riboprobes The method used is an adaptation of the method described by Simeone (1999).

Tissue preparation C57Bl/6 and UKO^{ex6} mouse embryos at days 8.5, 9.5, 10.5, 12.5, 14.5, 15.5 and of gestation (dpc) were dissected out of the yolk sac in ice-cold PBS under a dissecting microscope, except for early 8.5 and 9.5 dpc embryos which were fixed in the decidua. The embryos were transferred to a container with an excess volume of ice-cold freshly prepared 4% paraformaldehyde (PFA) solution in PBS and fixed o/n at 4°C in a rocking

table. The following morning, the embryos were taken through the following solutions:

1 X PBS	4° C	30min
0.85% (w/v) NaCl	4° C	30min
1:1 0.85% NaCl/100% ethanol	4° C	15min
70% ethanol (2X)	4° C	15min
85% ethanol	rt	30min
95% ethanol	rt	30min
100% ethanol (2X)	rt	30min
100% xylene (2X)	rt	30min
1:1 xylene/paraffin	60°C	45min
100% paraffin (3X)	60°C	45min

The last three 100% paraffin (BDH) washes were carried out inside a temperature controlled blocking unit (Blockmaster II, Raymon A Lamb). During this time the embryos were orientated inside plastic moulds (Raymond A Lamb) to obtain frontal or sagittal sections and then solidified on a cold stage and stored at 4 °C.

Preparation of sections 6µm serial sections were cut in a microtome (microtome 820, Spencer Instruments), floated in a 42 °C water bath (Raymond A Lamb) and collected on Superfrost slides (BDH). The slides had been previously treated with 3-aminopropyltriethoxy-silane (TESPA, Sigma) in order to firmly hold the sections during subsequent steps. Sections on slides were labelled and stored at rt until use.

Preparation and labelling of riboprobes A panel of riboprobes were prepared by cloning RT-PCR products corresponding to different regions of the

utrophin mRNA (primers used for each probe are listed in Table 2.5) into the pAMP vector. Sense and antisense probes were synthesised by *in vitro* transcription from the T7 or SP6 sites in the vector in the presence of α -S³⁵-UTP. Plastic tubes, tips, glass columns and glass wool were siliconized with (using Repelcoat, BDH-Merck) to avoid non-specific sticking of the ³⁵S labelled probes.

10ug of vector DNA for each construct were linearized with the *Accl* or *XbaI* restriction enzymes, ethanol precipitated and resuspended in 5ul of ddH₂O. 1-2ug of DNA were transcribed *in vitro* using 2 μ l (50U) of SP6 (sense probe) or T7 (antisense probe) RNA polymerase for 2hrs at 37°C in a 20ul reaction containing the following: 2 μ l of 10X transcription buffer (Roche-Boehringer Mannheim, 400mM Tris-HCl (pH 7.5), 60mM MgCl₂, 20mM spermidine, 100mM NaCl), 0.6mM dATP, dCTP and dGTP (Gibco BRL), 1ul of RNase inhibitor (Life Technologies), 4ul of α -³⁵S- UTP (ICN, 250uCi) and 10mM DTT (Roche-Boehringer Mannheim). Once transcription was complete, the template DNA was removed by adding 1 U of DNase (Life Technologies-Gibco BRL) and incubating at 37°C for 15 min. 3 μ g of total yeast RNA were added to the reactions to act as an RNA carrier. The RNA probes were alkali hydrolysed to a length of 100-400bp at 60 °C for times varying between 10 and 25 min in 50ul of a solution containing 10mM DTT, 80mM NaHCO₃ and 120mM Na₂CO₃. This procedure facilitates diffusion of the probe into the tissue. Hydrolysis was stopped by adding 50ul of a neutralising solution containing (10mM DTT, 200mM NaAc and 1% (v/v) acetic acid.

Primer	Sequence	Tm	PCR Size
U1-6-F U1-6-R	5'-CUACUACUACUAAAGTATGGGGACCTTGAAGCC-3' 5'-CAUCAUCAUCAU TTCATGACATCCTTCACCTGCC -3'	63°C	415bp
U31-34-F U31-34-R	5'-CUACUACUACUACTACAGAGGAACTTCGAGAGG-3' 5'-CAUCAUCAUCAUGCCTTCTGATGTGGATTTCTGC -3'	60°C	467bp
U56-59-F U56-59-R	5'-CUACUACUACU AACATCGACTGGATGACATGAACC -3' 5'-CAUCAUCAUCAU TTCAGAAGACTGCTTGCGCATGG-3'	60°C	411bp
U340-F U340-R	5'-CUACUACUACUACAGGCAATGTGAGCATCTATCC -3' 5'-CAUCAUCAUCAU TCATATTAGAAAGCCCCACCC-3'	60°C	339bp

Table 2.5 Primer pairs used to RT-PCR amplify the utrophin sequences corresponding to the riboprobes used for mRNA *in situ* hybridisation and referred to in chapter 6.

The labelled probe was separated from unincorporated nucleotides on a 5ml Sephadex G50 (Amersham Pharmacia check) column (a glass Pasteur pipette plugged with cotton wool) previously equilibrated with running buffer (10mM Tris-HCl pH 7.5, 5mM EDTA, 0.1% SDS and 10mM DTT) and total yeast RNA (50ug). The probe was added to the column and eluted in 200ul fractions of running buffer. The fractions containing the labelled probe were identified using a sensitive geiger counter. These were pooled into one tube, ethanol precipitated. The pellet was collected by centrifugation and resuspended thoroughly in an adequate volume of 100mM DTT solution. The amount of incorporated radioactivity (cpm/ μ l) was measured in scintillation liquid (National Diagnostics) in a β -particle scintillation counter (LKB Wallac Instruments) and the probe was diluted to c. 50000cpm/ μ l in hybridisation buffer (50% deionized formamide, 0.3M NaCl, 20mM Tris-HCl pH7.4, 5mM EDTA, 10mM NaHPO₄, 10% dextran sulphate 1X Denhardt's, 0.5mg/ml of total yeast RNA).

Pre-hybridisation treatment of sections All treatments were carried out in 250 ml glass boxes and with the slides arranged in raised-bottom glass racks. Prior to hybridisation, sections were treated with proteinase K (to increase the accessibility of the probe to the tissue) and with acetic anhydride to reduce non-specific electrostatic binding of the probe. In order to do this, the paraffin on the sections was removed with 100 % xylene in two washes and sections were hydrated through a decreasing series of ethanols (100% to 30%) followed by 0.85% NaCl (5 min), 1 x PBS (5 min) and 4% PFA (20 min). Diluted proteinase K (20ug/ml in 50mM Tris-HCl, 5mM EDTA, pH8) was directly applied to each section (c.20ul to cover the whole section) and sections were incubated for 7 min at rt. After this time, sections were fixed with 4% PFA for 5 min and rinsed

briefly in DEPC-H₂O and then transferred to a 0.25% (v/v) solution of acetic anhydride in 0.1M triethanolamine and incubated with stirring for 10 min. Sections were then washed with 1 x PBS for 5 min followed by 0.85% NaCl for 5 min and quickly dehydrated through an increasing series of ethanols (30% to 100%) and air dried until hybridised (1 to 2 hrs).

Prior to hybridisation, the riboprobes were denatured at 80° C in a water bath for 2 min and 20ul of probe were added directly to each section; the sections were covered with a coverslip and carefully arranged in a humid chamber containing a tissue soaked with 50% formamide and 4XSSC. The box was sealed and placed upright in a hybridisation oven and hybridisation was carried out o/n at 53 °C.

Post-hybridisation washes Washes were carried out in 250 ml glass boxes except for the formamide washes and RNase treatment which were carried out in 30ml coplin jars. All washes were carried out in water baths previously equilibrated to the required temperature.

After hybridisation the slides were washed under high stringency conditions as follows: coverslips were removed by immersing sections in 5XSSC, 10mM DTT in a 50° C water bath (20 min), this was followed by a wash in 50% formamide, 2 X SSC at 65 ° C for 45 min and two washes in 1 x NTE buffer (10 min each). Sections were then treated with a 20ug/ml solution of RNase A (Sigma) in 1 x NTE buffer at 37 °C for 30 min. Sections were then washed once with 1 x NTE buffer (5 min) and incubated again in 50% formamide, 22X SSC at 65 ° C for 45 min. Finally sections were consecutively washed in 2 X SSC and 0.1 X SSC at 37 ° C for 15 min each wash. The

washed sections were then dehydrated in an increasing series of ethanol solutions containing 0.3 M NH₄Ac and air dried.

Autoradiography Hybridisation signal was detected with a liquid photographic emulsion. Briefly, NTB-2 Kodak emulsion was melted prior to use in a 42 °C water bath; all radiographic procedures were carried out in a dark-room in safelight conditions (Wratten 2 filter). Bubbles in the emulsion were removed by dipping and swirling a clean slide inside the emulsion. Slides were then very gently dipped into the emulsion, to cover them with a thin and uniform layer of emulsion, and drained vertically. Excess emulsion on the back of the slides was removed with a tissue. The slides were then laid horizontally and the emulsion allowed to dry at rt for 2hrs. After this time, slides were placed, emulsion facing up, in a light-tight box containing a sachet of desiccant. The box was sealed, wrapped in foil paper and placed inside two light-tight bags and left to expose for 5 to 7 days at 4 °C. After that time, the slides were allowed to come to rt inside the box and, under safelight conditions, taken out of the box and transferred through Kodak Dektol developer (diluted 1:1) (3 min), dH₂O and fixer (undiluted 10 min). The developing reagents had been previously cooled to 15 °C in the cold-room and were used cold. The slides were then washed thoroughly in dH₂O, quickly transferred through 70% then 100% ethanol and air-dried. The dry slides were then counter-stained in toluidine blue for 2 min and transferred quickly through dH₂O, 70% ethanol, 100% ethanol and xylene (twice). Finally, slides were mounted in DPX and dried o/n before being examined under the microscope. Silver grains were visualised using dark-field optics on a Zeiss Axioplan microscope.

Chapter 3

Production of the Mupa Antibodies

Results

3.1 General comments

The present study was prompted by the work of our collaborators in Prof. Kay Davies lab in Oxford, who generated a utrophin knock-out mouse (Deconinck et al., 1997a) carrying an insertional mutation in exon 6 of the utrophin gene (section 1.10). The position of the mutation predicts that the UKO^{ex6} mice will be deficient for full-length utrophin but not for the short utrophin isoforms. Thus, UKO^{ex6} mice provided an ideal *in vivo* model to study the short utrophin isoforms and have been a crucial resource in the present study. The study of the Oxford team was not aimed at the short isoforms but focused on full-length utrophin.

In contrast, one of the main objectives of this thesis was to investigate the pattern of expression of the short utrophin isoforms in whole tissue extracts by Western blotting and their cellular localisation by immuno-histochemistry. To achieve this aim, reliable and specific antibodies were crucial. Several monoclonal and polyclonal antibodies have been raised against utrophin by other groups and some are commercially available such as the monoclonals DRP1 and DRP2 (raised against the most COOH-terminal 11 aminoacids (aa) and aa 1 to 261 of human utrophin respectively, Novocastra). Preliminary Western blots using these two monoclonal antibodies showed that they both detected a large number of non-specific components and neither of them efficiently detected high levels of full-length utrophin. Indeed, DRP1 and DRP2

are no longer recommended for Western blotting by Novocastra technical department. We also tested the monoclonals Mancho-3 and Mannut-, raised against the most COOH-terminal 329 aa and aa 113 to aa 371 of human utrophin respectively, (Nguyen et al., 1991, 1995). Both antibodies detected full-length utrophin but also a series of non-specific polypeptides. All four antibodies were raised in mouse and some non-specific crossreactivity might be predicted when used on Western blots of mouse tissue extracts. It seemed likely that other mouse monoclonal antibodies would also pose this problem.

In contrast, a limited series of blots using a polyclonal antibody, Urd40, raised against the distal rod domain of mouse utrophin, aa 2519 to 2867, (Blake et al., 1999) gave good results. Other polyclonal antibodies such as UT-2 (Imamura et al., 1998) and COOH-ter (Lumeng et al., 1999) were considered. However, these have been raised against the most COOH-terminal portion of utrophin and in order to distinguish one short isoform from another, a series of antibodies recognising different regions of utrophin were required. For this reason, it was decided to generate a panel of anti-mouse utrophin polyclonal antibodies.

Antibodies can be raised against short peptides or larger regions of purified proteins. There are advantages and disadvantages associated with each approach; anti-peptide antibodies can be synthesised easily and can target very specific regions of a protein. Their main disadvantage is that since they target a very short stretch of contiguous aminoacids they often do not recognise native protein. Thus, assays in which the protein is in its native conformation, such as immuno-histochemistry, may not work. On the other

hand, intact full-length protein or segments of protein are more laborious to generate.

Using DNA cloning techniques and bacterial expression systems it is possible to prepare polypeptide antigens corresponding to entire functional domains. Antibodies raised against such domains are suitable for functional studies and for immuno-histochemistry. Bearing these points in mind, it was decided to use a bacterial system to produce fusion proteins that would represent relatively large regions of mouse utrophin.

Four regions of utrophin were selected (Fig 3.1); utr-1, the actin binding domain from aa 24 to aa 320, an antibody raised against this region would detect full-length utrophin only; utr-2, aa 564 to 755, which encodes two spectrin repeats and a hinge region and would be present in full-length utrophin and in any unusual isoforms encoded by a transcript initiated upstream of exon 15. This region is downstream of the UKO^{ex6} targeted exon (exon 6) and the corresponding antibody would detect unconventional almost full-length utrophin polypeptides that might be produced in the UKO^{ex6} mice. Neither of the antibodies raised against utr-1 or utr-2 would detect Up140, G-utrophin or Up71.

utr-3, the distal rod domain (aa 2543 to 2738), was chosen to raise an antibody that would detect full-length utrophin, G-utrophin, and Up140 and any as yet undiscovered isoform translated from a position upstream of exon 56. An antibody to this region would not detect Up71, which is translated within exon 64. utr-4, comprising the most COOH-terminal sequence, aa 3095 to aa 3390, was also chosen to raise an antibody that would detect all utrophin isoforms including Up71.

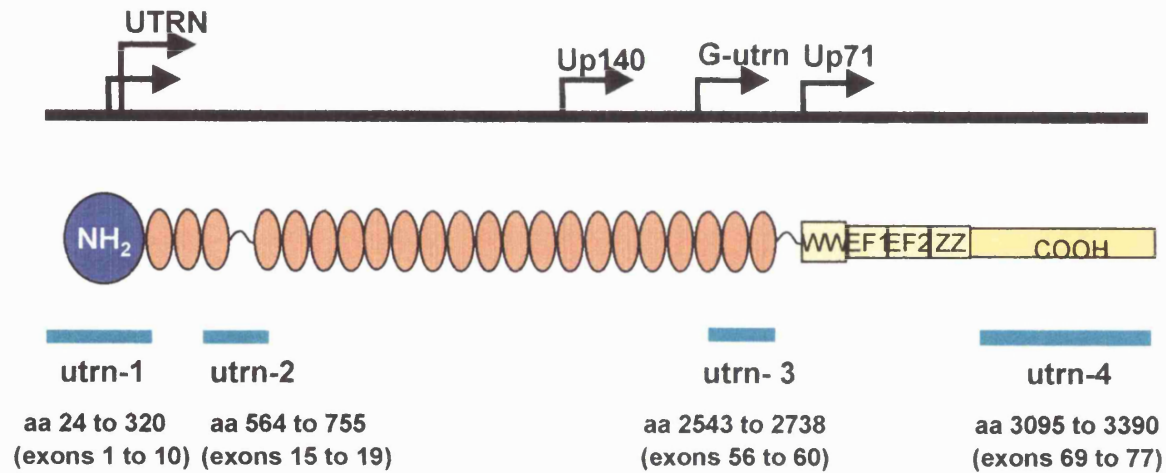


Fig 3.1 Relative positions of aa sequences used to raise mouse utrophin polyclonal antibodies are shown as green boxes relative to full-length utrophin protein. The positions of the 5' ends of known utrophin isoforms are indicated by arrows.

3.2 Preparation of the utrophin constructs

A variety of vectors and bacterial expression systems to produce fusion proteins are commercially available. I decided to use the Glutathione-S-Transferase (GST) Gene Fusion System (Amersham Pharmacia). This system consists of the pGEX plasmid vectors and a purification system based on sepharose affinity chromatography and site specific proteases.

In the pGEX vector (Fig 3.2), the complete coding sequence for GST is found upstream of the multiple cloning site. cDNA sequences cloned in the vector in the correct open reading are translated as a fusion protein with GST after induction of the tac promoter upstream of the GST sequence. Removal of GST from the fusion product is achieved by cleavage with proteases that recognise specific sites in sequences located between GST and the multiple cloning site (MCS). There are several slightly different versions of the pGEX vector; the pGEX-4T-1 vector, which has an expanded multiple cloning site and contains a thrombin cleavage sequence, was chosen for this study.

The strategy adopted for cloning the chosen segments of utrophin sequence was to RT-PCR amplify using primers flanking the exons of interest.

Recognition sequences for restriction enzymes with a site in the MCS are not present in the utr sequences and so were added to the 5' ends of the PCR primers, taking care to maintain the same reading frame as full-length utrophin (Fig 3.2); these primers are shown in Table 2.2. Two different enzymes were used so that the orientation of the inserts in the vector could be forced. RT-PCRs were carried out from mouse adult brain cDNA using primers positioned as follows ; utr-1 in exons 1 and 10, utr-2 in exons 15 and 19, utr-3 in exons 56 and 60 and utr-4 in exons 69 and 77. Products of the correct size were

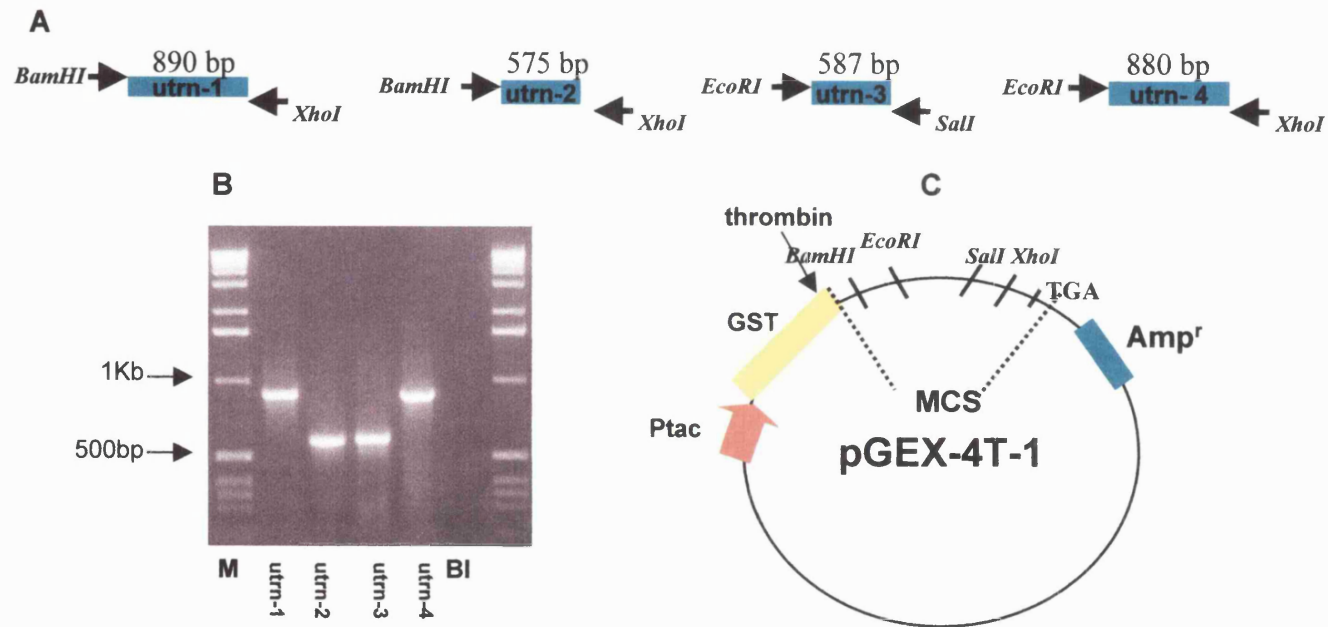


Fig 3.2 A, diagram to show the utrns polypeptides 1 to 4 indicating the restriction enzymes recognition sequences added at their 5' end (arrows). B, utrns-1-utrns-4 after RT-PCR. C, The pGEX-4T-1 vector showing the positions of restriction enzyme sites in the multiple cloning site (MCS) and other relevant elements including the position of the thrombin recognition sequence. bp=base-pair; Kb=kilo-base; M=DNA size marker; BI= no cDNA control; Ptac= *tac* promoter; GST= glutathione S-transferase sequence (with translation initiation codon); TGA=stop codons; Amp^r=ampicillin resistance element.

amplified (Fig 3.2), gel extracted and digested with the appropriate enzymes: *Bam*HI/*Xho*I for utr-1 and utr-2, *Eco*RI/*Sal*-I for utr-3 and *Eco*RI/*Xho*I for utr-4. The digested fragments were then ligated into the pGEX vector DNA prepared previously by digestion with the same pair of enzymes.

The recommended host bacterium for the expression of the fusion protein is the protease deficient *E.coli* strain, BL21. However, it became clear that these cells do not transform well; this was overcome by using 2 μ l of each ligation reaction to transform competent DH5 α cells with subsequent transfer of the recombinants into BL21 cells for expression. These DH5 α transformations were successful and DNA was prepared from 6 recombinants for each construct. The DNA was digested with the pair of enzymes used to clone each of the RT-PCR products (Fig 3.3). All of the four classes of recombinants gave the correct size insert (utr-1 890bp; utr-2 575 bp; utr-3 587 bp and utr-4 880 bp); only one out of six utr-4 recombinants contained the correct size insert.

One positive recombinant for each construct was sequenced, using vector specific primers that hybridise to sequences flanking the MCS in the vector (Table 2.2), to check that the inserts were in the correct open reading frame and that they contained the correct sequences. Plasmid DNAs from utr-1 to utr-4 were used to transform BL21 cells. Multiple clones were produced on transformation using purified plasmid DNAs. DNA was prepared from clones for each construct and the insert DNA was checked by restriction enzyme digestion. One recombinant containing each construct was selected to produce the fusion proteins and designated GSTutr-1, GSTutr-2, GSTutr-3 and GSTutr-4 (Fig 3. 3). The DNAs from GSTutr-1 to GSTutr-4 were again

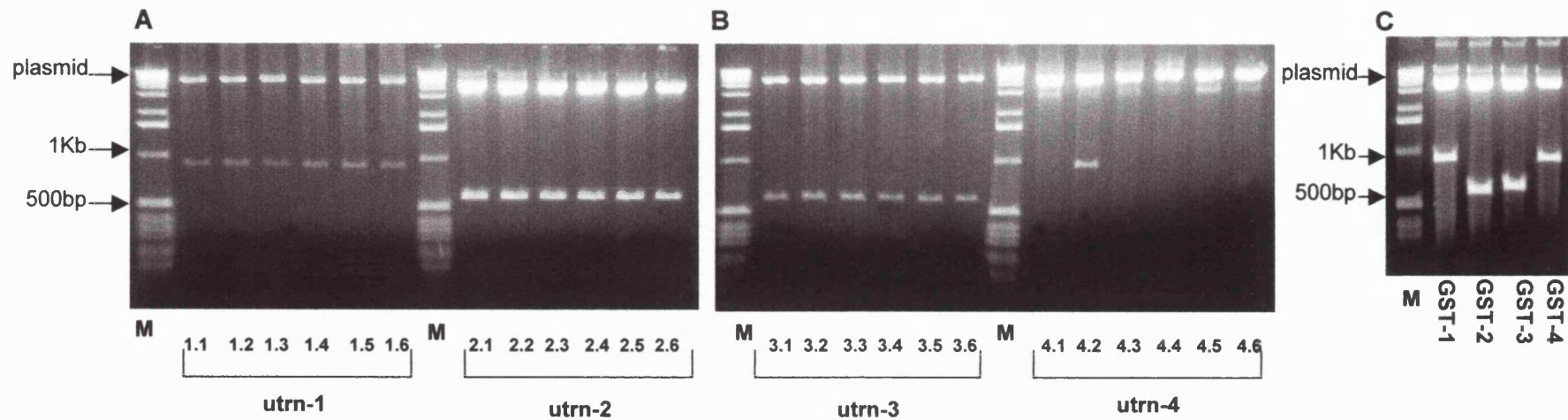


Fig 3.3 A, plasmid DNAs prepared transformed DH5 α recombinants (6 of each utrn type) digested with *Bam*Hi/*Xho*I (utrn-1 and 2) and B, *Eco*RI/*Sal*I (utrn-3) and *Eco*RI/*Xho*I (utrn-4). C, the same pair of restriction enzymes were used to digest plasmid DNAs from the BL21 recombinants. These were used to synthesise the GST-utrophin fusion proteins and were designated GSTutrn-1 to 4. bp=base-pair; Kb=kilo-base; M=DNA size marker

sequenced using vector primers to verify the reading frame before proceeding with the production of the antibodies. The recombinants were maintained and propagated throughout the experiment in BL21 cells on streaking L-agar plates with ampicillin.

3.3 Small-scale production of GST-fusion proteins

As a preliminary to large-scale protein production, small-scale experiments were carried out to determine the proteins optimal growing and induction conditions. This procedure, described in section 2.2, is shown diagrammatically in Fig 3.4. The results of the small-scale preparations of GSTutrn-1 and GSTutrn-2 are shown in Fig 3.5 and of GSTutrn-3 and GSTutrn-4 in Fig 3.6. The small-scale preparations were carried out in triplicate and were sampled at three stages (see Fig 3.4). Fraction A represents the total BL21 proteins, fraction B represents the insoluble proteins precipitated after sonication and centrifugation, and the EFP fraction represents the eluted fusion proteins after glutathione-sepharose affinity chromatography.

In all four cases, polypeptides of the correct size (c.62 kDa for GSTutrn-1 and GSTutrn-4 and c.50kDa for GSTutrn-2 and GSTutrn-3) were synthesised after induction with IPTG and were the major product in fraction A (Fig 3.5 lanes 1.1.A and 2.1.A and Fig 3.6 lanes 3.1.A and 4.1.A). Some of the fusion proteins remained in the insoluble fraction B (Fig 3.5 lanes 1.1.B and 2.1.B and Fig 3.6 lanes 3.1.B and 4.1.B). For GSTutrn-1, 3 and 4 most of the fusion protein was recovered in the soluble fraction after elution from glutathione-sepharose (Fig 3.5 lanes 1.1-1.3 and 2.1-2.3 and Fig 3.6 lanes 3.1-3.3). In contrast, the major

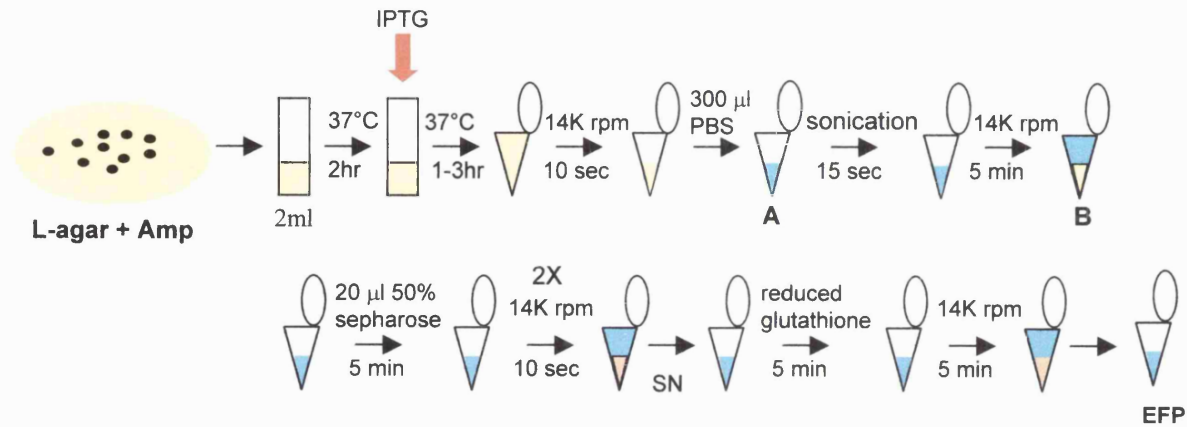


Fig 3.4 Diagram to show the steps of the small scale procedure to synthesise and purify fusion proteins using the GST system. amp= ampicillin; IPTG=isopropyl- β -thiogalactoside; K rpm=1000 revolutions per minute. When a sample was removed for analysis it is indicated as A, B or EFP. A=total BL21 proteins, B=insoluble proteins and cell debris after sonication and centrifugation. EFP= eluted fusion protein after affinity chromatography.

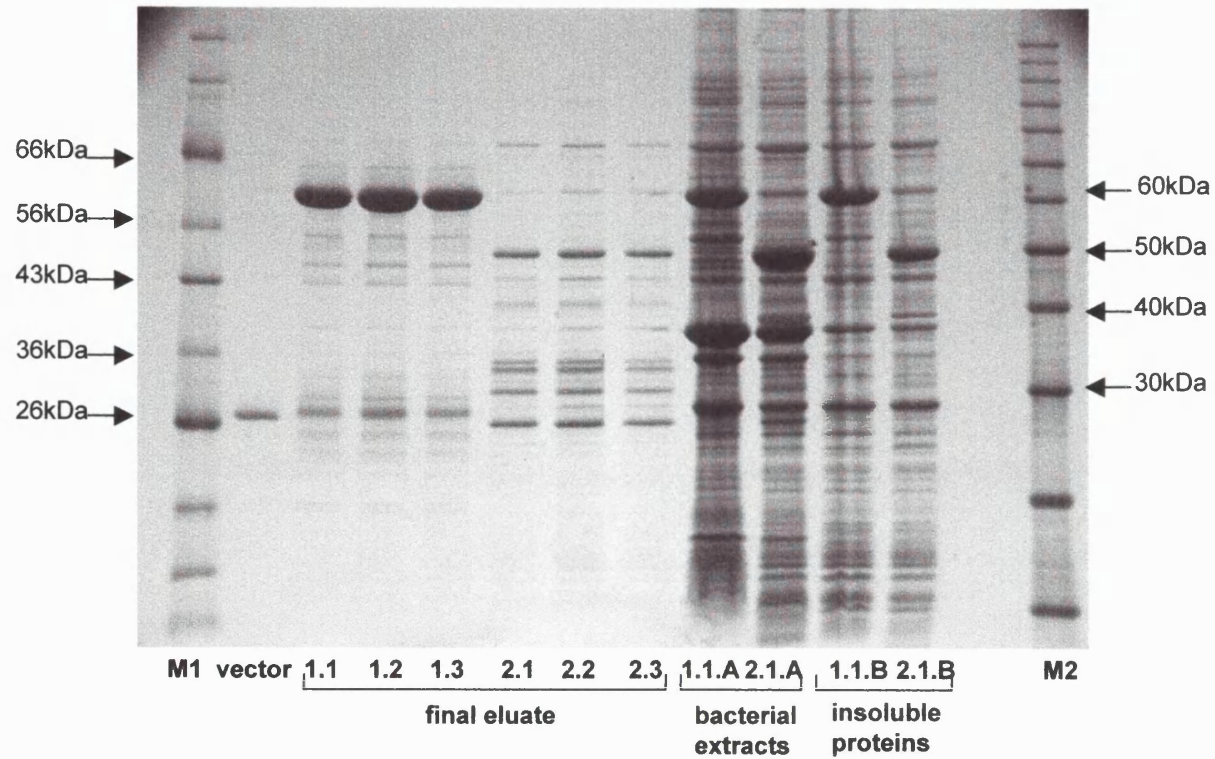


Fig 3.5 Small-scale preparation of GSTutrn-1 and GSTutrn-2 fusion proteins. The whole bacterial extracts correspond to fraction A in Fig 3.4; the insoluble proteins to fraction B and the final eluate to EFP. Three independent preparations were made, the final eluate for each of them is shown (lanes 1.1-1.3 and 2. 1.1-1.3) but only one example of fractions A (lanes 1.1.A and 2.1.A) and B (lanes 1.1.B and 2.1.B) are shown. Vector=GST protein purified from a BL21 clone containing vector without insert cDNA; M1= protein marker (New England Biolabs); M2=10kDa protein ladder (Gibco.BRL)

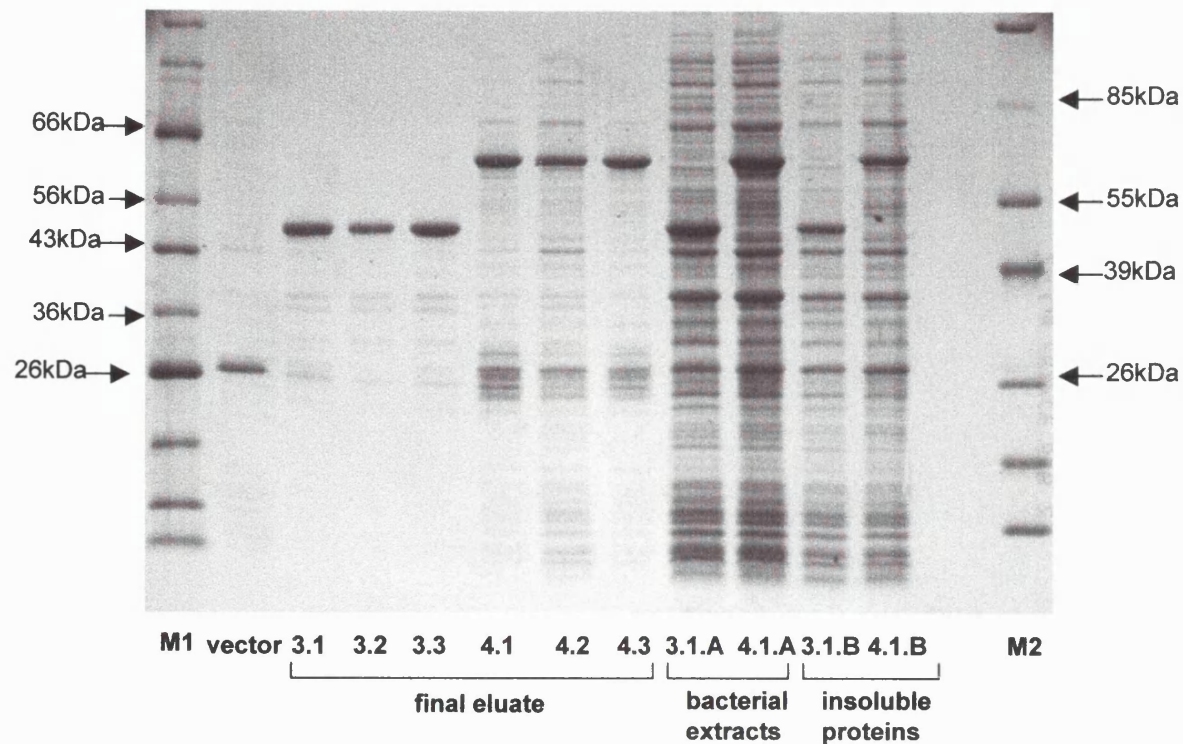


Fig 3.6 Small-scale preparation of GSTutrn-3 and GSTutrn-4 fusion proteins. The whole bacterial extracts correspond to fraction A in Fig 3.4; the insoluble proteins to fraction B and the final eluate to EFP. Three independent preparations were made, the final eluate for each of them is shown (lanes 3.1-3.3 and 4.1-4.3) but only one example of fractions A (lanes 3.1.A and 4.1.A) and B (lanes 3.1.B and 4.1.B) are shown. Vector=GST protein purified from a BL21 clone containing vector without insert cDNA; M1= protein marker (New England Biolabs); M2=protein marker ladder (Boehringer Mannheim)

part of GSTutrn-2 appeared to be insoluble and was retained in the insoluble pellet and only a small proportion was eluted (Fig 3.5 lanes 2.1-2.3).

Large-scale preparations of GSTutrn-1, 3 and 4 were undertaken and the problem of GSTutrn-2 was investigated further.

It seemed likely that the poor recovery of GSTutrn-2 was due to low solubility of the fusion protein or failure of the fusion protein to bind to the glutathione affinity resin. Various strategies were employed to improve the yield as follows:

- 1 In order to increase the binding of the fusion protein to glutathione sepharose:
 - DTT (5mM) was added to the bacterial cultures prior to sonication (Frangioni et al., 1993). However, this did not result in an increase in the amount of GSTutrn-2 recovered (data not shown).
 - An experiment was carried out in which lysozyme (1mg/ml) was added to the cell cultures before sonication. This prevents denaturation of the fusion protein during sonication by facilitating cell disruption and allows the use of shorter sonication times. These changes did not increase the amount of GSTutrn-2 recovered in the final eluate (data not shown).
- 2 In order to increase the total amount of fusion protein synthesised: the induction time of the small scale preparation was increased from 1.5hr to 3hr. This resulted in a noticeable increase in the amount of protein synthesised (Fig 3.7) although most of it remains in the insoluble fraction.

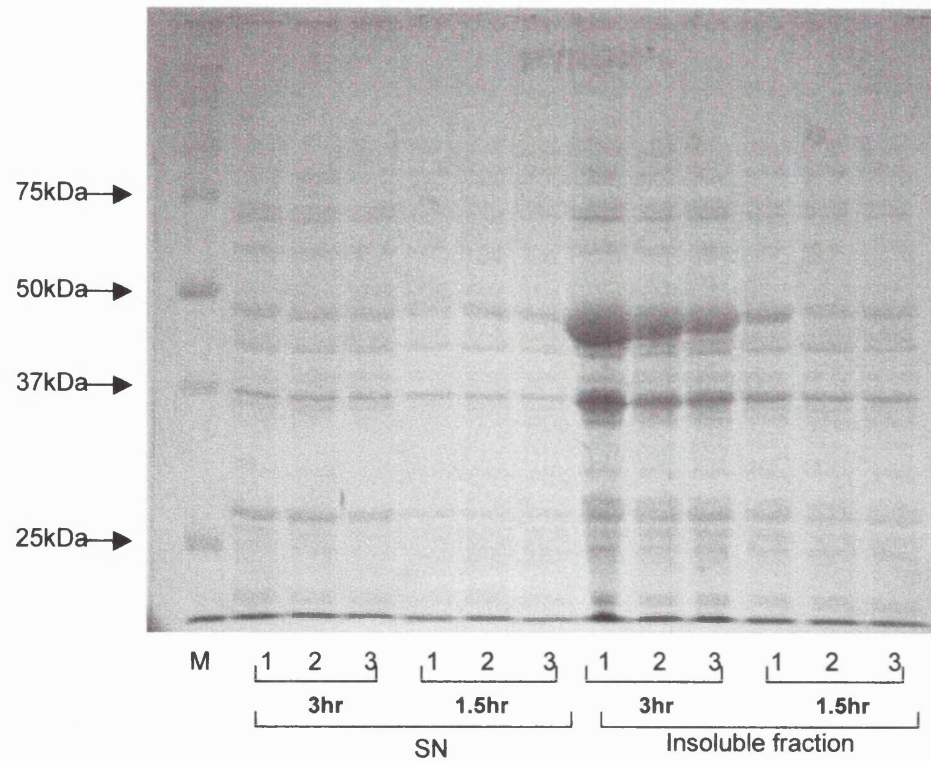


Fig 3.7 supernatants and pellets after sonication and precipitation of a small scale preparation of GSTutrn-2 using three different concentrations of IPTG: 0.1mM (1), 0.05mM (2) and 0.025mM (3) and either 3hrs or 1.5hr of induction. M: mw marker (Biorad).

3 Various strategies were tried to decrease the proportion of GSTutrn-2 in the insoluble pellet:

- The IPTG concentration was decreased from 0.1mM to 0.025mM (Fig.3.7). This decreased the amount of GSTutrn-2 in the insoluble pellet but increased the amount of GSTutrn-2 in the supernatant after sonication. A final concentration of 0.025mM was adopted for the subsequent experiments.
- An improved yield was achieved when the growing and induction temperature was decreased from 35°C to 32°C (data not shown) (Schein et al., 1990). A temperature of 32°C was adopted for the subsequent experiments.
- Addition of non-ionic detergents such as Triton X-100 before or after sonication was made to increase solubility. However, neither 1% or 0.1% Triton X-100 added before sonication resulted in an increase in the amount of purified GSTutrn-2 (Fig 3.8) but when Triton was added after sonication together with urea, the solubility of GSTutrn-2 increased. An experiment was carried out in which Triton X-100 (1% or 2% final concentrations) was added to the bacterial sonicates together with different concentrations of urea: 1M, 3M or 5M. The samples were incubated with rotation for 30 min at RT. The best results were achieved when using 1% Triton X-100 in combination with 3M urea (data not shown).

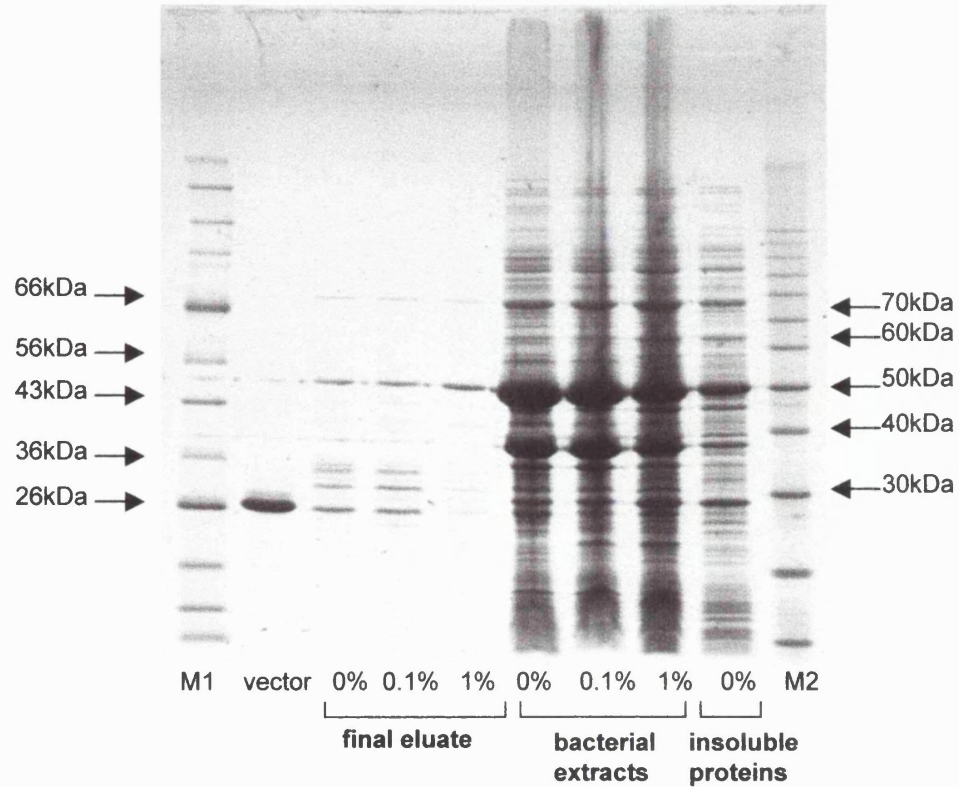


Fig 3.8 Small scale preparation of GSTutrn-2 treated with different Triton X-100 concentrations prior to sonication (0%, 0.1% and 1%). Vector =GST protein purified from a BL21 clone containing vector without insert cDNA. M1= mw marker (New England Biolabs); M2= 10kDa protein ladder (Gibco.BRL)

From these experiments, the following optimal conditions to produce GSTutrn-2 were adopted: grow cells at 32 °C, induce with 0.025mM IPTG for 3hr and treat the cultures after sonication for 30 min with 1% Triton x-100 and 3M urea.

These conditions were used in two small-scale preparations with Triton X-100 added to both but only one sample was treated with 3M urea. As shown in Fig 3.9, the amount of GSTutrn-2 (c.50kDa) in the supernatant plus 3M urea is greater than in the sample minus 3M urea. These conditions led to a much improved result compared to the earliest preparations (see Fig 3.5). However, by the time this was achieved, the immunisations and bleedings of the rabbits inoculated with utrn-1, utrn-3 and utrn-4 were completed and there was insufficient time to complete the preparation of the GSTutrn-2 antibody.

Analysis of the fractions collected during these small-scale preparations revealed a number of other prominent polypeptides in the total bacterial extracts and in the insoluble pellet. In particular, bands of 35kDa, 38kDa and 70kDa. These are likely to correspond to the *E.coli* chaperonins GrpE (Schönfeld et al., 1995) and DnaJ (Zylicz et al., 1985) and to the DnaK protein (Buchberger et al., 1996). These proteins have been shown to co-purify with GST fusion proteins (GST Gene Fusion System, Instructions booklet p 26) and make account for some of the weak non-specific bands seen in the affinity purified protein.

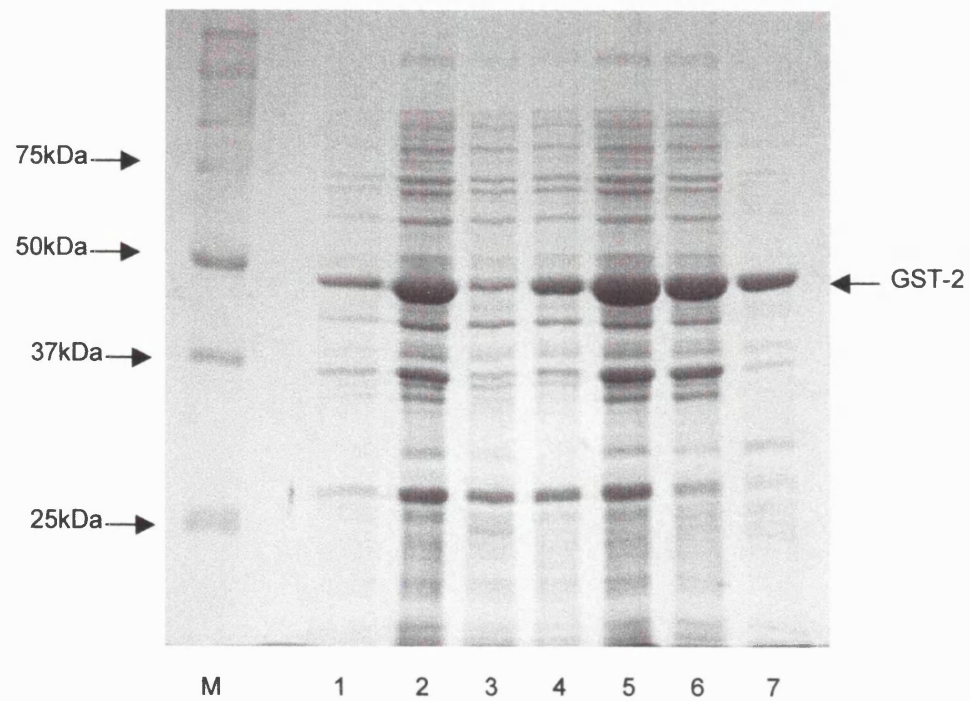


Fig 3.9 Small scale preparation of GSTutr-2 with and without 3M urea in the presence of 1% Triton X-100. 1=sample collected from the bacterial cultures after induction; 2=whole bacterial extract in PBS prior to sonication; 3 and 4=supernatant after sonication from sample not treated (3) and treated (4) with urea; 5 and 6=insoluble pellet from 3 and 4 respectively; 7=GSTutr-2. M=mw marker (Biorad).

3.4 Large scale production of GST-fusion proteins

It is estimated that 2.5mg of purified protein could be obtained from 1litre (l) of bacterial culture using the GST-system (GST Gene Fusion System instructions booklet, p. 11). For the large-scale production of GST-utrophin fusion proteins 1l or 2l culture volumes were routinely used. This procedure is described in detail in section 2.2 and as an "aide memoire" is shown diagrammatically in Fig 3.10.

The purified proteins and fractions collected at different stages of the purification procedure were analysed by SDS PAGE and Coomassie Blue staining. The utr-3 preparation is shown as an example in Fig. 3.11. Lane 1 represents the total protein content of the sonicated bacterial culture; the 50kDa band corresponds to GSTutr-3 fusion protein. The majority of GSTutr-3 remains in the supernatant after centrifugation (lane 2) but some is retained in the insoluble pellet (lane 3). Lane 4 is the supernatant after filtering through a 0.45 μ m filter and immediately prior to adding to the GST affinity column. The 50kDa polypeptide constitutes a major component of this fraction, approximately 5% of the total protein.

50ml of fraction 4 were applied to the GST affinity column and recycled twice. A small proportion of GSTutr-3 apparently did not bind and was collected in the first PBS wash (lane 6) but no further GSTutr-3 was collected in the second and third washes (lanes 7 and 8). 2.5 μ l and 5 μ l of a 1 in 10 dilution of the utr-3 eluate (total volume 500 μ l) after thrombin digestion are shown in lanes 11 and 12. After thrombin cleavage the protein designation loose their GST component and become utr-1 to 4. Thrombin digestion yielded

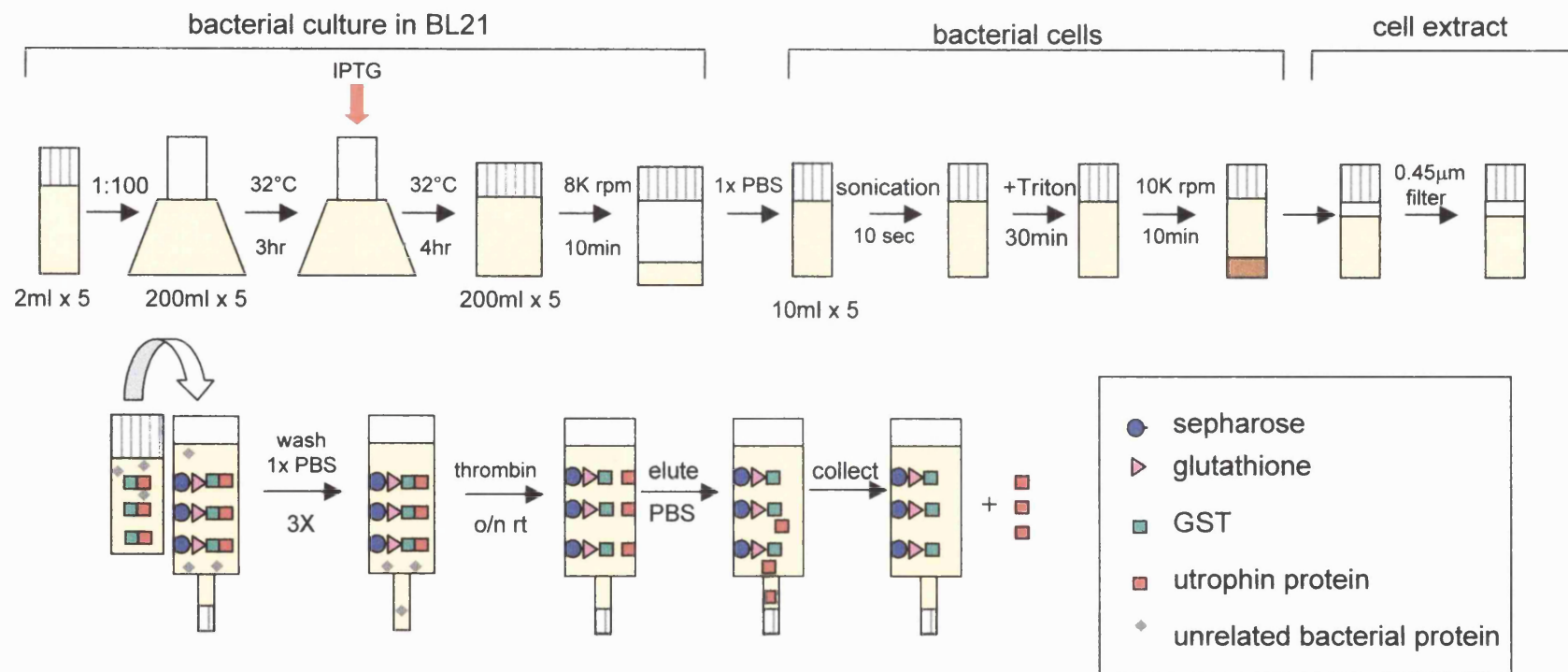


Fig 3.10 Diagrammatic representation of a large scale preparation and purification of GST-fusion proteins. o/n =overnight; rt=room-temperature; PBS=phosphate buffered saline; Triton=Triton X-100.

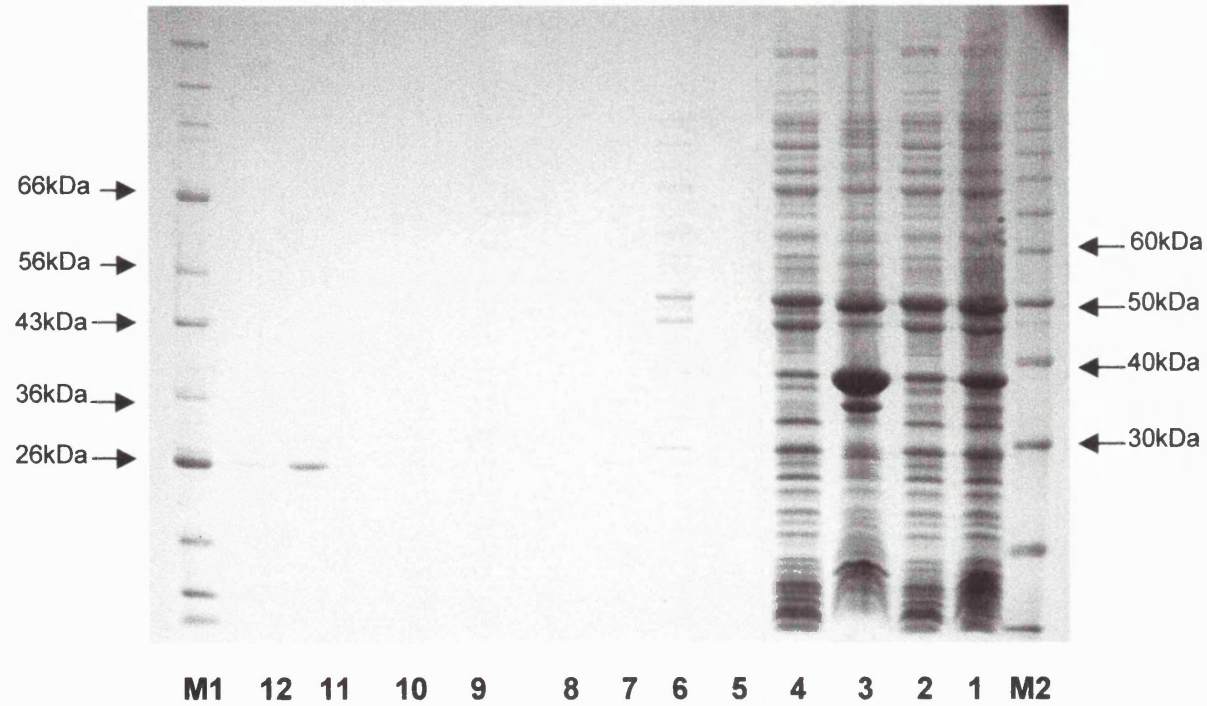


Fig 3.11 Large scale preparation of utrn-3. 2.5 μ l and 5 μ l of purified utrn-3 (lanes 12 and 11) and purified thrombin protein (lanes 10 and 9) and 10 μ l of a series of fractions collected at different stages of the preparation (lanes 1 to 8) were separated on a SDS PAGE and stained with Coomassie blue. M1 lane and M2 lane contain 20ul of New England Biolabs and Gibco BRL mw markers respectively.

a utrn protein of the correct mw of c. 24kDa. The calculated concentration of affinity purified utrn-3 was estimated spectrophotometrically as 5µg/µl. 2.5µl and 5µl of a 1 in 10 dilution of the purified thrombin protease protein were also loaded in the gel (lanes 9 and 10) to check whether these dilutions could be detected by Coomassie blue staining and whether they could contribute a band to those of the final eluate. As it turns out, these amounts were almost undetectable and did not appear to co-purify with utrn-3.

The same procedure was used to generate GSTutrn-1 and GSTutrn-4 fusion proteins. The concentrations of the affinity purified thrombin cleaved proteins were 10mg/ml for utrn-1 and 2.5mg/ml for utrn-4. Fig 3.12 shows 5 µg of each purified protein run on a SDS PAGE and stained with Coomassie blue; utrn-3 with a mw of 24kDa and utrn-4 with a mw of c.36kDa. Utrn-1 comprises two bands of 36kDa and 32kDa (the estimated mw for utrn-1 is 36kDa). Since the two bands appear only after thrombin digestion and were not apparent in the small-scale experiment (Fig.3.5), it was thought that there might be a weak recognition site for thrombin within the utrophin aa sequence. Examination of the aa sequence found a sub-optimal recognition motif (R K L L) 44 aa downstream of the thrombin cleavage site in the vector (the optimal sequence is P K L P₂ where P₂ is a non-acidic aa). If the sub-optimal sequence was being recognised by thrombin the mw difference between the two fragments would be 5kDa whereas the mw difference seen on Western blots is around 4kDa.

In order to investigate this further, the 36kDa and 32kDa bands from 5 µg of utrn-1 were separately excised from a SDS PAGE gel and eluted with PBS. The isolated bands were electrophoresed alongside a sample of utrn-1 which

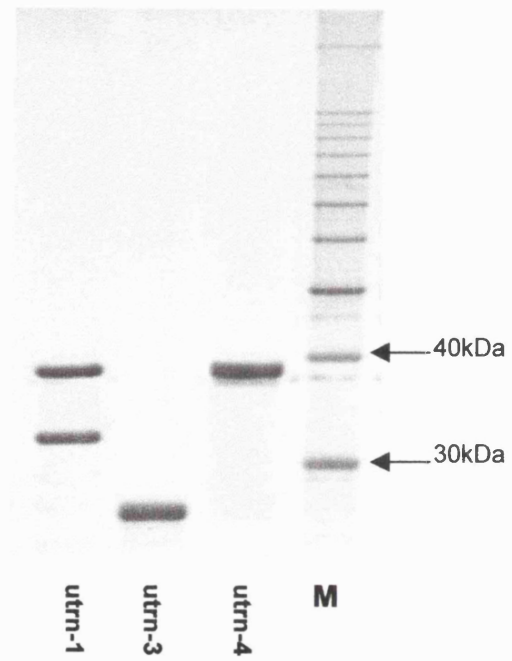


Fig 3.12 Purified utrn proteins after GST affinity chromatography and thrombin cleavage of the GST-utrn fusion proteins. M= mw marker (Gibco.BRL)

had not been eluted from a gel, and immunoblotted with two antibodies raised against the NH₂-terminus of utrophin; DRP2 (aa 1 to 261; Novocastra) and Mannut-1 (aa 113 to 371; Nguyen et al., 1995). The aa sequences used to raise these two antibodies overlap with that of utrn-1 (aa 24 to 320); therefore, both antibodies should detect both bands.

The results of this experiment were unexpected (Fig 3.13 A). Mannut-1 detected only the 36kDa band while DRP2 detected the 36Da and 32kDa bands. Interestingly, in the lane loaded with isolated 32kDa band lane, two bands of 36kDa and 32kDa are seen instead of a single 32kDa band. In Fig 3.13 B a second experiment was carried out; 500ng of utrn-1 were loaded and in this case Mannut-1 detected exclusively the 36Da band and DRP2 detected both the 36kDa and 32kDa bands. These experiments suggest that the two bands may represent two “conformations” of the same utrophin polypeptide.

The most likely explanation is that the 32kDa represents an intermediate “folded” form of GST-1 which cannot be detected by Mannut-1 because the aa sequence involved in the fold coincides with the binding site of Mannut-1, which must lie somewhere between aa 113 and 340. However, DRP2 interacts with a sequence, somewhere between aa 24 and 261 in utrn-1, that is available in both the “folded” and “unfolded” states. There is also the conversion of the fast mobility form “32kDa” to the “36kDa” form during electrophoresis (Fig 3.13 A lane 32kDa). It is difficult to explain how the 32kDa fast mobility polypeptide retains some structure in the presence of 0.5% SDS denaturing gel and suggests a very stable folding intermediate. Unfolding of most proteins is a two stage process with at least one folding intermediate involved (Creighton, 1997)

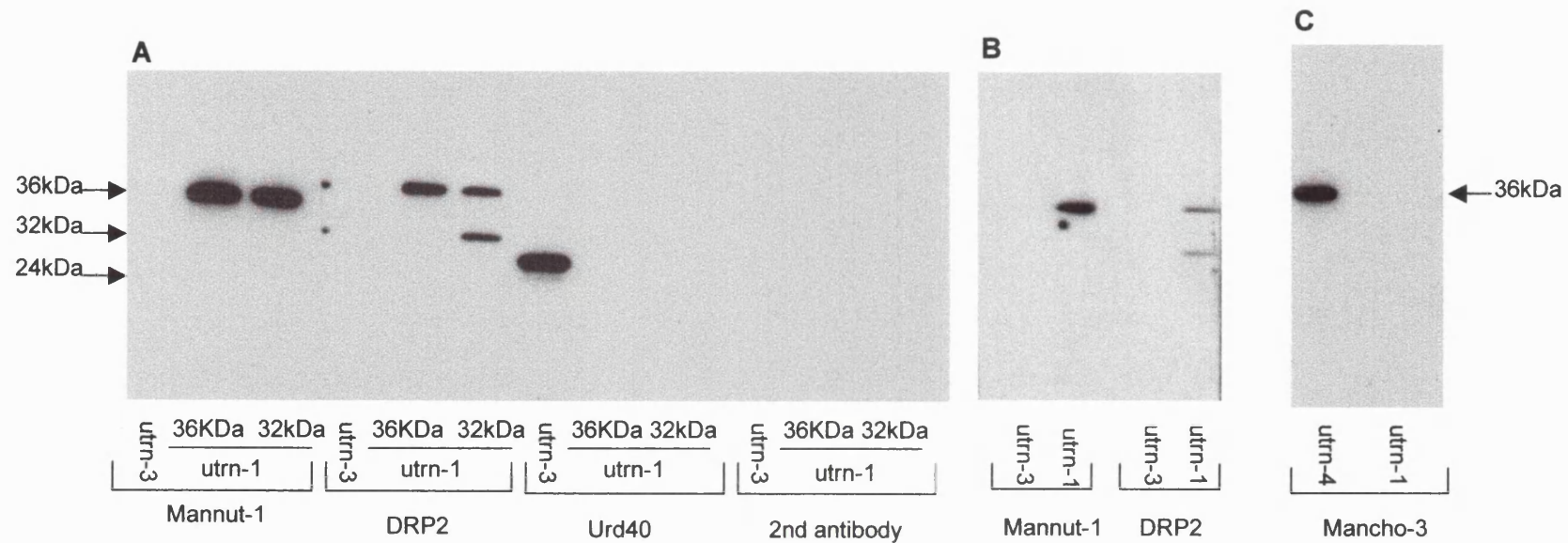


Fig 3.13 Western blots of purified proteins using utrophin specific monoclonal antibodies. A, the lower mw (32kDa) and higher mw (36kDa) bands that appeared after digestion of GSTutrn-1 with thrombin were run separately and probed with Mannut-1 and DRP2. utrn-3 was also run in this gel and was detected with Urd40. Incubation with second antibody failed to detect any band and confirmed the specificity of the antibody-antigen interactions. B, 500 ng of purified utrn-1 and utrn-3 probed with Mannut-1 and DRP2. C, purified utrn-4 and utrn-1 probed with Mancho-3.

and indeed monoclonal antibodies are used to study the conformational fluctuations of proteins (Creighton, 1997). There are several factors that may affect the shape of proteins on a SDS gel (and their electrophoretic mobility) and these include; presence of disulfide bonds, high proline content and very high or very low isoelectric points. An internal disulfide cannot form as there is only a single cysteine in utr-1; the proline content is not remarkable and the isoelectric point is 6.0 (neutral); so it is not obvious what factors lead to utr-1 folding.

To examine the specificities of utr-3 and utr-4, they were immunoblotted with the Urd40 and Mancho-3 antibodies which should detect utr-3 and utr-4 respectively. Exactly as might be expected Mancho-3 detected utr-4 but not utr-1 (Fig 3.13 C) and Urd40 detected utr-3 but not utr-1 (Fig 3.13 A).

3.5 Rabbit Immunisations

Antibodies were raised in New Zealand white rabbits by UCL Biological Services. 0.5mg of purified utr-1, utr-3 and utr-4 were used for the first immunisation and the boosts. To avoid numerical confusion in the animal house the rabbits were named "Cecilia", "Wendy" and "Yvonne" respectively. These antibodies were collectively named Mupa (mouse utrophin polyclonal antibodies). Particular attention must be paid to the naming of these antibodies and for their position in relation to the utrophin protein refer to Fig 4.2 A. The antibody raised against utr-1 corresponds to Mupa-1; however, because the GSTutr-2 preparation was not completed it was removed from the series and

the antibody raised against utr-3 corresponds to Mupa-2 and utr-4 antibody to Mupa-3.

The immune responses of the immunised rabbits were monitored by ELISA (for details see section 2.2). The pre-immune sera from all three rabbits did not recognise their corresponding utrophin antigens. This control was carried out to ensure that there were no immunoglobulins naturally present in the rabbits sera that could recognise utrophin.

The immune responses obtained with each utrophin protein were typical of a good humoral response. An example for the rabbit "Wendy" is shown in Fig 3.14. The primary response, after the first injection, was rather weak whereas the response to the second injection was dramatically different and antibody titres were remarkably higher. Antibody titre did not increase significantly after the 2nd and 3rd boosts. However, these repeated immunisations are necessary to obtain a highly specific antisera, since it is during this time that immunoglobulin class switching and affinity maturation occur (Delves, 1999).

3.6 Isolation of immunoglobulins from serum

Immunoglobulins were isolated from the serum of each of the immunised rabbits by repeated sodium sulphate precipitation, as described in chapter 2, section 2.2. The final precipitate was resuspended in 10 ml of PBS. The yield of IgG was calculated by spectrophotometric reading of the OD of the resuspended IgG solution at 280nm and 260nm. The yield of IgGs from the "Cecilia" serum was 12mg/ml, 8mg/ml for "Wendy" and 5.5 mg/ml for "Yvonne".

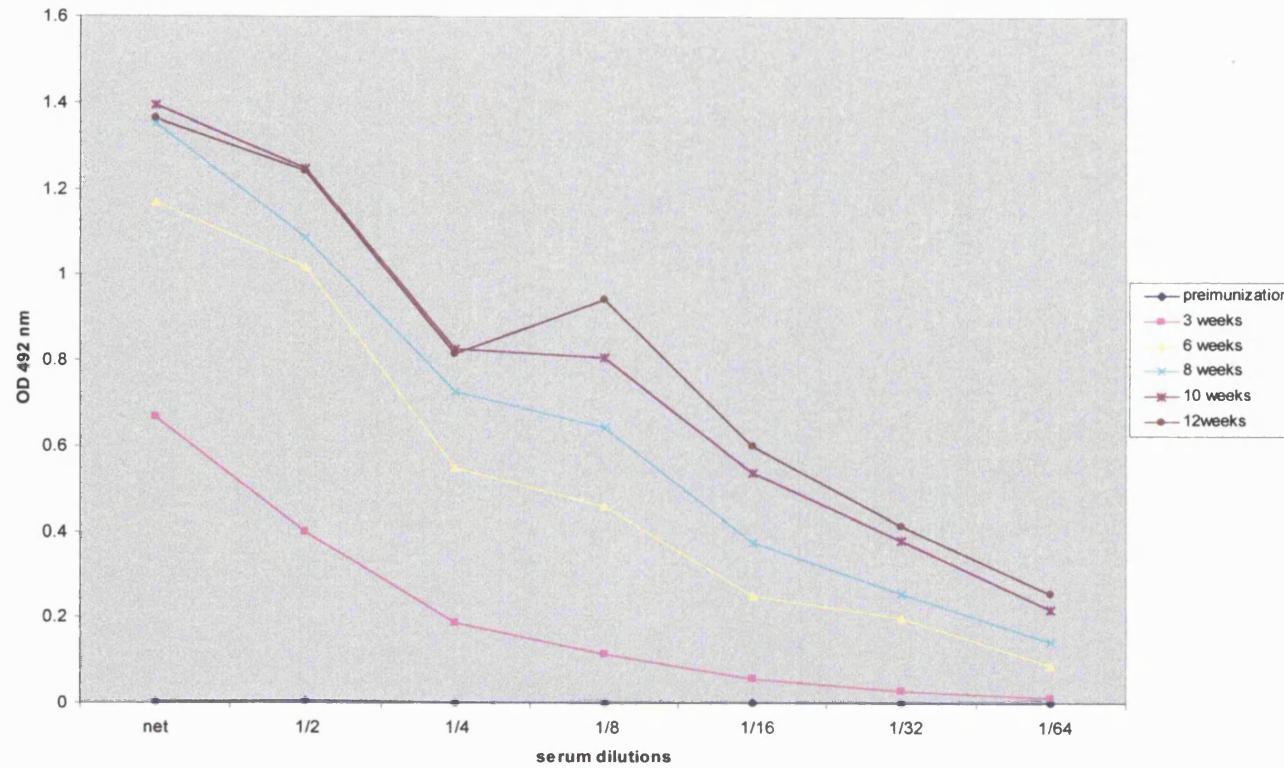


Fig 3.14 The immune response of a rabbit immunised with utr-3 monitored by ELISA. This graph shows the OD 492nm (peroxidase activity) of serial dilutions of the rabbit serum. Each curve represents a test bleed taken prior to each boost at a number of weeks (see key) from the first immunisation.

An aliquot (10 μ l) of the isolated IgGs and 1 μ l of the various supernatants from the sodium sulphate precipitations were run on an SDS PAGE and visualised by Coomassie blue staining; for example, Fig 3.15 shows the purification of IgGs from “Wendy” serum. For comparison, 10 μ l (1 μ g/ μ l) of commercial rabbit IgGs were run next to 10 μ l of a 1 μ g/ μ l dilution of the purified IgGs from “Wendy”. A major band of 50kDa , which represents the IgG heavy chain, can be seen in both lanes together with a smear in the region of 25kDa which corresponds to the IgG light chain. Bands corresponding to IgGs could not be seen in the lanes containing 1 μ l of a 1/10 dilution of non-precipitated proteins (SN 1, 2 and 3) whereas albumin (66kDa) was visible in these fractions at around 1mg/ml (estimated by comparison to serum albumin standards).

3.7 Affinity purification

The anti-utrophin IgG preparations were further purified by affinity chromatography. Affinity columns were prepared by immobilising the immunising antigens to AminoLink® or SulfoLink ® coupling gels (Pierce). Mupa-1 and Mupa-2 were purified using the corresponding thrombin cleaved utrn proteins and AminoLink® whereas Mupa-3 was purified using the fusion protein GSTutrn-4 coupled to SulfoLink ®, in order to take advantage of the four cysteine residues present in the GST tag for coupling the antigen to the affinity gel. The detailed procedures for both systems are described in chapter 2 section 2.2. As an example, the purification of specific IgGs from rabbit “Wendy” (antibody Mupa-2) are illustrated in Fig 3.16 A.

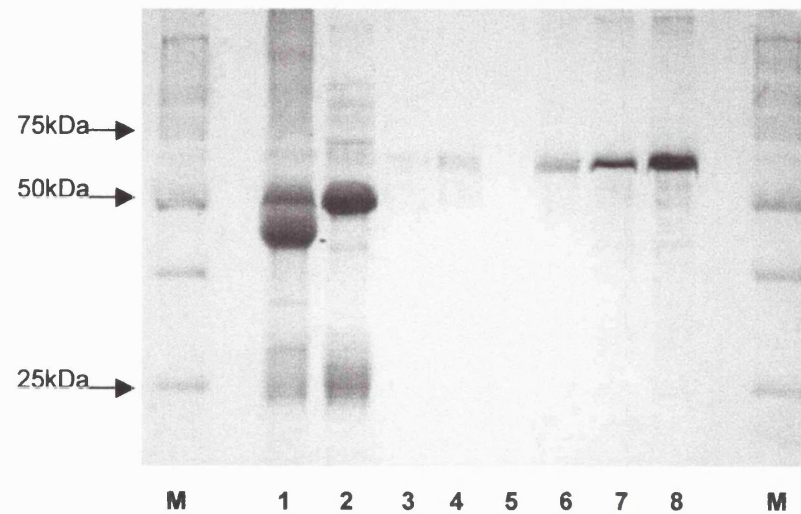


Fig 3.15 SDS PAGE stained with Coomassie blue showing: lane 1= 10 μ g of commercial rabbit IgGs; lane 2= isolated "Wendy's" IgGs (10 μ l of a 1 μ g/ μ l dilution) . lanes 3, 4 and 5 correspond to the supernatants 1 to 3 after sodium sulphate precipitation. lanes 6, 7 and 8 correspond to 1 μ g, 3 μ g and 5 μ g of bovine serum albumin. M1=mw marker (BioRad).

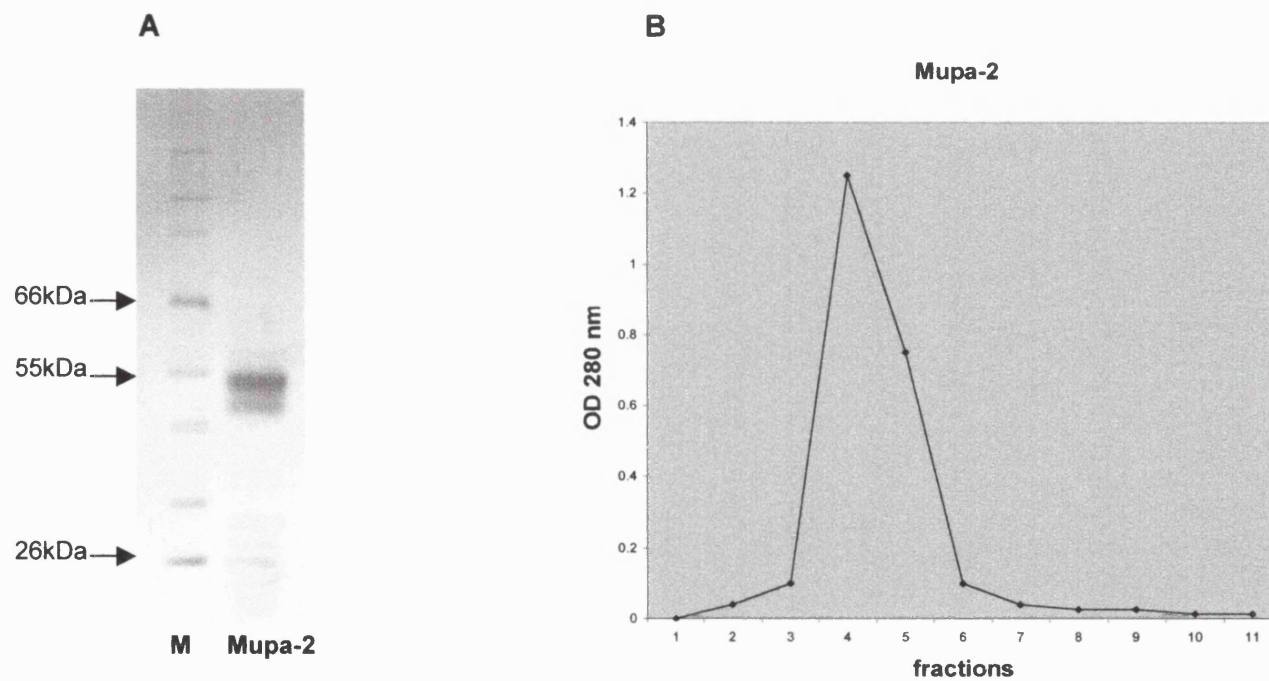


Fig 3.16 A, 10 μ g of affinity purified Mupa-2 electrophoresed on SDS PAGE and stained with Coomassie blue.
 B, Affinity purification of Mupa-2. The OD at 280nm for each of the fractions (1ml) eluted from the affinity column are shown.
 Fractions 3,4,5 and 6, which contain the specific antibodies, were selected and pooled together.
 M= mw marker (New England Biolabs).

The protein content of the collected fractions (10 fractions of 1ml) after affinity purification was estimated by measuring the OD at 280nm. These results for Mupa-2 are shown in Fig.3.16 B. Fractions 3,4, 5 and 6 contained most of the protein; these were pooled and dialysed against 1 x PBS. A total of 2.2 mg of Mupa-2 were purified from 28mg of total IgGs; 4.4 mg of Mupa-1 from 48 mg of total IgGs and 2.6mg of Mupa-3 from 22mg of total IgGs. The proportion of antigen specific antibodies within a polyclonal pool is around 10% (www.biotech.iastate.edu). The purified antibodies were aliquoted and stored at -70°C .

The results of the experiments using these antibodies on Western blots and immuno-histochemistry are described in chapters 4 and 5 respectively.

Discussion

3.8 General comments

There are numerous bacterial expression systems available for the large scale *in vivo* synthesis of protein as a fusion protein. In addition to the GST fusion system used in this study, the most commonly used are those in which proteins of interest are fused to His₆ or MBP (maltose-binding protein). His₆ fusion proteins are purified by metal affinity chromatography (e.g. TALON resin, Clontech; HiTrap resin, Amersham Pharmacia Biotech). Fusion to His₆ has the advantage that this tag does not need to be removed prior to immunisation because it is only poorly immunogenic and does not interfere with the structure of the fusion-partner.

The MBP system has been previously used to generate a utrophin specific antibody; the COOH-ter antibody (Lumeng et al., 1999) was raised against a utrophin-MBP fusion protein produced by cloning a COOH-terminal sequence into the pMAL-c vector (New England Biolabs, Beverley, MA). MBP-utrophin fusion proteins are purified by binding to an amylose affinity resin. It has been shown that fusion to MBP enhances the solubility of some proteins expressed in *E.coli* (Kapust et al., 1999). It may be sensible in future work to try this vector for the synthesis of GST-2 which was problematic because of its low solubility in the pGEX-4T-1 vector.

Another expression system that could be used to synthesise GST-2 is the Trx system (Novagen) in which the fusion tag is *E.coli* thioredoxin (trxA). It

has been shown that linkage to thioredoxin dramatically increases the solubility of otherwise insoluble proteins in *E.coli* (LaVallie et al., 1993).

It was unfortunate that the synthesis of GST-2 failed since an antibody raised against this region of utrophin (aa 564 to 755) would have been extremely useful on Western blots allowing the detection of full-length utrophin without crossreaction to other actin-binding proteins.

An interesting new protein expression system is the IMPACT system (New England Biolabs) which takes advantage of protein splicing. The expression vector in the IMPACT system contains adjacent sequences coding for an engineered intein (derived from *Saccharomyces cerevisiae* VMA intein) and for a chitin-binding domain from *Bacillus circulans* upstream of the cloning site. (Perler et al., 1994; Chong et al., 1998). The three part fusion protein is purified by binding to a chitin resin. Thereafter, the target protein is released by addition of DTT or β -mercaptoethanol which induces the intein to undergo self-cleavage. Thus, the protein of interest is recovered without the need for protease digestion. Protease digestion sometimes results in the non-specific cleavage of the target protein although this was not a problem in this particular study.

In general, the GST-fusion system proved to be adequate to produce the utrophin fusion proteins (with the exception of GST-2). However, since large amounts of purified protein (12mg) were required for immunisations and affinity purification it would have been an advantage to obtain a higher yield of fusion protein in all cases. As it was, several large scale preparations were necessary to achieve the appropriate amount. The manufacturers estimated yield of the GST-fusion system is 2.5mg per litre of initial bacterial culture (although it varies

from a protein to another). This figure is well below the yield that is claimed for the pMAL-MBP system (New England Biolabs) of 100mg per litre.

3.9 Thoughts on antibodies purification methods

A variety of methods for the purification of immunoglobulins have been described. These include; diethylaminoethyl (DEAE) ion exchange chromatography, which separates immunoglobulins from other serum proteins; gel filtration chromatography, which is most useful for separating IgM class immunoglobulins based on their larger size; affinity chromatography using immobilised protein A (derived from *Staphylococcus aureus*) or protein G (derived from β -haemolytic streptococci). Both affinity resins are very effective in the purification of rabbit antibodies and are good choices when the amount of pure antigen is limited.

In the present study, I chose to use a combination of sodium sulphate precipitation and antigen specific affinity chromatography. Sodium sulphate precipitation is useful for concentration of the anti-serum and yields a mixed pool of immunoglobulins of which c. 10% are specific for the antigen.

For the affinity chromatography, the solid support is usually sepharose carrying different chemical modifications depending on the particular affinity system. Some of the most widely used affinity resins are cyanogen bromide (CNBr) activated sepharose and N-hydroxy-succinimide –sepharose (NHS) both of which bind proteins via primary amines.

To obtain good quality antibodies which would give minimal background on Western blots and immuno-histochemistry, we decided to affinity purify the

Mupa polyclonal antibodies. After careful consideration of the advantages and disadvantages offered by each of the different coupling gels mentioned above, it was decided to use AminoLink® and SulfoLink® (Pierce) because both had been used to purify similar antibodies, e.g. Urd40 (Blake et al., 1999) and their binding capacities were reasonable. The advantage of SulfoLink® over AminoLink® is that in the first method the four cysteine residues present in the GST tag can be used to bind to the gel (it is not necessary to remove the tag from the immunogen) and it does not require handling of cyanoborohydride which is toxic. In all cases, affinity purification of the Mupa antibodies resulted in the expected yields and quality of specific IgGs.

Chapter 4

Western blots and 5' RACE

Results

Western blots

4.1 General comments

While there is good evidence that the short utrophins are transcribed (Schofield et al., 1993; Blake et al., 1995; Wilson et al., 1999; Lumeng et al., 1999) it remains unclear whether these transcripts are translated into protein, whether RNA and protein levels are correlated and whether all of the short utrophin isoforms have been identified. If short utrophin isoforms are present, it will be important to establish the profile of isoforms present in each tissue. In order to look for polypeptides corresponding to the utrophin mRNAs and to resolve some of these questions a series of Western blots were carried out using the newly synthesised antibodies described in chapter 3. Blots from SDS PAGE gels were used so that the polypeptides could be distinguished from each other by size.

Western blotting was carried out using Mupa-1, Mupa-2, Mupa-3 polyclonal antibodies (chapter 3). The positions of the aa residues used to raise each of these antibodies are shown in Fig 4.2 A. Two antibodies not made in our laboratory were also used, these were Mancho-3 and Urd40 (Table 2.3). Mancho-3 was raised in mouse against the last 329 aa of the human utrophin protein (Nguyen et al., 1991). Our early experiments with this antibody showed that it is not totally reliable on Western blots because it crossreacts with a set of

low molecular weight (mw, 66 to 24 kDa) mouse proteins. However, it does detect utrophin polypeptides, does not crossreact with dystrophin and in a comparative analysis is a useful resource. Urd40 is a polyclonal antibody raised in rabbit against a fusion protein that contained aa 2519 to 2867 of mouse utrophin. This antibody had been pre-absorbed against the corresponding dystrophin fusion protein (Blake et al., 1999) prior to use. Mupa antibodies are not pre-absorbed against dystrophin because preliminary experiments showed that at dilutions lower than 1 in 250 there was no crossreactivity with dystrophin (dilutions of 1 in 750 and 1 in 1000 were routinely used). The positions of three further antibodies, K5B1 (Fabbrizio et al., 1995), COOH-ter, (Lumeng et al., 1999) and Ut43 (Knuesel et al., 2000) used in immunoblot analysis of utrophin by other groups are also shown in Fig 4.2 A.

SDS-denatured tissue extracts were prepared from freshly killed adult C57Bl and UKO^{ex6} mice and embryos (14.5 to 16.5 dpc) (section 2.2). Equal amounts of protein were extracted in the same volume of SDS dissolving buffer and the amount of protein in each extract was checked by SDS PAGE and Coomassie blue staining; an example is shown in Fig 4.1. Immunoblots were also stained with Ponceau S immediately prior to blocking and incubation with the primary antibody.

In order to confirm that positive immunoreactivity seen on the blots was due to interaction with primary antibodies, identical gels were incubated in the presence or absence of each of the primary antibodies before incubation with the second antibody. The blots treated with second antibody alone showed no immunoreactive polypeptides in all cases; this experiment for Mupa-2 is shown as an example in Fig 4.3.

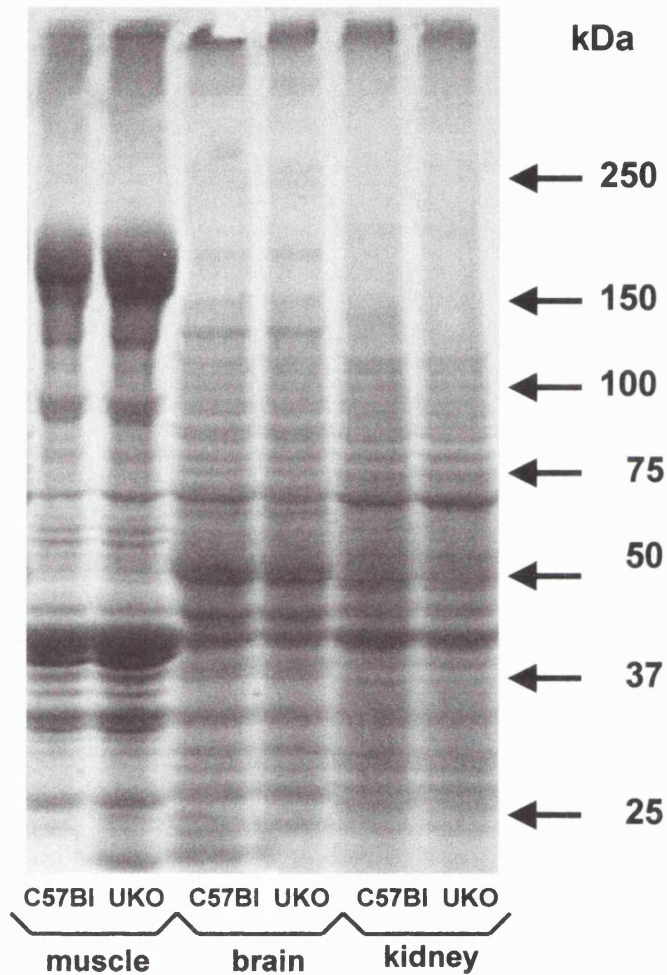


Fig 4.1 SDS PAGE gel of adult C57BI and UKO^{ex6} (UKO) mouse tissue extracts stained with Coomassie blue. Tissues were extracted at a standard wt/vol relation of tissue and extraction buffer. Equal amounts (20 μ l) were loaded on the gel. Markers (not shown) were BioRad precision broad range size standards and their positions on the membrane were recorded prior to staining

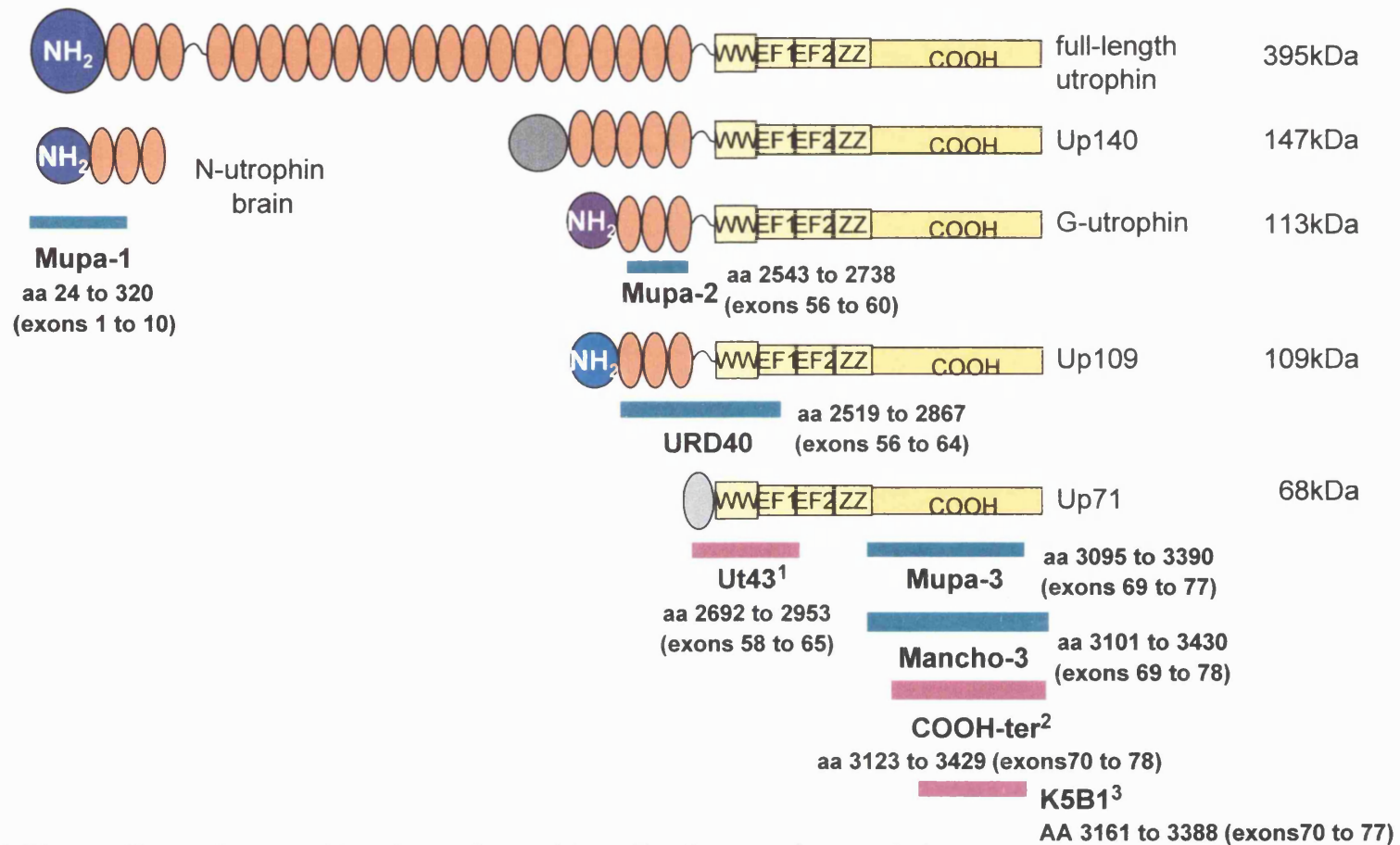


Fig 4.2 A The positions of aa used to raise anti-utrophin antibodies are shown relative to the known utrophin isoforms (green boxes). The corresponding positions for other antibodies referred to in the text are also shown (purple boxes). 1: Knuesel et al. (2000); 2: Lumeng et al. (1999); 3: Fabrizio et al. (1995).

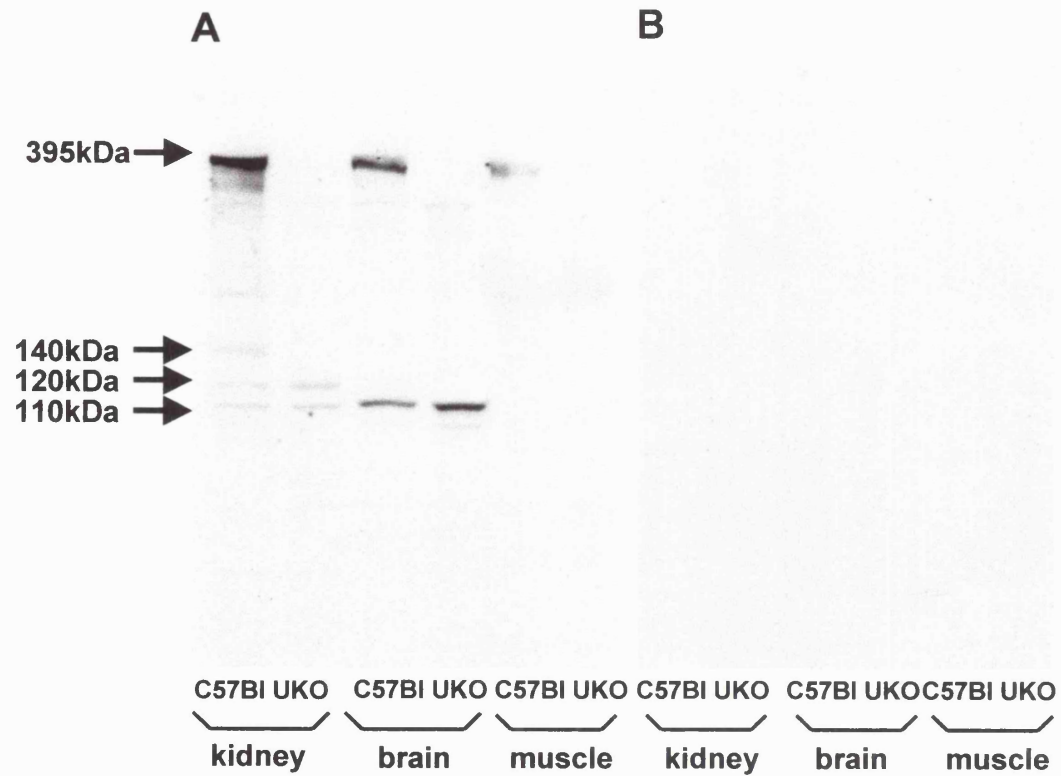


Fig 4.3 Western blot of C57BI and UKO^{ex6} (UKO) adult mouse protein extracts. A, using Mupa-2 antibody and B, in the absence of Mupa-2

It was immediately obvious that each of the various antibodies detected a number of bands, some of which were difficult to interpret. It was decided that to aid the interpretation of Western blots, the bands detected with each antibody would be classified according to whether they were present in control and/or UKO^{ex6} tissues and whether they were detected with one or more antibodies. This rationale is summarised in Table 4.1. Category A contains bands detected only in control tissues that are not full-length utrophin (395kDa) but are detected by more than one antibody. It is most likely that these bands represent degradation products of full-length utrophin although they could also represent short isoforms that are not expressed in UKO^{ex6} mice in the absence of full-length utrophin. This latter seems relatively unlikely since the short isoforms appear to be transcribed from distinct promoters embedded within genomic sequence adjacent to the transcription start site and their transcription is not likely to be affected by loss of full-length protein.

Category B contains bands that are larger than 65kDa, detected in control and UKO^{ex6} tissues but only with a single antibody. 65kDa was chosen as a reference mw because polypeptides of that size and larger would be detected not only by Mupa-3 and Mancho-3 but also by Urd40.

If such bands are detected only by a single antibody, the most likely explanation is that they are the result of crossreactivity of that particular antibody with non-utrophin protein(s) in one or more tissues (see Fig 4.2 B which shows the estimated minimum sizes of utrophin polypeptides that could be detected by the Mupa antibodies, Urd40 and Mancho-3).

category	criteria	symbol	interpretation	example
A	expressed in C57Bl only, <395kDa, & detected with more than 1 antibody	§	utrophin 395 kDa degradation products	140kDa Fig.4.4
B	expressed in C57Bl & UKO ^{ex6} , >65kDa detected with a single antibody	†	cross-reactivity with non-utrophin protein	260kDa Fig.4.4
C	expressed in C57Bl & UKO ^{ex6} , <65kDa detected with a single antibody	‡	cross-reactivity or short utrophin isoform	50kDa Fig.4.11
D	expressed in C57Bl & UKO ^{ex6} , detected with more than 1 antibody	*	short utrophin isoform	120kDa Fig.4.4

Table 4.1 Criteria for the classification of polypeptides detected on Western blots. The symbols shown are used to indicate this classification on the blots

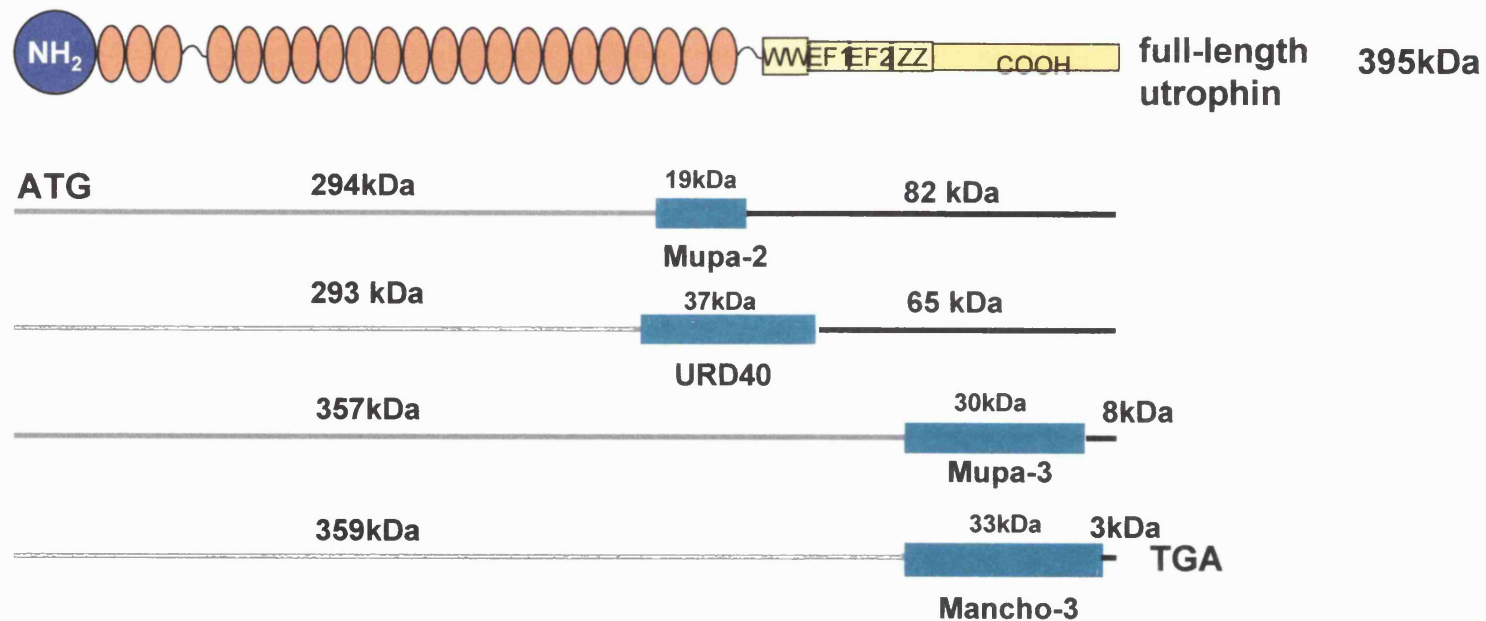


Fig 4.2 B Estimated minimum sizes of polypeptides that could be detected with each of the C-terminal antibodies (green boxes). Those polypeptides translated from full-length utrophin ATG are represented as solid grey lines and C-terminal isoforms are represented as solid black lines. Calculations were made using the program "pepstats" and full-length utrophin aa sequence and considering that at least 20aa of these polypeptides should be contained within the sequences used to raise each of the antibodies in order to be detected by each antibody. The difference between 395kDa (full-length utrophin mw) and the addition of the two mw given for each antibody represents the mw of the polypeptides used to raise each antibody and are shown in small font above each antibody.

Category C contains those bands detected in control and UKO^{ex6} tissues, smaller than 65kDa and detected with only one antibody. COOH-terminal isoforms of that size would only be detected by Mupa-3 and Mancho-3 but are too small to be detected by Urd40 or Mupa-2. In this category is difficult to be certain whether bands detected only with the most COOH-terminal antibodies represent a genuine short utrophin isoform or are the result of crossreactivity of Mupa-3 and Mancho-3 with a protein different to utrophin.

Finally, in category D were placed those polypeptides that are detected in control and UKO^{ex6} tissues with more than one antibody, in a reproducible manner. Amongst the different categories of bands these are the only firm candidates for short utrophin isoforms and were the focus of attention in this study.

Examples of polypeptides belonging to each category are shown in Figs 4.4 to 4.12 and explained in detail. I would like to emphasise that this approach is not strict and exclusive but merely a strategy to identify and acknowledge bands of interest and to simplify the analysis by discarding bands that are non-specific or uncertain in origin.

The banding patterns in a variety of tissues were examined. On the basis of the band classification and information obtained from previous and published RNA studies (Schofield et al., 1993; Blake et al., 1995; Wilson et al., 1999; Lumeng et al., 1999) a few tissues were selected for a detailed analysis. These were kidney, brain, muscle, testis and foetal hands.

4.2 Western blot analysis of a selection of tissues

Kidney Kidney shows a very interesting pattern of polypeptides and illustrates well the complexity of the Western blotting results. Fig 4.4 A shows the analysis of extracts of adult mouse kidney incubated with all the different antibodies. Fig 4.4 B shows 16.5 dpc kidney extracts incubated with Mupa-2 and Mupa-3. Full-length utrophin (395 kDa) is abundant in both control adult and foetal kidney and is detected with Mupa-1, Mupa-2, Urd40, Mancho-3 and Mupa-3; this isoform is absent from UKO^{ex6} kidney. It was noticeable that Mupa-1 and Mancho-3 gave less intense staining of the 395kDa band than the other antibodies. Adult kidney shows the highest levels of full-length utrophin amongst the tissues analysed followed by lung (Fig 4.4 C) and liver (not shown). Full-length utrophin is less abundant in foetal kidney than in adult kidney, this may suggest that full-length utrophin expression increases with development. In addition to full-length utrophin, several other polypeptides of mw between 260kDa and 110kDa were consistently seen and were classified according to the criteria shown in Table 4.1.

The polypeptide detected only with Mupa-1 of mw c. 260kDa is seen not only in kidney but is also detected in other tissues including lung, brain, liver, heart and muscle. This band was placed in category B and protein databases were searched for possible sequence homologies with utrophin aa 24 to 320, used to raise Mupa-1. This search revealed that β -spectrin (erythrocytic and non-erythrocytic) shows relatively high similarity to the NH₂-terminus of utrophin across several stretches of approximately 10 to 20 aa that could well constitute epitopes for Mupa-1 recognition (Fig 4.5). This was not unexpected since

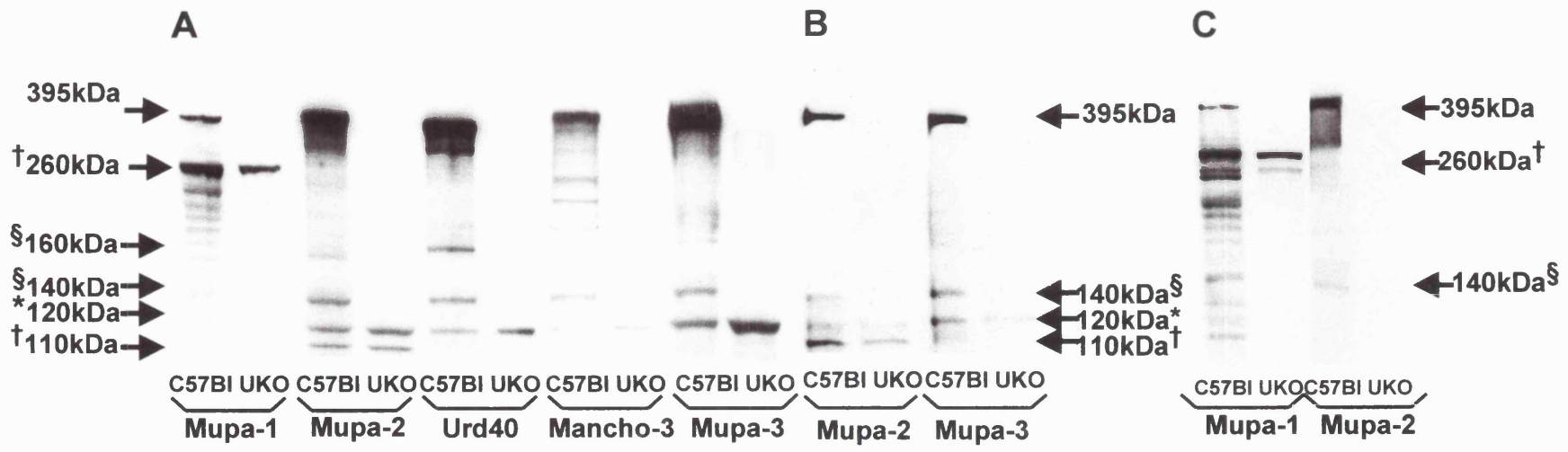


Fig 4.4 Western blot analysis of kidney and lung extracts of C57BI and UKO^{ex6} mice (UKO). A, adult using Mupa-1, Mupa-2, Mupa-3, Urd40 and Mancho-3 antibodies. B, 16.5dpc embryos using Mupa-2 and Mupa-3 antibodies. C, adult lung extracts immunoblotted with Mupa-1 and Mupa-2.
 § category A, †category B, *category D (Table 4.1)

```

Utrophin : 4  SDEHNDVQKKTF TKWINARFSKSGKPPISDMPXXXXXXXXXXXXXXXXXXXXXXXXXPKR-RGS 62
+DE VQKKTF TKW+N+ ++ I+D++ PK +G
β-spectrin: 49 ADEREAVQKKTF TKWVNSHLARVSCR-ITDLYTDLRDGRMLIKLLEVLSCERLPKPTKGR 107

Utrophin: 63  TRVHALNNVNVFLQVLHQNNVDLVNIGGTDIVAGNPKLTLGLLWSIILHWQVKDVMKDIM 122
R+H L NV++ LQ L + V L N+G DIV GN +LTLGL+W+IIL +Q++D+ +
β-spectrin: 108 MRIHCLENVDKALQFLKEQRVHLENMGSHDIVDGNHRLTLGLIWTIILRFQIQDISVETE 167

Utrophin: 123 SDLQQTNSEKILLSWVRQTTTRPYSQVNVLNFTTSWTDGLAFNAVLHRHKPDLFDWDEMVK 182
+ ++ +++ LL W + T Y VN+ NFTTSW DG+AFNA++H+H+PDL D+D++ K
β-spectrin: 168 DNKEKKSARDALLWCQMKTAGYPNVNIHNFTTSWRDGMAFNALIHKHRPDLIDFDKLLK 227

Utrophin: 183 MSPIERLDHAFDKAHTSLGIEKLLSPETVAVHLPDKSIIIMYLSLF 229
+ L +AF+ A LG+ KLL PE ++V PD+KSII Y+ + +
β-spectrin: 228 SNAHYNLQNAFNLAEQHLGLTKLLDPEDISVDHPDEKSIITYVVTYY 274

```

Fig 4.5 aa alignment between mouse utrophin aminoacids

24 to 320 used to raise Mupa-1 and mouse β -spectrin, non-erythroid (accession: Q62261). The areas in blue indicate aa sequences where there is some similarity between the two proteins. += conservative substitution x= residue masked by BLAST to prevent artefactual hits - =insertion or deletion of a single aa

β -spectrin and utrophin are both members of the dystrophin/spectrin superfamily (Tinsley et. al, 1993). Mouse β -spectrin non-erythrocytic (the murine homologue of the human β -spectrin non-erythrocytic 1) is the best candidate for this polypeptide since its molecular weight is 274kDa. α -actinin is another member of the dystrophin/spectrin superfamily but was excluded from considerations since it has a mw of 103kDa. β -spectrin is most abundant in brain and is also expressed in kidney and in all tissues in which a band of this size is detected by Mupa-1 including lung, muscle and heart.

While the likelihood of the 260kDa band being β -spectrin is high, the alternative explanation that it is a novel utrophin isoform with the same NH₂-terminus but terminating prior to the aa sequence corresponding to Urd40 and Mupa-2 might be considered. An argument against this view is that if this hypothetical novel transcript contained sequence corresponding to the targeted exon in UKO^{ex6} mice it would not be translated in UKO^{ex6} samples as is the case for full-length utrophin. Furthermore, no evidence of such an unusual isoform was found by RT-PCR (chapter 5 section 5.3).

The 110kDa polypeptide detected in adult and foetal kidney (Fig 4.4) by Mupa-2 only was placed in the same category as the 260kDa band (category B). However, in this case no good candidate proteins were identified in the protein databases which could be responsible for crossreactivity. Such a candidate may emerge as data analyses from the Human Genome Sequencing project are completed.

Bands of 160kDa and 140kDa are detected with all the antibodies but occur only in control tissue. These bands are interpreted as degradation products of full-length utrophin (category A) since they are absent in UKO^{ex6}

kidney and other UKO^{ex6} tissues, but are detected in kidney and all control tissues rich in full-length utrophin. If this interpretation is correct then it suggests that degradation occurs in such a way that the breakdown products retain the actin binding domain intact and are preferentially detected with Mupa-1. A ladder of bands is also seen in association with the 260kDa component which suggests that β -spectrin is also susceptible to degradation. As might be predicted, in this case, breakdown products are also seen in UKO^{ex6} samples where β -spectrin is expressed as in control tissues.

Another weak possibility is that the 160kDa and 140kDa bands are genuine short utrophin isoforms (Up140 predicted mw is 147 kDa) which are lost in the absence of full-length utrophin. This could be explained if for example they were involved in a membrane protein complex alongside full-length utrophin and the DAPs; when the complex no longer assembles, as in UKO^{ex6} mice, these isoforms are no longer stable and degrade. This hypothesis seems unlikely because the 140kDa/160kDa bands are detected, albeit weakly, by Mupa-1, the NH₂-terminal antibody, (Fig 4.4 A and C). Genuine short isoforms, would not contain the epitope corresponding to the actin-binding domain, whereas some breakdown products of full-length utrophin might contain such sequences. Thus, the best explanation is that these bands are degradation products of full-length utrophin but other scenarios cannot be excluded.

One band of 120 kDa was placed in category D (Fig 4.4 A and B) as a promising candidate for short utrophin isoform. This band was detected with all the antibodies except for the NH₂-terminal antibody Mupa-1 and was consistently present in both control and UKO^{ex6} adult and foetal kidney. It was not detected in any other tissue and thus appears to be a short utrophin isoform

that is kidney specific. A band of similar mw was reported by Nguyen et al. (1995) in a kidney derived cell line (COS) extract and by Rafael et al. (1999) in the kidney of the double dystrophin/utrophin knock-out mouse (dko^{ex6}) using Mancho-3. In their illustration the 120 kDa band is missing from the control kidney. However, careful scrutiny of Figs shown in Loh et al. (2000) finds a component of c. 120kDa in control kidney extracts after immunoprecipitation with Urd40.

It is interesting to note that in the adult kidney (Fig 4.4 A), this 120kDa polypeptide appears upregulated in UKO^{ex6} compared to the control sample and this is most evident with Urd40 and Mancho-3. 5'RACE was carried out in an attempt to isolate the transcript corresponding to this short isoform from adult kidney. These experiments are described later in this chapter in sections 4.4 and 4.5.

In summary, immunoblot analysis of mouse kidney extracts suggests that at least two different utrophin proteins might be co-expressed in this tissue, full-length utrophin and a 120kDa novel short utrophin isoform.

Brain Expression of full-length utrophin RNA and protein in the mouse brain is well documented (Blake et al., 1995; Khurana et al., 1992; Kamakura et al., 1994; Lumeng et al., 1999). There is good evidence from mRNA *in situ* hybridisation experiments and Northern blotting for the presence of the short transcript, G-utrophin, in specific areas of the mouse and rat brain and in the trigeminal and dorsal root-ganglia (Blake et al., 1995; Knuesel et al., 2000). There is also some data from RT-PCR about the expression of Up140 and Up71 in adult and foetal mouse and human brain (Wilson et al., 1999).

However, information about whether these transcripts are being translated in neuronal tissues is controversial. Fabbri et al. (1995) and Lumeng et al. (1999) both reported bands on immunoblots which could correspond to Up71. These occur in rabbit sciatic nerve and mouse brain extracts respectively and were detected using two different anti-human and anti-mouse COOH-terminal antibodies, K5B1 and COOH-ter respectively (see Fig 4.2 A). The authors did not detect G-utrophin in these tissues. In contrast, Knuesel et al. (2000) detected high levels of a polypeptide, the correct size for G-utrophin, in rat brain using a polyclonal antibody against the distal rod domain of rat utrophin, Ut43, (see Fig 4.2 A) but failed to detect any bands that might correspond to Up71.

Using the Mupa antibodies on Western blots, full-length utrophin was detected in adult and foetal C57Bl brain extracts but was absent from UKO^{ex6} samples. In Fig 4.6, full-length utrophin can be seen (395kDa) in control brain with Mupa-1, Mupa-2, Mupa-3 and Mancho-3 but is not seen in UKO^{ex6} brain. Note that full-length utrophin appears as a very weak band with Mupa-1 in comparison to that seen with Mupa-2 and Mupa-3, a situation very similar to that described in kidney. Overall, brain expresses lower levels of full-length utrophin than kidney and lung but higher levels than muscle. Brain shows a similar complexity of bands as kidney and the bands were categorised as described previously (Table 4.1) in order to aid the interpretation of the banding patterns.

A 260 kDa polypeptide is detected only with Mupa-1 in control and UKO^{ex6} extracts and here, as in kidney, it probably corresponds to mouse β -spectrin non-erythrocytic which is preferentially expressed in brain (category B).

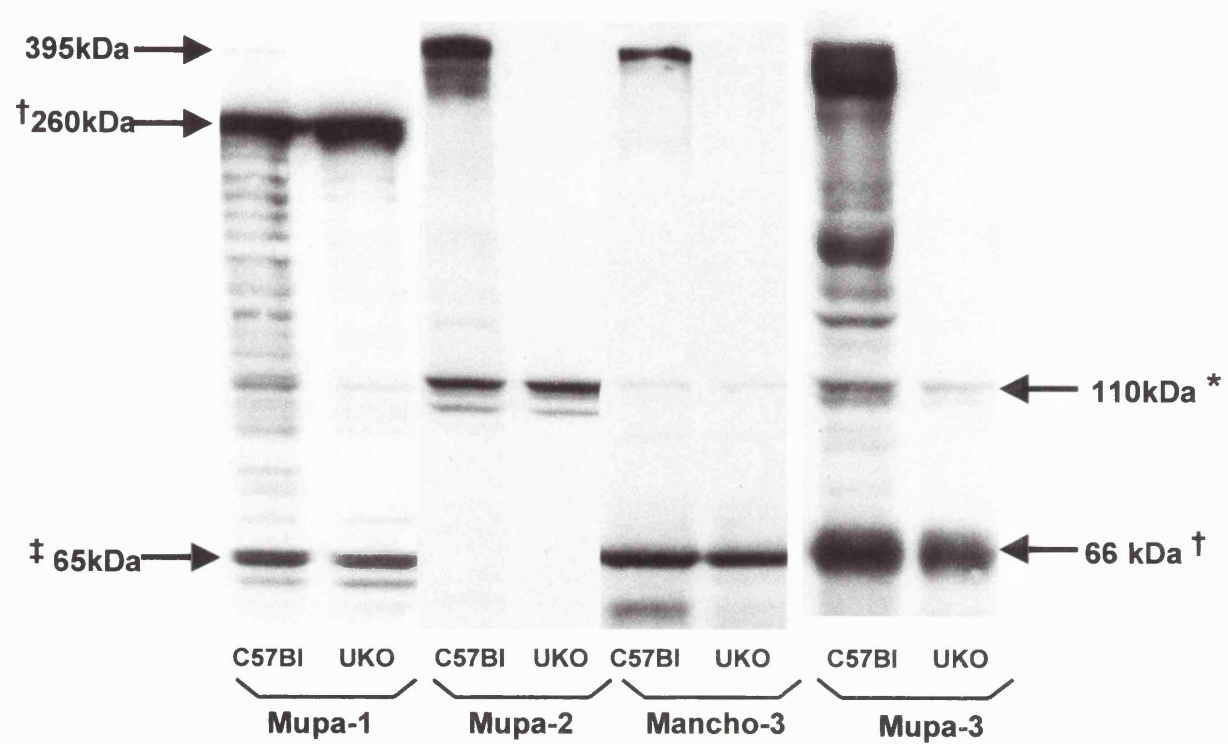


Fig 4.6 Western blot of brain extracts from C57BI and UKO^{ex6} (UKO) adult mice using Mupa-1, Mupa-2, Mancho-3 and Mupa-3 as primary antibodies. Bands have been categorised according to Table 4.1

Note that the associated ladder of smaller bands, probably representing breakdown products of β -spectrin, is also present.

A strong component of 65 kDa is detected in control and UKO^{ex6} extracts but only with Mupa-1 (category C). It is of interest that a band of 62 kDa was detected by Nguyen et al. (1995) in C6 glioma cells using an N-terminal antibody against utrophin, Mannut-1. This report was followed by the identification of a short N-terminal utrophin mRNA and protein by Zuellig et al. (2000). Zuellig and colleagues describe a 3.7Kb transcript encoding a 62kDa protein detected in Northern and Western blots respectively. It appears that this isoform arises because intron 14 is not spliced out during the processing of this mRNA and this leads to a Val residue and a stop codon being introduced 3' to the normal utrophin sequence from exon 1 to exon 14. This results in an isoform containing the actin-binding domain and two spectrin-like repeats only. Is the 65kDa band seen with Mupa-1 this N-utrophin? This seems unlikely since N-utrophin mRNA would contain the targeted exon in UKO^{ex6} mice and would be affected by this mutation in the same way as full-length utrophin. Thus, it is more likely that the 65kDa polypeptide is the product of crossreactivity of this antibody with a non-specific protein. A search of the protein databases identified a protein of the correct size and with some homology to the aa sequence used to raise Mupa-1 (Fig 4.7). This protein is plastin (T isoform), an actin binding protein that is expressed in several tissues including brain and has a mw of 70kDa.

However, in contrast to β -spectrin, the homology between utrophin and plastin is low and involves only very short contiguous runs of aa sequences

```

Utrophin: 70 NVNRLVQLVHQNVDLVNIGGTDIVAGNPKLTLGLLWSIILHWQVKDV-----M 118
              N+N L      +VNIG D+ AG P L LGLLW II      D+      +
Plastin: 193 NLNLALNSASAIGCHVVNIGAEDLRAGKPHLVLGLLWQIIKIGLFADIELSRNEALAALL 252

Utrophin: 119 KD--IMSDLQQTNSEKILLSWVRQTRPYSQVNVLNFTTSWTDGLAFNAVLHRHKP---- 172
              +D + +L + + E++LL W      + NF+ D A+ +L++ P
Plastin: 253 RDGETLEELMKLSPPELLLRWANFHLNSGWQKINNPSADIKDSKAYFHLNQLIAPKGQK 312

Utrophin: 173 -----DLFDWDEMVKMSPIERLDHAFDKAHTSLGIEKLLSPETVAVHLPDKKSIIMY 224
              ++ ++E + E + DK LG + ++P V P K + +
Plastin: 313 EGEPRIDINMSGFNETDDLKRAESMLQQADK----LGCRRQFVTPADVVSQNP--KLNLAF 366

Utrophin: 225 LTSLFEVLP 233
              + +LF P
Plastin: 367 VANLFNKYP 375

```

Fig 4.7 aa alignment between mouse utrophin aminoacids 24 to 320 used to raise Mupa-1 and T-plastin (accession: P13797). The areas in blue indicate aa sequences where there is some similarity between the two proteins.

+ =conservative substitution, x=residue masked by BLAST to prevent artefactual hits, - = insertion or deletion of a single aa

(5 aa), and thus it is also possible that this 65kDa polypeptide represents an as yet unidentified protein.

A 110kDa polypeptide is detected with Mupa-2, Mupa-3, and Urd40 (data not shown) and weakly with Mancho-3 (Fig 4.6) in control and UKO^{ex6} brain extracts. This category D polypeptide seems very likely to correspond to G-utrophin, based on size (G-utrophin is 113kDa) and in line with previous studies on cultured Schwannoma cell lines and mouse embryos (Blake et al., 1995). Furthermore, Knuesel et al. (2000) reported a >110kDa polypeptide in rat brain extracts using a COOH-terminal antibody, Ut43 (Fig 4.2 A).

Mancho-3 and Mupa-3 detect a band of 66kDa (Fig 4.6) in control and UKO^{ex6} brain. This could well correspond to one of the bands of 78 and 82 kDa reported by Lumeng et al. (1999) using the COOH-ter (Fig 4.2 A) antibody, although it seems rather small. The 66kDa band is detected in all tissues with Mancho-3 but only in brain and testis with Mupa-3. Although this band could represent Up71 it is not detected by Urd40. Because of the uncertainty, this band was placed in category B and regarded as crossreactivity with a non-specific protein. The relative weakness of the 110kDa and 70kDa bands in the Mupa-3 UKO^{ex6} lane compared to the control lane (Fig 4.6) is probably due to an experimental inaccuracy in loading the gel, other blots do not show this effect.

A 100kDa is detected only with Mupa-2 (Fig 4.6) in both control and UKO^{ex6} brain and seems likely to be due to non-specific crossreactivity of this antibody (category B).

Taken together, these experiments indicate that G-utrophin is probably translated in adult brain and is relatively abundant.

Skeletal Muscle

Expression of full-length utrophin protein in skeletal

muscle has been widely studied by immunological methods and human and mouse skeletal muscle extracts have been analysed using several utrophin antibodies (Nguyen et al., 1991, 1995; Tanaka et al., 1991; Clerk et al., 1993). These studies have shown that full-length utrophin is expressed in adult skeletal muscle but is more abundant in foetal muscle. In general, these studies focused on the detection of full-length utrophin and rarely mention smaller bands on Western blots. Tanaka et al. (1991) reported bands of 120kDa and 70KDa in muscle extracts which were classified as artefacts of the detection system or degradation of full-length utrophin. Lumeng et al. (1999) and Peters et al. (1997) detected a band of 140 kDa in muscle using COOH-terminal antibodies which they believe may represent a short utrophin isoform.

In the present study, Western blotting of C57Bl and UKO^{ex6} skeletal muscle revealed a pattern of bands much less complex than those shown by kidney and brain. Full-length utrophin was detected at moderate levels in adult control muscle (Fig 4.8). Mupa-1 again gave the weakest signal. A strong 100kDa component is seen exclusively with Mupa-1 in the control and UKO^{ex6} lanes (category B) (Fig 4.8 A) and probably results from the interaction of Mupa-1 with a non-utrophin protein. It is interesting to note that this band is also detected by Mupa-1 in heart (data not shown) and thus may represent a striated muscle actin-binding protein. A search of the protein databases showed that α -actinin which belongs to the spectrin superfamily and has a mw of 103 kDa, has some homology, as expected, to utrophin actin-binding domain (across four stretches of up to 10 aa), (Fig 4.9). Amongst the three α -actinin isoforms α -actinin 3 is the best candidate for the 100kDa band seen with Mupa-1 since it is expressed in both skeletal and cardiac muscle.

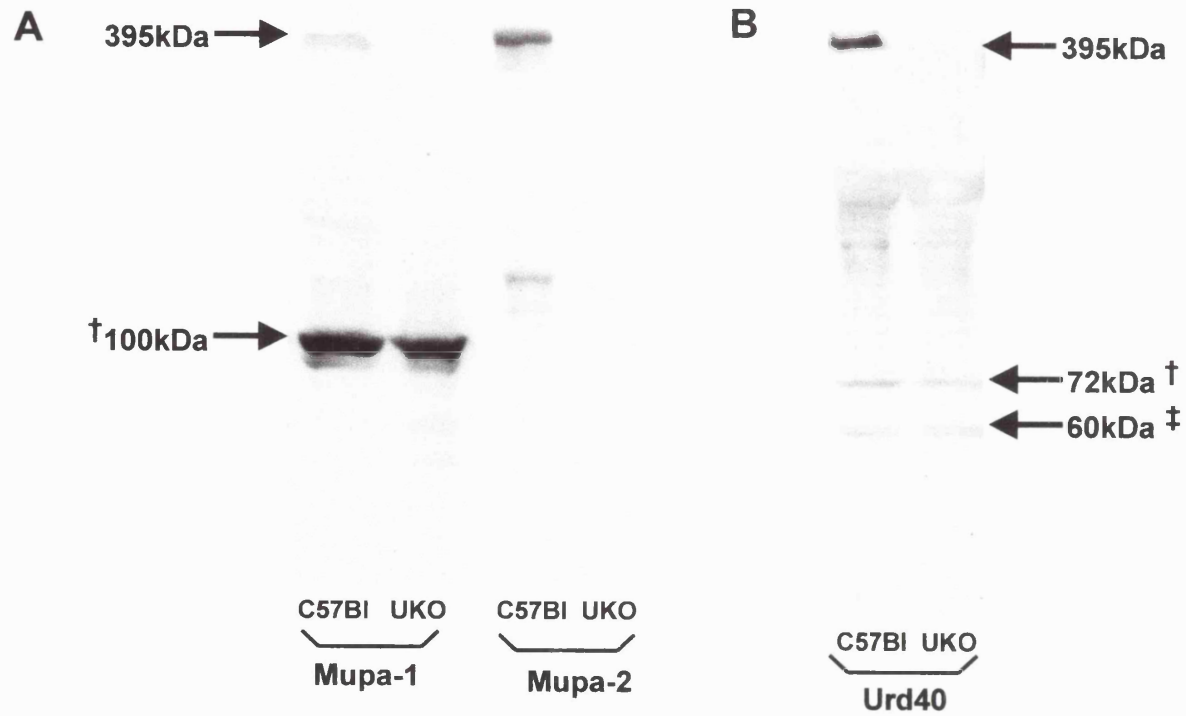


Fig 4.8 Western blotting of adult control (C57BI) and UKO^{ex6} (UKO) skeletal muscle extracts A, using Mupa-1 and Mupa-2 and B, using Urd40.

```

Utrophin: 11 QKKTFTKWINARFSGKGPISDMFXXXXXXXXXXXXXXXXXXXXXXXXXPK-ERGSTRVHALN 69
Q+KTFT W N+ K+G I ++ PK +RG R H +
α-actinin: 40 QRKTFTAUCNSHLRKAGTQ-IENIEEDFRNGLKLMLELVISGERLPKPDGRGKMRPHKIA 98
Utrophin: 70 NVNRYLQVLHQMVVDLVNIGGTDIVAGNPKLTLGLLWSIILHUQVKDVMKDIMSLLQQTN 129
NVN+ L + V LV+IG +IV GN K+TLG++W+IIL + ++D+ +++T+
α-actinin: 99 NVNKALDYIASKGVKLVSIGAEIIVDGNVVKMTLGMIWTIILRFAIQDI-----SWEETS 152
Utrophin: 130 SEKILLSWVRQTTTRPYSQVNVLNFTTSWTDGLAFNAVLHRRHKPDLFDWDEMVKMSPIERL 189
+++ LL W ++ T PY VN+ NF TSW DGL A++HRH+PDL D+ ++ K PI +
α-actinin: 153 AKEGLLLWCQRKTAAPYRNWNIQNFHTSWKDGLGLCALIHRHRPDLIDYSKLNKDDPIGNI 212
Utrophin: 190 DHAFDKAHTSLGIEKLLSPETVA-VHLPDKKSIIMVLTSLFEVL--PQQVTIDAIREVET 246
+ A + A L I K+L E + PD+++I+ Y++ + +Q A R +
α-actinin: 213 NLAMEIAEKHLDIPKMLDAEDIVNTPKPDERAIMTYVSCFYHAFAGAEQAETAANRICKV 272

Utrophin: 247 LPRKYKKECEEEIHIQSAVLAE 269
L + E EE ++ L E
α-actinin: 273 LAVNQENERLMEEYERLASELLE 295

```

Fig 4.9 aa alignment between mouse utrophin aminoacids 24 to 320 used to raise Mupa-1 and human α -actinin 2 (accession: P35609). The areas in blue indicate aa sequences where there is some similarity between the two proteins. += conservative substitution, x= residue masked by BLAST to prevent artefactual hits, - = insertion or deletion of a single aa

72kDa and 60kDa bands are detected in control and UKO^{ex6} extracts with Urd40 only (Fig 4.8 B). The 72kDa component could correspond to the short isoform, Up71 but if this was the case it should also be detected with the other COOH-terminal antibodies Mupa-3 and Mancho-3 and it is not. Mancho-3 detects a 66kDa band in muscle, but this same band is detected by this antibody in all tissues and is regarded as a non-specific component, not to be confused with either the 72kDa or 60kDa bands seen in muscle with Urd40. Although Up71 mRNA expression in muscle has been detected by RT- PCRs, and indeed Up71 mRNA occurs in all tissues, there have been no reports of this isoform in skeletal muscle in numerous Western blot analyses carried out in other laboratories. Therefore it is likely that the 72kDa band represents crossreactivity of Urd40 with a protein different to utrophin (category B). The same conclusion was made regarding the 60kDa band which was placed into category C.

In summary, full-length utrophin is moderately expressed in adult skeletal muscle and there is no evidence for translation of any short utrophin isoform in this tissue.

Testis There is some information already present in the literature to suggest that utrophin might be expressed in testis. Lumeng et al. (1999) found expression of full-length utrophin and perhaps G-utrophin mRNAs in mouse adult testis by Northern blot analysis, and in Western blot analysis using the COOH-ter antibody (Fig 4.2 A) they detected full-length utrophin and two short isoforms. Wilson et al. (1999) reported the expression of the short transcripts Up71 and Up140 in foetal and adult testis by RT-PCR and Schofield et al. (1993) detected mRNA in the

developing gonad of 14.5dpc embryos by mRNA *in situ* hybridisation. None of these observations have been followed up by a detailed study.

Western blots of adult mouse testis extracts showed that full-length utrophin is moderately expressed, but is relatively lower compared to lung and kidney, and that low mw bands are present in control and UKO^{ex6} testis and are detected with more than one C-terminal antibody (category D) and could correspond to short utrophin isoforms.

Examples of Western blots of testis extracts with Mupa-1, Mupa-2 and Mupa-3 are shown in Fig 4.10. Full-length utrophin is present in control testis as a relatively weak band but is absent in UKO^{ex6} testis. In addition, a doublet of bands of approximately 103kDa and 97kDa is detected by Mupa-2 (Fig 4.10). The 103kDa band is also detected with Mupa-3 and Urd40 (data not shown) and may represent a novel short utrophin isoform (category D). These two bands could correspond to the 90kDa and 97kDa bands reported by Lumeng et al. (1999) using the COOH-ter antibody. If that is the case then perhaps the 97kDa band detected here (corresponding to Lumeng et al. 90 kDa band) should also be placed in category D.

Mupa-2 and Mupa-3 also detect a 66kDa component in control and UKO^{ex6} testis. This band detected by Mupa-3 could correspond to Up71 but is not detected by Urd40 and thus it was placed in category B. The 66kDa band detected with Mupa-2 is likely to be different to the band detected with Mupa-3 since the minimum size of a C-terminal polypeptide that could be detected by Mupa-2 is 82kDa (Fig 4.2 B). Thus, it was interpreted as non-specific crossreactivity product of Mupa-2 with a non-utrophin protein (category B) and different to the 66kDa band seen with Mupa-3. While G-utrophin and Up140 mRNAs are thought to be expressed in testis

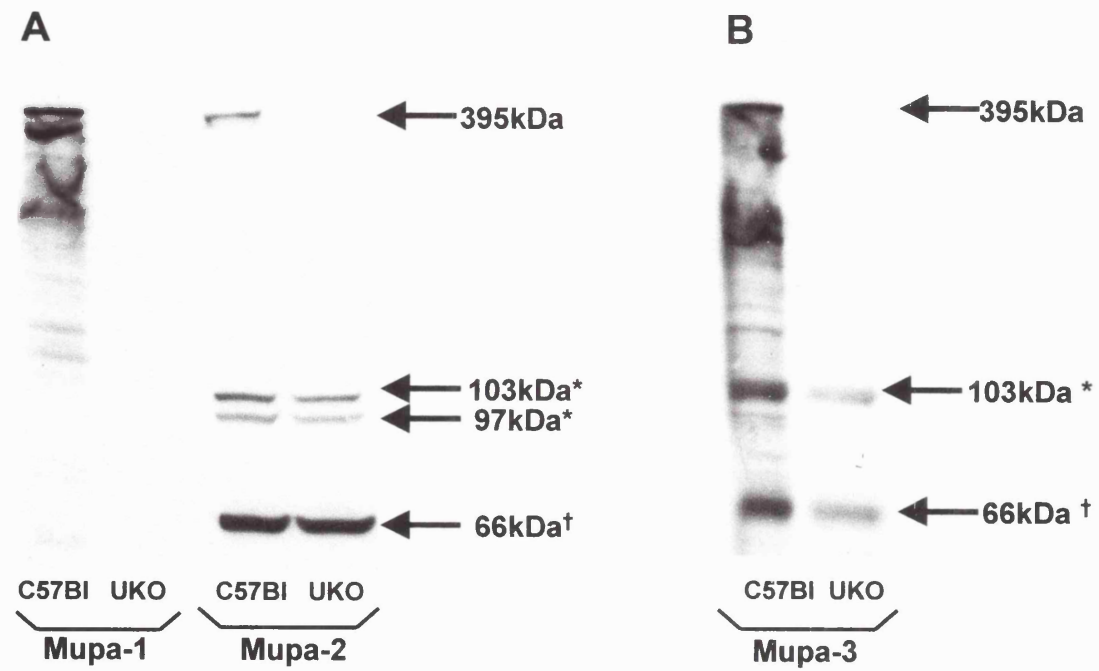


Fig 4.10 Western blotting of adult C57BI and UKO^{ex6} (UKO) testis extracts A, using Mupa-1 and Mupa-2 and B, using Mupa-3

(Lumeng et al., 1999; Wilson et al., 1999) polypeptides of the correct sizes for these isoforms, 113kDa and 147kDa respectively, were not seen on Western blots.

In brief, full-length utrophin is expressed in testis and at least one novel short isoform of 103kDa, and perhaps a second of 97kDa, is also expressed.

Foetal hands

Previous reports of mRNA *in situ* hybridisation to mouse embryo sections (Schofield et al., 1993) revealed strikingly high levels of utrophin mRNA in the tendon primordia of the developing digits of the hand and foot-plates. That mRNA could correspond to full-length utrophin or to a short transcript. Expression of G-utrophin mRNA was not detected in the tendon primordia with a G-utrophin specific probe (Blake et al., 1995). Thus, Up140, Up71 or an as yet unidentified short utrophin could be expressed in the developing digits. In order to investigate which utrophin isoform is expressed in the tendon primordia, extracts were prepared from whole foetal hands and feet from UKO^{ex6} and control embryos and analysed by Western blotting. These experiments revealed that both control and UKO^{ex6} extracts exhibited a 109kDa polypeptide which could be detected in control and UKO^{ex6} foetal extracts at different stages of development and with more than one of the COOH-terminal antibodies (Mupa-2, Mupa-3 and Urd40), (category D).

Fig 4.11 shows extracts of control and UKO^{ex6} 16.5 dpc embryonic hands immunoblotted with Mupa-2 and Mupa-3. The 109kDa polypeptide is detected with Mupa-2 and Mupa-3 (it was not detected with Mupa-1, data not shown). Mupa-3 detects a doublet of bands (109kDa and 112kDa) in this position as does Urd40 (Fig 4.12). Mupa-3 and Urd40 were raised against aa sequences that are more COOH-terminal than that used to raise Mupa-2 and might both show specificity for a utrophin epitope not detected by Mupa-2. One possibility is that the 112/109kDa

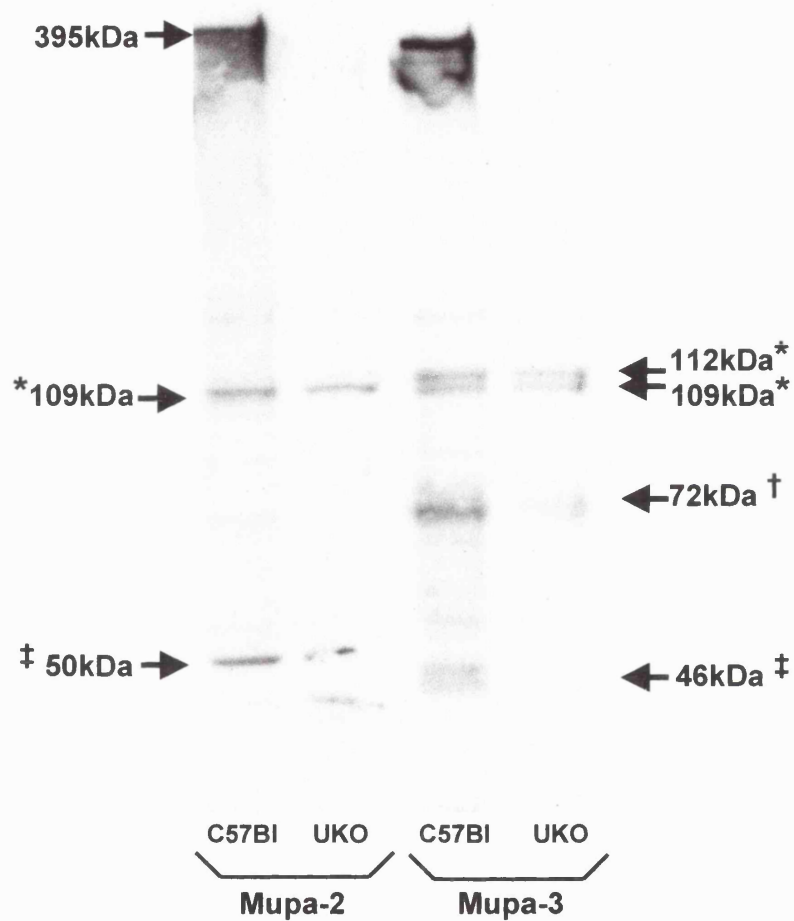


Fig 4.11 16.5 dpc hands extracts from C57BI and UKO^{ex6} (UKO) embryos were analysed by western blotting using Mupa-2 and Mupa-3

forms represent the same isoform which is post-translationally modified (e.g. by phosphorylation) in a way that alters its apparent molecular size. A 72kDa band seen only with Mupa-3 qualifies as non-specific category B band and a 50kDa band detected by Mupa-2 only was placed in category C (see Fig 4.12).

Fig 4.12 A shows immunoblots of UKO^{ex6} 15.5dpc, 16.5 dpc and newborn hands extracts. Note that the 109kDa band is significantly less prominent in newborn hands. This is not due to a lower total protein content of the extract as judged by Coomassie blue staining of an identical gel (Fig 4.12 B). Other smaller bands are also detected in the immunoblots, these include the minor 50kDa band, noted previously and seen in 15.5dpc and 16.5 dpc UKO^{ex6} and control hands with Mupa-2, and a strong 46kDa band detected in newborn hands also only with Mupa-2. The 46kDa band was also placed in category C as a non-specific crossreactivity product. Weak and fuzzy bands of mw 44-46kDa were seen in control foetal hands extracts (Fig 4.11) with Mupa-3 but not with Mupa-2 and were placed in category C as non-specific bands different to utrophin or of uncertain origin.

In summary, in the developing hand, in addition to full-length utrophin, a short isoform of 109kDa is expressed at high levels in control and UKO^{ex6} foetal hands which may be downregulated during development and perinatally. This isoform is detected with three different COOH-terminal antibodies, Mupa-2, Mupa-3 and Urd40 and perhaps undergoes post-translational modification.

Immunoblot analysis of a variety of foetal tissues suggested that this 109kDa isoform is also expressed in foetal brain, lung, muscle and heart where it is detected by Mupa-2 and Mupa-3 (data not shown). However, these foetal tissues were not analysed in detail. The size of this protein was used to design a 5' RACE experiment to look for its corresponding mRNA. This experiment, described in detail later in

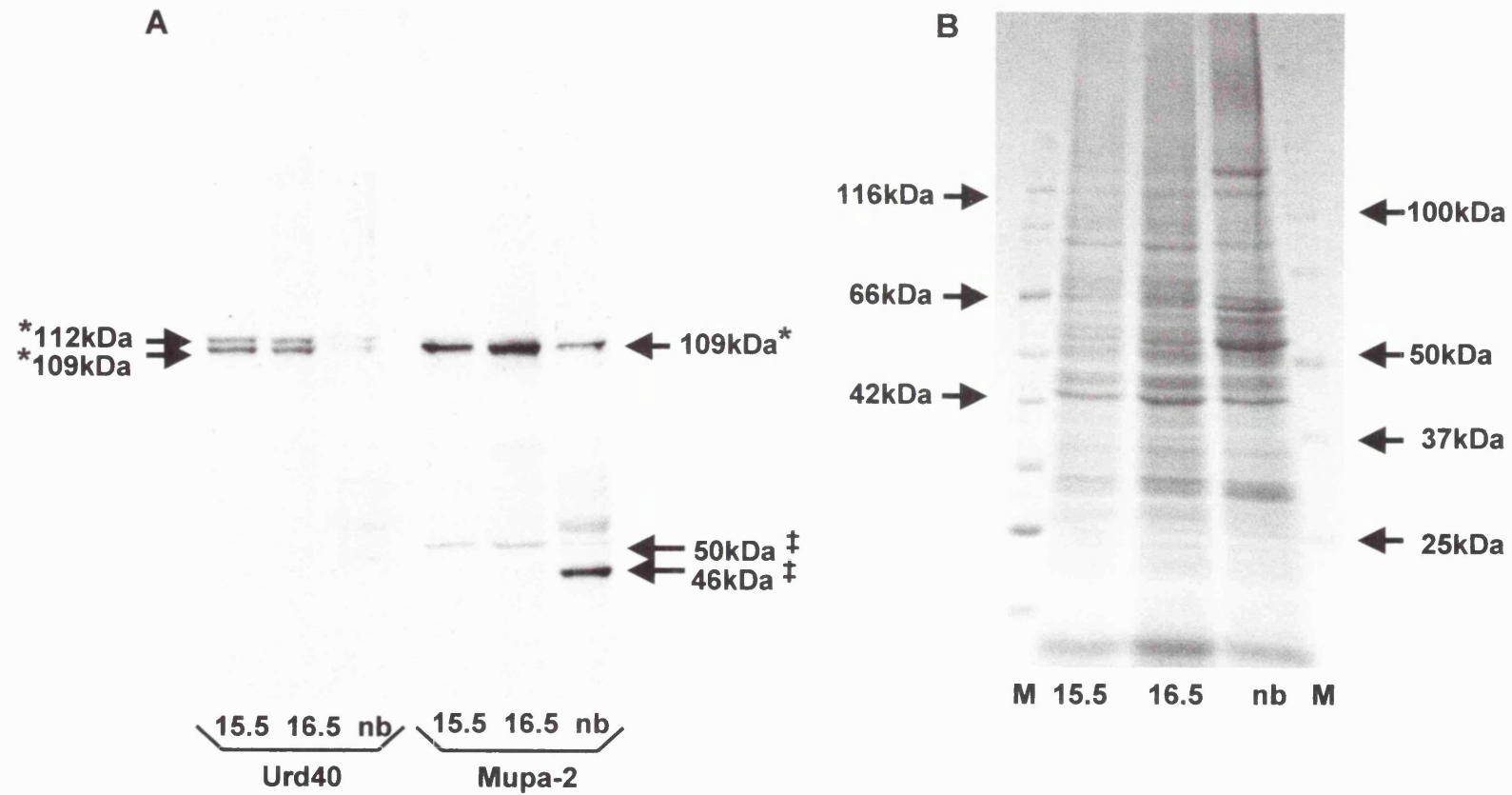


Fig 4.12 UKO^{ex6} foetal (15.5dpc and 16.5 dpc) and newborn (nb) hands extracts A, analysed with Urd40 and Mupa-2 and B resolved in SDS PAGE and stained with Coomassie blue after. M=mw marker

sections 4.4 and 4.5, led to the isolation of a novel short isoform of a predicted molecular weight of 109kDa that was named Up109.

4.3 Summary of Western blots results

The results described in this section are summarised in Table 4.2 and show that the Mupa antibodies have been useful in the analysis of utrophin isoforms by Western blotting. Each of them detects full-length utrophin although Mupa-1 does not show such a high specificity as the other antibodies. The antibodies have also detected short utrophins in certain control and UKO^{ex6} tissues. Because of the complexity of the utrophin protein and the consequent high probability of non-specific crossreactivity with other proteins in whole tissue extracts, the combined use of several antibodies has proved to be an essential and informative approach.

The results confirm that full-length utrophin is ubiquitously expressed and that its abundance varies from tissue to tissue being particularly abundant in kidney and lung and present at low levels only in muscle and brain. Amongst the known utrophin isoforms only G-utrophin seems to be translated. No firm evidence for the translation of Up71 or Up140 was found in this study. There is evidence that novel short isoforms of 120kDa and of 109kDa may be translated in kidney and foetal hands respectively and that the 109kDa isoform is also present perhaps in other foetal tissues.

kDa	tissue	antibody	mouse	identity
395	all	all	C57Bl	Fl
120	kidney	Mupa-2, Mupa-3, Urd40, Mancho-3	C57Bl, UKO ^{ex6}	Up120 novel isoform
110	brain	Mupa-2, Mupa-3, Urd40, Mancho-3	C57Bl, UKO ^{ex6}	G-utrophin
103/97	testes	Mupa-2, Mupa-3 Urd40	C57Bl, UKO ^{ex6}	Up103/97 novel isoform
109	foetal hands	Mupa-2, Mupa-3 Urd40	C57Bl, UKO ^{ex6}	Up109 novel isoform
260	all	Mupa-1	C57Bl, UKO ^{ex6}	spectrin Xreact
160	lung, kidney	all	C57Bl	Fl degradation
140	lung, kidney, muscle	all	C57Bl	Fl degradation
100	muscle	Mupa-1	C57Bl, UKO ^{ex6}	α -actinin Xreact
65	brain	Mupa-1	C57Bl, UKO ^{ex6}	plastin Xreact

Table 4.2 Summary of Western blot results. Fl = full-length utrophin, Xreact= crossreactivity. The utrophin proteins identified in this study are in the top section of the table and the non-specific bands in the bottom section

5' RACE

4.4 5' RACE in the region of exons 54 and 55

In an attempt to isolate the short utrophin transcripts corresponding to the 109kDa foetal hands and 120kDa adult kidney polypeptides seen on Western blots a 5' rapid amplification of cDNA ends (5'RACE) experiment was carried out using mRNA from UKO^{ex6} 15.5 dpc hands and adult kidney (Fig 4.13). It was estimated that COOH-terminal isoforms of these sizes might be transcribed from positions immediately upstream of exons 54 or 55. A summary of the 5' RACE procedure, given in detail in section 2.2, is shown in Fig 4.14, the positions of the utrophin specific primers used in this experiment are shown in Fig 4.15 and their sequences are given in Table 2.4.

In brief, first strand cDNA was synthesised using 1.5 µg of total RNA from adult kidney and foetal hands and a primer, UT56R1, corresponding to sequence in exon 56 (Fig 4.15). The mRNA template was removed by treatment with RNase H and RNase T1. After addition of a 5' poly-C_n tail, using terminal-deoxynucleotidyl transferase (TdT), the cDNA was amplified in two separate reactions, using UT56R1 (annealing temperature, T_A, 45° C) and UT55R2 (T_A 55°C) and a forward G-tailed anchor primer, (Fig 4.16 A). Two control samples were included in this first round PCR; a cDNA prepared in the absence of reverse transcriptase (-RT), to test the presence or absence of genomic DNA in the RNA preparations, and a cDNA without a poly-C_n tail (-TdT), which provided a control for the specificity of the G-tailed anchor primer. Throughout all 5' RACE experiments, no product was seen in the -RT control

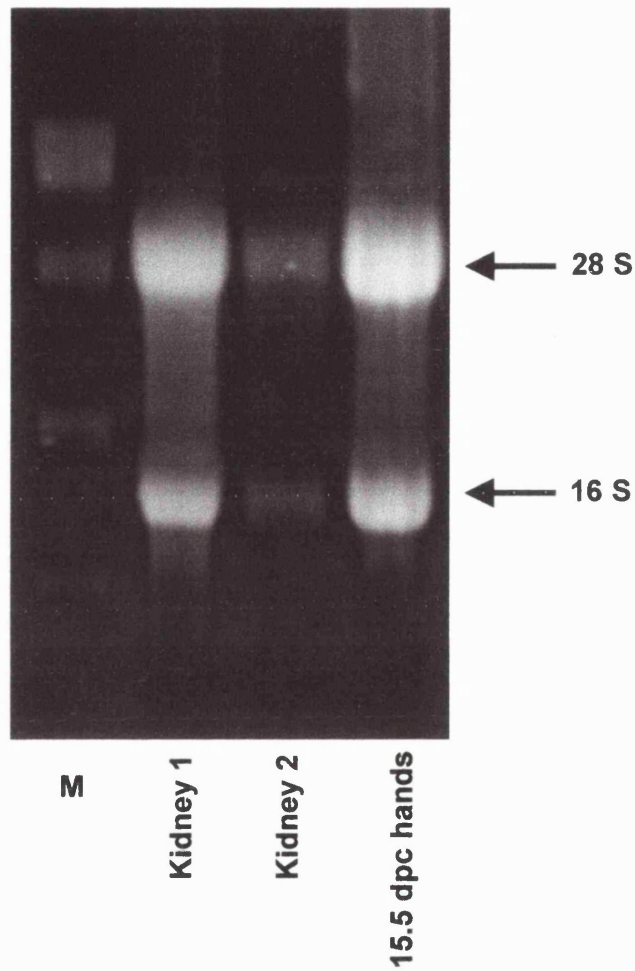


Fig 4.13 RNA preparations (5 μ g) from UKO^{ex6} adult kidney and foetal hands resolved on a 1% agarose gel stained with EtBr. Kidney1 and the hands mRNA were used as templates for 5'RACE experiments. M= RNA size ladder (5 μ l)

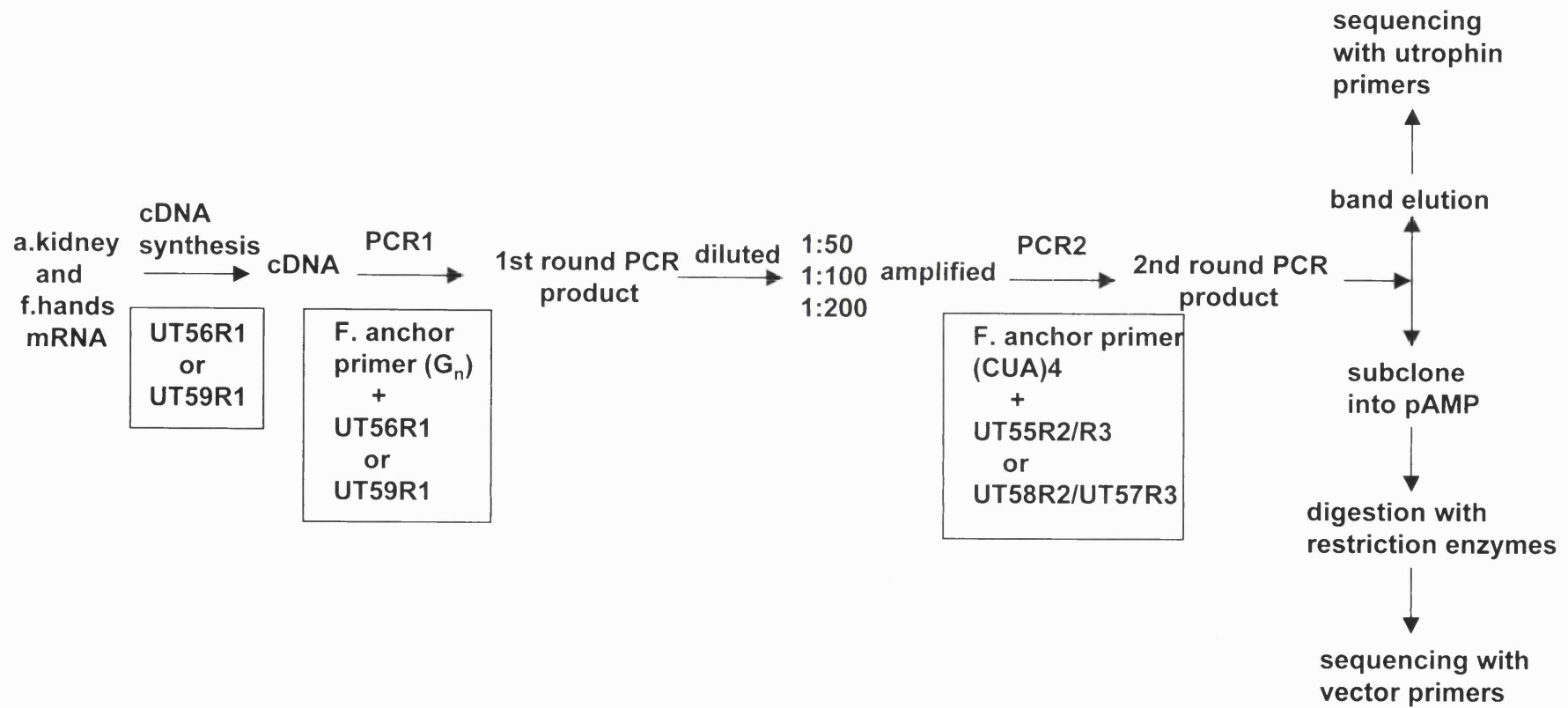


Fig 4.14. Diagram outlining the 5'RACE procedure. The primers used at each stage are shown in boxes and their sequences are given in Table 2.4. F= forward primer.

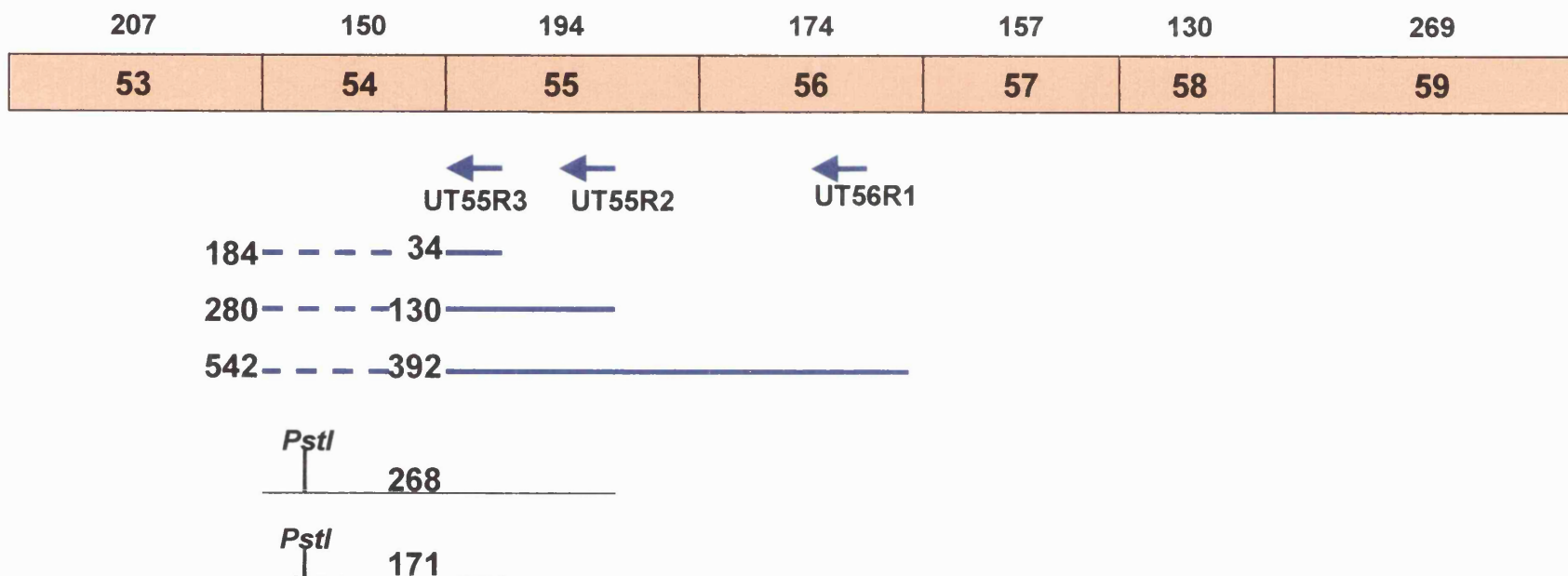


Fig 4.15 Positions in the utrophin mRNA of the specific primers used for 5'RACE. The length in base pairs from the 3' end of each primer to exons 53/54 and exons 54/55 boundaries is shown diagrammatically by discontinuous and solid blue lines respectively. Exons are shown as boxes, and their length in bp is shown above. The *Pst*I site in exon 54 is also indicated relative to the PCR products and the sizes of the expected digestion products is given.

confirming that the RNA preparations were free from contaminating genomic DNA.

Amplification with UT55R2 failed to produce a visible product (Fig 4.16 A). This is not an uncommon finding at this stage of the 5'RACE procedure and is usually associated with a scarcity of the specific mRNA being amplified.

Amplification using UT56R1 gave a smear of signal but this is likely to represent non-specific products, since it appears in samples amplified from a cDNA containing the poly-C_n tail (+) and in the –TdT control.

A second round of nested amplification was carried out. The nested primers were UT55R2 in the case of products amplified in the first round using UT56R1 (UT56R1/UT55R2 combination) or UT55R3 for products amplified using UT55R2 in the first round (UT55R2/UT55R3 combination). Since the plan was to clone the nested products from these amplifications, a universal forward anchor primer with four CUA repeats at its 5' end, necessary for uracil DNA glycosylase mediated cloning into the pAMP vector, was used in combination with the nested primers. Nested amplification with UT55R2 of various dilutions of the kidney samples produced a strong band of approximately 350bp and a diffuse smear (Fig 4.16 B). Bands ranging from 700bp to 200bp were amplified in the foetal hands samples (Fig 4.16 B). Amplification with UT55R3 gave no products in the kidney samples and a smear of bands (200bp to 2Kb) in the foetal hands samples (Fig 4.16 B). In all cases the same results were obtained for the 1:50, 1:100 and 1:200 dilutions.

2µl of the 1:100 products were cloned into the pAMP vector and 1µl and 5µl of the corresponding ligation reactions were used to transform competent

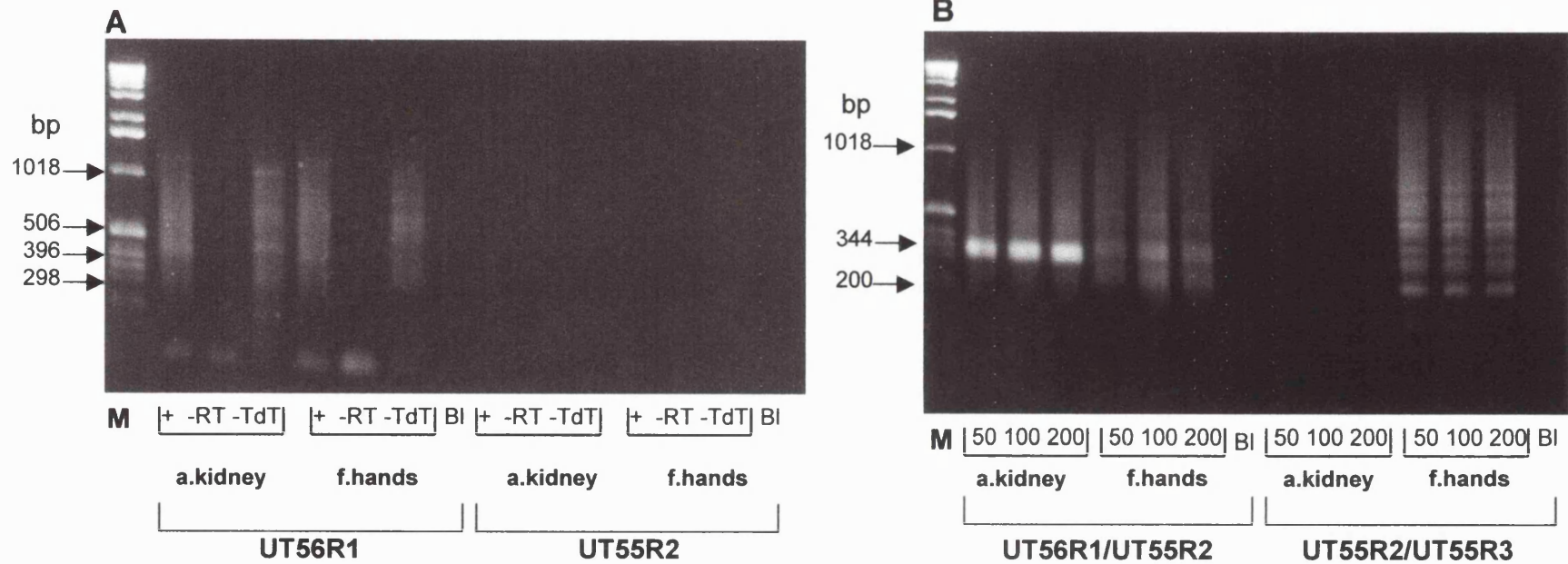


Fig 4.16 A, First round PCR products of the Poly- C_n tailed cDNA (+) using either UT56R1 or UT55R2 in combination with the forward primer. B, Nested amplification of various dilutions (1:50, 1:100 and 1:200) of the kidney and hands first round PCR products using UT55R2 or UT55R3.
 -RT= A cDNA sample prepared in the absence of reverse transcriptase; -TdT= non Poly- C_n tailed cDNA
 BI= no DNA control; bp= base-pairs; M=DNA size marker

DH5 α cells. More than 100 clones grew overnight. DNA was prepared from clones from each plate and electrophoresed after digestion with *EcoRI* and *HindIII*. This procedure demonstrated the sizes of the cloned products (Fig 4.17 A). The kidney recombinants showed insert sizes varying from 170 bp to 600 bp, the 350bp band seen in the nested PCR using UT55R2 (Fig 4.16 B) was represented by 25% of the recombinants examined. The foetal hands recombinants showed inserts ranging from 150bp to 470bp.

The recombinant DNAs were also digested with *PstI* (Fig 4.17 B). Full-length utrophin has a *PstI* site in exon 54 and there is a unique *PstI* site in the pAMP multiple cloning site. Therefore recombinants that give products of the correct sizes (268bp if amplified with UT55R2 and 171bp if amplified with UT55R3) must contain exon 54 and cannot represent novel sequence initiated in intron 54. However, they could contain novel sequence derived from intron 53. Clones that are not digested or show unusual size bands are likely to represent novel sequences. Recombinants with inserts too short to encompass exon 54 *PstI* site could represent either known utrophin sequence or a novel sequence.

48 clones from the foetal hands samples were analysed in this way; 26 (55%) appeared to contain exon 54, 17 (35%) contained inserts too short to cross exons 54/55 boundary and 5 (10%) gave unusual banding patterns. 24 kidney recombinants were also analysed; 12 (50%) contained exon 54, 7 (30%) were very short and 5 (20%) showed unusual banding patterns. On the basis of the sizes of the inserts after *EcoRI* and *HindIII* digestion and the results from the *PstI* digestion, 16 recombinants (12 hands and 4 kidney) were selected

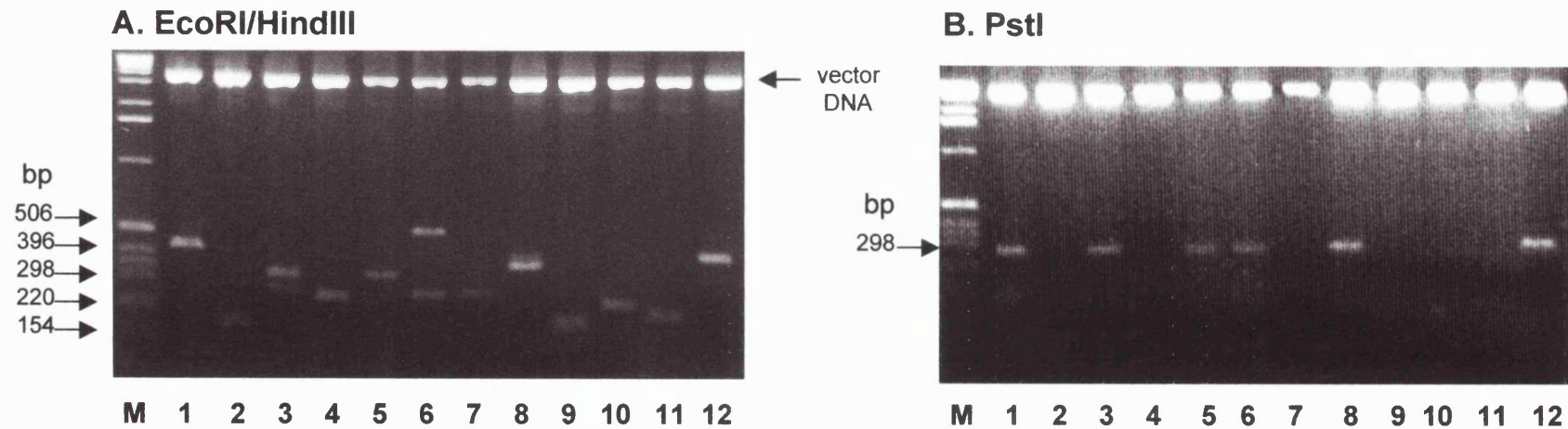


Fig 4.17 An example of *EcoRI/HindIII* and *PstI* digests of DNA from foetal hands 5' RACE recombinants. Recombinants 1, 3, 5, 6, 8 and 12 gave a *PstI* product of the expected size if exon 54 is present. Recombinant 6 corresponds to utrophin sequence extending to exon 52 where there is a *HindIII* site. Recombinants 4, 7 and 10 could correspond to utrophin or to a novel sequence and clones 2, 9 and 11 contained very short inserts. M=DNA size marker

to be sequenced. Of four kidney recombinants sequenced, three contained sequence totally unrelated to utrophin. A search of the databases using BLAST showed that one had homology to an unrelated testis cDNA and another clone had some similarity to a putative tumour suppresser mRNA (LUCA 15). The remaining recombinant clone contained sequence extending into exon 54 to a position 34 bp downstream of exons 53/54 boundary. Of the twelve foetal hands recombinants sequenced, eight contained known utrophin sequence; five extended into exon 54 and three into exon 53. The remaining recombinants were unrelated to utrophin; one had homology with an unrelated brain cDNA, another with the MSX2 cDNA and the third showed no significant homology to any sequence in the database. The sequence of DNA from the remaining clone could not be successfully analysed and was discarded.

In retrospect, it might have been sensible to gel extract and sequence some of the major PCR products seen after the nested amplification, particularly the 350bp kidney product (Fig 4.16 B), although it was assumed that it would be adequately represented in the recombinants. Unfortunately, that sample was lost and could not be analysed.

Clearly this experiment was problematic. A relatively high proportion (37%) of the 5' RACE products tested were unrelated to utrophin indicating that the "gene specific" primers were annealing to unrelated cDNAs non-specifically. Perhaps, this was not surprising since the primer (UT56R1) that was used to synthesise the cDNAs (RT step at 42°C) and for the first round of PCR, has a very low melting temperature and was annealed to the template cDNA at the relatively low temperature of 45°C. Note that the only kidney recombinants

which were sequenced were products amplified with UT56R1. Another problem was that small size PCR products were preferentially cloned.

Nonetheless, all the utrophin sequences recovered (63% of all those sequenced) contained exon 54 and 25% of those also contained exon 53. Thus, although this experiment was not exhaustive, it found no evidence of novel utrophin mRNAs transcribed from regions within introns 53 and 54.

4.5 5' RACE in the region of exons 56 and 57

Attention was turned further downstream and a second 5' RACE experiment was designed to examine the intron 55/exon 56 and intron 56/exon57 boundaries. This was considered a reasonable experiment to do since transcripts encoding the 120kDa kidney and 109kDa foetal hands isoforms could have novel first exons which encode protein that would contribute to the polypeptide mw determined by SDS PAGE. The positions of the utrophin primers used in this second 5' RACE experiment are shown in Fig 4.18 and their sequences are given in Table 2.4.

A first amplification was carried out (T_A 56°C), from cDNAs synthesised with UT59R1 as template. As before, the G-tailed anchor primer was the forward primer and UT59R1 or UT58R2 the reverse primers (Fig 4.19). Electrophoresis of the first round PCR products gave a 400bp band, equally prominent in both types of sample, in the UT59R1 amplifications. No product was visible in samples amplified with UT58R2. The 400bp band was gel extracted and sequenced using UT59R1 but unfortunately this sequencing reaction failed twice. This was not pursued further since it seemed likely that

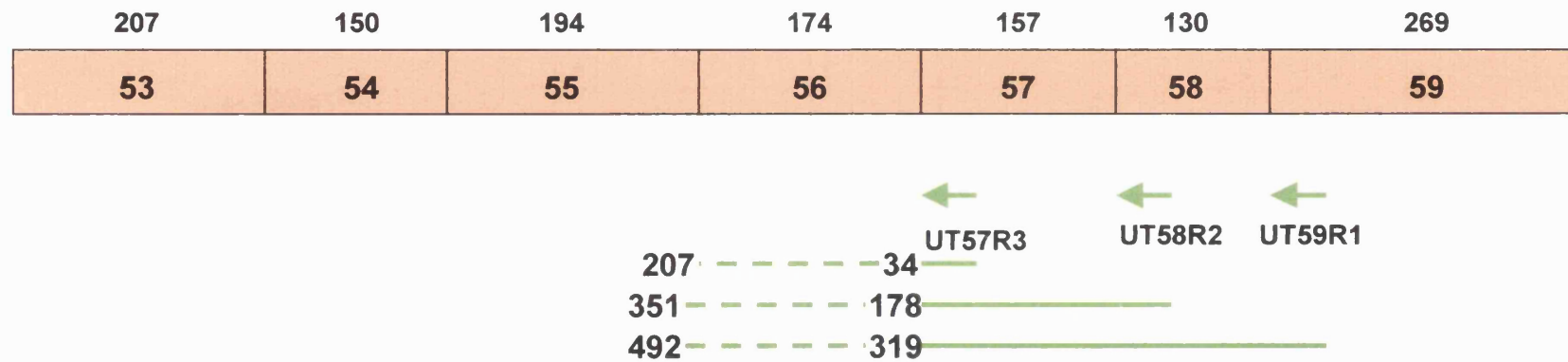


Fig 4.18 Positions of the utrophin specific primers used for the second 5'RACE experiment. The length in base pairs from the 3' end of each primer to the exons 55/56 and exons 56/57 boundaries is shown diagrammatically by discontinuous and solid green lines respectively. Exons are shown in boxes and their length in bp indicated above.

this band represents a non-specific product; had it been utrophin, a prominent product of 259bp would have been amplified with the nested primer UT58R2 (situated 141 bp upstream of the 3' end of UT59R1, Fig 4.18) and this was not the case (Fig 4.19).

As in the first experiment, a second round of PCR (T_A 56°C) was carried out using 1:50, 1:100 and 1:200 dilutions of the first round products. UT58R2 and UT57R3 were used as reverse primers for the first round products amplified with UT59R1 (shown as UT59R1/UT58R2 and UT59R1/UT57R3 in Fig 4.19 B) and UT57R3 for the first round products amplified using UT58R2 (UT58R2/UT57R3 in Fig 4.19.B). UT59R1/UT58R2 and UT59R1/UT57R3 combinations produced a series of bands ranging in size from 100bp to 800bp in kidney samples and 100bp to 1Kb in foetal hands samples. The UT58R2/UT57R3 combination also produced a number of bands, somewhat more clearly defined, the largest being around 600 bp in kidney. In all cases there were no differences between the three dilutions amplified.

It was decided that this second round amplification may be relatively non-specific and this was explored by repeating the nested PCR experiment at a higher annealing temperature, 58°C instead of 56°C, using the 1:50 dilution of the first round products. Overall, this did not lead to a reduction in the number of components, particularly in the UT59R1/UT58R2 and UT59R1/UT57R3 products, although certain larger mw bands appeared more prominent (Fig 4.20 A). These include; in the UT59R1/UT58R2 combination, bands of 900bp and 800bp amplified from hands and kidney cDNAs respectively, while in the UT59R1/UT57R3 combination, a 750bp was clearly visible in the hands sample. The UT58R2/UT57R3 combination gave a much improved banding pattern for

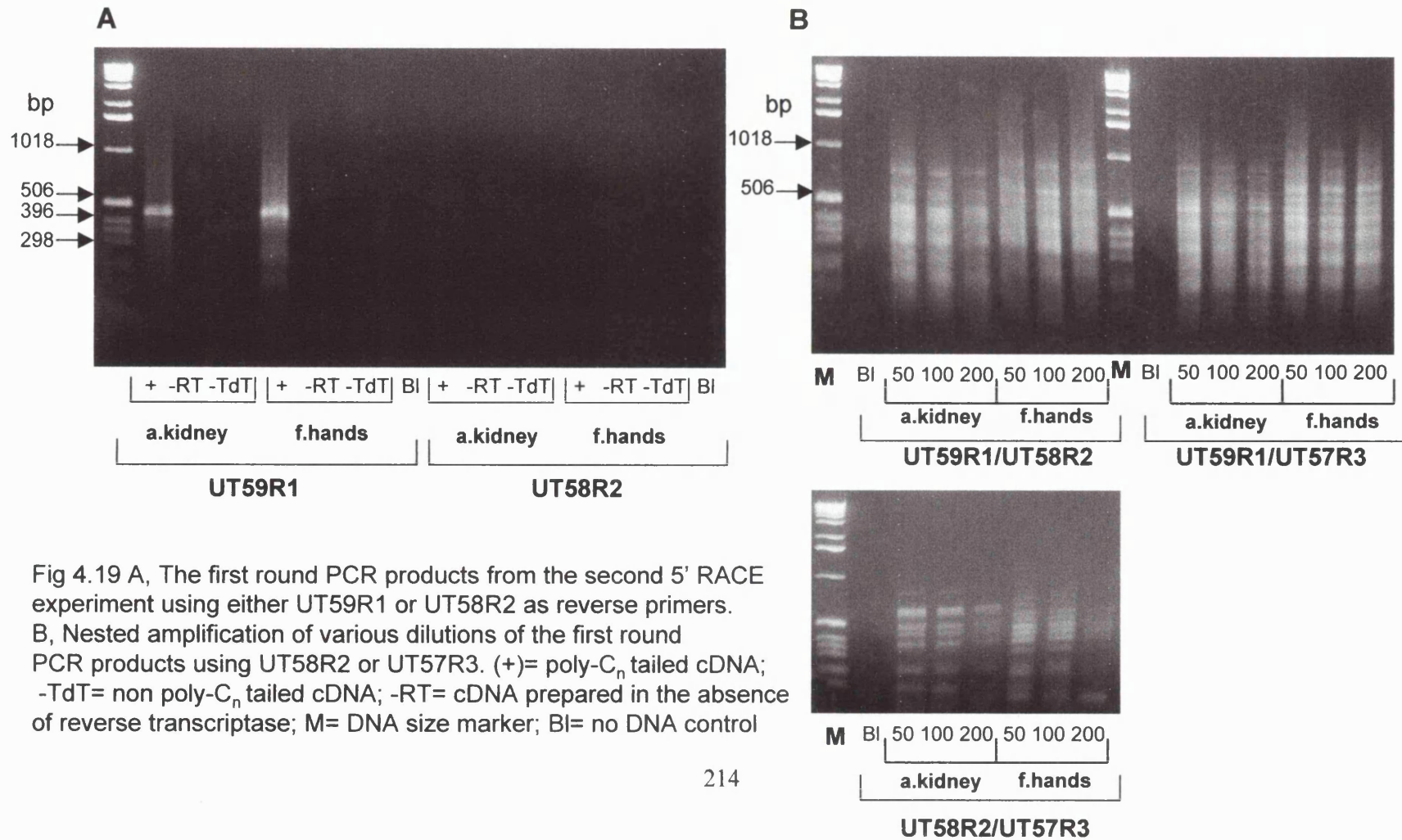


Fig 4.19 A, The first round PCR products from the second 5' RACE experiment using either UT59R1 or UT58R2 as reverse primers. B, Nested amplification of various dilutions of the first round PCR products using UT58R2 or UT57R3. (+)= poly-C_n tailed cDNA; -TdT= non poly-C_n tailed cDNA; -RT= cDNA prepared in the absence of reverse transcriptase; M= DNA size marker; BI= no DNA control

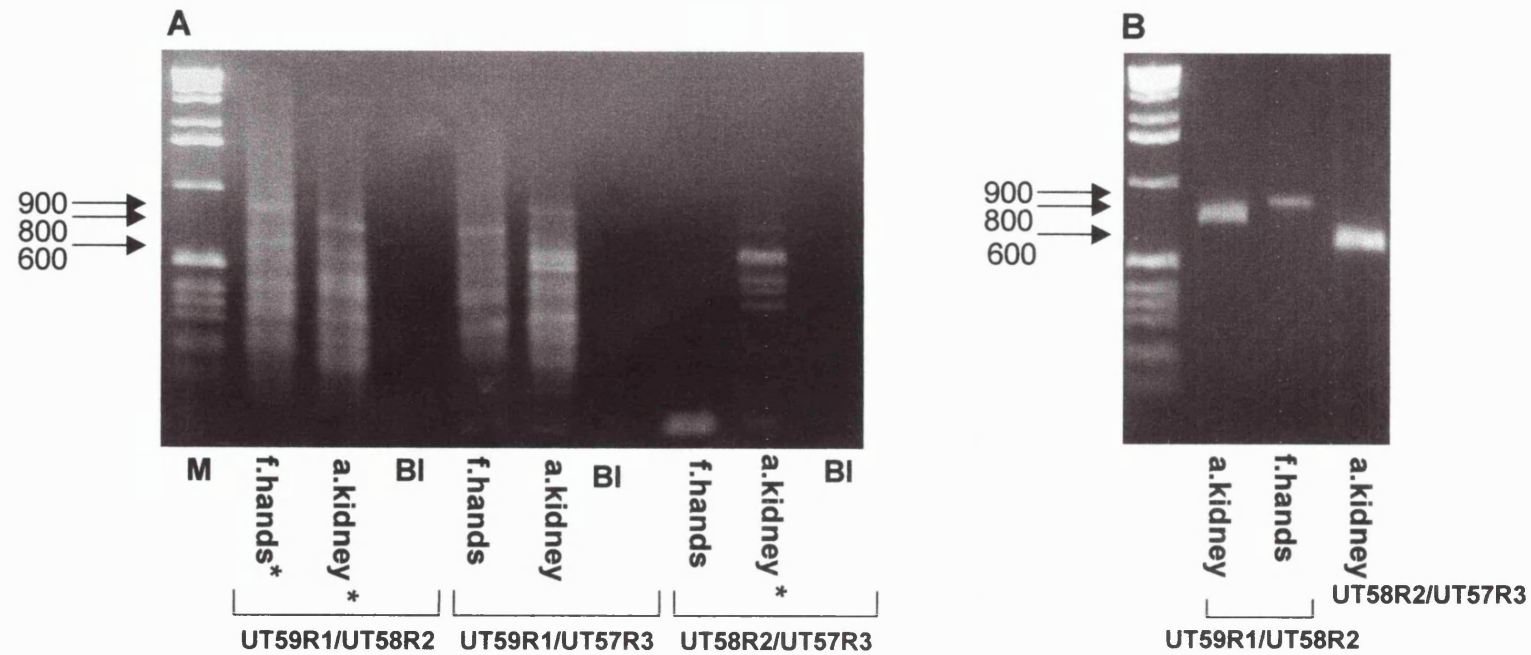


Fig 4.20 A, nested amplification at 58°C of the 1:50 dilutions of the first PCR products from adult kidney and foetal hands cDNAs using UT58R2 or UT57R3. The asterisked bands (hands UT59R1/UT58R2 900bp, kidney UT59R1/UT58R2 800bp and kidney UT58R2/UT57R3 600bp) were re-amplified and gel extracted and are shown in B. M=DNA size marker; BI=no DNA

the kidney in which a 600bp band was clearly resolved although, no products were detected in the hands.

Because of the problems encountered in the earliest 5' RACE experiment it was decided to recover bands by cutting them out from the gel and eluting the DNA, in addition to cloning the PCR products. Accordingly, the large bands mentioned above were recovered from the agarose gel and re-amplified using the nested primers UT58R2 or UT57R3. The 750bp hands band did not re-amplify and was not pursued; the 800bp kidney and 900bp hands bands were both re-amplified with UT58R2 and the 600bp kidney band with UT57R3. These three isolated bands are shown in Fig 4.20 B after gel purification. The extracted DNA was sequenced using either UT58R2 or UT57R3 as reverse primers. Both the 800bp and 600bp kidney bands contained known utrophin sequence spanning from exons 58 or 57 to exons 54 or 53 (Fig 4.21) with no evidence of deviation from known sequence. In contrast, the hands 900bp sequence contained all of exons 57 and 56 but diverged from the known utrophin sequence at a point exactly coincident with the exon 56/intron 55 boundary (Fig 4.21). Fig 4.22 shows the sequence of this band alongside the sequence of the 600bp kidney band for comparison. This suggests that the hands mRNA represents a novel short utrophin transcript, whose transcription begins in intron sequence upstream of exon 56.

In addition to the analysis of individual eluted bands, the second round PCR products (Fig 4.19 B) were cloned into the pAMP vector, DNA was prepared from 24 recombinant and digested with *EcoRI/Hind III* as described for the first 5' RACE experiment. The sizes of the inserts ranged from 200bp to 600bp and twelve recombinants (6 hands and 6 kidney) were sequenced.

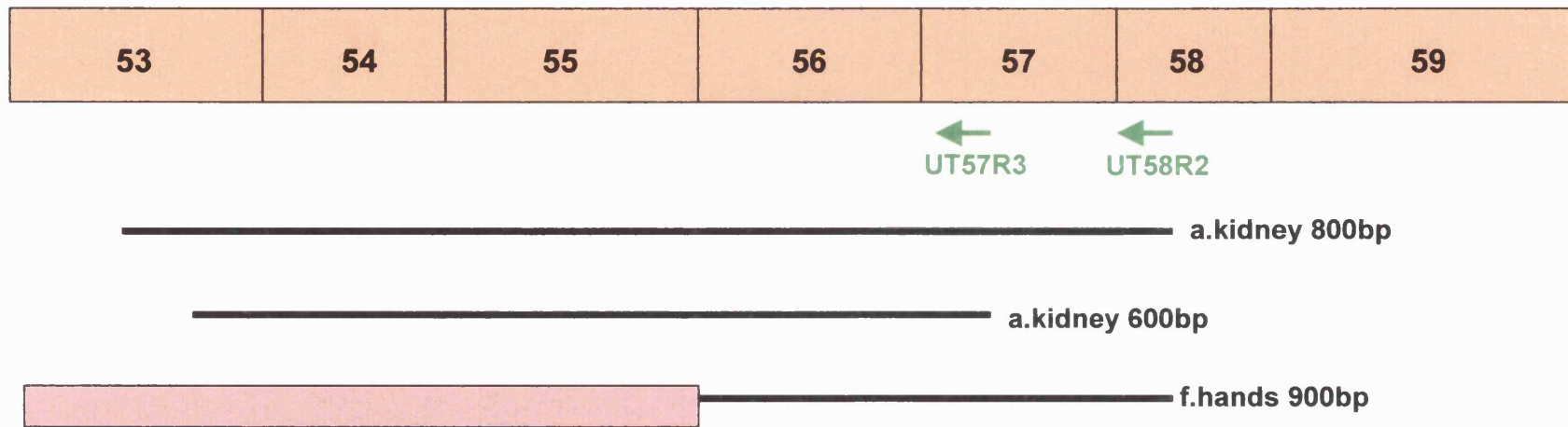


Fig 4.21 A diagram showing the extent of the mRNA sequences isolated by 5' RACE in the region of exons 59 to 56. The position of the sequencing primers UT58R2 and UT57R3 are shown. The sequence of products containing known utrophin sequence is shown by a solid black line and novel sequence upstream of exon 56 is indicated by a coloured box

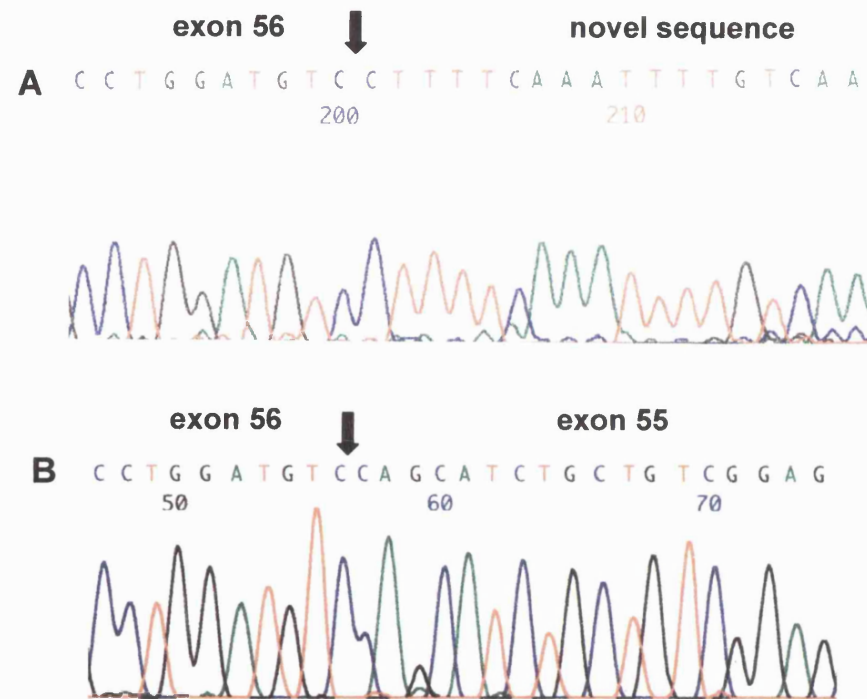


Fig 4.22 A, shows how the novel sequence isolated from foetal hands mRNA diverges from full length utrophin at the exons 56/55 boundary. B, sequence from the 600 bp kidney band that contains exon 55. These sequencing reactions were carried out using UT57R3 as the primer.

Of the 6 hands recombinants, five (83%) contained sequence corresponding to known utrophin and one (17%) was unrelated sequence. One of the five recombinants containing utrophin sequence (20%) showed novel sequence immediately upstream of utrophin exon 56 that corresponded to the sequence identified in the hands 900bp band. This may seem a small proportion but since small size PCR products were preferentially cloned, a realistic estimate of what proportion of the total transcripts in foetal hands corresponds to this novel sequence cannot be inferred from this experiment. Of the 6 kidney recombinants, four (67%) contained known utrophin sequence extending into exon 55 and two were completely unrelated sequences (33%).

At this stage the decision was made to concentrate efforts in the analysis of the foetal hands novel isolated sequence and to put aside the search for the kidney novel short mRNA.

4.6 Characterisation of the novel 109kDa isoform (Up109)

5' novel sequence of Up109 The foetal hands 900bp product band was cloned into the pAMP vector and sequenced with the M13 forward and reverse primers which lie at each side of the multiple cloning site (Table 2.4). In all there were 460 basepairs (bp) upstream of the exon 56/intron 55 boundary (Fig 4.23). The novel sequence includes a reading frame that stays open for 138 bp 5' of the known intron/exon junction where a TAG stop codon is encountered. There is an in frame translation initiation codon, ATG, 51 bp 5' of the intron/exon junction which lies in a moderately favourable Kozak sequence (Kozak et al., 1995), GCCACCAUGG, with a critical purine, A, preceding the

```

tttcctttctgctgtgtgtaattgagaccaaactctaagcctgggctctgaagagaacag 60
                Up109F1           Up109Rs1
tggtaggctgcaggtcttttagggaggccggcagaaagagatcctgggcttcccagggcaa 120
aaaaggagaccatgccagcctcgtggaacacagctacaagaaaacacagaagcaggtctc 180
tgctgcccagctccgaagtccgtgaggaaacggacccaaggtggggtggctaaaatgtc 240
ccagcgcaagctgctgatgctcatgggcccaccgctcaagggcaaggattgaaaaggattt 300
                ↓
tacgaaggagttgaaagtatagctagtgaagatacgggttttaaaagttggacgttgttg 360
tctgaaggaagtttgccaggaagatgtaggcttcaagggctcccggacg***ATGATTGGTCT 420
                Exon 56      M I G L
GAACTTCAGCTTACGAGAATTGTTGACAAAATTTGAAAAGGACATCCAGGCAGAAATGA 480
                ↑
    N F S L R E L L T K F E K D I Q A E I D
TCCCCACAATGACATATTTAAAAGCATCGATGGAAACCGGCAGAAGATGGTGAAAGCTCT 540
    A H N D I F K S I D G N R Q K M V K A L
    EcoRI
    |
GGGGAATCTGAGGAAGCAACAATGCTTCAACATCGACTGGATGACATGAACCAAAGATG 600
                Up109R1
    G N S E E A T M L Q H R L D D M N Q R W
GAATGATTGAAGGCAAAATCTGCTAGCATCAG
    N D L K A K S A S I

```

Fig 4.23. The 5' sequence and conceptual translation of Up109 cDNA. The point at which Up109 differs from full-length utrophin at the exon 56 boundary is indicated by an arrow. The translation initiation ATG codon is asterisked and an in frame stop codon is indicated by a solid arrow. The sequences of the forward primer Up109F1 and reverse primers Up109R1 and Up109Rs1 are underlined. The single *EcoRI* site in exon 56 is also indicated.

ATG codon by three nucleotides. Thus the novel sequence comprises 51 bp of translated sequence and 409 nt of 5' UTR.

The conceptual translation of the novel sequence predicts a protein of 109kDa (Fig 4.23) and this isoform was designated Up109 in line with previous utrophin (Up) and dystrophin (Dp) isoforms. The Up109 sequence diverges from full-length utrophin at exactly the same point as one of the short utrophin isoforms, G-utrophin (Blake et al., 1995), and the dystrophin homologue Dp116 (Byers et al., 1993), diverges from full-length dystrophin. However, the unique first exons of G-utrophin, Dp116 and Up109 are quite different. The Up109 protein sequence includes an SLR motif (aa 7 to 9) that constitutes a potential phosphorylation site for protein kinase C (PKC), two potential phosphorylation sites for casein kinase II (aa 7 to 10 and 13 to 16), a N-myristoylation site (aa 3 to 8) and a N-glycosylation site (aa 5 to 8) all predicted by PROSITE peptide analysis program. The unique 5' sequence of Up109 and the deduced NH₂-terminal amino acid sequence have no significant homology to any protein or mRNA sequence listed in the current databases.

Expression of Up109 mRNA

The expression of Up109mRNA was investigated by RT-PCR using cDNAs prepared from a limited selection of control and UKO^{ex6} adult and foetal tissues. cDNAs were amplified using a forward primer situated within the unique sequence of Up109, Up109F1 (Table 2.4, Fig 4.23) and a reverse primer in exon 57 of utrophin, (expected size of the PCR product is 665bp). In order to test the quality of the cDNA preparations and to allow a rough comparison of the levels of mRNA, cDNA was also amplified using primers for the ubiquitously expressed phosphoglucomutase 2, *pgm2*,

mouse gene (Wijnen et al., 1977) which is the homologue of the human *PGM1* gene (Whitehouse et al., 1992).

Fig 4.24. shows the results of this experiment; all tissues show a similar abundance of *pgm2* mRNA (Fig 4.24 B); Up109 mRNA is expressed in foetal hands and also in other foetal tissues (Fig 4.24 C). Foetal hands, kidney and brain express moderate levels of Up109 mRNA while in foetal muscle Up109 is only weakly expressed. Up109 mRNA was barely detected in adult tissues and was absent from adult muscle. There were no differences in the abundance of Up109 mRNA message in control and UKO^{ex6} tissues. Samples amplified in the absence of reverse transcriptase (-RT) confirmed that amplification could not be ascribed to contaminating DNA (Fig 4.24 B and C).

A minor band (<10% of the major 665bp product) of c. 430 bp was also seen in these RT-PCR experiments. Increasing the annealing temperature (gradually from 56°C to 65°C) and using a hot start PCR procedure (consists of a initial denaturation step of 15 min at 95°C, so that the primers do not anneal to the cDNA before the enzyme starts to work) using HotStar Taq polymerase did not result in the disappearance of this small band. Both bands, the 665 bp corresponding to Up109 and the 430 bp band, were gel extracted and sequenced with the forward Up109 specific primer and the reverse primer UT57R3.

The 665 bp band contained, as expected, Up109 novel sequence. The 430bp product diverged from the known utrophin sequence at the intron 55/exon 56 boundary and was different to the previous Up109 sequence (Up109a) in that it lacked the 239 bp of Up109 sequence which lie immediately upstream of exon 56. In this case the exon 56 sequence abutted directly to bp

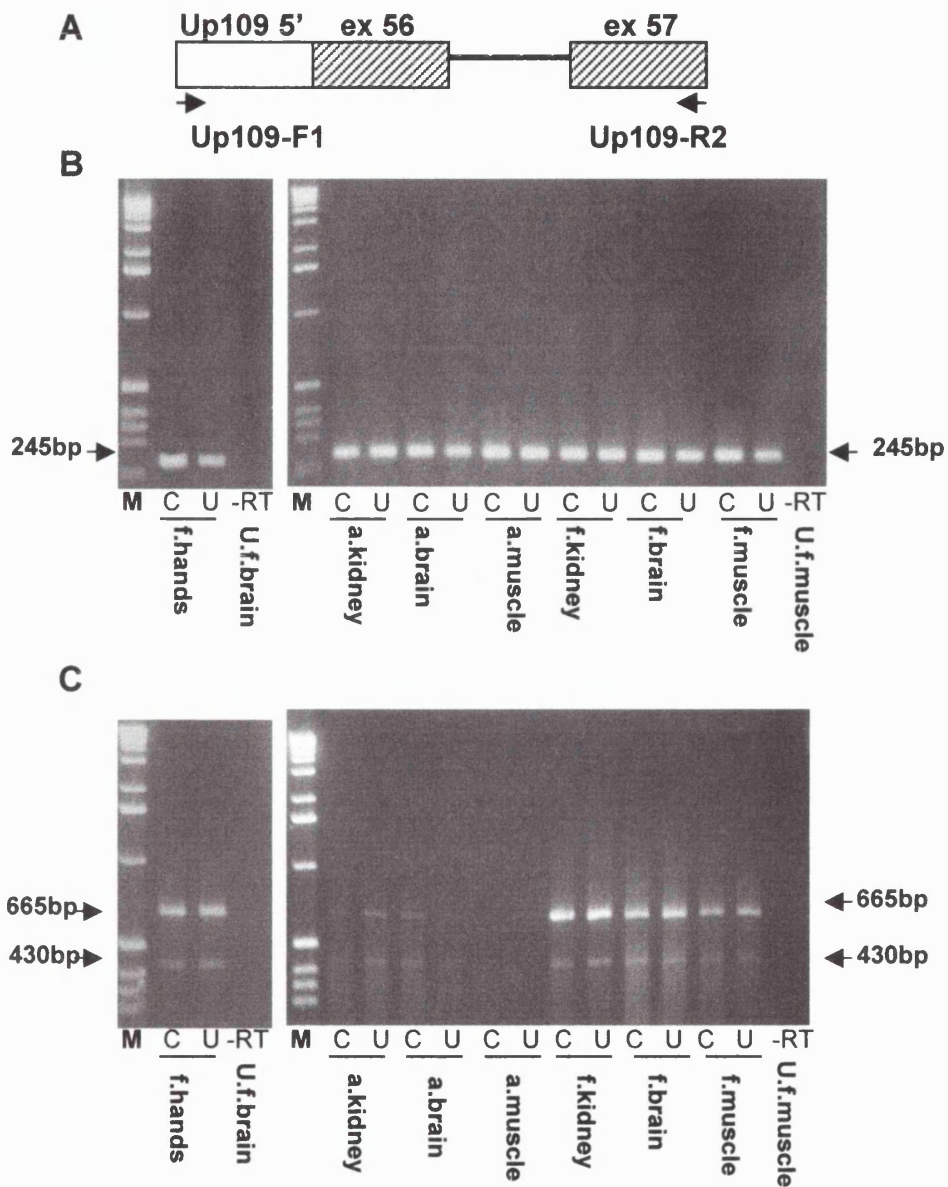


Fig 4.24 A, position of the primers Up109F1 and Up109R2 used in RT-PCR of control and UKO^{ex6} adult and foetal tissues. B, amplification using mouse *pgm2* primers. C, amplification using Up109 specific primer. The foetal hands PCR products were run on a separate gel but were amplified in the same PCR reaction as the other tissues. The same amount of amplified product (15 μ l) was run in all cases. M=DNA size marker C=C57Bl; U=UKO^{ex6}; -RT=cDNA prepared without reverse transcriptase

221 of the Up109 sequence (Fig 4.23). This observation suggests that the 430 bp product is a minor transcript (Up109b) in which the sequence between bp 222 and bp 460 of the Up109 sequence has been spliced out. Indeed, the 5' (AAG/GT) and 3' (AG/G) splice sites conform to the consensus splice donor and acceptor sites sequences. Therefore, it is possible that during mRNA processing these intermediate 239 bp are regarded as an intron by the splicing machinery and are removed, this is illustrated in Fig 4.25. Up109b lacks the sequence encoding for the unique 17 aa of Up109a. However, it contains an in frame ATG codon 91 bp upstream of the junction with exon 56. Translation is not likely to be initiated from this ATG since there is an in frame stop codon 73 bp downstream. The next in frame ATG is found in exon 56 and if Up109b is translated it would be 39 aa shorter than Up109a, that is 4.5 kDa smaller. There are other cases of similar alternative splicing events involving the 5' end of genes in the literature. One example is the carbonic anhydrase I gene (*CA1*), (Barlow et al., 1987) where a sequence of 54 nt in the 5' UTR is either present or absent. There are many instances of alternative splicing within exons, the luteinizing hormone receptor mRNA (Reinholz et al., 2000) is a good example of this type.

Position of Up109 first exon in the utrophin gene In order to investigate the position of Up109 unique sequence in the utrophin gene and to obtain genomic sequence corresponding to the proximal promoter, a mouse genomic library (λ -DASH I-129) was screened using as probe a ³²P labelled *EcoRI/HindIII* 540 bp fragment of Up109 that contained 460 bp of unique sequence and the first 80 bp of exon 56 (this work was carried out as a

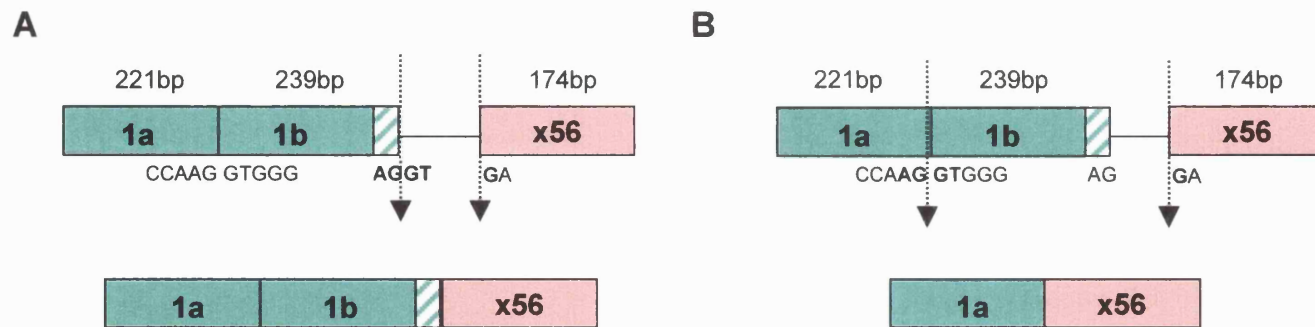


Fig 4.25 Alternative splicing events in the first exon of Up109. In A, 460 bp of unique 5' sequence (1a+1b) are spliced to exon 56 whereas in B, the most 221 bp (1a) are spliced to exon 56 and the intervening 239 bp behave as intron sequence. Discontinuous arrows indicate splicing and the nucleotides that are involved in the splice junction sites used in A and B are shown in bold type. The hatched area represents Up109 unique aa sequence. X56=utrophin exon 56; bp=base pairs.

collaborative effort with Wendy Putt in the lab). DNA from a positive recombinant, U109G-2, was prepared and digested with *EcoRI*, this seemed a sensible strategy since in the sequence comprised in the probe there is a single *EcoRI* site (Fig 4.23; Fig 4.26).

Southern blotting using the *EcoRI* /*HindIII* 540 bp probe identified a major 6.8Kb *EcoRI* fragment that contained the Up109 sequence (data not shown). This fragment was gel extracted (Fig 4.26 A) and sequenced using forward (Up109F1) and reverse (Up109Rs1) primers. Both primers are situated near the 5' end of Up109 sequence and are indicated in Fig 4.23. Sequencing with Up109F1 showed that this fragment contained Up109 sequence up to the intron 55/exon 56 boundary. The sequence then diverged from the known utrophin sequence into unknown sequence. In this experiment, c.40 bp downstream of the boundary could be read with confidence. This sequence is shown in Fig 4.26 B.

To explore the possibility that the Up109 sequence does not lie immediately adjacent to exon 56 a PCR amplification of mouse genomic DNA and foetal hands cDNA was carried out using Up109F1, situated at the 5' end of Up109 and Up109R1, situated in exon 56, (see Fig 4.23 for primer positions). If the first exon of Up109 lies immediately adjacent to exon 56 in the genome, the same size product (541bp) should be amplified from genomic DNA and cDNA. However, a product of the expected size amplified from cDNA but no product was seen after amplification of genomic DNA (Fig 4.26 C1). This result could not have been due to poor quality of the DNA sample since the same sample amplified well giving the correct size product using primers for the *pgm2* gene.

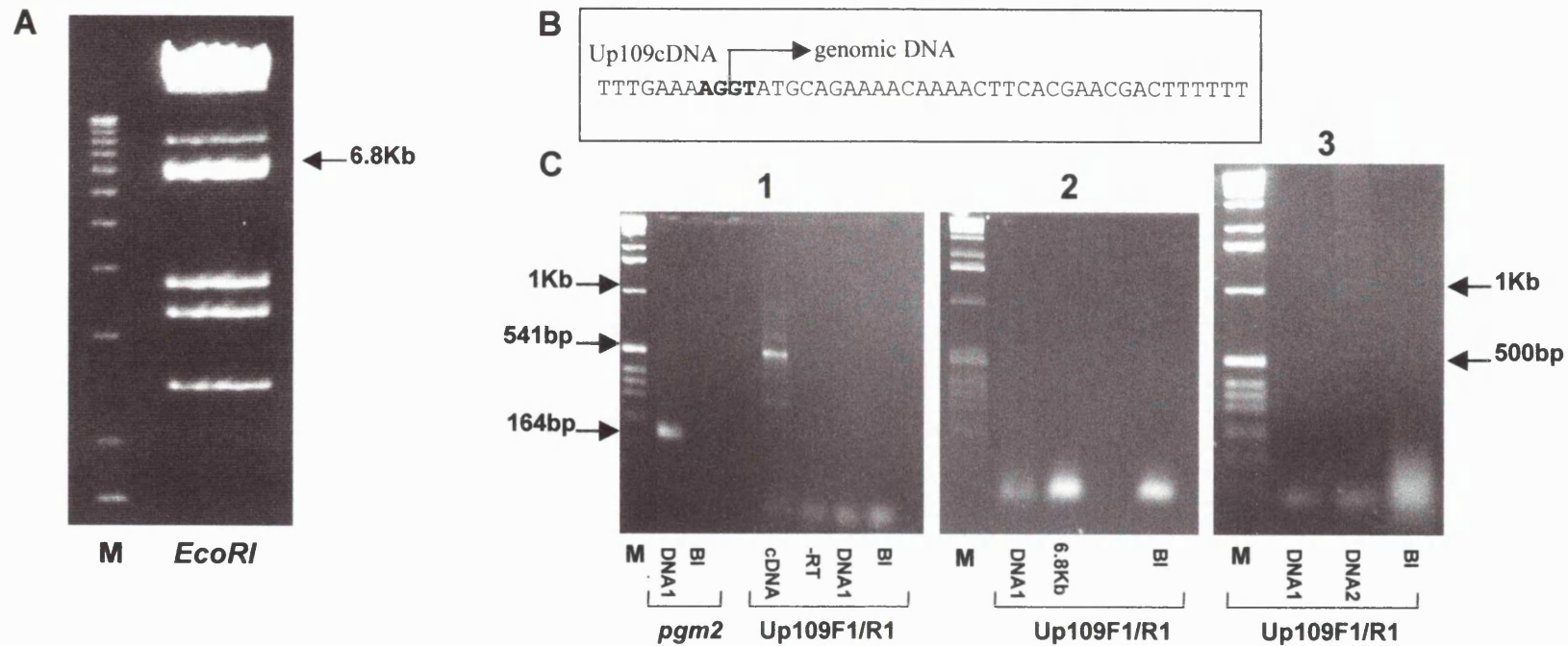


Fig 4.26 A, *EcoRI* digestion of the genomic recombinant, U109G-2. Southern blotting and autoradiography identified the 6.8Kb fragment as the major hybridising fragment. This band was gel extracted and sequenced with Up109 primers.

B, sequencing of the 6.8Kb fragment revealed unknown sequence downstream of the 3' end of the unique Up109 sequence (arrow) suggesting that Up109 novel sequence is separated from exon 56 by intron sequence. C.1, PCR of mouse genomic DNA (DNA1) with *pym2* primers to test the integrity of the DNA and PCR of DNA1 and foetal hands cDNA with Up109 specific primers. C.2, PCR of DNA1 and the 6.8Kb *EcoRI* fragment with Up109 specific primers. C.3, PCR of two genomic DNA samples, DNA1 and DNA2 with Up109 specific primers. M=DNA size marker; -RT=no-reverse transcriptase; BI=no DNA control

This PCR reaction was repeated using independent genomic DNA samples and the isolated 6.8Kb genomic fragment as templates with the same negative result (Fig 4.26 C2 and C3). These experiments support the results of the sequence analysis and together suggest that Up109 first exon is not adjacent or close to exon 56 but lies further away within intron 55.

In order to establish the position of the unique sequence within intron 55, and to determine whether the Up109 sequence is conserved between the mouse and the human genes, the human genome was searched for the 5' unique sequence of Up109. This search revealed a match with a chromosome 6 genomic clone in the high throughput database (HTG), (accession no: AC073979). The AC073979 sequence is designated a "working draft sequence" and is presented as 17 contiguous, apparently non-overlapping, fragments. The Up109 first exon lies between 125028 bp and 125488 bp of this sequence within fragment 16. The human sequence showed 87% identity with the mouse sequence (Fig 4.27). The start codon in Up109 coding sequence is conserved between both species and the identity at the aa level is 94% with only one aa change (serine in mouse and asparagine in human). Thus, it seems that the unique NH₂-terminus of Up109 is highly conserved and is important for the function of this isoform.

In order to determine the orientation of the Up109 sequence and to gain an idea of the size of intron 55, the human genomic sequence was searched for exons 55 and 56. These comparisons showed that exon 55 lies between 54203 bp and 54393 bp, (80% identity to the mouse sequence) and exon 56 sequence is between 182140 bp and 183315 bp (92% identity to the mouse sequence). These findings suggest that the size of utrophin intron 55 is >128Kb.

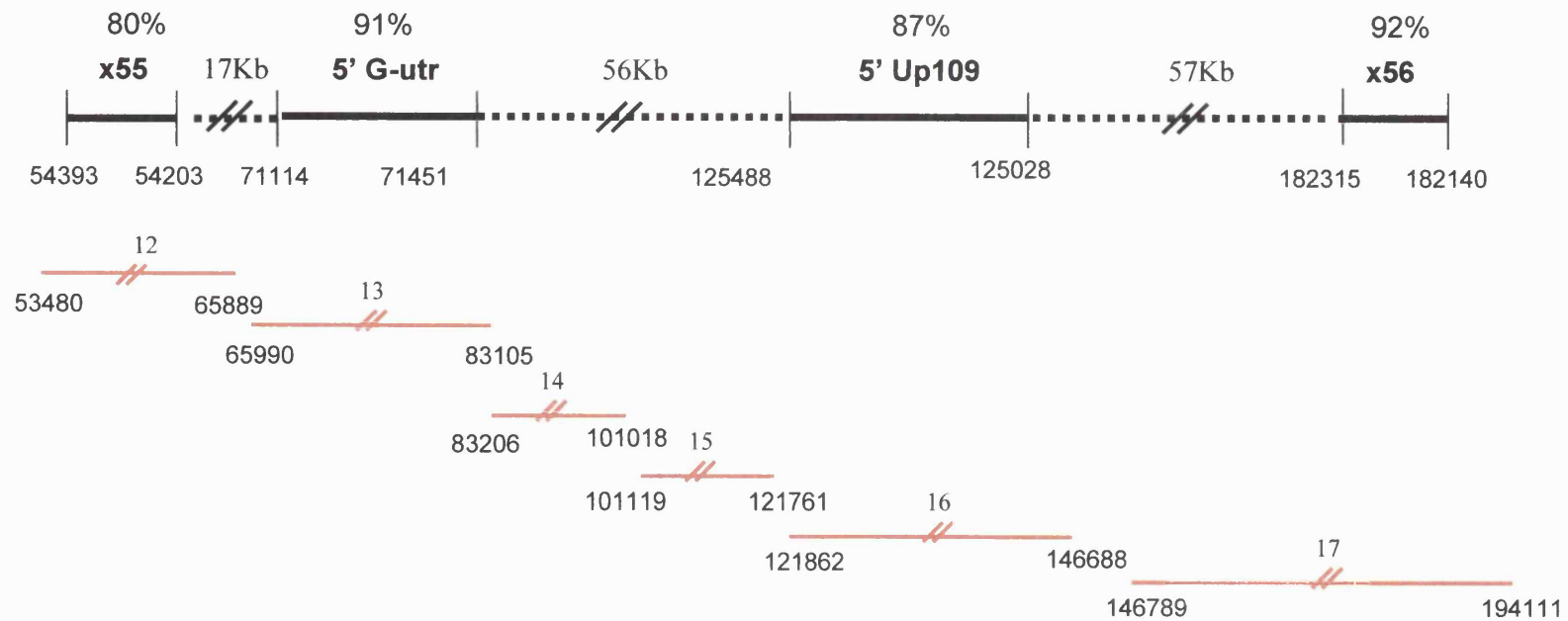


Fig 4.27. Diagram showing the relative positions of exon 55, exon 56, G-utrophin and Up109 first exons on the human AC073979 sequence. The percentage identity between the mouse and human sequences is shown above. Intronic sequence is represented as discontinuous black lines. The positions of the AC073979 fragments 12 to 17 are shown relative to this region of the utrophin gene as red lines. x: exon; Kb: kilobase

These data also indicate that the sequence which comprises Up109 first exon lies 57Kb upstream of exon 56.

The identification of a human genomic sequence containing the utrophin gene also allowed us to predict the position of G-utrophin first exon which is also thought to lie within intron 55 (Blake et al., 1995) but has not been firmly positioned. Comparison of the published G-utrophin exon 1 (accession no. X83506, Blake et al., 1995) with the AC073979 sequence located this exon between 71114 bp and 71451 bp (91% identity to mouse sequence). However, this sequence which is in fragment 13, is in the opposite orientation compared with the first exon of Up109 and exons 55 and 56 which lie in fragments 16, 12 and 17 respectively. Given that AC073979 is a “working draft”, it may be that this particular fragment which has no apparent overlap with fragments at either side has been entered in the database in the incorrect orientation.

Taken together, these observations suggest that the structure of the utrophin gene in the region of exon 55-56 may be as shown in Fig 4.27.

5' flanking sequence of Up109

Sequencing of the 6.8Kb *EcoRI*

fragment, isolated from a mouse genomic library (Fig 4.26 A), with the primer Up109Rs1 (Table 2.4, Fig 4.23) extended the Up109 sequence by 298 bp towards the 5' end. This sequence, which could constitute the proximal promoter of Up109 was analysed using the Signal Scan program for the presence of promoter elements and transcription factor binding sites (Fig 4.28).

The GC content of this region flanking Up109 is 45%. Thus, there is no indication that Up109 is characterised by a CpG island, as for example, is found in the proximal promoter of the short dystrophin transcript Dp71. However,

Up109 is developmentally regulated and it is not expected to be regulated in a manner typical of a housekeeping gene. There is an Initiator sequence (Inr) at –129 bp (numbers given are from the 5' end of the 5'RACE product). This sequence, which is conserved from *Drosophila* to mammals (Burke et al., 1997), is often found at the start of transcription (A is position +1) and is a variant of the consensus sequence PyPyCAPuPu (Strachan, Read, p.174, 1999). If transcription is initiated at this position it means that the sequence obtained through the 5'RACE experiment was not complete but was 129 nt short of the 5' end of the mRNA.

To acknowledge both possibilities of initiation of transcription, the positions of promoter elements are given below in bp from the end of the 5' RACE product and in brackets from the Inr sequence. No conventional TATA box and CCAAT box was found. However, it has been shown that TATA less promoters can initiate transcription from a GC box where the transcription factor Sp1 binds (Smale et al., 1997). There is a potential Sp1 binding site at position –206; they are usually found within 100bp of the transcription initiation site, and if we consider the A in the Inr sequence (-131) as the start of transcription, this GC box will then be at position -75. There is a binding site for the general initiator of transcription TFIID at position –89 (+ 42); This motif has been shown to be functional in the core promoter of the myelin basic protein gene (Tamura et al., 1988), for example. In the case of Up109 this motif would lie in the 5'UTR. In addition, at position –39 (+ 92) there is a binding site for MAZ, a Zinc-finger type DNA-binding protein that is involved in the regulation of expression of the *c-myc* gene (Bossone et al., 1992) and that has been found to be important in

-298 atgaaactagcttggtggtcaccatacaactgtgcttctgctgtctggga
 CACC **c-myc**

-248 gaatggaagctggtggtctcgtgtctcgggtttttgggcgcttccagc
 CACC **Sp1**

-198 taggagcacactcctgcttactggaactctacataagccctgctgtttta

AP1 →

-148 aaattggtccttgactcagacttttttttttttctgtcttttcttttt
 F2F **Inr** **PEA3** **PEA3**

-98 tctttttgaaggcagcctgaatggaggaagtggtaatgcttggcttttt
 TFDII

-48 ttccctcccttctctcttgcaagtttcaggctatagctttttccccctt →

MAZ

Fig 4.28. 5' flanking sequence of Up109. The two potential transcriptional start sites are indicated by arrows. Potential binding sites for transcription factors are indicated. The numbering is from the 5' end of the largest 5' RACE product.

the regulation of genes that lack a TATA box, for example as described for the serotonin 1a receptor gene (Parks et al., 1996).

Other promoter elements identified include two potential CACC boxes at positions –233 (-102) and –281 (- 150). These sequences are recognition sites for the erythroid Krüppel-like factor (EKLF) which is a zinc-finger DNA- binding protein (Miller et al., 1993) and for the ht β factor that is involved in the regulation of T-cell receptor genes (Wang Y. et al., 1996). CACC boxes are found in the regulatory sequence of a large number of genes including the β -globin gene (Mantovani et al., 1988). There are also binding sites for other ubiquitous transcription factors such as c-myc, position – 266 (-135), a cell cycle regulator; F2F a general transcriptional repressor (Jackson et al., 1992) and AP-1. Near this AP-1 binding site there are two sequences, -113 and –103 (+ 19 and + 29 respectively), that may constitute binding sites for PEA3 transcription factor that has been shown to interact synergistically with AP1 to increase transcription levels (Gutman et al., 1990).

In hands, Up109 appears to be developmentally regulated, such that it is most abundant between 15 and 16 dpc and declines to low or absent levels after birth (see Fig 4.11 and 4.12). However, binding sites for transcription factors known to be important during development were not identified.

Transcription factors which are crucial for the development of the limb and digits are for instance the 5' most members of the *Hoxa* and *Hoxd* gene clusters, *Lmx1* and also T-box transcription factors such as *Tbx4* and *Tbx5* (Schwabe et al., 1998). No binding site for any of these transcription factors are found in Up109 proximal promoter; on the contrary, the majority of the identified promoter elements are binding sites for ubiquitous transcription factors.

Discussion

4.7 General comments

Western blot analysis has been a central technique in the study of utrophin since it became the focus of research in the context of its similarity to dystrophin and the muscular dystrophies (Hoffman et al., 1989a; Love et al., 1989). Early studies showed that utrophin was more widely distributed than dystrophin and prompted the analysis of other non-muscle tissues such as brain (Khurana et al., 1992), peripheral nerve (Matsumura et al., 1993a) and lung (Matsumura et al., 1993b). During the course of these studies, researchers came across smaller mw bands on Western blots but these were regarded as degradation products of full-length utrophin (Matsumura et al., 1993a; Nguyen et al., 1991) or as non-specific bands (Tanaka et al., 1991). It was only after short dystrophin isoforms were isolated (Bar et al., 1990; Byers et al., 1993; Lidov et al., 1995), that the existence of short utrophin isoforms was considered.

The cloning and sequencing of the human utrophin cDNA was completed in 1992 (Tinsley et al., 1992) and various laboratories raised antibodies against different regions of the human protein in an attempt to look for potential short isoforms. But little progress has been made.

In the case of dystrophin, the availability of samples from the *mdx* mouse and the null mutations in DMD patients had helped to resolve full-length dystrophin from short dystrophins and dystrophin specific from non-specific products. A similar approach became possible for utrophin with the generation of utrophin null mice (Deconinck et al., 1997a; Grady et al., 1997a), and the study described here was initiated.

4.8 The origin of the multiple bands seen on Western blots

Earlier studies undertaken in other labs on normal human and mouse tissues had recognised various problems with using a Western blot approach; these included, degradation of full-length utrophin, crossreactivity of utrophin specific antibodies with related proteins and the limitations of monoclonal antibodies, all of which have been encountered in this study. Two of these problems, degradation of full-length utrophin and crossreactivity with related proteins, appear to be inherent to the structure of utrophin and are difficult to avoid.

Degradation of full-length utrophin Full-length utrophin and dystrophin, are giant proteins (427kDa and 395kDa respectively) and thus are particularly susceptible to degradation. There are several examples in the literature where small mw bands, likely to correspond to breakdown products of these proteins, have been detected on Western blots by dystrophin and utrophin specific antibodies.

Koenig et al. (1990) detected a c.200kDa band in skeletal muscle extracts using antibodies against the NH₂-terminus and against the rod domain of dystrophin. This polypeptide could be generated experimentally by limited proteolysis of dystrophin. Voit et al. (1991) reported a similar 220kDa band in DMD muscle extracts using a utrophin crossreacting antibody to dystrophin. The authors ascribed this band to a breakdown product of full-length utrophin since dystrophin was absent from this patient's muscle. Because these polypeptides were more prominent in DMD and BMD muscle Voit et al. (1991) further suggested that dystrophin and utrophin could be particularly susceptible

to degradation by site specific proteases in diseased muscle. These authors and Hoffman et al. (1988) also reported a dystrophin and utrophin doublet ,with mobility slightly faster than the full-length polypeptides, which they also attributed to degradation.

Nguyen et al. (1991, 1992) have reported bands which they ascribe to degradation of full-length dystrophin and utrophin detected with monoclonal antibodies. They describe in particular a ladder of bands ranging in size between 60kDa and 180kDa in several cell lines extracts including glioma, Schwannoma, skin fibroblasts and Hela epithelial like cells (Nguyen et al., 1992).

A ladder of bands in association with the degradation of β -spectrin (270kDa) seen in this study supports the argument that large proteins are more susceptible to degradation.

It is worth mentioning, that throughout the Western blots carried out in this thesis, degradation products of utrophin were detected with the NH₂-terminal antibody, Mupa-1, and were much less apparent with the COOH-terminal antibodies. This suggests a gradual truncation from the COOH-terminus. A similar pattern of degradation with the identification of protease-sensitive regions has been described for dystrophin (Hori et al., 1995).

Since the utmost care was taken in preparing tissue extracts and avoiding repeated thawing, we must conclude that rapid degradation takes place in the tissues immediately on death and before extraction.

Crossreactivity with related proteins Immunogenic crossreactivity occurs when different proteins share antigenic determinants and is most likely

to occur between related proteins belonging to the same family. Crossreactivity has been described for numerous protein families; for example, the glycoproteins hormones which include thyroid stimulating hormone (TSH), luteinizing hormone (LH), follicle stimulating hormone (FSH), and chorionic gonadotropin hormone (CGH). These hormones are formed by a common α -chain and a hormone "specific" β -chain encoded by different genes on different chromosomes. However, antibodies against the β -chain of TSH have been shown to cross-react with the β -chain of LH, FSH and CGH (Baluja et al., 2000).

Another example is provided by the eight member family of metabotropic glutamate receptors (mGluRs). The protein consists of a large conserved extracellular NH₂-terminal domain, a hydrophobic region of seven transmembrane domains and an intracellular COOH-terminal domain. Antibodies raised against sequences from the NH₂-terminal and COOH-terminal regions crossreact with other glutamate receptors both in Western blots and immuno-histochemistry (Peltekova et al., 2000).

Utrophin belongs to the spectrin superfamily which also includes spectrin, actinin, dystrophin (Pascual et al., 1997), dystrophin-related protein 2 (DRP2), (Roberts et al., 1996) and dystrobrevin (Blake et al., 1996a). Dystrophin and utrophin share homology with spectrin β chain (see section 1.4) and with α -actinin (section 1.4) at the actin binding domain (percentage identity at the aa level is c. 55%) and in the central region of spectrin repeats (percentage identity at the aa level is c. 35%), (Davison et al., 1988; Tinsley et al., 1993b).

There are other proteins not members of the spectrin superfamily that also contain an actin binding domain similar to the one found in dystrophin and

utrophin (overall percentage identity at the aa level 35-40%). For example; fimbrin, 70kDa (Bretscher et al., 1980), filamin, 280kDa (Koteliansky et al., 1982) and plastin, 70kDa (Lin C. et al., 1993). Given adequate regions of identity, these proteins may also crossreact with utrophin and/or dystrophin antibodies.

The possibility that antibodies raised against dystrophin/utrophin may crossreact with members of the spectrin superfamily is well acknowledged in the literature. This is best illustrated by the work of Hoffman et al. (1987b, 1989) on dystrophin. The authors reported that an antibody against the rod domain of dystrophin crossreacted on Western blots with a c.90kDa polypeptide corresponding to an isoform of cytoskeletal α -actinin. Examination of α -actinin in extensor digitorum longus (EDL) muscle extracts showed that in this tissue it was c.1000 fold more abundant than dystrophin. As a further experiment, α -actinin was immunoprecipitated with an α -actinin polyclonal antibody and the purified protein Western blotted and detected with the dystrophin antibody, thus confirming the crossreactivity.

In addition, utrophin was detected as a dystrophin-crossreacting protein, before being isolated and recognised as a dystrophin homologue (Fardeau et al., 1990; Pons et al., 1991). Prior to the cloning of utrophin, this crossreactivity of some dystrophin antibodies was used to study the tissue distribution of utrophin and the conservation of the structural domains between the two proteins (Voit et al., 1991).

In the present study, we have proposed that Mupa-1 antibody (raised against the actin binding domain of utrophin) crossreacts with β -spectrin and possibly α -actinin and plastin. The likelihood of β -spectrin being the 260kDa

band seen in brain, kidney and muscle extracts is high since a sequence of almost 20 aa is shared between spectrin and utrophin in the region used to raise Mupa-1; this number of residues is regarded as sufficient to constitute an antigenic determinant (Catty, 1989).

However, the possibility of crossreactivity with α -actinin and plastin in striated muscle and brain is more difficult to explain since sequence alignments showed that in both cases only very short contiguous aa sequences (5 aa) of high identity occur. It may be that in these tissues α -actinin and plastin are much more abundant than utrophin and weak interactions may still result in bands of moderate to high intensities.

Two monoclonal antibodies raised against the NH₂-terminus of human utrophin have been described; Mannut-1 (Nguyen et al., 1995), aa 113-371, and DRP2 (Novocastra), aa 1-261. In addition, a polyclonal antibody, UT-11, has been raised against aa 2-594 of rat utrophin (Knuesel et al., 2000). These antibodies are raised against similar regions of the actin binding domain that are also potential crossreacting antigenic determinants. However, the individual clones from which Mannut-1 and DRP2 are derived may not necessarily recognise those sequences. Preliminary Western blots made in our lab with Mannut-1 showed that this antibody detects a 100kDa band in human striated muscle. This is very similar to the non-specific (perhaps α -actinin) band seen in our study in skeletal and cardiac muscle using Mupa-1. However, Nguyen et al. (1995) did not encounter such a crossreactivity problem in their work using Mannut-1. Similarly, there is no evidence from the literature that Mannut-1 or DRP2 crossreact with β -spectrin (Nguyen et al., 1995; Grady et al., 1997a).

In glioma cells, Mannut-1 and UT-11 each detect a 62kDa band (Nguyen et al., 1995; Zuellig et al., 2000). It was proposed that this polypeptide represents a short NH₂-terminal utrophin isoform containing the actin-binding domain and three spectrin repeats. However, it seems reasonable to ask whether this polypeptide represents crossreaction with an actin binding protein, as seems to be the case for the 65 kDa band detected with Mupa-1 in brain extracts in the course of the present study.

The problems of crossreactivity could be resolved, in the case of monoclonal antibodies, by selecting clones that do not interact with crossreacting partners; either using an ELISA based assay or Western blotting. This would be time consuming and perhaps not entirely foolproof as some crossreacting partners could not be predicted. Similarly, polyclonal antibodies could be preabsorbed against immobilised polypeptides from the region of identity between the crossreacting proteins. For example, the utrophin polyclonal antibodies, Urd40 (Blake et al., 1999) and UT-2 (Imamura et al., 1998) were preabsorbed against dystrophin to avoid crossreactivity. In practical terms, it would be too unwieldy to preabsorb utrophin antisera against all the members of the spectrin superfamily and actin binding protein families and indeed such repeated preabsorption is likely to result in the loss of specific activity.

Other crossreactivities Other crossreacting proteins for which no firm candidates could be identified are more difficult to explain and their origin may lie in the nature of the Mupa antibodies, Urd40 and Mancho-3. These antibodies have all been raised against large proteins with the advantage that they

recognise native utrophin and therefore can be used in a wider range of techniques such as immunoprecipitation and immuno-histochemistry. The obvious disadvantage is that they interact with a larger number of antigen determinants and are more likely to crossreact with other proteins. This point emphasises the advantage of antibodies raised against synthetic peptides (linear antigen determinants) which is that they can detect very specific regions of a protein. However, this type of antibody provides a good resource mainly for Western blotting, in denaturing conditions, and are not always effective with naturally folded protein.

Monoclonals are sometimes preferred because each clone is homogenous in specificity, activity and detects a single antigenic determinant, whereas polyclonal antibodies, are heterogeneous with many IgGs interacting with different epitopes and the specificity and affinity of a polyclonal antibody may vary from one immunised animal to another. Mancho-3 is a monoclonal antibody unlike the Mupa antibodies and Urd40.

Preliminary trials with Mancho-3 showed that this antibody detected in addition to full-length utrophin a series of bands in all tissues. Some of these bands could represent mouse immunoglobulins (IgGs) present in blood contaminating the extracts. This would be in line with a report by Nguyen et al. (1992) of a band of c. 50kDa (the mw of IgG heavy chain) detected using Mancho-3 and Mancho-7 in mouse cell extracts. Although this band was present in all cells it was most intense in a hybridoma cell line which is likely to contain large amounts of mouse IgGs. The IgGs in this case would have been detected by the anti-mouse IgG second antibody. Nguyen et al. (1992) did not check this possibility.

However, it seems likely that the bands detected in the present study with Mancho-3 are not mouse IgGs since they were not seen when the blots were incubated with the second antibody only. Therefore they seem more likely to be the result of Mancho-3 recognising an unidentified family of mouse proteins. Since this difficulty could not be readily overcome, Mancho-3 was not used extensively in the present study.

4.9 Short utrophin isoforms

Analysis of mouse tissue extracts by Western blotting with the newly prepared Mupa antibodies has provided valuable information about short utrophin isoforms and their regulation. Analysis of UKO^{ex6} tissues has been a crucial aspect of this study, effectively removing the complexity associated with degradation of full-length utrophin. As a result, we have been able to identify with some confidence potential short isoforms. Our study has emphasised the diversity of utrophin isoforms and the complexity of the regulation of the utrophin gene. The most relevant findings are discussed below.

Are Up140 and Up71 translated?

The Western blots described in this study found no firm evidence of polypeptides corresponding to the short utrophin isoforms Up140 and Up71. Nevertheless, a handful of isolated reports hint that there might be translation of these transcripts in certain tissues. Lumeng et al. (1999) detected a band of 140kDa in adult skeletal muscle and in testis and bands that could correspond to Up71 in brain. All three of these tissues were examined in the present study without detecting such components. A band of 80kDa, which might correspond to Up71, has been reported in

peripheral nerve and in isolated rabbit arteries and veins (Fabbrizio et al., 1995; Rivier et al., 1997). These special tissues were not isolated and tested in the present study. Taken together, the available data show that expression of Up71 and Up140 as proteins is not abundant or widespread although some expression might be confined to a few special sites.

The absence, or undetectable levels, of Up140 and Up71 polypeptides is in contrast with the distribution of their mRNAs which have been found in a wide variety of adult and foetal tissues (Wilson et al., 1999; Lumeng et al., 1999) by RT-PCR. While RT-PCR provides a rapid method for examining the expression of transcripts and requires very small amounts of RNA (cDNA synthesis and amplification from 1 µg of total RNA versus 5 to 10 µg for loading on a Northern blot) it is also an extremely sensitive technique. Single or a few mRNA molecules can be amplified and this may mean that low abundance messages might be detected by RT-PCR which would not be detected by Northern blotting. Other laboratories using Northern blotting have detected full-length and G-utrophin transcripts, 13Kb and 5.5 Kb respectively (Blake et al., 1995, Lumeng et al. 1999), but not Up140 or Up71 transcripts (6.5Kb, or, 4.9Kb).

The differences in sensitivities between techniques such as Northern and Western blotting and RT-PCR have been raised previously in connection with expression of the short dystrophin isoforms. On the basis of Northern and Western blot analysis Dp140 mRNA was believed to be restricted to brain, kidney and retina (Lidov et al., 1995; Rodius et al., 1997) and Dp71 to liver, testis, lung, kidney and retina (Bar et al., 1990; Lederfein et al., 1993; Rapaport et al., 1992; Blake et al., 1992; Claudepierre et al., 1999). However, Tokarz et al. 1998 using RT-PCR demonstrated Dp140 and Dp71 mRNAs in several

tissues not previously described and argued that their distribution had been underestimated.

In the case of utrophin, RT-PCRs predict a wide tissue distribution for Up140 and Up71 mRNAs. However, the actual pattern of translation of these transcripts appears to be much more restricted. This discrepancy between RNA and protein levels may conceal interesting mechanisms of post-transcriptional processing.

Although initiation of transcription is considered the primary control point for the regulation of gene expression this is not always the case; there may be variation in mRNA transport and stability, translation, protein targeting, stability and processing. Variable levels of translation may be controlled by RNA-binding proteins interacting with sequences in mRNA untranslated regions. Protein binding may promote or repress translation and in addition, may regulate the stability of the mRNA molecule. For example, this has been shown for the connective tissue growth factor/hypertrophic chondrocyte specific 24 (ctgf/hcs24) mRNA which has an element within its 3' UTR which acts as a cis-acting element binding to a nuclear factor, which has not been identified yet, which represses translation (Kubota et al., 2000). Similar regulatory sequences are also found in the 5' UTR of the iron binding protein, ferritin, mRNA. These sequences, known as iron-response elements (IRE), bind IRE-binding proteins and these interactions are important for the maintenance of iron homeostasis (Klausner et al., 1993). Iron metabolism provides a good example of translational control of gene expression; elevated blood iron levels result in an increase in the synthesis of ferritin protein without changes in the levels of its mRNA (Klausner et al., 1993).

An example more relevant to this thesis is the post-transcriptional regulatory mechanism which controls the expression of Dp140 in the developing rat retina; while the nature of the control mechanism is unknown, it results in an increase in Dp140 protein levels without a change in levels of Dp140 mRNA (Rodius et al., 1997). There is no direct evidence for such regulatory mechanisms controlling the expression of Up140 and Up71.

The absence or undetectable levels of Up140 and Up71 proteins might be explained in a number of other ways

- a) The protein products are very unstable
 - b) The sequences necessary for translation initiation are not in a favourable environment resulting in poor translation.
 - c) The transcript is functional as an mRNA and not as a protein
- a) There is some evidence to suggest that proteins which are normally associated with membranes may be unstable and more susceptible to degradation if they are unable to bind (Bijlmakers et al., 2000; Loo et al., 1998; Yates et al., 1997; Manilal et al., 1998). Thus, utrophin (and dystrophin) stability may depend on the formation of a DAP complex and the correct assembly of this complex. It has been demonstrated that the converse is true; loss of dystrophin results in a dramatic reduction of sarcolemmal DAPs (Ervasti et al., 1990; Ohlendieck et al., 1991a; Sewry et al., 1994a).

Another pathological situation is illustrated by Emery-Dreifuss muscular dystrophy. In some cases, a truncated emerin protein lacking the hydrophobic COOH-terminal tail, which anchors emerin to the nuclear membrane, results from mutation (Manilal et al., 1998). The truncated protein cannot be detected

by Western blotting despite normal mRNA levels. The authors suggest that a truncated emerin is unstable because it cannot integrate into the membrane.

Up140 and Up71 possess the domains needed for association with the DAPs and are likely to form a DAP complex. The short dystrophin isoform Dp71 is known to assemble DAPs since its exogenous expression in skeletal muscle of *mdx* mice restores the DAP complex to the membrane, although this results in a more severe muscle phenotype (Greenberg et al., 1994). It could be postulated that in normal muscle competition exists between full-length utrophin and the short utrophins for available sites in the DAP complex. Full-length utrophin would be preferentially recruited to the complex and unbound Up140 and Up71 rapidly degraded. However, this idea does not explain their absence in the UKO^{ex6} mice.

The argument could be extended so that in UKO^{ex6} mice full-length dystrophin may substitute for full-length utrophin preferentially to Up140 and Up71. If this were the case then it could be further argued that Up140 and Up71 polypeptides will be detected in tissues of the double knock-out mice, dko^{ex6} (Deconinck et al., 1997b, section 1.10).

There is some information on this particular point from the work of Rafael et al. (1999). Western blot analysis of dko^{ex6} tissues show no evidence for synthesis of Up140 and Up71. This finding argues against the idea that Up140 and Up71 are translated but degraded if not assembled into a DAP complex.

The blots of the dko^{ex6} show a protein of some interest; this was a band in dko^{ex6} kidney extracts which was absent in control mice and appears to correspond to the Up120 isoform described in the present study. It is not clear

why it was not seen in the control mice extracts but this could be in line with the view that Up120 is upregulated in the absence of full-length utrophin.

b) Are Up140 and Up71 poorly translated?

Both Up140 and Up71 translation initiation codons lie in weak consensus sequences (ideal Kozak consensus is gccGCCG/ACCAUG, Kozak et al., 1995). However, both have a critical G and A respectively at position –3 to the most likely translation initiation codons. The ATG codons in G-utrophin and Up109 are within similar sequences which also do not conform the ideal Kozak consensus, but both seem to be translated. Therefore, deviation from the consensus sequence is not sufficient to prevent translation and other translational or post-translational factors must be involved.

c) Up140 and Up71 may function as transcripts and not as proteins

There are several examples of mRNA-like transcripts (spliced and with a poly-A tail) that are not translated into proteins and are believed to function at the RNA level. One of these is *Xist*, X inactive specific transcript, which is expressed exclusively from the inactive X chromosome and is a processed RNA for which no protein product has been identified. The transcript is not exported from the nucleus and is found associated with the X-chromosome. It has been postulated that it might have a role in chromatin remodelling (Erdmann et al., 1999).

Another example is the *gas5* mRNA, expressed in the growth arrest phase of the cell cycle, with only a short open reading frame (ORF) encoding a polypeptide of 41 aa. Antibodies raised against those 41 aa failed to detect a

protein product by Western blotting in cultured cell lines or mouse tissue extracts. However, protein synthesised *in vitro* was detected (Raho G et al., 2000). Comparison of mouse and rat gas5 showed that the ORF is not conserved. Many other non-coding RNAs have been identified in animals and plants (Erdmann et al., 1999). A common characteristic of these transcripts is that they lack an obvious ORF or only have putative very short ORFs with little or no conservation across species.

In the final discussion section a novel idea for the role of Up140 and Up71 mRNAs will be discussed.

Confirmation that G-utrophin is a neuronal specific utrophin isoform The Western blot data presented in this chapter show that in contrast to Up140 and Up71, a polypeptide corresponding to G-utrophin (113kDa) was consistently detected in control and UKO^{ex6} brain extracts. These data are in line with previously published studies; together, they confirm that G-utrophin expression is restricted to neural tissues (Blake et al. 1995; Lumeng et al., 1999; Knuesel et al. 2000). There is only one previous report of protein studies; Knuesel et al. (2000) detected a 113kDa band in rat brain extracts using an antibody raised against the COOH-terminus.

What is the function of G-utrophin in the neurone? mRNA *in situ* hybridisation experiments on brain sections (Blake et al., 1995; Knuesel et al., 2000) localise G-utrophin to neurones rather than glia or microvasculature, where full-length utrophin seems to be the major isoform (Knuesel et al., 2000). The sites of expression include; the large neurones of the facial nuclei, all the neurones of the pontine, vestibular and anterior olfactory nuclei, pyramidal

neurones of the cerebral cortex and secretory neurones of the hypothalamus. In dorsal-root and trigeminal ganglia G-utrophin is expressed in unipolar sensory neurones.

From immuno-histochemistry, it seems most likely that G-utrophin is localised at the postsynaptic membrane of the dendrites (Kamakura et al., 1994, Knuesel et al., 2000). Since G-utrophin contains the cysteine rich and carboxy-terminal domains involved in interaction with the DAPs it could form part of a specialised post-synaptic membrane complex. This is likely to involve β 2-syntrophin since its pattern of expression overlaps that of G-utrophin (Peters et al., 1994, Gorecki et al., 1997) and perhaps β -dystrobrevin which associates with dystrophin in neurones (α -dystrobrevin-1 does not occur in neurones, Blake et al., 1999). β -dystroglycan is not likely to be part of the G-utrophin complex since its expression does not overlap that of G-utrophin (Schofield et al., 1995b).

The G-utrophin complex could play a role in the establishment and maintenance of the synapse and/or in the clustering of neurotransmitter receptors. This might be similar to the function of full-length utrophin in the clustering of acetylcholine receptors (AChR) at the muscle NMJ. Alternatively, these complexes could also be involved in signalling processes via nNOS bound to syntrophin (Brenman et al., 1996; Hillier et al., 1999) but in either case it should be remembered that G-utrophin, unlike full-length utrophin, does not have the NH₂-terminal domain for linking to the cytoskeleton.

At the start of this project the position of the G-utrophin unique first exon and 5' flanking sequence were unknown. Sequence including this part of the utrophin gene has now appeared in the Human Genome Project high

throughput database, and sequence comparison places the first exon of human G-utrophin in intron 55, 113Kb upstream of exon 56. It is of some interest that the percentage identity between the mouse and human first exon sequences is 91%. This degree of identity is substantially higher than for Up140 (70%) and Up71 (60%) (Wilson thesis, 1999) and suggests perhaps greater selective pressure on the G-utrophin sequence.

Where is the promoter of Up120?

The studies described here point to the existence of a novel tissue specific isoform of utrophin: a 120kDa kidney specific isoform. Taken together with evidence from work in other labs which report bands of a similar size in kidney (Nguyen et al., 1992; Rafael et al., 1999; Loh et al., 2000), the evidence for this isoform is strong. The size of the polypeptide suggests that the transcript must initiate in intron 53 or intron 54, however, I was not able to recover a novel mRNA species by 5' RACE.

This failure must result from inadequacies in the design of these particular 5' RACE experiments. For instance, there was clear evidence of non-specific binding of the gene specific primer during the reverse transcription step, the end result of which was that a relatively large proportion of the recovered sequences were unrelated to utrophin. This problem could be prevented in future studies by carrying out the nested PCR steps at higher annealing temperature or by redesigning the gene-specific primers.

This difficulty was probably compounded by the strategy of cloning the PCR products which led to the preferential selection of small products. Very few of the utrophin sequences recovered in this way extended 5' beyond exon 53 and therefore the possibility that Up120 mRNA initiates from intron 53 could not

be excluded. It is also possible that the Up120 transcript may initiate within intron 51 or 52 and this area might be a target for future 5' RACE studies.

While the intensities of the bands seen on Western blots indicate that Up120 protein levels are comparable to full-length utrophin it is not necessarily the case that the mRNA is at corresponding levels and indeed Up120 mRNA may represent a very small proportion of kidney mRNAs. It may be sensible in future 5' RACE experiments to use an increased amount of template RNA.

Perhaps the most productive approach to take in future studies would be to screen kidney cDNA libraries using either cDNA probes or if an expression cDNA library is available, Mupa-2, Mupa-3 and Urd40 antibodies as probes. It might be particularly powerful to screen the filters consecutively with more than one antibody and with a short cDNA representing the unique sequence of Up120. In this way, recombinants containing full-length utrophin and other short utrophins would be identified and could be put aside and Up120 recombinants selected.

Does Up120 have a role in kidney ?

Utrophin expression has been demonstrated in several areas of the kidney; collecting ducts and tubules, glomerulus and Bowman's capsule (Loh et al., 2000) and in a kidney epithelial cell line (MDCK) (Kachinsky et al., 1999). Loh et al., (2000) showed by immunohistochemistry and immunoprecipitation, using Urd40 and isoform-specific dystrobrevin and syntrophin antibodies, that in each of these sites utrophin is forming a specialised complex with different syntrophin and dystrobrevin isoforms. Up120 could be part of one or some of those complexes since it contains the necessary sequences to interact with DAPs (but lacks the actin

binding NH₂-terminal domain). Full-length utrophin or Up120 may serve different purposes in each kidney structure. Up120 may be complexed with β -dystrobrevin; careful scrutiny of Figs shown in Loh et al. (2000) revealed a band of c.120kDa that is immunoprecipitated with a β -dystrobrevin specific antibody.

A novel short isoform(s) in testis

The results from the present study indicate that a novel testis specific utrophin isoform (s) may exist. There has been one previous report concerning utrophin in testis; Lumeng et al. (1999) detected bands of 97kDa and 90kDa. The 103kDa and 97kDa polypeptides seen in the present study could correspond to those bands seen by Lumeng et al. (1999).

In order to further investigate this short transcript, a testis mRNA 5' RACE experiment could be carried out focusing on the region of exon 56-57, alternatively, the cDNA could be isolated by screening testis specific cDNA libraries.

Up109: A novel foetal utrophin isoform

A novel short utrophin transcript, Up109, has been identified during the course of this study. Previously published mRNA *in situ* hybridisation experiments in control embryos (Schofield et al., 1993) provided the first clue that a novel transcript could be expressed at high levels in the tendons in foetal hands. This was followed by the detection of a major polypeptide of 109kDa in foetal hands extracts by Western blotting and finally the corresponding cDNA was isolated by 5' RACE.

Comparison of utrophin cDNA sequence with the sequence information available from the Human Genome high-throughput database indicates that

intron 55 is 130Kb long; the exceptional size of this intron makes it less surprising that two distinct promoters transcribing two separate transcripts, G-utrophin and Up109, could emerge in this position of the utrophin gene. Further comparisons showed that Up109 and G-utrophin first exons are 57Kb and 113Kb upstream of exon 56 respectively. The sizes of other utrophin introns have not yet been determined, but such large introns are not unusual in the dystrophin gene, although there is no evidence for multiple promoters within a single intron of the dystrophin gene.

An interesting observation is that while both G-utrophin and U109 first exons lie some distance upstream of exon 56, the first exons of Up140 and Up71 are immediately adjacent to exons 45 and 63 respectively. However, the promoters for Dp140 and Dp71 lie somewhere within introns 44 (Lidov et al., 1995) and 62 (Lederfein et al., 1993) in the dystrophin gene (exact position not yet known). These observations confirm that sequences which are functional in RNA transcription may arise at any position where the sequence context is favourable.

The percentage identity between the mouse and human Up109 unique sequence is 87% (this thesis) which is higher than for Up140 (70%) and Up71 (60%) first exons (Wilson thesis, 1999). It is tempting to speculate that this high degree of conservation supports the view that this isoform is functional and necessary for the cells in which it is expressed.

The mRNA and protein expression data presented in this study indicate that Up109 is preferentially expressed in foetal tissues and is developmentally regulated. mRNA *in situ* hybridisation experiments (Schofield et al., 1993) suggests that Up109 mRNA accumulates in the tendon primordia. However,

immuno-histochemical analysis of foetal hands sections with Mupa antibodies, which will be described in detail in the next chapter (section 5.2, Fig 5.22, 5.23) rather suggests that Up109 protein may be localised not to the tendon primordia but to the deepest strata of the epidermis and to the epidermal-dermal junction. Thus, in the case of Up109 the mRNA and protein do not appear to co-localise.

There are other instances where mRNA and protein do not co-localise. For instance, in the large intestine, carbonic anhydrase I (CA 1) mRNA localises to the upper half of the mucosal crypts whereas the protein is found in the luminal epithelium (Sowden et al., 1993). In this case, it seems that transcription occurs as the cells migrate and differentiate en route to the luminal surface, while translation occurs once the cells reach the luminal surface and mature. Another example is the neuronal enzyme PGP9.5 in the mouse embryo (Schofield et al., 1995a). While PGP9.5 mRNA is most abundant in the superficial layers of the cerebral cortex, the highest levels of protein are found in the deeper layers of the cortex. The different localisation of Up109 mRNA and protein would imply cell migration or some mechanism of mRNA or protein translocation, perhaps involving ribonuclear protein particles which could mask the RNA or protein from probe or antibody interactions.

Up109 could also be responsible for the signal detected by mRNA *in situ* hybridisation in other foetal tissues by Schofield et al. (1993) with a 3'UTR probe and in the present study with the U56-59 and U340 riboprobes (chapter 6 section 6.2). It will be of great interest to investigate the distribution of Up109 during development by mRNA *in situ* hybridisation using a Up109 specific riboprobe (there are 460 bp of unique sequence in Up109 exon 1).

Thoughts on the function of Up109

The Up109 protein contains the domains necessary for binding to β -dystroglycan, syntrophin and dystrobrevin and therefore could assemble with DAPs. There may be undiscovered developmental isoforms of DAPs which might be involved in embryonic/foetal specific complexes. The unique aa sequence of Up109 has a phosphorylation site for protein kinase C and two phosphorylation sites for casein kinase II (PROSITE program). As yet there is no evidence that these sites are functional, but if they are, their phosphorylation could modulate the assembly of these complexes. Up109 unique coding sequence also contains a N-myristoylation site where a myristate group (C_{14} fatty acid chain) could be added. This type of post-translational modification is associated with the anchoring of proteins to membranes (Stratchan, Read, 1999, p 21). However, these sites occur frequently in proteins and are not necessarily functional (PROSITE program).

The unique NH_2 -terminus of Up109 is notably hydrophobic (11 out of 17 aa are hydrophobic). This type of short hydrophobic NH_2 -terminal aa sequence could correspond to a signal peptide responsible for guiding proteins to the plasma or mitochondrial membranes and which is subsequently cleaved (Stratchan, Read, 1999, p 21). However, the 17 unique aa of Up109 were not recognised as a plausible signal peptide by the prediction programs Sigcleave and SIGNAL (HGMP).

Up109 proximal promoter

The proximal promoter of Up109 is without a CpG island, unlike full-length utrophin (Dennis et al., 1996) and Dp71 (Lederfein et al., 1993), and without TATA box and there is some evidence from this study that suggests that Up109 may be developmentally regulated. Several

genes that are regulated during development or differentiation, including the *Drosophila* homeotic genes ultrabithorax (Biggin et al., 1988) antennapedia (Perkins et al., 1988) and engrailed (Soeller et al., 1988), also lack an apparent TATA box and a CpG island.

The presence of an initiator sequence 131 bp upstream of the 5' end of the 5' RACE product suggests that the 5' RACE product does not correspond to the full-length cDNA and that transcription is initiated at this more 5' position. If that were the case then some of the potential *cis*-acting regulatory elements would lie in the 5' UTR. Thus, the binding site for TFIID would be at position +42, the binding site for MAZ would be at position +92 and the two binding sites for PEA3 would be at positions +19 and +29.

How does this affect the interpretation of transcription of Up109? It is not unusual to find regulatory sequences have been identified in transcribed leader sequences; these have been found in *Drosophila* and mammalian genes. For instance, the downstream promoter element (DPE) is a 7bp conserved sequence found at position +30 in the TATA-less promoters of the antennapedia gene and the human and mouse interferon regulatory factor-1 genes (Burke et al., 1997). A study where partial deletions in the ultrabithorax gene promoter were carried out showed that sequences between -154 and +41 were crucial for the expression of this gene (Biggin et al., 1988) and other studies on this same promoter showed that sequences between -200 to +989 were sufficient to modulate the temporal levels of expression of ultrabithorax in the *Drosophila* embryo (Bienz et al., 1998). Thus, the upstream initiator sequence remains the best candidate site for initiation of transcription of Up109.

So far, short utrophin isoforms have been identified after their dystrophin homologues. A question inevitably arises; is there a Dp109? Although it is a possibility, there is no evidence for such a short dystrophin from the vast amount of Western blots that have been carried out to date with dystrophin antibodies.

Chapter 5

Immuno-histochemistry

Results

5.1 General comments

Adult and foetal skeletal muscle, adult kidney, adult testis and foetal hands were selected for immuno-histochemical analysis using the new Mupa antibodies. The analysis of adult skeletal muscle was undertaken largely to confirm the specificity and sensitivity of the antibodies. In addition, it was hoped that the analysis of adult kidney and testis and foetal muscle and hands would reveal more about the distribution and relative abundance of short utrophin isoforms in these tissues.

The technique of immuno-histochemistry was not available in my own lab and I am very grateful to Dr. Susan Brown, Hammersmith Hospital, Neuromuscular Unit, for teaching me this technique and allowing me to carry out some of the experiments in her lab. Experiments that were carried out at the Hammersmith Hospital are indicated in the captions of the corresponding Figs.

5.2 Immuno-histochemical analysis of a selection of tissues

Adult muscle The ability of the Mupa antibodies to interact with native utrophin on tissue cryosections and their optimal dilutions for immuno-histochemistry were tested on adult skeletal muscle sections from control and *mdx* mice. Antibody dilutions that provided clear staining of neuromuscular

junctions (NMJ) with no sarcolemmal staining and minimal background were selected.

Fig 5.1 shows staining of control quadriceps sections with 1/200, 1/400 and 1/800 dilutions of Mupa-1. Utrophin immunoreactivity was detected using a biotinylated anti-rabbit IgG followed by Texas red conjugated-streptavidin. NMJs were independently localised by labelling with fluorescein-conjugated α -bungarotoxin. All three dilutions of Mupa-1 gave high levels of utrophin staining at NMJs. The 1/200 dilution also weakly stained the sarcolemma and this was attributed to crossreactivity with dystrophin; however, at higher dilutions virtually no sarcolemmal labelling was visible. A 1/800 dilution of Mupa-1 was routinely used for immuno-histochemistry.

Mupa-1 also detected utrophin in blood-vessels, capillaries and peripheral nerves (Fig 5.1 A, E and Fig 5.2 A, C) as previously reported using other anti-utrophin antibodies (Khurana et al., 1991; Helliwell et al., 1992; Nguyen et al., 1995; Rivier et al., 1997).

In muscle from *mdx* mice, Mupa-1 at 1/800 dilution gave signal at the NMJ and at the sarcolemma (Fig 5.2). Both signals are likely to be due to utrophin and the signal at the sarcolemma implies upregulation of utrophin in the absence of dystrophin. Location of utrophin at the sarcolemma has been previously described in both *mdx* and DMD muscle (e.g. Nguyen et al., 1991; Helliwell et al., 1992; Matsumura et al., 1992; Taylor et al., 1997).

Very similar distributions of signal were obtained using Mupa-2 (1/200 dilution) and Mupa-3 (1/800 dilution), (Fig 5.3). In general, Mupa-2 and Urd40 showed lower affinity for their epitopes than Mupa-1 and Mupa-3 in all tissues

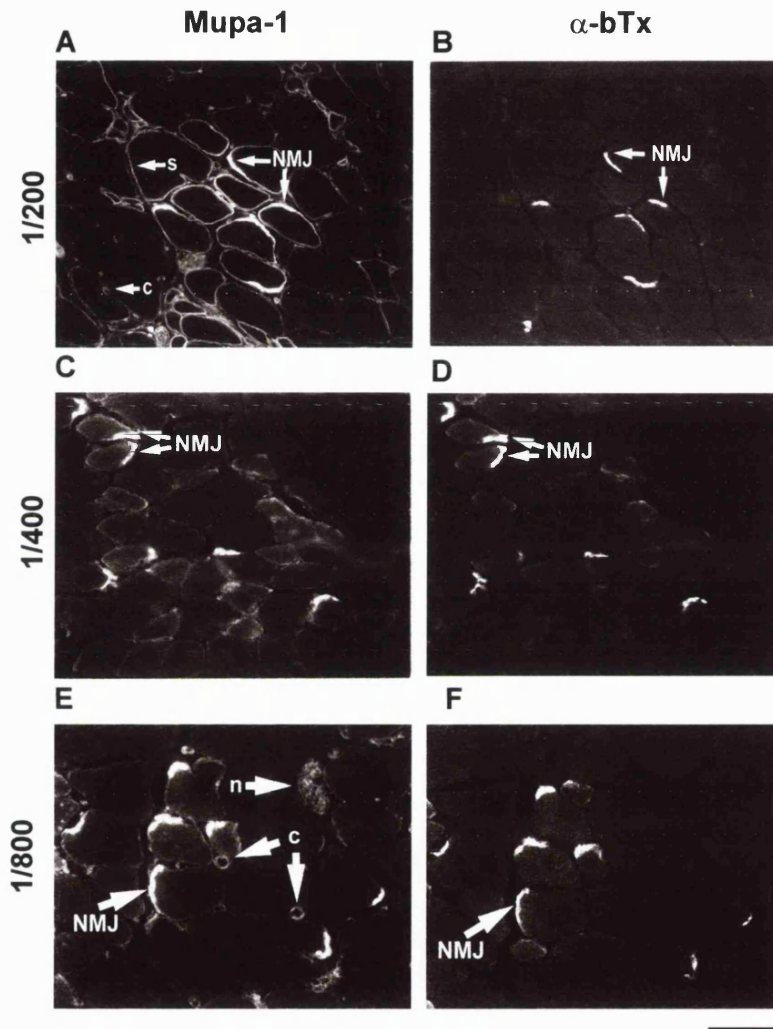


Fig 5.1 Indirect immuno-fluorescence of control mouse quadriceps sections with 1/200, 1/400 and 1/800 dilutions of Mupa-1 (A,C,E) and with α -bungarotoxin, α -bTx, (B, D, F). Mupa-1 was detected with a streptavidin-Texas Red conjugate and α -bungarotoxin was conjugated to fluorescein. All three dilutions of Mupa-1 detect utrophin at the neuromuscular junction (NMJ). At the 1/200 dilution Mupa-1 crossreacts with dystrophin and weakly labels the sarcolemma (s). Mupa-1 also detects utrophin in peripheral nerves (n) and capillaries (c). Bar = 120 μ m.

* This experiment was carried out at the Hammersmith Hospital.

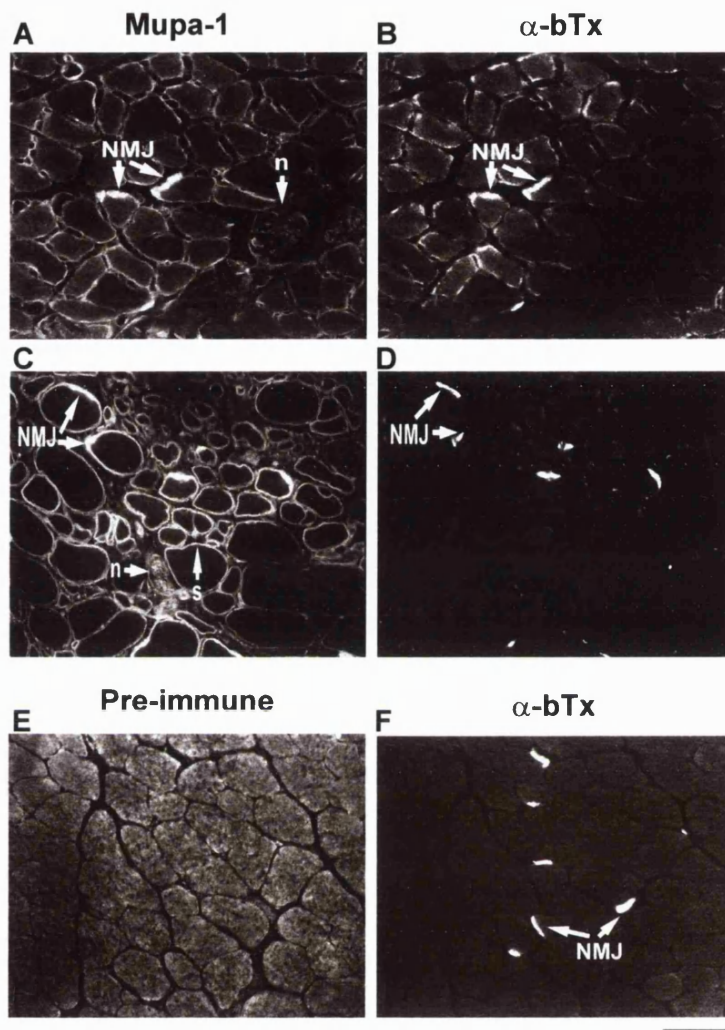


Fig 5.2 Immunolabelling of *mdx* mouse quadriceps sections with Mupa-1 (A,C) and α -bungarotoxin, α -bTx (B,D,F). Utrophin was visualised with a streptavidin Texas-red conjugate and α -bTx was conjugated to fluorescein. Utrophin is detected at the neuromuscular junctions (NMJ), intramuscular nerves (n) and at the sarcolemma (s). No signal was detected when the pre-immune antiserum was used (E). Bar = 120 μ m.

* This experiment was carried out at the Hammersmith Hospital.

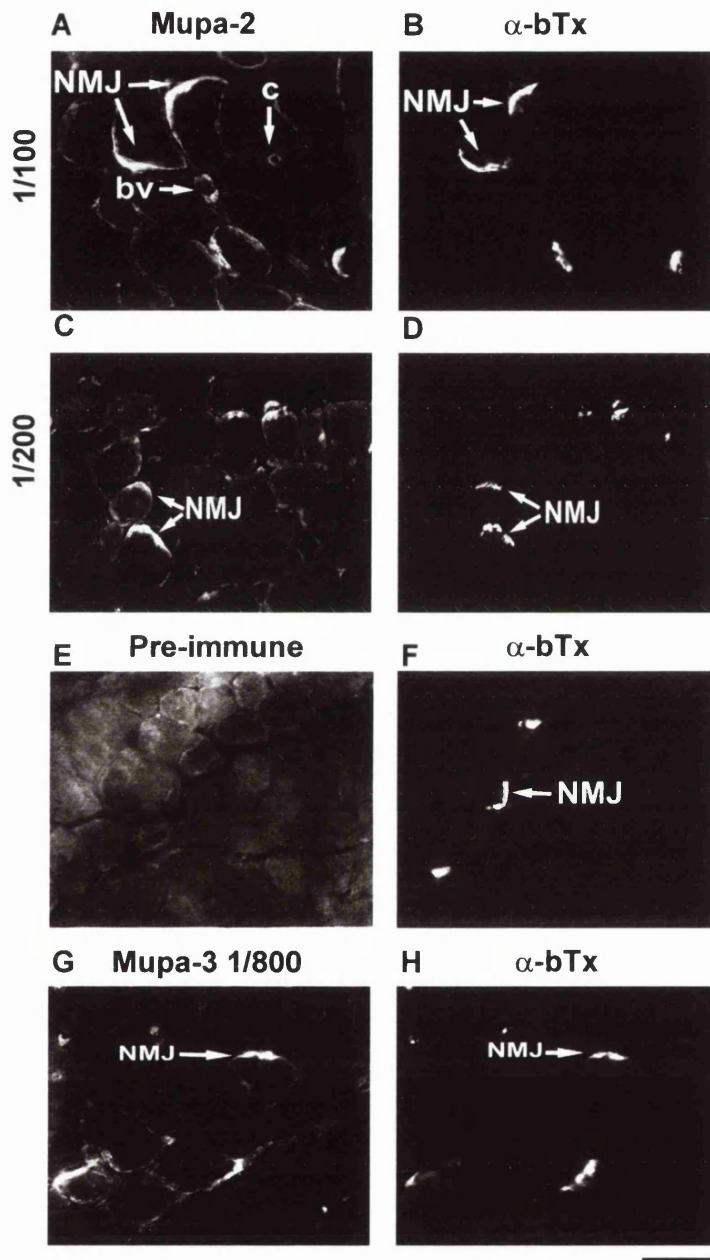


Fig 5.3 Immunohistochemistry using *mdx* (A, B, C, D, E and F) and control (G, H) quadriceps sections and 1/100 and 1/200 dilutions of Mupa-2 (A,C); Mupa-2 pre-immune serum (E); 1/800 dilution of Mupa-3 (G) and fluorescein-conjugated α -bungarotoxin (B,D,F and H). Utrophin is detected by both antibodies at the neuromuscular junction (NMJ), in blood vessels (bv) and capillaries (c). No labelling could be seen with the pre-immune serum (E). Bar = 120 μ m.

*This experiment was carried out at the Hammersmith Hospital

examined. This may reflect differences in accessibility of the aa sequences used to raise each of these antibodies in native utrophin.

In no case was signal detected using the pre-immune sera (Fig 5.2 E, Fig 5.3 E, Fig 5.4 A) or when the primary antibody step was omitted from the immuno-histochemistry procedure (Fig 5.4 D).

Double immuno-histochemical labelling of C57Bl quadriceps sections was used to check for Mupa antibodies crossreactivity with dystrophin using the anti-dystrophin monoclonal Dys2, (Novocastra, fluorescein-conjugated anti-mouse IgG) and Mupa-1, -2 and -3 at their working dilutions (biotinylated anti-rabbit IgG and Texas red conjugated streptavidin). The dystrophin specific antibody was raised against the COOH-terminus of dystrophin and detects all dystrophin isoforms. Fig 5.5 shows that while utrophin and dystrophin are co-detected at the NMJ by the antibodies (Miike et al., 1989; Ohlendieck et al., 1991a; Nguyen et al., 1991) only the anti-dystrophin antibody detects signal at the sarcolemma. No utrophin labelling at the sarcolemma was seen with the Mupa antibodies.

Utrophin was detected in sections of C57Bl muscle in large and small veins and arteries, in capillaries and peripheral nerves (both at the perineurium and nerve fibre) with Mupa-1, Mupa-2 and Mupa-3 (for example: Fig 5.1 A and E, Fig 5.2 A and C, Fig 5.3 A and Fig 5.6). The signal seen at these locations was of very similar intensities with all three antibodies; this suggests that full-length utrophin is present at these locations rather than short isoforms. This was confirmed by the absence of signal in blood vessels, nerves and capillaries in UKO^{ex6} sections with any of the Mupa antibodies.

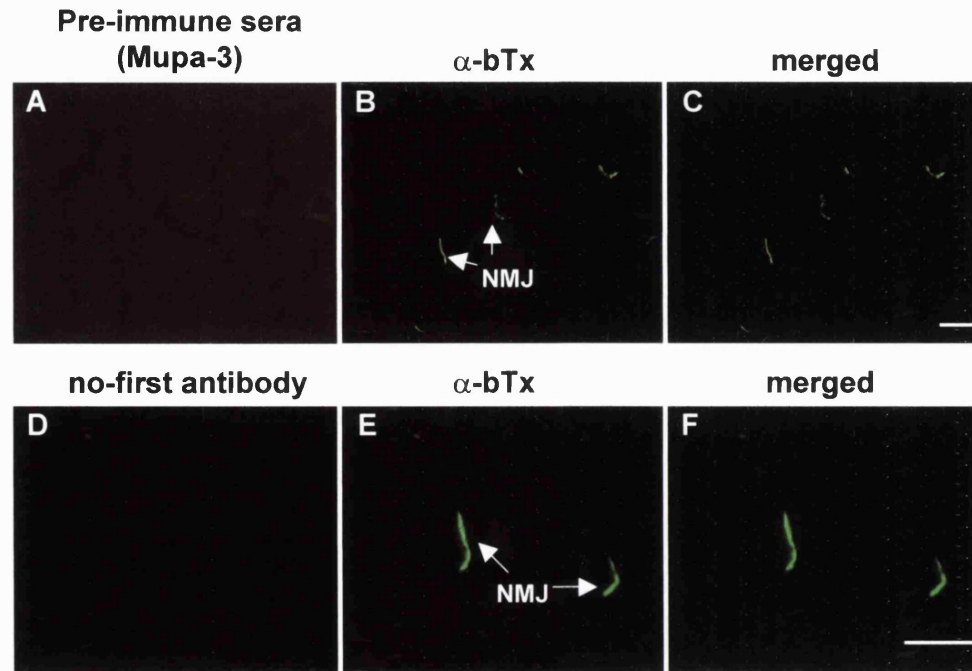


Fig 5.4 C57Bl quadriceps sections immunostained with α -bungarotoxin (B,E), the pre-immune serum corresponding to Mupa-3 (A) or the second antibody only, goat anti-rabbit IgG (D). The superimposed images are shown in C and F respectively. No signal is detected using Mupa-3 pre-immune serum (A) or if the first antibody is omitted (D). NMJ=neuromuscular junction; α -bTx= α -bungarotoxin. Bar = 60 μ m.

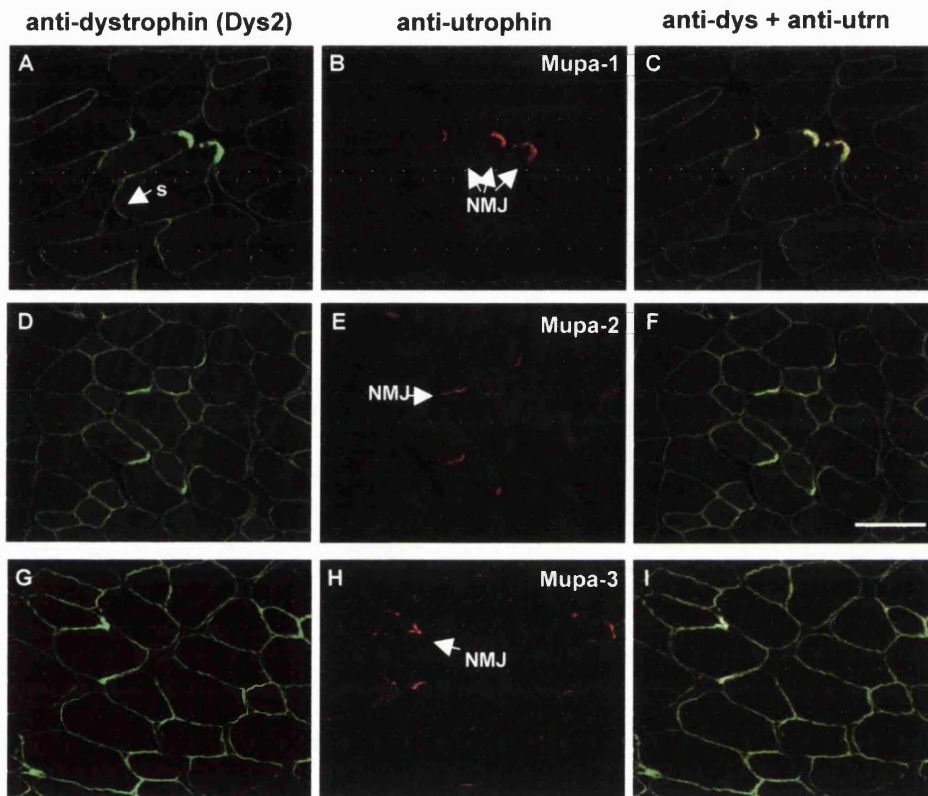


Fig 5.5 Double immunofluorescence of C57Bl quadriceps sections with antibodies against dystrophin (Dys2, Novocastra, signal detected with fluorescein-conjugated anti mouse Ig ; A,D, G) and utrophin antibodies (Mupa-1(B), -2 (E) and -3 (H)); signal detected using a biotinylated anti-rabbit Ig and Texas red-conjugated streptavidin. The superimposition of the images corresponding to each fluorochrome (C,F,I) confirmed the labelling of the neuromuscular junction by both antibodies (yellow), whereas the sarcolemma was positive only for dystrophin (green). Bar =120 μ m.

In control muscle sections, the endomysial capillary network was brightly labelled with all three Mupa antibodies. As an example, immuno-detection by Mupa-2 of capillaries adjacent to a muscle fibre is shown in detail in Fig 5.6. Here, utrophin seems to localise to the endothelial cells detected by labelling their nuclei with the fluorescent DNA binding reagent 4', 6 diamidino-2-phenylindole (DAPI). Utrophin expression at this site may account for a considerable proportion of the total utrophin signal detected in skeletal muscle. In general, reports in the literature underestimate the expression of utrophin in capillaries (Tanaka et al., 1991; Pons et al., 1991; Ohlendieck et al., 1991). Although some authors have draw special attention to the labelling of capillaries (Helliwell et al., 1992; Clerk et al., 1993). This discrepancy may be due to differences in affinities amongst the antibodies used in each case. For instance, both Helliwell et al. (1992) and Clerk et al. (1993) used the monoclonal Mancho-7.

Experiments shown in Figs 5.1, 5.2 and 5.3 were carried out at the Hammersmith Hospital, Neuromuscular Unit, and examined using a Leica microscope equipped with epifluorescence optics and sections were photographed. All subsequent experiments were carried out in UCL using a Zeiss microscope equipped with epifluorescence optics, a six positions filter wheel (Chroma, USA) and a CCD camera (Photometrics, Tucson, US). Image analysis was performed using the QuipsTM SmartCapture software (Digital Scientific, Cambridge, UK).

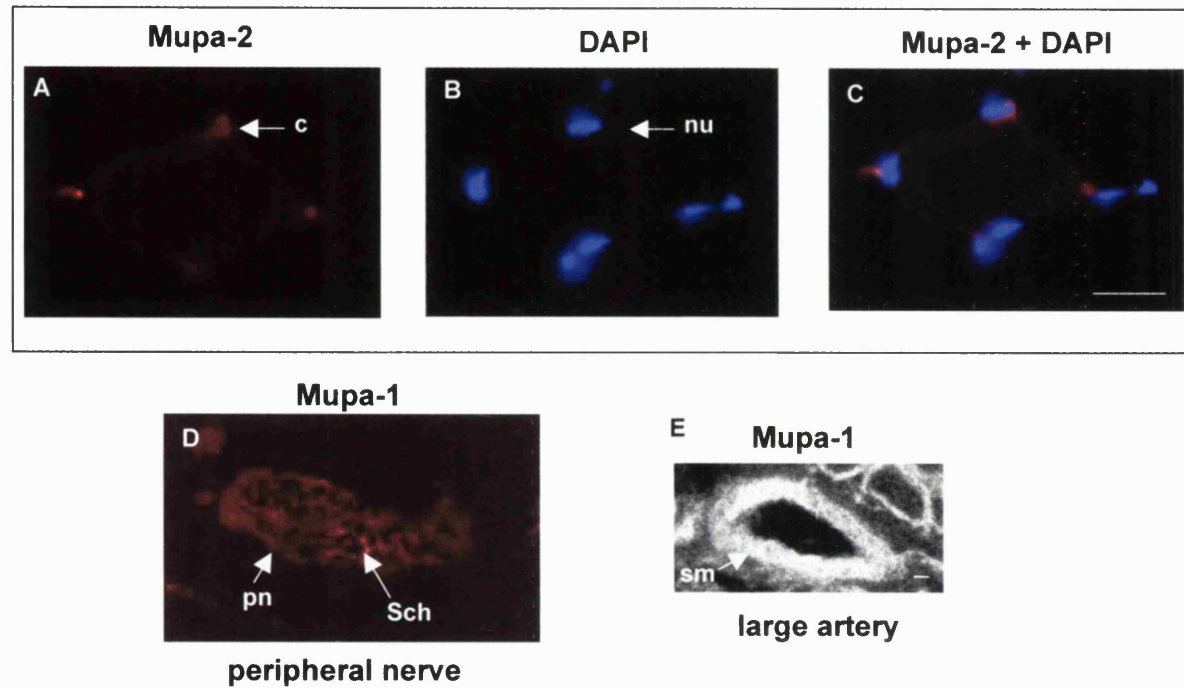


Fig 5.6 Expression of utrophin in capillaries' endothelial cells detected by immuno-labelling with Mupa-2 (A). Nuclei are also labelled by the DNA binding fluorescent dye DAPI (B). The merged image is shown in (C); Mupa-1 immuno-labelling of utrophin in the perineurium (pn) and Schwann cells (Sch) of a intramuscular nerve and in the smooth muscle wall of a large blood-vessel is also shown in D and E respectively. c = capillary; nu=nucleus; pn=perineurium; Sch=Schwann cell; sm =smooth muscle. Bar = 30 μ m

It seemed particularly important to establish an optimal exposure time before proceeding. It became apparent that UCL capture system is very sensitive and that even very low intensity signals, almost invisible to the eye, could be magnified by overexposure during image capture if exposure times between 5 to 10 seconds were used.

Experiments with control sections showed that the UCL system gave similar results to those obtained at the Hammersmith Hospital, when an exposure time of 2 seconds (sec) was used. A comparative analysis of UKO^{ex6} and C57BI skeletal muscle was then undertaken.

Surprisingly, all antibodies gave signal at the NMJ in UKO^{ex6} sections. However, there was a marked difference in the intensity of utrophin labelling between C57BI and UKO^{ex6} sections. This effect is clearly demonstrated in Figs 5.7 and 5.8 and 5.9 which show the immuno-staining of control and UKO^{ex6} muscle sections with Mupa-1, Urd40 and Mupa-2 respectively. From these images the signal appears to be at least eight to ten fold more abundant at C57BI NMJ compared to UKO^{ex6} NMJ. A total of four C57BI and UKO^{ex6} muscle samples from different mice were analysed in this way with similar results.

Fig 5.7 and Fig 5.8 also illustrate the importance of optimising the image capturing settings, particularly the exposure time, when using a digital system. These Figs show that when longer exposure times (5 sec) were used the levels of expression of utrophin at the NMJ of UKO^{ex6} and C57BI sections seemed comparable (compare in Fig 5.7 A to F with G to L and in Fig 5.8 B, D, F with G,H,I), an entirely artificial result.

A series of low exposure experiments indicated that weak signal is detected at the NMJ in UKO^{ex6} skeletal muscle by both NH₂-terminal and

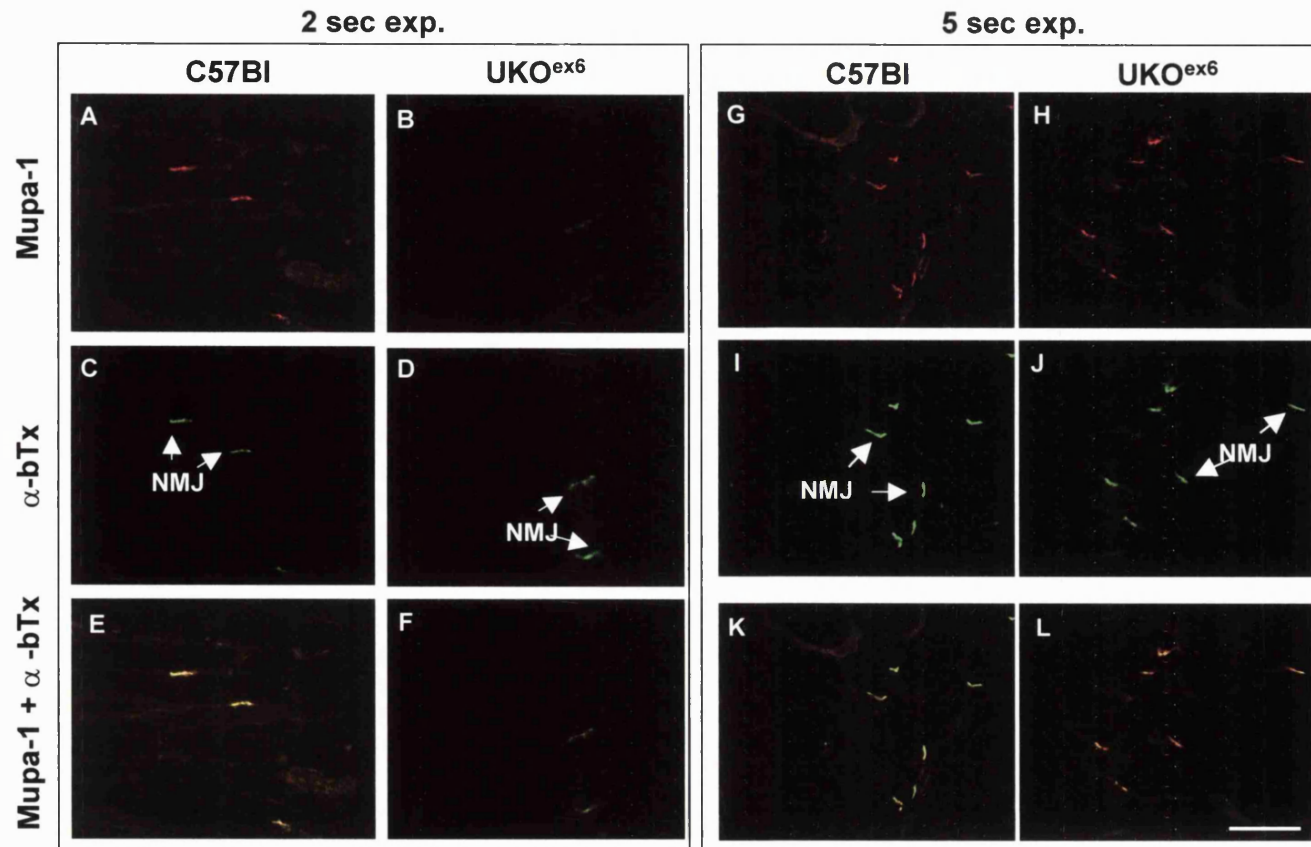


Fig 5.7 Double immuno-histochemical staining of C57BI (A,C,E,G,I,K) and UKO^{ex6} (B,D,F,H,J,L,) quadriceps sections with fluorescein-conjugated α -bungarotoxin (α -bTx) and Mupa-1 visualised with a Texas Red conjugate. These images were captured using either 2 sec (A to F) or 5 sec (G to L) exposure times. Bar=120 μ m

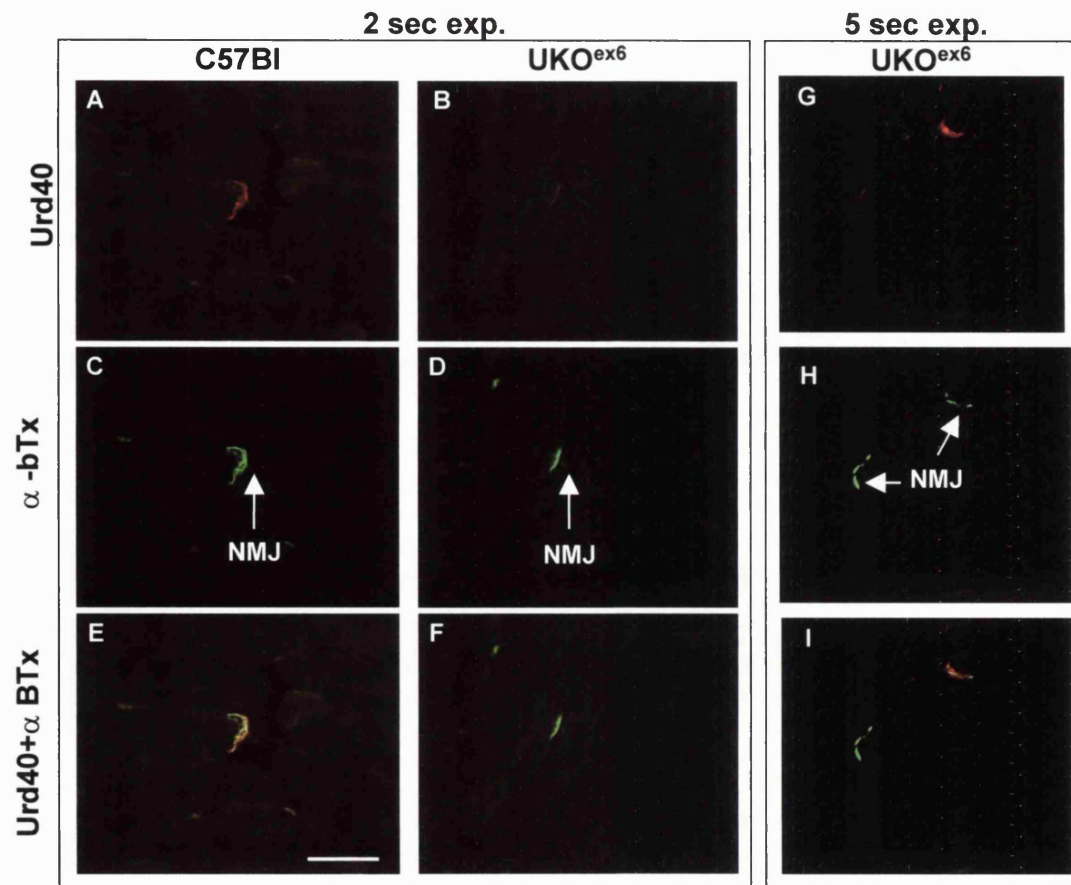


Fig 5.8 Double immuno-histochemical staining of C57BI (A,C,E) and UKO^{ex6} (B,D,F,G,H,I) quadriceps sections with fluorescein-conjugated α -bungarotoxin (α -bTx) and Urd40 visualised with a Texas Red conjugate. These images were captured using either 2 sec (A to F) or 5 sec (G to I) exposure times. Bar = 100 μ m

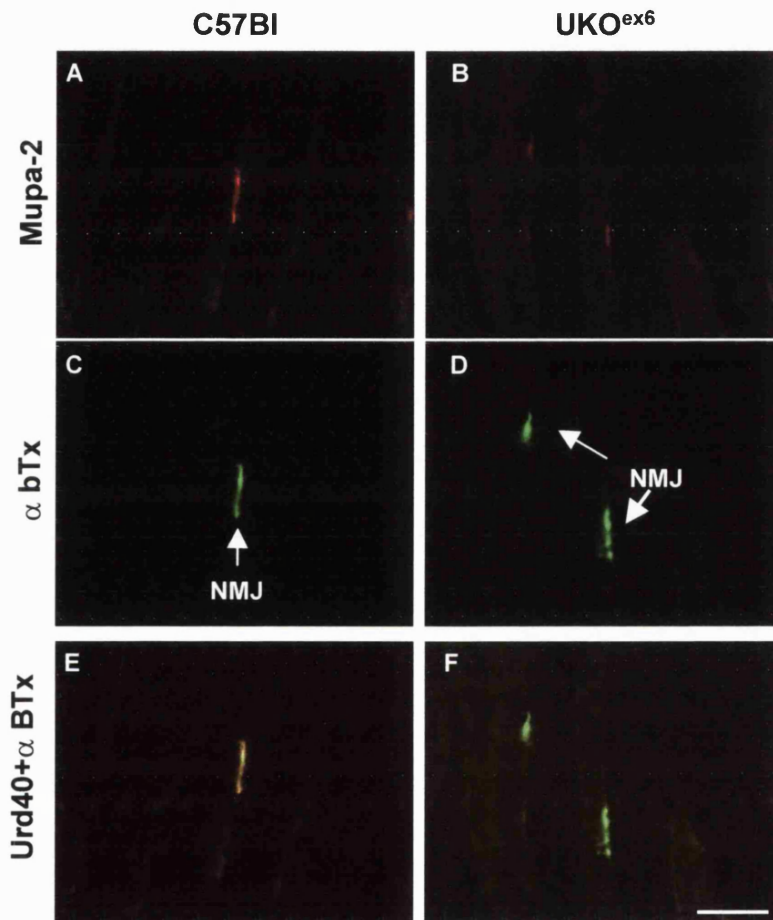


Fig 5.9 Longitudinal sections of C57BI (A,C,E) and UKO^{ex6} (B,D,F) quadriceps stained with Mupa-2 (A,B) and α -bungarotoxin (C,D). 2 sec exposure time and identical camera settings were used to capture both C57BI and UKO images. The signal detected in UKO^{ex6} muscle (B) is weaker than in control muscle (A) and this difference in intensities is revealed in the merged images (E,F). NMJ= neuromuscular junction α bTx= α -bungarotoxin . Bar = 30 μ m.

COOH-terminal antibodies. Detection of utrophin in UKO^{ex6} tissue by the COOH-terminal antibodies alone would imply the expression of a short isoform, maybe upregulated in the absence of full-length utrophin, although, there is no evidence for such an isoform from the Western blots presented in this study (section 4.2, Fig 4.8). However, the detection of the same signal by the NH₂-terminal antibody Mupa-1 is more difficult to explain.

The origin of this signal was explored in various ways. One possibility was that the signal derives from some unusual splice variant form of utrophin. In order to test this idea, RT-PCR amplification of RNA from UKO^{ex6} and control tissues was carried out using primers on either side of the “knock-out” targeted exon, exon 6 (see Table 2.1 for primers sequence). This RT-PCR was carried out using RNA prepared from the remaining female UKO^{ex6} mouse tissue in the OCT block, from which sections were cut for immuno-histochemistry, and from embryos born to the same UKO^{ex6} female mouse which had been stored at -70 °C. These tissues were used to confirm the genotype of the material used for immuno-histochemistry.

A striking result was seen; a band of 492 bp was amplified from control muscle as expected whereas in the UKO^{ex6} samples a shorter product of 319 bp was amplified (Fig 5.10 A). Sequencing of this short RT-PCR product revealed that the size difference was due to the skipping of the disrupted exon 6 in UKO^{ex6} tissues; with exon 5 spliced to exon 7 (Fig 5. 10 B, C, D). This splicing event results in the disruption of the open reading frame (ORF) and in the introduction of a premature stop codon 45 bp into exon 7. If such a transcript were translated it would encode a truncated 17kDa utrophin protein containing only part of the actin-binding domain.

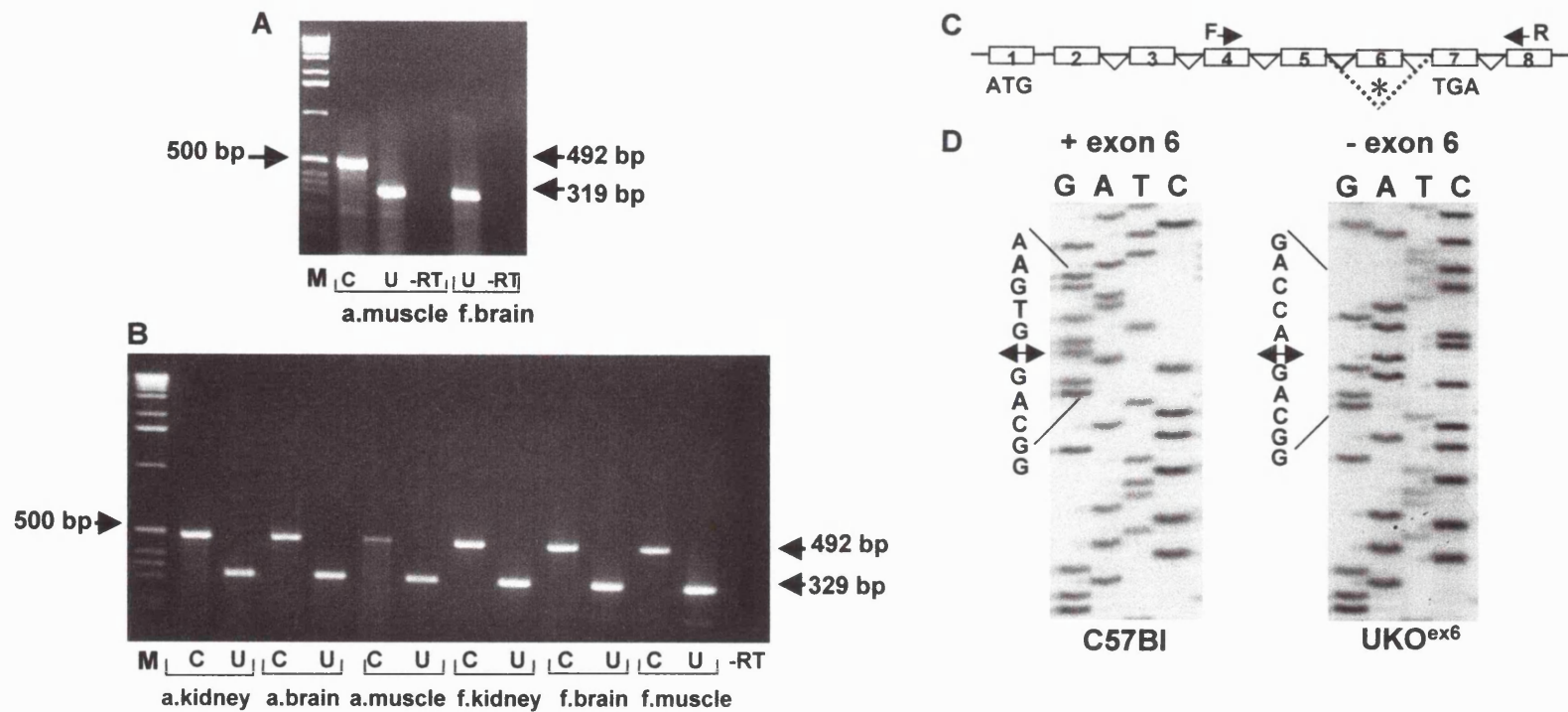


Fig 5.10 A, RT-PCR from C57BI (C) and UKO^{ex6} (U) adult skeletal muscle and UKO^{ex6} foetal brain RNA using primers in exons 4 and 8. D, sequence of the products shown in A. The exon5/exon6 and exon5/exon7 boundaries are indicated by an arrow. C, diagrammatic representation of exon 6 skipping. The premature stop codon in exon 7 is indicated. B, RT-PCR amplification using the same primer pair and a selection of C57BI and UKO^{ex6} adult (a) and foetal (f) tissues demonstrated that skipping of exon 6 is not restricted to skeletal muscle. bp=base-pair; M=DNA size marker. -RT=control sample without reverse transcriptase. F=forward PCR primer; R=reverse PCR primer.

Other experiments were designed to test whether alternative splicing at the 5' end of the UKO^{ex6} utrophin gene was occurring in such a way that the ORF is maintained and a shortened isoform is synthesised which could bind at the NMJ. For example, if exon 5 were spliced to exon 10 the ORF would be maintained and a shortened protein would be produced. This idea is given strength by the observation of more than 10 alternative splicing events in the 5' region of the dystrophin gene (Surono et al., 1997). For instance, exon 2 can be spliced to exons 8, 10, 17 and 18 in human skeletal muscle (Dwi Pramono et al., 2000). In addition, it has been reported in DMD patients with frameshift mutations, that the dystrophin ORF is restored by exon skipping (Nicholson et al., 1992). In order to investigate whether similar splicing events take place in the utrophin gene, RT-PCRs were carried out from a selection of adult and foetal C57Bl and UKO^{ex6} tissues using forward primers situated in exons 2, 4 and 8 and reverse primers in exons 5, 12 and 15 (Table 2.1, Fig 5.11). However, no evidence for differential splicing in either UKO^{ex6} or control tissues was found other than that involving the mutated exon 6.

An alternative explanation for the weak signal detected with Mupa-1 in UKO^{ex6} mice is that it is the result of low level crossreactivity with dystrophin. Although Mupa-1 does not detect dystrophin at the sarcolemma (Fig 5.1 and Fig 5.5), it may have enough affinity to detect dystrophin at the NMJ where it is concentrated in UKO^{ex6} muscle. In order to test this idea our collaborators in Prof.K.Davies lab in Oxford used Mupa-1 to investigate NMJ signal in utrophin-dystrophin double knock-out mice (dko^{ex6}). They found that Mupa-1 detects signal at the NMJ in UKO^{ex6} mice but not in dko^{ex6} mice and that Mupa-1 labels the sarcolemma of dko^{ex6} revertant fibres which are also labelled with

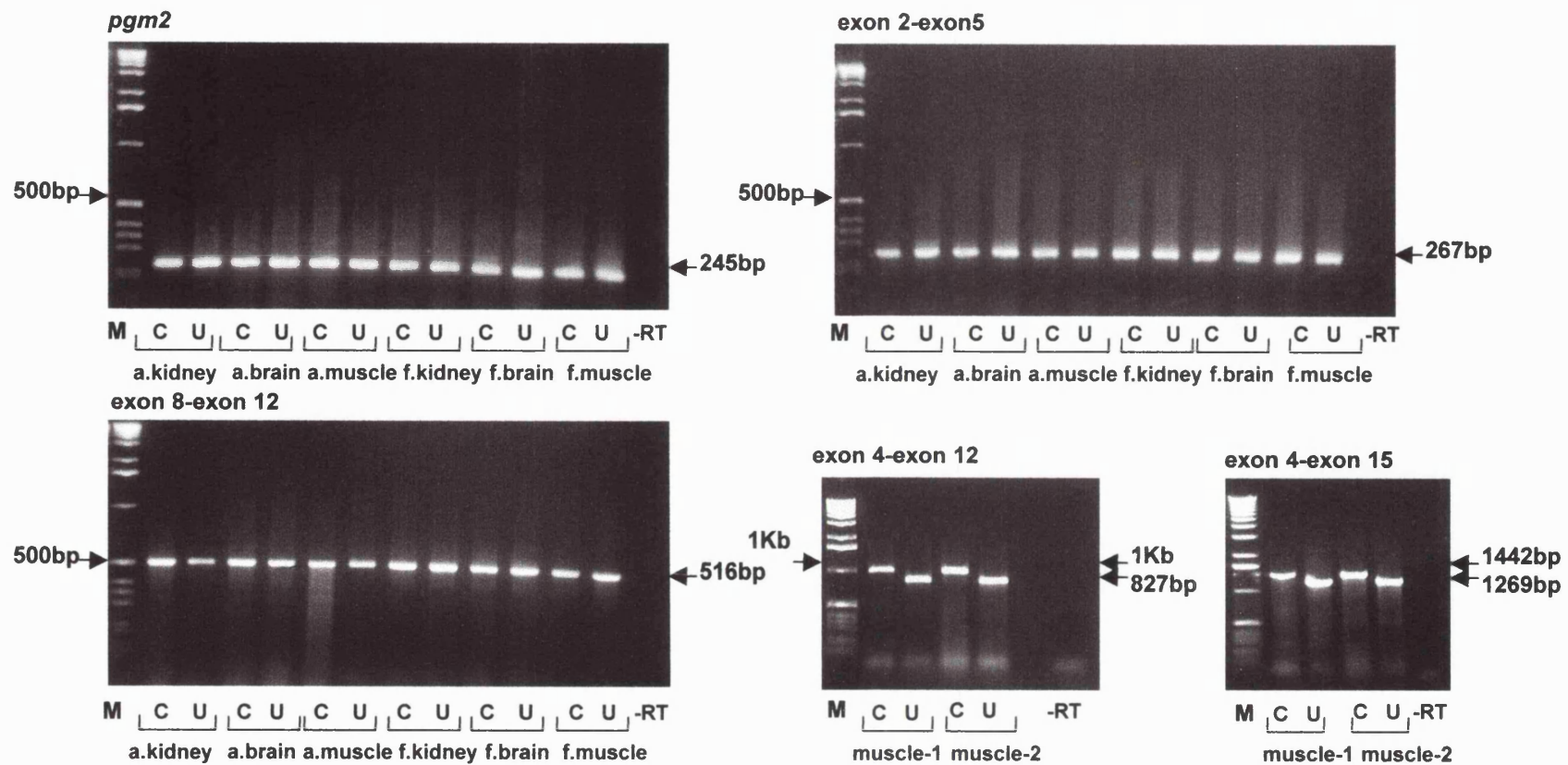


Fig 5.11 RT-PCRs using various primer combinations and mRNAs from adult (a) and foetal (f) C57Bl (C) and UKO^{ex6} (U) tissues. Two skeletal muscle samples from two further mice (1 and 2) were also amplified. The size difference between control and UKO^{ex6} amplified products in exon 4-exon 12 and exon 4-exon 15 corresponds to the size of exon 6. Amplification with *pgm2* primers was used to check the integrity and quantity of mRNA.

dystrophin specific antibody (Dr. Andrew Weir, personal communication). These experiments support the idea that Mupa-1 may crossreact at low levels with dystrophin under the conditions used for immuno-histochemistry.

One proposal to explain the NMJ signal in UKO^{ex6} mice with Mupa-2, Mupa-3 and Urd40 is that it corresponds to a short utrophin isoform which is weakly expressed in the absence of full-length utrophin and which was not detected by Western blotting. Since this weak signal is detected by Mupa-2 (which does not detect Up71), Up140 is currently the best candidate for detection. However, there is no evidence of a band of that size in Western blots of UKO^{ex6} muscle (section 4.2, Fig 4.8)

In the absence of dystrophin, the DAP complex at the muscle fibre sarcolemma does not assemble and several members of the complex are absent (Ervasti et al., 1990; Ohlendieck et al., 1991b). In contrast, it appears that in the absence of full-length utrophin the expression of β -dystroglycan, dystrophin and rapsyn at the NMJ are normal compared to control mice (Deconinck et al., 1997a).

Immuno-staining of C57Bl and UKO^{ex6} mice skeletal muscle sections in the present study confirmed these findings. The levels of expression of α - and β -dystroglycan, β -sarcoglycan and dystrophin are comparable in control and UKO^{ex6} mice, both at the cell membrane and NMJ (Fig 5. 12). In Fig 5.12 C and F the NMJ appears brightly labelled by anti α - and β -dystroglycan antibodies; the labelling at the sarcolemma cannot be seen because the brightness of these two figures was lowered in order to visualise the NMJ.

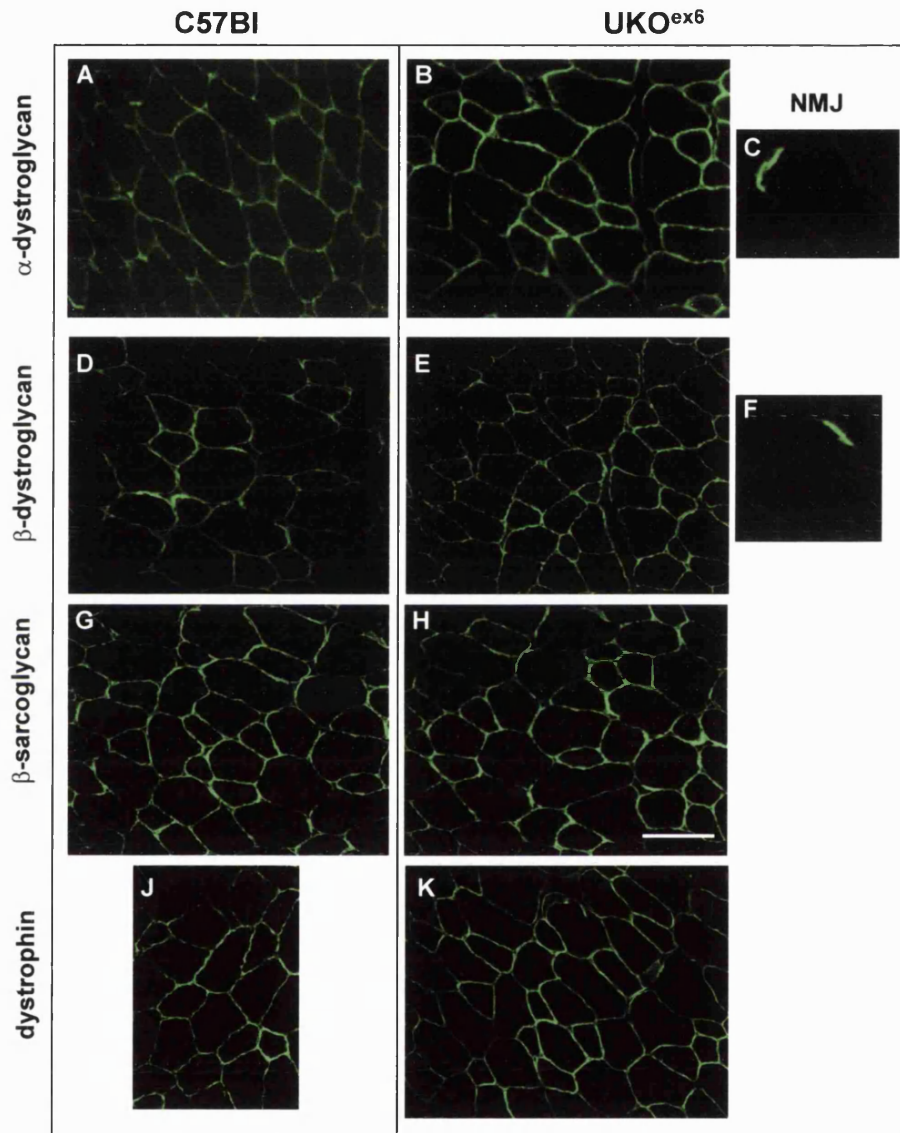


Fig 5.12 Immuno-labelling of the DAP complex at the sarcolemma and NMJ in C57BI and UKO^{ex6} skeletal muscle sections. The antibodies used were VIA4-1(α -dystroglycan), NCL-b-DG (β -dystroglycan), NCL-b-SARC (β -Sarcoglycan) and Dys2 (dystrophin) (Table 2.3). The brightness of the image was decreased in C and F until the NMJ was just visible. Bar =120 μ m.

Thus, as proposed by Deconinck et al. (1997a) and Grady et al. (1997a) full-length utrophin is not necessary for the correct assembly and maintenance of the DAP complex at the NMJ, finding in line with the mild muscle defects shown by UKO^{ex6} mice and the overall normal structure and function of their NMJs .

Foetal skeletal muscle There is a substantial body of evidence that utrophin is developmentally regulated at the sarcolemma (Khurana et al., 1991; Clerk et al., 1993; Koga et al., 1993; Mora et al., 1996; Lin S. et al., 2000). In the present study, a single stage of development, 16.5dpc, was examined. In these embryos the NMJs are established and the mature layout of the muscle blocks is in place (Ontell et al., 1984; Kieny et al., 1986). At this stage, the predominant myosin heavy chain (MyHC) isoform is the embryonic form (Lu et al., 1999; Whalen et al., 1981; Vivarelli et al., 1988) but some perinatal MyHC protein is also present. Lu et al. (1999) demonstrated that by 16.5 dpc it was also possible to detect mRNAs encoding for the three adult fast MyHC isoforms (IIa, IIb and IIc/x), (MyHC IIb most abundant) and for β myosin heavy chain.

The Mupa antibodies and Urd40 detected utrophin at the sarcolemma of myotubes in anterior limb sections from C57Bl embryos (Fig 5.13; Fig 5.14). Utrophin was also abundant in blood vessels and peripheral nerves (Fig 5.13 B) and at the myotendinous junction (Fig 5.13 A).

Comparison of signal intensities seen in control mice with the different antibodies was not informative in regard to the expression of short isoforms in control mice (Fig 5.13; 5.14;-as before, labelling was weakest with Urd40 and Mupa-2). However, analysis of UKO^{ex6} muscle provided a hint that a short

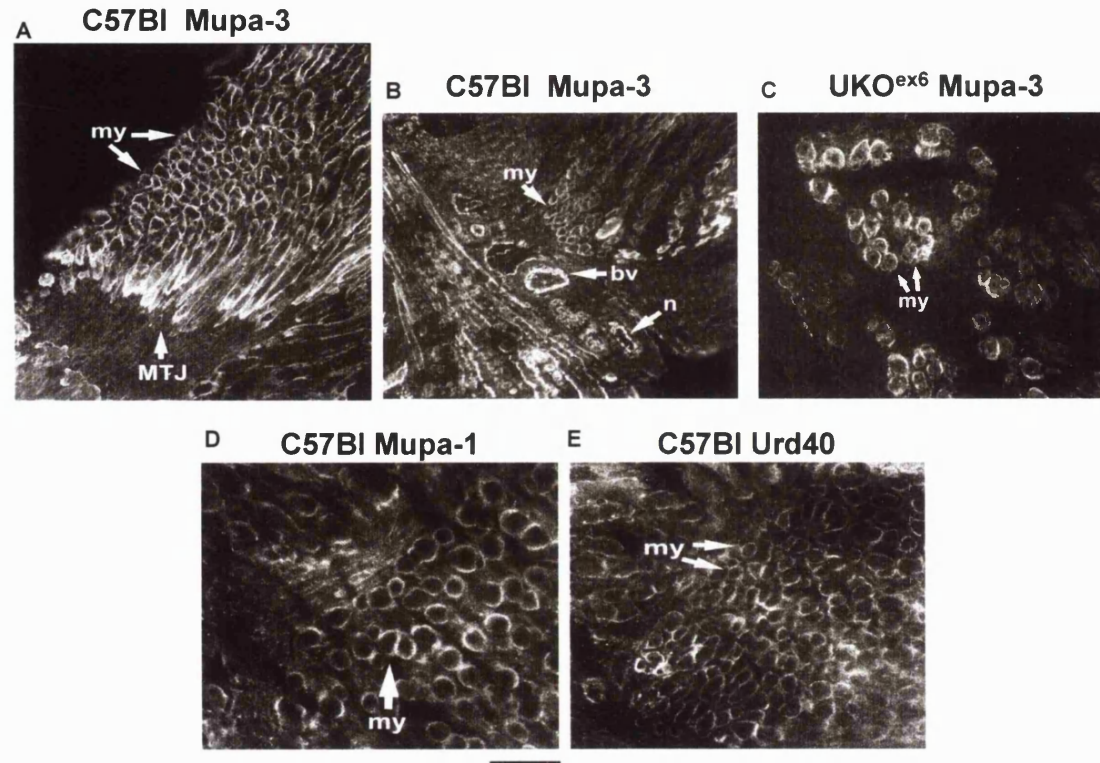


Fig 5.13 Upper limb sections of C57Bl (A, B, D, E) and UKO^{ex6} (C) 16.5 dpc embryos stained with Mupa-3 (A,B, C), Mupa-1 (D) and Urd40 (E). Expression of utrophin at the myotendinous junction (MTJ) is shown in A. Utrophin is expressed at the sarcolemma in C57Bl myotubes and in blood vessels and nerves. In UKO^{ex6} foetal muscle utrophin was detected at the sarcolemma of immature myotubes with Mupa-3 (C) .my=myotubes; bv=blood-vessel; n=nerve; sm=smooth-muscle. Bar = 80µm.

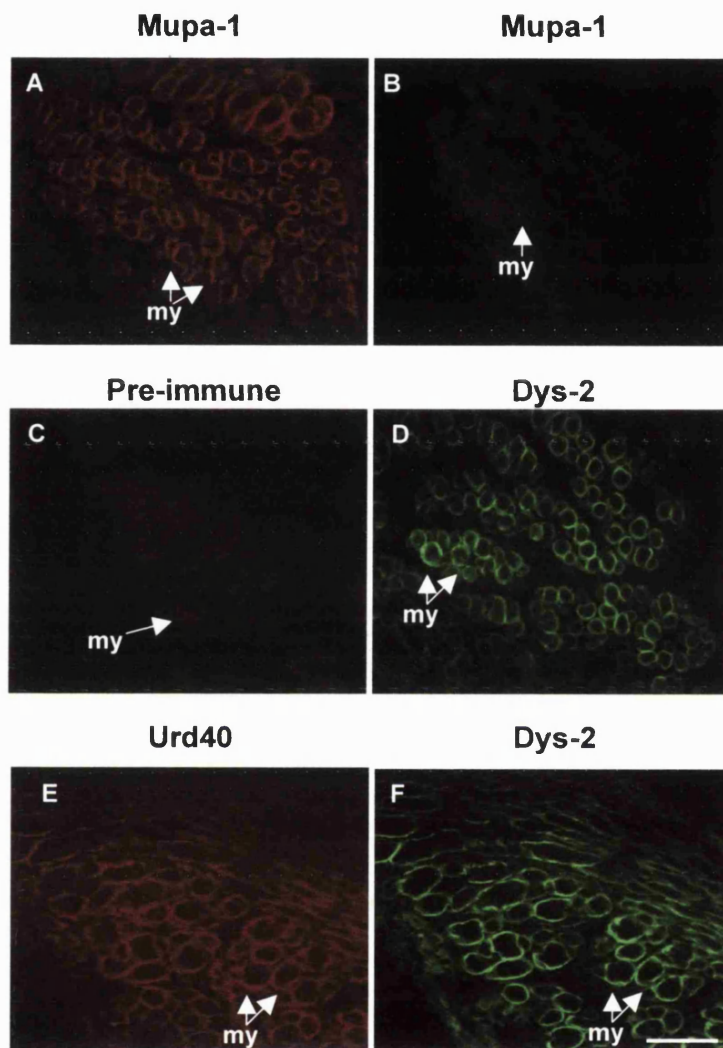


Fig 5.14 Immuno-histochemical labelling of C57Bl (A,C,E, F) and UKO^{ex6} (B,D) 16.5 dpc foetal muscle sections using Mupa-1, Urd40 and Dys-2 antibodies. my=myotube. Bar = 80 μ m.

Panel E and F represent an identical section doubly-labelled with Urd40 and Dys-2.

utrophin isoform might be expressed in foetal muscle. In foetal UKO^{ex6} sections, no signal was detected with Mupa-1 (Fig 5.14 B), Mupa-2 and Urd40 (data not shown); however, Mupa-3 gave a clear signal at the sarcolemma (Fig 5.13 C). An attractive proposition is that this signal corresponds to Up109 which was detected in C57Bl and UKO^{ex6} foetal muscle on Western blots by Mupa-3 (data not shown). However, Up109 should also be detected by Mupa-2; indeed, this was the case for Western blots but not for immuno-histochemistry. Perhaps the signal from Mupa-2 is too weak to be detected.

Adult kidney. There is a considerable body of evidence, largely derived from Western blots, that utrophin is expressed at high levels in kidney (for example: Love et al., 1991; Nguyen et al., 1992; Lumeng et al., 1999). In addition, Grady et al. (1997a) used immuno-histochemical analysis to localise utrophin in mouse kidney to the glomerulus basal lamina. Loh et al, (2000) also reported utrophin in glomeruli, distal convoluted tubules of the cortex and collecting ducts of the medulla and Raats et al. (2000) investigated the precise localisation of utrophin in rat and human renal cortex by immuno-histochemistry and immunoelectron microscopy. These authors found that utrophin is present in the cytoplasm of the podocyte (specialised epithelial cell in the visceral side of Bowman's capsule) foot processes and in the basal side of epithelial cells of distal tubules. These signals seen in these studies seem due to full-length utrophin since utrophin signal was detected with antibodies against the NH₂-terminus of the protein.

Data from Western blots, from both the present study (section 4.2, Fig 4.4) and previous reports (Nguyen et al., 1995; Rafael et al., 1999) suggest that

in addition to the full-length isoform, a short utrophin isoform, Up120, is expressed in kidney. This was further investigated using the panel of Mupa antibodies and immuno-histochemical analysis of UKO^{ex6} kidney sections.

As expected, in C57Bl kidney, Mupa-1 and Mupa-3 gave high levels of signal in the glomerulus, convoluted tubules and collecting ducts (Fig 5.15; 5.16 respectively). The levels of utrophin signal detected with Urd40 and Mupa-2 were substantially lower than those obtained with Mupa-1 and Mupa-3 (data not shown) as noted previously on skeletal muscle immuno-histochemistry. In UKO^{ex6} kidney, Mupa-1 gave no signal but Mupa-3 gave weak signal in the UKO^{ex6} glomerulus (Fig 5.15; 5.16). These results suggest that in the glomerulus and convoluted tubules full-length utrophin is the major isoform but that a short isoform may also be expressed in the glomerulus.

The signal seen in UKO^{ex6} glomerulus was weak. In order to determine whether this was genuine signal, sections were immuno-stained using a signal amplification system; biotinylated anti-rabbit IgG followed by fluorescein-conjugated streptavidin. The results are shown in Fig 5.17. The modified labelling system gave unacceptable levels of non-specific background in the renal cortex. This is probably due to the presence of endogenous biotin or biotin binding proteins. However, incubation of sections with pre-immune serum instead of the primary antibody showed that the non-specific signal is confined to the renal tubules and was barely detectable within the glomerulus. Bearing this in mind comparison of Fig 5.17 panel B (UKO^{ex6}) with C (C57Bl) shows detectable utrophin signal in UKO^{ex6} glomerulus.

These results allow the tentative suggestion that a short utrophin isoform may be expressed in kidney. This idea would be in line with the data derived

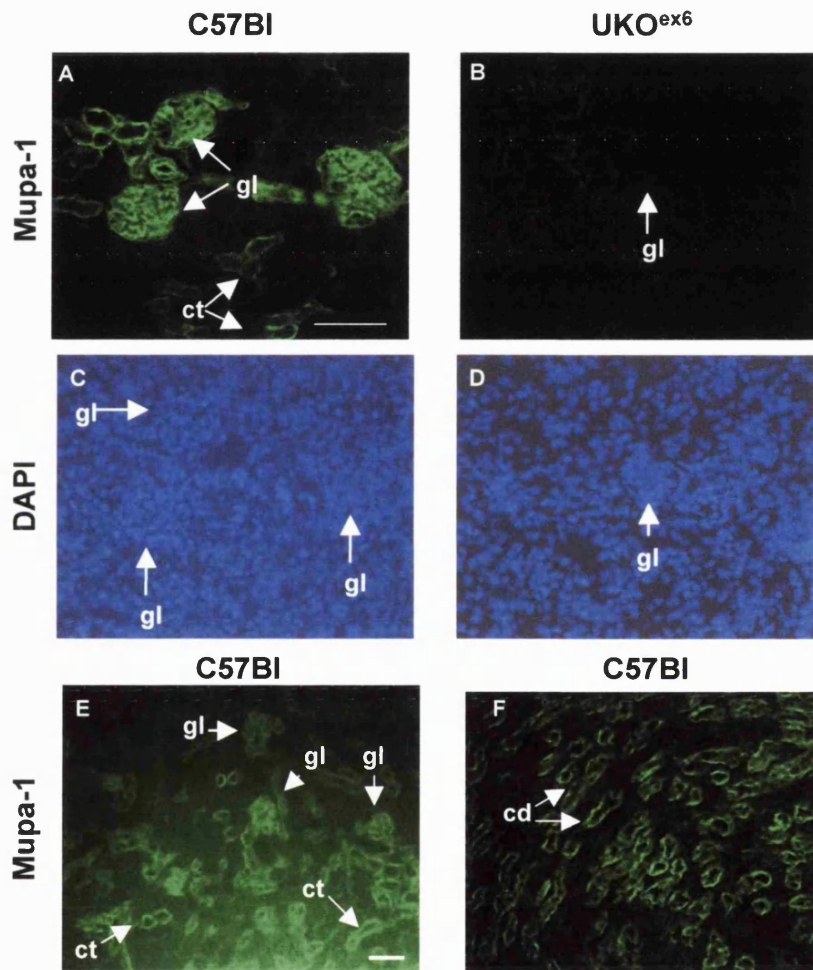


Fig 5.15 Immuno-histochemistry of C57Bl (A,E,F) and UKO^{ex6} (B) adult kidney sections with Mupa-1. This antibody detects utrophin in glomeruli (gl) and convoluted tubules (ct) in C57Bl kidney (A) but not in UKO^{ex6} kidney (B). The positions of the glomeruli in A and B are revealed by DAPI staining (C,D). Sections through the cortex (E) and medulla (F) of a C57Bl mouse labelled with Mupa-1 showing utrophin expression in glomeruli (gl) and distal convoluted tubules (E) and in the collecting ducts (cd) (F). Bar=80 μ m.

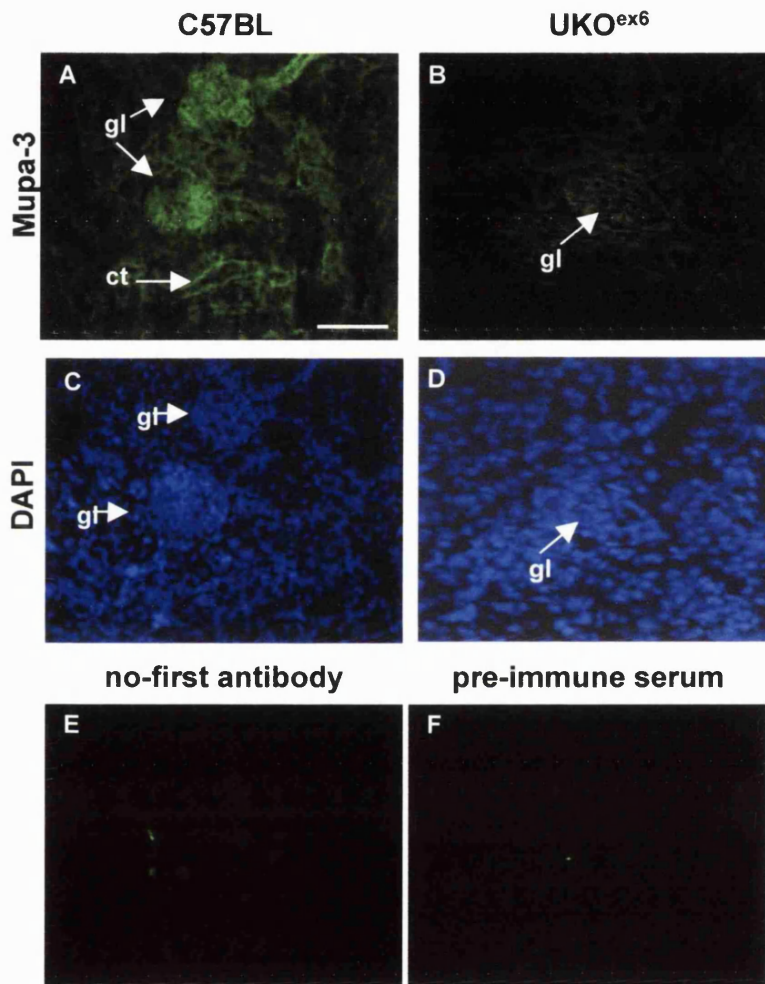


Fig 5.16 C57BL (A,C) and UKO^{ex6} (B,D) adult kidney sections labelled with Mupa-3. This antibody gives high levels of immuno-signal in glomeruli and convoluted tubules in C57BL kidney (A). Weak signal can be detected in glomeruli but not in tubules of UKO^{ex6} kidney. C and D correspond to the DAPI labelling of the sections in A and B respectively. E, C57BL kidney section incubated with the second antibody only or F with a pre-immune serum and fluorescein-conjugated anti-rabbit IgG (D). gl=glomerulus; ct=convoluted tubule. Bar =80 μ m.

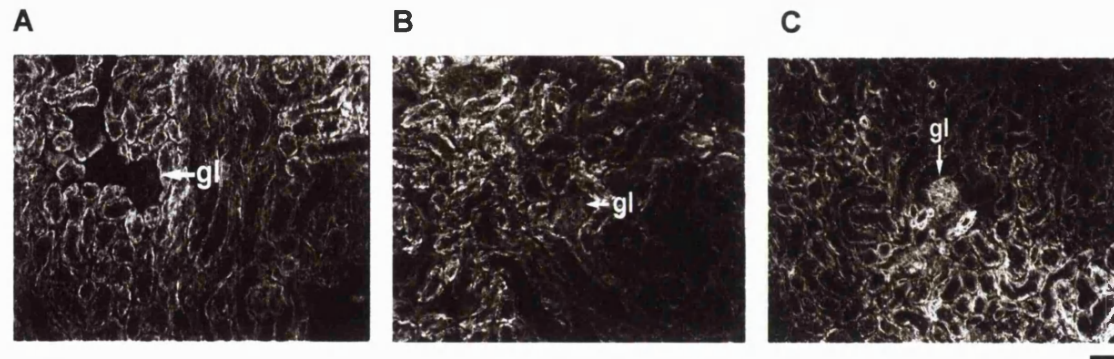


Fig 5.17 Sections through the renal cortex of C57Bl (A,C) and UKO^{ex6} (B) mice labelled with a pre-immune serum (A) or with Mupa-3 (B,C). This experiment was carried out using a biotinylated anti-rabbit IgG and fluorescein-conjugated streptavidin and thus the high levels of non-specific labelling of the cortex in A. By comparison, some weak expression of utrophin can be seen in UKO^{ex6} kidney (B) and high levels of utrophin expression in C57Bl kidney. gl=glomerulus. Bar = 80 μ m.

from Western blots (section 4.2, Fig 4.4) in which Up120 emerges as a likely candidate for upregulation in the UKO^{ex6} kidney.

The distribution of dystrophin in kidney was explored using the P6 antibody (Table 2.3) and was not detected in glomeruli, convoluted tubules or collecting ducts but was confined to blood-vessels (Fig 5.18). This observation is in agreement with the findings of Loh et al. (2000) who examined control mouse adult kidney sections with P6 antibody.

Taken together, immuno-histochemistry in kidney suggest that in adult kidney full-length utrophin is the major utrophin isoform and is expressed in cortical glomeruli and tubules and in the medulla, and a short utrophin isoform, perhaps Up120, may also be expressed in the glomerulus.

Adult testis Western blot analysis of testis extracts (section 4.2, Fig 4.10) showed that full-length utrophin is expressed at moderate levels in this tissue and suggested that a short isoform(s) of 97kDa/103kDa is also expressed. This latter observation prompted us to examine utrophin in adult testes by immuno-histochemistry. High levels of utrophin signal were detected by Mupa-1 (Fig 5. 19), Mupa-2 (Fig 5.20) and Mupa-3 (Fig 5.21) in C57Bl testis in the connective tissue between seminiferous tubules (intertubular tissue) and in a population of large polyhedral cells (Fig 5.19 E,F and 5.21 A). These latter are Leydig cells which are of mesenchymal origin, are found isolated or in small clusters and secrete testosterone. The intertubular tissue also contains mesenchyme-like pluripotent cells, mononuclear cells and fibrocytes. These may also express utrophin but could not be clearly identified.

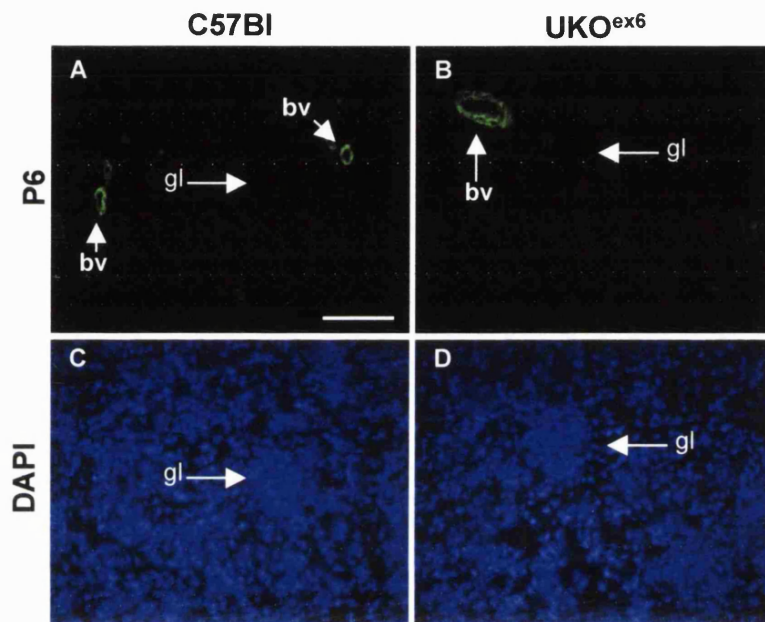


Fig 5.18 Immuno-labelling of C57BI (A) and UKO^{ex6} (B) kidney sections with the anti-dystrophin polyclonal antibody P6. This antibody detects dystrophin in small blood-vessels (bv) in C57BI and UKO^{ex6} kidney but not in the glomerulus (gl). C and D show the DAPI staining of A and B respectively; the position of glomeruli is indicated by arrows . Bar =80 μ m.

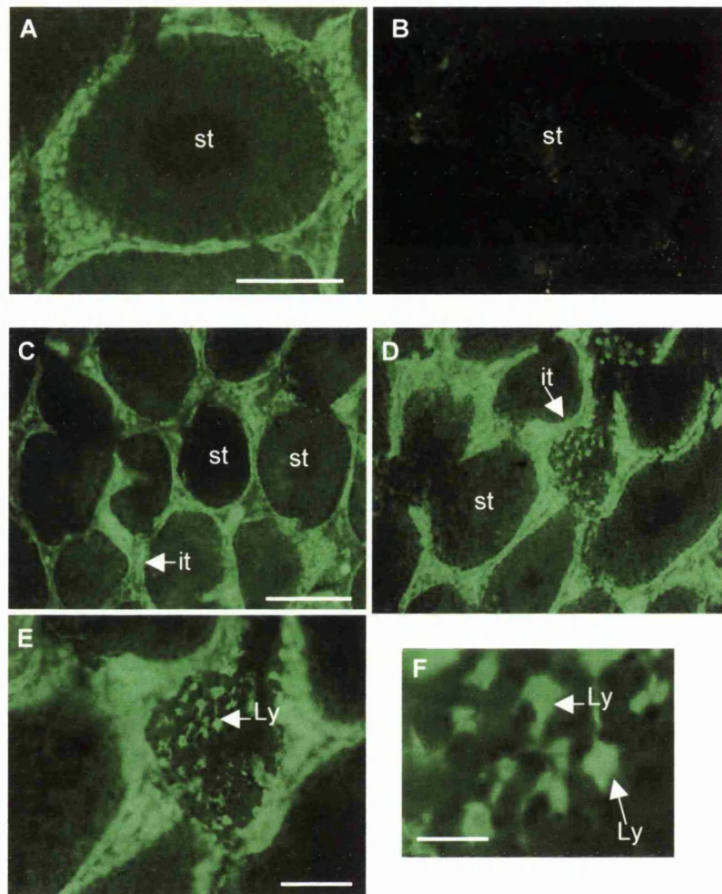


Fig 5. 19 Immuno-histochemical analysis of C57BI (A,C,D,E,F) and UKO (B) adult testis using Mupa-1. In C57BI testis utrophin is expressed in the intertubular tissue surrounding the seminiferous tubules (A,C,D, E) and in Leydig cells (E, F). E represents a detail of D and F is a close-up of E to illustrate the polyhedral shape of utrophin expressing cells. Utrophin was not detected in UKO kidney (B). st=seminiferous tubule; it=intertubular tissue; Ly=Leydig cell. Bar (A) =100 μ m; Bar (C) =200 μ m; Bar (E) =80 μ m ; Bar (F) =16 μ m.

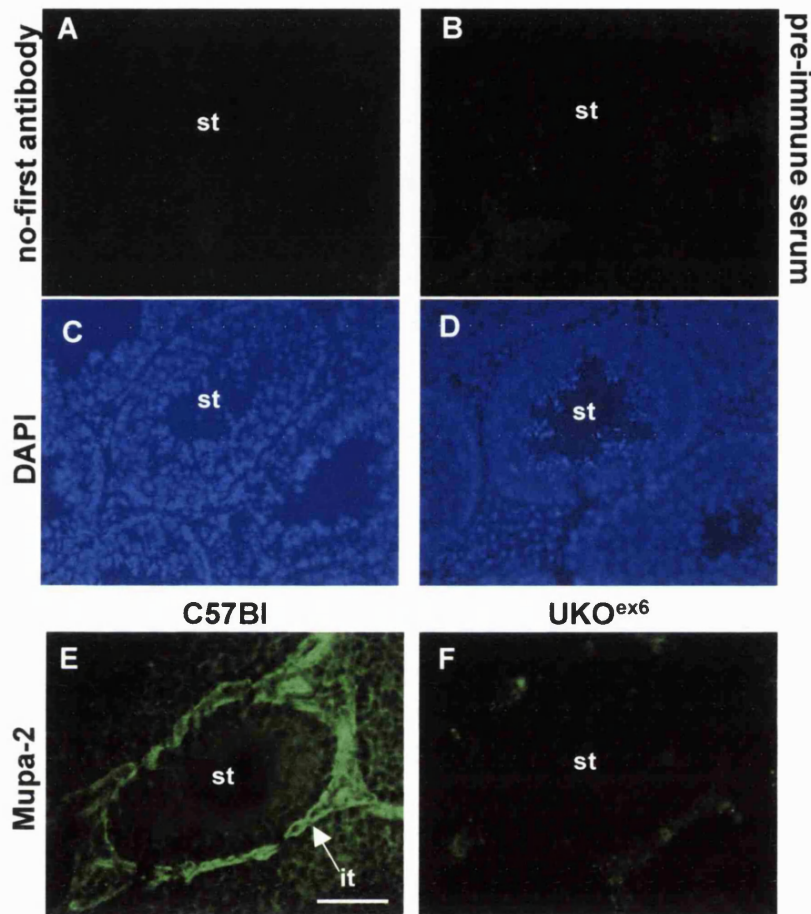


Fig 5.20 A, C57BI adult testis labelled with fluorescein-conjugated anti-rabbit IgG and B, with a pre-immune serum followed by incubation with fluorescein-conjugated anti-rabbit IgG. The position of seminiferous tubules in A and B was revealed by DAPI staining (C,D respectively). E, C57BI adult testis immuno-labelled with Mupa-2 showing utrophin expression in the intertubular tissue (it). F, Mupa-2 immuno-labelling of UKO^{ex6} adult testis showing the absence of signal. Bar= 100 μ m.

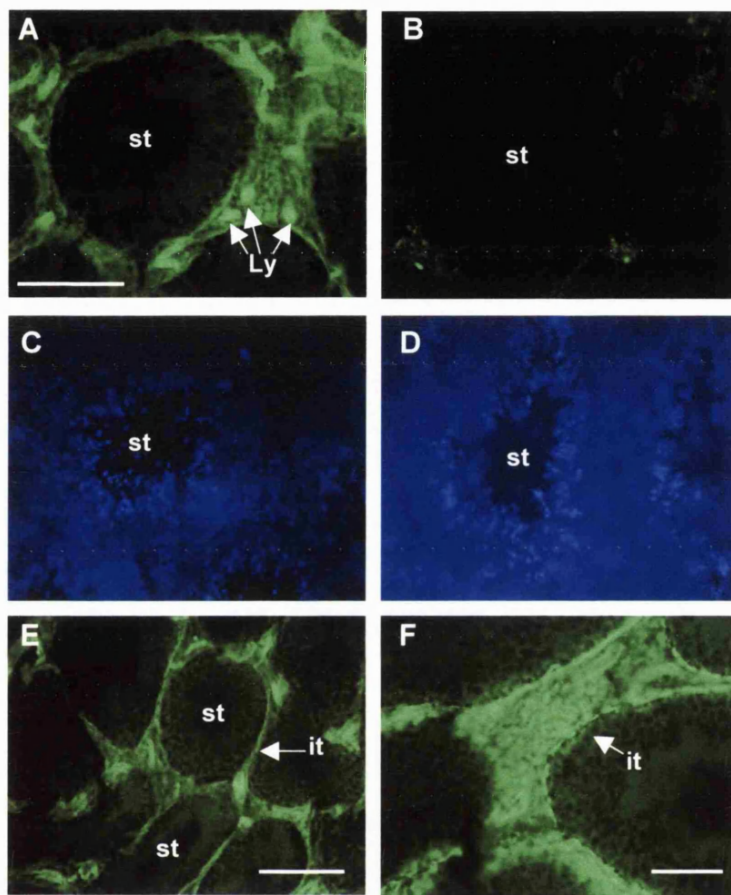


Fig 5.21 Labelling of C57Bl (A,C,E,F) and UKO^{ex6} (B,D) adult testis sections with Mupa-3. Utrophin is expressed in the intertubular tissue (it) and Leydig cells (Ly) in C57Bl testis but is absent in UKO^{ex6} testis. The DAPI staining of A and B are shown in C and D respectively to demonstrate the presence of a seminiferous tubule (st). E shows an area with several seminiferous tubules and F shows a detail of the space between two tubules. Bar (A) = 100 μ m; Bar (E)=200 μ m Bar (F)= 80 μ m.

Levels of signal in testis were so high that Mupa-2, which gave very weak or no signal in other tissues, gave detectable levels in testis (Fig 5.20 E).

No signal could be detected in UKO^{ex6} testis with any of the antibodies; this suggests that full-length utrophin is the major utrophin isoform in this tissue and that short 97kDa/103kDa isoforms are not expressed. If the 97kDa/103kDa bands are not some unusual artefact of the SDS PAGE/Western blotting procedure, then it is necessary to propose that these proteins are not detected in their native form within the testis. It may also suggest that the proteins are dispersed at low levels throughout the cytoplasm of testicular cells and may be more difficult to detect than if concentrated in a particular structure.

Foetal hands

Western blot analysis of foetal hands extracts

demonstrated expression of full-length utrophin and Up109 in this tissue (section 4.2, Fig 4.11, Fig 4.12). Published mRNA *in situ* hybridisation studies (Schofield et al., 1993) and the present study (see section 6.2 and Fig 6.12) suggest that the mRNA accumulates in the tendon primordia. In order to investigate the cellular distribution of these isoforms hand sections were prepared from embryos at two stages of development, 15.5dpc and 16.5dpc. An antibody against collagen type I, [$\alpha 1(I)$]₂ $\alpha 2$ (Table 2.3), was also used as a tendon marker to stain adjacent sections.

Fig 5.22 shows transverse sections through the tip of the digits of 15.5dpc C57Bl and UKO^{ex6} embryos stained with anti-collagen I antibody (A) Mupa-3 (E) and Mupa-2 (G). The anti-collagen I antibody and the utrophin specific antibodies gave a very different staining pattern. Collagen I signal is punctuate and accumulates in two areas dorsally and ventrally to the ossifying

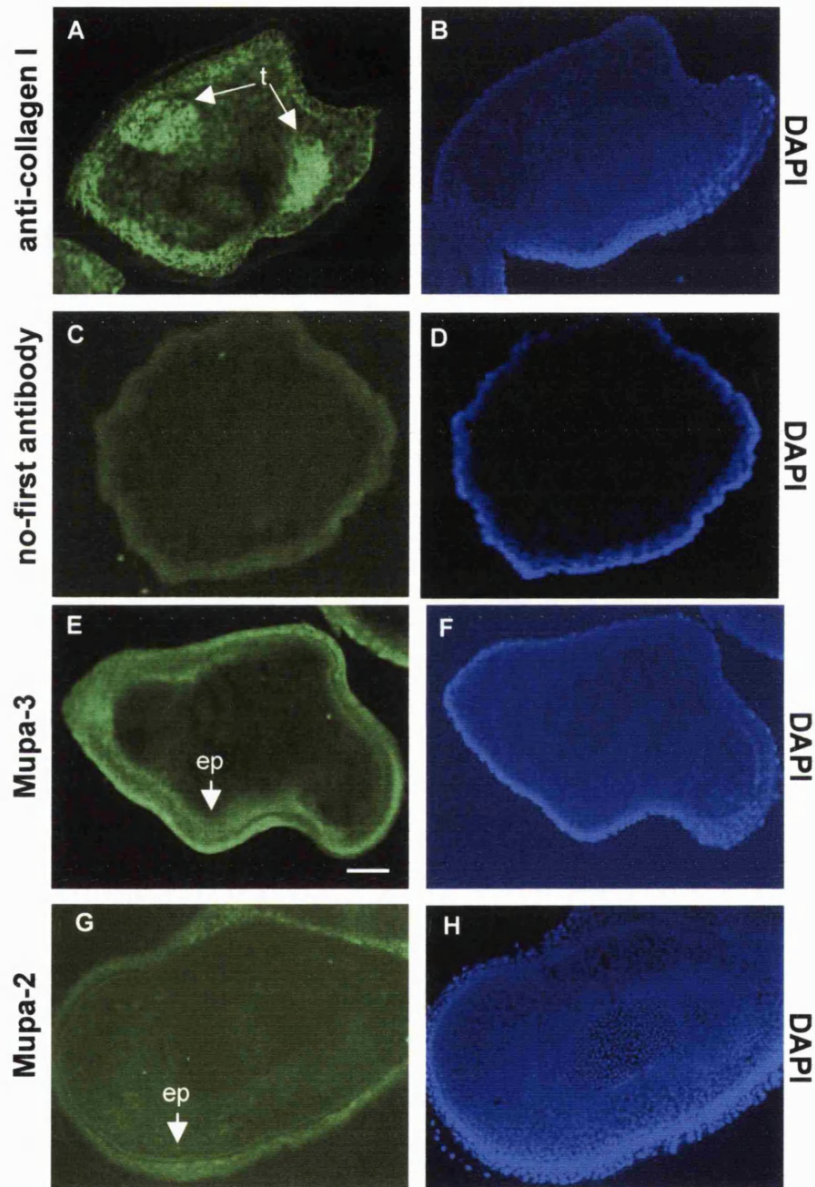


Fig 5.22 Transverse sections through the tips of the digits of 15.5 dpc UKO^{ex6} (A-F) and C57Bl (G,H) embryos: section A is labelled with anti-collagen type I antibody; C with the second antibody only; E with Mupa-3 and G with Mupa-2. DAPI staining corresponding to A,C, E and G is shown in B, D, F and H respectively. ep=epidermis; t=tendon. Bar = 200 μ m.

cartilages in regions that correspond to the tendon primordia and highest abundance of utrophin mRNA seen in the mRNA *in situ* hybridisation experiments (Schofield et al., 1993). Some signal was also detected in a broad band of cells in the dermis. In contrast, the anti-utrophin antibodies detected signal exclusively in epidermal and dermal layers of cells. The levels of non-specific background were determined by staining adjacent sections in the absence of the first antibody or with a pre-immune serum (Fig 5.22 C). The skin is a tissue prone to show non-specific fluorescence, particularly keratinocytes in the most superficial layer of the epidermis; however, while the signal detected with the weak antibody Mupa-2 may be ascribed entirely to background signal, the signal detected with Mupa-3 is well above background levels and shows a differential distribution. It is confined to an outer layer of cells, maybe 2-3 cells thick, in the epidermis and then less abundantly to a more diffuse inner layer.

By 16.5dpc the pattern of protein distribution has changed. For example, Fig 5.23 shows a series of longitudinal sections through the most distal half of 16.5 dpc C57Bl (E) and UKO^{ex6} (A, C) hands labelled with Mupa-1 (E) and Mupa-3 (C). Strong signal is seen in a narrow cell layer in the deepest strata of the epidermis rather than in the more superficial layers seen a 15.5 dpc. Now in contrast, the more superficial layer shows only a weak signal. The strong signal appears in a layer of cells which could correspond to the epidermal-dermal junction. This is a specialised basement membrane that links the membrane of epidermal cells to the extracellular matrix of the dermis (Bannister, 1995, p 397). This signal is present in both control and UKO^{ex6} mice but in UKO^{ex6} mice, Mupa-1, the NH₂-terminal antibody did not detect signal. Even at this stage of development no protein is seen in the tendon.

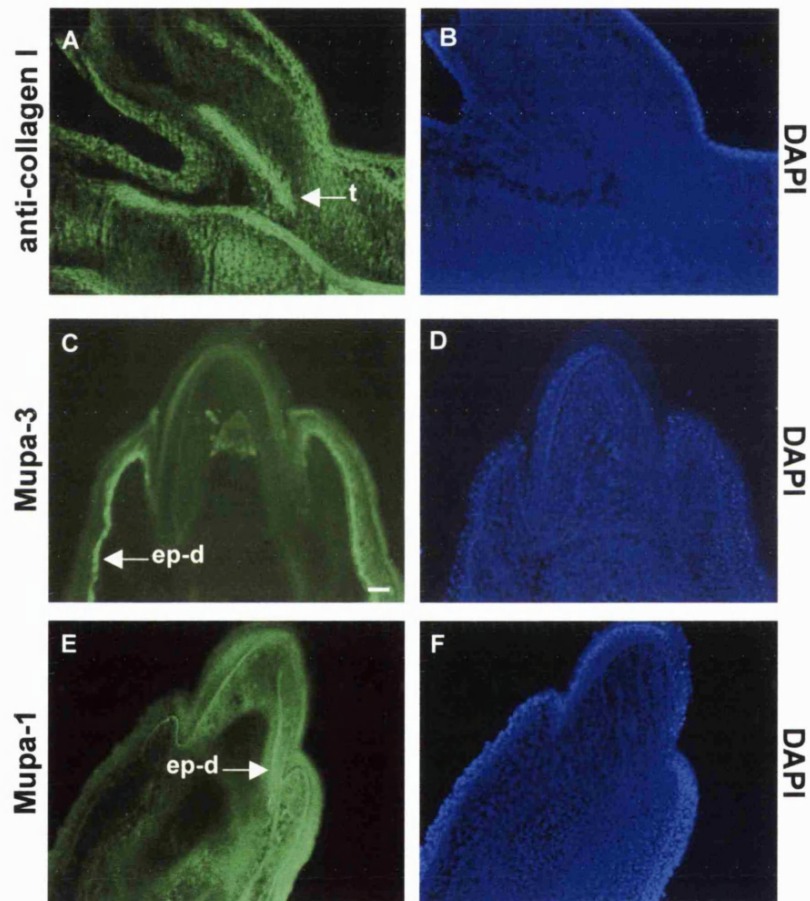


Fig 5.23 Longitudinal sections through the distal half of 16.5 dpc UKO^{ex6} (A,B,C,D) and C57Bl (E,F) hands immuno-labelled with A, anti-collagen I antibody; C, Mupa-3; E, Mupa-1. DAPI staining corresponding to and A,C, E is shown in B,D, F. ep-d=epidermal-dermal junction; t=tendon. Bar = 200 μ m.

The observation that Mupa-3 detects utrophin in both UKO^{ex6} and control tissue whereas Mupa-1 detects the same signal but only in controls could be explained by proposing that both Up109 and full-length utrophin share the same distribution in the developing hand. These data are limited by the small number of foetal hands sections analysed, nonetheless, they suggest that Up109 does not co-locate with its mRNA in tendons and accumulates in the epidermis possibly at the epidermal-dermal junction.

Summary

The results described in this section are summarised in Table 5.1. In brief it appears that full-length utrophin is the major form of utrophin in normal adult skeletal muscle, kidney and testis. Full-length utrophin is also abundant at in the smooth muscle of blood vessels and in nerves. In UKO^{ex6} muscle, weak signal at the NMJ detected with the COOH-terminal antibodies has been interpreted as accumulation of a short isoform, perhaps Up140. In developing muscle full-length utrophin is expressed at the sarcolemma, - possibly together with a short isoform, Up109.

Full-length utrophin is also the major form in normal adult kidney and accumulates in glomeruli, tubules and collecting ducts. However both the immunohistochemistry and Western blot data support the view that the short form Up120 is also expressed in glomeruli. In testis, full-length utrophin is abundant in intertubular tissue and Leydig cells. The short isoforms (103/97kDa) seen on Western blots of testis were not detectable by immunohistochemistry. Analysis of foetal hands sections revealed that both full-length utrophin and Up109 are co-expressed at the epidermis.

Tissue	mice	Mupa-1	Mupa-2	Mupa-3	isoform	
vasculature	-smooth muscle	control UKO ^{ex6}	++++ -	+++ -	++++ -	Fl-utrn
	-endothelium	control UKO ^{ex6}	+++ -	++ -	+++ -	Fl-utrn
peripheral nerve	control UKO ^{ex6}	+++ -	++ -	+++ -	Fl-utrn	
skeletal muscle	-NMJ	control UKO ^{ex6}	++++ -	+++ +	++++ +	Fl-utrn + Up140
	-myotube sarcolemma	control UKO ^{ex6}	++++ -	++ -	++++ ++	Fl-utrn + Up109
kidney	-glomeruli	control UKO ^{ex6}	++++ -	++ -	++++ ++	Fl-utrn + Up120
	-tubules/ducts	control UKO ^{ex6}	+++ -	+ -	+++ -	Fl-utrn
testis	-intertubular tissue	control UKO ^{ex6}	++++ -	+++ -	++++ -	Fl-utrn
	-Leydig cells	control UKO ^{ex6}	++++ -	+++ -	++++ -	Fl-utrn
limb	-epidermis	control UKO ^{ex6}	+++ -	+ +	+++ +++	Fl-utrn + Up109

Table 5.1 Summary of immuno-histochemistry experiments. The relative intensities of immunoreactive staining detected with each antibody are indicated by - or +, with + = weak and ++++= very strong.

Discussion

5.3 Utrophin isoforms in skeletal muscle

General comments The expression of full-length utrophin in skeletal muscle is well documented by numerous immuno-histochemistry studies (Khurana et al., 1991; Ohlendieck et al., 1991a; Nguyen et al., 1991,1995; Helliwell et al., 1992; Matsumura et al., 1992). The main objective of the immuno-histochemical analysis of adult and foetal muscle presented in this study was to characterise the new Mupa antibodies and in addition, to ask whether short isoforms are expressed in UKO^{ex6} muscle in the absence of the full-length isoform.

The Mupa antibodies interact well with native utrophin; Mupa-1 and Mupa-3 are particularly efficient whereas Mupa-2 gave a general weaker signal. This may reflect differences in the accessibility of the aa sequences used to raise each of these antibodies. Perhaps, the NH₂- and COOH-termini are more exposed at the surface of native utrophin and thus more accessible to antibodies than the central region of spectrin repeats. It is interesting to note that in direct contrast to the findings made by immuno-histochemical analysis, Mupa-1 gave the weakest signal on Western blots (see Fig 4.4, 4.6 and 4.8). Thus it seems that Mupa-1 appears to recognise a conformational epitope and has higher affinity for native utrophin than for the denatured aa sequence.

This observation highlights the possibility that antibodies efficiency and suitability vary from one technique to another. For instance, Nguyen et al. (1991) raised a panel of monoclonal antibodies against the COOH-terminus of

utrophin which, when tested on Western blots and immuno-histochemistry, showed variable results. In particular, Mancho-7 behaved in a manner similar to Mupa- 1 labelling utrophin intensely on sections but giving only a faint band on Western blots. Mancho 16 and 17, on the other hand, worked well on Western blots but failed to label neuromuscular junctions on sections.

The immuno-histochemical analysis of adult skeletal muscle presented in this study confirms that full-length utrophin is the major muscle isoform and that is also abundant in blood-vessels, intramuscular nerves and in the capillary network as previously described (Helliwell et al., 1992; Nguyen et al., 1995). Full-length utrophin is also expressed at the sarcolemma of regenerating fibres confirming that this isoform is upregulated in the absence of dystrophin.

The present studies have also confirmed by examination of utrophin in UKO^{ex6} muscle that full-length utrophin is the sole utrophin isoform in nerves, blood-vessels and capillaries. Despite the absence of utrophin in nerve fibres, UKO^{ex6} mice do not suffer from muscle weakness and exhibit no symptoms of peripheral neuropathy and no obvious morphological abnormalities upon histological examination of muscle sections (Deconinck et al., 1997a). This suggests that either full-length utrophin is not necessary for the function of nerves and blood-vessels or that a related protein is compensating for its absence in UKO^{ex6} mice. Fabrizio et al. (1995) demonstrated the co-expression of Dp116 (but not full-length dystrophin) and full-length utrophin in sciatic nerve fibres. Thus Dp116 could be partially compensating for the loss of full-length utrophin in UKO^{ex6} peripheral nerve.

In blood-vessels, Rivier et al. (1997) showed that the distribution of full-length utrophin and dystrophin does not coincide and proposed different roles

for both proteins in muscle vasculature. Utrophin is expressed in large and small arteries and veins whereas dystrophin is associated with arteries but is not found in small veins. These authors proposed that dystrophin plays a mechanical role in arteries which have an active work in circulation whereas utrophin has a rather architectural role in the assembly of smooth muscle membrane protein complexes. The difference in cell-type location implies that dystrophin would have to be *de novo* synthesised in small veins in order to be considered as compensating for the lack of utrophin in blood-vessels.

A short utrophin isoform is expressed at the NMJ in UKO^{ex6} mice It was surprising to find that in UKO^{ex6} muscle, weak levels of utrophin signal were detected at the NMJ. Although it can be argued that the signal detected with Mupa-1 represents crossreactivity with dystrophin, that cannot explain the signal detected with Urd40 (preabsorbed against dystrophin) or with Mupa-2 (epitope aa region has very low homology to dystrophin). Thus, it seems probable that a short utrophin isoform is expressed at the NMJ in UKO^{ex6} mice. Such a short isoform must correspond to a mRNA transcribed from a position upstream of exon 56 as judged by its antibody reactivity.

However, no good candidate short utrophin isoform was detected on Western blots of UKO^{ex6} muscle extracts. It is possible that this isoform was not detected on Western blots because it is only very weakly expressed. During immuno-histochemistry experiments the NMJs were the focus of attention, highlighted by labelling with α -bungarotoxin. NMJs represent only a small proportion of muscle tissue and a protein exclusively expressed at this site may be at such low levels in a general tissue extract that it is undetectable by

Western blotting. It is relevant to note that full-length utrophin, the major isoform, is detected as a rather weak band (in comparison with other tissues) on blots (Fig 4.8).

These results are in contrast to previous analysis of UKO^{ex6} skeletal muscle by Deconinck et al. (1997a). These authors did not detect significant levels of utrophin at the NMJ in UKO^{ex6} mice neither with the NH₂-terminal antibody DRP3 (Novocastra) nor with the COOH-terminal antibody DRP1 (Novocastra, a monoclonal raised against a short peptide corresponding to the 11 most COOH-terminal aa). As discussed in section 3.1 antibodies to short peptides may not recognise, or may interact less well, with the native protein. Thus, this previous work does not entirely exclude the expression of a short utrophin isoform at UKO^{ex6} NMJ.

There is a difference between the two strains of UKO mice that points towards the presence of a short utrophin isoform at the NMJ. Both UKO^{ex6} and UKO^{ex64} have been crossed with the *mdx* mouse to generate utrophin-dystrophin deficient mice (dko), (Deconinck et al., 1997b; Grady et al., 1997b, section 1.10). The analysis of the DAP complex at the NMJ in both types of dko mice by immuno-histochemistry showed that while in dko^{ex6} the expression of the synaptic protein β 2-syntrophin was normal, in dko^{ex64} β 2-syntrophin was nearly undetectable.

Since the only difference between both double knock-outs is the presence or absence of the short utrophins, this observation may imply that a short utrophin isoform (they all contain the syntrophin binding domain) is important for the correct localisation of β 2-syntrophin in the NMJ DAP complex. It is relevant to note that the levels of β 2-syntrophin were not reduced in the

UKO^{ex64} single knock-out (Grady et al., 1997a) perhaps suggesting that dystrophin associates with β 2-syntrophin in the absence of all utrophin isoforms. This leads on to the proposal that is only in the absence of full-length utrophin and full-length dystrophin that a short utrophin isoform is recruited as partner of β 2-syntrophin in a DAP complex in UKO^{ex6} NMJs.

In addition, short utrophin isoforms may also have a signalling role in striated muscle mediated by interactions with syntrophin and NOS. This idea is supported by the observation that dko^{ex64} mice, but not dko^{ex6} mice, show a cardiomyopathy associated with a decrease in nNOS and an increase in the induced NOS (iNOS) in cardiac muscle (Bia et al., 1999).

Is this short isoform important for NMJ structure and function? It is tempting to speculate that a short utrophin isoform may be partly compensating for the absence of full-length utrophin and may be allowing the DAP complex at the NMJ to assemble, as does Dp71 in *mdx* mice (Greenberg et al., 1994). Even low levels of expression may be sufficient to provide this compensation. An argument against such a view is UKO^{ex64} mice, deficient for all utrophin isoforms (Grady et al., 1997a), are thought not to show more severe abnormalities of the NMJ than UKO^{ex6} mice, although, in fact they do show a reduced number of junctional folds and acetyl-choline receptors (AChR). These data suggest that in UKO^{ex6} mice, short utrophin isoforms may occur but their absence does not completely disable the function of the neuromuscular junction.

Is a short isoform expressed in foetal muscle?

The analysis of

16.5 dpc foetal muscle sections with the Mupa antibodies showed that full-length utrophin was detected in normal foetal muscle at the sarcolemma of myotubes, in nerves and in large blood-vessels; no signal was detected in capillaries (Takemitsu et al., 1991; Khurana et al., 1991; Clerk et al., 1993). The lack of expression in capillaries was noted by Clerk et al. (1993) who found that utrophin expression in capillaries was not apparent until 41 weeks gestation in human embryos, at a stage when utrophin was no longer present at the sarcolemma of myotubes.

Interestingly, the labelling of UKO^{ex6} foetal muscle sarcolemma with Mupa-3 but not with Mupa-1 points to the expression of a short utrophin isoform in the developing muscle. This isoform could correspond to Up109 which was detected on Western blots by Mupa-3 and Mupa-2 and by Up109 specific RT-PCR, albeit weakly, from foetal muscle mRNA. Taken together, the Western blots and immuno-histochemistry results point towards the co-expression of full-length utrophin and a short isoform in foetal muscle rather than an upregulation of a short isoform in UKO^{ex6} mice in the absence of full-length utrophin.

There is no firm evidence in the literature for a short utrophin isoform in foetal muscle. However, a band of 120kDa was described by Takemitsu et al. (1991) and by Koga et al. (1993) on Western blots of mouse foetal muscle extracts but dismissed as an artefact as it was detected even when the antiserum had been preabsorbed with the immunising peptide. Careful examination of the Figs shown in both of these reports revealed that the 120kDa polypeptide was more abundant in younger foetal extracts (14.5 dpc and 15.5 dpc, compared to 20 dpc, 1 week old mouse and adult mouse

extracts) and in human primary myogenic cultures compared to human adult skeletal muscle. This apparent developmentally differentiated pattern of expression argues against the identification of the “120kDa” band as an artefact and leaves open the question of a short utrophin isoform in foetal muscle.

It seems relevant to note that the presence of a short dystrophin isoform(s) in foetal muscle has been demonstrated. These studies, which used antibodies raised against different regions of dystrophin in immunohistochemical analyses of foetal skeletal muscle (Clerk et al., 1992; Lin S. et al. (2000), suggest that Dp71 is expressed at the sarcolemma of myotubes prior to the appearance of full-length dystrophin at the sarcolemma.

Direct experiments to examine the profile of expression of Dp71 showed that indeed, it is expressed at early stages in muscle development and is absent in adult skeletal muscle (Lambert et al., 1993; Schofield et al., 1994), whereas full-length dystrophin expression is initially low but increases towards birth (Clerk et al., 1992). Both isoforms may be co-expressed for a short time during development and because of their structural differences are likely to have different functions.

Some information on the role of Dp71 comes from a study of its localisation in C₂C₁₂ myoblasts (Howard et al., 1999). In these cells, Dp71 localises with bundles of actin microfilaments and precipitates with the microfilament fraction whereas full-length dystrophin fractionates with the sarcolemma fraction. These authors suggest that Dp71 has a role in actin cytoskeleton remodelling.

In the case of utrophin, if full-length and say Up109 were co-expressed in foetal muscle they are likely to play different roles. In future studies, it would be

of interest to analyse in detail the relative intracellular distribution of full-length utrophin and Up109 by immuno-histochemistry (maybe using an antibody raised against the unique aa sequence of Up109) and by protein solubilization and fractionation studies.

The results presented in this chapter confirm that utrophin and dystrophin are both expressed at the sarcolemma in foetal muscle as reported previously (Clerk et al., 1992, 1993; Lin S. et al., 2000).

Is this short isoform compensating for the loss of full-length utrophin in

UKO^{ex6} foetal muscle?

UKO^{ex6} muscle development seems to have occurred normally, these mice do not show signs of muscle weakness at birth despite the absence of full-length utrophin. Deconinck et al. (1997a) reported that UKO^{ex6} mice are born with a normal weight and size. However, personnel at UCL Biological Services and myself have consistently observed that UKO^{ex6} mice are relatively smaller than their control counterparts. This observation may imply that UKO^{ex6} foetal development is not entirely normal. A short isoform such as Up109 could be partially compensating for the absence of full-length utrophin in UKO^{ex6} mice. However, such an isoform, as mentioned earlier, has important structural differences with full-length utrophin and is likely not to fulfil all the functions of full-length utrophin.

In the present study, a limited number of sections and a single developmental stage have been analysed and the data are preliminary. In future studies, analysis of human and mouse foetal muscle sections at different stages of development might throw more light on the pattern of expression and possible role of Up109 in the developing muscle.

5. 4 Full-length utrophin and Up120 are expressed in kidney

The results presented in this study show that full-length utrophin is the major utrophin isoform in adult kidney and is found in the glomeruli and convoluted tubules of the cortex and in the collecting ducts of the medulla. Previous analyses have detected utrophin in the glomeruli of mouse, rat and human kidney (Grady et al., 1997a; Loh et al., 2000; Raats et al., 2000). The glomerular cell wall is made up of podocytes, glomerular basement membrane and fenestrated endothelium and forms a barrier preventing the passage of plasma proteins into the urinary space during glomerular filtration. Raats et al. (2000) demonstrated by immunoelectron microscopy that podocytes are the major source of utrophin expression in the renal glomerulus. More precisely, utrophin localised to the foot-processes which are in direct contact with the endothelial cells of the glomerulus.

The present study also provides good evidence that in addition to full-length utrophin a short utrophin isoform is expressed in kidney; while no signal was detected in UKO^{ex6} kidney with Mupa-1, low level signal could be detected with Mupa-3 in glomeruli. This isoform is likely to be Up120, a utrophin isoform detected on Western blots of C57Bl and UKO^{ex6} adult and foetal kidney extracts with four different COOH-terminal utrophin specific antibodies.

What are the functions of full-length utrophin and Up120 in kidney?

Full-length utrophin and Up120 both contain the domains necessary for interacting with dystroglycan, syntrophins and dystrobrevins and thus are likely to be complexed with such proteins in the kidney. However, Up120 lacks the

NH₂-terminal domain and would not be involved in those functions which require interactions with the cytoskeleton via actin.

Several DAPs have been reported in kidney. Loh et al. (2000) analysed by immuno-histochemistry and immunoprecipitation the composition of dystrobrevin-associated complexes in mouse kidney and found that utrophin is part of four distinct complexes; in endothelial cells utrophin is found with α -dystrobrevin-1 and β 2-syntrophin, in podocytes with β -dystrobrevin and β 2-syntrophin, in distal convoluted tubules with β -dystrobrevin, β 2-syntrophin, α -syntrophin and the Dp71 isoform (exon 78 spliced out, Dp71 Δ C) and in collecting ducts with β -dystrobrevin, β 1- and β 2-syntrophin, α -syntrophin and Dp71 Δ C.

Loh and colleagues (2000) did not consider the possibility of a short utrophin isoform in kidney and as yet there is no evidence to say whether the various DAP complexes listed above are formed in the presence of full-length utrophin or short utrophin isoforms or both.

Kachinsky et al. (1999) demonstrated the association of utrophin with dystrobrevin and β 2-syntrophin in a canine kidney epithelial cell line. They found that this complex localises at the basolateral membrane of epithelial cells and they proposed that it linked the actin cytoskeleton of the epithelial cell to the extracellular matrix and thus helps maintain the membrane integrity. This would be an important function in glomerular cells which are subject to mechanical stress from the high blood pressure that drives glomerular filtration; in this case, such an interaction would require full-length utrophin.

Thus far there is no direct evidence that utrophin and dystroglycan form a complex in adult kidney despite the identification of α - and β - dystroglycan in

the glomerular basement membrane and in Bowman's capsule and proximal and distal tubules (Durbeej et al., 1998). Raats et al. (1999) found that utrophin and dystroglycan are located in different regions of glomerular podocytes; utrophin accumulates in areas of contact with the basement membrane while α - and β -dystroglycan localise to the lateral and apical membrane of the podocyte.

Durbeej et al. (1999) made a careful analysis of the dystroglycan complex in adult and foetal kidney epithelial cells by density gradient centrifugation and could not demonstrate an association between dystroglycan and utrophin in adult kidney, but showed that these two proteins were associated in foetal kidney. This suggests that different types of DAPs-utrophin complexes exist in the developing and mature kidney and it is likely that the full-length isoform and Up120 take part in these protein-protein interactions.

The observation that Up120 is upregulated in glomeruli in the absence of full-length utrophin indicates that this isoform may play a special role in kidney filtration. Given the expression of several DAPs in kidney, Up120 may have several functions independent of cytoskeleton interactions and based solely on protein-protein interactions. For instance, a Up120-DAPs complex could recruit proteins to the membrane via the PDZ and PH domains of syntrophin (Touhara et al., 1994; Yao et al., 1994). Such a complex could also play a signalling role via NOS, which is known to bind to syntrophin (Brenman et al., 1996), and be important for regulation of renal vascular tone and for glomerular filtration. NO has been shown to be an important mediator of renal blood flow (Rahman et al., 2001). Another possibility is that a Up120-DAPs complex could play a role in cell-cell contact maintaining the integrity of the glomerular barrier necessary for efficient glomerular filtration.

Whatever the function of full-length utrophin and Up120 in kidney, it does not seem to be crucial for glomerular filtration. A study of the UKO^{ex6} and UKO^{ex64} mice, deficient for full-length utrophin and for all utrophin isoforms respectively (Deconinck et al., 1997a; Grady et al., 1997a), failed to find any histologically visible kidney abnormalities or abnormal kidney function.

A possible explanation for the lack of pathology in the absence of full-length utrophin and short utrophin isoforms is that dystrophin isoforms are compensating for this loss. However, full-length dystrophin is not likely to play a compensatory role since it is not expressed in kidney cortex or in medulla (Grady et al., 1997a; Loh et al., 2000). Furthermore, dko mice (section 1.10) do not show kidney abnormalities.

Dp140 is a possible substitute, however, there is some controversy regarding the expression of Dp140 in adult kidney (Durbeej et al., 1997; Lidov et al., 1998). The present study, Grady et al. (1997a) and Loh et al. (2000) did not detect dystrophin signal in glomeruli using antibodies which would have detected Dp140.

Dp71, however, has been located in the glomeruli, cortical tubules and Bowman's capsule by immuno-histochemistry using an antibody raised against the unique COOH-terminus of Dp71 (Loh et al., 2000). Thus, Dp71 could be taking the place of longer utrophin isoforms in crucial protein-protein interactions. However, an argument against this scenario comes from the study of the offspring from a cross between UKO^{ex6} and *mdx*^{3CV} mice; the homozygous offspring appear to have normal kidney function and morphology (Rafael et al., 1999). Thus, it seems that neither full-length dystrophin nor short dystrophin isoforms are likely to replace full-length utrophin.

This leaves two possible explanations; another member of the dystrophin gene family is compensating for the loss of utrophin isoforms or no utrophin isoform is essential for normal kidney functioning.

Amongst the dystrophin related proteins, dystrobrevin (Blake et al., 1996a, 1998) and dystrophin-related protein 2 (DRP2) (Roberts et al., 1996) might be considered since they are both expressed in kidney (Loh et al., 2000; Dixon et al., 1997). However, both lack the NH₂-terminal and all (dystrobrevin) or nearly all (DRP2) spectrin repeat domains (Blake et al., 1996a, 1998; Roberts et al., 1996) and thus are not likely to have the same functions as full-length utrophin but may compensate for loss of short utrophins.

With the idea that utrophin and the DAPs play a important role in kidney, Raats et al. (2000) analysed immuno-histochemically the expression of α - and β -dystroglycan, agrin and utrophin in an experimental rat model for proteinuric glomerulopathy (adriamycin induced nephropathy, ADN). The authors found that the expression of all of these proteins was reduced in the glomerulus of ADN rats compared to control rats. However, it appears that this decrease is most likely to be due to a decrease in podocyte membrane surface as a result of the podocyte foot fusion, a common finding in glomerulopathies.

Therefore, despite the high levels of full-length utrophin in kidney, and the expression of Up120, there is no evidence that they play crucial roles in this tissue.

5.5 Full-length utrophin is expressed in testis intertubular tissue and in Leydig cells

The data presented in this section show that full-length utrophin is abundant in testis and localises to the intertubular tissue separating seminiferous tubules and in Leydig cells. A search of the literature indicates that this is the first report of the cellular localisation of utrophin in testis and that there is only one other report of utrophin expression in mouse testis as judged by Western blotting (Lumeng et al., 1999).

The identification of the isoform detected by immuno-histochemistry as full-length utrophin is made on the basis of its presence in control testis and its absence in UKO^{ex6} testis. Full-length utrophin was also detected as a strong testis component on Western blots (section 4. 2, Fig 4.10). In addition, two short utrophins of 97kDa/103kDa were seen on immunoblots and these are similar to two short isoforms, 90kDa/97Kda, detected by Lumeng et al (1999) in the same way. However, there is no immuno-histochemical evidence for such isoforms in testis.

These short isoforms cannot be entirely dismissed since there are other examples of proteins identified by Western blotting but undetectable by immuno-histochemistry. For instance, Durbeej et al. (1999) were able to demonstrate the presence of γ -sarcoglycan in lung by Western blotting but could not detect signal by immuno-histochemistry using the same antibodies. The possibility that the 97kDa/103kDa intracellular utrophin polypeptides are not accessible to the antibodies could be investigated in future studies by trying to expose the surface antigens, for example, by treating the sections with detergent (e.g. 1% Triton X-100).

One other possibility is that the section fixation procedure may be affecting the folding of the short isoforms. Because the testis morphology was not easily retained without fixation, the sections were fixed with acetone for 7 min prior to immuno-histochemistry. Acetone fixation denatures proteins by coagulation and can result in antigen disruption and epitope masking (<http://chemicom.com/resource/>). Although a relatively short fixation time was used it is possible that structural, biochemical or environmental differences between full-length utrophin and the 97kDa/103kDa isoforms may be sufficient to result in different sensitivities to acetone. This possibility could also be investigated in future studies.

Immuno-histochemistry and Western blotting studies indicate that full-length utrophin is abundant in testis. From the present study, utrophin appears to localise to the intertubular tissue which comprises a loose, supportive, connective tissue containing blood-vessels and various cell types including peritubular cells, pluripotent mesenchyme cells, fibrocytes, Leydig cells and mononuclear cells (macrophages, lymphocytes and monocytes), (Wrobel et al., 1988). Fibrocytes, peritubular cells and Leydig cells are all derived from the pluripotent mesenchyme cells (Wrobel et al., 1988).

In the present study, all the components of the intertubular tissue were brightly labelled by the anti-utrophin antibodies; however, Leydig cells labelling was particularly intense. Leydig cells are primarily hormone secreting cells; they synthesise and secrete testosterone and other androgens. Hormones are secreted by exocytosis. In a typical hormone secreting cell, secretory granules are transported to the cell apical membrane, the granule and cell membranes

fuse and the contents of the granules are released to the extracellular space (Karp, 1999, p 322).

Could utrophin be involved in secretion? It is possible to speculate that utrophin might be involved in secretion by interacting with the cytoskeleton via actin and functioning to transport secretory granules containing testosterone to the apical membrane of Leydig cells.

There is a body of immuno-cytochemical and biochemical evidence to support a motile role of the cytoskeleton in the directional transport of secretory granules from the Golgi apparatus to the cell membrane. For instance, actin and actinin filaments have been found in association with granules membrane and, together with myosin and tropomyosin, are known to accumulate directly beneath the apical plasma membrane in cells actively involved in exocytosis. Cytoskeleton driven granule transport is likely to involve calcium dependent actin filament shortening. (Tartakoff, 1987).

Pharmacological studies also support the role of actin and microtubules in exocytosis. In these studies, treatment of cells, such as the exocrine cells of the pancreas, with microtubule or actin specific poisons, colchicine and cytochalasin respectively, inhibit exocytosis (Oliver and Berlin, 1979).

It is relevant to note that utrophin is expressed in other hormone secreting tissues. In the embryo, utrophin mRNA is detected in Rathke's pocket (Schofield et al., 1993) which will become the glandular part of the pituitary which contains cells that synthesise and secrete glucocorticoid hormones including luteinizing hormone (LH), thyroid-stimulating hormone (TSH) and follicle-stimulating hormone (FSH). Utrophin protein has also been detected in

the neurohypophysis where neurones produce and secrete vasopresin and oxytocin (Dorbani-Mamine et al., 1998).

In future studies, a priority would be to establish the precise cellular and sub-cellular localisation of utrophin in Leydig cells and in intertubular tissue cells. This could be done for instance by immunoelectron microscopy. The analysis of utrophin in Leydig cells may be facilitated by growing the cells in culture as described in the literature (Denduchis et al., 1996). There is also a non-tumorigenic Leydig cell line, TM3, which is commercially available (Mather et al., 1982).

It would also be important to examine the composition of testis specific utrophin-DAPs complexes. This could be approached initially by immunohistochemistry and immunoprecipitation using the existing antibodies against the known DAPs; α - and β -dystroglycan and the different sarcoglycans, dystrobrevin and syntrophin isoforms. Alternatively, novel testis specific DAPs could be looked for and isolated by screening testis cDNA libraries with DNA probes containing sequences conserved within each group of DAPs.

There is already some information regarding the expression of dystroglycan in the mouse testis. Durbeej et al. (1998) reported expression of α - and β -dystroglycan in the seminiferous tubule basement membrane. Dystroglycan expression was also weakly detected in the spermatogonia in the layer immediately adjacent to the basement membrane. However, these authors did not detect dystroglycan in the intertubular tissue. Taken together with the results in the present study, it appears that dystroglycan and utrophin do not co-localise in testis and thus are not likely to be part of the same DAP complex. A similar scenario to that described in adult kidney (Durbeej et al.,

1999). Thus, it is possible that in Leydig and other intertubular cells utrophin may be associated with an as yet unidentified transmembrane protein similar to dystroglycan.

Examination of the Figs in Durbeej et al. (1998) revealed that the pattern of expression of the integrin $\alpha 6$ subunit closely resembles that obtained in the present study with the Mupa antibodies.

Integrins are transmembrane heterodimers consisting of combinations of α and β chains. To date, 17 and 8 different α and β chains respectively have been identified. Both the α and β integrin chains have a large extracellular domain that binds to extracellular matrix proteins, a transmembrane domain and a short cytoplasmic domain that binds to the actin cytoskeleton via other proteins such as vinculin and talin (Karp, 1999, p. 263).

In the marmoset, Husen et al. (1999) found that $\alpha 5$, $\alpha 6$ and $\beta 1$ integrin subunits are all expressed in sertoli cells and basal compartment of seminiferous tubules and in addition, $\alpha 5$ alone is expressed in the intertubular tissue. The pattern of $\alpha 5$ labelling shown in Husen et al. (1999) is very similar to that shown by Durbeej et al. (1998) for $\alpha 6$ integrin subunit and this may reflect a difference between rodents and primates in the identification of integrin subunits.

These observations leave open the possibility of an association between utrophin and integrin in the formation of an extracellular matrix/transmembrane link. There is no evidence in the literature for the association of utrophin with integrin. However, this possibility could be investigated in future studies by protein overlay assays, also known as Far-Western blotting (Dunbar, 1994). Using this technique, Durbeej et al. (1999) demonstrated the direct association

of α -dystroglycan and laminin in rabbit kidney. Alternatively, utrophin bound integrin protein complexes could be immunoprecipitated and detected with an anti-integrin antibody.

How does the absence of full-length utrophin affect UKO^{ex6} mice

testis?

Leydig cells secrete testosterone which is responsible for the control of testicular vasculature, for secondary sexual changes at puberty and for sexual/mating behaviour (Bannister and Dyson, 1995). It would be of interest to examine the functional status of Leydig cells in UKO^{ex6} mice by measuring levels of serum testosterone perhaps with anti-testosterone antibodies (Romeo et al., 1999). If full-length utrophin played a crucial role in testosterone secretion, it might be expected that in its absence infertility and/or abnormal sexual development and behaviour would result. Although UKO^{ex6} mice are fertile and there have been no reports in the literature of fertility problems, UCL Biological Services staff noted that at least twice the number of UKO^{ex6} male/female pairs had to be set up to obtain the same number of successful matings (marked by vaginal plugs) as achieved for C57Bl mice.

Such an enigmatic abnormality may be due to impaired Leydig cell function and reduced testosterone levels. Other observations with regard to UKO^{ex6} breeding success were also made. There was a consistent reduction in UKO^{ex6} litter size (6 pups in UKO^{ex6} versus 8 in C57Bl) and a smaller newborn body size. There was also some evidence for a 0.5 day developmental delay most obvious at early stages (8.5 and 9.5dpc) in UKO^{ex6} embryos compared to C57Bl embryos and a comparatively smaller body size of adult UKO^{ex6} mice.

The significance of these observations will need further investigation in future studies.

In summary, in testis full-length utrophin is expressed in the intertubular tissue and is particularly abundant in Leydig cells where it could play a role in hormone secretion. Utrophin was undetectable in UKO^{ex6} mice which although fertile may exhibit subtle sexual behaviour abnormalities. Although no blatant pathologies are seen in mice deficient for utrophin, the recognition that high levels of utrophin are expressed in this tissue opens the door to a consideration of the role of utrophin in infertility in man.

5.6 Expression of utrophin in the skin

The immuno-histochemical study of developing mouse hands presented in this study shows that both full-length utrophin and a short utrophin isoform are expressed in the epidermis. The short utrophin isoform is likely to correspond to Up109, a novel isoform detected in foetal hands extracts by Western blotting (chapter 4 Fig 4.11, 4.12) and which was subsequently isolated as a cDNA and sequenced.

The staining patterns detected in control hands with Mupa-1 and in UKO^{ex6} hands with Mupa-3 were similar indicating that full-length utrophin and Up109 co-localise. In 15.5 dpc embryos, signal was detected in rather superficial layers of the epidermis (maybe stratum granulosum or spinosum). This signal is not likely to represent non-specific background since it was stronger than the low level signal detected in the absence of primary antibody and was not localised to the most superficial stratum corneum which is where non-specific signal was seen.

In 16.5 dpc embryonic hands, utrophin signal accumulated in a deeper cell layer that could be interpreted as the epidermal-dermal junction. This is the area of contact between epidermal keratinocytes and the underlying dermis (Bannister, 1995, p 397). Full-length utrophin and Up109 could have complementary roles here; full-length utrophin could form a link between the cytoskeleton of the keratinocyte and the extracellular matrix of the dermis providing a stable substratum for the epidermis whereas Up109 could be responsible for the organisation of DAP complexes in the basal membrane of the keratinocyte involved for example in cell to cell contact, hemidesmosomes are abundant in the epidermal-dermal junction (Mackie et al. 1988), or in cell signalling processes.

Utrophin expression has been reported in epithelial cells in lung and kidney (Durbeej et al., 1999; Kachinsky et al., 1999) and always in close association with basement membranes. Dystroglycan could be part of an epidermal utrophin complex(es) since it is expressed in all layers of the epidermis, except for the stratum corneum, and is also found in the epidermal-dermal junction (Durbeej et al., 1998). Such a dystroglycan-utrophin complex could bind to an extracellular matrix glycoprotein (in a similar way that it binds agrin in the NMJ). Tenascin is a good candidate for such a dystroglycan-utrophin partner since it is found at the epidermal-dermal junction (Mackie et al., 1988). Tenascin is thought to be involved in epidermal cell migration and wound healing since its expression at the epidermal-dermal junction was markedly upregulated after skin injury (Mackie et al., 1988). However, a search of the literature did not find any report of a known association between tenascin and a member of the DAPs.

The most intriguing finding from the immuno-histochemistry experiments shown in this section is that the distribution of utrophin protein does not correlate with the distribution of the mRNA determined by mRNA *in situ* hybridisation (Schofield et al., 1993). Utrophin mRNA seemed to accumulate in the tendon primordia, however, utrophin was not detected in the developing tendons with the Mupa antibodies. In addition, anti-collagen type I antibody, which gave signal in tendons, and anti-utrophin antibodies gave a completely different labelling pattern.

This observation implies that utrophin mRNA or protein migrates from a central position within the digit to the epidermis. There are other examples of different distributions of mRNA and protein; in particular the example of carbonic anhydrase I in the large intestine (Sowden et al., 1993) and PGP9.5 in the cerebral cortex (Schofield et al., 1995a) were discussed previously in section 4.9.

In summary, immuno-histochemical analysis of foetal (only 15.5 and 16.5 embryos were analysed) hands sections has revealed that full-length utrophin and Up109 are expressed in the skin and in particular in the epidermal-dermal junction and not in the developing tendons as anticipated

Chapter 6

Expression of utrophin mRNAs during embryogenesis

Results

6.1 General comments

In addition to immunological methods, mRNA *in situ* hybridisation of UKO^{ex6} tissues also has the potential to be very informative with regard to the expression of short utrophins. The emphasis of the initial analysis of UKO^{ex6} mice by the Oxford team was to establish the effects of the deficiency of full-length utrophin protein, in particular in skeletal muscle. Protein analysis by immuno-histochemistry was the major technique used and no reference was made to short isoforms. However, mRNA *in situ* hybridisation will only be informative in UKO^{ex6} mice if the mutated mRNA is absent or at considerably reduced levels. In most reported cases, insertional mutations result in complete absence of the mutated RNA; for example, using mRNA *in situ* hybridisation, Zhao et al. (2000) showed that in A3 adenosin receptor (A3AR) knock-out mice tissue, A3 mRNA was undetectable; both α - and β -sarcoglycan mRNAs were undetectable in the α -sarcoglycan and the β -sarcoglycan knock-out mice (Duclos et al., 1998; Araishi et al., 1999). In a few instances, the genetic manipulation results in a marked reduction in the level of the mutated mRNA; this is the case for the *Eya1* knock-out mice which show a reduction of at least 50% of normal levels of the *Eya1* mRNA (Johnson et al., 1999).

More relevant to this thesis is the observation that only drastically reduced levels of dystrophin mRNA are present in *mdx* and *mdx*^{3CV} mice tissues - both mice carry nonsense mutations. Dystrophin transcripts were barely

detectable on Northern blots of RNAs prepared from dystrophin deficient tissues and RNase protection assays showed that *mdx* and *mdx*^{3CV} tissues contain <20% of the normal levels of dystrophin mRNA (Sincinski et al., 1989; Cox et al., 1993b).

What is the mechanism of this mRNA loss? Special attention has been paid to mutations that, as in the case of UKO^{ex6} mice, result in the introduction of a premature stop codon. There is now a considerable body of evidence from the study of nonsense mutations in numerous other genes to suggest that a prematurely terminated mRNA is rapidly degraded by the cellular mechanism of nonsense-mediated mRNA decay (NMD) (Frischmeyer et al., 1999). These include, the β -globin, fibrillin 1 and CFTR genes (Frischmeyer et al., 1999). It appears that splicing plays a crucial role in NMD and that the juxtaposition of an intron downstream to the premature termination codon triggers NMD (Neu-Yilik et al., 2001).

The NMD phenomenon is also important in human genetic diseases caused by nonsense mutations and underlies for example the mechanism which results in mutations at the 5' end of the β -globin gene giving low levels of the nonsense mRNA, no protein product and a recessive form of inheritance (haploinsufficiency) whereas mutations in the last exon giving normal levels of a nonsense transcript, an abnormal truncated β -globin chain and a dominant-negative mode of inheritance (Thein et al., 1990).

NMD of mRNA is likely to be the mechanism active in UKO^{ex6} mice. Deconinck et al. (1997a) reported that the mutation in the UKO^{ex6} utrophin gene resulted in differential splicing of mRNA and skipping of the targeted exon in the utrophin mRNA with the introduction of a premature stop codon in the

immediately downstream exon and the disruption of the open reading frame. As part of the present study, the skipping of exon 6 in mRNAs transcribed in all UKO^{ex6} tissues was confirmed (Fig 5.10, 5. 11).

Thus, we can predict that the NMD process is initiated by the nonsense mutation in exon 7 and the proximity of intron 7 (71bp downstream of the premature stop codon) and that UKO^{ex6} mice will show only low levels or no mutated mRNA (no truncated protein). There is now good evidence that no truncated protein is synthesised (Deconinck et al., 1997a, chapter 4 Figs 4.4 to 4.12) and the proposition that mutated mRNA is rapidly degraded was confirmed by RNase protection assays carried out by our collaborators in Oxford who found that utrophin mRNA levels are substantially reduced in UKO^{ex6} tissues (Deconinck et al., 1997a; A. Weir, personal communication).

Taking into account these facts it was decided to conduct a series of mRNA *in situ* hybridisation experiments using mouse embryo sections with the view that any mRNAs that were abundant in both control and UKO^{ex6} tissues would correspond to short transcripts.

Before describing the experiments and their results it is relevant to review what was already known about the distribution of utrophin mRNA in normal foetal tissues. Only two detailed studies of utrophin expression during normal development have been reported. Schofield et al. (1993) examined mouse embryos by mRNA *in situ* hybridisation using a riboprobe derived from the 3' UTR of the utrophin gene. Numerous sites of utrophin expression were identified including neural tube, dorsal-root and trigeminal ganglia, vibrissae, digits and kidney (more details will be given later in section 6.2). However, because of the position of this probe it is impossible to tell whether the signal

was due to full-length utrophin mRNA or to short transcripts. Blake et al. (1995) carried-out a more focused study using a G-utrophin-specific probe and showed that expression of this transcript accounts for the hybridisation signal in a subset of the sites described by Schofield et al. (1993). In addition, Love et al. (1991) showed by Northern blotting that full-length utrophin mRNA is weakly expressed in human foetal skeletal muscle (24 weeks old foetus) and by slot blotting that mRNAs are abundant in several human foetal tissues such as heart, liver, placenta and gut. Since a 3' UTR probe was used in the slot blots it is not possible to tell whether those mRNAs correspond to the full-length or to short transcripts. More recently, RT-PCR analysis of RNAs from human and mouse foetal tissues showed that Up140 and Up71 appear to be ubiquitously expressed (Wilson et al., 1999); however, since these experiments were not quantitative, it is difficult to judge the relative levels of mRNA in each cell type. In the present study, short polypeptides of 109kDa and 120kDa were detected by Western blotting in foetal hands and kidney extracts respectively (Fig 4.4; Fig 4.11; Fig 4.12).

6.2 mRNA *in situ* hybridisation

It was hoped that mRNA *in situ* hybridisation might tell us something about the short utrophin isoforms - are they transcribed in foetal tissues in the absence of full-length utrophin?, is their expression altered in UKO^{ex6} embryos?, do they show tissue/stage specific expression?

It was also hoped that by using multiple probes it would be possible to determine which transcript is expressed in each tissue. Four probes were prepared: probe U340 (10279bp-10618bp) in the 3'UTR which would detect all

utrophin transcripts (full-length, Up140, Up120, G-utrophin, Up109, Up71), probe U56-59 (7581bp –7992bp) designed to detect all transcripts except for Up71, probe U31-34 (4255bp-4722bp) and probe U1-6 (7bp-422bp) to detect full-length mRNA only.

The positions of these probes relative to the transcription start sites of the known utrophin transcripts are shown in Fig 6.1. They were prepared by RT-PCR amplification of the corresponding utrophin sequences from C57Bl mRNAs. Primers that included deoxy-UMP residues at their 5' end were used in order to allow directional cloning into the multiple cloning site of the pAMP vector (Gibco.BRL, Fig 6.2). The RT-PCR primers (Table 2.5) were positioned as follows: U1-6 in exons 1 and 6; U31-34 in exons 31 and 34; U56-59 in exons 56 and 59 and U340 in exon 79 at the 3'UTR. In all cases, products of the correct size were amplified (Fig 6.2) and were ligated to pAMP vector; ligation reactions were used to transform competent DH5 α cells. The transformations were successful as judged by restriction digestion with *EcoRI* and *HindIII* of DNAs prepared from recombinants of each type of construct (data not shown). DNA from recombinants for each probe was sequenced using vector primers flanking the inserts to check their orientation and sequence. In all four cases the cloned utrophin sequences were correct. Antisense or sense radiolabelled riboprobes were synthesised by *in vitro* transcription from the T7 or SP6 RNA polymerase promoters present in the vector in the presence of ³⁵S-UTP (Fig 6.2).

Control (C57Bl) and UKO^{ex6} embryos were collected at different stages of development (8.5dpc-15.5 dpc), embedded in paraffin and sections prepared.

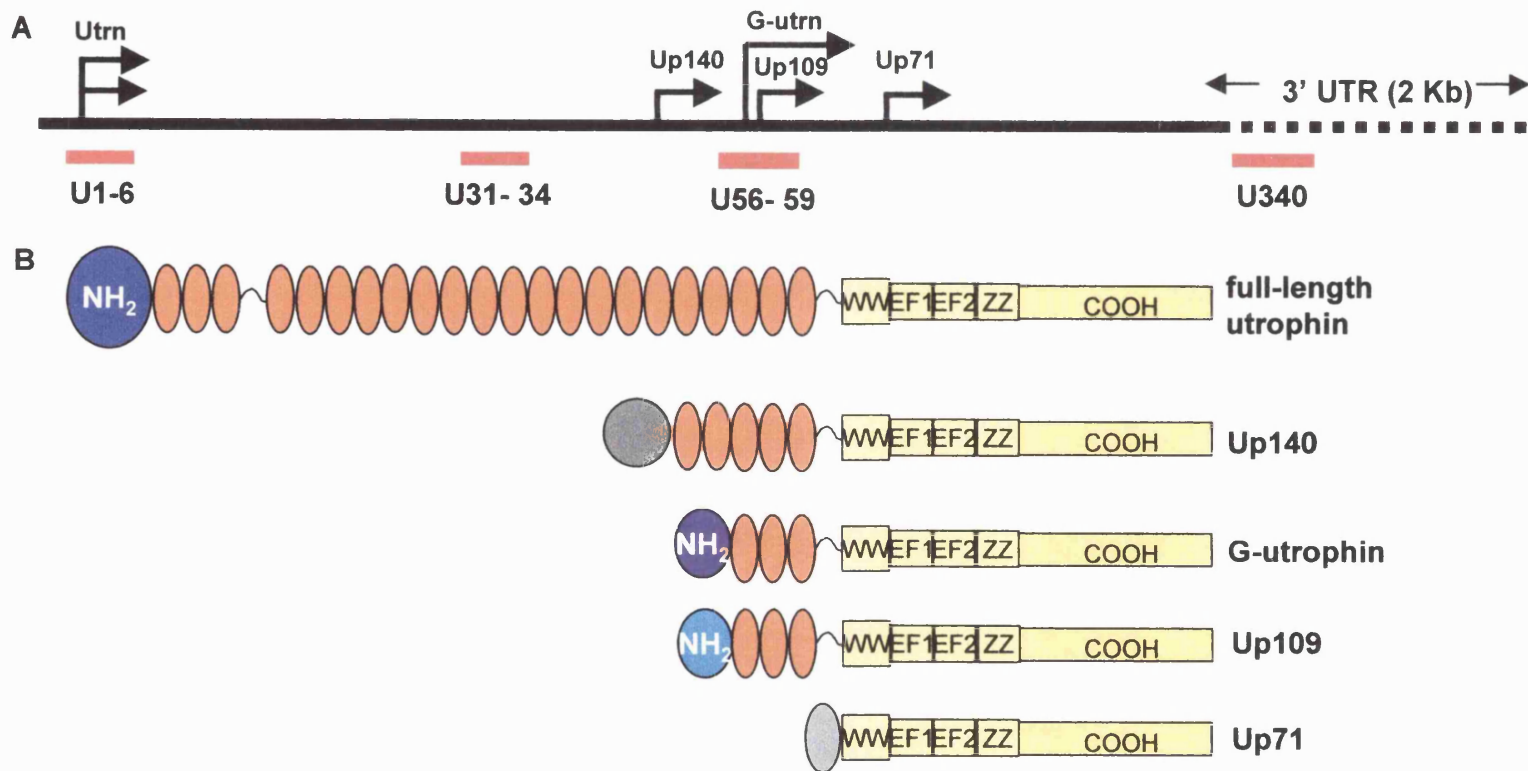


Fig 6.1 Diagram showing the positions of the riboprobes (red boxes) for mRNA *in situ* hybridisation relative to the transcription start site (arrows) for each transcript (A) and protein structure of each isoform (B) .

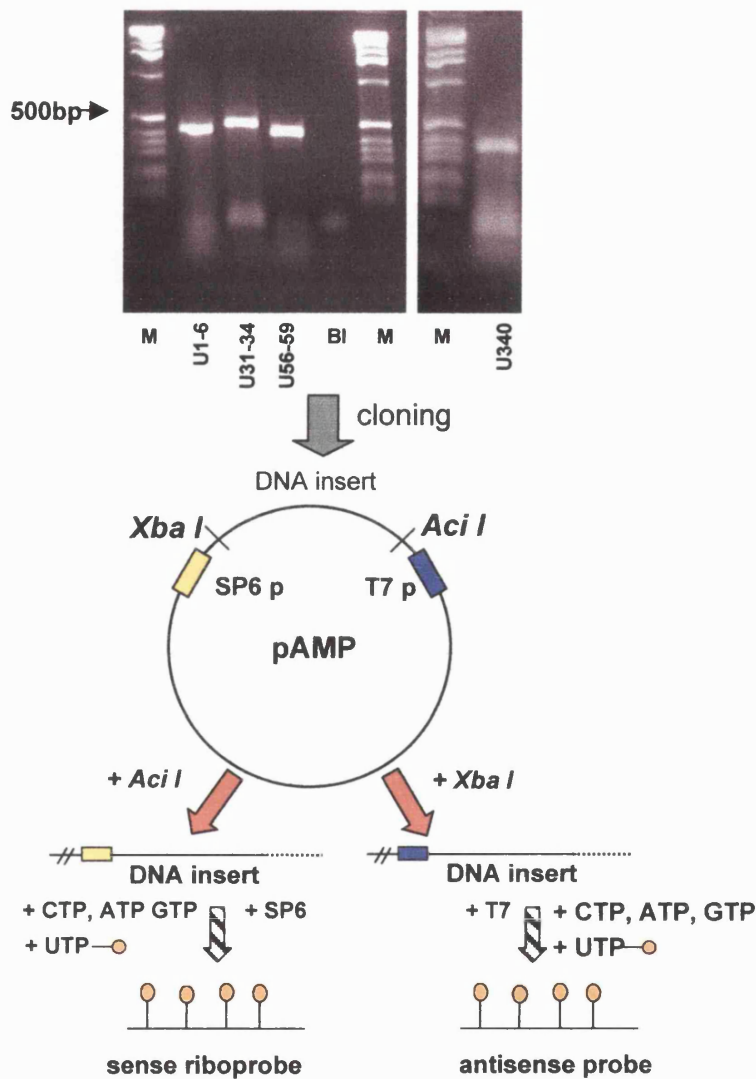


Fig 6.2 Production of riboprobes for mRNA *in situ* hybridisation. RT-PCR amplification of the utrophin sequences corresponding to U1-6 (415bp); U31-34 (467bp); U56-59 (411bp) and U340 (340bp). RT-PCR products were cloned into the pAMP vector that contains promoters (p) for SP6 and T7 RNA polymerase. Riboprobes were synthesised using plasmid linearised with either *AccI* or *XbaI* by *in vitro* transcription with SP6 (sense probes) or T7 (antisense probe) polymerase in the presence of dNTPs and ^{35}S -labelled UTP.

○ = ^{35}S ; M=DNA marker; BI= no DNA control



As a guide, Fig 6.3 illustrates diagrammatically some of the orientations of transverse, sagittal and frontal sections shown in the subsequent Figs.

The specificities of the utrophin antisense riboprobes were confirmed by the absence of signal using the corresponding sense probes as controls, examples are shown in Figs 6.5 and 6.12.

Two unexpected problems emerged which made the analysis of the mRNA *in situ* hybridisation experiments more complex than expected. Firstly, the exon 1-6 sequence appeared to be largely unsuccessful as a probe, at best it occasionally gave a very weak although specific signal. Nevertheless, this probe was routinely included in each series of experiments (see for example Fig 6.4). This meant that the U31-34 probe became the major source of information about the distribution of full-length utrophin mRNA in control tissues. Secondly, although full-length utrophin protein has been detected in some control embryonic tissues (Khurana et al., 1991; Clerk et al., 1993; Koga et al., 1993; Nguyen et al., 1995), there was little indication that this was matched by accumulation of mRNA at those sites; This appears to point to a rapid rate of mRNA turnover but relatively high protein stability.

Foetal stage 8.5 -10.5dpc

The early mouse embryo body is "S" shaped and during or shortly after the period between 8 and 8.5 dpc it rotates 180° along its longitudinal axis, a process known as "turning", and the embryo becomes "C" shaped (Rugh, 1968, p102).

The neural tube forms at the beginning of this stage by fusion of the neural folds on either side of the neural plate. The neural tube will become the brain and spinal cord and will give rise to the peripheral nervous system. The

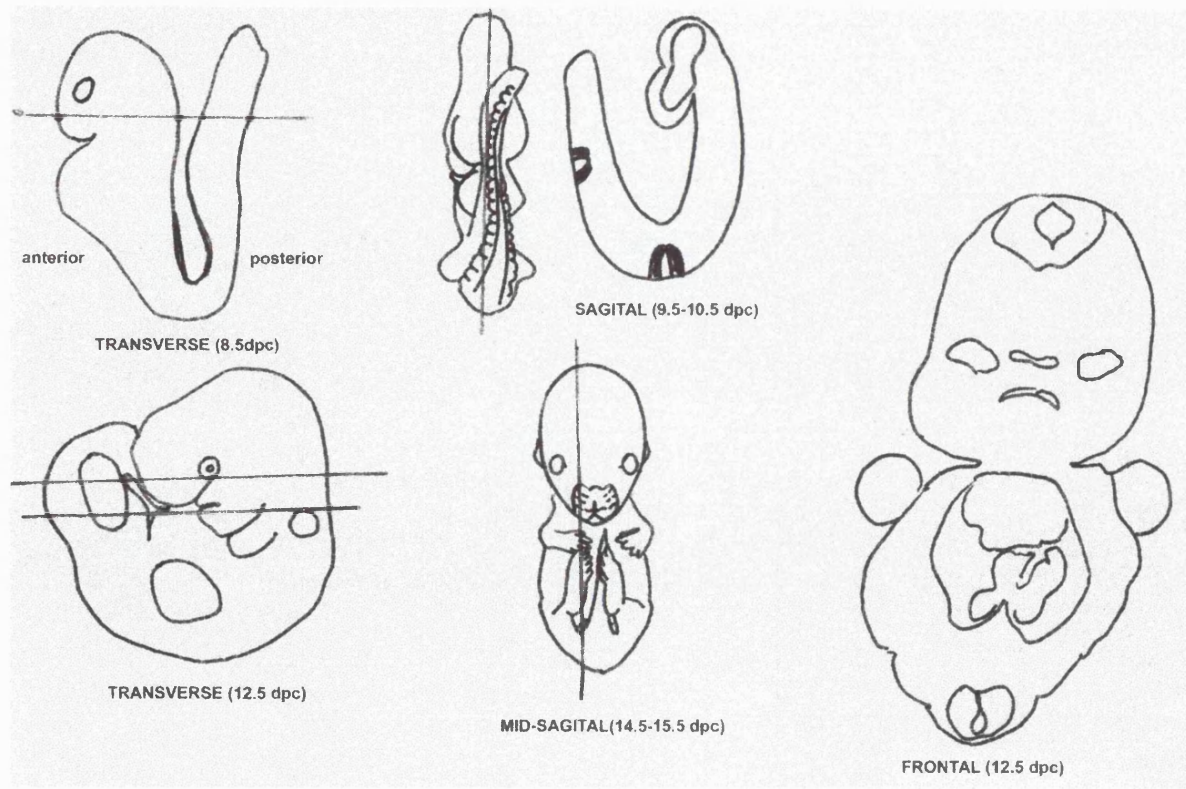


Fig 6.3 Examples of the orientation of sections, transverse, frontal and sagittal, shown in Figs 6.4 to 6.16.

neural tube closes by elevation of the sides of the plate, forming in the ventral surface, the neural groove. Closure occurs in a rostro-caudal fashion such that by 9.5 dpc the rostral extremity is closing while the caudal end is still open. The neural tube is almost completely closed along its entire length by 11 dpc (Rugh, 1968, p 97). Thus, the cephalic (anterior) region of the embryo is developmentally more advanced than the caudal (posterior) region.

Utrophin mRNA is first detected in the UKO^{ex6} embryo at 8.5 dpc and is distributed in the medial and lateral portions of the neural plate. As the neural tube begins to form, mRNA is confined to the most medial region of the neural groove. This observation is in agreement with that of Schofield et al. (1993) who also reported utrophin expression in the neural groove of 8.5dpc C57Bl embryos using a 3' UTR probe.

Both neural plate and groove mRNAs are detected with U340 probe (detects all utrophin mRNAs) (Fig 6.4). However, the neural plate mRNA is not detected with U56-59 probe indicating that this early mRNA is Up71 (Fig 6.4). In contrast, the neural groove mRNA is detected with U340 and U56-59 probes but was not detected with the 5' probes U1-6 or U31-34 (Fig 6.4) suggesting that the signal in the neural groove must correspond to a short utrophin mRNA; Up140, Up109, G-utrophin or a novel transcript. This transcript appears to replace Up71, which is developmentally downregulated as the neural tube forms, and goes on to be expressed throughout the neural tube at later stages. By 9.5 and 10.5dpc utrophin mRNA is abundant along the whole length of the spinal neural tube and is present in the ventricular floor-plate of the developing brain (Fig 6.5 and Fig 6.6); both U340 and U56-59 continue to give the same levels of signal.

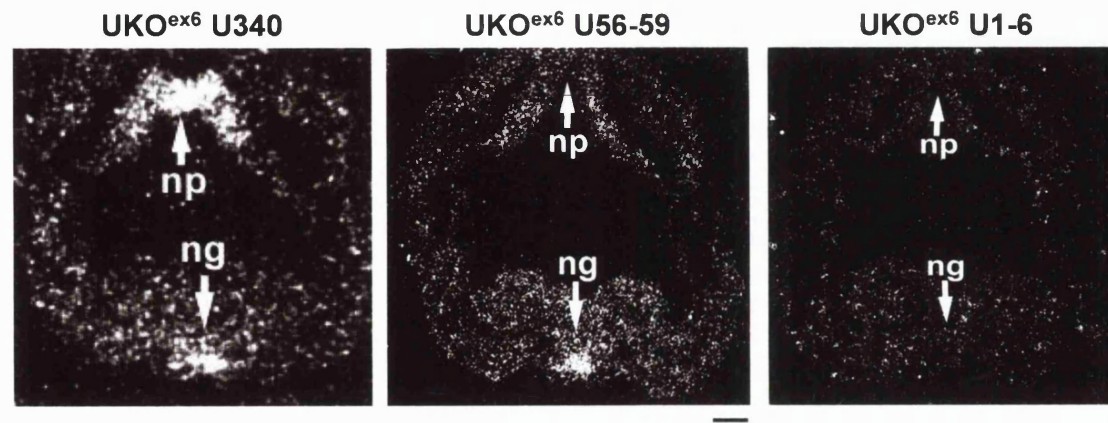


Fig 6.4 Dark-field micrographs of transverse sections through a 8.5 dpc UKO^{ex6} embryo probed with U340, U56-59 or U1-6. The anterior end of the embryo is at the bottom of the Fig and the posterior at the top. ng=neural-groove; np=neural plate. Bar=35 μ m.

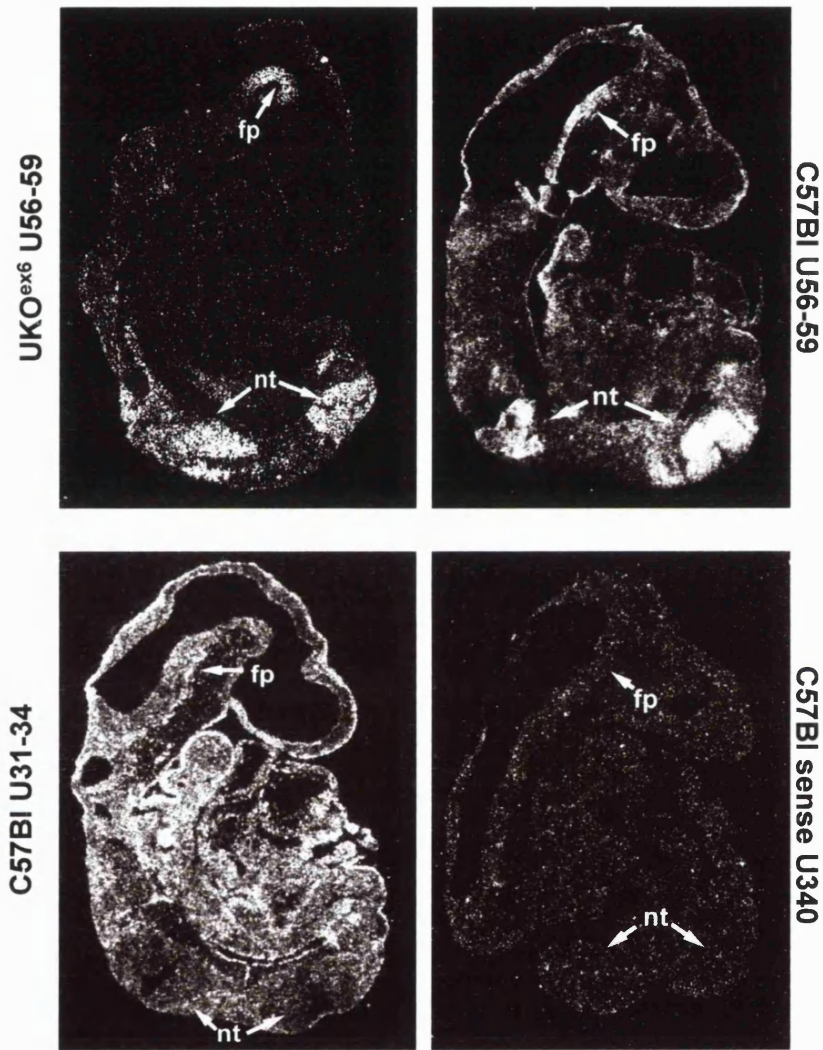


Fig 6.5 Dark-field micrographs of sagittal sections trough 9.5dpc UKO^{ex6} and 10.5dpc C57BI embryos probed with U56-59 or U31-34 probes. A section hybridised to the sense U340 probe is also shown. Expression is indicated in neural tube (nt) and floor-plate (fp). Bar=200 μ m.

At this stage of development, hybridisation of UKO^{ex6} sections with U31-34 probe gave no signal and was comparable to the negative control (Fig 6.5). However, hybridisation of control mouse sections with the same probe gave a low level signal all over the embryo (Fig 6.5); a feature previously noted in control mice by Schofield et al. (1993) using a 3' UTR probe. The complete absence of hybridisation in UKO^{ex6} mice suggests that this signal could represent low level ubiquitous expression of full-length utrophin mRNA in control tissues. Significantly, U31-34 probe did not detect the mRNA present in the neural tube (Fig 6.5, Fig 6.6) thereby confirming that the signal in neural tube corresponds to a short transcript.

Expression of utrophin is observed in control and UKO^{ex6} embryos in the dorsal-root ganglia (drg) soon after they start to form by condensation of neural crest cells at 10 dpc (Kaufman, 1992, p 92) and persists throughout development. Utrophin signal in dorsal-root ganglia was detected with U56-59 and U340 probes but not with U31-34 probe (Fig 6.6). This suggests that a short utrophin isoform different from Up71 is expressed in dorsal-root ganglia. This is in line with previous findings; Blake et al. (1995) demonstrated that G-utrophin is the most abundant transcript in dorsal-root ganglia using a transcript specific probe.

Schofield et al. (1993) reported expression of utrophin transcripts in the developing hand in control embryos at 14.5 dpc but not in the developing bud at earlier stages. The limb buds develop from a group of cells known as the "limb field" which derive from the somites and lateral plate mesoderm. In the present study, utrophin transcripts were detected in the developing forelimb shortly after the bud first becomes evident at approximately 9 dpc (Kaufman, 1992, p 75).

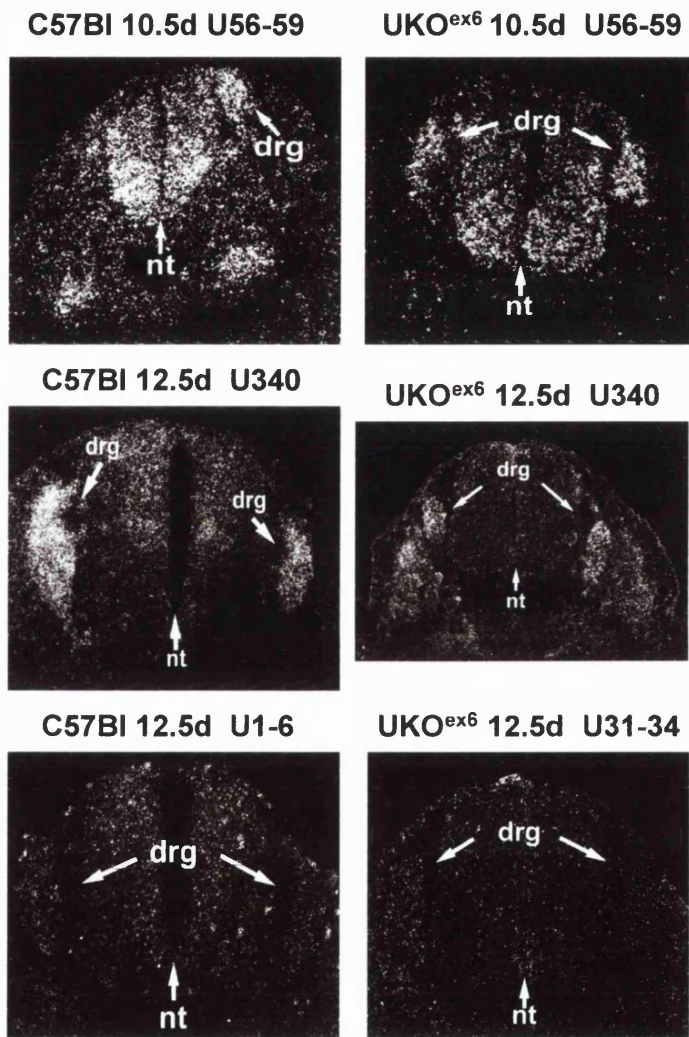


Fig 6.6 Dark-field micrographs of frontal sections of 10.5 and 12.5 dpc C57Bl and UKO^{ex6} embryos. U56-59 and U340 probes detect signal in the neural tube (nt) and developing dorsal-root ganglia (drg) in the C57Bl and UKO^{ex6} embryo . U31-34 and U1-6 probes do not detect signal in either of these sites. Bar=100 μ m.

Utrophin mRNA was detected in the forelimb with U340 (Fig 6.7) and U56-59 probes (data not shown) with equal intensity in both control and UKO^{ex6} embryos (Figs 6.7 and 6.12). At this stage, there was no specific regional distribution of expression in the limb bud.

The heart is the first organ to differentiate and function and is the most prominent organ in the 9.5-10.5 dpc embryo. However, utrophin mRNAs were not detected in the developing heart at this stage apart from the low level and dispersed signal seen with U31-34 probe in control embryos (Fig 6.5).

Foetal stage 12.5 dpc During this stage of development, the back of the embryo straightens and its overall shape begins to adopt more “adult-like” features (Rugh, 1968, p 183). The kidney is now clearly visible, although it is still largely tubular with no signs of glomeruli, and the gonads are still undifferentiated (Kaufman, 1992, p 145). No utrophin mRNA was seen in either kidney or testis at this stage of their differentiation.

By 12.5 dpc, expression in the spinal neural tube has become restricted to the most caudal end (Fig 6.6) as described previously by Schofield et al. (1993) in control mice. This is illustrated in Fig 6.6; hybridisation signal can be seen in the more caudal (neural tube still slightly open) control embryo section but no signal can be seen in the slightly more anterior UKO^{ex6} section of the same age embryo.

At this stage, the differentiation of the forelimb is well underway and the hand plate is no longer paddle-shaped but shows early signs of the developing digits (Kaufman, 1992, p 145). Utrophin expression is now localised to the distal region of the developing forelimb in a region that seems to correspond to the

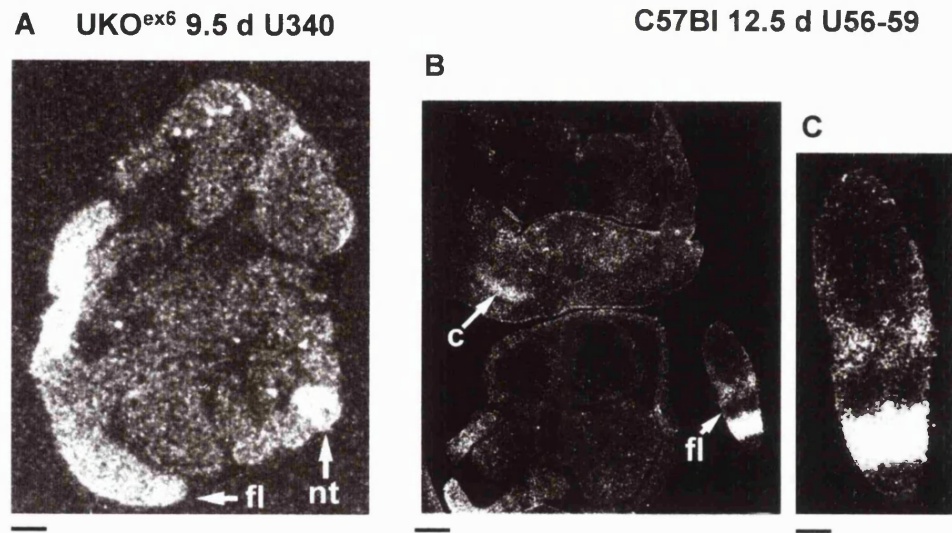


Fig 6.7 Utrophin signal in the developing forelimb bud (fl). A, sagittal section of a 9.5 dpc UKO^{ex6} embryo hybridised with U340. B, frontal section of a 12.5 dpc C57Bl embryo hybridised with U56-59. C, close-up of B showing the area of positive hybridisation signal in the forelimb bud. Bar in A=200 μ m; B=285 μ m C=120 μ m. nt=neural tube; c= cartilage primordia.

zone of polarising activity, ZPA (Fig 6.7). This is a group of specialised mesodermal cells found at the posterior margin of the limb bud that are responsible for establishing the anteroposterior axis of the limb (Riddle et al., 1993). At 10.5 and 12.5 dpc the mRNA levels in the limb bud were identical in control and UKO^{ex6} embryos and showed the same pattern of hybridisation; positive with U56-59 and U340 probes and negative with U31-34 probe. These results suggest that a short utrophin isoform transcribed from a position upstream of exon 56 is responsible for the signal seen in the ZPA.

By 12.5 dpc, the highest levels of utrophin expression are found in the trigeminal (Fig 6.8) and dorsal-root (Fig 6.9) ganglia and persist at high levels in later stages. The pattern of probe hybridisation is identical to that seen at 10.5 dpc. It is most likely that this signal can be ascribed to G-utrophin whose transcription initiates in intron 55 (in agreement with the study of Blake et al., 1995 in control mice).

The pattern of utrophin expression has expanded such that hybridisation signals are also now apparent in other parts of the anterior region of the embryo, particularly in Rathke's pocket (Fig 6.8), which will eventually become the anterior pituitary gland, cartilage of the nose and in the tongue (Fig 6.10). Utrophin mRNA in Rathke's pocket and nose was detected in both control and UKO^{ex6} embryos with U56-59 and U340 probes but not with U31-34 probe and thus cannot be attributed to full-length utrophin. In contrast, in the tongue, hybridisation signal was only detected in control embryos (Fig 6.10) and not in UKO^{ex6}; this points straight to the expression of full-length utrophin in tongue striated muscle. There is some evidence in the literature for full-length utrophin

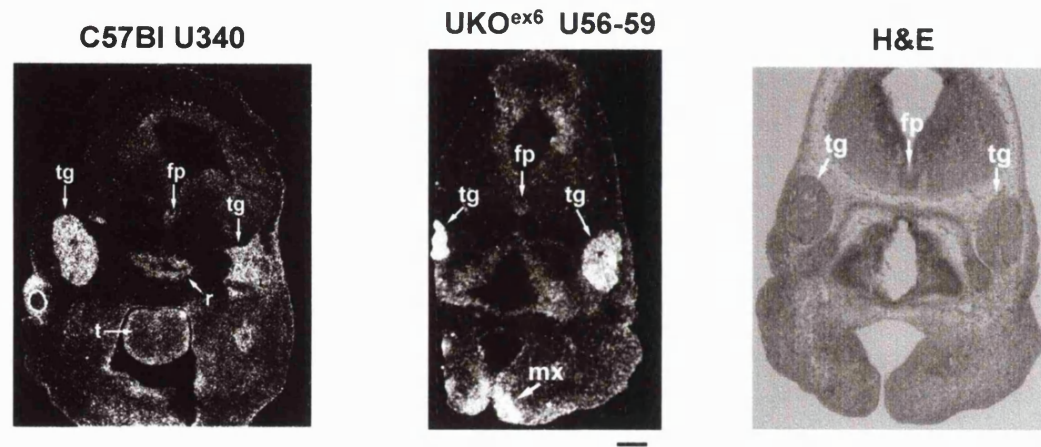
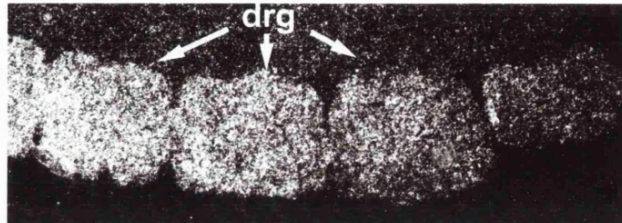
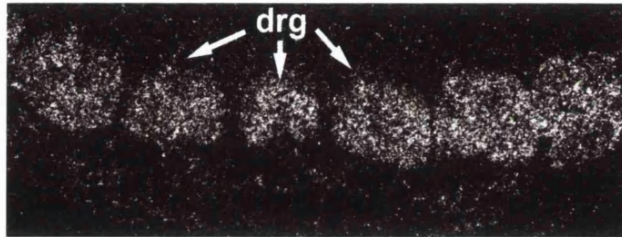


Fig 6.8 Dark-field micrographs of frontal sections of 12.5 dpc control and UKO^{ex6} embryos probed with the U56-59 and U340 probes. A bright-field photograph of an adjacent section stained with haematoxylin and eosin (H&E) is also shown. The signal in the trigeminal ganglia (tg) is indicated by arrows. U56-59 also detects utrophin signal in Rathke's pocket (r), floor-plate (fp) and maxilla (mx). t= tongue. Bar=350 μ m.

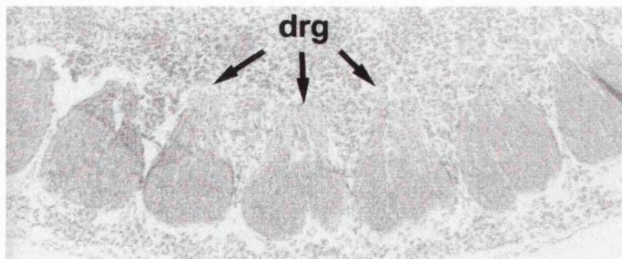
C57Bl 14.5d U340



UKO^{ex6} 12.5d 56-59



H&E



6.9 Sagittal sections through the lumbar region of a 14.5 dpc C57Bl embryo probed with U340 and a 12.5 dpc UKO^{ex6} embryo probed with U56-59. Both probes detect high levels of signal in the dorsal-root ganglia (drg) in C57Bl and UKO^{ex6} embryos. Bright-field micrograph of an adjacent section stained with H&E. Bar=45 μ m.

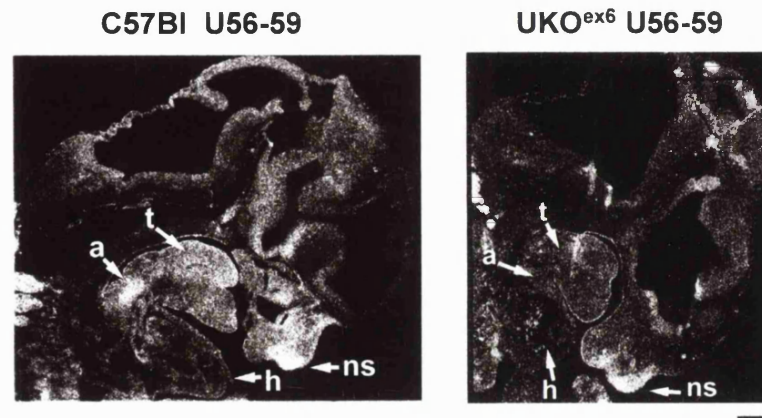


Fig 6.10 Sagittal sections through the head region of 12.5 dpc C57BI and UKO^{ex6} embryos probed with U56-59 probe showing signal in the tip of the nose (ns) in both embryos. There is signal in the C57BI embryo tongue (t) but not in the UKO^{ex6} embryo. There is also signal in the aortic region (a) of the heart (h) in the C57BI embryo which is absent in the UKO^{ex6} embryo. Bar=340 μ m

in tongue from the work of Lin S. et al. (1999) who detected protein in the tongue of rat embryos using an NH₂-terminal anti-utrophin antibody.

At 12.5 dpc signal was detected in a group of cells in the outflow region of the heart in control embryos but not in UKO^{ex6} embryos (Fig 6.10); this mRNA thus also seems likely to correspond to full-length utrophin mRNA. Utrophin mRNA in this position was not detected at earlier (10.5dpc) or later (14.5 dpc) stages. Schofield et al. (1993) reported the same pattern of expression of utrophin mRNA in these cells in the same region in 11.5dpc control embryos using the 3' UTR probe. Thus, full-length utrophin appears to be transiently expressed in the outflow region of the heart between 11.5 and 12.5 days.

Foetal stage 14.5 –15.5 dpc

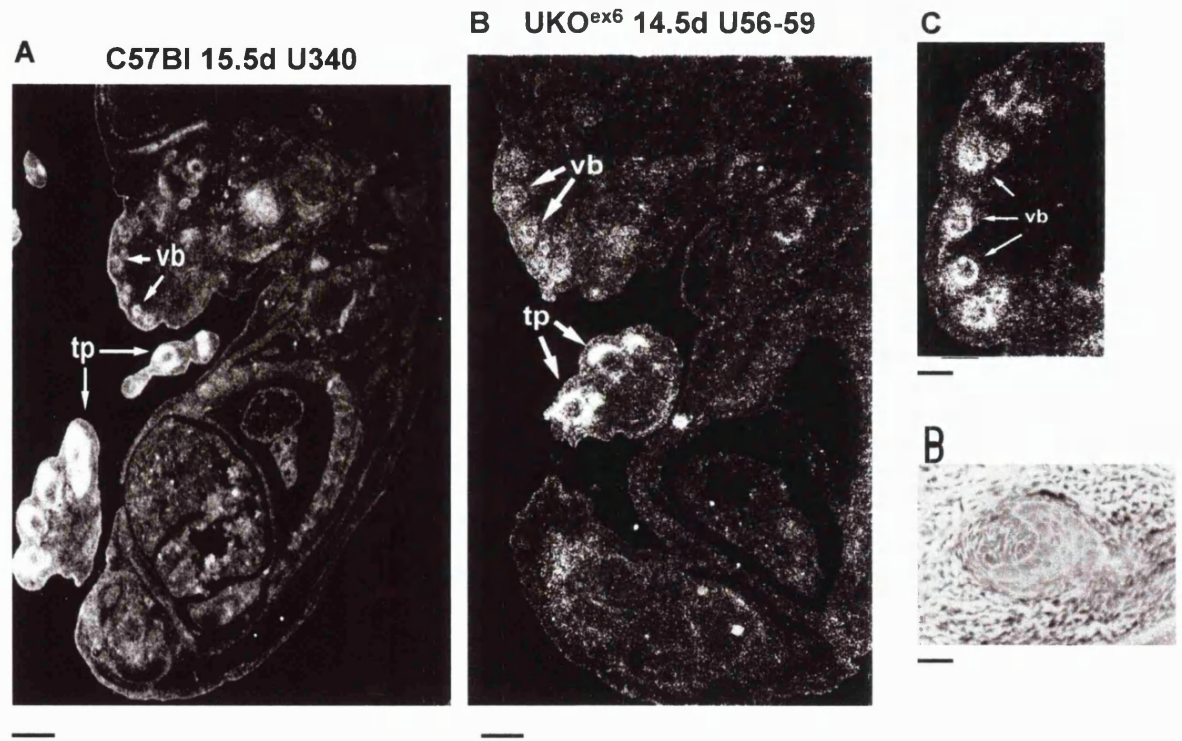
In the 14.5-15.5 dpc embryo many of the “adult” structures are in place and there is a noticeably “rodent-like” face (Rugh, 1968, p 195). Between 12.5 and 14.5 dpc the hands and feet have undergone a dramatic change in morphology, the digits are separated and in the limbs the cartilaginous primordia of the long bones are present (Kaufman, 1992, p 211). The cranial ganglia and nerves are prominent and the choroid plexii, which were visible from 13 dpc, have increased considerably in volume. The inner ear components are well differentiated in the 14.5 dpc embryo (Kaufman, 1992, p 215). The lumen of the stomach is very large and occupies, together with the liver, most of the peritoneal cavity. The pyloric sphincter at the gastro-duodenal junction is particularly clear at this stage. The lung and diaphragm are completely differentiated (Kaufman, 1992, p 214).

Primitive glomeruli are seen in the kidney at the beginning of this stage and the kidney cortex and medulla are well defined by 15.5 dpc. In the testis,

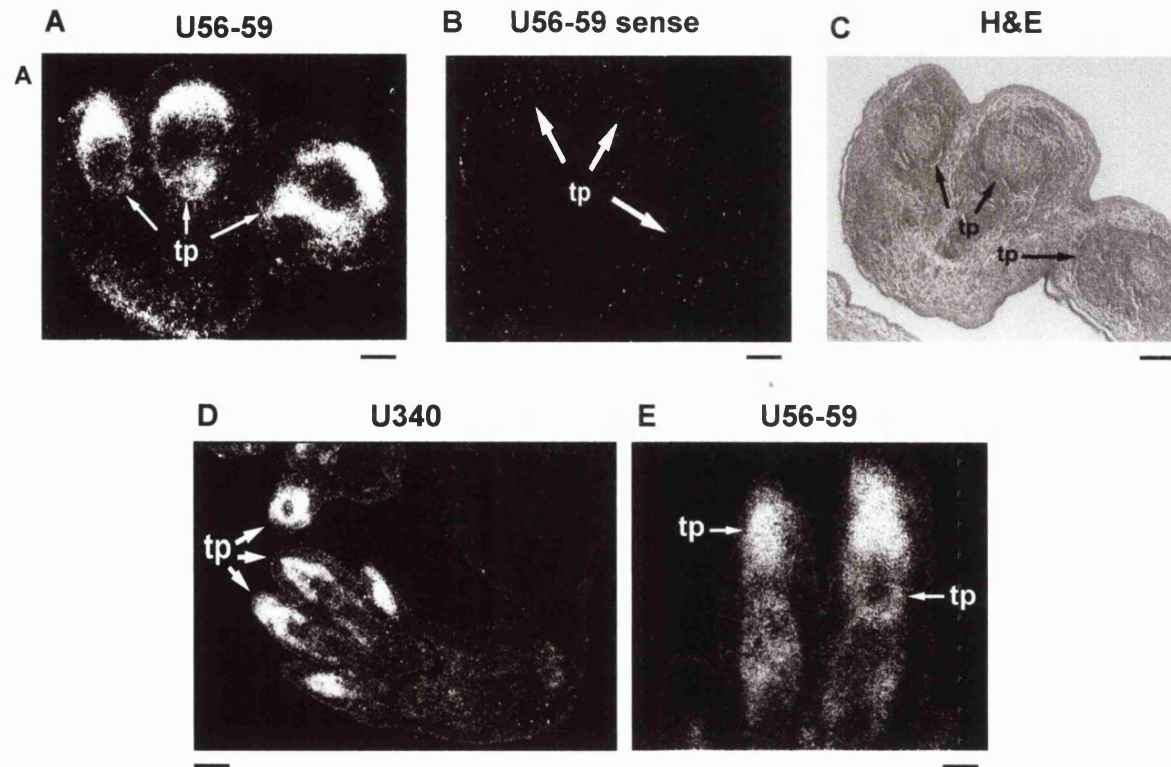
primitive seminiferous tubules appear in the 14.5 dpc embryo in the form of testicular cords; 24hrs later, differentiation is well advanced and the testis has increased in size compared to the ovary (Kaufman, 1992, p 216). In the 14.5-15.5 dpc embryo, centres of ossification appear, for instance, in the pectoral and pelvic girdles and ribs (Kaufman, 1992, p 217).

At 14.5-15.5 dpc utrophin transcripts become even more widely expressed, for example in the developing follicles of the vibrissae (Fig 6.11) which are tactile hairs, whiskers, in the adult mouse. Utrophin here is detected with both U56-59 and U340 probes with equal intensity in both UKO^{ex6} and C57Bl embryos but not with U31-34 probe. Expression in the vibrissae was also detected in control mice by Schofield et al. (1993) with a 3'UTR probe but not by Blake et al. (1995) using a G-utrophin specific probe. Thus G-utrophin and Up71 can be excluded as the source of signal in the vibrissae.

Utrophin mRNA accumulation persists in both UKO^{ex6} and control limb buds at identical levels. At this stage, the signal is much stronger than at 12.5dpc which suggests that expression in these cells is increasing. mRNA is confined now to the digits of developing hands and feet and gives the same pattern of hybridisation with the various probes as seen at earlier stages of development (Fig 6.11 and Fig 6.12). When Blake and colleagues (1995) examined control mice at this stage using the G-utrophin specific probe they did not observe hybridisation to the digits. The signal in the digits seems to localise to the mesenchyme cells differentiating into tendon dorsally and ventrally to the forming phalangeal bones. In these cells it appears to be a short utrophin transcript different from G-utrophin and Up71. Expression of Up109 mRNA in the tendon primordia would be in line with results from the Western blots



6.11 Dark-field micrographs of mid-sagittal sections through 15.5 dpc C57BI (A) and 14.5 dpc UKO^{ex6} (B) embryos hybridised with U340 or U56-59 probes. The signal in the tendon primordia in the digits (tp) and vibrissae (vb) is indicated by arrows. C shows higher magnification of the vibrissae. D, bright-field micrograph of a vibrissae follicle stained with H&E. Bar (A,B)=500µm; Bar (C)=200µm; Bar (D)=100µm.



6.12 Utrophin expression in the tendon primordia (tp) of the developing digits of the hand (A,B) and foot (D,E) of UKO^{ex6} 14.5 dpc embryos. Signal in the digits is detected with U56-59 (A,E) and U340 (D) probes but is not detected with a sense probe (B). C = bright-field micrograph of an adjacent section stained with H&E. Bar (A,B,C,E)=250 μ m; Bar (D)=500 μ m.

(chapter 4 Fig 4.11 and 4.12) in which Up109 polypeptide was detected in 15.5 and 16.5dpc hands extracts. Full-length utrophin protein was also detected in 16.5 control hands extracts (Fig 4.11), however, full-length utrophin mRNA was not detected in control embryos with U31-34 probe and there were no significant differences in the intensities of signal between control and UKO^{ex6} embryos. This suggests that in foetal hands, as in skeletal muscle, levels of full-length utrophin mRNA are low or that the mRNA is unstable or confined within the cells and undetectable by mRNA *in situ* hybridisation with the weak 5' probes.

Expression of utrophin mRNA is visible at this stage of development in the semicircular canals of the inner ear in both control and UKO^{ex6} sections (Fig 6.13). This site of expression has not been noted previously. This mRNA was detected with the U340 and U56-59 probes (Fig 6.13) but not with the 5' probes (data not shown). G-utrophin expression in the inner ear was not detected by Blake et. al (1995) but it is not clear that the appropriate sections were analysed. Thus, the signal in the semicircular canals could correspond to G-utrophin, Up140, Up109 or to a novel short transcript.

At this stage, utrophin mRNA accumulates in the kidney and testis as reported previously for control mice by Schofield et al. (1993). Both U56-59 and U340 probes detected this signal (Fig 6.14) and it seems likely that a short transcript is abundant in the developing kidney and testis. G-utrophin can be excluded since the G-utrophin specific probe did not detect mRNA in either of these two tissues (Blake et al., 1995). The short transcript expressed in kidney could correspond to Up120 which was detected in foetal kidney extracts by Western blotting (chapter 4 Fig 4.4). The position of the transcription initiation

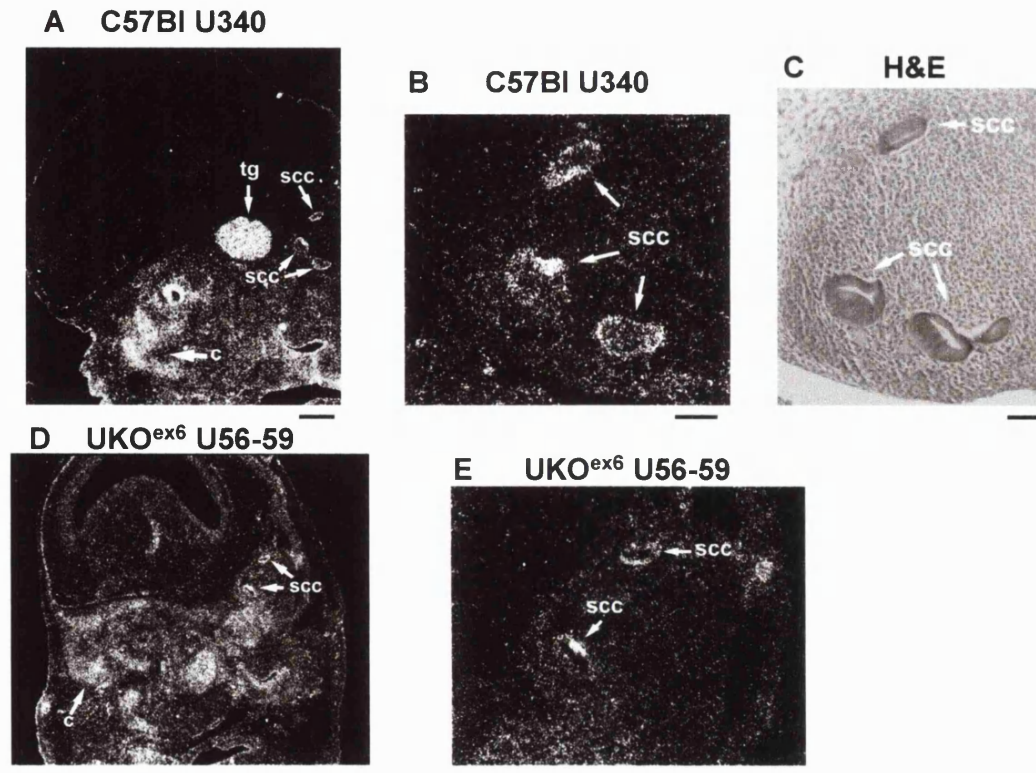


Fig 6.13 Utrophin expression in the semicircular canals (scc) of the inner ear in 15.5 dpc C57BI and 14.5 dpc UKO^{ex6} embryos. Sections were hybridised to U340 or U56-59 probes. B and E show the semicircular canals at higher magnification. C, Bright-field photograph of the scc stained with H&E. tg=trigeminal ganglia. Utrophin signal in the cartilage primordia (c) of the nasal septum is also shown. Bar (A,D) = 500µm; Bar (B,C,E) =250 µm.

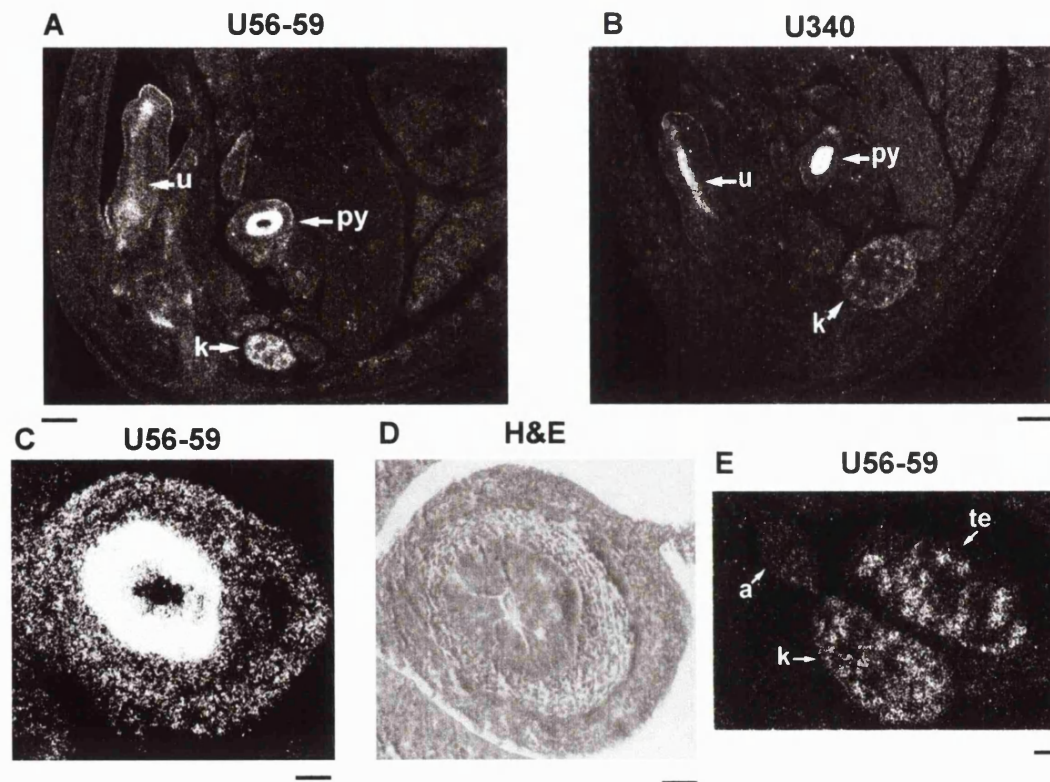


Fig 6.14 Dark-field micrographs of sections through the abdomen of 14.5 dpc UKO^{ex6} embryos showing utrophin signal in the pyloric sphincter (py), kidney (k), testis (te) and urethra (u). Signal is detected at these sites with U56-59 (A,C, E) and U340 probes (B). C, detail of the signal in the pyloric sphincter and D, bright-field micrograph of the pyloric sphincter stained with H&E. E, signal in the kidney (k) and testis (te) and weak signal in the adrenal gland (a). Bar (A,B) = 200 μm; Bar (C,D) = 40 μm; Bar (E) = 130 μm.

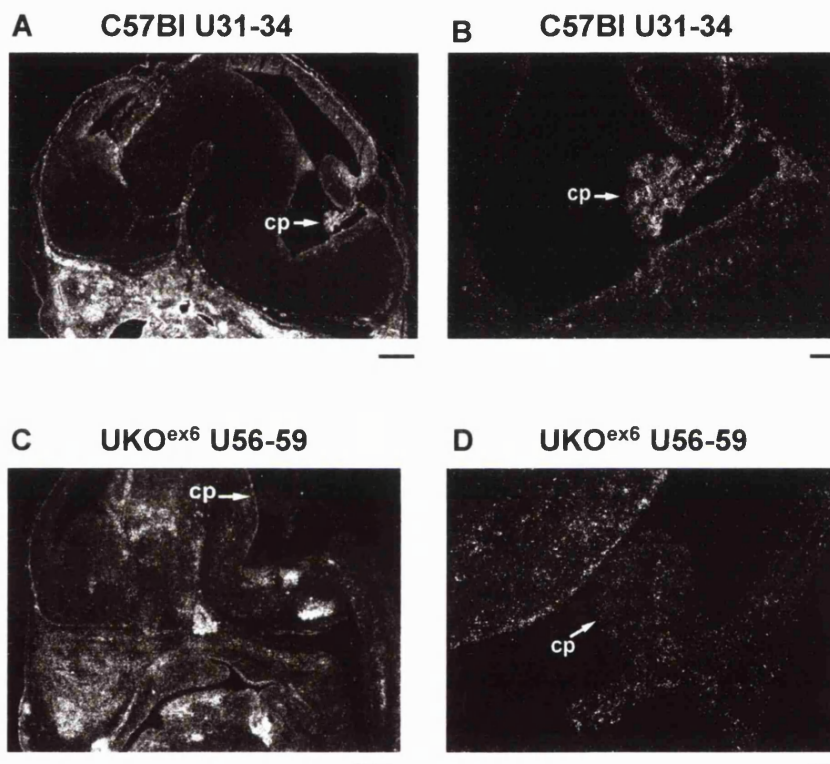


Fig 6.15 Sagittal sections through the head of 14.5 dpc C57Bl and UKO^{ex6} embryos probed with U31-34 or U56-59 probes. The choroid plexus (cp) in the brain is indicated by arrows. Bar (A,C)=300 μ m. Bar (B,D) =75 μ m.

There was evidence for expression of utrophin mRNAs in facial cartilages. The individual cartilages were difficult to recognise and are only specifically labelled when identified with some confidence, otherwise, they are simply indicated with a “c” where the identification was uncertain. It was also difficult to achieve identical sections in the UKO^{ex6} and control mice and cross-comparison for individual cartilages was restricted. Overall, it appears that both a short transcript and full-length utrophin mRNA are expressed in facial cartilages since both U31-34 and the 3' probes detected hybridisation signal in control mice but signal with the U31-34 probe was absent in UKO^{ex6} (Fig 6.16).

In passing it should be noted that utrophin mRNAs were also detected in the thyroid gland and in tooth primordia in control and UKO^{ex6} embryos (Fig 6.16); utrophin expression in these sites has been previously reported in control embryos by Schofield et al. (1993).

6.3 Summary of results

Table 6.1 summarises the major findings from the mRNA *in situ* hybridisation experiments. Data regarding G-utrophin expression in control mouse embryos (Blake et al., 1995) as well as data from the work of Schofield et al. (1993) are also included. Using information about the relative position of each riboprobe (Fig 6.1) the data are combined to determine which of the known utrophin isoforms is likely to be expressed in each tissue. In compiling this table it has been assumed that no other as yet unidentified transcript exist and may require modification if further short isoforms come to light.

In summary, it appears that short utrophin mRNAs are transcribed and are abundant in a variety of embryonic/foetal tissues. In contrast, full-length

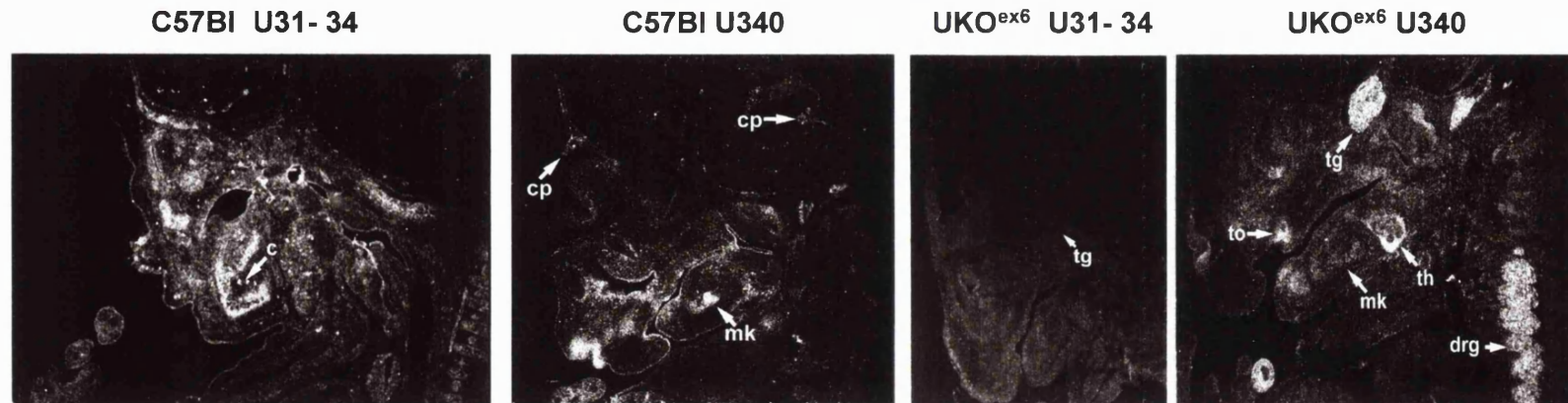


Fig 6.16 Sagittal sections through the head of 14.5 dpc C57Bl and UKO^{ex6} embryos hybridised with U31-34 and U340 probes showing signal in facial cartilages, including Meckel's cartilage (mk), tooth primordia (to) and thyroid gland (th). The trigeminal (tg) and dorsal-root ganglia (drg) in C are also indicated. Bar=300 μ m.

TISSUE	MICE	U31-34	U56-59	U340	G-utr ⁿ ^a	3' UTR ^b	TRANSCRIPT
neural groove	control	nt	nt	nt	-	++	Up140/Up109
	UKO ^{ex6}	-	++	++			
neural plate	control	nt	nt	nt	-	nt	Up71
	UKO ^{ex6}	-	-	+++			
neural tube	control	-	+++	+++	-	+++	Up140/Up109
	UKO ^{ex6}	-	+++	+++			
sensory ganglia	control	-	++++	++++	++++	++++	G-utrophin
	UKO ^{ex6}	-	++++	++++			
tongue	control	nt	+	+	-	+	FI-utr ⁿ
	UKO ^{ex6}	-	-	-			
heart outflow tract	control	nt	+	+	-	+	FI-utr ⁿ
	UKO ^{ex6}	-	-	-			
tendon primordia	control	-	+++	++++	-	++++	Up109
	UKO ^{ex6}	-	++++	++++			
vibrissae	control	-	+++	+++	-	+++	Up140/Up109
	UKO ^{ex6}	-	+++	+++			
semicircular canals	control	-	+++	+++	-	nt	Up140/Up109
	UKO ^{ex6}	-	+++	+++			
kidney	control	-	++	++	-	++	Up120
	UKO ^{ex6}	-	++	++			
testis	control	-	++	++	-	++	Up140/Up109
	UKO ^{ex6}	-	++	++			
pyloric sphincter	control	nt	nt	nt	nt	nt	Up140/Up109
	UKO ^{ex6}	-	++++	++++			
urethra	control	nt	nt	nt	nt	nt	Up140/Up109
	UKO ^{ex6}	-	+++	+++			
choroid plexii	control	+	+	+	-	+	FI-utr ⁿ
	UKO ^{ex6}	-	-	-			
facial cartilages	control	+	++	++	-	nt	FI-utr ⁿ + Up140
	UKO ^{ex6}	-	++	++			

Table 6 .1 Summary of mRNA *in situ* hybridisation experiments. The relative intensities of signals detected with each riboprobe are indicated. - = no signal; +=low; ++++=very strong; nt= the appropriate sections were not tested.

a- taken from Schofield et al. (1993) or b- taken from Blake et al. (1995). Both studies were done on control mice only.

utrophin mRNA is abundant only in the striated muscle of the tongue, the outflow region of the heart and choroid plexii and in some facial cartilage primordia. It seems likely that full-length utrophin mRNA is present at low levels in many other tissues, apparent as high level background signal with the U31-34 probe. Data from Western blots and immuno-histochemistry shows that full-length utrophin is expressed in the developing hands, kidney and skeletal muscle in control embryos but too diffuse within the cell or at too low levels to be detected by mRNA *in situ* hybridisation.

There was no evidence of large scale up- or down-regulation of short transcripts in UKO^{ex6} tissues in the absence of full-length utrophin.

The different short transcripts show temporal and tissue specific patterns of expression. Up71 is expressed during early neurulation and then is replaced by another short transcript, presumed to be Up140, which continues to be expressed in the neural tube at later stages. In dorsal-root and trigeminal ganglia G-utrophin is the major utrophin transcript. In the developing digits a novel transcript, Up109, is likely to represent the major utrophin mRNA while Up120 may be expressed in kidney. In vibrissae, semicircular canals, urethra, testis and pyloric sphincter Up140 appears to be the major transcript although Up109 could also be expressed in all these tissues.

Discussion

6.4 General comments

The mRNA *in situ* hybridisation experiments using UKO^{ex6} mouse sections presented in this section have shown that different utrophin transcripts have tissue and temporal specific patterns of expression during mouse embryogenesis. They suggest that short transcripts are the predominant mRNAs in most foetal tissues although accumulation of full-length utrophin mRNA has been demonstrated in a few control tissues.

What can be said regarding individual utrophin transcripts? It is striking that while there is overwhelming evidence from protein studies for expression of full-length utrophin in foetal skeletal muscle it is difficult to demonstrate this by mRNA *in situ* hybridisation. The contrast between the detection of protein and mRNA in tissue sections may result from the relatively concentrated localisation of stable protein at the NMJ and sarcolemma; whereas the mRNA may be more diffusely localised within the muscle cell and less stable. Where full-length utrophin mRNA is detected by mRNA *in situ* hybridisation it is presumably relatively very abundant, this will also be true for short utrophin isoforms. The full-length utrophin mRNA is abundant in the choroid plexii, the striated muscle of the tongue, facial cartilages and transiently in the outflow tract of the heart. Full-length utrophin is also widely present at lower levels in most cell types in the earlier stages of development.

Up71 appears to be the first utrophin transcript expressed during development and accumulates in the neural plate; this mRNA is not at detectable levels in any particular tissue later in development. Previous

published RT-PCR studies demonstrated low levels of Up71 mRNA in foetal testis, lung, muscle and kidney (Wilson et al., 1999). This discrepancy can be explained by the significantly higher sensitivity of RT-PCR technique compared to mRNA *in situ* hybridisation. G-utrophin transcription, as previously reported, is confined to sensory ganglia (Blake et al. (1995). Short transcripts initiated from a position upstream of exon 56 and downstream of exon 34 (possibly Up140, Up109 and Up120) are abundantly expressed in a variety of tissues such as the neural tube, pyloric sphincter and facial cartilages. The wide tissue distribution of Up140 mRNA during development is in line with previous RT-PCR studies (Wilson et al., 1999). On the basis of the Western blotting results and RT-PCR, Up109 is likely to be the short mRNA expressed in the tendon primordia and together with Up140 are the best candidates for expression in the remaining tissues, apart from kidney where Up120 seems to be the most likely transcript as judged from Western blotting data. However, the possibility that other unidentified short mRNAs exist in those tissues cannot be excluded.

6.5 Utrophin mRNAs detected in selected tissues

Neural tube The cells in the neural tube constitute the neuroepithelium which will give rise to neurones, motor nerves, neuroglia and ependymal cells (Carlson, 1994, p 205). The neural plate represents the first location where utrophin mRNA is expressed in the developing embryo. Utrophin transcripts are detected as early as 8.5dpc in UKO^{ex6} and control embryos, when the neural tube is starting to form, and are located in the posterior neural plate and in the most medial part of the neural groove. Expression of utrophin mRNA in the

neural groove might be induced by the underlying notochord which is known to influence expression of genes in the neural tube via signalling molecules such as sonic hedgehog (MacMahon et al., 1998). The transcript expressed in the neural plate has been identified as Up71. As the sides of the neural tube lift to form the neural tube, Up71 mRNA declines and is replaced by a different short transcript, perhaps Up140 or Up109, which is found throughout and along the length of the tube by 9.5 and 10.5 dpc.

Expression of utrophin mRNA in the neural tube changes during development with a progressive loss of mRNA in a rostrocaudal direction. By 12.5dpc mRNA is restricted to the most caudal end, around the caudal neuropore, which is the last region to close, although signal is retained in the floor-plate of the brain ventricles up to 12.5 dpc. It is relevant to compare this pattern of expression with that of Dp71 which is first detected along the length of the neural tube by 12.5dpc; thus, it could be postulated that Dp71 replaces the short utrophin transcript expressed in neural tube.

The pattern of utrophin expression in the neural tube is similar to that of neuronal cell adhesion molecules (NCAMs). These proteins mediate adhesive interactions between neural cells and other cells by a self-binding mechanism. NCAMs are expressed in the neuroepithelium of the caudal neural tube and are believed to play a role in providing positional information along the rostrocaudal axis of the neural tube and/or in neural tube closure (Bally-Cuif et al., 1993). This similarity between the expression pattern in the neural tube of utrophin and NCAMs suggest that they may both come under the control of the same regulatory mechanisms or that they may have similar functions. Thus, it is tempting to speculate that a short utrophin isoform expressed in the neural tube

prior to closure may have a role in neural tube closure (although at present there is no evidence that this transcript is translated). There are no signs in either the UKO^{ex6} or the UKO^{ex64} mice of neural tube defects although it is not clear if minor problems such as late closure of the posterior neuropore have been deliberately looked for.

A firm identification of the utrophin transcript expressed in the neural tube could be made by screening an early embryo (8.5 dpc) cDNA library (for example the one generated by Gearhart, Johns Hopkins Hospital, Baltimore, USA); this would be unequivocal since utrophin transcripts are not expressed anywhere else in the embryo at this stage.

Dorsal-root and cranial ganglia In the present study abundant utrophin mRNA was seen in the dorsal-root and cranial ganglia in both control and UKO^{ex6} mice. The dorsal-root ganglia form by condensation of trunk neural crest cells at both sides of the neural tube (Kaufman, 1992 p 120) and are first evident by 10dpc. The trigeminal ganglia form earlier, by 8dpc, and derive from cranial neural crest cells (Kaufman, 1992 p 74). Utrophin transcripts were identified in these sites in control mice embryo by Schofield et al. (1993) using a 3' riboprobe, and Blake et al. (1995) results demonstrated that this could be ascribed to G-utrophin. The present study, using multiple riboprobes and UKO^{ex6} sections, confirms these findings. There is a hint that a distinct short transcript might be present in dorsal root ganglia prior to G-utrophin expression. Using the U340 and U56-59 probes a utrophin mRNA was detectable in the dorsal-root ganglia as early as 10.5dpc whereas the G-utrophin specific probe did not detect G-utrophin until 11.5dpc (Blake et al., 1995). Thus, it is possible

that a different short transcript (perhaps Up140 or Up109) precedes the expression of G-utrophin in dorsal-root ganglia. However, this finding could also be explained by differences in the sensitivity of the various probes.

Choroid plexii The present study has demonstrated that the utrophin mRNA expressed in choroid plexii is the full-length transcript. This identification was made on the basis that utrophin signal was detected in C57Bl embryos with the most 5' probes but was absent in UKO^{ex6} embryos.

The expression of full-length utrophin in adult brain choroid plexii has been previously described by Knuesel et al. (2000) who used mRNA *in situ* hybridisation and a 5' probe. In addition, high levels of full-length utrophin protein in the choroid plexii were demonstrated using an NH₂-terminal anti-utrophin antibody (Knuesel et al., 2000). Taken together, all of data indicate that expression of full-length utrophin in the choroid plexii is established during development and continues in the adult. The choroid plexii develop from an invagination of the roof of the myelencephalon in 11 dpc mouse embryos (Berry, Bannister and Standring, 1995, p 1203; Rugh, 1968, p, 308), however, utrophin mRNA is not detected until a relative late stage of organogenesis, 14.5dpc. Knuesel et al. (2000) showed that utrophin protein localises precisely to the basolateral membrane of the epithelial cells which constitute the tissue structure. Thus, full-length utrophin could play an architectural role in maintaining the polarity of the choroid epithelium by establishing ion channels and transporters complexes across the basolateral membrane of the epithelial cells; alternatively, utrophin could be involved in cell-cell junctions which preserve the integrity of the brain-blood barrier (for details of choroid plexus

structure and function see Berry, Bannister and Standing (1995). These complexes are not likely to involve dystroglycan, at least in the embryo, since dystroglycan mRNA is not detectable in choroid plexii in control mice (Schofield et al., 1994).

The tongue A tongue primordia is first seen at 11 dpc as a pair of lateral swellings associated with the dorsal surface of the mandibular component of the first pharyngeal arch (Kaufman, 1992, p 241). The current mRNA *in situ* studies have identified abundant utrophin mRNA in the foetal tongue at 12.5dpc. Schofield et al. (1993) had earlier reported expression of both utrophin and dystrophin mRNAs in the neonatal mouse tongue. Data from UKO^{ex6}/control comparison clarifies that the tongue utrophin mRNA can be attributed to full-length utrophin. This accords well with the detection of full-length utrophin protein in the tongue of E12 rat embryos by immuno-histochemistry by Lin S. et al. (2000). The dystrophin mRNA is also probably full-length since it was detected using a 5' riboprobe (Schofield et al., 1993). The tongue striated muscle groups have a distinct three dimensional arrangement not found in any other muscle and the predominant fibre type is II. In addition to utrophin, nitric oxide synthase and β -dystroglycan have been detected by immuno-histochemistry at the NMJs in neonatal rat tongue (Christova et al., 1997) and it appears that the utrophin-DAP complex is similar to that in other muscles. It is not clear why the levels of mRNA are so much higher in the tongue; either the density of NMJs is significantly greater or utrophin has some other role perhaps in association with sensory receptors serving the tongue taste buds.

Limb bud/digits

In the present study, a short utrophin transcript was detected as a diffuse signal in the limb bud at 10 dpc which by 14.5 dpc was restricted to specific areas of the developing digits. Judging by their relative position, these areas appear to be the developing digital tendons. Schofield et al. (1993) also reported high levels of utrophin mRNA in the regions identified as tendon primordia. However, these authors did not note expression of utrophin in the developing limb before 14.5dpc.

As described in sections 4.4 and 4.5, based on the very high levels of utrophin mRNA in foetal hands described by Schofield et al. (1993), a special study of utrophin expression in the developing digits was undertaken which led to the isolation of a novel short utrophin mRNA, Up109. The pattern of hybridisation signal seen with the different riboprobes in the mRNA *in situ* hybridisation experiments agrees well with the identification of this signal as Up109.

The development of the vertebrate limb has been thoroughly studied by numerous groups and is well understood. In brief, limbs arise from the lateral plate mesoderm and initially consist of a mass of undifferentiated mesodermal cells covered by a thick layer of ectoderm, the apical ectodermal ridge. Interaction between the mesoderm and the overlying ectoderm drives outgrowth of the limb whereas morphogenesis is controlled solely by the mesoderm. The ectodermal ridge keeps the distal most mesenchyme cells in an undifferentiated state and promotes proliferation (Carlson, 1994, p 182-201; Schwabe et al., 1998). A subset of mesenchyme cells that derive exclusively from the lateral plate mesoderm will give rise to the tendons.

In all stages examined, utrophin mRNA in the limb bud was confined to the distal portion of the bud. However, there are some indications that the domains of utrophin mRNA expression change during limb development or that more than one short transcript is expressed. At 12.5dpc utrophin mRNA appears to localise to a region that corresponds to the zone of polarising activity (ZPA) which controls the development of the limb bud in the anteroposterior axis by releasing a morphogen (Schwabe et al., 1998). In contrast, in the 14.5 dpc hand utrophin mRNA accumulates in the tendon primordia in a dorsoventral orientation.

A tendon is a highly organised connective tissue that connects the muscle to the bone (Salmons, 1995, p 781). Although I have proposed that utrophin is expressed in the tendons, a firm identification of the tissue/cell type has not been made. A more extensive series of mRNA *in situ* hybridisations and immuno-histochemical studies are needed to make a firm identification; for the latter, cultured fibroblasts (the major cell type in tendons) and a tendon marker such as collagen type I may be useful.

Semicircular canals The present study has shown for the first time that utrophin mRNA occurs in the semicircular canals of the inner ear.

The hybridisation pattern to the different riboprobes seen on both C57Bl and UKO^{ex6} sections indicate that a short transcript, perhaps Up140 or Up109, is the major transcript in this location. The utrophin signal in the semicircular canals is not diffuse but corresponds to an inner layer along the whole circumference of the canals. Each semicircular canal has a terminal swelling known as the ampulla which represents its sensory area. The sensory epithelium consists of

mechanoreceptive cells, hair cells, with some non-sensory supporting cells scattered amongst them. The hair cells form synapses at their base with afferent and efferent endings of the vestibular nerve. The role of these cells is to detect the orientation of the head and changes in head movement, and they are responsible for the control of equilibrium and position (Berry, Bannister and Standing, 1995, p 1367).

At present the exact location of utrophin in the semicircular canals is not known. However, one proposal worth of further investigation is that a short utrophin isoform is expressed in the basal membrane in these mechanoreceptor cells at the synapse forming an inner ear specific DAP complex, similar to the skeletal muscle NMJ DAP complex, where it might have a role in the clustering of neurotransmitters receptors. Innervation of the vestibular labyrinth is thought to be mainly cholinergic and neutrinergic and both acetylcholine receptors and NOS, which occur at the NMJ, have been found to be expressed in the vestibular sensory epithelium (Lustig et al., 1999; Lysakowski et al., 2000).

It is of relevance to note that full-length dystrophin and Dp116 are expressed in the hair cells of the organ of Corti, which is the part of the cochlea responsible for hearing (Dodson et al., 1995). Using immuno-histochemistry these authors determined that in the hair cells these dystrophins localise to the cuticular plate, lateral membrane and to the synaptic regions. Using antibodies against different regions of the dystrophin protein they showed that Dp116 predominates in the synaptic region. Dodson et al. (1995) proposed that dystrophin in the cochlea could have a role in maintaining the stability of the cell membrane upon acoustic stimulation and also in nervous transmission.

Could the utrophin mRNA in the semicircular canals be attributed to the utrophin homologue of Dp116, G-utrophin? This is an idea which merits further investigation although at present G-utrophin appears to be a neuronal-specific utrophin isoform. The Blake et al. (1995) study using a G-utrophin specific probe is not helpful since it is not clear whether sections containing the semicircular canals were analysed. At least at present, the idea that G-utrophin is the transcript expressed in the semicircular canals cannot be excluded.

There are various ways in which a firm identification of the semicircular canal transcript could be made in future studies. One possibility is to carry out careful mRNA *in situ* hybridisation experiments using riboprobes specific for G-utrophin, Up109 or Up140.

Perhaps more importantly, the inner ear should be analysed by immunohistochemistry using either appropriate sections and/or vestibular sensory epithelium cells grown in culture. Milhaud et al. (1999) have described appropriate cell lines. Antibodies against proteins which are expressed in sensory cells could be used as cell type markers. For instance, calmodulin and spectrin which are expressed in semicircular canals sensory epithelium (Ogata et al., 1998; Pirvola et al., 1990).

Another sensible approach will be to screen inner ear cDNA libraries for specific utrophin cDNAs. Such libraries have recently become available. For example Verpy et al. (2000) generated a vestibular specific cDNA library by dissecting the vestibular apparatus (including the semicircular canals) from the cochlea of newborn mice and separating the sensory areas from the non-sensory areas and cartilage.

Pyloric sphincter A short utrophin mRNA, Up140 or Up109 (or an as yet unidentified transcript) is expressed at high levels in the pyloric sphincter which lies between the stomach and the small intestine. This is the first report of utrophin expression at this site.

The overall histological organisation of the pyloric sphincter is similar to that found in other parts of the gastro-intestinal tract; the main layers of the wall are: the mucosa - the innermost layer formed by columnar epithelial cells with secretory and absorptive functions; the submucosa - a connective tissue with abundant collagen and elastin fibres that supports the mucosa and its nerve, vascular and lymphatic supply; the *muscularis externa* - consists of inner circular and outer longitudinal smooth muscle layers (Bannister, 1995, p 1747). The pyloric sphincter is distinguished from the rest of the digestive tract by a thickening of the circular smooth muscle layer of the *muscularis externa*. Contraction of the pyloric sphincter occludes the lumen delaying stomach emptying and thereby permitting food breakdown before passage into the small intestine (Bannister, 1995, p 1747). The short utrophin mRNA localises to the broad band of cells immediately adjacent to the lumen corresponding to the mucosa.

In the context of gut and its genetic control the work of Zákány et al. (1999) is of particular interest. They generated mice “knocked-out” for the majority of the *Hoxd* genes; these mice lacked all sphincters along the intestinal tract and had severe alterations of smooth muscle and epithelia in the region of the pyloric sphincter. It might be proposed that the transcription of Up140 or Up109 might be regulated by *Hoxd* genes. Binding sites for *Hoxd* factors are not present in the 1Kb of human Up140 5' flanking sequence currently available

(Wilson thesis, 2000). Several sites for the binding of GATA transcription factors are present (Wilson thesis 2000); these factors are expressed in the gastrointestinal epithelia and are known to be important in intestinal development (Laverriere et al., 1994). In the present study no binding sites for *Hoxd* or GATA factors were identified in the short, 300 bp, Up109 5' flanking sequence analysed (section 4.6). The identification of regulatory sequences for Up140 and Up109 need much more extensive investigation before a relationship, if any, with *Hoxd* genes can be established.

Urogenital system During the course of this study, utrophin transcripts have been demonstrated in three components of the urogenital system: the kidney, the testis and the urethra. While expression of utrophin mRNA in embryonic kidney and testis was reported by Schofield et al. (1993), this is the first report of expression of utrophin in the urethra. The hybridisation pattern seen in the present study points towards the expression of a transcript initiated from a position upstream of exon 56 in all three sites. G-utrophin was not detected in any of these structures and can be excluded (Blake et al., 1995). Up140 and Up120 are a possibility but firm identification of the kidney/urethra /testis transcript(s) requires further study. One obvious strategy would be to screen tissue specific cDNA libraries with the U340 and U56-59 sequences.

The urogenital system derives from intermediate mesoderm. Both the kidney and the testis derive from the nephros and are developmentally and phylogenetically related. The kidney starts to differentiate before the gonads and goes through three major stages, pronephros (9 dpc), mesonephros (10.5 dpc) and metanephros (12dpc). A mature vertebrate kidney with a differentiated

cortex and medulla is in place by 15 dpc (Carlson, 1994, p 344). In the present study, utrophin mRNA was not seen in kidney before 14.5 dpc although Schofield et al. (1993) reported utrophin expression in kidney by 12.5dpc.

Major sites of utrophin mRNA expression in the foetal kidney are the collecting ducts and glomeruli; both of these structures arise from the mesenchyme which condenses to form the mesonephric duct, which will become the collecting ducts, and the blastema which in turn will become the glomeruli. During the differentiation of the glomeruli a population of cells are induced to form polarised epithelial cells. This transition is believed to involve changes in the collagen and laminin make up of the extracellular matrix and interactions between the latter and an integral glycoprotein called uvomorulin (Carlson, 1994, p 344). Could a short utrophin transcript have a role in these interactions perhaps forming part of the link between uvomorulin and the extracellular matrix? Isolation of the glomerular utrophin protein and its detailed localisation will be required in order to answer this question.

The testis begins to differentiate from a group of mesodermal cells proximal to the degenerating mesonephros. Cells in the caudal part of this mesodermal mass become the coelomic epithelium which will form the genital ridge (11 dpc). Primordial cells migrate into the genital ridge, and the coelomic epithelium sends out projections which become the primitive seminiferous tubules. By 14.5 dpc, the stage at which a utrophin mRNA is detected, the testis has prominent primitive seminiferous tubules and the germinal epithelium and the intertubular tissue are clearly defined (Rugh, 1968, p 282). The testosterone secreting Leydig cells, fibrocytes and mononuclear cells of the intertubular

tissue have all derived from a common population of mesenchyme cells (Wrobel et al., 1988).

At this stage it is not easy to ascertain the cellular localisation of the short utrophin transcript from the pattern of signal seen on the testis sections by mRNA *in situ* hybridisation. However, it appears to localise to the primitive seminiferous tubules (Rugh, 1968, p 282). This is in contrast to full-length utrophin protein seen in the mature testis which by immuno-histochemistry (chapter 5 section 5.2) localises to the intertubular tissue. Thus it is possible that a short transcript is expressed in the seminiferous tubules in foetal testis while full-length utrophin is confined to the fully differentiated intertubular tissue in adult testis.

The urethra constitutes the outlet of the bladder and is divided into four parts, a preprostatic urethra, from the bladder to the urethra, a prostatic urethra that runs through the prostate, a membranous short urethra and a penile urethra that runs within the penis (Dyson, 1995, p 1842). The urethra is basically a canal lined ventrally with stratified squamous epithelium and dorsally with low cuboidal epithelium. Mucus secreting cells are common throughout the epithelium and occur frequently in the penile urethra. The epithelium rests on a highly vascularised loose connective tissue which in turn is surrounded by striated muscle (Dyson, 1995, p 1842). The prostatic and membranous urethra derive from the upper urogenital sinus and the penile urethra from the lower urogenital sinus and the genital folds.

The short utrophin transcript detected in the present study accumulates in the penile urethra. It is not clear whether the signal is associated with the striated muscle of the urethra or the internal layer of epithelial cells. A much

more detailed and deliberate study of the penis sections needs to be undertaken and of course it will be essential to determine whether this short transcript and that seen in foetal testis are translated.

6.6 Final remarks

The mRNA *in situ* hybridisation experiments presented in this section clearly indicate the presence of short utrophin transcripts in foetal tissues. However, it is important to consider these findings in the context of the protein studies described in chapters 4 and 5. These latter, while largely confined to adult tissues, provide little evidence that short utrophin isoforms are actually translated. There are important exceptions to this; Up109 is translated in foetal hands and foetal muscle, Up120 in adult and foetal kidney, G-utrophin in brain and a short isoform(s) of 97kDa/103kDa may be expressed in testis. Furthermore, the preliminary and incomplete protein analysis of foetal tissues extracts carried out in the present study together with RT-PCRs (section 4.6) suggest that Up109 is also expressed in foetal brain, lung and heart. Expression of Up109 in hands significantly decreased towards birth and a polypeptide corresponding to Up109 was not seen in any of the adult tissues examined. Thus, it is possible to speculate that Up109 is a foetal utrophin isoform and corresponds to the mRNAs seen not only in the tendon primordia but also in other sites such as neural tube and pyloric sphincter. In future studies, mRNA *in situ* hybridisation using a Up109 specific probe will help resolve this question.

Nevertheless, there is an urgent need to clarify this situation by much more extensive protein studies on foetal tissues in order to establish whether

the high levels of mRNA are reflected in high/moderate levels of protein or not.

Meanwhile, we must consider two scenarios:

a-The short transcripts are not extensively translated but may have a role as mRNAs – this interesting hypothesis is not discussed here but in the final discussion.

b-The short utrophin mRNAs expressed in foetal tissues are translated at a level concomitant with the mRNA levels and extensive protein studies of foetal tissues needs to be carried out. If this is the case, the cellular distribution and potential function of those isoforms could be explored in future studies. For example, the present study provides evidence that G-utrophin is translated in brain and that its mRNA is expressed at high levels in ganglia and may also be expressed in the inner ear. The dystrophin homologue of G-utrophin, Dp116, is expressed in both tissues. On the basis of this evidence, in future studies it would be sensible to give priority to the investigation of whether G-utrophin is translated in dorsal-root ganglia and semicircular canals.

Recently, Masaki et al. (2000) demonstrated the expression of Dp116 in satellite cells in dissected rat dorsal-root ganglia. Using an antibody against the COOH-terminus of dystrophin the authors detected Dp116 in dorsal-root ganglia extracts and this was followed by the detection of an immunoreactive protein in sections. Dp116 localises to the outer membrane of satellite cells but is not expressed in the ganglia neurones (Masaki et al., 2000). β -dystroglycan was also detected in those cells where it co-localised with Dp116. The ECM protein laminin-2 was detected in dorsal-root ganglia sections in the basal lamina surrounding the satellite cells and laminin overlay assays indicated an association with α -dystroglycan. In summary, that study showed that a

specialised Dp116-DAP complex exists in dorsal-root ganglia satellite cells. This complex is likely to link the membrane of these cells to the basal lamina through the interaction with laminin-2. A similar study could be carried out using the new Mupa antibodies in order to establish if G-utrophin is translated in foetal and mature dorsal-root ganglia. The association of G-utrophin with DAPs could be investigated by immuno-histochemistry and immunoprecipitation experiments using antibodies against DAPs.

It is interesting to note that in contrast to the adult tissue, Dp116 mRNA was not detected in ganglia in embryos by mRNA *in situ* hybridisation using a Dp116 specific riboprobe (Schofield et al., 1994); thus, it is possible that G-utrophin is expressed in foetal ganglia and Dp116 in adult ganglia or alternatively, G-utrophin is expressed in ganglia neurones (as in the brain, Blake et al., 1995) and Dp116 in satellite cells and each of them is part of a different DAP complex.

Regarding the expression of G-utrophin in the semicircular canals, in future studies the inner ear of embryos, when technically feasible, and adult mice could be dissected and analysed by Western blotting and immuno-histochemistry with the Mupa antibodies. This has been done for dystrophin (Dodson et al. 1995). These authors showed that Dp116 is expressed in the hair cells of the cochlea where it localises to the synaptic regions of the membrane. These authors used Western blotting and immuno-histochemistry to cochlea whole mounts. Alternatively, whole embryo cryosections containing the semicircular canals could be looked at first by mRNA *in situ* hybridisation (using digoxigenin labelled riboprobes) followed by immuno-histochemistry, as for example described by Jowett (1999), to make a firm comparison of mRNA and protein levels. If a short utrophin protein was identified, these experiments could

be taken further by investigation of DAPs in the inner ear in order to determine the composition of a potential sensory cell specific DAP complex.

The expression of a utrophin isoform in the inner ear could be important towards the identification of human pathologies associated with utrophin deficiency. Regarding dystrophin, there have been two reports of families with hereditary hearing loss mapped to the DMD locus (Lalwani et al., 1994; Pfister et al., 1998, 1999) and there is some evidence that cochlear function is impaired in *mdx* mice (Raynor et al., 1997). If the short utrophin isoform transcribed in the developing inner ear is important for sensory cell function and for transmission of positional information to the brain, we would expect its absence to result in abnormal behaviour and dysequilibrium. However, UKO^{ex64} mice, deficient for all utrophins (Grady et al., 1997a) do not show any apparent abnormal behaviour. However, the identification of such a phenotype may require special tests such as those carried out in *mdx* mice by Raynor et al. (1997) including measurements of the brainstem auditory evoked response; these may not be performed if the involvement of a short utrophin in inner ear function is not suspected.

Despite the uncertainty regarding the translation and functional significance of the mRNAs detected in this study it can be said that utrophin transcripts are expressed in a wide variety of developing organ systems with different embryonic origins and cell type composition as summarised in Table 6.2. Utrophin transcripts are abundant in a variety of neural crest derivatives (c. 33% of the sites of utrophin expression) such as ganglia, developing teeth, facial cartilages, vibrissae and heart outflow and in mesodermally (c.33%) derived tissues. Utrophin mRNAs are slightly less abundant in ectodermally derived

TISSUE	EMBRYONIC ORIGIN	CELL TYPE	TRANSCRIPT
NERVOUS SYSTEM			
neural tube & floor-plate	ectoderm	neurones & nerves & glia	Up7/Up140/Up109
dorsal-root & trigeminal ganglia	neural crest	neurones	G-utrophin
choroid plexii	ectoderm	epithelia (secretory)	full-length
Rathke's pocket	ectoderm	epithelia (secretory)	Up140/Up109
SKELETAL TISSUES			
tongue	mesoderm	striated muscle	full-length
facial cartilages	neural crest	condrocytes	full-length + Up140
tendon primordia	mesoderm	fibroblasts	Up109
tooth primordia	neural crest	epithelia (+/-secretory)	Up140/Up109
DIGESTIVE SYSTEM			
mucosa of the pyloric sphincter	endoderm	epithelia (+/-secretory)	Up140/Up109
SENSORY ORGANS			
semicircular canals	ectoderm	epithelia	Up140/Up109
follicles of vibrissae	neural crest	epithelia/neurones	Up140/Up109
UROGENITAL SYSTEM			
Kidney (glomeruli/tubules)	mesoderm	epithelia	Up120
Testis (seminiferous tubules)	mesoderm	epithelia, germinal cells	Up140/Up109
urethra	mesoderm	epithelia/striated muscle	Up140/Up109
CIRCULATORY SYSTEM			
Heart outflow tract	neural crest	smooth muscle, angioblast	full-length

Table 6.2. Summary of the foetal tissues expressing abundant utrophin mRNAs detected by mRNA *in situ* hybridisation; their embryonic origin and major cell types that form each tissue. +/-secretory indicates that only some cells are secretory. The most likely utrophin transcript expressed in each location is listed.

tissues (c.27%), and the mucosa of the pyloric sphincter represents the only tissue of utrophin expression of endodermal origin (c.7%).

To conclude, the present study has also attempted to identify which of the several short utrophin transcripts is the major utrophin form in each foetal tissue. A firm identification will not be made until studies using transcript specific riboprobes, screening of tissue specific cDNA libraries or 5' RACE and comprehensive Western blotting and immuno-histochemistry have been carried out.

Chapter 7

Final Results and Conclusions

7.1 General conclusions

The overall aim of this project was to characterise the known short utrophin isoforms, G-utrophin (Blake et al., 1995), Up140, and Up71 (Wilson et al., 1999). The expression of these short transcripts have previously only been partially investigated; in the case of Up140 and Up71 only at the mRNA level and only by RT-PCR (Wilson et al., 1999). Much remained to be learnt about the tissue distribution of these forms at both RNA and protein levels.

It was believed that one of the reasons why Up140, G-utrophin and Up71 proteins had remained elusive in the past was because of the lack of appropriate antibodies to analyse mouse protein preparations and because of the propensity of full-length utrophin to breakdown into smaller products that confused the interpretation of the results. As a consequence, two fundamental strategies were adopted for the present study:

- i) To generate a new panel of anti-mouse utrophin polyclonal antibodies for use in Western blotting and immuno-histochemistry.
- ii) To make use of the utrophin deficient mice UKO^{ex6} which it was believed would express only the short utrophin isoforms.

In addition, it was also hoped that these strategies would allow the identification of other novel short isoforms should they occur.

The most significant advances and findings to come out of this work are listed below and summarised in Table 7.1 (pg 371b):

Tissue	395kDa				Up140				Up120			G-utrn				Up109				Up71				Figs	data in thesis
	RT ¹	IS ²	W	IHC	RT ¹	IS	W	IH	IS	W	IHC	RT ⁴	IS	W	IHC	RT	IS	W	IHC	RT ¹	IS	W	IHC		
a.kidney	+		+	+	+		-	-		+	+	+		-	-	-	-	-	-	+		-	-	4.4, 5.15-5.17	179, 281
f.kidney	+	-	+	nt	+	+	-	nt	+	+	nt	nt	-	-	nt	+	+	-	nt	+	-	-	nt	4.4, 6.14	179, 342, 345
a.brain	+		+	nt	+		-	nt		-	nt	+		+	nt	-		-	nt	+		-	nt	4.6	184
f.brain	+	+	nt	nt	+	+	nt	-	-	nt	nt	-	-	nt	nt	+	+	nt	+	+	-	nt	nt	6.5, 6.8, 6.15	198, 327, 345
a.sk. muscle	+		+	+	+		-	+		-	-	-		-	-	-		-	-	+		-	-	4.8, 5.1-5.12	190
f.striated muscle	+	+	nt	+	+	-	nt	-	-	nt	-	-	-	nt	-	+	-	nt	+	+	-	-	nt	5.12, 5.14, 6.10	278, 334, 351
a.testis	+		+	+	+		-	-		-	-	nt		-	-	nt		-	-	+		-	-	4.10, 5.19-5.21	193, 286
f.testis	+	-	nt	nt	+	-	nt	nt	-	nt	nt	nt	-	nt	nt	nt	-	nt	nt	+	-	nt	nt	6.14	342
f.hands	nt	-	+	+	nt	-	-	-	-	-	-	nt	-	-	-	+	+	+	+	nt	-	-	-	4.11, 4.12, 5.22 5.23, 6.11, 6.12	196, 291 332, 334, 342

Tissue ⁵	395kDa	Up140	Up120	G-utrn	Up109	Up71	Figs	data in thesis
neural tube	-	+	-	-	+	+	6.4, 6.5, 6.6	327, 332
f.ganglia	-	-	-	+	-	-	6.6, 6.8, 6.9	330, 334
f.inner ear	-	+	-	nt	+	-	6.13	342
f.urethra	-	+	-	-	+	-	6.14	345
f.pyloric sphincter	-	+	-	-	+	-	6.14	345
f.heart	+	-	-	-	-	-	6.10	338
vibrissae	-	+	-	-	+	-	6.11	339

footnotes

¹ Taken from Wilson et al. (1999); ² mRNA *in situ* hybridisation experiments were only carried out on embryo sections and not on adult tissues; ³ RT-PCRs using Up120 specific primers have not been carried out because the unique Up120 5' sequence has not yet been isolated; ⁴ RT-PCR experiments (not published) were carried out in the lab using G-utrophin specific primers; ⁵ All tissues in this section of the Table were analysed by mRNA *in situ* hybridisation only (see pg 365-366).

Table 7.1 Expression profiles of utrophin mRNAs and proteins. Summary of the data given in Tables 4.2, 5.1 and 6.1. The pages on which the results are described are given, along with the corresponding figure numbers. RT= reverse transcriptase PCR; IS= mRNA *in situ* hybridisation; W= Western blots; IHC= immuno-histochemistry. nt = not tested; - = not detected; + = detected.

1. A new resource of anti-utrophin polyclonal antibodies has been generated. Mupa-1 appears to be an excellent antibody for immunohistochemistry when used at high dilutions. However, this antibody does not detect denatured protein well and is not useful for standard SDS PAGE immunoblots. In contrast, Mupa-2 is ideal for Western blotting but not for immunohistochemistry because it interacts more efficiently with the denatured utrophin epitope. Mupa-3 at high dilutions, is very useful for both Western blotting and immunohistochemistry. These antibodies have now been made available to our collaborators in Oxford and in the Hammersmith Hospital and are accessible to any research group.

2. Combining data from this thesis and from the literature (Love et al., 1991; Kamakura et al., 1994; Knuesel et al., 2000) indicates that full-length utrophin, both RNA and protein, is more abundant in adult tissues than during development. Skeletal muscle is exceptional in this regard showing higher levels of expression during muscle differentiation (Koga et al., 1993; Clerk et al., 1993).

3. In contrast, the short utrophin mRNAs appear to be more abundant in foetal than in adult life, although it is not clear at present whether protein levels will be similarly elevated. These RNAs are transcribed at normal levels in mice knocked-out for full-length utrophin.

4. The translation of the short utrophins is apparently not commensurate with the abundance of RNA. In particular, there is no unequivocal evidence for

translation of Up140 and Up71, although expression of low levels in some tissues cannot be excluded (for example there is a hint that Up140 may be weakly expressed at low levels in the UKO^{ex6} NMJ).

5. The present study has confirmed that the major utrophin in kidney glomeruli, cortical tubules and collecting ducts is the full-length form.

6. The present study has shown for the first time that full-length utrophin localises to the intertubular tissue surrounding the seminiferous tubules and accumulates in Leydig cells. Since Leydig cells are the source of testosterone, this raises the question of a possible role of full-length utrophin in secretion. This finding has also prompted the suggestion that the subtle mating/breeding abnormalities observed in UKO^{ex6} mice may reflect utrophin deficiency. Furthermore, this finding may have implications for human male infertility and testis associated pathologies.

7. Two novel short isoforms, Up109 and Up120 have been identified, thereby contributing towards the completion of the utrophin transcriptional map. These two short isoforms are translated at modest levels. A cDNA for Up109 has been isolated and characterised. This isoform contains a unique 17 aa NH₂-terminus which is highly hydrophobic and has phosphorylation and myristoylation sites. These motifs may be involved in guiding Up109 to membranes. Up109 appears to be a foetal isoform. Except for the differences in their NH₂-termini, Up109 and G-utrophin are structurally identical. Up120 has

been identified as a kidney specific polypeptide. This isoform is found in glomeruli and increases in the absence of full-length utrophin.

8. The present work has confirmed that G-utrophin expression is confined to neuronal tissues and has positioned the G-utrophin first exon within intron 55 113Kb upstream of exon 56.

Some interesting issues which derive from these findings are discussed below:

7.2 Other genes containing alternative promoters

The use of alternative promoters within a single gene is an important source of functional diversity in mammalian cells. Such promoters fall into two types; Firstly, there are those at the 5' end of genes which transcribe alternative mRNAs whose products have identical or very similar functions. The presence of these promoters allows for the temporal and tissue diversification of expression of what it is essentially the same product. Secondly, there are promoters which lie within the body of a gene, usually within an intron, and transcribe truncated versions of mRNAs which yield proteins shortened from the NH₂-terminus.

The diversity of promoters in a single gene and their interactions with distinct panels of transcription factors is one important way in which animals of distinct species are genetically different from one another and achieve varying complexity of cell differentiation. This partly explains why the human genome contains only 25000 to 40000 genes (around 100000 genes were initially

estimated), only about twice the number of genes needed to make a fruitfly, worm and plant. In other words, complexity does not depend on the number of genes but on gene expression regulatory mechanisms.

There are many examples of genes which make use of alternative promoters at their 5' end - insulin-like growth factor II (Lee et al., 1999), progesterone receptor (Kim et al., 1999) and of course, dystrophin (Blake et al., 1996b). Two genes are particularly interesting to mention because they are related to dystrophin/utrophin in some way. Plectin is one example; the gene covers 32Kb of DNA and its protein product (500kDa) contains an NH₂-terminal actin-binding domain with homology to the dystrophin/utrophin domain (Fuchs et al., 1999). Plectin is a versatile cytoskeletal linker and localises at cell-cell contact areas of membranes such as the intercalated discs of cardiac muscle, hemi-desmosomes and desmosomes, Z -line structures and dense plaques of striated and smooth muscle (Kolmerer et al., 1996). The various isoforms display a diversity of sites of expression and functions; for example, the adult skeletal muscle isoform contains a novel actin-binding domain which confers it with higher actin-binding activity than other isoforms (Fuchs et al., 1999). This diversity is achieved by 11 alternative promoters in combination with differential splicing (Fuchs et al., 1999).

A second example is the α -dystrobrevin gene which has three promoters within the 5' 270Kb of the gene, that are active in a tissue specific manner (Holzfeind et al., 1999). The distal brain promoter is 120Kb away from the muscle promoter and a third promoter is found 70K downstream of the muscle promoter and 80Kb upstream of the first coding exon 1. The isoforms are very similar in their structure but show tissue specific expression. The α -dystrobrevin

gene is very large (440Kb) with 23 coding exons occupying 170Kb of that sequence.

There are some examples of internal distal promoters transcribing short isoforms of gene products but these are much less common than alternative 5' promoters. One example is the collagen type III gene which has a full-length and a short transcript of 5.7Kb and 4Kb respectively. The short mRNA is transcribed from an alternative promoter situated within intron 23, 20Kb downstream of the upstream promoter (Zhang et al., 1997). The alternative transcript contains a unique first exon, situated 699 bp upstream of intron23/exon 24 boundary, which splices to exon 24. The predicted size of the truncated protein is 20kDa and it lacks various domains essential to normal collagen function, i.e. a signal peptide, the NH₂-terminal propeptide and one third of the triple helical domain. The alternative promoter within intron 23 confers tissue specificity since the short transcript, in contrast to the full-length transcript, is expressed in the growth cartilages during endochondral ossification (Zhang et al., 1999).

The sodium independent anion exchanger AE2 gene is another example. This gene encodes three transcripts, two of which are transcribed from internal promoters in introns 2 and 5. The first exon of one of the short transcripts encodes for three unique aa whereas the other one contains exclusively 5' UTR (Wang Z. et al., 1996).

Apart from these examples only a few other genes containing several distal promoters exist. What makes utrophin and dystrophin special?

Both genes are huge and even more important they have unusually large introns (the mRNAs of dystrophin and utrophin represent only 0.15% and 1.4%

respectively of the size of the genes). The very long introns provide a sequence resource where promoters may arise by chance during evolution; thus, the promoter for Dp140 has arisen in intron 44, which is 220Kb long, and the Dp71 promoter in intron 62, which is 65Kb long (Nobile et al., 1995, 1997; McNaughton et al., 1998).

Although there is very little published information about utrophin introns, a comparison of the utrophin cDNA sequence and the genomic sequences in the human genome database indicate the presence of some large introns; for example, utrophin intron 55 is around 130Kb long. It is within this intron that the promoters for G-utrophin and Up109 are found. The size of utrophin intron 55 is quite a bit larger than the corresponding dystrophin intron which is <55Kb (Nobile et al., 1995), and confirms that intron sizes vary between utrophin and dystrophin. Some utrophin introns must be smaller than their dystrophin counterparts since the overall size of the gene is around 50% of the dystrophin gene (Pearce et al., 1993).

It is of interest to ask about the order in which the multiple promoters of dystrophin and utrophin arose during evolution; was a short transcript the ancestral progenitor or a full-length transcript? Dystrophin/utrophin-like genes have been found in several invertebrate species including amphioxus, starfish, sea urchin (Wang J. et al., 1998; Roberts et al., 1998), fruitfly (Neuman et al., 2001) and *C. elegans* (Bessou et al., 1998). The current view is that the three classes of dystrophin-like sequences, namely dystrophins, utrophins and DRP2, diverged before the vertebrate radiation (around 500×10^6 years ago). All the available evidence points towards a full-length (rather than a short form) utrophin-like gene as the ancestral form; for example, a full-length isoform is

found in *Drosophila* and *C.elegans* (Bessou et al., 1998; Neuman et al., 2001). In addition, the isolation of a G-utrophin/Dp116 homologue from the sea urchin (Wang J. et al., 1998) provides evidence that at least the G-utrophin/Dp116 promoter was already in place in the ancestral gene prior to the divergence of utrophin and dystrophin. There is also evidence of a 140kDa protein detected in the striated muscle of the leech which could correspond to the ancestral form of Dp140/Up140 (Royuela et al., 1999). There is however no evidence for Dp71/Up71 like transcripts in invertebrates, which indicates that these promoters arose at some time during vertebrate evolution but before the duplication event that gave rise to dystrophin and utrophin (maybe before the radiation of the fishes 300×10^6 years ago).

Dystrophin homologues of Up109 and Up120 utrophin isoforms have not been reported; similarly a utrophin homologue of Dp260 could not be identified. It seems possible that these promoters arose after the utrophin/dystrophin duplication.

7.3 If short utrophins are not translated do they have another function?

There is little evidence that Up140 and Up71 are translated and while G-utrophin, Up120 and Up109 are translated, the levels of protein appear to be low relative to mRNA levels, particularly if distribution in foetal hands and ganglia is considered. These observations have led us to the idea that translation is not a major feature of the short utrophin (and short dystrophin) transcripts and that they either function as mRNAs or are a secondary product of some other cellular function. According to the latest figures on the human

genome only 5% of the transcribed portion of the human genome sequence encodes protein (Baltimore, D., 2001).

The function of non-protein-coding RNAs (ncRNAs) is diverse and they are most likely to be involved in specific recognition of nucleic acid sequences via complementary base pairing; leaving aside the well known transfer, ribosomal, small nucleolar and nuclear RNAs. Other ncRNAs can be involved in various cellular processes such as transcription, translation and RNA processing. Some RNAs have specific cellular functions such as telomerase RNA, which functions as a template for adding more telomeres, and the signal recognition particle RNA, which is involved in translocating proteins across the endoplasmic reticulum (Eddy et al., 1999).

There is a short mitochondrial RNA which has a function perhaps relevant to this discussion. This is transcribed from the mitochondrial L-strand in the D-loop region and acts as a template for the synthesis of the H-strand displacing the old H-strand as replication proceeds (Grossman et al., 1996). The D-loop, a 1Kb regulatory region, contains the origin of replication of the H-strand and the promoters for transcription for both the H- and L-strands. Thus, in the mitochondrion, replication of DNA is coupled to transcription so that the L-strand transcript serves as a primer for the replication of the H-strand (Clayton et al., 1992). It seems particularly relevant to point out that rare and unusually large deletions of mitochondrial DNA, associated with inflammatory myopathies, occur in the region of the origin of replication of the L-strand. Other deletions occur in the “major region” located between the origin of replication of the H- and L-strands (Bank et al., 2000).

Could the short utrophin (and dystrophin) transcripts be associated with origins of replication and act as templates during the replication of DNA? In complex organisms, which have to copy a large amount of DNA during the S phase of the cell cycle, fast replication is achieved by increasing the number of origins of replication (Bogan et al., 2000) and these are estimated to occur in mammalian genes at 300-500Kb intervals (Verbovaia et al., 1997). Replication origins increase efficiency of replication by facilitating the assembly of multiprotein replication complexes (ORC) at specific sites.

Origins of replication appear in particular DNA sequences, for example, they occur quite frequently in close proximity to transcription promoters or directly downstream of transcribed genes (Bogan et al., 2000). It has been proposed that the proximity of origins of replication to transcription promoters could be due to the ability of the ORC to use binding sites for transcription factors in the DNA or transcription factors themselves to assemble. This mechanism would provide the flexibility to increase the rate of replication by incorporating "reserve" origins of replication when replication needs to be carried out fast, for example in embryos. However, except for one example regarding *Sacharomyces cerevisiae* origins, there is no evidence that transcription factors are required *per se* for origin activity (Bogan et al., 2000). Alternatively, it is possible that origins are situated near promoters because they use the mRNAs transcribed from such promoters as templates.

The origins of replication in the utrophin gene have not been mapped but they are known in the dystrophin gene (Verbovaia et al., 1997). Interestingly, they have been roughly mapped to the regions of intron 7, intron 28, intron 46 to 48 and intron 64. Except for intron 7, all these regions are close to alternative

promoters transcribing the short dystrophins, Dp260, Dp140 and Dp71 respectively. Thus, it is possible to speculate that in the utrophin and dystrophin genes, as in the mitochondrial DNA, replication is coupled to transcription. The short mRNAs transcribed from promoters in these regions may simply be adventitious transcription of the mRNA or they may act as templates for the replicatory process. It is also possible that the promoters in utrophin introns 44 and 62 are only active and involved in replication when high rates of DNA synthesis are required, for example, in rapidly dividing foetal cells. This idea would be in complete agreement with the detection of high levels of short mRNAs in embryos from very early stages detected in the present study by mRNA *in situ* hybridisation.

This phenomenon has not yet been described in the nuclear genome – however it will be confined to very large genes which are relatively rare.

It is worth drawing attention to the fact that in dystrophin the majority of the deletions are found in intron 1, 7 and 44 where the promoters for the three major full-length dystrophins and for the short isoform Dp140 are found. This could be ascribed to the presence of vulnerable single stranded DNA during DNA replication. It is not yet clear whether the utrophin gene is vulnerable to deletion in the same way as dystrophin.

7.4 Implications for manipulation of utrophin transcription in DMD patients

What implications does the foregoing have for the proposed therapeutic approach to DMD which involves upregulation of utrophin transcription? If small molecules, which have a generalised effect on chromatin structure, are used there may be some outcome which affects the origins of replication. The origins

of replication are thought to use regions where chromatin is in a relaxed configuration and this might be enhanced by such treatment. From the proposal that origins of replication are associated with transcription start sites it is a short step to envisage that transcription of the short mRNAs may be increased when chromatin structure is changed.

In this thesis, no evidence for expression of short isoforms in skeletal and cardiac muscle could be found so overexpression of short isoforms is not likely to present a problem in these tissues. There is a little negative data already available on this point; upregulation of utrophin by injection into *mdx* mice muscle of L-arginine and NO (section 1.11) results in a significant increase in the levels of full-length utrophin (Chaubourt et al., 1999, 2000). In this case, the authors did not report the appearance of short isoforms, however, it is not absolutely clear whether short isoforms were present in the treated muscles or not since in the Fig shown in the paper only the high mw part of the Western blots are shown.

However, upregulation of full-length utrophin in non-muscle tissues may present a problem. If the idea that full-length utrophin binds with higher affinity to the DAPs is correct then, abnormally high levels of full-length utrophin might displace short isoforms, such as Up120 in kidney and G-utrophin in brain, from DAP complexes. Would the loss of these short isoforms matter? UKO^{ex64} mice do not show any signs of abnormal brain or kidney functioning and thus it is difficult to say whether Up120 and G-utrophin are important; however, it must be born in mind that in UKO^{ex64} mice short dystrophins might be compensating in brain and kidney and until a knock-out mouse deficient for all utrophins and all dystrophins has been generated this question will remain unanswered.

It would certainly be of interest to monitor the relative rates of synthesis of the various utrophin transcripts and rates of DNA replication in all tissues.

If small molecules or transcription factors which are specific to the muscle promoter are used to upregulate utrophin in DMD (or *mdx*) cells then no unexpected outcomes are likely.

7.5 Utrophin and disease

Although mouse models are a very useful tool to study the function of proteins and to predict the consequences of their absence, certain limitations exist; in some cases the phenotype of the mouse model does not closely resemble the human disorder (reviewed by Wynshaw-Boris et al., 1996), this is well illustrated by the relatively mild clinical phenotype of *mdx* mice compared to DMD patients. This could be due to differences in the contribution of modifier genes, longevity and gene regulation and expression. Differences exist in the embryonic pattern of expression of developmental and disease genes between mouse and men, for example, the *WNT7A* gene and the calpain 3 gene (*CAPN3* - the locus of limb-girdle muscular dystrophy 2A; Fourgerousse et al., 2000). Thus, the lack of an obvious phenotype in utrophin null mice does not necessarily mean that in humans, mutations in the utrophin gene are completely benign. Such condition would be inherited in an autosomal recessive fashion and would be relatively rare.

Bearing this in mind it is possible to speculate about potential pathologies caused by mutations in the utrophin gene. For example, given the high levels of full-length utrophin in brain and peripheral nerve and of G-utrophin in brain and ganglia, mutations in the utrophin gene could result in a form of hereditary

motor and sensory neuropathy (HMSN). Examples of autosomal recessive HMSN which have not been assigned a locus include; HMSN with excessive myelin folding complex (OMIM 256855), peripheral neuropathy and optic atrophy (OMIM 601152) and nerve deafness and distal neurogenic amyotrophy (OMIM 258650). Amongst these autosomal recessive HMSN there is one which is particularly interesting; HMSN with deafness, mental retardation and absent sensory large myelinated fibres (OMIM 214370). This represents an early onset peripheral neuropathy which was first reported by Mancardi et al. (1992) in two brothers whose parents were first cousins.

Both full-length utrophin and Up109 appear to localise to the epidermal-dermal junction in mouse embryos where they may take part of two different DAP complexes with different functions. Mutations in the utrophin gene might possibly result in an autosomal recessive form of epidermolysis bullosa (EB). This is a group of inherited mechano-bullous disorders characterised by blistering and erosions of the skin caused by separation of the epidermis from the dermis. This idea is attractive because mutations in both the plectin gene (OMIM 226670) and laminins $\alpha 3$, $\beta 3$ and $\gamma 2$ (OMIM 226700, 150310, 150292) are associated with EB.

In addition, given that a short utrophin transcript, Up140 or Up109, is expressed in the pyloric sphincter, it is also relevant to mention here that an autosomal recessive form of EB caused by mutations in either the $\alpha 6$ or $\beta 4$ integrin genes is associated with pyloric atresia (OMIM 226730) which is characterised by a membranous diaphragmatic obstruction of the pyloric lumen.

Since utrophin isoforms (Up140 or Up109) are also expressed in facial cartilages mutations could also result in facial dysmorphology.

The present study has shown that full-length utrophin, and maybe a short isoform(s), are expressed in the Leydig cells of the testis and therefore it is appropriate to discuss here the possible implications of utrophin deficiency in the context of infertility and/or hypogonadism. Leydig cells produce testosterone which enters the seminiferous tubules and triggers spermatogenesis (Bannister, Dyson, 1995). Testosterone and Leydig cell function are crucial for sperm production and abnormalities in its production lead to infertility/sexual disorders such as Kallman's syndrome (OMIM 14950) and the "fertile eunuch" syndrome (OMIM 228300). This syndrome is peculiar because patients are fertile but show markedly reduced serum levels of testosterone and LH, abnormalities in sperm count and mobility and hypogonadism.

In future studies it should be a priority to examine the UKO^{ex6} and UKO^{ex64} mice in more detail; to measure serum testosterone and LH levels and sperm count and to examine the morphology and mobility of sperm in both strains of UKO mice.

Finally, the detection of a short utrophin transcript in the semicircular canals of the developing inner ear is intriguing. Could mutations in the 3' end of the utrophin gene result in an autosomal recessive form of dysequilibrium or vestibulopathy? Such conditions do exist, for example, the dysequilibrium syndrome (OMIM 224050) which is an autosomal recessive trait characterised by disturbed dysequilibrium, mental retardation, severely retarded motor development and muscular hypotonia. Perhaps the possibility that utrophin could be involved in such disorders should not be overlooked.

References

- Abdulrazzak, H., Noro, N., Simons, J. P., Goldspink, G., Barnard, E. A., and Gorecki, D. C. (2001). Structural diversity despite strong evolutionary conservation in the 5'-untranslated region of the p-type dystrophin transcript. *Mol Cell Neurosci* **17**:500-513.
- Adams, M. E., Butler, M. H., Dwyer, T. M., Peters, M. F., Murnane, A. A., and Froehner, S. C. (1993). Two forms of mouse syntrophin, a 58 kd dystrophin-associated protein, differ in primary structure and tissue distribution. *Neuron* **11**:531-540.
- Adams, M. E., Kramarcy, N., Krall, S. P., Rossi, S. G., Rotundo, R. L., Sealock, R., and Froehner, S. C. (2000). Absence of alpha-syntrophin leads to structurally aberrant neuromuscular synapses deficient in utrophin. *J Cell Biol* **150**:1385-1398.
- Ahn, A. H. and Kunkel, L. M. (1995). Syntrophin binds to an alternatively spliced exon of dystrophin. *J Cell Biol* **128**:363-371.
- Allen, D. L. and Leinwand, L. A. (2001). Postnatal myosin heavy chain isoform expression in normal mice and mice null for IIb or IId myosin heavy chains. *Dev Biol* **229**:383-395.
- Amann, K. J., Renley, B. A., and Ervasti, J. M. (1998). A cluster of basic repeats in the dystrophin rod domain binds F-actin through an electrostatic interaction. *J Biol Chem* **273**:28419-28423.
- Amann, K. J., Guo, A. W., and Ervasti, J. M. (1999). Utrophin lacks the rod domain actin binding activity of dystrophin. *J Biol Chem* **274**:35375-35380.
- Ambrose, H. J., Blake, D. J., Nawrotzki, R. A., and Davies, K. E. (1997). Genomic organization of the mouse dystrobrevin gene: comparative analysis with the dystrophin gene. *Genomics* **39**:359-369.
- Anderson, J. T., Rogers, R. P., and Jarrett, H. W. (1996). Ca²⁺-calmodulin binds to the carboxyl-terminal domain of dystrophin. *J Biol Chem* **271**:6605-6610.
- Arahata, K., Hoffman, E. P., Kunkel, L. M., Ishiura, S., Tsukahara, T., Ishihara, T., Sunohara, N., Nonaka, I., Ozawa, E., and Sugita, H. (1989). Dystrophin diagnosis: comparison of dystrophin abnormalities by immunofluorescence and immunoblot analyses. *Proc Natl Acad Sci U S A* **86**:7154-7158.

- Araishi, K., Sasaoka, T., Imamura, M., Noguchi, S., Hama, H., Wakabayashi, E., Yoshida, M., Hori, T., and Ozawa, E. (1999). Loss of the sarcoglycan complex and sarcospan leads to muscular dystrophy in beta-sarcoglycan-deficient mice. *Hum Mol Genet* **8**:1589-1598.
- Araki, E., Nakamura, K., Nakao, K., Kameya, S., Kobayashi, O., Nonaka, I., Kobayashi, T., and Katsuki, M. (1997). Targeted disruption of exon 52 in the mouse dystrophin gene induced muscle degeneration similar to that observed in Duchenne muscular dystrophy. *Biochem Biophys Res Commun* **238**:492-497.
- Arsanto, J. P., Caubit, X., Rivier, F., Hugon, G., Thouveny, Y., and Mornet, D. (1999). Expression patterns of dystrophin products, especially of apodystrophin-1/Dp71, in the neural retina of Amphibian urodele *Pleurodeles waltl*. *Int J Dev Biol* **43**:75-83.
- Austin, R. C., Morris, G. E., Howard, P. L., Klamut, H. J., and Ray, P. N. (2000). Expression and synthesis of alternatively spliced variants of Dp71 in adult human brain. *Neuromuscul Disord* **10**:187-193.
- Bally-Cuif, L., Goridis, C., and Santoni, M. J. (1993). The mouse NCAM gene displays a biphasic expression pattern during neural tube development. *Development* **117**:543-552.
- Baltimore, D. (2001). Our genome unveiled. *Nature* **409**:814-816.
- Baluja, C., I, Brito Moreno, A. I., Amores, S., I, and Acosta, B. C. (2000). Production and characterization of specific monoclonal antibodies of the human thyroid stimulating hormone [In Process Citation]. *Hybridoma* **19**:335-338.
- Bank, C., Soulimane, T., Schroder, J. M., Buse, G., and Zanssen, S. (2000). Multiple deletions of mtDNA remove the light strand origin of replication. *Biochem Biophys Res Commun* **279**:595-601.
- Bannister L.H. and Dyson M. (1995). Reproductive system. In "Gray's Anatomy" (Williams P.L, Ed.), pp. 1853, Churchill Livingstone.
- Bannister L.H. (1995). Integumental system. In "Gray's Anatomy" (Williams P.L, Ed.), pp. 397, Churchill Livingstone.
- Bannister L.H. (1995). Alimentary System. In "Gray's Anatomy" (Williams P.L, Ed.), pp. 1683-1812, Churchill Livingstone.

- Banwell, B. L., Russel, J., Fukudome, T., Shen, X. M., Stilling, G., and Engel, A. G. (1999). Myopathy, myasthenic syndrome, and epidermolysis bullosa simplex due to plectin deficiency. *J Neuropathol Exp Neurol* **58**:832-846.
- Bar, S., Barnea, E., Levy, Z., Neuman, S., Yaffe, D., and Nudel, U. (1990). A novel product of the Duchenne muscular dystrophy gene which greatly differs from the known isoforms in its structure and tissue distribution. *Biochem J* **272**:557-560.
- Bardoni, A., Felisari, G., Sironi, M., Comi, G., Lai, M., Robotti, M., and Bresolin, N. (2000). Loss of Dp140 regulatory sequences is associated with cognitive impairment in dystrophinopathies. *Neuromuscul Disord* **10**:194-199.
- Barlow, J. H., Lowe, N., Edwards, Y. H., and Butterworth, P. H. (1987). Human carbonic anhydrase I cDNA. *Nucleic Acids Res* **15**:2386.
- Bartlett, R. J., Stockinger, S., Denis, M. M., Bartlett, W. T., Inverardi, L., Le, T. T., thi, M. N., Morris, G. E., Bogan, D. J., Metcalf-Bogan, J., and Kornegay, J. N. (2000). In vivo targeted repair of a point mutation in the canine dystrophin gene by a chimeric RNA/DNA oligonucleotide. *Nat Biotechnol* **18**:615-622.
- Barton-Davis, E. R., Cordier, L., Shoturma, D. I., Leland, S. E., and Sweeney, H. L. (1999). Aminoglycoside antibiotics restore dystrophin function to skeletal muscles of mdx mice. *J Clin Invest* **104**:375-381.
- Beggs, A. H., Hoffman, E. P., Snyder, J. R., Arahata, K., Specht, L., Shapiro, F., Angelini, C., Sugita, H., and Kunkel, L. M. (1991). Exploring the molecular basis for variability among patients with Becker muscular dystrophy: dystrophin gene and protein studies. *Am J Hum Genet* **49**:54-67.
- Bennett, V. (1990). Spectrin-based membrane skeleton: a multipotential adaptor between plasma membrane and cytoplasm. *Physiol Rev* **70**:1029-1065.
- Berry, M. M., Stranding S.M., and Bannister L.H. (1995). Nervous System. In "Gray's Anatomy" (Williams P.L, Ed.), pp. 901-1398, Churchill Livingstone.
- Bessou, C., Giuglia, J. B., Franks, C. J., Holden-Dye, L., and Segalat, L. (1998). Mutations in the *Caenorhabditis elegans* dystrophin-like gene *dys-1* lead to hyperactivity and suggest a link with cholinergic transmission. *Neurogenetics* **2**:61-72.

- Bewick, G. S., Nicholson, L. V., Young, C., O'Donnell, E., and Slater, C. R. (1992). Different distributions of dystrophin and related proteins at nerve- muscle junctions. *Neuroreport* **3**:857-860.
- Bia, B. L., Cassidy, P. J., Young, M. E., Rafael, J. A., Leighton, B., Davies, K. E., Radda, G. K., and Clarke, K. (1999). Decreased myocardial nNOS, increased iNOS and abnormal ECGs in mouse models of Duchenne muscular dystrophy. *J Mol Cell Cardiol* **31**:1857-1862.
- Bienz, M., Saari, G., Tremml, G., Muller, J., Zust, B., and Lawrence, P. A. (1988). Differential regulation of Ultrabithorax in two germ layers of *Drosophila*. *Cell* **53**:567-576.
- Bies, R. D., Phelps, S. F., Cortez, M. D., Roberts, R., Caskey, C. T., and Chamberlain, J. S. (1992). Human and murine dystrophin mRNA transcripts are differentially expressed during skeletal muscle, heart, and brain development. *Nucleic Acids Res* **20**:1725-1731.
- Biggin, M. D. and Tjian, R. (1988). Transcription factors that activate the Ultrabithorax promoter in developmentally staged extracts. *Cell* **53**:699-711.
- Bijlmakers, M. J. and Marsh, M. (2000). Hsp90 is essential for the synthesis and subsequent membrane association, but not the maintenance, of the Src-kinase p56(lck). *Mol Biol Cell* **11**:1585-1595.
- Blake, D. J., Love, D. R., Tinsley, J., Morris, G. E., Turley, H., Gatter, K., Dickson, G., Edwards, Y. H., and Davies, K. E. (1992). Characterization of a 4.8kb transcript from the Duchenne muscular dystrophy locus expressed in Schwannoma cells. *Hum Mol Genet* **1**:103-109.
- Blake, D. J., Tinsley, J. M., and Davies, K. (1994). The emerging family of dystrophin-related proteins. *Trends in Cell Biology* **4**:19-23.
- Blake, D. J., Schofield, J. N., Zuellig, R. A., Gorecki, D. C., Phelps, S. R., Barnard, E. A., Edwards, Y. H., and Davies, K. E. (1995). G-utrophin, the autosomal homologue of dystrophin Dp116, is expressed in sensory ganglia and brain. *Proc Natl Acad Sci U S A* **92**:3697-3701.

- Blake, D. J., Nawrotzki, R., Peters, M. F., Froehner, S. C., and Davies, K. E. (1996a). Isoform diversity of dystrobrevin, the murine 87-kDa postsynaptic protein. *J Biol Chem* **271**:7802-7810.
- Blake, D. J., Tinsley, J. M., and Davies, K. E. (1996b). Utrophin: a structural and functional comparison to dystrophin. *Brain Pathol* **6**:37-47.
- Blake, D. J., Nawrotzki, R., Loh, N. Y., Gorecki, D. C., and Davies, K. E. (1998). beta-dystrobrevin, a member of the dystrophin-related protein family. *Proc Natl Acad Sci U S A* **95**:241-246.
- Blake, D. J., Hawkes, R., Benson, M. A., and Beesley, P. W. (1999). Different dystrophin-like complexes are expressed in neurons and glia. *J Cell Biol* **147**:645-658.
- Bloch, R. J. and Morrow, J. S. (1989). An unusual beta-spectrin associated with clustered acetylcholine receptors. *J Cell Biol* **108**:481-493.
- Bogan, J. A., Natale, D. A., and Depamphilis, M. L. (2000). Initiation of eukaryotic DNA replication: conservative or liberal? *J Cell Physiol* **184**:139-150.
- Boland, B. J., Silbert, P. L., Groover, R. V., Wollan, P. C., and Silverstein, M. D. (1996). Skeletal, cardiac, and smooth muscle failure in Duchenne muscular dystrophy. *Pediatr Neurol* **14**:7-12.
- Bonnemann, C. G., Modi, R., Noguchi, S., Mizuno, Y., Yoshida, M., Gussoni, E., McNally, E. M., Duggan, D. J., Angelini, C., and Hoffman, E. P. (1995). Beta-sarcoglycan (A3b) mutations cause autosomal recessive muscular dystrophy with loss of the sarcoglycan complex. *Nat Genet* **11**:266-273.
- Bossone, S. A., Asselin, C., Patel, A. J., and Marcu, K. B. (1992). MAZ, a zinc finger protein, binds to c-MYC and C2 gene sequences regulating transcriptional initiation and termination. *Proc Natl Acad Sci U S A* **89**:7452-7456.
- Boxer, L. M., Miwa, T., Gustafson, T. A., and Kedes, L. (1989). Identification and characterization of a factor that binds to two human sarcomeric actin promoters. *J Biol Chem* **264**:1284-1292.
- Boyce, F. M., Beggs, A. H., Feener, C., and Kunkel, L. M. (1991). Dystrophin is transcribed in brain from a distant upstream promoter. *Proc Natl Acad Sci U S A* **88**:1276-1280.

Breitbart, R. E. and Nadal-Ginard, B. (1987). Developmentally induced, muscle-specific trans factors control the differential splicing of alternative and constitutive troponin T exons. *Cell* **49**:793-803.

Brenman, J. E., Chao, D. S., Xia, H., Aldape, K., and Brecht, D. S. (1995). Nitric oxide synthase complexed with dystrophin and absent from skeletal muscle sarcolemma in Duchenne muscular dystrophy. *Cell* **82**:743-752.

Brenman, J. E., Chao, D. S., Gee, S. H., McGee, A. W., Craven, S. E., Santillano, D. R., Wu, Z., Huang, F., Xia, H., Peters, M. F., Froehner, S. C., and Brecht, D. S. (1996). Interaction of nitric oxide synthase with the postsynaptic density protein PSD-95 and alpha1-syntrophin mediated by PDZ domains. *Cell* **84**:757-767.

Bretscher, A. and Weber, K. (1980). Fimbrin, a new microfilament-associated protein present in microvilli and other cell surface structures. *J Cell Biol* **86**:335-340.

Brown, S. C. and Lucy, J. A. (1993). Dystrophin as a mechanochemical transducer in skeletal muscle. *Bioessays* **15**:413-419.

Brussee, V., Tardif, F., Roy, B., Goulet, M., Sebille, A., and Tremblay, J. P. (1999). Successful myoblast transplantation in fibrotic muscles: no increased impairment by the connective tissue. *Transplantation* **67**:1618-1622.

Buchberger, A., Schroder, H., Hestekamp, T., Schonfeld, H. J., and Bukau, B. (1996). Substrate shuttling between the DnaK and GroEL systems indicates a chaperone network promoting protein folding. *J Mol Biol* **261**:328-333.

Buckle, V. J., Guenet, J. L., Simon-Chazottes, D., Love, D. R., and Davies, K. E. (1990). Localisation of a dystrophin-related autosomal gene to 6q24 in man, and to mouse chromosome 10 in the region of the dystrophin muscularis (dy) locus. *Hum Genet* **85**:324-326.

Bulfield, G., Siller, W. G., Wight, P. A., and Moore, K. J. (1984). X chromosome-linked muscular dystrophy (mdx) in the mouse. *Proc Natl Acad Sci U S A* **81**:1189-1192.

Burke, T. W. and Kadonaga, J. T. (1997). The downstream core promoter element, DPE, is conserved from *Drosophila* to humans and is recognized by TAFII60 of *Drosophila*. *Genes Dev* **11**:3020-3031.

- Burridge, K. and Feramisco, J. R. (1981). Non-muscle alpha actinins are calcium-sensitive actin-binding proteins. *Nature* **294**:565-567.
- Burton, E. A., Tinsley, J. M., Holzfeind, P. J., Rodrigues, N. R., and Davies, K. E. (1999). A second promoter provides an alternative target for therapeutic up-regulation of utrophin in Duchenne muscular dystrophy. *Proc Natl Acad Sci U S A* **96**:14025-14030.
- Bushby, K. M., Gardner-Medwin, D., Nicholson, L. V., Johnson, M. A., Haggerty, I. D., Cleghorn, N. J., Harris, J. B., and Bhattacharya, S. S. (1993). The clinical, genetic and dystrophin characteristics of Becker muscular dystrophy. II. Correlation of phenotype with genetic and protein abnormalities. *J Neurol* **240**:105-112.
- Bushby, K. M., Appleton, R., Anderson, L. V., Welch, J. L., Kelly, P., and Gardner-Medwin, D. (1995). Deletion status and intellectual impairment in Duchenne muscular dystrophy. *Dev Med Child Neurol* **37**:260-269.
- Bushby, K. M., Hill, A., and Steele, J. G. (1999). Failure of early diagnosis in symptomatic Duchenne muscular dystrophy. *Lancet* **353**:557-558.
- Byers, T. J., Kunkel, L. M., and Watkins, S. C. (1991). The subcellular distribution of dystrophin in mouse skeletal, cardiac, and smooth muscle. *J Cell Biol* **115**:411-421.
- Byers, T. J., Lidov, H. G., and Kunkel, L. M. (1993). An alternative dystrophin transcript specific to peripheral nerve. *Nat Genet* **4**:77-81.
- Campbell, K. P. and Kahl, S. D. (1989). Association of dystrophin and an integral membrane glycoprotein. *Nature* **338**:259-262.
- Carlson B.M. (1994), Human Embryology and Developmental Biology, Mosby.
- Carr, C., Fischbach, G. D., and Cohen, J. B. (1989). A novel 87,000-Mr protein associated with acetylcholine receptors in Torpedo electric organ and vertebrate skeletal muscle. *J Cell Biol* **109**:1753-1764.
- Carugo, K. D., Banuelos, S., and Saraste, M. (1997). Crystal structure of a calponin homology domain [letter]. *Nat Struct Biol* **4**:175-179.
- Catty, D, (1989), Antibodies: a practical approach, Oxford University Press.

- Chan, R. Y., Boudreau-Lariviere, C., Angus, L. M., Mankal, F. A., and Jasmin, B. J. (1999). An intronic enhancer containing an N-box motif is required for synapse- and tissue-specific expression of the acetylcholinesterase gene in skeletal muscle fibers. *Proc Natl Acad Sci U S A* **96**:4627-4632.
- Chao, D. S., Gorospe, J. R., Brenman, J. E., Rafael, J. A., Peters, M. F., Froehner, S. C., Hoffman, E. P., Chamberlain, J. S., and Bredt, D. S. (1996). Selective loss of sarcolemmal nitric oxide synthase in Becker muscular dystrophy. *J Exp Med* **184**:609-618.
- Chapman, V. M., Miller, D. R., Armstrong, D., and Caskey, C. T. (1989). Recovery of induced mutations for X chromosome-linked muscular dystrophy in mice. *Proc Natl Acad Sci U S A* **86**:1292-1296.
- Chaubourt, E., Fossier, P., Baux, G., Leprince, C., Israel, M., and de La, P. S. (1999). Nitric oxide and l-arginine cause an accumulation of utrophin at the sarcolemma: a possible compensation for dystrophin loss in Duchenne muscular dystrophy. *Neurobiol Dis* **6**:499-507.
- Chaubourt, E., Voisin, V., Fossier, P., Baux, G., Israel, M., and de La, P. S. (2000). The NO way to increase muscular utrophin expression? *C R Acad Sci III* **323**:735-740.
- Chelly, J., Kaplan, J. C., Maire, P., Gautron, S., and Kahn, A. (1988). Transcription of the dystrophin gene in human muscle and non-muscle tissue. *Nature* **333**:858-860.
- Chelly, J., Gilgenkrantz, H., Lambert, M., Hamard, G., Chafey, P., Recan, D., Katz, P., de la Chapelle, A., Koenig, M., and Ginjaar, I. B. (1990). Effect of dystrophin gene deletions on mRNA levels and processing in Duchenne and Becker muscular dystrophies. *Cell* **63**:1239-1248.
- Chelly, J., Hamard, G., Koulakoff, A., Kaplan, J. C., Kahn, A., and Berwald-Netter, Y. (1990). Dystrophin gene transcribed from different promoters in neuronal and glial cells. *Nature* **344**:64-65.
- Chen, D. H., Takeshima, Y., Ishikawa, Y., Ishikawa, Y., Minami, R., and Matsuo, M. (1999). A novel deletion of the dystrophin S-promoter region cosegregating with mental retardation. *Neurology* **52**:638-640.

- Chen, H. I. and Sudol, M. (1995). The WW domain of Yes-associated protein binds a proline-rich ligand that differs from the consensus established for Src homology 3-binding modules. *Proc Natl Acad Sci U S A* **92**:7819-7823.
- Chiurazzi, P., Pomponi, M. G., Pietrobono, R., Bakker, C. E., Neri, G., and Oostra, B. A. (1999). Synergistic effect of histone hyperacetylation and DNA demethylation in the reactivation of the FMR1 gene. *Hum Mol Genet* **8**:2317-2323.
- Chong, S., Montello, G. E., Zhang, A., Cantor, E. J., Liao, W., Xu, M. Q., and Benner, J. (1998). Utilizing the C-terminal cleavage activity of a protein splicing element to purify recombinant proteins in a single chromatographic step. *Nucleic Acids Res* **26**:5109-5115.
- Christova, T., Grozdanovic, Z., and Gossrau, R. (1997). Nitric oxide synthase (NOS) I during postnatal development in rat and mouse skeletal muscle. *Acta Histochem* **99**:311-324.
- Claudepierre, T., Mornet, D., Pannicke, T., Forster, V., Dalloz, C., Bolanos, F., Sahel, J., Reichenbach, A., and Rendon, A. (2000). Expression of Dp71 in Muller glial cells: a comparison with utrophin- and dystrophin-associated proteins. *Invest Ophthalmol Vis Sci* **41**:294-304.
- Claudepierre, T., Rodius, F., Frasson, M., Fontaine, V., Picaud, S., Dreyfus, H., Mornet, D., and Rendon, A. (1999). Differential distribution of dystrophins in rat retina. *Invest Ophthalmol Vis Sci* **40**:1520-1529.
- Clayton, D. A. (1992). Transcription and replication of animal mitochondrial DNAs. *Int Rev Cytol* **141**:217-232.
- Clerk, A., Strong, P. N., and Sewry, C. A. (1992). Characterisation of dystrophin during development of human skeletal muscle. *Development* **114**:395-402.
- Clerk, A., Morris, G. E., Dubowitz, V., Davies, K. E., and Sewry, C. A. (1993). Dystrophin-related protein, utrophin, in normal and dystrophic human fetal skeletal muscle. *Histochem J* **25**:554-561.
- Cohen, D. R., Ferreira, P. C., Gentz, R., Franza, B. R., and Curran, T. (1989). The product of a fos-related gene, fra-1, binds cooperatively to the AP-1 site with Jun: transcription factor AP-1 is comprised of multiple protein complexes. *Genes Dev* **3**:173-184.

- Coleman, T. R., Fishkind, D. J., Mooseker, M. S., and Morrow, J. S. (1989). Contributions of the beta-subunit to spectrin structure and function. *Cell Motil Cytoskeleton* **12**:248-263.
- Corrado, K., Rafael, J. A., Mills, P. L., Cole, N. M., Faulkner, J. A., Wang, K., and Chamberlain, J. S. (1996). Transgenic mdx mice expressing dystrophin with a deletion in the actin-binding domain display a "mild Becker" phenotype. *J Cell Biol* **134**:873-884.
- Cox, G. A., Cole, N. M., Matsumura, K., Phelps, S. F., Hauschka, S. D., Campbell, K. P., Faulkner, J. A., and Chamberlain, J. S. (1993a). Overexpression of dystrophin in transgenic mdx mice eliminates dystrophic symptoms without toxicity. *Nature* **364**:725-729.
- Cox, G. A., Phelps, S. F., Chapman, V. M., and Chamberlain, J. S. (1993b). New mdx mutation disrupts expression of muscle and nonmuscle isoforms of dystrophin. *Nat Genet* **4**:87-93.
- Cox, G. A., Sunada, Y., Campbell, K. P., and Chamberlain, J. S. (1994). Dp71 can restore the dystrophin-associated glycoprotein complex in muscle but fails to prevent dystrophy [see comments]. *Nat Genet* **8**:333-339.
- Creighton, T. E. , (1997), Protein Structure: a practical approach, IRL Press
- Crosbie, R. H., Heighway, J., Venzke, D. P., Lee, J. C., and Campbell, K. P. (1997). Sarcospan, the 25-kDa transmembrane component of the dystrophin-glycoprotein complex. *J Biol Chem* **272**:31221-31224.
- Crosbie, R. H., Lebakken, C. S., Holt, K. H., Venzke, D. P., Straub, V., Lee, J. C., Grady, R. M., Chamberlain, J. S., Sanes, J. R., and Campbell, K. P. (1999). Membrane targeting and stabilization of sarcospan is mediated by the sarcoglycan subcomplex. *J Cell Biol* **145**:153-165.
- D'Souza, V. N., Nguyen, T. M., Morris, G. E., Karges, W., Pillers, D. A., and Ray, P. N. (1995). A novel dystrophin isoform is required for normal retinal electrophysiology. *Hum Mol Genet* **4**:837-842.
- Danieli, G. A. and Barbujani, G. (1984). Duchenne muscular dystrophy. Frequency of sporadic cases. *Hum Genet* **67**:252-256.

Davies, K. E., Smith, T. J., Bunday, S., Read, A. P., Flint, T., Bell, M., and Speer, A. (1988). Mild and severe muscular dystrophy associated with deletions in Xp21 of the human X chromosome. *J Med Genet* **25**:9-13.

Davis, R. L., Cheng, P. F., Lassar, A. B., and Weintraub, H. (1990). The MyoD DNA binding domain contains a recognition code for muscle-specific gene activation. *Cell* **60**:733-746.

Davison, M. D. and Critchley, D. R. (1988). alpha-Actinins and the DMD protein contain spectrin-like repeats [letter]. *Cell* **52**:159-160.

DeChiara, T. M., Bowen, D. C., Valenzuela, D. M., Simmons, M. V., Poueymirou, W. T., Thomas, S., Kinetz, E., Compton, D. L., Rojas, E., Park, J. S., Smith, C., DiStefano, P. S., Glass, D. J., Burden, S. J., and Yancopoulos, G. D. (1996). The receptor tyrosine kinase MuSK is required for neuromuscular junction formation in vivo. *Cell* **85**:501-512.

Deconinck, A. E., Potter, A. C., Tinsley, J. M., Wood, S. J., Vater, R., Young, C., Metzinger, L., Vincent, A., Slater, C. R., and Davies, K. E. (1997a). Postsynaptic abnormalities at the neuromuscular junctions of utrophin- deficient mice. *J Cell Biol* **136**:883-894.

Deconinck, A. E., Rafael, J. A., Skinner, J. A., Brown, S. C., Potter, A. C., Metzinger, L., Watt, D. J., Dickson, J. G., Tinsley, J. M., and Davies, K. E. (1997b). Utrophin-dystrophin-deficient mice as a model for Duchenne muscular dystrophy. *Cell* **90**:717-727.

Deconinck, N., Tinsley, J., De Backer, F., Fisher, R., Kahn, D., Phelps, S., Davies, K., and Gillis, J. M. (1997). Expression of truncated utrophin leads to major functional improvements in dystrophin-deficient muscles of mice. *Nat Med* **3**:1216-1221.

Deconinck, N., Rafael, J. A., Beckers-Bleukx, G., Kahn, D., Deconinck, A. E., Davies, K. E., and Gillis, J. M. (1998). Consequences of the combined deficiency in dystrophin and utrophin on the mechanical properties and myosin composition of some limb and respiratory muscles of the mouse. *Neuromuscul Disord* **8**:362-370.

Delves, P. J., (1997), Antibody production: essential techniques, John Wiley and Sons.

Demarchez, M., Hartman, D.J., Herbage D., VilleG., Prunieras M. (1987). Wound healing of skin transplanted onto the nude mouse. II. An immunohistological and

ultrastructural study of the epidermal basement membrane zone reconstruction and connective tissue reorganization. *Dev Biol* **121**: 119-29

Denduchis, B., Schteingart, H., Cigorraga, S., Vianello, S. E., Casanova, M. B., and Lustig, L. (1996). Immunodetection of cell adhesion molecules and extracellular matrix proteins in rat Leydig cell cultures. *Int J Androl* **19**:353-361.

Dennis, C. L., Tinsley, J. M., Deconinck, A. E., and Davies, K. E. (1996). Molecular and functional analysis of the utrophin promoter. *Nucleic Acids Res* **24**:1646-1652.

DeWolf, C., McCauley, P., Sikorski, A. F., Winlove, C. P., Bailey, A. I., Kahana, E., Pinder, J. C., and Gratzner, W. B. (1997). Interaction of dystrophin fragments with model membranes. *Biophys J* **72**:2599-2604.

Dixon, A. K., Tait, T. M., Campbell, E. A., Bobrow, M., Roberts, R. G., and Freeman, T. C. (1997). Expression of the dystrophin-related protein 2 (Drp2) transcript in the mouse. *J Mol Biol* **270**:551-558.

Dodson, H. C., Piper, T. A., Clarke, J. D., Quinlivan, R. M., and Dickson, G. (1995). Dystrophin expression in the hair cells of the cochlea. *J Neurocytol* **24**:625-632.

Dorbani-Mamine, L., Stoeckel, M. E., Jancsik, V., Ayad, G., and Rendon, A. (1998). Dystrophins in neurohypophysial lobe of normal and dehydrated rats: immunolocalization and biochemical characterization. *Neuroreport* **9**:3583-3587.

Duclert, A., Savatier, N., Schaeffer, L., and Changeux, J. P. (1996). Identification of an element crucial for the sub-synaptic expression of the acetylcholine receptor epsilon-subunit gene. *J Biol Chem* **271**:17433-17438.

Duclos, F., Straub, V., Moore, S. A., Venzke, D. P., Hrstka, R. F., Crosbie, R. H., Durbeej, M., Lebakken, C. S., Ettinger, A. J., van der, M. J., Holt, K. H., Lim, L. E., Sanes, J. R., Davidson, B. L., Faulkner, J. A., Williamson, R., and Campbell, K. P. (1998). Progressive muscular dystrophy in alpha-sarcoglycan-deficient mice. *J Cell Biol* **142**:1461-1471.

Duhaiman, A. S. and Bamberg, J. R. (1984). Isolation of brain alpha-actinin. Its characterization and a comparison of its properties with those of muscle alpha-actinins. *Biochemistry* **23**:1600-1608.

Dunbar B.S. (1994), Protein blotting: A practical approach, IRL Press

- Dunckley, M. G., Wells, K. E., Piper, T. A., Wells, D. J., and Dickson, G. (1994). Independent localization of dystrophin N- and C-terminal regions to the sarcolemma of mdx mouse myofibres in vivo. *J Cell Sci* **107**:1469-1475.
- Dunckley, M. G., Manoharan, M., Villiet, P., Eperon, I. C., and Dickson, G. (1998). Modification of splicing in the dystrophin gene in cultured Mdx muscle cells by antisense oligoribonucleotides. *Hum Mol Genet* **7**:1083-1090.
- Durbeej, M., Jung, D., Hjalt, T., Campbell, K. P., and Ekblom, P. (1997). Transient expression of Dp140, a product of the Duchenne muscular dystrophy locus, during kidney tubulogenesis. *Dev Biol* **181**:156-167.
- Durbeej, M., Henry, M. D., Ferletta, M., Campbell, K. P., and Ekblom, P. (1998). Distribution of dystroglycan in normal adult mouse tissues. *J Histochem Cytochem* **46**:449-457.
- Durbeej, M. and Campbell, K. P. (1999). Biochemical characterization of the epithelial dystroglycan complex. *J Biol Chem* **274**:26609-26616.
- Durbeej, M., Cohn, R. D., Hrstka, R. F., Moore, S. A., Allamand, V., Davidson, B. L., Williamson, R. A., and Campbell, K. P. (2000). Disruption of the beta-sarcoglycan gene reveals pathogenetic complexity of limb-girdle muscular dystrophy type 2E. *Mol Cell* **5**:141-151.
- Dwi Pramono, Z. A., Takeshima, Y., Surono, A., Ishida, T., and Matsuo, M. (2000). A novel cryptic exon in intron 2 of the human dystrophin gene evolved from an intron by acquiring consensus sequences for splicing at different stages of anthropoid evolution. *Biochem Biophys Res Commun* **267**:321-328.
- Dyson M. (1995). Urinary System. In "Gray's Anatomy" (Williams P.L, Ed.), pp. 1813-1846, Churchill Livingstone.
- Ebihara, S., Guibinga, G. H., Gilbert, R., Nalbantoglu, J., Massie, B., Karpati, G., and Petrof, B. J. (2000) Differential effects of dystrophin and utrophin gene transfer in immunocompetent muscular dystrophy (mdx) mice *Physiol Genomics* **3**:133-144.
- Eddy, S. R. (1999). Noncoding RNA genes. *Curr Opin Genet Dev* **9**:695-699.
- Ellis, R. J. and van der Vies, S. M. (1991). Molecular chaperones. *Annu Rev Biochem* **60**:321-347.

Emery, A. E. (1991). Population frequencies of inherited neuromuscular diseases--a world survey. *Neuromuscul Disord* **1**:19-29.

England, S. B., Nicholson, L. V., Johnson, M. A., Forrest, S. M., Love, D. R., Zubrzycka-Gaarn, E. E., Bulman, D. E., Harris, J. B., and Davies, K. E. (1990). Very mild muscular dystrophy associated with the deletion of 46% of dystrophin. *Nature* **343**:180-182.

Erdmann, V. A., Szymanski, M., Hochberg, A., de Groot, N., and Barciszewski, J. (1999). Collection of mRNA-like non-coding RNAs. *Nucleic Acids Res* **27**:192-195.

Ervasti, J. M., Ohlendieck, K., Kahl, S. D., Gaver, M. G., and Campbell, K. P. (1990). Deficiency of a glycoprotein component of the dystrophin complex in dystrophic muscle. *Nature* **345**:315-319.

Ervasti, J. M., Kahl, S. D., and Campbell, K. P. (1991). Purification of dystrophin from skeletal muscle. *J Biol Chem* **266**:9161-9165.

Ervasti, J. M. and Campbell, K. P. (1991). Membrane organization of the dystrophin-glycoprotein complex. *Cell* **66**:1121-1131.

Fabrizio, E., Latouche, J., Rivier, F., Hugon, G., and Mornet, D. (1995). Re-evaluation of the distributions of dystrophin and utrophin in sciatic nerve. *Biochem J* **312**:309-314.

Fanin, M., Melacini, P., Angelini, C., and Danieli, G. A. (1999). Could utrophin rescue the myocardium of patients with dystrophin gene mutations? *J Mol Cell Cardiol* **31**:1501-1508.

Fardeau, M., Tome, F. M., Collin, H., Augier, N., Pons, F., Leger, J., and Leger, J. (1990). [Presence of dystrophine-like protein at the neuromuscular junction in Duchenne muscular dystrophy and in "mdx" mutant mice] Presence d'une proteine de type dystrophine au niveau de la jonction neuromusculaire dans la dystrophie musculaire de Duchenne et la souris mutante "mdx". *C R Acad Sci III* **311**:197-204.

Feener, C. A., Koenig, M., and Kunkel, L. M. (1989). Alternative splicing of human dystrophin mRNA generates isoforms at the carboxy terminus. *Nature* **338**:509-511.

Ferlini, A., Sewry, C., Melis, M. A., Mateddu, A., and Muntoni, F. (1999). X-linked dilated cardiomyopathy and the dystrophin gene. *Neuromuscul Disord* **9**:339-346.

Ferns, M., Deiner, M., and Hall, Z. (1996). Agrin-induced acetylcholine receptor clustering in mammalian muscle requires tyrosine phosphorylation. *J Cell Biol* **132**:937-944.

Fitzgerald, K. M., Cibis, G. W., Giambone, S. A., and Harris, D. J. (1994). Retinal signal transmission in Duchenne muscular dystrophy: evidence for dysfunction in the photoreceptor/depolarizing bipolar cell pathway. *J Clin Invest* **93**:2425-2430.

Fougerousse, F., Bullen, P., Herasse, M., Lindsay, S., Richard, I., Wilson, D., Suel, L., Durand, M., Robson, S., Abitbol, M., Beckmann, J. S., and Strachan, T. (2000). Human-mouse differences in the embryonic expression patterns of developmental control genes and disease genes. *Hum Mol Genet* **9**:165-173.

Frangioni, J. V. and Neel, B. G. (1993). Solubilization and purification of enzymatically active glutathione S-transferase (pGEX) fusion proteins. *Anal Biochem* **210**:179-187.

Frischmeyer, P. A. and Dietz, H. C. (1999). Nonsense-mediated mRNA decay in health and disease. *Hum Mol Genet* **8**:1893-1900.

Froehner, S. C. (1991). The submembrane machinery for nicotinic acetylcholine receptor clustering. *J Cell Biol* **114**:1-7.

Frohman, M. A. (1993). Rapid amplification of complementary DNA ends for generation of full-length complementary DNAs: thermal RACE. *Methods Enzymol* **218**:340-356.

Fuchs, P., Zorer, M., Reznicek, G. A., Spazierer, D., Oehler, S., Castanon, M. J., Hauptmann, R., and Wiche, G. (1999). Unusual 5' transcript complexity of plectin isoforms: novel tissue-specific exons modulate actin binding activity. *Hum Mol Genet* **8**:2461-2472.

Galvagni, F. and Oliviero, S. (2000). Utrophin transcription is activated by an intronic enhancer. *J Biol Chem* **275**:3168-3172.

Galvagni, F., Capo, S., and Oliviero, S. (2001). Sp1 and Sp3 physically interact and cooperate with GABP for the activation of the utrophin promoter. *J Mol Biol* **306**:985-996.

Gautam, M., Noakes, P. G., Moscoso, L., Rupp, F., Scheller, R. H., Merlie, J. P., and Sanes, J. R. (1996). Defective neuromuscular synaptogenesis in agrin-deficient mutant mice. *Cell* **85**:525-535.

Gautam, M., DeChiara, T. M., Glass, D. J., Yancopoulos, G. D., and Sanes, J. R. (1999). Distinct phenotypes of mutant mice lacking agrin, MuSK, or rapsyn. *Brain Res Dev Brain Res* **114**:171-178.

Geng, Y., Sicinski, P., Gorecki, D., and Barnard, P. J. (1991). Developmental and tissue-specific regulation of mouse dystrophin: the embryonic isoform in muscular dystrophy. *Neuromuscul Disord* **1**:125-133.

Gilbert, R., Nalbanoglu, J., Tinsley, J. M., Massie, B., Davies, K. E., and Karpati, G. (1998). Efficient utrophin expression following adenovirus gene transfer in dystrophic muscle. *Biochem Biophys Res Commun* **242**:244-247.

Gilbert, R., Nalbantoglu, J., Petrof, B. J., Ebihara, S., Guibinga, G. H., Tinsley, J. M., Kamen, A., Massie, B., Davies, K. E., and Karpati, G. (1999). Adenovirus-mediated utrophin gene transfer mitigates the dystrophic phenotype of mdx mouse muscles. *Hum Gene Ther* **10**:1299-1310.

Gofflot, F., Hall, M., and Morriss-Kay, G. M. (1998). Genetic patterning of the posterior neuropore region of curly tail mouse embryos: deficiency of Wnt5a expression. *Int J Dev Biol* **42**:637-644.

Gonzalez, E., Montanez, C., Ray, P. N., Howard, P. L., Garcia-Sierra, F., Mornet, D., and Cisneros, B. (2000). Alternative splicing regulates the nuclear or cytoplasmic localization of dystrophin Dp71. *FEBS Lett* **482**:209-214.

Gorecki, D., Geng, Y., Thomas, K., Hunt, S. P., Barnard, E. A., and Barnard, P. J. (1991). Expression of the dystrophin gene in mouse and rat brain. *Neuroreport* **2**:773-776.

Gorecki, D. C., Monaco, A. P., Derry, J. M., Walker, A. P., Barnard, E. A., and Barnard, P. J. (1992). Expression of four alternative dystrophin transcripts in brain regions regulated by different promoters. *Hum Mol Genet* **1**:505-510.

Gorecki, D. C. and Barnard, E. A. (1995). Specific expression of G-dystrophin (Dp71) in the brain. *Neuroreport* **6**:893-896.

Grady, R. M., Merlie, J. P., and Sanes, J. R. (1997a). Subtle neuromuscular defects in utrophin-deficient mice. *J Cell Biol* **136**:871-882.

Grady, R. M., Teng, H., Nichol, M. C., Cunningham, J. C., Wilkinson, R. S., and Sanes, J. R. (1997b). Skeletal and cardiac myopathies in mice lacking utrophin and dystrophin: a model for Duchenne muscular dystrophy. *Cell* **90**:729-738.

Grady, R. M., Zhou, H., Cunningham, J. M., Henry, M. D., Campbell, K. P., and Sanes, J. R. (2000) Maturation and maintenance of the neuromuscular synapse: genetic evidence for roles of the dystrophin--glycoprotein complex. *Neuron* **25**:279-293.

Gramolini, A. O., Dennis, C. L., Tinsley, J. M., Robertson, G. S., Cartaud, J., Davies, K. E., and Jasmin, B. J. (1997). Local transcriptional control of utrophin expression at the neuromuscular synapse. *J Biol Chem* **272**:8117-8120.

Gramolini, A. O., Burton, E. A., Tinsley, J. M., Ferns, M. J., Cartaud, A., Cartaud, J., Davies, K. E., Lunde, J. A., and Jasmin, B. J. (1998). Muscle and neural isoforms of agrin increase utrophin expression in cultured myotubes via a transcriptional regulatory mechanism. *J Biol Chem* **273**:736-743.

Gramolini, A. O., Angus, L. M., Schaeffer, L., Burton, E. A., Tinsley, J. M., Davies, K. E., Changeux, J. P., and Jasmin, B. J. (1999a). Induction of utrophin gene expression by heregulin in skeletal muscle cells: role of the N-box motif and GA binding protein. *Proc Natl Acad Sci U S A* **96**:3223-3227.

Gramolini, A. O., Karpati, G., and Jasmin, B. J. (1999b). Discordant expression of utrophin and its transcript in human and mouse skeletal muscles. *J Neuropathol Exp Neurol* **58**:235-244.

Gramolini, A. O. and Jasmin, B. J. (1999c). Expression of the utrophin gene during myogenic differentiation. *Nucleic Acids Res* **27**:3603-3609.

Gramolini, A. O., Wu, J., and Jasmin, B. J. (2000). Regulation and functional significance of utrophin expression at the mammalian neuromuscular synapse. *Microsc Res Tech* **49**:90-100.

Greenberg, D. S., Sunada, Y., Campbell, K. P., Yaffe, D., and Nudel, U. (1994). Exogenous Dp71 restores the levels of dystrophin associated proteins but does not alleviate muscle damage in mdx mice [see comments]. *Nat Genet* **8**:340-344.

Grossman, L. I. and Shoubridge, E. A. (1996). Mitochondrial genetics and human disease. *Bioessays* **18**:983-991.

GST, Gene Fusion System; Instructions Booklet, (1999), Amersham Pharmacia Biotech.

Guo, W. X., Nichol, M., and Merlie, J. P. (1996). Cloning and expression of full length mouse utrophin: the differential association of utrophin and dystrophin with AChR clusters. *FEBS Lett* **398**:259-264.

Gussoni, E., Soneoka, Y., Strickland, C. D., Buzney, E. A., Khan, M. K., Flint, A. F., Kunkel, L. M., and Mulligan, R. C. (1999). Dystrophin expression in the mdx mouse restored by stem cell transplantation. *Nature* **401**:390-394.

Gutman, A. and Wasylyk, B. (1990). The collagenase gene promoter contains a TPA and oncogene-responsive unit encompassing the PEA3 and AP-1 binding sites. *EMBO J* **9**:2241-2246.

Hall, B. K. and Miyake, T. (2000). All for one and one for all: condensations and the initiation of skeletal development. *Bioessays* **22**:138-147.

Hanks, M., Wurst, W., Anson-Cartwright, L., Auerbach, A. B., and Joyner, A. L. (1995). Rescue of the En-1 mutant phenotype by replacement of En-1 with En-2 [see comments]. *Science* **269**:679-682.

Harris R.A and Crabb D.W (1997). Metabolic interrelationships. In "Textbook of Biochemistry with clinical correlations" (Devlin T.M., Ed.), pp. 525, Wiley-Liss.

Hashida-Okumura, A., Okumura, N., Iwamatsu, A., Buijs, R. M., Romijn, H. J., and Nagai, K. (1999). Interaction of neuronal nitric-oxide synthase with alpha1-syntrophin in rat brain. *J Biol Chem* **274**:11736-11741.

Helliwell, T. R., Man, N. T., Morris, G. E., and Davies, K. E. (1992). The dystrophin-related protein, utrophin, is expressed on the sarcolemma of regenerating human skeletal muscle fibres in dystrophies and inflammatory myopathies. *Neuromuscul Disord* **2**:177-184.

Henry, M. D. and Campbell, K. P. (1998). A role for dystroglycan in basement membrane assembly. *Cell* **95**:859-870.

Hillier, B. J., Christopherson, K. S., Prehoda, K. E., Bretz, D. S., and Lim, W. A. (1999). Unexpected modes of PDZ domain scaffolding revealed by structure of nNOS-syntrophin complex. *Science* **284**:812-815.

- Hoffman, E. P., Brown, R. H. J., and Kunkel, L. M. (1987a). Dystrophin: the protein product of the Duchenne muscular dystrophy locus. *Cell* **51**:919-928.
- Hoffman, E. P., Knudson, C. M., Campbell, K. P., and Kunkel, L. M. (1987b). Subcellular fractionation of dystrophin to the triads of skeletal muscle. *Nature* **330**:754-758.
- Hoffman, E. P., Kunkel, L. M., and Brown, R. H. J. (1988). Proteolytic fragment or new gene product? [letter]. *Nature* **336**:210.
- Hoffman, E. P., Beggs, A. H., Koenig, M., Kunkel, L. M., and Angelini, C. (1989a). Cross-reactive protein in Duchenne muscle *Lancet* **2**:1211-1212.
- Hoffman, E. P., Watkins, S. C., Slayter, H. S., and Kunkel, L. M. (1989b). Detection of a specific isoform of alpha-actinin with antisera directed against dystrophin. *J Cell Biol* **108**:503-510.
- Holzfeind, P. J., Ambrose, H. J., Newey, S. E., Nawrotzki, R. A., Blake, D. J., and Davies, K. E. (1999). Tissue-selective expression of alpha-dystrobrevin is determined by multiple promoters. *J Biol Chem* **274**:6250-6258.
- Hopkins CR and Duncan CJ., (1979), *Secretory mechanisms*, Cambridge University Press.
- Hori, S., Ohtani, S., Nguyen, T. M., and Morris, G. E. (1995). The N-terminal half of dystrophin is protected from proteolysis in situ. *Biochem Biophys Res Commun* **209**:1062-1067.
- Houzelstein, D., Lyons, G. E., Chamberlain, J., and Buckingham, M. E. (1992). Localization of dystrophin gene transcripts during mouse embryogenesis. *J Cell Biol* **119**:811-821.
- Howard, P. L., Dally, G. Y., Ditta, S. D., Austin, R. C., Worton, R. G., Klamut, H. J., and Ray, P. N. (1999). Dystrophin isoforms DP71 and DP427 have distinct roles in myogenic cells. *Muscle Nerve* **22**:16-27.
- Hu, R. J., Watanabe, M., and Bennett, V. (1992). Characterization of human brain cDNA encoding the general isoform of beta-spectrin. *J Biol Chem* **267**:18715-18722.

Hu, X. Y., Ray, P. N., Murphy, E. G., Thompson, M. W., and Worton, R. G. (1990). Duplicational mutation at the Duchenne muscular dystrophy locus: its frequency, distribution, origin, and phenotype-genotype correlation. *Am J Hum Genet* **46**:682-695.

Huang, X., Poy, F., Zhang, R., Joachimiak, A., Sudol, M., and Eck, M. J. (2000). Structure of a WW domain containing fragment of dystrophin in complex with beta-dystroglycan. *Nat Struct Biol* **7**:634-638.

Hugnot, J. P., Gilgenkrantz, H., Vincent, N., Chafey, P., Morris, G. E., Monaco, A. P., Berwald-Netter, Y., Koulakoff, A., Kaplan, J. C., and Kahn, A. (1992). Distal transcript of the dystrophin gene initiated from an alternative first exon and encoding a 75-kDa protein widely distributed in nonmuscle tissues. *Proc Natl Acad Sci U S A* **89**:7506-7510.

Hull, M. G., Glazener, C. M., Kelly, N. J., Conway, D. I., Foster, P. A., Hinton, R. A., Coulson, C., Lambert, P. A., Watt, E. M., and Desai, K. M. (1985). Population study of causes, treatment, and outcome of infertility. *Br Med J (Clin Res Ed)* **291**:1693-1697.

Husen, B., Giebel, J., and Rune, G. (1999). Expression of the integrin subunits alpha 5, alpha 6 and beta 1 in the testes of the common marmoset. *Int J Androl* **22**:374-384.

Ikuta, T., Ausenda, S., and Cappellini, M. D. (2001). Mechanism for fetal globin gene expression: role of the soluble guanylate cyclase-cGMP-dependent protein kinase pathway. *Proc Natl Acad Sci U S A* **98**:1847-1852.

Imamura, M. and Ozawa, E. (1998). Differential expression of dystrophin isoforms and utrophin during dibutyryl-cAMP-induced morphological differentiation of rat brain astrocytes. *Proc Natl Acad Sci U S A* **95**:6139-6144.

Imamura, M., Araishi, K., Noguchi, S., and Ozawa, E. (2000). A sarcoglycan-dystroglycan complex anchors Dp116 and utrophin in the peripheral nervous system. *Hum Mol Genet* **9**:3091-3100.

Jackson, S. M., Keech, C. A., Williamson, D. J., and Gutierrez-Hartmann, A. (1992). Interaction of basal positive and negative transcription elements controls repression of the proximal rat prolactin promoter in nonpituitary cells. *Mol Cell Biol* **12**:2708-2719.

Jacobson, C., Cote, P., Rossi, S., Rotundo, R., and Carbonetto, S. (2001). The Dystroglycan Complex Is Necessary for Stabilization of Acetylcholine Receptor

Clusters at Neuromuscular Junctions and Formation of the Synaptic Basement Membrane. *J Cell Biol* **152**:435-450.

James, M., Nuttall, A., Ilsley, J. L., Ottersbach, K., Tinsley, J. M., Sudol, M., and Winder, S. J. (2000). Adhesion-dependent tyrosine phosphorylation of (beta)-dystroglycan regulates its interaction with utrophin. *J Cell Sci* **113**:1717-1726.

Jane, S. M. and Cunningham, J. M. (1998). Understanding fetal globin gene expression: a step towards effective HbF reactivation in haemoglobinopathies. *Br J Haematol* **102**:415-422.

Johnson, K. R., Cook, S. A., Erway, L. C., Matthews, A. N., Sanford, L. P., Paradies, N. E., and Friedman, R. A. (1999). Inner ear and kidney anomalies caused by IAP insertion in an intron of the *Eya1* gene in a mouse model of BOR syndrome. *Hum Mol Genet* **8**:645-653.

Jowett T (1999). Two colour in situ hybridization. *In* "In situ hybridization: A practical approach" (Wilkinson D.G., Ed.), pp. 107-126, Oxford University Press..

Jung, D., Filliol, D., Metz-Boutigue, M. H., and Rendon, A. (1993). Characterization and subcellular localization of the dystrophin-protein 71 (Dp71) from brain. *Neuromuscul Disord* **3**:515-518.

Jung, D., Yang, B., Meyer, J., Chamberlain, J. S., and Campbell, K. P. (1995). Identification and characterization of the dystrophin anchoring site on beta-dystroglycan. *J Biol Chem* **270**:27305-27310.

Kachinsky, A. M., Froehner, S. C., and Milgram, S. L. (1999). A PDZ-containing scaffold related to the dystrophin complex at the basolateral membrane of epithelial cells. *J Cell Biol* **145**:391-402.

Kalaydjieva, L., Hallmayer, J., Chandler, D., Savov, A., Nikolova, A., Angelicheva, D., King, R. H., Ishpekova, B., Honeyman, K., Calafell, F., Shmarov, A., Petrova, J., Turnev, I., Hristova, A., Moskov, M., Stancheva, S., Petkova, I., Bittles, A. H., Georgieva, V., Middleton, L., and Thomas, P. K. (1996). Gene mapping in Gypsies identifies a novel demyelinating neuropathy on chromosome 8q24. *Nat Genet* **14**:214-217.

Kalaydjieva, L., Gresham, D., Gooding, R., Heather, L., Baas, F., de Jonge, R., Blechschmidt, K., Angelicheva, D., Chandler, D., Worsley, P., Rosenthal, A., King, R.

- H., and Thomas, P. K. (2000). N-myc downstream-regulated gene 1 is mutated in hereditary motor and sensory neuropathy-Lom. *Am J Hum Genet* **67**:47-58.
- Kamakura, K., Tadano, Y., Kawai, M., Ishiura, S., Nakamura, R., Miyamoto, K., Nagata, N., and Sugita, H. (1994). Dystrophin-related protein is found in the central nervous system of mice at various developmental stages, especially at the postsynaptic membrane. *J Neurosci Res* **37**:728-734.
- Kameya, S., Araki, E., Katsuki, M., Mizota, A., Adachi, E., Nakahara, K., Nonaka, I., Sakuragi, S., Takeda, S., and Nabeshima, Y. (1997). Dp260 disrupted mice revealed prolonged implicit time of the b-wave in ERG and loss of accumulation of beta-dystroglycan in the outer plexiform layer of the retina. *Hum Mol Genet* **6**:2195-2203.
- Kameya, S., Miyagoe, Y., Nonaka, I., Ikemoto, T., Endo, M., Hanaoka, K., Nabeshima, Y., and Takeda, S. (1999). alpha1-syntrophin gene disruption results in the absence of neuronal-type nitric-oxide synthase at the sarcolemma but does not induce muscle degeneration. *J Biol Chem* **274**:2193-2200.
- Kapust, R. B. and Waugh, D. S. (1999). Escherichia coli maltose-binding protein is uncommonly effective at promoting the solubility of polypeptides to which it is fused. *Protein Sci* **8**:1668-1674.
- Karp G. Cell and Molecular Biology, 2nd ed, 1999, John Wiley & Sons.
- Karpati, G., Carpenter, S., Morris, G. E., Davies, K. E., Guerin, C., and Holland, P. (1993). Localization and quantitation of the chromosome 6-encoded dystrophin-related protein in normal and pathological human muscle. *J Neuropathol Exp Neurol* **52**:119-128.
- Kaufman M.H., (1992), The Atlas of Mouse Development, Academic Press.
- Keep, N. H., Norwood, F. L., Moores, C. A., Winder, S. J., and Kendrick-Jones, J. (1999). The 2.0 A structure of the second calponin homology domain from the actin-binding region of the dystrophin homologue utrophin. *J Mol Biol* **285**:1257-1264.
- Khurana, T. S., Watkins, S. C., Chafey, P., Chelly, J., Tome, F. M., Fardeau, M., Kaplan, J. C., and Kunkel, L. M. (1991). Immunolocalization and developmental expression of dystrophin related protein in skeletal muscle. *Neuromuscul Disord* **1**:185-194.

Khurana, T. S., Watkins, S. C., and Kunkel, L. M. (1992). The subcellular distribution of chromosome 6-encoded dystrophin-related protein in the brain. *J Cell Biol* **119**:357-366.

Khurana, T. S., Prendergast, R. A., Alameddine, H. S., Tome, F. M., Fardeau, M., Arahata, K., Sugita, H., and Kunkel, L. M. (1995a). Absence of extraocular muscle pathology in Duchenne's muscular dystrophy: role for calcium homeostasis in extraocular muscle sparing. *J Exp Med* **182**:467-475.

Khurana, T. S., Kunkel, L. M., Frederickson, A. D., Carbonetto, S., and Watkins, S. C. (1995b). Interaction of chromosome-6-encoded dystrophin related protein with the extracellular matrix. *J Cell Sci* **108**:173-185.

Kieny, M., Pautou, M. P., Chevallier, A., and Mauger, A. (1986). Spatial organization of the developing limb musculature in birds and mammals. *Bibl Anat* 65-90.

Kim, J. J., Wang, J., Bambra, C., Das, S. K., Dey, S. K., and Fazleabas, A. T. (1999). Expression of cyclooxygenase-1 and -2 in the baboon endometrium during the menstrual cycle and pregnancy. *Endocrinology* **140**:2672-2678.

Klamut, H. J., Gangopadhyay, S. B., Worton, R. G., and Ray, P. N. (1990). Molecular and functional analysis of the muscle-specific promoter region of the Duchenne muscular dystrophy gene. *Mol Cell Biol* **10**:193-205.

Klamut, H. J., Bosnoyan-Collins, L. O., Worton, R. G., and Ray, P. N. (1997). A muscle-specific enhancer within intron 1 of the human dystrophin gene is functionally dependent on single MEF-1/E box and MEF-2/AT-rich sequence motifs. *Nucleic Acids Res* **25**:1618-1625.

Klausner, R. D., Rouault, T. A., and Harford, J. B. (1993). Regulating the fate of mRNA: the control of cellular iron metabolism. *Cell* **72**:19-28.

Knuesel, I., Mastrocola, M., Zuellig, R. A., Bornhauser, B., Schaub, M. C., and Fritschy, J. M. (1999). Short communication: altered synaptic clustering of GABA_A receptors in mice lacking dystrophin (mdx mice). *Eur J Neurosci* **11**:4457-4462.

Knuesel, I., Bornhauser, B. C., Zuellig, R. A., Heller, F., Schaub, M. C., and Fritschy, J. M. (2000). Differential expression of utrophin and dystrophin in CNS neurons: an in situ hybridization and immunohistochemical study. *J Comp Neurol* **422**:594-611.

Knuesel, I., Zuellig, R. A., Schaub, M. C., and Fritschy, J. M. (2001). Alterations in dystrophin and utrophin expression parallel the reorganization of GABAergic synapses in a mouse model of temporal lobe epilepsy. *Eur J Neurosci* **13**:1113-1124.

Kobzik, L., Reid, M. B., Bredt, D. S., and Stamler, J. S. (1994). Nitric oxide in skeletal muscle. *Nature* **372**:546-548.

Koenig, M. (1987). Complete cloning of the Duchenne muscular dystrophy (DMD) cDNA and preliminary genomic organization of the DMD gene in normal and affected individuals. *Cell* **50**:509-517.

Koenig, M., Monaco, A. P., and Kunkel, L. M. (1988). The complete sequence of dystrophin predicts a rod-shaped cytoskeletal protein. *Cell* **53**:219-226.

Koenig, M., Beggs, A. H., Moyer, M., Scherpf, S., Heindrich, K., Bettecken, T., Meng, G., Muller, C. R., Lindlof, M., and Kaariainen, H. (1989). The molecular basis for Duchenne versus Becker muscular dystrophy: correlation of severity with type of deletion. *Am J Hum Genet* **45**:498-506.

Koenig, M. and Kunkel, L. M. (1990). Detailed analysis of the repeat domain of dystrophin reveals four potential hinge segments that may confer flexibility. *J Biol Chem* **265**:4560-4566.

Koga, R., Ishiura, S., Takemitsu, M., Kamakura, K., Matsuzaki, T., Arahata, K., Nonaka, I., and Sugita, H. (1993). Immunoblot analysis of dystrophin-related protein (DRP). *Biochim Biophys Acta* **1180**:257-261.

Koike, S., Schaeffer, L., and Changeux, J. P. (1995). Identification of a DNA element determining synaptic expression of the mouse acetylcholine receptor delta-subunit gene. *Proc Natl Acad Sci U S A* **92**:10624-10628.

Koteliansky, V. E., Shirinsky, V. P., Gneushev, G. N., and Smirnov, V. N. (1981). Filamin, a high relative molecular mass actin-binding protein from smooth muscles, promotes actin polymerization. *FEBS Lett* **136**:98-100.

Kozak, M. (1995). Adherence to the first-AUG rule when a second AUG codon follows closely upon the first [published erratum appears in Proc Natl Acad Sci U S A 1995 Jul 18;92(15):7134]. *Proc Natl Acad Sci U S A* **92**:2662-2666.

- Kramarcy, N. R., Vidal, A., Froehner, S. C., and Sealock, R. (1994). Association of utrophin and multiple dystrophin short forms with the mammalian M(r) 58,000 dystrophin-associated protein (syntrophin). *J Biol Chem* **269**:2870-2876.
- Kramarcy, N. R. and Sealock, R. Syntrophin isoforms at the neuromuscular junction: developmental time course and differential localization. (2000) *Mol Cell Neurosci* **15**:262-274.
- Krebs, C. J., Dey, B., and Kumar, G. (1996). The cerebellum-enriched form of nuclear factor I is functionally different from ubiquitous nuclear factor I in glial-specific promoter regulation. *J Neurochem* **66**:1354-1361.
- Kruh, J. (1982). Effects of sodium butyrate, a new pharmacological agent, on cells in culture. *Mol Cell Biochem* **42**:65-82.
- Kubota, S., Kondo, S., Eguchi, T., Hattori, T., Nakanishi, T., Pomerantz, R. J., and Takigawa, M. (2000). Identification of an RNA element that confers post-transcriptional repression of connective tissue growth factor/hypertrophic chondrocyte specific 24 (ctgf/hcs24) gene: similarities to retroviral RNA-protein interactions [In Process Citation]. *Oncogene* **19**:4773-4786.
- Laemmli, U. K., Beguin, F., and Gujer-Kellenberger, G. (1970). A factor preventing the major head protein of bacteriophage T4 from random aggregation. *J Mol Biol* **47**:69-85.
- Lalwani, A. K., Brister, J. R., Fex, J., Grundfast, K. M., Pikus, A. T., Ploplis, B., San Agustin, T., Skarka, H., and Wilcox, E. R. (1994). A new nonsyndromic X-linked sensorineural hearing impairment linked to Xp21.2. *Am J Hum Genet* **55**:685-694.
- Lambert, M., Chafey, P., Hugnot, J. P., Koulakoff, A., Berwald-Netter, Y., Billard, C., Morris, G. E., Kahn, A., Kaplan, J. C., and Gilgenkrantz, H. (1993). Expression of the transcripts initiated in the 62nd intron of the dystrophin gene. *Neuromuscul Disord* **3**:519-524.
- Larsson, S. H., Charlieu, J. P., Miyagawa, K., Engelkamp, D., Rassoulzadegan, M., Ross, A., Cuzin, F., van Heyningen, V., and Hastie, N. D. (1995). Subnuclear localization of WT1 in splicing or transcription factor domains is regulated by alternative splicing. *Cell* **81**:391-401.

Lassar, A. B., Davis, R. L., Wright, W. E., Kadesch, T., Murre, C., Voronova, A., Baltimore, D., and Weintraub, H. (1991). Functional activity of myogenic HLH proteins requires hetero-oligomerization with E12/E47-like proteins in vivo. *Cell* **66**:305-315.

LaVallie, E. R., DiBlasio, E. A., Kovacic, S., Grant, K. L., Schendel, P. F., and McCoy, J. M. (1993). A thioredoxin gene fusion expression system that circumvents inclusion body formation in the *E. coli* cytoplasm. *Biotechnology (N Y)* **11**:187-193.

Laverriere, A. C., MacNeill, C., Mueller, C., Poelmann, R. E., Burch, J. B., and Evans, T. (1994). GATA-4/5/6, a subfamily of three transcription factors transcribed in developing heart and gut. *J Biol Chem* **269**:23177-23184.

Law, D. J., Allen, D. L., and Tidball, J. G. (1994). Talin, vinculin and DRP (utrophin) concentrations are increased at mdx myotendinous junctions following onset of necrosis. *J Cell Sci* **107**:1477-1483.

Lederfein, D., Levy, Z., Augier, N., Mornet, D., Morris, G., Fuchs, O., Yaffe, D., and Nudel, U. (1992). A 71-kilodalton protein is a major product of the Duchenne muscular dystrophy gene in brain and other nonmuscle tissues. *Proc Natl Acad Sci U S A* **89**:5346-5350.

Lederfein, D., Yaffe, D., and Nudel, U. (1993). A housekeeping type promoter, located in the 3' region of the Duchenne muscular dystrophy gene, controls the expression of Dp71, a major product of the gene. *Hum Mol Genet* **2**:1883-1888.

Lenk, U., Hanke, R., Thiele, H., and Speer, A. (1993). Point mutations at the carboxy terminus of the human dystrophin gene: implications for an association with mental retardation in DMD patients. *Hum Mol Genet* **2**:1877-1881.

Lescaudron, L., Peltekian, E., Fontaine-Perus, J., Paulin, D., Zampieri, M., Garcia, L., and Parrish, E. (1999). Blood borne macrophages are essential for the triggering of muscle regeneration following muscle transplant. *Neuromuscul Disord* **9**:72-80.

Lidov, H. G., Byers, T. J., Watkins, S. C., and Kunkel, L. M. (1990). Localization of dystrophin to postsynaptic regions of central nervous system cortical neurons. *Nature* **348**:725-728.

Lidov, H. G., Selig, S., and Kunkel, L. M. (1995). Dp140: a novel 140 kDa CNS transcript from the dystrophin locus. *Hum Mol Genet* **4**:329-335.

- Lidov, H. G. and Kunkel, L. M. (1997). Dp140: alternatively spliced isoforms in brain and kidney. *Genomics* **45**:132-139.
- Lidov, H. G. and Kunkel, L. M. (1998). Dystrophin and Dp140 in the adult rodent kidney. *Lab Invest* **78**:1543-1551.
- Liechti-Gallati, S., Koenig, M., Kunkel, L. M., Frey, D., Boltshauser, E., Schneider, V., Braga, S., and Moser, H. (1989). Molecular deletion patterns in Duchenne and Becker type muscular dystrophy. *Hum Genet* **81**:343-348.
- Lin, C. S., Park, T., Chen, Z. P., and Leavitt, J. (1993). Human plastin genes. Comparative gene structure, chromosome location, and differential expression in normal and neoplastic cells. *J Biol Chem* **268**:2781-2792.
- Lin, S. and Burgunder, J. M. (2000). Utrophin may be a precursor of dystrophin during skeletal muscle development. *Brain Res Dev Brain Res* **119**:289-295.
- Loh, N. Y., Ambrose, H. J., Guay-Woodford, L. M., DasGupta, S., Nawrotzki, R. A., Blake, D. J., and Davies, K. E. (1998). Genomic organization and refined mapping of the mouse beta-dystrobrevin gene. *Mamm Genome* **9**:857-862.
- Loh, N. Y., Newey, S. E., Davies, K. E., and Blake, D. J. (2000). Assembly of multiple dystrobrevin-containing complexes in the kidney. *J Cell Sci* **113**:2715-2724.
- Loo, M. A., Jensen, T. J., Cui, L., Hou, Y., Chang, X. B., and Riordan, J. R. (1998). Perturbation of Hsp90 interaction with nascent CFTR prevents its maturation and accelerates its degradation by the proteasome. *EMBO J* **17**:6879-6887.
- Love, D. R., Hill, D. F., Dickson, G., Spurr, N. K., Byth, B. C., Marsden, R. F., Walsh, F. S., Edwards, Y. H., and Davies, K. E. (1989). An autosomal transcript in skeletal muscle with homology to dystrophin. *Nature* **339**:55-58.
- Love, D. R., Morris, G. E., Ellis, J. M., Fairbrother, U., Marsden, R. F., Bloomfield, J. F., Edwards, Y. H., Slater, C. P., Parry, D. J., and Davies, K. E. (1991). Tissue distribution of the dystrophin-related gene product and expression in the mdx and dy mouse. *Proc Natl Acad Sci U S A* **88**:3243-3247.
- Lu, B. D., Allen, D. L., Leinwand, L. A., and Lyons, G. E. (1999). Spatial and temporal changes in myosin heavy chain gene expression in skeletal muscle development. *Dev Biol* **216** :312-326.

- Lumeng, C. N., Phelps, S. F., Rafael, J. A., Cox, G. A., Hutchinson, T. L., Begy, C. R., Adkins, E., Wiltshire, R., and Chamberlain, J. S. (1999). Characterization of dystrophin and utrophin diversity in the mouse *Hum Mol Genet* **8**:593-599.
- Lustig, L. R., Hiel, H., and Fuchs, P. A. (1999). Vestibular hair cells of the chick express the nicotinic acetylcholine receptor subunit alpha 9. *J Vestib Res* **9**:359-367.
- Lyons, G. E., Ontell, M., Cox, R., Sassoon, D., and Buckingham, M. (1990). The expression of myosin genes in developing skeletal muscle in the mouse embryo. *J Cell Biol* **111**:1465-1476.
- Lysakowski, A. and Singer, M. (2000). Nitric oxide synthase localized in a subpopulation of vestibular efferents with NADPH diaphorase histochemistry and nitric oxide synthase immunohistochemistry. *J Comp Neurol* **427**:508-521.
- Macias, M. J., Hyvonen, M., Baraldi, E., Schultz, J., Sudol, M., Saraste, M., and Oschkinat, H. (1996). Structure of the WW domain of a kinase-associated protein complexed with a proline-rich peptide. *Nature* **382**:646-649.
- Mackie, E. J., Halfter, W., and Liverani, D. (1988). Induction of tenascin in healing wounds. *J Cell Biol* **107**:2757-2767.
- MacLennan, P. A. and Edwards, R. H. (1990). Protein turnover is elevated in muscle of mdx mice in vivo. *Biochem J* **268**:795-797.
- Mancardi, G. L., Di Rocco, M., Schenone, A., Veneselli, E., Doria, M., Abbruzzese, M., Tabaton, M., and Borroni, C. (1992). Hereditary motor and sensory neuropathy with deafness, mental retardation and absence of large myelinated fibers. *J Neurol Sci* **110**:121-130.
- Manilal, S., Recan, D., Sewry, C. A., Hoeltzenbein, M., Llense, S., Leturcq, F., Deburgrave, N., Barbot, J., Man, N., Muntoni, F., Wehnert, M., Kaplan, J., and Morris, G. E. (1998). Mutations in Emery-Dreifuss muscular dystrophy and their effects on emerin protein expression. *Hum Mol Genet* **7**:855-864.
- Mann, C. J., Honeyman, K., Cheng, A. J., Ly, T., Lloyd, F., Fletcher, S., Morgan, J. E., Partridge, T. A., and Wilton, S. D. (2001). Antisense-induced exon skipping and synthesis of dystrophin in the mdx mouse. *Proc Natl Acad Sci U S A* **98**:42-47.

Mantovani, R., Malgaretti, N., Nicolis, S., Giglioni, B., Comi, P., Cappellini, N., Bertero, M. T., Caligaris-Cappio, F., and Ottolenghi, S. (1988). An erythroid specific nuclear factor binding to the proximal CACCC box of the beta-globin gene promoter. *Nucleic Acids Res* **16**:4299-4313.

Mar, J. H. and Ordahl, C. P. (1990). M-CAT binding factor, a novel trans-acting factor governing muscle-specific transcription. *Mol Cell Biol* **10**:4271-4283.

Masaki, T., Matsumura, K., Hirata, A., Yamada, H., Hase, A., Shimizu, T., Yorifuji, H., Motoyoshi, K., and Kamakura, K. (2001). Expression of dystroglycan complex in satellite cells of dorsal root ganglia. *Acta Neuropathol (Berl)* **101**:174-178.

Mather, J. P. (1982). Ceruloplasmin, a copper-transport protein, can act as a growth promoter for some cell lines in serum-free medium. *In Vitro* **18**:990-996.

Matsumura, K., Ervasti, J. M., Ohlendieck, K., Kahl, S. D., and Campbell, K. P. (1992). Association of dystrophin-related protein with dystrophin-associated proteins in mdx mouse muscle. *Nature* **360**:588-591.

Matsumura, K., Yamada, H., Shimizu, T., and Campbell, K. P. (1993a). Differential expression of dystrophin, utrophin and dystrophin-associated proteins in peripheral nerve. *FEBS Lett* **334**:281-285.

Matsumura, K., Shasby, D. M., and Campbell, K. P. (1993b). Purification of dystrophin-related protein (utrophin) from lung and its identification in pulmonary artery endothelial cells. *FEBS Lett* **326**:289-293.

McKay, B. S., Irving, P. E., Skumatz, C. M., and Burke, J. M. (1997). Cell-cell adhesion molecules and the development of an epithelial phenotype in cultured human retinal pigment epithelial cells. *Exp Eye Res* **65**:661-671.

McMahon, J. A., Takada, S., Zimmerman, L. B., Fan, C. M., Harland, R. M., and McMahon, A. P. (1998). Noggin-mediated antagonism of BMP signaling is required for growth and patterning of the neural tube and somite. *Genes Dev* **12**:1438-1452.

McNaughton, J. C., Cockburn, D. J., Hughes, G., Jones, W. A., Laing, N. G., Ray, P. N., Stockwell, P. A., and Petersen, G. B. (1998). Is gene deletion in eukaryotes sequence-dependent? A study of nine deletion junctions and nineteen other deletion breakpoints in intron 7 of the human dystrophin gene. *Gene* **222**:41-51.

- Megeney, L. A., Kablar, B., Garrett, K., Anderson, J. E., and Rudnicki, M. A. (1996). MyoD is required for myogenic stem cell function in adult skeletal muscle. *Genes Dev* **10**:1173-1183.
- Merlini, L., Villanova, M., Sabatelli, P., Trogu, A., Malandrini, A., Yanakiev, P., Maraldi, N. M., and Kalaydjieva, L. (1998). Hereditary motor and sensory neuropathy Lom type in an Italian Gypsy family. *Neuromuscul Disord* **8**:182-185.
- Miike, T., Miyatake, M., Zhao, J., Yoshioka, K., and Uchino, M. (1989). Immunohistochemical dystrophin reaction in synaptic regions. *Brain Dev* **11**:344-346.
- Milasin, J., Muntoni, F., Severini, G. M., Bartoloni, L., Vatta, M., Krajinovic, M., Mateddu, A., Angelini, C., Camerini, F., Falaschi, A., Mestroni, L., and Giacca, M. (1996). A point mutation in the 5' splice site of the dystrophin gene first intron responsible for X-linked dilated cardiomyopathy. *Hum Mol Genet* **5**:73-79.
- Milhaud, P. G., Nicolas, M. T., Bartolami, S., Cabanis, M. T., and Sans, A. (1999). Vestibular semicircular canal epithelium of the rat in culture on filter support: polarity and barrier properties. *Pflugers Arch* **437**:823-830.
- Miller, I. J. and Bieker, J. J. (1993). A novel, erythroid cell-specific murine transcription factor that binds to the CACCC element and is related to the Kruppel family of nuclear proteins. *Mol Cell Biol* **13**:2776-2786.
- Milner, R. E., Busaan, J. L., Holmes, C. F., Wang, J. H., and Michalak, M. (1993). Phosphorylation of dystrophin. The carboxyl-terminal region of dystrophin is a substrate for in vitro phosphorylation by p34cdc2 protein kinase. *J Biol Chem* **268**:21901-21905.
- Mimura, N. and Asano, A. (1987). Further characterization of a conserved actin-binding 27-kDa fragment of actinogelin and alpha-actinins and mapping of their binding sites on the actin molecule by chemical cross-linking. *J Biol Chem* **262**:4717-4723.
- Moizard, M. P., Billard, C., Toutain, A., Berret, F., Marmin, N., and Moraine, C. (1998). Are Dp71 and Dp140 brain dystrophin isoforms related to cognitive impairment in Duchenne muscular dystrophy? *Am J Med Genet* **80**:32-41.
- Monaco, A. P., Neve, R. L., Colletti-Feener, C., Bertelson, C. J., Kurnit, D. M., and Kunkel, L. M. (1986). Isolation of candidate cDNAs for portions of the Duchenne muscular dystrophy gene. *Nature* **323**:646-650.

Moores, C. A. and Kendrick-Jones, J. (2000). Biochemical characterisation of the actin-binding properties of utrophin. *Cell Motil Cytoskeleton* **46**:116-128.

Mora, M., Di Blasi, C., Barresi, R., Morandi, L., Brambati, B., Jarre, L., and Cornelio, F. (1996). Developmental expression of dystrophin, dystrophin-associated glycoproteins and other membrane cytoskeletal proteins in human skeletal and heart muscle. *Brain Res Dev Brain Res* **91**:70-82.

Morris, G. E., Sedgwick, S. G., Ellis, J. M., Pereboev, A., Chamberlain, J. S., and Nguyen, t. M. (1998). An epitope structure for the C-terminal domain of dystrophin and utrophin. *Biochemistry* **37**:11117-11127.

Morris, G. E., Nguyen, T. M., Nguyen, T. N., Pereboev, A., Kendrick-Jones, J., and Winder, S. J. (1999). Disruption of the utrophin-actin interaction by monoclonal antibodies and prediction of an actin-binding surface of utrophin. *Biochem J* **337**:119-123.

Moscoso, L. M., Chu, G. C., Gautam, M., Noakes, P. G., Merlie, J. P., and Sanes, J. R. (1995). Synapse-associated expression of an acetylcholine receptor-inducing protein, ARIA/heregulin, and its putative receptors, ErbB2 and ErbB3, in developing mammalian muscle. *Dev Biol* **172**:158-169.

Muntoni, F., Cau, M., Ganau, A., Congiu, R., Arvedi, G., Mateddu, A., Marrosu, M. G., Cianchetti, C., Realdi, G., Cao, A., and (1993). Brief report: deletion of the dystrophin muscle-promoter region associated with X-linked dilated cardiomyopathy. *N Engl J Med* **329**:921-925.

Muntoni, F., Gobbi, P., Sewry, C., Sherratt, T., Taylor, J., Sandhu, S. K., Abbs, S., Roberts, R., Hodgson, S. V., Bobrow, M., and (1994). Deletions in the 5' region of dystrophin and resulting phenotypes. *J Med Genet* **31**:843-847.

Muntoni, F., Wilson, L., Marrosu, G., Marrosu, M. G., Cianchetti, C., Mestroni, L., Ganau, A., Dubowitz, V., and Sewry, C. (1995). A mutation in the dystrophin gene selectively affecting dystrophin expression in the heart. *J Clin Invest* **96**:693-699.

Navankasattusas, S., Zhu, H., Garcia, A. V., Evans, S. M., and Chien, K. R. (1992). A ubiquitous factor (HF-1a) and a distinct muscle factor (HF-1b/MEF-2) form an E-box-independent pathway for cardiac muscle gene expression. *Mol Cell Biol* **12**:1469-1479.

- Nawrotzki, R., Loh, N. Y., Ruegg, M. A., Davies, K. E., and Blake, D. J. (1998). Characterisation of alpha-dystrobrevin in muscle. *J Cell Sci* **111**:2595-2605.
- Neu-Yilik, G., Gehring, N. H., Thermann, R., Frede, U., Hentze, M. W., and Kulozik, A. E. (2001). Splicing and 3' end formation in the definition of nonsense-mediated decay-competent human beta-globin mRNPs. *EMBO J* **20**:532-540.
- Neuman, S., Kaban, A., Volk, T., Yaffe, D., and Nudel, U. (2001). The dystrophin / utrophin homologues in *Drosophila* and in sea urchin. *Gene* **263**:17-29.
- Nguyen, T. M., Ellis, J. M., Love, D. R., Davies, K. E., Gatter, K. C., Dickson, G., and Morris, G. E. (1991). Localization of the DMDL gene-encoded dystrophin-related protein using a panel of nineteen monoclonal antibodies: presence at neuromuscular junctions, in the sarcolemma of dystrophic skeletal muscle, in vascular and other smooth muscles, and in proliferating brain cell lines. *J Cell Biol* **115**:1695-1700.
- Nguyen, T. M., Le, T. T., Blake, D. J., Davies, K. E., and Morris, G. E. (1992). Utrophin, the autosomal homologue of dystrophin, is widely-expressed and membrane-associated in cultured cell lines. *FEBS Lett* **313**:19-22.
- Nguyen, T. M., Helliwell, T. R., Simmons, C., Winder, S. J., Kendrick-Jones, J., Davies, K. E., and Morris, G. E. (1995). Full-length and short forms of utrophin, the dystrophin-related protein. *FEBS Lett* **358**:262-266.
- Nicholson, L. V., Bushby, K. M., Johnson, M. A., den Dunnen, J. T., Ginjaar, I. B., and van Ommen, G. J. (1992). Predicted and observed sizes of dystrophin in some patients with gene deletions that disrupt the open reading frame. *J Med Genet* **29**:892-896.
- Nicholson, L. V., Bushby, K. M., Johnson, M. A., Gardner-Medwin, D., and Ginjaar, I. B. (1993). Dystrophin expression in Duchenne patients with "in-frame" gene deletions. *Neuropediatrics* **24**:93-97.
- Nigro, V., Piluso, G., Belsito, A., Politano, L., Puca, A. A., Papparella, S., Rossi, E., Viglietto, G., Esposito, M. G., Abbondanza, C., Medici, N., Molinari, A. M., Nigro, G., and Puca, G. A. (1996). Identification of a novel sarcoglycan gene at 5q33 encoding a sarcolemmal 35 kDa glycoprotein. *Hum Mol Genet* **5**:1179-1186.
- Nishio, H., Takeshima, Y., Narita, N., Yanagawa, H., Suzuki, Y., Ishikawa, Y., Ishikawa, Y., Minami, R., Nakamura, H., and Matsuo, M. (1994). Identification of a novel first

exon in the human dystrophin gene and of a new promoter located more than 500 kb upstream of the nearest known promoter. *J Clin Invest* **94**:1037-1042.

Nobile, C., Galvagni, F., Marchi, J., Roberts, R., and Vitiello, L. (1995). Genomic organization of the human dystrophin gene across the major deletion hot spot and the 3' region. *Genomics* **28**:97-100.

Nobile, C., Marchi, J., Nigro, V., Roberts, R. G., and Danieli, G. A. (1997). Exon-intron organization of the human dystrophin gene. *Genomics* **45**:421-424.

Nomura, A., Shigemoto, R., Nakamura, Y., Okamoto, N., Mizuno, N., and Nakanishi, S. (1994). Developmentally regulated postsynaptic localization of a metabotropic glutamate receptor in rat rod bipolar cells. *Cell* **77**:361-369.

Nudel, U., Zuk, D., Einat, P., Zeelon, E., Levy, Z., Neuman, S., and Yaffe, D. (1989). Duchenne muscular dystrophy gene product is not identical in muscle and brain. *Nature* **337**:76-78.

Ogata, Y. and Slepecky, N. B. (1998). Immunocytochemical localization of calmodulin in the vestibular end-organs of the gerbil. *J Vestib Res* **8**:209-216.

Ohlendieck, K., Ervasti, J. M., Matsumura, K., Kahl, S. D., Leveille, C. J., and Campbell, K. P. (1991a). Dystrophin-related protein is localized to neuromuscular junctions of adult skeletal muscle. *Neuron* **7**:499-508.

Ohlendieck, K., Ervasti, J. M., Snook, J. B., and Campbell, K. P. (1991b). Dystrophin-glycoprotein complex is highly enriched in isolated skeletal muscle sarcolemma. *J Cell Biol* **112**:135-148.

Ohtsuka, Y., Udaka, K., Yamashiro, Y., Yagita, H., and Okumura, K. (1998). Dystrophin acts as a transplantation rejection antigen in dystrophin-deficient mice: implication for gene therapy. *J Immunol* **160**:4635-4640.

Ontell, M. and Kozeka, K. (1984). The organogenesis of murine striated muscle: a cytoarchitectural study. *Am J Anat* **171**:133-148.

Parks, C. L. and Shenk, T. (1996). The serotonin 1a receptor gene contains a TATA-less promoter that responds to MAZ and Sp1. *J Biol Chem* **271**:4417-4430.

Partridge, T. A., Morgan, J. E., Coulton, G. R., Hoffman, E. P., and Kunkel, L. M. (1989). Conversion of mdx myofibres from dystrophin-negative to -positive by injection of normal myoblasts. *Nature* **337**:176-179.

Pascual, J., Castresana, J., and Saraste, M. (1997). Evolution of the spectrin repeat. *Bioessays* **19**:811-817.

Pearce, M., Blake, D. J., Tinsley, J. M., Byth, B. C., Campbell, L., Monaco, A. P., and Davies, K. E. (1993). The utrophin and dystrophin genes share similarities in genomic structure. *Hum Mol Genet* **2**:1765-1772.

Pelteková, V., Han, G., Soleymanlou, N., and Hampson, D. R. (2000). Constraints on proper folding of the amino terminal domains of group III metabotropic glutamate receptors. *Brain Res Mol Brain Res* **76**:180-190.

Perkins, K. K., Dailey, G. M., and Tjian, R. (1988). In vitro analysis of the Antennapedia P2 promoter: identification of a new Drosophila transcription factor. *Genes Dev* **2**:1615-1626.

Perler, F. B., Davis, E. O., Dean, G. E., Gimble, F. S., Jack, W. E., Neff, N., Noren, C. J., Thorner, J., and Belfort, M. (1994). Protein splicing elements: inteins and exteins--a definition of terms and recommended nomenclature. *Nucleic Acids Res* **22**:1125-1127.

Perrine, S. P. and Faller, D. V. (1993). Butyrate-induced reactivation of the fetal globin genes: a molecular treatment for the beta-hemoglobinopathies. *Experientia* **49**:133-137.

Peters, M. F., Kramarcy, N. R., Sealock, R., and Froehner, S. C. (1994). beta 2-Syntrophin: localization at the neuromuscular junction in skeletal muscle. *Neuroreport* **5**:1577-1580.

Peters, M. F., Adams, M. E., and Froehner, S. C. (1997). Differential association of syntrophin pairs with the dystrophin complex. *J Cell Biol* **138**:81-93.

Pfister, M. H., Apaydin, F., Turan, O., Bereketoglu, M., Bylgen, V., Braendle, U., Zenner, H. P., and Lalwani, A. K. (1998). A second family with nonsyndromic sensorineural hearing loss linked to Xp21.2: refinement of the DFN4 locus within DMD. *Genomics* **53**:377-382.

Pfister, M. H., Apaydin, F., Turan, O., Bereketoglu, M., Bilgen, V., Braendle, U., Kose, S., Zenner, H. P., and Lalwani, A. K. (1999). Clinical evidence for dystrophin dysfunction as a cause of hearing loss in locus DFN4. *Laryngoscope* **109**:730-735.

Phillips, W. D., Noakes, P. G., Roberds, S. L., Campbell, K. P., and Merlie, J. P. (1993). Clustering and immobilization of acetylcholine receptors by the 43-kD protein: a possible role for dystrophin-related protein. *J Cell Biol* **123**:729-740.

Pillers, D. M., Bulman, D. E., Weleber, R. G., Sigesmund, D. A., Musarella, M. A., Powell, B. R., Murphey, W. H., Westall, C., Panton, C., Becker, L. E., and . (1993). Dystrophin expression in the human retina is required for normal function as defined by electroretinography. *Nat Genet* **4**:82-86.

Pirvola, U., Ylikoski, J., and Virtanen, I. (1990). Immunohistochemical localization of nonerythroid spectrin (fodrin) in the sensory cells of the vestibular end organs of the rat and guinea pig. *ORL J Otorhinolaryngol Relat Spec* **52**:127-132.

Pons, F., Augier, N., Leger, J. O., Robert, A., Tome, F. M., Fardeau, M., Voit, T., Nicholson, L. V., Mornet, D., and Leger, J. J. (1991). A homologue of dystrophin is expressed at the neuromuscular junctions of normal individuals and DMD patients, and of normal and mdx mice. Immunological evidence. *FEBS Lett* **282**:161-165.

Pons, F., Robert, A., Fabbrizio, E., Hugon, G., Califano, J. C., Fehrentz, J. A., Martinez, J., and Mornet, D. (1994). Utrophin localization in normal and dystrophin-deficient heart. *Circulation* **90**:369-374.

Ponting, C. P., Blake, D. J., Davies, K. E., Kendrick-Jones, J., and Winder, S. J. (1996). ZZ and TAZ: new putative zinc fingers in dystrophin and other proteins. *Trends Biochem Sci* **21**:11-13.

Porter, J. D., Rafael, J. A., Ragusa, R. J., Brueckner, J. K., Trickett, J. I., and Davies, K. E. (1998a). The sparing of extraocular muscle in dystrophinopathy is lost in mice lacking utrophin and dystrophin. *J Cell Sci* **111**:1801-1811.

Porter, J. D. (1998b). Commentary: extraocular muscle sparing in muscular dystrophy: a critical evaluation of potential protective mechanisms. *Neuromuscul Disord* **8**:198-203.

Prigojin, H., Brusel, M., Fuchs, O., Shomrat, R., Legum, C., Nudel, U., and Yaffe, D. (1993). Detection of Duchenne muscular dystrophy gene products in amniotic fluid and chorionic villus sampling cells. *FEBS Lett* **335**:223-230.

Puca, A. A., Nigro, V., Piluso, G., Belsito, A., Sampaolo, S., Quaderi, N., Rossi, E., Di Iorio, G., Ballabio, A., and Franco, B. (1998). Identification and characterization of a novel member of the dystrobrevin gene family. *FEBS Lett* **425**:7-13.

Pulkkinen, L., Smith, F. J., Shimizu, H., Murata, S., Yaoita, H., Hachisuka, H., Nishikawa, T., McLean, W. H., and Uitto, J. (1996). Homozygous deletion mutations in the plectin gene (PLEC1) in patients with epidermolysis bullosa simplex associated with late-onset muscular dystrophy. *Hum Mol Genet* **5**:1539-1546.

Raats, C. J., van den, B. J., Bakker, M. A., Oppers-Walgreen, B., Pisa, B. J., Dijkman, H. B., Assmann, K. J., and Berden, J. H. (2000). Expression of agrin, dystroglycan, and utrophin in normal renal tissue and in experimental glomerulopathies. *Am J Pathol* **156**:1749-1765.

Rafael, J. A., Sunada, Y., Cole, N. M., Campbell, K. P., Faulkner, J. A., and Chamberlain, J. S. (1994). Prevention of dystrophic pathology in mdx mice by a truncated dystrophin isoform. *Hum Mol Genet* **3**:1725-1733.

Rafael, J. A., Cox, G. A., Corrado, K., Jung, D., Campbell, K. P., and Chamberlain, J. S. (1996). Forced expression of dystrophin deletion constructs reveals structure-function correlations. *J Cell Biol* **134**:93-102.

Rafael, J. A., Tinsley, J. M., Potter, A. C., Deconinck, A. E., and Davies, K. E. (1998). Skeletal muscle-specific expression of a utrophin transgene rescues utrophin-dystrophin deficient mice. *Nat Genet* **19**:79-82.

Rafael, J. A., Trickett, J. I., Potter, A. C., and Davies, K. E. (1999). Dystrophin and utrophin do not play crucial roles in nonmuscle tissues in mice. *Muscle Nerve* **22**:517-519.

Rafael, J. A. and Brown, S. C. (2000). Dystrophin and utrophin: genetic analyses of their role in skeletal muscle. *Microsc Res Tech* **48**:155-166.

Rafael, J. A., Townsend, E. R., Squire, S. E., Potter, A. C., Chamberlain, J. S., and Davies, K. E. (2000). Dystrophin and utrophin influence fiber type composition and post-synaptic membrane structure. *Hum Mol Genet* **9**:1357-1367.

Rahman, M. M., Varghese, Z., and Moorhead, J. F. (2001). Paradoxical increase in nitric oxide synthase activity in hypercholesterolaemic rats with impaired renal function and decreased activity of nitric oxide. *Nephrol Dial Transplant* **16**:262-268.

Raho, G., Barone, V., Rossi, D., Philipson, L., and Sorrentino, V. (2000). The gas 5 gene shows four alternative splicing patterns without coding for a protein [In Process Citation]. *Gene* **256**:13-17.

Rando, T. A., Disatnik, M. H., and Zhou, L. Z. (2000). Rescue of dystrophin expression in mdx mouse muscle by RNA/DNA oligonucleotides. *Proc Natl Acad Sci U S A* **97**:5363-5368.

Rapaport, D., Lederfein, D., den Dunnen, J. T., Grootsholten, P. M., van Ommen, G. J., Fuchs, O., Nudel, U., and Yaffe, D. (1992). Characterization and cell type distribution of a novel, major transcript of the Duchenne muscular dystrophy gene. *Differentiation* **49**:187-193.

Raynor, E. M. and Mulroy, M. J. (1997). Sensorineural hearing loss in the mdx mouse: a model of Duchenne muscular dystrophy. *Laryngoscope* **107**:1053-1056.

Read, A. P., Mountford, R. C., Forrest, S. M., Kenwick, S. J., Davies, K. E., and Harris, R. (1988). Patterns of exon deletions in Duchenne and Becker muscular dystrophy. *Hum Genet* **80**:152-156.

Reinholz, M. M., Zschunke, M. A., and Roche, P. C. (2000). Loss of alternately spliced messenger RNA of the luteinizing hormone receptor and stability of the follicle-stimulating hormone receptor messenger RNA in granulosa cell tumors of the human ovary. *Gynecol Oncol* **79**:264-271.

Riddle, R. D., Johnson, R. L., Laufer, E., and Tabin, C. (1993). Sonic hedgehog mediates the polarizing activity of the ZPA. *Cell* **75**:1401-1416.

Rivier, F., Robert, A., Hugon, G., and Mornet, D. (1997). Different utrophin and dystrophin properties related to their vascular smooth muscle distributions. *FEBS Lett* **408**:94-98.

Roberts, R. G., Coffey, A. J., Bobrow, M., and Bentley, D. R. (1992). Determination of the exon structure of the distal portion of the dystrophin gene by vectorette PCR. *Genomics* **13**:942-950.

Roberts, R. G., Coffey, A. J., Bobrow, M., and Bentley, D. R. (1993). Exon structure of the human dystrophin gene. *Genomics* **16**:536-538.

Roberts, R. G., Freeman, T. C., Kendall, E., Vetrie, D. L., Dixon, A. K., Shaw-Smith, C., Bone, Q., and Bobrow, M. (1996). Characterization of DRP2, a novel human dystrophin homologue. *Nat Genet* **13**:223-226.

Roberts, R. G. and Bobrow, M. (1998). Dystrophins in vertebrates and invertebrates. *Hum Mol Genet* **7**:589-595.

Rodgers, G. P., Dover, G. J., Uyesaka, N., Noguchi, C. T., Schechter, A. N., and Nienhuis, A. W. (1993). Augmentation by erythropoietin of the fetal-hemoglobin response to hydroxyurea in sickle cell disease. *N Engl J Med* **328**:73-80.

Rodius, F., Claudepierre, T., Rosas-Vargas, H., Cisneros, B., Montanez, C., Dreyfus, H., Mornet, D., and Rendon, A. (1997). Dystrophins in developing retina: Dp260 expression correlates with synaptic maturation. *Neuroreport* **8**:2383-2387.

Romeo, R. and Marcello, M. F. (1999). Some considerations on the human Leydig cell (immunohistochemical observations). *Arch Ital Urol Androl* **71**:143-148.

Rosa, G., Ceccarini, M., Cavaldesi, M., Zini, M., and Petrucci, T. C. (1996). Localization of the dystrophin binding site at the carboxyl terminus of beta-dystroglycan. *Biochem Biophys Res Commun* **223**:272-277.

Royuela, M., Paniagua, R., Rivier, F., Hugon, G., Robert, A., and Mornet, D. (1999). Presence of invertebrate dystrophin-like products in obliquely striated muscle of the leech, *Pontobdella muricata* (Annelida, Hirudinea). *Histochem J* **31**:603-608.

Rubenstein, R. C. and Zeitlin, P. L. (1998). A pilot clinical trial of oral sodium 4-phenylbutyrate (Buphenyl) in deltaF508-homozygous cystic fibrosis patients: partial restoration of nasal epithelial CFTR function. *Am J Respir Crit Care Med* **157**:484-490.

Rudnicki, M. A., Braun, T., Hinuma, S., and Jaenisch, R. (1992). Inactivation of MyoD in mice leads to up-regulation of the myogenic HLH gene Myf-5 and results in apparently normal muscle development. *Cell* **71**:383-390.

Rudnicki, M. A. and Jaenisch, R. (1995). The MyoD family of transcription factors and skeletal myogenesis. *Bioessays* **17**:203-209.

Rugh R. (1968), *The Mouse, its reproduction and development*, Burgess Publishing Company.

Sadoulet-Puccio, H. M., Khurana, T. S., Cohen, J. B., and Kunkel, L. M. (1996). Cloning and characterization of the human homologue of a dystrophin related phosphoprotein found at the Torpedo electric organ post-synaptic membrane. *Hum Mol Genet* **5**:489-496.

Sadoulet-Puccio, H. M., Rajala, M., and Kunkel, L. M. (1997). Dystrobrevin and dystrophin: an interaction through coiled-coil motifs. *Proc Natl Acad Sci U S A* **94**:12413-12418.

Salanova, M., Stefanini, M., De, C., I, and Palombi, F. (1995). Integrin receptor alpha 6 beta 1 is localized at specific sites of cell-to-cell contact in rat seminiferous epithelium. *Biol Reprod* **52**:79-87.

Salmons S. (1995). Muscle. In "Gray's Anatomy" (Williams P.L, Ed.), pp. 737-900, Churchill Livingstone.

Sander, M., Chavoshan, B., Harris, S. A., Iannaccone, S. T., Stull, J. T., Thomas, G. D., and Victor, R. G. (2000). Functional muscle ischemia in neuronal nitric oxide synthase-deficient skeletal muscle of children with Duchenne muscular dystrophy. *Proc Natl Acad Sci U S A* **97**:13818-13823. {

Sanger, F., Nicklen, S., and Coulson, A. R. (1977). DNA sequencing with chain-terminating inhibitors. *Proc Natl Acad Sci U S A* **74**:5463-5467.

Savage, G. N. and Kerr, J. B. (1995). Effect of seminiferous tubule size on hCG-induced regeneration of peritubular Leydig cells in hypophysectomized, EDS-treated rats. *Int J Androl* **18**:35-45.

Schein, C. H. (1990). Solubility as a function of protein structure and solvent components. *Biotechnology (N Y)* **8**:308-317.

Schofield, J., Houzelstein, D., Davies, K., Buckingham, M., and Edwards, Y. H. (1993). Expression of the dystrophin-related protein (utrophin) gene during mouse embryogenesis. *Dev Dyn* **198**:254-264.

Schofield, J. N., Blake, D. J., Simmons, C., Morris, G. E., Tinsley, J. M., Davies, K. E., and Edwards, Y. H. (1994). Apo-dystrophin-1 and apo-dystrophin-2, products of the

Duchenne muscular dystrophy locus: expression during mouse embryogenesis and in cultured cell lines. *Hum Mol Genet* **3**:1309-1316.

Schofield, J. N., Day, I. N., Thompson, R. J., and Edwards, Y. H. (1995a). PGP9.5, a ubiquitin C-terminal hydrolase; pattern of mRNA and protein expression during neural development in the mouse. *Brain Res Dev Brain Res* **85**:229-238.

Schofield, J. N., Gorecki, D. C., Blake, D. J., Davies, K., and Edwards, Y. H. (1995b). Dystroglycan mRNA expression during normal and mdx mouse embryogenesis: a comparison with utrophin and the apo-dystrophins. *Dev Dyn* **204**:178-185.

Schonfeld, H. J., Schmidt, D., Schroder, H., and Bukau, B. (1995). The DnaK chaperone system of *Escherichia coli*: quaternary structures and interactions of the DnaK and GrpE components. *J Biol Chem* **270**:2183-2189.

Schwabe, J. W., Rodriguez-Esteban, C., and Izpisua Belmonte, J. C. (1998). Limbs are moving: where are they going? *Trends Genet* **14**:229-235.

Sewry, C. A., Matsumura, K., Campbell, K. P., and Dubowitz, V. (1994a). Expression of dystrophin-associated glycoproteins and utrophin in carriers of Duchenne muscular dystrophy. *Neuromuscul Disord* **4**:401-409.

Sewry, C. A., Sansome, A., Matsumura, K., Campbell, K. P., and Dubowitz, V. (1994b). Deficiency of the 50 kDa dystrophin-associated glycoprotein and abnormal expression of utrophin in two south Asian cousins with variable expression of severe childhood autosomal recessive muscular dystrophy. *Neuromuscul Disord* **4**:121-129.

Sewry, C. A., Man, N. T., Lynch, T., and Morris, G. E. (2001). Absence of utrophin in intercalated discs of human cardiac muscle. *Histochem J* **33**:9-12.

Sharp, N. J., Kornegay, J. N., Van Camp, S. D., Herbstreith, M. H., Secore, S. L., Kettle, S., Hung, W. Y., Constantinou, C. D., Dykstra, M. J., Roses, A. D., and . (1992). An error in dystrophin mRNA processing in golden retriever muscular dystrophy, an animal homologue of Duchenne muscular dystrophy. *Genomics* **13**:115-121.

Sherratt, T. G., Vulliamy, T., and Strong, P. N. (1992). Evolutionary conservation of the dystrophin central rod domain. *Biochem J* **287**:755-759.

Sicinski, P., Geng, Y., Ryder-Cook, A. S., Barnard, E. A., Darlison, M. G., and Barnard, P. J. (1989). The molecular basis of muscular dystrophy in the mdx mouse: a point mutation. *Science* **244**:1578-1580.

Simeone A (1998) Detection of mRNA in tissue sections with radiolabelled probes. *In* "In situ hybridization: A practical approach" (Wilkinson D.G., Ed.), pp. 69-87 Oxford University Press.

Slater, C. R., Young, C., Wood, S. J., Bewick, G. S., Anderson, L. V., Baxter, P., Fawcett, P. R., Roberts, M., Jacobson, L., Kuks, J., Vincent, A., and Newsom-Davis, J. (1997). Utrophin abundance is reduced at neuromuscular junctions of patients with both inherited and acquired acetylcholine receptor deficiencies. *Brain* **120**:1513-1531.

Smale, S. T. (1997). Transcription initiation from TATA-less promoters within eukaryotic protein-coding genes. *Biochim Biophys Acta* **1351**:73-88.

Soeller, W. C., Poole, S. J., and Kornberg, T. (1988). In vitro transcription of the *Drosophila engrailed* gene. *Genes Dev* **2**:68-81.

Southern, E. M. (1975). Detection of specific sequences among DNA fragments separated by gel electrophoresis. *J Mol Biol* **98**:503-517.

Sowden, J., Leigh, S., Talbot, I., Delhanty, J., and Edwards, Y. (1993). Expression from the proximal promoter of the carbonic anhydrase 1 gene as a marker for differentiation in colon epithelia. *Differentiation* **53**:67-74.

Stedman, H., Wilson, J. M., Finke, R., Kleckner, A. L., and Mendell, J. (2000). Phase I clinical trial utilizing gene therapy for limb girdle muscular dystrophy: alpha-, beta-, gamma-, or delta-sarcoglycan gene delivered with intramuscular instillations of adeno-associated vectors. *Hum Gene Ther* **11**:777-790.

Stedman, H. H., Sweeney, H. L., Shrager, J. B., Maguire, H. C., Panettieri, R. A., Petrof, B., Narusawa, M., Leferovich, J. M., Sladky, J. T., and Kelly, A. M. (1991). The mdx mouse diaphragm reproduces the degenerative changes of Duchenne muscular dystrophy. *Nature* **352**:536-539.

Strachan, T and Read, A. P., (1999), Human Molecular Genetics, Bios Scientific Publishers Ltd.

- Stradal, T., Kranewitter, W., Winder, S. J., and Gimona, M. (1998). CH domains revisited. *FEBS Lett* **431**:134-137.
- Strehler, E. E. and Zacharias, D. A. (2001). Role of alternative splicing in generating isoform diversity among plasma membrane calcium pumps. *Physiol Rev* **81**:21-50.
- Sudol, M., Chen, H. I., Bougeret, C., Einbond, A., and Bork, P. (1995). Characterization of a novel protein-binding module--the WW domain. *FEBS Lett* **369**:67-71.
- Sunada, Y., Bernier, S. M., Kozak, C. A., Yamada, Y., and Campbell, K. P. (1994). Deficiency of merosin in dystrophic dy mice and genetic linkage of laminin M chain gene to dy locus. *J Biol Chem* **269**:13729-13732.
- Surono, A., Takeshima, Y., Wibawa, T., Pramono, Z. A., and Matsuo, M. (1997). Six novel transcripts that remove a huge intron ranging from 250 to 800 kb are produced by alternative splicing of the 5' region of the dystrophin gene in human skeletal muscle. *Biochem Biophys Res Commun* **239**:895-899.
- Suzuki, A., Goll, D. E., Singh, I., Allen, R. E., Robson, R. M., and Stromer, M. H. (1976). Some properties of purified skeletal muscle alpha-actinin. *J Biol Chem* **251**:6860-6870.
- Takemitsu, M., Ishiura, S., Koga, R., Kamakura, K., Arahata, K., Nonaka, I., and Sugita, H. (1991). Dystrophin-related protein in the fetal and denervated skeletal muscles of normal and mdx mice. *Biochem Biophys Res Commun* **180**:1179-1186.
- Tamura, T., Miura, M., Ikenaka, K., and Mikoshiba, K. (1988). Analysis of transcription control elements of the mouse myelin basic protein gene in HeLa cell extracts: demonstration of a strong NFI-binding motif in the upstream region. *Nucleic Acids Res* **16**:11441-11459.
- Tamura, T., Yoshioka, K., Jinno, Y., Niikawa, N., and Miike, T. (1993). Dystrophin isoforms expressed in the mouse retina. *J Neurol Sci* **115**:214-218.
- Tanaka, H., Ikeya, K., and Ozawa, E. (1990). Difference in the expression pattern of dystrophin on the surface membrane between the skeletal and cardiac muscles of mdx carrier mice. *Histochemistry* **93**:447-452.

Tanaka, H., Ishiguro, T., Eguchi, C., Saito, K., and Ozawa, E. (1991). Expression of a dystrophin-related protein associated with the skeletal muscle cell membrane.

Histochemistry **96**:1-5.

Tartakoff A.M. (1987), *The secretory and endocytic paths*, John Wiley & Sons.

Taylor, J., Muntoni, F., Dubowitz, V., and Sewry, C. A. (1997). The abnormal expression of utrophin in Duchenne and Becker muscular dystrophy is age related.

Neuropathol Appl Neurobiol **23**:399-405.

Tennyson, C. N., Dally, G. Y., Ray, P. N., and Worton, R. G. (1996). Expression of the dystrophin isoform Dp71 in differentiating human fetal myogenic cultures. *Hum Mol Genet* **5**:1559-1566.

Thein, S. L., Hesketh, C., Taylor, P., Temperley, I. J., Hutchinson, R. M., Old, J. M., Wood, W. G., Clegg, J. B., and Weatherall, D. J. (1990). Molecular basis for dominantly inherited inclusion body beta-thalassemia. *Proc Natl Acad Sci U S A* **87**:3924-3928.

The Recombinant Protein Handbook, 2000, Amersham Pharmacia Biotech

Thomas, G. D., Hansen, J., and Victor, R. G. (1997). ATP-sensitive potassium channels mediate contraction-induced attenuation of sympathetic vasoconstriction in rat skeletal muscle. *J Clin Invest* **99**:2602-2609.

Thomas, G. D., Sander, M., Lau, K. S., Huang, P. L., Stull, J. T., and Victor, R. G. (1998). Impaired metabolic modulation of alpha-adrenergic vasoconstriction in dystrophin-deficient skeletal muscle. *Proc Natl Acad Sci U S A* **95**:15090-15095.

Tinsley, J. M., Blake, D. J., Roche, A., Fairbrother, U., Riss, J., Byth, B. C., Knight, A. E., Kendrick-Jones, J., Suthers, G. K., and Love, D. R. (1992). Primary structure of dystrophin-related protein. *Nature* **360**:591-593.

Tinsley, J. M., Blake, D. J., and Davies, K. E. (1993a). Apo-dystrophin-3: a 2.2kb transcript from the DMD locus encoding the dystrophin glycoprotein binding site. *Hum Mol Genet* **2** :521-524.

Tinsley, J. M., Blake, D. J., Pearce, M., Knight, A. E., Kendrick-Jones, J., and Davies, K. E. (1993b). Dystrophin and related proteins. *Curr Opin Genet Dev* **3**:484-490.

- Tinsley, J. M., Potter, A. C., Phelps, S. R., Fisher, R., Trickett, J. I., and Davies, K. E. (1996). Amelioration of the dystrophic phenotype of mdx mice using a truncated utrophin transgene. *Nature* **384**:349-353.
- Tinsley, J., Deconinck, N., Fisher, R., Kahn, D., Phelps, S., Gillis, J. M., and Davies, K. (1998). Expression of full-length utrophin prevents muscular dystrophy in mdx mice. *Nat Med* **4**:1441-1444.
- Tokarz, S. A., Duncan, N. M., Rash, S. M., Sadeghi, A., Dewan, A. K., and Pillers, D. A. (1998). Redefinition of dystrophin isoform distribution in mouse tissue by RT-PCR implies role in nonmuscle manifestations of duchenne muscular dystrophy. *Mol Genet Metab* **65**:272-281.
- Tommasi, d., V, Di Zenzo, G., Sudol, M., Cesareni, G., and Dente, L. (2000). Contribution of the different modules in the utrophin carboxy-terminal region to the formation and regulation of the DAP complex. *FEBS Lett* **471**:229-234.
- Torrente, Y., Tremblay, J. P., Pisati, F., Belicchi, M., Rossi, B., Sironi, M., Fortunato, F., El Fahime, M., D'Angelo, M. G., Caron, N. J., Constantin, G., Paulin, D., Scarlato, G., and Bresolin, N. (2001). Intraarterial Injection of Muscle-derived CD34(+)Sca-1(+) Stem Cells Restores Dystrophin in mdx Mice. *J Cell Biol* **152**:335-348.
- Touhara, K., Inglese, J., Pitcher, J. A., Shaw, G., and Lefkowitz, R. J. (1994). Binding of G protein beta gamma-subunits to pleckstrin homology domains. *J Biol Chem* **269**:10217-10220.
- Tremblay, J. P. (2000) Planning of a new clinical trial of myoblast transplantation in DMD patients Myology 2000 conference proceedings.
- van Deutekom, J. C., Floyd, S. S., Booth, D. K., Oligino, T., Krisky, D., Marconi, P., Glorioso, J. C., and Huard, J. (1998). Implications of maturation for viral gene delivery to skeletal muscle. *Neuromuscul Disord* **8**:135-148.
- Verbovaia, L. V. and Razin, S. V. (1997). Mapping of replication origins and termination sites in the Duchenne muscular dystrophy gene. *Genomics* **45**:24-30.
- Verpy, E., Leibovici, M., Zwaenepoel, I., Liu, X. Z., Gal, A., Salem, N., Mansour, A., Blanchard, S., Kobayashi, I., Keats, B. J., Slim, R., and Petit, C. (2000). A defect in harmonin, a PDZ domain-containing protein expressed in the inner ear sensory hair cells, underlies Usher syndrome type 1C. *Nat Genet* **26**:51-55.

- Vivarelli, E., Brown, W. E., Whalen, R. G., and Cossu, G. (1988). The expression of slow myosin during mammalian somitogenesis and limb bud differentiation. *J Cell Biol* **107**:2191-2197.
- Voit, T., Haas, K., Leger, J. O., Pons, F., and Leger, J. J. (1991). Xp21 dystrophin and 6q dystrophin-related protein. Comparative immunolocalization using multiple antibodies. *Am J Pathol* **139**:969-976.
- Wagner, K. R., Cohen, J. B., and Haganir, R. L. (1993). The 87K postsynaptic membrane protein from Torpedo is a protein-tyrosine kinase substrate homologous to dystrophin. *Neuron* **10**:511-522.
- Wakefield, P. M., Tinsley, J. M., Wood, M. J., Gilbert, R., Karpati, G., and Davies, K. E. (2000). Prevention of the dystrophic phenotype in dystrophin/utrophin-deficient muscle following adenovirus-mediated transfer of a utrophin minigene. *Gene Ther* **7**:201-204.
- Wang, B., Li, J., and Xiao, X. (2000). Adeno-associated virus vector carrying human minidystrophin genes effectively ameliorates muscular dystrophy in mdx mouse model. *Proc Natl Acad Sci U S A* **97**:13714-13719.
- Wang, J., Pansky, A., Venuti, J. M., Yaffe, D., and Nudel, U. (1998). A sea urchin gene encoding dystrophin-related proteins. *Hum Mol Genet* **7**:581-588.
- Wang, Y. F. and Yu-Lee, L. Y. (1996). Multiple stat complexes interact at the interferon regulatory factor-1 interferon-gamma activation sequence in prolactin-stimulated Nb2 T cells. *Mol Cell Endocrinol* **121**:19-28.
- Wang, Z., Schultheis, P. J., and Shull, G. E. (1996). Three N-terminal variants of the AE2 Cl⁻/HCO₃⁻ exchanger are encoded by mRNAs transcribed from alternative promoters. *J Biol Chem* **271**:7835-7843.
- Wells, D. J., Wells, K. E., Asante, E. A., Turner, G., Sunada, Y., Campbell, K. P., Walsh, F. S., and Dickson, G. (1995). Expression of human full-length and minidystrophin in transgenic mdx mice: implications for gene therapy of Duchenne muscular dystrophy. *Hum Mol Genet* **4**:1245-1250.
- Whalen, R. G., Sell, S. M., Butler-Browne, G. S., Schwartz, K., Bouveret, P., and Pinset-Harstom, I. (1981). Three myosin heavy-chain isozymes appear sequentially in rat muscle development. *Nature* **292**:805-809.

Whitehouse, D. B., Putt, W., Lovegrove, J. U., Morrison, K., Hollyoake, M., Fox, M. F., Hopkinson, D. A., and Edwards, Y. H. (1992). Phosphoglucomutase 1: complete human and rabbit mRNA sequences and direct mapping of this highly polymorphic marker on human chromosome 1. *Proc Natl Acad Sci U S A* **89**:411-415.

Wijnen, L. M., Grzeschik, K. H., Pearson, P. L., and Meera, K. P. (1977). The human PGM-2 and its chromosomal localization in man-mouse hybrids. *Hum Genet* **37**:271-278.

Williamson, R. A., Henry, M. D., Daniels, K. J., Hrstka, R. F., Lee, J. C., Sunada, Y., Ibraghimov-Beskrovnya, O., and Campbell, K. P. (1997). Dystroglycan is essential for early embryonic development: disruption of Reichert's membrane in Dag1-null mice. *Hum Mol Genet* **6**:831-841.

Wills N., Reuss L., and Lewis S.A. Epithelial transport, 1996, Chapman & Hall.

Wilson, J., Putt, W., Jimenez, C., and Edwards, Y. H. (1999). Up71 and up140, two novel transcripts of utrophin that are homologues of short forms of dystrophin. *Hum Mol Genet* **8**:1271-1278.

Winder, S. J., Hemmings, L., Bolton, S. J., Maciver, S. K., Tinsley, J. M., Davies, K. E., Critchley, D. R., and Kendrick-Jones, J. (1995). Calmodulin regulation of utrophin actin binding. *Biochem Soc Trans* **23**:397S.

Winder, S. J. (1997). The membrane-cytoskeleton interface: the role of dystrophin and utrophin. *J Muscle Res Cell Motil* **18**:617-629.

Wright, W. E., Sassoon, D. A., and Lin, V. K. (1989). Myogenin, a factor regulating myogenesis, has a domain homologous to MyoD. *Cell* **56**:607-617.

Wrobel, K. H., Dostal, S., and Schimmel, M. (1988). Postnatal development of the tubular lamina propria and the intertubular tissue in the bovine testis. *Cell Tissue Res* **252**:639-653.

Wynshaw-Boris, A. (1996). Model mice and human disease. *Nat Genet* **13**:259-260.

Yamamoto, K., Yuasa, K., Miyagoe, Y., Hosaka, Y., Tsukita, K., Yamamoto, H., Nabeshima, Y. I., and Takeda, S. (2000). Immune response to adenovirus-delivered antigens upregulates utrophin and results in mitigation of muscle pathology in mdx mice. *Hum Gene Ther* **11**:669-680.

- Yao, L., Kawakami, Y., and Kawakami, T. (1994). The pleckstrin homology domain of Bruton tyrosine kinase interacts with protein kinase C. *Proc Natl Acad Sci U S A* **91**:9175-9179.
- Yates, J. R. (1997). 43rd ENMC International Workshop on Emery-Dreifuss Muscular Dystrophy, 22 June 1996, Naarden, The Netherlands. *Neuromuscul Disord* **7**:67-69.
- Yoshida, T., Hanada, H., Iwata, Y., Pan, Y., and Sigekawa, M. (1996). Expression of a dystrophin-sarcoglycan complex in serum-deprived BC3H1 cells and involvement of alpha-sarcoglycan in substrate attachment. *Biochem Biophys Res Commun* **225**:11-15.
- Youssoufian, H., McAfee, M., and Kwiatkowski, D. J. (1990). Cloning and chromosomal localization of the human cytoskeletal alpha-actinin gene reveals linkage to the beta-spectrin gene. *Am J Hum Genet* **47**:62-71.
- Zakany, J. and Duboule, D. (1999). Hox genes and the making of sphincters. *Nature* **401**:761-762.
- Zhang, Y., Niu, Z., Cohen, A. J., Nah, H. D., and Adams, S. L. (1997). The chick type III collagen gene contains two promoters that are preferentially expressed in different cell types and are separated by over 20 kb of DNA containing 23 exons. *Nucleic Acids Res* **25**:2470-2477.
- Zhang, Y., Niu, Z., Cohen, A. J., and Adams, S. L. (1999). The internal chondrocyte-specific promoter of the chick type III collagen gene is activated by AP1 and is repressed in fibroblasts by a complex containing an LBP1-related protein. *Nucleic Acids Res* **27**:4090-4099.
- Zhao, Z., Makaritsis, K., Francis, C. E., Gavras, H., and Ravid, K. (2000). A role for the A3 adenosine receptor in determining tissue levels of cAMP and blood pressure: studies in knock-out mice. *Biochim Biophys Acta* **1500**:280-290.
- Zuellig, R. A., Bornhauser, B. C., Knuesel, I., Heller, F., Fritschy, J. M., and Schaub, M. C. (2000). Identification and characterisation of transcript and protein of a new short N-terminal utrophin isoform. *J Cell Biochem* **77**:418-431.
- Zylicz, M. and Georgopoulos, C. (1984). Purification and properties of the Escherichia coli dnaK replication protein. *J Biol Chem* **259**:8820-8825.

Up71 and Up140, two novel transcripts of utrophin that are homologues of short forms of dystrophin

James Wilson, Wendy Putt, Cecilia Jimenez and Yvonne H. Edwards*

MRC Human Biochemical Genetics Unit, University College London, Wolfson House, 4 Stephenson Way, London NW1 2HE, UK

Received February 15, 1999; Revised and Accepted April 1, 1999

Utrophin is a large protein which accumulates at the neuromuscular synapse and myotendinous junctions in adult skeletal muscle, and is widely expressed in several non-skeletal muscle tissues. Evidence from a variety of sources suggests that a successful strategy for treatment of Duchenne muscular dystrophy patients will be to increase expression of utrophin in muscle. There is still much to be learnt about utrophin gene regulation, in particular regarding alternative isoforms, their promoters and role in muscle and non-muscle tissues. Using 5'-RACE we have identified two novel transcripts of utrophin, Up71 and Up140, with unique first exons and promoters located in intron 62 and intron 44, respectively. These transcripts appear to be structural homologues of the short dystrophin transcripts, Dp140 and Dp71, emphasizing the high degree of structural conservation between the utrophin and dystrophin genes. RT-PCR shows that Up71 and Up140 are widely expressed in both human and mouse tissues, including skeletal muscle. We present evidence for transcript-specific differential mRNA splicing of exon 71, in both Up71 and Up140, similar to that described for dystrophin. No evidence for splicing of exon 78 of utrophin was found. This is in contrast to dystrophin and may reflect a subtle functional difference in patterns of phosphorylation between the two proteins.

INTRODUCTION

Utrophin is a large protein (395 kDa) which is widely expressed and most abundant in several non-skeletal muscle tissues, for example lung, intestine, embryonic neural tube, sensory ganglia, tendons and ossifying cartilages (1–3). Utrophin is the autosomal (chromosome 6q24) homologue of dystrophin (4,5), the protein absent or abnormal in X-linked Duchenne and Becker's muscular dystrophies (DMD and BMD, respectively).

In adult muscle, utrophin accumulates at the neuromuscular synapse (NMJ) and myotendinous junctions (MTJ) (6,7). At the NMJ, utrophin contributes to the maintenance of the post-synaptic membrane and clustering of acetylcholine receptors

by interacting with a sub-neuronal complex of proteins; these include F-actin, several of the 'dystrophin-associated proteins' (DAPs; dystroglycan, dystrobrevins, syntrophins and sarcoglycans) (8–10) and the synapse-associated proteins rapsyn and agrin (11). In contrast to utrophin, dystrophin in muscle is most abundant at the sarcolemma. Here it also interacts with DAPs to form a link between the sub-membraneous network of non-muscle actin and the extracellular matrix and thereby maintains the integrity of the sarcolemma (8–10).

Utrophin is an important focus for research in DMD because of its structural and functional similarities to dystrophin and its therapeutic potential (12). The finding that in developing and regenerating muscle fibres utrophin protein locates not only to the NMJ and MTJ but also to the sarcolemma (13–15), suggests that utrophin might functionally replace dystrophin. This idea is supported by the demonstration that overexpression of utrophin in dystrophin-deficient (*mdx*) mice leads to the widespread appearance of utrophin at the sarcolemma and amelioration of the muscle phenotype (16). Recently, it was shown that the severe muscle phenotype exhibited by dystrophin/utrophin doubly deficient mice is also corrected by overexpression of utrophin (17). These important observations all support the view that increased expression of utrophin might be a successful therapeutic strategy for the treatment of DMD (16,18).

Compared with dystrophin there is relatively little information about utrophin gene regulation, in particular with regard to alternative isoforms and their promoters. Regulation of the dystrophin gene is complex, with at least seven promoters that determine the expression of multiple isoforms. There are three full-length (427 kDa) isoforms: muscle dystrophin confined to skeletal, cardiac and smooth muscle (19), C-dystrophin found in cortical neurons and P-dystrophin in cerebellar Purkinje cells (20,21). There are also four shorter apo-dystrophin isoforms: Dp71 (22) expressed in a wide variety of tissues, Dp140 (23) in brain glial cells, Dp116 (24) found in fetal brain and adult peripheral nerve and Dp260 (25) in the retina and regions of the CNS.

Given the structural homology between utrophin and dystrophin it seems very likely that utrophin will show similar complexity (12). At present only a single full-length utrophin isoform has been described. This is transcribed from a TATA box-less promoter associated with a CpG island at the 5' end of the transcript and is expressed in skeletal muscle and several other tissues (26). Direct injection of promoter/gene reporter constructs into muscle demonstrated that this promoter func-

*To whom correspondence should be addressed. Tel: +44 171 504 502; Fax: +44 171 387 3496; Email: yedwards@hgmp.mrc.ac.uk

tions in a synapse-specific way (27). One other utrophin isoform has been reported and designated G-utrophin. This 5.5 kb mRNA is transcribed from a promoter, which probably lies in intron 55, and is expressed in sensory dorsal root and cranial ganglia and is a major utrophin in the brain (28). An important point about G-utrophin is that its sequence diverges from full-length utrophin at the same point that the short dystrophin transcript, Dp116, diverges from full-length dystrophin. This suggests that the position of the Dp116 promoter is conserved between the two genes and that utrophin homologues of other dystrophin alternative promoters, Dp260, Dp71 and Dp140, may be found. This possibility is strengthened by reports of 140 and 80 kDa utrophin-immunoreactive proteins in extracts of skeletal muscle and peripheral nerve (29,30) that may represent homologues of the dystrophin transcripts Dp140 and Dp71.

In the present study we have explored this possible functional conservation further. Using 5'-RACE we have searched for structural homologues of the short dystrophin isoforms and have identified two novel utrophin transcripts. These transcripts appear to be the utrophin counterparts of Dp71 and Dp140; each shows a unique 5' exon, wide tissue distribution and evidence for differential mRNA splicing.

RESULTS

The 5'-RACE procedure was used to identify utrophin transcripts that differ from the published utrophin sequence at their 5' ends. Human fetal brain mRNA was chosen as the starting material and in the first instance, reverse transcription was carried out using primers specific for utrophin exons 63 and 45 (exon numbering as for dystrophin). These primers were designed specifically to look for the utrophin homologues of dystrophin Dp71 and Dp140.

Isolation and characterization of the novel utrophin transcript Up71

After 5'-RACE using nested primers specific for exon 63, two extension products of 360 and 250 bp were isolated and subcloned. The sequence of the 360 bp product corresponded to that expected for full-length utrophin extending across exons 63 and 62, while the 250 bp product contained novel sequence upstream of the exon 63 sequence (Fig. 1A). The novel sequence diverges from the known mRNA sequence at a point exactly coincident with the junction between exon 63 and intron 62. This is the same point at which the short dystrophin transcript Dp71 diverges from full-length dystrophin sequence. The novel utrophin transcript is designated Up71.

Up71 has 169 nt of unique 5' sequence. This includes 101 nt of open reading frame but it is not certain that this sequence is translated. There is an ATG codon situated 116 nt from the 5' end of the transcript within the open reading frame, but this is in a suboptimal sequence context. In particular, the critical purine in position -3 of the Kozak translation initiation consensus (31) is absent. Furthermore, if this ATG were functional as an initiation codon then the 5' sequence would encode an N-terminal sequence unusually rich in Phe (shown in small caps in Fig. 1A). The next ATG is 90 bp further downstream in exon 63 and here the sequence context is more favourable for translation initiation. If translation initiates from this downstream

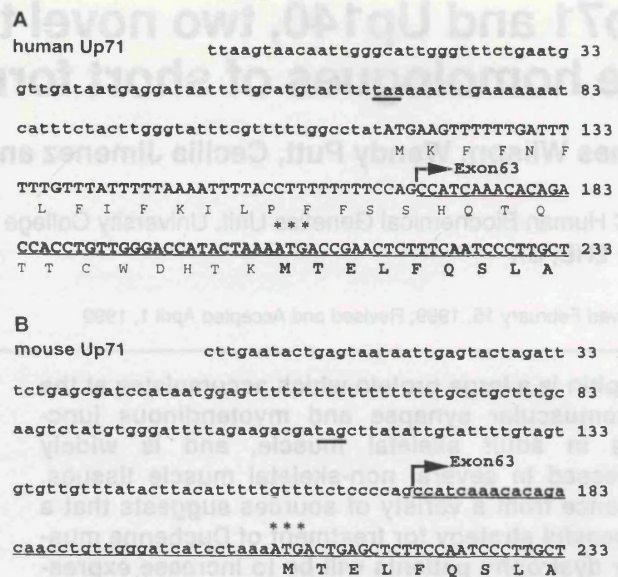


Figure 1. (A) The 5' sequence of human Up71 cDNA. The arrow indicates the point at which Up71 differs from full-length utrophin and the position of the boundary between intron 62 and exon 63 in the full-length transcript. The most likely translation initiation ATG codon is denoted by asterisks and the deduced amino acid sequence is shown in bold. Amino acid sequence from another more upstream ATG is also shown, as non-bold text; however, this is in a relatively unfavourable Kozak consensus sequence. The downstream ATG is conserved in the mouse Up71 sequence that is shown for comparison (B). The first stop codons in the 5'-UTR, upstream of the ATG codon, are underlined. Exon numbering as for dystrophin

codon the novel Up71 sequence would comprise entirely 5'-untranslated sequence.

Sequence comparisons show that in the mouse, the upstream ATG of the human sequence is not present, while the downstream ATG in exon 63 is conserved between the two species (Fig. 1B). The novel first exons of the human and mouse sequences show 56% nucleotide homology, whereas the adjacent coding exon 62 shows 91% homology across species. This supports the view that the 5' exon of Up71 is untranslated and that the downstream ATG is the major site of translation initiation.

Isolation and characterization of the novel utrophin transcript, Up140

After 5'-RACE using exon 45-specific primers, four extension products of different sizes were isolated and subcloned (Fig. 2). Sequence analysis showed two products, of 480 and 370 bp, containing sequence corresponding to exons 44 and 45 of the full-length utrophin transcript. In contrast, the other products, of 550 and 630 bp, contained novel sequence 5' of exon 45 (Fig. 3A) and identical in the two clones where they overlapped. The novel 5' sequence diverges from the known full-length utrophin transcript at a point exactly coincident with the junction between exon 45 and intron 44 and continues 5' for a further 507 nt. This short utrophin transcript has been designated Up140, in line with the dystrophin transcript (Dp140) whose transcription is initiated in intron 44 (23). The reading frame of Up140 stays open for 86 nt 5' of the junction with exon 45, before a TAA stop codon is encountered, but does not

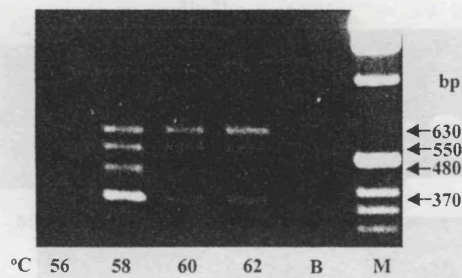


Figure 2. The 5'-RACE products amplified from human fetal brain mRNA using hGSP3-Up140 5'-TGCACAATCCCATCCCCAGTTCG and the anchor primer GGCCACGCGTCGACTAGTACGG₁₈. Amplification was carried out at various annealing temperatures ranging from 56 to 62°C. B, amplification carried out in the absence of cDNA; M, DNA size marker track.

contain a translation initiation codon. The first ATG lies within exon 46, 709 nt downstream from the 5' end of the transcript. The relatively long 5'-untranslated region (5'-UTR) of Up140 is a feature held in common with dystrophin Dp140, which is also translated from a downstream ATG located in exon 51. However, in the case of Dp140 the unique 5' sequence does not lie immediately adjacent to the exon 45/intron 44 boundary but derives from a region further within intron 44 (23).

Sequence comparisons (Fig. 3B) show that the level of nucleotide homology between the novel sequence in human and mouse is 70% across 200 bp immediately upstream of exon 45. This is relatively low for coding sequence but is similar to that found when the adjacent coding exons 45 and 46 are compared (71% nucleotide identity and only 61% amino acid identity). Thus, the region around exon 45 is not highly conserved between man and mouse and, indeed, the ATG codon in the human sequence is absent from the mouse sequence. An ATG situated a further 177 nt downstream (in exon 47) is conserved between the two species and is presumably the functional translation start site in the mouse. The differences in the positions of the translation start sites mean that in man Up140 has 58 extra amino acids at its N-terminus compared with mouse (Fig. 3).

Alignment of full-length utrophin and dystrophin cDNA sequences in the region adjacent to the Up140/Dp140 promoters shows that in exons 48 and 49, utrophin lacks 113 amino acids present in dystrophin. These amino acids correspond to the rod domain repeat 19 unit, encompassing the hinge 3 region which is absent in utrophin. These comparisons contribute to the view that the region close to the Up140/Dp140 promoters is susceptible to mutation and loss of sequence conservation.

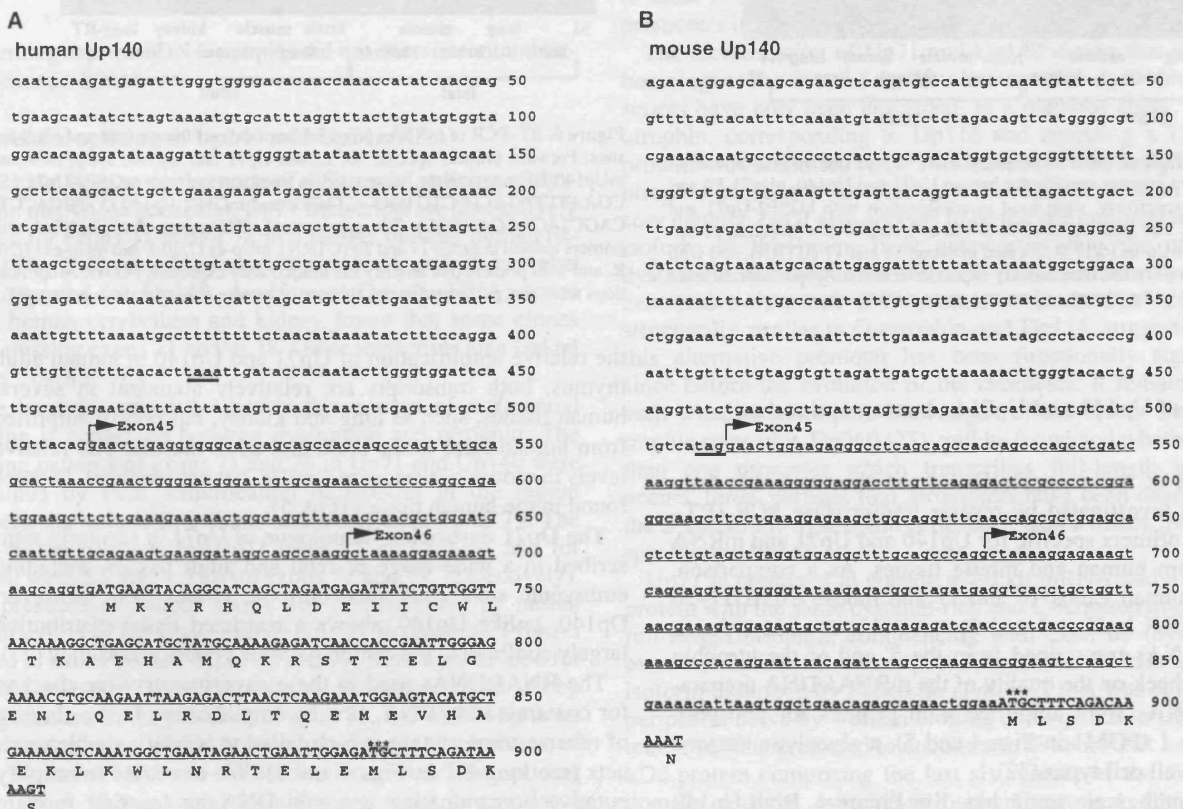


Figure 3. (A) The 5' sequence of human Up140 cDNA. Arrows indicate the positions of the boundaries between intron 44 and exon 45, and intron 45 and exon 46. The arrow marking exon 45 indicates the point at which Up140 differs from full-length utrophin. The deduced amino acid sequence is shown in uppercase. The upstream ATG codon of the human sequence is not conserved in the mouse sequence (B) although the next ATG downstream (asterisks) is conserved. The first stop codons in the 5'-UTR, upstream of the ATG codon, are underlined.

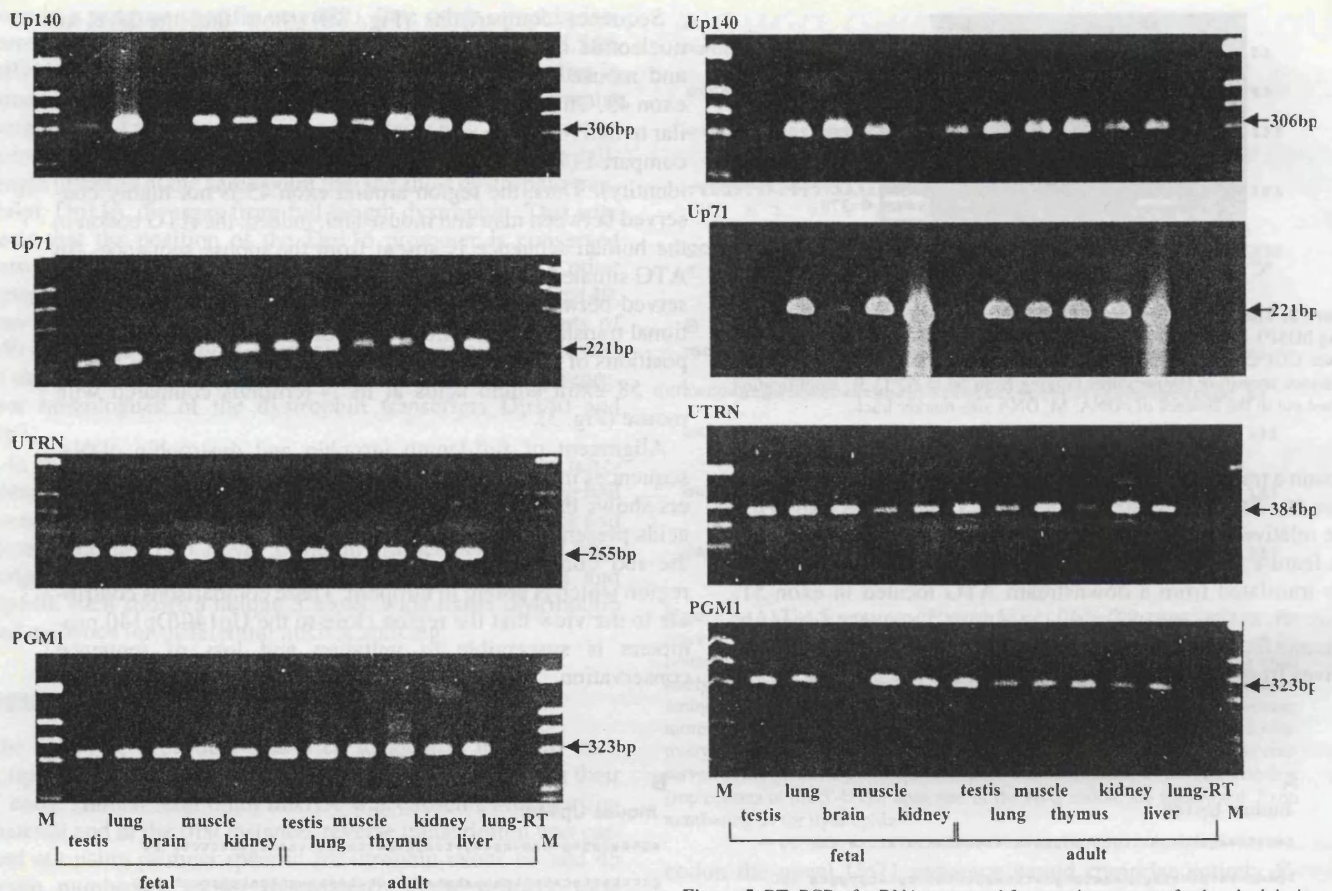


Figure 4. RT-PCR of mRNAs prepared from various human fetal and adult tissues. Forward primers specific for human Up71 and Up140, hUp71-F4 and hUp140-F6, respectively, were used in combination with hGSP2-Up71 and hGSP3-Up140. The same set of cDNAs was also amplified with primers hUp-ex16/17-F and hUp-ex16/17-R, located in exons 16 and 17 (UTRN), and with primers that amplify the ubiquitously expressed PGM1. Amplifications were also performed in the absence of reverse transcriptase; one example is shown here, lung-RT.

Expression of Up140 and Up71 in human and rodent tissues

The patterns of tissue expression of the short utrophin transcripts were investigated by reverse transcriptase PCR (RT-PCR) using primers specific for Up140 and Up71 and mRNA prepared from human and mouse tissues. As a comparison, primers in human exons 16 and 17 and mouse exons 17–20 (marked UTRN in Figs 4 and 5) were also used in order to amplify mRNAs transcribed from the 5' end of the utrophin gene. As a check on the quality of the mRNA/cDNA preparation the cDNAs were amplified with primers for phosphoglucomutase 1 (PGM1 in Figs 4 and 5), a glycolytic enzyme expressed in all cell types (32).

Typical findings are summarized in Figure 4. Both Up140 and Up71 mRNAs are amplified in all the adult and fetal tissues tested, including skeletal muscle, and neither shows particular tissue specificity. While the two short transcripts appear to differ in the detail of their distribution, for example compare

Figure 5. RT-PCR of mRNAs prepared from various mouse fetal and adult tissues. Forward primers specific for mouse Up71 and Up140, mUp71-F8 and mUp140-F4, respectively, were used in combination with mGSP2-Up71 (5'-CGAATTTGATTGCTGTGCGGTAGG) and mGSP2-Up140 (5'-TCCACCTCAGCTACAAGAGTGC). The same set of cDNAs was also amplified with primers located in exons 17 and 20 (UTRN), mUp-ex17/20-F and mUp-ex17/20-R, and with primers that amplify the ubiquitously expressed PGM1. Amplifications were also performed in the absence of reverse transcriptase, e.g. lung-RT.

the relative amplification of Up71 and Up140 in human adult thymus, both transcripts are relatively abundant in several human tissues, such as lung and kidney, but poorly amplified from human fetal testis, brain and adult muscle. The relative levels in mouse tissues were similar, but not identical, to those found in the human tissues (Fig. 5).

The Dp71 dystrophin homologue of Up71 is similarly transcribed in a wide range of fetal and adult tissues, including embryonic stem cells and chorionic villous (33). However, Dp140, unlike Up140, shows a restricted tissue distribution largely confined to the central nervous system and kidney (23).

The RNA/cDNAs used in these experiments were checked for contaminating DNA, first by amplification in the absence of reverse transcriptase, which failed to amplify visible products (see lung-RT in Figs 4 and 5). We also tried to amplify putative contaminating genomic DNA by locating forward primers in the adjacent 5' intron sequence while keeping the reverse primer within exon sequence (either exon 63 or exon 45). This primer combination did not amplify products from tissue cDNAs but readily amplified genomic DNA, thereby

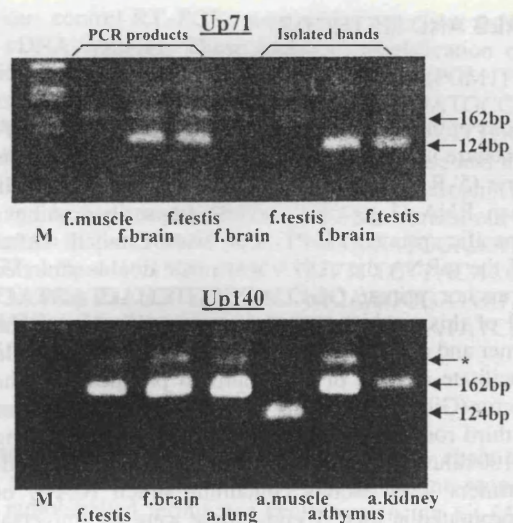


Figure 6. PCR to demonstrate the presence and absence of exon 71 in alternatively spliced forms of human Up71 and Up140 cDNA. Amplification of the transcript-specific cDNAs using the primers Ux70-F (5'-CAGGTGCGAAGAA-GTACTTTGCC) and Ux72-R (5'-GGTGTGCATCATGAAACAGTTGAGG) leads to a 162 bp product in the presence of exon 71, and a 124 bp product in the absence of exon 71. The nucleotide sequence of spliced forms was checked by direct analysis of DNA eluted from separated bands excised from agarose gels ('isolated bands'). The band indicated by an asterisk was also isolated and sequenced and is a non-specific PCR product.

confirming that the cDNA samples did not contain contaminating genomic DNA.

Differential splicing of Up140 and Up71 mRNA

There have been several reports of differential splicing of dystrophin mRNA; in particular, Dp71 transcripts are alternatively spliced for exons 71 and/or 78 in a variety of adult human tissues (34). Differential splicing of exons 71 and 78 has also been reported for Dp140. Analysis of Dp140 cDNA clones from human cerebellum and kidney found that some clones were missing exons 71 and/or 78. Other transcripts also lacked exons 71–74 (35).

We have investigated whether this pattern of differential splicing is conserved between dystrophin and utrophin. The splicing patterns of exons 71 and 78 in Up71 and Up140 were examined by PCR amplification of cDNAs in the region between the unique first exons and either exon 72 or 79. The sizes of the products for Up71 were 1.2 and 2.0 kb, and for Up140 were 3.7 and 4.5 kb (to exons 72 and 79, respectively). The presence of spliced forms was demonstrated by nested amplification of the transcript-specific PCR products. Primers placed in exons 70 and 72, or 70 and 79, were used to look for splicing of exons 71 and 78, respectively; a product of 162 bp was generated in the presence of exon 71, and of 124 bp in its absence. A product of 216 bp was generated in the presence of exon 78, and of 184 bp in its absence. No evidence for splicing out of exon 78 was found for either transcript in any tissue (data not shown); however, exon 71 was alternatively spliced in a transcript- and tissue-specific manner.

For Up71, several fetal and adult tissues contain a mixture of transcripts spliced and unspliced for exon 71, although the pro-

portion of spliced and unspliced forms varies from tissue to tissue. For example, fetal muscle contains predominantly the unspliced form while fetal brain and testis contain predominantly the spliced form (Fig. 6). Adult testis and thymus showed no evidence of splicing, and fetal lung contained only mRNA spliced out for exon 71 (data not shown).

For Up140 the unspliced form is the major isoform in most tissues, although splicing out of exon 71 occurs at very low levels in several tissues. In contrast, the spliced form is the major Up140 transcript in adult skeletal muscle (Fig. 6). The nucleotide sequence of spliced forms was checked by direct sequence analysis of DNA eluted from separated bands excised from agarose gels ('isolated bands' in Fig. 6); this also confirmed that the splicing out of exon 71 occurs exactly at the known exon/intron boundaries.

DISCUSSION

In this study we describe two novel transcripts of the utrophin gene, Up71 and Up140, whose promoters are located in the distal half of the gene. Both mRNAs are distinguished by a novel first exon comprising untranslated sequence (Up71, 206 nt; Up140, 709 nt). The Up140 and Up71 mRNA sequences diverge from that of full-length utrophin at the same positions as the short dystrophin transcripts, Dp140 and Dp71, diverge from full-length dystrophin sequence. These findings provide good evidence that the gene duplication event which gave rise to these two genes occurred after the appearance of multiple promoters in the ancestral gene.

The identification of Up71 and Up140 means that utrophin homologues for three of the four known short dystrophin transcripts have now been described. In a previous study, a short utrophin, corresponding to Dp116 and encoding a 113 kDa protein, was identified (28). This transcript was designated G-utrophin because of its relatively abundant expression in sensory ganglia, but it also appears to be the predominant utrophin isoform in the brain. It is noteworthy that the utrophin/dystrophin homologue identified in the sea urchin *Strongylocentrotus purpuratus* (36) transcribes an internal transcript structurally similar to G-utrophin and Dp116, suggesting that this alternative promoter has been functionally significant since before the evolution of the chordates. It remains to be seen whether a utrophin homologue of the fourth short dystrophin transcript, Dp260 (25), will be found and whether more than one promoter which transcribes full-length utrophin occurs; three, perhaps four, promoters have been described at the 5' end of the dystrophin gene, each with a distinctive tissue specificity (19,21).

Up71 is predicted to encode a 4.0 kb mRNA and a 71 kDa protein with the same cysteine-rich and C-terminal domains as full-length utrophin, commencing with exon 63 (dystrophin exon numbering). It seems probable that an 80 kDa utrophin isoform described by Fabbrizio *et al.* (37) that was detected in peripheral nerve by western blotting corresponds to Up71 protein. Up140 is predicted to encode a 6.75 kb mRNA and a 155 kDa protein comprising the last six repeats of the distal rod domain and the cysteine-rich and C-terminal domains of utrophin. This seems likely to be the equivalent of the mouse 140 kDa utrophin isoform detected by Peters *et al.* (29) after immunoaffinity purification of muscle fibre extracts. In a recent paper, Lumeng *et al.* reported multiple small utrophin

isoforms in adult mouse tissues, seen after western blotting using a C-terminal region antibody (38). Amongst these they identified a possible utrophin homologue of the short dystrophin isoform Dp71 in brain and a possible homologue of Dp140 in testis, muscle and other tissues. Taken together, these observations support the view that the Up71 and Up140 transcripts are translated into functional protein in some tissues.

What is the functional significance of Up71 and Up140? These short transcripts are predicted to encode proteins that have lost the N-terminal actin-binding domain and part or all of the long spectrin-like rod region. Both retain sequences that encode the C-terminal domains that mediate binding to membrane proteins and it seems probable that their cellular function will involve interactions with cell membranes. Utrophin and dystrophin share 74% amino acid identity in their membrane protein-binding domains and both are able to bind β -dystroglycan, syntrophin and dystrobrevin (10,39,40). It is possible that their sequence differences confer some discrete role in cellular function. This may be particularly true for Dp140 and Up140, which each contain a portion of the rod region where their protein homology is much less well conserved. However, it is also reasonable to propose that in tissues where short utrophin and dystrophin isoforms are co-expressed, they may be functionally redundant. This idea is attractive. It would help to explain why in Duchenne muscular dystrophy patients where internal promoters are lost by deletion there is not a severe clinical outcome in non-muscle tissues known to express short dystrophin isoforms. [Singularly amongst the short dystrophin isoforms, the loss of Dp260 has been linked to an ocular phenotype associated with an abnormal electroretinogram (25).] It would also help to explain why there is very little or no difference in clinical phenotype between mice knocked-out for utrophin in such a way that only full-length utrophin expression is ablated (41) and those in which the insertional mutation prevents transcription of all utrophin transcripts (42).

The importance of assigning splice patterns to particular isoforms of dystrophin was recognized once it was established that distinct mRNAs were being transcribed from alternative promoters and that differential splicing of dystrophin was transcript-specific (34,35). In the present study, we demonstrate that utrophin is also transcribed from multiple promoters and that the various transcripts show different patterns of mRNA splicing. Our findings regarding the splicing of exon 71 and the lack of differential splicing of exon 78 coincide exactly with those of Lumeng *et al.* (38), although in that study no information was given about which transcripts were subject to differential splicing. The alternative splicing of exon 71 in Up71 and Up140 may have functional significance since this exon is close to and upstream of the syntrophin/dystrobrevin-binding domains and may play a role in membrane-cytoskeletal interactions. It may be of significance that no evidence for alternative splicing of exon 78 was found for these short isoforms, although this is a feature of their dystrophin counterparts, Dp71 and Dp140 (34,35). In dystrophin, one of two consensus p34^{cdc2} phosphorylation sites is located in exon 78 and it has been proposed that alternative splicing of exon 78 may modulate phosphorylation, resulting in differential dystrophin-protein interactions. For utrophin, this mechanism would not have a functional outcome since the phosphorylation site in exon 78 is not conserved (34).

MATERIALS AND METHODS

5'-RACE

The 5' regions of utrophin cDNAs were amplified using the 5'-RACE procedure under conditions exactly as specified by the manufacturer (5'-RACE system; Gibco BRL, Paisley, UK). In brief, human RNA (1 μ g) was reverse transcribed using a utrophin-specific primer GSP1 and was C-tailed. After removal of the mRNA the cDNA was made double-stranded using the anchor primer GGCCACGCTCGACTAGTACGG₁₈; 5 μ l of this product were further amplified using the anchor primer and a nested utrophin-specific primer, GSP2. In order to facilitate cloning of the amplified products into the pAMP1 vector (Gibco BRL) using the uracil DNA glycosylase method, a third round of amplification was carried out using 5 μ l of a 1:100 dilution of the second round amplification product and primers with codons containing uracil (CAU₄ or CUA₄) incorporated at their 5' ends; these were the universal primer and either GSP2 or GSP3.

The primers used were: hGSP1-Up71, 5'-CTGTACGGTAGG-CAGAAAACG; hGSP2-Up71, 5'-CATTATTCAGGTCAGC-AAGGG; hGSP1-Up140, 5'-TCCCAGCGTTGGTTTAAACCT-GCC; hGSP2-Up140, 5'-GCTTCCATCTGCCTGGAGAG; hGSP3-Up140, 5'-TGCACAATCCCATCCCCAGTTCCG.

Isolation of human and mouse utrophin genomic clones

Human genomic clones containing utrophin sequence were isolated from the ICRF-sorted chromosome 6 library (ICRF reference C109; 13), by hybridization with a 288 bp ³²P-labelled PCR product amplified using hGSP2-Up140 located in exon 45 and hUp140-F6 (5'-CCTGATGACATTCATGAAGGTGG) located in the novel sequence. Mouse genomic clones were isolated from a λ DASH library (a gift from Dr A. Reith, UCL, London, UK) by hybridization with ³²P-labelled PCR products as probes; these were a 159 bp fragment amplified from exon 45 using mUp45-F2 (5'-GAACTGGAAGAGGGCCTCAGC) and mUp45-R2 (5'-TCCACCTCAGCTACAAGAGTGG) and a 62 bp fragment amplified from exon 63 using mUp63-R6 (5'-CAAGGGATT-GGAAGAGCTCAGTC) and mUp63-F5 (5'-CCATCAAACA-CAGACAACCTG). DNA was prepared from these recombinant clones using maxi-preparation kits from Qiagen.

RT-PCR

Human and mouse post-mortem tissues were collected and flash frozen in liquid nitrogen. The fetal mouse samples were taken between 11.5 and 15.5 days post-coitum and the human fetal samples were between 14 and 20 weeks gestation. RNA was isolated from tissue that had been powdered under liquid nitrogen and homogenized in RNazolB reagent (Biogenesis, Poole, UK). RNA RT-PCR was carried out using random oligonucleotide primers to generate first strand cDNA. In order to ensure that in the subsequent PCR, amplification of cDNA aliquots was specific for each utrophin isoform, the forward primers contained only sequence from the unique first exon of each alternative transcript. These primers were as follows: hUp71-F4, 5'-ATTGGCATTGGGTTTCTGAATGG; mUp71-F8, 5'-CTAGATT-TCTGAGCGATCC; hUp140-F6, 5'-GCCTGATGACATTCA-GAAGGTGG; mUp140-F4, 5'-AAGACATTATAGCCCTA-CCCCG.

Various control RT-PCRs were also carried out using the same cDNA samples. These included amplification of the ubiquitously expressed phosphoglucomutase (PGM1) gene (32) using the primers PGM1-1F (5'-AACAAAGATGCCCTTGGGAGCTGTGA) and PGM1-1R (5'-GAACTGATTGGACAGAAGGCACTAG), which amplify both mouse and human PGM1. In addition, amplification across human utrophin exons 16/17 and mouse utrophin exons 17-20 was carried out using the primers: hUp-ex16/17-F, 5'-GGAAGACATGGAAATGAGCGT; hUp-ex16/17-R, 5'-GCTTGTCTCTTACACGAA-CAGTC; mUp-ex17/20-F, 5'-GAGAACAAGGGATGGTGAAGAAGC; mUp-ex17/20-R, 5'-GCTGCTGAGATATCATC-TTCC.

DNA sequence analysis

DNA sequences were determined by the dideoxy chain termination method of Sanger *et al.* (43) using thermo-sequenase and a radiolabelled terminator cycle sequencing kit (Amersham Life Sciences, Little Chalfont, UK).

ACKNOWLEDGEMENTS

J.W. was supported by an MRC post-graduate studentship and C.J. by a research training grant from the EEC.

REFERENCES

- Tinsley, J.M., Blake, D.J., Roche, A., Fairbrother, U., Riss, J., Byth, B.C., Knight, A.E., Kendrick-Jones, J., Suthers, G.K., Love, D.R., Edwards, Y.H. and Davies, K.E. (1992) Primary structure of dystrophin-related protein. *Nature*, **360**, 591-592.
- Love, D.R., Morris, G.E., Ellis, J.M., Fairbrother, U., Marsden, R.F., Bloomfield, J.F., Edwards, Y.H., Slater, C.P., Parry, D.J. and Davies, K.E. (1991) Tissue distribution of the dystrophin-related gene product and expression in the *mdx* and *dy* mouse. *Proc. Natl Acad. Sci. USA*, **88**, 3243-3247.
- Schofield, J.N., Houzelstein, D., Davies, K., Buckingham, M. and Edwards, Y.H. (1993) Expression of the dystrophin-related protein (Utrophin) gene during mouse embryogenesis. *Dev. Dyn.*, **198**, 254-264.
- Koenig, M., Monaco, A.P. and Kunkel, L.M. (1988) The complete sequence of dystrophin predicts a rod-shaped cytoskeletal protein. *Cell*, **53**, 210-228.
- Ahn, A.H. and Kunkel, L.M. (1993) The structural and functional diversity of dystrophin. *Nature Genet.*, **3**, 283-291.
- Bewick, G.S., Nicholson, L., Young, C., O'Donnell, E. and Slater, C.R. (1992) Different distributions of dystrophin and related proteins at nerve muscle junctions. *Neuroreport*, **3**, 857-860.
- Law, D.J., Allen, D.L. and Tidball, J.G. (1994) Talin, vinculin and DRP (utrophin) concentrations are increased at the *mdx* myotendinous junctions following onset of necrosis. *J. Cell Sci.*, **107**, 1477-1483.
- Ervasti, J.M., Kahl, S.D. and Campbell, K.P. (1991) Purification of dystrophin from skeletal muscle. *J. Biol. Chem.*, **266**, 9161-9165.
- Matsumura, K. and Campbell, K.P. (1994) Dystrophin-glycoprotein complex: its role in the molecular pathogenesis of muscular dystrophies. *Muscle Nerve*, **17**, 2-15.
- Sadoulet-Puccio, H., Rajala, M. and Kunkel, L. (1997) Dystrobrevin and dystrophin: an interaction through coiled-coil motifs. *Proc. Natl Acad. Sci. USA*, **94**, 12413-12418.
- Campanelli, J.T., Roberds, S.L., Campbell, K.P. and Scheller, R.H. (1994) A role for dystrophin associated glycoproteins and utrophin in Agrin-induced AChR clustering. *Cell*, **77**, 663-674.
- Blake, D.J., Tinsley, J.M. and Davies, K.E. (1996) Utrophin: a structural and functional comparison to dystrophin. *Brain Pathol.*, **6**, 37-47.
- Clerk, A., Morris, G.E., Dubowitz, V., Davies, K.E. and Sewry, C.A. (1993) Dystrophin-related protein, utrophin, in normal and dystrophic human fetal skeletal muscle. *Histochem. J.*, **25**, 554-561.
- Karpati, G., Carpenter, S., Morris, G.G.E., Davies, K.E., Guerin, C. and Holland, P. (1993) Localisation and quantitation of the chromosome 6-encoded dystrophin-related protein in normal and pathological human muscle. *J. Neuropathol. Exp. Neurol.*, **52**, 119-128.
- Helliwell, T.R., Man, N.T., Morris, G.E. and Davies, K.E. (1992) The dystrophin-related protein, utrophin, is expressed on the sarcolemma of regenerating human skeletal muscle fibres in dystrophies and inflammatory myopathies. *Neuromusc. Disord.*, **2**, 177-184.
- Tinsley, J.M., Potter, A.C., Phelps, S.R., Fisher, R., Trickett, J.I. and Davies, K.E. (1996) Amelioration of the dystrophic phenotypes of *mdx* mice using a truncated utrophin transgene. *Nature*, **384**, 349-353.
- Rafael, J., Tinsley, J., Potter, A., Deconinck, A. and Davies, K. (1998) Skeletal muscle specific expression of a utrophin transgene rescues utrophin-dystrophin deficient mice. *Nature Genet.*, **19**, 79-82.
- Roush, W. (1997) Backup gene may help muscles help themselves. *Science*, **276**, 35-36.
- Klamut, K.J., Gangopadhyay, S.B., Worton, R.G. and Ray, P.N. (1990) Molecular and functional analysis of the muscle-specific promoter region of the Duchenne muscular dystrophy gene. *Mol. Cell. Biol.*, **10**, 193-205.
- Nudel, U., Zuk, D., Einat, P., Zeelon, E., Levy, Z., Neuman, S. and Yaffe, D. (1989) Duchenne muscular dystrophy gene product is not identical in muscle and brain. *Nature*, **337**, 76-78.
- Gorecki, D., Monaco, A., Derry, J., Walker, A., Barnard, E. and Barnard, P. (1992) Expression of four alternative dystrophin transcripts in brain regions regulated by different promoters. *Hum. Mol. Genet.*, **1**, 505-510.
- Bar, S., Barnea, E., Levy, Z., Neuman, S., Yaffe, D. and Nudel, U. (1990) A novel product of the Duchenne muscular dystrophy gene which greatly differs from the known isoforms in its structure and tissue distribution. *Biochem. J.*, **272**, 557-560.
- Lidov, H.G.W., Selig, S. and Kunkel, L.M. (1995) Dp140: a novel 140 kDa CNS transcript from the dystrophin locus. *Hum. Mol. Genet.*, **4**, 329-335.
- Byers, T.J., Lidov, H.G.W. and Kunkel, L.M. (1993) An alternative dystrophin transcript specific to peripheral nerve. *Nature Genet.*, **4**, 77-93.
- Kameya, S., Araki, E., Katsuki, M., Mizota, A., Adachi, E., Nakahara, K., Nonaka, I., Sakuragi, S., Takeda, S. and Nabeshima, Y.-I. (1997) Dp260 disrupted mice revealed prolonged implicit time of the b-wave in ERG and loss of accumulation of β -dystroglycan in the outer plexiform layer of the retina. *Hum. Mol. Genet.*, **6**, 2195-2203.
- Dennis, C.L., Tinsley, J.M., Deconinck, A.E. and Davies, K.E. (1996) Molecular and functional analysis of the utrophin promoter. *Nucleic Acids Res.*, **24**, 1646-1652.
- Gramolini, A., Dennis, C., Tinsley, J., Robertson, G., Cartaud, J., Davies, K. and Jasmin, B. (1997) Local transcriptional control of utrophin expression at the neuromuscular synapse. *J. Biol. Chem.*, **272**, 8117-8120.
- Blake, D.J., Schofield, J.N., Zuellig, R.A., Gorecki, D.C., Phelps, S.R., Barnard, E.A., Edwards, Y.H. and Davies, K.E. (1995) G-utrophin the autosomal homologue of dystrophin Dp116, is expressed in sensory ganglia and brain. *Proc. Natl Acad. Sci. USA*, **92**, 3697-3701.
- Peters, M., Adama, M. and Froehner, S. (1997) Differential association of syntrophin with the dystrophin complex. *J. Cell Biol.*, **138**, 81-93.
- Fabbrizio, E., Latouche, J., Rivier, F., Hugon, G. and Mornet, D. (1995) Re-evaluation of the distributions of dystrophin and utrophin in sciatic nerve. *Biochem. J.*, **312**, 309-314.
- Kozak, M. (1995) Adherence to the first-AUG rule when a second AUG codon follows closely upon the first. *Proc. Natl Acad. Sci. USA*, **92**, 2662-2666.
- Whitehouse, D.B., Putt, W., Lovegrove, J., Morrison, K., Hollyoake, M., Fox, M., Hopkinson, D.A. and Edwards, Y.H. (1992) Phosphoglucomutase 1: complete human and rabbit mRNA sequences and direct mapping of this highly polymorphic marker on human chromosome 1. *Proc. Natl Acad. Sci. USA*, **89**, 411-415.
- Lederfein, D., Yaffe, D. and Nudel, U. (1993) A housekeeping type promoter, located in the 3' region of the Duchenne muscular dystrophy gene, controls the expression of Dp71, a major product of the gene. *Hum. Mol. Genet.*, **2**, 1883-1888.
- Austin, R.C., Howard, P.L., D'Sousa, V.N., Kalmut, H.J. and Ray, P.N. (1995) Cloning and characterisation of alternatively spliced isoforms of Dp71. *Hum. Mol. Genet.*, **4**, 1475-1483.
- Lidov, H.G. and Kunkel, L.M. (1997) Dp140 alternatively spliced isoforms in brain and kidney. *Genomics*, **45**, 132-139.
- Wang, J., Pansky, A., Venuti, J.M., Yaffe, D. and Nudel, U. (1998) A sea-urchin gene encoding dystrophin-related proteins. *Hum. Mol. Genet.*, **7**, 581-588.

37. Fabrizio, E., Nudel, U., Hugon, G., Robert, A., Pons, F. and Mornet, D. (1995) Characterisation and localization of a 77 kDa protein related to the dystrophin gene family. *Biochem. J.*, **299**, 359–365.
38. Lumeng, C., Phelps, S., Rafael, J., Cox, G., Hutchinson, T., Begy, C., Adkins, E., Wiltshire, R. and Chamberlain, J. (1999) Characterization of dystrophin and utrophin diversity in the mouse. *Hum. Mol. Genet.*, **8**, 593–599.
39. Chamberlain, J.J., Corrado, K., Rafael, J.J., Cox, G.A., Hauser, M. and Lumeng, C. (1997) Interactions between dystrophin and the sarcolemma membrane. *Soc. Gen. Physiol. Ser.*, **52**, 19–29.
40. Peters, M.F., Sadoulet-Puccio, H.M., Grady, M.R., Kramarcy, N.R., Kunkel, L.M., Sanes, J.R., Sealock, R. and Froehner, S.C. (1998) Differential membrane localisation and intermolecular associations of alpha-dystrobrevin isoforms in skeletal muscle. *J. Cell Biol.*, **142**, 1269–1278.
41. Deconinck, A.E., Potter, A.C., Tinsley, J.M., Wood, S.J., Vater, R., Young, C., Metzinger, L., Vincent, A., Slater, C.R. and Davies, K.E. (1997) Postsynaptic abnormalities at the neuromuscular junctions of utrophin-deficient mice. *J. Cell Biol.*, **136**, 883–894.
42. Grady, R.M., Merlie, J.P. and Sanes, J.R. (1997) Subtle neuromuscular defects in utrophin-deficient mice. *J. Cell Biol.*, **136**, 871–882.
43. Sanger, F., Nicklen, S. and Coulson, A.R. (1977) DNA sequencing with chain terminating inhibitors. *Proc. Natl Acad. Sci. USA*, **74**, 5436–5467.